COMPLETED

3. N88:25/3319

Westinghouse Hanford Company

NUREG/CR-3319
HEDL-TME 85-3

LWR PRESSURE VESSEL SURVEILLANCE DOSIMETRY IMPROVEMENT PROGRAM:

LWR POWER REACTOR SURVEILLANCE PHYSICS-DOSIMETRY DATA BASE COMPENDIUM

ORIGINAL

Edited by:
W.N. McElroy

Hanford Engineering Development Laboratory
Operated by
Westinghouse Hanford Company

Prepared for
U.S. Nuclear Regulatory Commission

U.S. Nuclear Regulatory Commission

BEST COPY AVAILABLE

NUREG/CR-3319
HEDL-TME 85-3
R5

LWR PRESSURE VESSEL SURVEILLANCE DOSIMETRY IMPROVEMENT PROGRAM:

LWR POWER REACTOR SURVEILLANCE PHYSICS-DOSIMETRY DATA BASE COMPENDIUM

Edited by:
W.N. McElroy

Manuscript Completed: July 1985
Date Published: August 1985

Hanford Engineering Development Laboratory

Operated by Westinghouse Hanford Company
P.O. Box 1970 Richland, WA 99352
A Subsidiary of Westinghouse Electric Corporation

Prepared for Division of Engineering Technology
Office of Nuclear Regulatory Research
U.S. Nuclear Regulatory Commission
Washington, DC 20555
NRC FIN No. B5988

I

NOTICE

This report was prepared as an account of work sponsored by an agency of the United States Government. Neither the United States Government nor any agency thereof, or any of their employees, makes any warranty, expressed or implied, or assumes any legal liability of responsibility for any third party's use, or the results of such use, of any information, apparatus, product or process disclosed in this report, or represents that its use by such third party would not infringe privately owned rights.

NOTICE

Availability of Reference Materials Cited in NRC Publications

Most documents cited in NRC publications will be available from one of the following sources:

1. The NRC Public Document Room, 1717 H Street, N.W.
   Washington, DC 20555
2. The Superintendent of Documents, U.S. Government Printing Office, Post Office Box 37082, Washington, DC 20013-7082
3. The National Technical Information Service, Springfield, VA 22161

Although the listing that follows represents the majority of documents cited in NRC publications, it is not intended to be exhaustive.

Referenced documents available for inspection and copying for a fee from the NRC Public Document Room include NRC correspondence and internal NRC memoranda; NRC Office of Inspection and Enforcement bulletins, circulars, information notices, inspection and investigation notices; Licensee Event Reports; vendor reports and correspondence; Commission papers; and applicant and licensee documents and correspondence.

The following documents in the NUREG series are available for purchase from the NRC/GPO Sales Program: formal NRC staff and contractor reports, NRC-sponsored conference proceedings, and NRC booklets and brochures. Also available are Regulatory Guides, NRC regulations in the *Code of Federal Regulations*, and *Nuclear Regulatory Commission Issuances*.

Documents available from the National Technical Information Service include NUREG series reports and technical reports prepared by other federal agencies and reports prepared by the Atomic Energy Commission, forerunner agency to the Nuclear Regulatory Commission.

Documents available from public and special technical libraries include all open literature items, such as books, journal and periodical articles, and transactions. *Federal Register* notices, federal and state legislation, and congressional reports can usually be obtained from these libraries.

Documents such as theses, dissertations, foreign reports and translations, and non-NRC conference proceedings are available for purchase from the organization sponsoring the publication cited.

Single copies of NRC draft reports are available free, to the extent of supply, upon written request to the Division of Technical Information and Document Control, U.S. Nuclear Regulatory Commission, Washington, DC 20555.

Copies of industry codes and standards used in a substantive manner in the NRC regulatory process are maintained at the NRC Library, 7920 Norfolk Avenue, Bethesda, Maryland, and are available there for reference use by the public. Codes and standards are usually copyrighted and may be purchased from the originating organization or, if they are American National Standards, from the American National Standards Institute, 1430 Broadway, New York, NY 10018.

LWR POWER REACTOR SURVEILLANCE PHYSICS-DOSIMETRY
DATA BASE COMPENDIUM

FOREWORD

The Light Water Reactor Pressure Vessel Surveillance Dosimetry Improvement Program (LWR-PV-SDIP) has been established by NRC to improve, test, verify, and standardize the physics-dosimetry-metallurgy, damage correlation, and associated reactor analysis methods, procedures, and data used to predict the integrated effect of neutron exposure to LWR pressure vessels and their support structures. A vigorous research effort attacking the same measurement and analysis problems exists worldwide; and strong cooperative links between US NRC-supported activities at HEDL, ORNL, NBS, and MEA and those supported by CEN/SCK (Mol, Belgium), EPRI (Palo Alto, CA, USA), KFA (Jülich, Germany), and several UK laboratories have been extended to other countries. These cooperative links are strengthened by the active membership of the scientific staff from many countries and laboratories in the ASTM E10 Committee on Nuclear Technology and Applications. Several ASTM E10 subcommittees are responsible for preparation of LWR surveillance standards.

The primary objective of this multilaboratory program is to prepare an updated and improved set of physics-dosimetry-metallurgy, damage correlation, and associated reactor analysis ASTM standards for LWR pressure vessel and support structure irradiation surveillance programs. Supporting this objective are a series of analytical and experimental validation and calibration studies in "Standard, Reference, and Controlled Environment Benchmark Fields," research reactor "Test Regions," and operating power reactor "Surveillance Positions."

These studies will establish and certify the precision and accuracy of the measurement and predictive methods recommended in the ASTM standards and used for the assessment and control of present and end-of-life (EOL) conditions of pressure vessel and support structure steels. Consistent and accurate measurement and data analysis techniques and methods, therefore, will be developed, tested, and verified along with guidelines for required neutron field calculations to correlate changes in material properties with characteristics of the neutron radiation field. Application of established ASTM standards should permit the reporting of measured materials property changes and neutron exposures to an accuracy and precision within 10% to 30%, depending on the measured metallurgical variable and neutron environment.

Assessment of the radiation-induced degradation of material properties in a power reactor requires accurate definition of the neutron field from the outer region of the reactor core to the outer boundaries of the pressure vessel. The accuracy of measurements on neutron flux and spectrum is associated with two distinct components of LWR irradiation surveillance procedures: 1) proper application of calculational estimates of the neutron exposure at in- and ex-vessel surveillance positions, various locations in the vessel wall and in ex-vessel support structures, and 2) understanding the relationship between material property changes in reactor vessels and their support structures, and in metallurgical test specimens irradiated in test reactors and at accelerated neutron flux positions in operating power reactors.

The first component requires verification and calibration experiments in a variety of neutron irradiation test facilities, including LWR-PV mockups, power reactor surveillance positions, and related benchmark neutron fields. The benchmarks serve as a permanent reference measurement for neutron flux and fluence detection techniques. The second component requires serious extrapolation of an observed neutron-induced mechanical property change from research reactor "Test Regions" and operating power reactor "Surveillance Positions" to locations inside the body of the pressure vessel wall and to ex-vessel support structures. The neutron flux at the vessel inner wall is up to one order of magnitude lower than at surveillance specimen positions and up to two orders of magnitude lower than at test reactor positions. At the vessel outer wall, the neutron flux is one order of magnitude or more lower than at the vessel inner wall. Further, the neutron spectra at, within, and leaving the vessel are substantially different.

To meet reactor pressure vessel radiation monitoring requirements, a variety of neutron flux and fluence detectors are employed, most of which are passive. Each detector must be validated for application to the higher flux and harder neutron spectrum of the research reactor "Test Region" and to the lower flux and degraded neutron spectrum at "Surveillance Positions." Required detectors must respond to neutrons of various energies so that multigroup spectra can be determined with accuracy sufficient for adequate damage response estimates. Detectors being used, developed, and tested for the program include radiometric (RM) sensors, helium accumulation fluence monitor (HAFM) sensors, solid state track recorder (SSTR) sensors, and damage monitor (DM) sensors.

The necessity for pressure vessel mockup facilities for physics-dosimetry investigations and for irradiation of metallurgical specimens was recognized early in the formation of the NRC program. Experimental studies associated with high- and low-flux versions of a pressurized water reactor (PWR) pressure vessel mockup are in progress in the US, Belgium, France, and United Kingdom. The US low-flux version is known as the ORNL Poolside Critical Assembly (PCA) and the high-flux version is known as the Oak Ridge Research Reactor (ORR) Poolside Facility (PSF), both located at Oak Ridge, Tennessee. As specialized benchmarks, these facilities provide well-characterized neutron environments where active and passive neutron dosimetry, various types of LWR-PV and support structure neutron field calculations, and temperature-controlled metallurgical specimen exposures are brought together.

The two key low-flux pressure vessel mockups in Europe are known as the Mol-Belgium-VENUS and Winfrith-United Kingdom-NESDIP facilities. The VENUS Facility is being used for PWR core source and azimuthal lead-factor studies, while NESDIP is being used for PWR cavity and azimuthal lead-factor studies. A third and important low-fluence pressure vessel mockup in Europe is identified with a French PV-simulator at the periphery of the Triton reactor. It served as the irradiation facility for the DOMPAC dosimetry experiment to study surveillance capsule perturbations and through-PV-wall radial fluence and damage profiles (gradients) for PWRs of the Fessenheim 1 type.

Results of measurement and calculational strategies outlined here will be made available for use by the nuclear industry as ASTM standards. Federal Regulations 10CFR50 (Cf83) already requires adherence to several ASTM standards that establish a surveillance program for each power reactor and incorporate metallurgical specimens, physics-dosimetry flux-fluence monitors, and neutron field evaluation. Revised and new standards in preparation will be carefully updated, flexible, and, above all, consistent.

ACKNOWLEDGMENTS

The success of the LWR Pressure Vessel Surveillance Dosimetry Improvement Program (LWR-PV-SDIP) continues to depend on the efforts and the free exchange of ideas and views by representatives of a large number of research, service, regulatory, vendor, architect/engineer, and utility organizations. The information reported herein could not have been developed without the continuing support of the respective funding organizations and their management and technical staffs. Special acknowledgment is due to C. Z. Serpan of NRC for having identified the need for an international program such as the LWR-PV-SDIP and for making it possible by taking a strong overall support and management lead.

Additional acknowledgment is due to B. R. Hayward, R. L. Knecht, W. F. Sheely, and H. H. Yoshikawa of HEDL for their constructive comments and help in the preparation and review of program documentation. Contributions to this handbook resulting from interactions with other LWR-PV-SDIP participants are also acknowledged. Very special acknowledgment is given to J. M. Dahlke who edited this document; to D. C. Smith of the HEDL Irradiation Environment Group; and to the HEDL Technical Publications, Word Processing, Graphics, and Duplicating personnel who contributed to its preparation.

Authors and contributors for specific sections are:

S.0, 1.0.1, 1.0.2, 1.0.2.2, 4.1, 4.1.2, 4.1.3, 4.1.4, 4.2 - 4.5, 5.1, 5.2	WN McElroy (HEDL)
1.0.2.1	PN Randall (NRC)
1.1, 1.0.2.2, 2.1, 3.1, 5.5	SL Anderson, TR Mager, SE Yanichko (W-NTD); WN McElroy (HEDL)
1.2, 2.2, 3.2, 5.6	JP Higgins, JN Kass, G. Martin (GE); WN McElroy (HEDL)
1.3, 2.3, 3.3, 5.7	JJ Koziol (CE); WN McElroy (HEDL)
1.4, 2.4, 3.4, 5.8	CL Whitmarsh, AL Lowe Jr, HS Palme (B&W); WN McElroy (HEDL)
3.5, 5.10	MP Manahan, RS Denning, RG Jung, LM Lowry (BMI)
3.6, 5.9	EB Norris (SwRI)
4.1.1	JA Grundl, ED McGarry (NBS)
4.1.2, 5.1	EP Lippincott, WN McElroy (HEDL)
4.1.2, 4.1.3, 4.2 - 4.5	RL Simons, WN McElroy (HEDL)
4.1.4	FH Ruddy, WN McElroy (HEDL)
5.3	FW Stallmann (ORNL)
5.4	AL Aronson, JF Carew (BNL)
Bibliography	JM Dahlke (HEDL)

CONTENTS

Page

Foreword iii

Acknowledgments vi

Acronyms xii

S.0 SUMMARY S-1

1.0 NUCLEAR REACTOR PRESSURE VESSEL AND SUPPORT STRUCTURES SURVEILLANCE 1.0-1

- 1.0.1 Introduction 1.0-1
  - 1.0.1.1 NRC and EPRI Physics-Dosimetry-Metallurgy Data Base Compendia 1.0-1
  - 1.0.1.2 Background 1.0-2
- 1.0.2 Codes, Standards, and Regulatory Rules 1.0-3
  - 1.0.2.1 NRC Regulations and Licensing Requirements 1.0-4
  - 1.0.2.2 ASTM Standards 1.0-5

1.1 WESTINGHOUSE (W) REACTORS 1.1-1

- 1.1.1 Surveillance Programs 1.1-1
  - 1.1.1.1 Surveillance Capsules 1.1-1
  - 1.1.1.2 Capsule Removal 1.1-5
  - 1.1.1.3 Neutron Flux Monitors 1.1-5

1.2 GENERAL ELECTRIC (GE) REACTORS 1.2-1

- 1.2.1 Surveillance Programs 1.2-1
  - 1.2.1.1 Surveillance Capsules 1.2-1
  - 1.2.1.2 Capsule Removal 1.2-2
  - 1.2.1.3 Neutron Flux Monitors 1.2-2
  - 1.2.1.4 Potential Surveillance Program Modifications 1.2-2

1.3 COMBUSTION ENGINEERING (CE) REACTORS 1.3-1

- 1.3.1 Surveillance Programs 1.3-1
  - 1.3.1.1 Surveillance Capsules 1.3-3
  - 1.3.1.2 Capsule Removal 1.3-11
  - 1.3.1.3 Neutron Flux and Correlation Monitors 1.3-11

CONTENTS (Cont'd)

Page

1.4 BABCOCK AND WILCOX (B&W) REACTORS 1.4-1

1.4.1 Surveillance Programs 1.4-1

1.4.1.1 Surveillance Capsules 1.4-6
1.4.1.2 Capsule Removal 1.4-9
1.4.1.3 Nuclear Flux Monitors 1.4-9

2.0 PHYSICS-DOSIMETRY SURVEILLANCE PROGRAMS FOR PWR AND BWR 2.0-1

2.1 W-NTD CAPSULE PHYSICS-DOSIMETRY 2.1-1

2.1.1 Surveillance Capsules 2.1-1
2.1.2 Reactor Physics Calculations 2.1-1
2.1.3 Results of Reactor Physics Calculations 2.1-5

2.2 GE CAPSULE PHYSICS-DOSIMETRY 2.2-1

2.2.1 Surveillance Capsules 2.2-1
2.2.2 Reactor Physics Calculations 2.2-1
2.2.3 Results of Reactor Physics Calculations 2.2-1

2.3 CE CAPSULE PHYSICS-DOSIMETRY 2.3-1

2.3.1 Surveillance Capsules 2.3-1
2.3.2 Reactor Physics Calculations 2.3-1
2.3.3 Results of Reactor Physics Calculations 2.3-1

2.4 B&W CAPSULE PHYSICS-DOSIMETRY 2.4-1

2.4.1 Surveillance Capsules 2.4-1
2.4.2 Reactor Physics Calculations 2.4-1
2.4.3 Results of Reactor Physics Calculations 2.4-1

3.0 EVOLUTION OF PWR AND BWR REACTOR SURVEILLANCE DATA PROCESSING 3.0-1

3.1 SURVEILLANCE DOSIMETRY DATA PROCESSING AT W-NTD 3.1-1

3.1.1 Neutron Dosimetry 3.1-1
3.1.2 Comparison of Measurement and Calculations 3.1-1

3.2 SURVEILLANCE DOSIMETRY DATA PROCESSING AT GE 3.2-1

3.3 SURVEILLANCE DOSIMETRY DATA PROCESSING AT CE 3.3-1

CONTENTS (Cont'd)

Page

3.4 SURVEILLANCE DOSIMETRY DATA PROCESSING AT B&W 3.4-1

3.4.1 Analytical Fluence Calculations 3.4-1
3.4.2 Dosimeter Activity Calculations and Measurements 3.4-3
3.4.3 Normalization of Calculations 3.4-5
3.4.4 Calculation Benchmarks 3.4-5

3.5 SURVEILLANCE DOSIMETRY DATA PROCESSING AT BMI 3.5-1

3.5.1 Approach 3.5-1
3.5.2 Radiochemistry and Counting Procedures 3.5-3
3.5.3 Neutronics Analyses 3.5-4

3.6 SURVEILLANCE DOSIMETRY DATA PROCESSING AT SwRI 3.6-1

3.6.1 Evolution of Processing Procedures 3.6-1
3.6.2 Evaluation of Dosimeter Activities 3.6-1
3.6.3 Calculation of Spectrum-Averaged Cross Sections 3.6-2
3.6.4 Determination of Surveillance Capsule Fluence 3.6-4
3.6.5 Calculation Benchmarks 3.6-5

4.0 DETERMINATION OF EXPOSURE PARAMETER VALUES AND UNCERTAINTIES FOR OPERATING PWR AND BWR POWER PLANTS 4.0-1

4.1 DATA ANALYSIS METHODS 4.1-1

4.1.1 Examination of Individual Detector Responses Using National Bureau of Standards Procedures 4.1-2

4.1.1.1 Exposure Parameters from Individual Detectors 4.1-5
4.1.1.2 Consideration of Errors 4.1-10

4.1.2 HEDL National Reactor Dosimetry Center Procedures 4.1-12

4.1.2.1 Introduction 4.1-12
4.1.2.2 Description of the FERRET-SAND II Analysis and Input Data 4.1-12

CONTENTS (Cont'd)

Page

4.1.2.3 Calculated Flux-Spectral Data 4.1-15
4.1.2.4 Cross-Section Data 4.1-15
4.1.2.5 Comparison of FERRET-SAND II Analysis and Individual Detectors 4.1-15

4.1.3 Reactor Surveillance Capsule Analysis Procedures and Results 4.1-17

4.1.3.1 Introduction 4.1-17
4.1.3.2 Analysis Procedures 4.1-17
4.1.3.3 Results 4.1-23

4.1.4 Reactor Cavity Analysis Procedures and Results 4.1-27

4.1.4.1 Introduction 4.1-27
4.1.4.2 Recommended Dosimetry Sets 4.1-28
4.1.4.3 Dosimetry Capsules and Thermal Neutron Shields 4.1-29
4.1.4.4 Placement of Dosimeters 4.1-30
4.1.4.5 Measurement of Dosimetry Sensor Reaction Products 4.1-30
4.1.4.6 Data Analysis 4.1.31
4.1.4.7 Benchmarking and Uncertainty Evaluation 4.1-31
4.1.4.8 Status of Work and Results for Cavity Surveillance Dosimetry 4.1.32

4.2 WESTINGHOUSE SURVEILLANCE CAPSULES: SPECIFIC DETAILS 4.2-1

4.3 COMBUSTION ENGINEERING SURVEILLANCE CAPSULES: SPECIFIC DETAILS 4.3-1

4.4 BABCOCK AND WILCOX SURVEILLANCE CAPSULES: SPECIFIC DETAILS 4.4-1

4.5 GENERAL ELECTRIC SURVEILLANCE CAPSULES: SPECIFIC DETAILS 4.5-1

5.0 SURVEILLANCE DATA DEVELOPMENT, EVALUATION, AND SPACIAL AND TEMPORAL EXTRAPOLATIONS 5.0-1

5.1 DETERMINATION OF NEUTRON DAMAGE 5.1-1

5.1.1 Introduction 5.1-1
5.1.2 Evaluation of Neutron Damage 5.1-2
5.1.3 Physics-Dosimetry Nuclear Data Needs 5.1-3

CONTENTS (Cont'd)

Page

5.1.4 Physics-Dosimetry-Metallurgy Standards 5.1-5
5.1.5 Conclusions 5.1-6

5.2 TREND CURVE DATA DEVELOPMENT, TESTING, AND APPLICATIONS 5.2-1

5.3 THE USE OF ADJUSTMENT METHODS AND RELATED STATISTICAL ANALYSIS FOR THE EVALUATION OF PRESSURE VESSEL SURVEILLANCE RESULTS 5.3-1

5.3.1 Introduction 5.3-1
5.3.2 Statistical Analysis in Support of Dosimetry for Metallurgical Tests 5.3-2
5.3.3 Statistical Analysis for the Verification of Reactor Calculations and Extrapolation to End-of-Life Conditions 5.3-4
5.3.4 Summary and Recommendations 5.3-5

5.4 EVALUATION OF METHODS FOR REDUCING PRESSURE VESSEL FLUENCE 5.4-1

5.4.1 Pressure Vessel Radiation Embrittlement Calculations Programs 5.4-1
5.4.2 Benchmarking of Pressure Vessel Fluence Calculations 5.4-2

5.5 W-NTD PROCEDURES 5.5-1

5.6 GE PROCEDURES 5.6-1

5.7 CE PROCEDURES 5.7-1

5.8 B&W PROCEDURES 5.8-1

5.8.1 Plant Specific Fluence 5.8-1
5.8.2 Radial and Azimuthal Gradients 5.8-1
5.8.3 Fluence Lead Factors 5.8-4
5.8.4 Fluence Uncertainty 5.8-4

5.9 SwRI PROCEDURES 5.9-1

5.9.1 Determination of Vessel Wall Exposure 5.9-1
5.9.2 Verification of Fluence Rate Calculations 5.9-1

5.10 BMI PROCEDURES 5.10-1

BIBLIOGRAPHY B-1

ACRONYMS

ANO-1	Arkansas Nuclear One Reactor
ASME	American Society of Mechanical Engineers
ASTM	American Society for Testing and Materials
BMI	Battelle Memorial Institute, Columbus, Ohio
BSR	Bulk Shielding Reactor
BWR	Boiling Water Reactor
B&W	Babcock & Wilcox
CE	Combustion Engineering
CEN/SCK	Centre d'Etude de l'Energie Nucleaire, Mol, Belgium
CR-3	Crystal River-3 Reactor
DETAN	A Computer Code that Calculates Integral Cross Sections by Folding Cross Section Data Over a Neutron Spectrum
DM	Damage Monitor
DOE	Department of Energy
DOMPAC	Triton Reactor Thermal Shield and Pressure Vessel Mockup, Forenay-aux-Roses, France
EFPY	Effective Full-Power Years
ENDF	Evaluated Nuclear Data File
EOL	End-of-Life
EPRI	Electric Power Research Institute, Pal Alto, California
FERRET	Least-Squares Adjustment Code
FFTF	Fast Flux Test Facility
FSAR	Final Safety Analysis Report
FWHM	Full Width, Half Maximum
GE	General Electric Company
HAFM	Helium Accumulation Fluence Monitor
HEDL	Hanford Engineering Development Laboratory, Richland, WA
HSST	Heavy Section Steel Technology
IAEA	International Atomic Energy Agency, Vienna, Austria
ISNF	Intermediate-Energy Standard Neutron Field (at NBS)
KFA	Kernforshungsanlage Jülich GmbH, Federal Republic of Germany
LBP	Lump Burnable Poison

BEST COPY AVAILABLE

ACRONYMS (Cont'd)

LRC	Lynchburg Research Center
LWR	Light Water Reactor
MEA	Materials Engineering Associates Inc, Oxen Hill, Maryland
MP	Midplane
MPC	Metal Properties Council
NBS	National Bureau of Standards, Gaithersburg, Maryland
NDTT	Nil Ductility Transition Temperature
ΔNDTT	Nil Ductility Transition Temperature Shift
NESDIP	NESTOR Shielding and Dosimetry Improvement Program, UK
NRC	Nuclear Regulatory Commission
NRDC	National Reactor Dosimetry Center (at HEDL)
NRE	Nuclear Research Emulsion
NSSS	Nuclear Steam Supply Systems
NUREG	Nuclear Regulatory Commission Report Designation
ORNL	Oak Ridge National Laboratory
ORR	Oak Ridge (Research) Reactor (at ORNL)
ORR-PSF	Oak Ridge (Research) Reactor - Poolside Facility
PCA	Poolside Critical Assembly (at ORNL)
PF	Perturbation Factor
PSF	Poolside Facility (at ORNL)
PTS	Pressurized Thermal Shock
PV	Pressure Vessel
PVS	Pressure Vessel Simulator
PWR	Pressurized Water Reactor
RM	Radiometric Monitor
RPD	Relative Power Density
RPV	Reactor Pressure Vessel
RT_{NDT}	Reference Nil-Ductility Temperature
RVSP	Reactor Vessel Surveillance Program
SAILOR	Shielding- and -Application-Independent Libraries for Operating Reactors
SAND II	Spectrum Analysis by Neutron Detectors, Version II (A Multiple-Foil Adjustment Code)

ACRONYMS (Cont'd)

SDIP	Surveillance Dosimetry Improvement Program
SDMF	Simulated Dosimetry Measurement Facility
SPVC	Simulated Pressure Vessel Capsule
SSC	Simulated Surveillance Capsule
SSTR	Solid State Track Recorder
SUNY-NSTF	State University of New York - Nuclear Science and Technology Facilities, Buffalo, NY
SwRI	Southwest Research Institute, San Antonio, Texas
TS	Thermal Shield
UK	United Kingdom
US	United States
VENUS	PV Mockup (at Mol, Belgium)
W	Westinghouse
West2LP	Westinghouse 2-Loop Plant
W-NTD	Westinghouse - Nuclear Technology Division

LWR POWER REACTOR SURVEILLANCE PHYSICS-DOSIMETRY

DATA BASE COMPENDIUM

S.0 SUMMARY

This NRC physics-dosimetry compendium (Sections 1.0 through 4.0) is a collation of information and data developed from available research and commercial light water reactor vessel surveillance program (RVSP) documents and related surveillance capsule reports. The Section 4.0 data represents the results of the HEDL least-squares FERRET-SAND II Code re-evaluation of exposure units and values for 47 PWR and BWR surveillance capsules for W, B&W, CE, and GE power plants (see Figure S.1). Using a consistent set of auxiliary data and dosimetry-adjusted reactor physics results, the revised fluence values (Table 4.1.3.3 of Section 4.1.3) for E > 1 MeV averaged 25% higher than the originally reported values. The range of fluence values (new/old) was from a low of 0.80 to a high of 2.38.

These HEDL-derived FERRET-SAND II exposure parameter values are being used for NRC-supported HEDL and other PWR and BWR trend curve data development and testing studies, as discussed in Sections 4.0 and 5.0. These studies are providing results to support Revision 2 of Regulatory Guide 1.99. As stated by Randall (Ra84), the Guide is being updated to reflect recent studies of the physical basis for neutron radiation damage and efforts to correlate damage to chemical composition and fluence.

The information in this document is also being made available to the ASTM E10 Committee, to the Metal Properties Council (MPC) Subcommittee 6 on Materials for Nuclear Reactors, and to others developing improved data bases and trend curves. These curves are used by the utilities and by the NRC to account for neutron radiation damage in setting pressure/temperature limits, in making fracture analysis, and in predicting neutron-induced changes in reactor PV steel fracture toughness and embrittlement during the vessel's service life.

The status of the development and application of new advancements in LWR reactor surveillance programs, such as cavity physics-dosimetry for improving the reliability of current and end-of-life (EOL) predictions on the metallurgical conditions of pressure vessels and their support structures, is discussed in Sections 4.0 and 5.0 with appropriate referencing to the current literature, federal and NRC regulations and rules, and the new series of 21 ASTM LWR Surveillance Standards. Application of established ASTM standards is expected to permit the reporting of measured materials property changes and neutron exposures to an accuracy and precision within bounds of 10% to 30%, depending on the measured metallurgical variable and neutron environment.

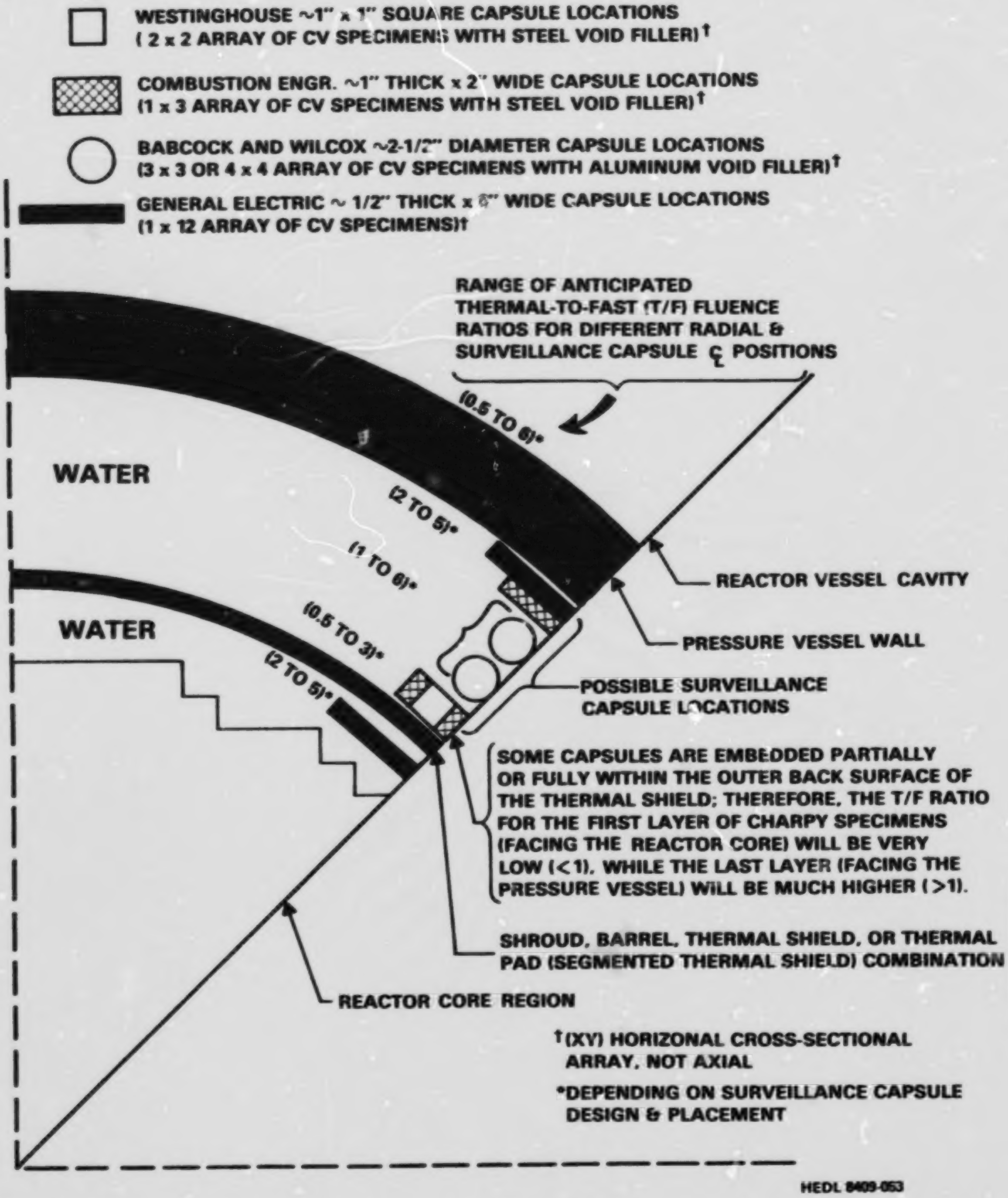
☐ WESTINGHOUSE ~1" x 1" SQUARE CAPSULE LOCATIONS
(2 x 2 ARRAY OF CV SPECIMENS WITH STEEL VOID FILLER)†
▨ COMBUSTION ENGR. ~1" THICK x 2" WIDE CAPSULE LOCATIONS
(1 x 3 ARRAY OF CV SPECIMENS WITH STEEL VOID FILLER)†
○ BABCOCK AND WILCOX ~2-1/2" DIAMETER CAPSULE LOCATIONS
(3 x 3 OR 4 x 4 ARRAY OF CV SPECIMENS WITH ALUMINUM VOID FILLER)†
■ GENERAL ELECTRIC ~ 1/2" THICK x 6" WIDE CAPSULE LOCATIONS
(1 x 12 ARRAY OF CV SPECIMENS)†
RANGE OF ANTICIPATED THERMAL-TO-FAST (T/F) FLUENCE RATIOS FOR DIFFERENT RADIAL & SURVEILLANCE CAPSULE ℄ POSITIONS
(0.5 TO 6)*
(2 TO 5)*
(1 TO 6)*
(0.5 TO 3)*
(2 TO 5)*
WATER
WATER
REACTOR VESSEL CAVITY
PRESSURE VESSEL WALL
POSSIBLE SURVEILLANCE CAPSULE LOCATIONS
SOME CAPSULES ARE EMBEDDED PARTIALLY OR FULLY WITHIN THE OUTER BACK SURFACE OF THE THERMAL SHIELD; THEREFORE, THE T/F RATIO FOR THE FIRST LAYER OF CHARPY SPECIMENS (FACING THE REACTOR CORE) WILL BE VERY LOW (<1), WHILE THE LAST LAYER (FACING THE PRESSURE VESSEL) WILL BE MUCH HIGHER (>1).
SHROUD, BARREL, THERMAL SHIELD, OR THERMAL PAD (SEGMENTED THERMAL SHIELD) COMBINATION
REACTOR CORE REGION
†(XY) HORIZONAL CROSS-SECTIONAL ARRAY, NOT AXIAL
*DEPENDING ON SURVEILLANCE CAPSULE DESIGN & PLACEMENT
HEDL 8409-053

FIGURE S.1. Schematic Representation of In-Vessel Surveillance Capsule Designs and Locations for Operating PWRs and BWRs.

1.0 NUCLEAR REACTOR PRESSURE VESSEL AND SUPPORT STRUCTURES SURVEILLANCE

1.0.1 Introduction

1.0.1.1 NRC and EPRI Physics-Dosimetry-Metallurgy Data Base Compendia

This NRC LWR Power Reactor Surveillance Physics-Dosimetry Data Base Compendium provides, in loose-leaf form, new or re-evaluated exposure rate [total ($E > 0.0$ eV), thermal ($E < 0.414$ eV), and fast ($E > 0.1$ and $E > 1.0$ MeV) neutron flux levels and dpa/s in iron] and exposure [neutron fluence ($E > 1.0$ MeV) and dpa in iron] values based on multiple foil reaction rate measurements for individual surveillance capsules removed from operating PWR and BWR power plants. As reactor vessel surveillance program (RVSP) reports received by NRC from utilities are re-evaluated with FERRET-SAND II or other least-squares-type codes, this document will be periodically revised. These RVSP reports are prepared under mandate of the Nuclear Regulatory Commission (NRC) to assess the extent of radiation embrittlement in the pressure vessel steels of commercial nuclear power plants.

The corresponding "irradiated" and "unirradiated" metallurgical data bases are provided in the loose-leaf EPRI NP-2428, "Irradiated Nuclear Pressure Vessel Steel Data Base" (Mc82c) and EPRI NP-933, "Nuclear Pressure Vessel Steel Data Base" (Se78) reports, respectively. The current exposure parameter values provided in EPRI NP-2428 are flux ($E > 1.0$ MeV) and fluence ($E > 1.0$ MeV), in general, based on only the measured ^{54}Fe(n,p)^{54}Mn reaction rate and the associated calculated iron spectral averaged cross section.

The RVSP reports are the primary source of the physics-dosimetry information and input data used for the FERRET-SAND II least-squares code analyses reported herein. The assessment and re-evaluation of the reliability, consistency, and accuracy of the input data have been a joint cooperative effort among staff members of the HEDL National Reactor Dosimetry Center (NRDC), Oak Ridge National Laboratory (ORNL), the National Bureau of Standards (NBS), the Nuclear Regulatory Commission (NRC), the Electric Power Research Institute (EPRI), and the four reactor vendors and two other service laboratories that have prepared the RVSP reports for the utilities who operate the PWR and BWR Nuclear Steam Supply Systems (NSSS).

The surveillance programs developed by each of the four reactor vendors for their particular type of reactors are reviewed in Sections 1.1 through 1.4 and 2.1 through 2.4. Evolution of the reactor surveillance data processing program offered to the utilities by each of the six service laboratories (W,, GE, CE, B&W, BMI, and SwRI) is discussed in Sections 3.1 through 3.6.

The methods used, the determination of re-evaluated exposure parameter values with uncertainties, and the documentation of the HEDL FERRET-SAND II least-squares code results are provided in Section 4.0 according to reactor type

(W, GE, CE, or B&W). The key results are summarized in Table 4.1.3.3 of Section 4.1.3.

Sections 4.1.4 and 5.0 consider more recent advances in surveillance data development, testing, and applications; low-leakage core flux reduction methods; and spacial and temporal extrapolations based on work that has been accomplished by the reactor vendors, utilities, service laboratories, and other LWR Pressure Vessel Surveillance Dosimetry Improvement Program (LWR-PV-SDIP) participants.

It is anticipated that a NRC "LWR Test Reactor Physics-Dosimetry Data Base Compendium" (NUREG/CR-3322) will be prepared to present results from FERRET-SAND II, LSL, and other least-squares-type code analyses of physics-dosimetry for US (BSR, PSF, SUNY-NSTF Buffalo, Virginia, etc.); UK (DIDO, HERALD, etc.), Belgium (BR-2, etc.); France (Melusine, etc.); Germany (FRJ1, FRJ2, etc.), and other participating countries. Associated with this would be another NRC document (NUREG/CR-3326), "LWR Test Reactor Irradiated Nuclear Pressure Vessel and Support Structure Steel Data Base Compendium," that would reference and/or present data and results for selected metallurgical experiments performed in the above mentioned test reactors.

With the NUREG/CR-3322 test reactor physics-dosimetry data, NUREG/CR-3326 would provide: 1) a more precisely defined and representative research reactor physics-dosimetry-metallurgy data base, 2) a better understanding of the mechanisms causing neutron damage, and 3) tested and verified exposure data and physical damage correlation models, all of which are needed to support the preparation and acceptance of ASTM Standard E706(IE), Damage Correlation, and ASTM Standard E706(IIF), ΔNDTT with Fluence, standards and future revisions of Regulatory Guide 1.99.

1.0.1.2 Background

To account for neutron radiation damage in setting pressure/temperature limits and making fracture analysis, neutron-induced changes in reactor PV steel fracture toughness and embrittlement must be predicted and then checked by extrapolation of surveillance program data during the vessel's service life. Uncertainties in the predicting methodology can be significant. The main variables of concern are associated with:

- Steel chemical composition and microstructure
- Steel irradiation temperature
- Power plant configurations and dimensions - core edge to surveillance to vessel wall to support structure positions
- Core power distribution
- Reactor operating history
- Reactor physics computations
- Selection of neutron exposure units

- Dosimetry measurements
- Neutron spectral effects
- Neutron dose rate effects.

Variables associated with the physical measurements of PV steel property changes are not considered here and are addressed separately in Appendices G and H of 10CFR50 (Cf83); in ASTM Standards; in NRC, EPRI, ASTM, and IAEA Special Reports; and in other appropriate references.

The US NRC has estimated that, without remedial action, a few operating early-generation US pressurized water reactors (PWR) could have beltline materials with marginal toughness, relative to the existing requirements of Appendices G and H of 10CFR50 and Regulatory Guide 1.99 (Re77), sometime within their presently licensed service life (Nr80,Ra83,Ra84), i.e., in the range up to about 32 years. This is of particular concern for safety, licensing, and regulatory issues related to pressurized thermal shock (PTS) (Di82).

As older vessels become more highly irradiated, the predictive capability for changes in fracture toughness and embrittlement must improve, particularly for plants operated beyond their current design service life, i.e., in the range above about 32 years. Since, during the vessel's service life, an increasing amount of information will be available from research reactor tests and power reactor surveillance programs, better procedures to evaluate and use this information can and must be developed. The most appropriate way to make information available on these procedures is through voluntary consensus standards, such as those now being developed by ASTM Committee E10 on Nuclear Technology and Applications (As84,He82,Mc84); these are discussed in Section 1.0.2.2.

Additional background information is provided in References (St83a,Mc82a, Mc84,Mc85,Pe84,As84).

1.0.2 Codes, Standards, and Regulatory Rules

Guiding many of the surveillance programs described in Reference (St83a) are changes in codes, standards, and regulatory guides developed largely since the 1970 publication of the first edition of the Metal Properties Council (MPC) surveillance review. Though much of the information required for such rule-making documents was in hand in 1970, several years were required for full development and implementation. A synoptic introduction to these documents is provided in Ref. (St83a) on a chronological base with ASTM Standards first, then ASME Code changes and, finally, regulatory guides (rules).

A brief discussion is provided in Section 1.0.2.1 on pertinent documents used by the NRC in reviewing license applications and addressing regulatory issues. Section 1.0.2.2 provides a brief report on the status of the preparation and applications of the set of 21 ASTM LWR surveillance standards.

1.0.2.1 NRC Regulations and Licensing Requirements

Pertinent documents used by the NRC in reviewing license applications and ensuring the reactor vessel integrity of operating reactors are listed here as convenient references for the uninitiated. Additional and more detailed background information is provided by Steele in Reference (St83a), Chapter 1.

1) Code of Federal Regulations, Title 10: "Energy," Part 50: "Domestic Licensing of Production and Utilization Facilities," Appendix A: "General Design Criteria for Nuclear Power Plants" (cited as 10CFR50, App A), Criterion 31: "Fracture Prevention of Reactor Coolant Pressure Boundary" presents the basic requirements for the prevention of fracture in this boundary.

2) 10CFR50, App G: "Fracture Toughness Requirements" presents these requirements for the reactor coolant pressure boundary during both normal operation and "anticipated operational occurrences." Such AOOs are defined in 10CFR50, App A as normal operating conditions that are expected to occur one or more times during the life of a nuclear power unit. At present no regulations govern fracture toughness requirements during accident conditions, i.e., conditions of lower expected frequency than AOOs. The closest thing to such regulation is the pressurized thermal shock rule, based on a report SECY 82-465 (Di82) to the NRC dated November 18, 1982. The commission approved the final rule, SECY 85-60, on June 20, 1985. Publication in the Federal Register will follow.

3) 10CFR50, App G also incorporates, by reference, portions of the ASME Boiler and Pressure Vessel Code, Section III: "Rules for Construction of Nuclear Power Plant Components," Section XI: "Rules for Inservice Inspection of Nuclear Power Plant Components," and Appendix G: "Protection Against Nonductile Failure." The ASME Code does not give guidance for the treatment of radiation damage in setting pressure/temperature limits or other fracture-prevention procedures. That is one of the principal purposes of 10CFR50, App G.

4) 10CFR50, App H: "Reactor Vessel Material Surveillance Program Requirements," is a mid-1983 revision of 10CFR50, App G with emphasis on material surveillance.

5) 10CFR50, App H incorporates, by reference, ASTM Standard E185-82: "Standard Practice for Conducting Surveillance Tests for Light-Water-Cooled Nuclear Power Reactor Vessels." Most technical details concerning materials, specimen types, test procedures, withdrawal schedules, etc. are now contained in both ASTM E185-79 and E185-82. The 1982 edition is the same as the 1979 except that a printer's omission from paragraph 9.2.3 was corrected. This standard is item IF of ASTM E706-84, "Master Matrix for Light Water Reactor Pressure Vessel Surveillance Standards."

6) Regulatory Guide 1.99 (Rev. 1), "Effects of Residual Elements on Predicted Radiation Damage to Reactor Vessel Materials," was used as the basis for an evaluation of shift and of upper-shelf decrease that contributes to the updating of pressure/temperature limits for reactor plants every few years. Regulatory Guide 1.99 (Rev. 2) is being developed and has grown out of the pressurized thermal shock effort. Guthrie fitted a PWR surveillance data base with an expression that was the product of a chemistry-dependent factor and fluence raised to a fixed power. The chemistry factor was a linear combination of an additive constant (copper) and a copper-nickel product term. The data base used for this work is published in SECY 82-465 (Di82) and in NUREG/CR-2805, Vol. 1 (Gu82b). Subsequently, two steps have been taken to avoid overshoot in the high-fluence, high-copper, high-nickel region where the data base is sparce (Ra84). One step modified the copper-nickel product term (the precise operation has not yet been chosen). The other step modified the fluence exponent. Instead of a constant term (which traditionally ranged from 0.2 to 0.5), the exponent has the form: $a - b \ln f$. This form produces trend curves concave downward when plotted on log-log paper.

7) Standard Review Plan, NUREG-0800, (St81), provides the basis for implementation of the NRC regulations in the review of license applications for new plants. The following sections are of specific interest:

- Section 4.3: Nuclear Design.
  (Paragraph III.8 outlines review procedures for neutron flux calculations that are important to reactor vessel embrittlement and to design of the surveillance program.)
- Section 5.3.1: Reactor Vessel Materials.
- Section 5.3.2: Pressure/Temperature Limits.
- Section 5.3.3: Reactor Vessel Integrity.

1.0.2.2 ASTM Standards

The master matrix standard, ASTM E706-84 [Ref.(As82)], describes a series of 20 ASTM standard practices, guides, and methods for the determination of neutron-induced changes in LWR pressure vessel and support structure steels throughout a nuclear power plant's service life (Figures 1.0.1 and 1.0.2). Some of these are existing ASTM standards; some are ASTM standards that have been modified; and some are newly proposed ASTM standards. More detailed information, justification, and specific requirements for the nine practices, six guides, and five methods are provided in Ref. (As82,As84).

The reader is referred to the ASTM E853-84, "Standard Practice for Analyses and Interpretation of Nuclear Reactor Surveillance Results," (As84),

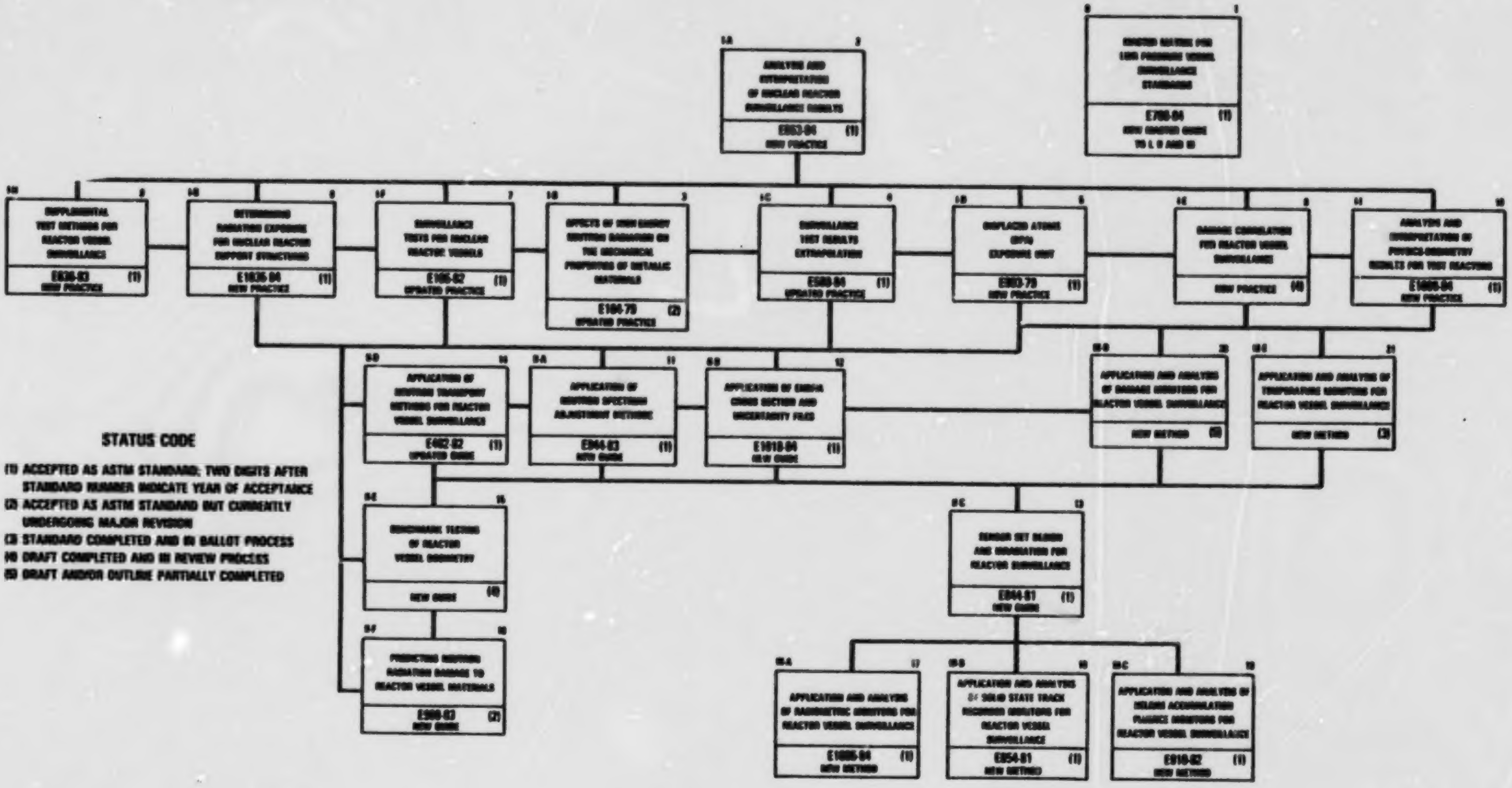
ANALYSIS AND INTERPRETATION OF NUCLEAR REACTOR SURVEILLANCE RESULTS
E853-84 (1)
NEW PRACTICE
MASTER MATRIX FOR LWR PRESSURE VESSEL SURVEILLANCE STANDARDS
E706-84 (1)
NEW MASTER GUIDE TO I, II AND III
SUPPLEMENTAL TEST METHODS FOR REACTOR VESSEL SURVEILLANCE
E636-83 (1)
NEW PRACTICE
DETERMINING RADIATION EXPOSURE FOR NUCLEAR REACTOR SUPPORT STRUCTURES
E1035-84 (1)
NEW PRACTICE
SURVEILLANCE TESTS FOR NUCLEAR REACTOR VESSELS
E185-82 (1)
UPDATED PRACTICE
EFFECTS OF HIGH ENERGY NEUTRON RADIATION ON THE MECHANICAL PROPERTIES OF METALLIC MATERIALS
E184-79 (2)
UPDATED PRACTICE
SURVEILLANCE TEST RESULTS EXTRAPOLATION
E560-84 (1)
UPDATED PRACTICE
DISPLACED ATOMS (DPA) EXPOSURE UNIT
E693-79 (1)
NEW PRACTICE
DAMAGE CORRELATION FOR REACTOR VESSEL SURVEILLANCE
NEW PRACTICE (4)
ANALYSIS AND INTERPRETATION OF PHYSICS-DOSIMETRY RESULTS FOR TEST REACTORS
E1006-84 (1)
NEW PRACTICE
APPLICATION OF NEUTRON TRANSPORT METHODS FOR REACTOR VESSEL SURVEILLANCE
E482-82 (1)
UPDATED GUIDE
APPLICATION OF NEUTRON SPECTRUM ADJUSTMENT METHODS
E944-83 (1)
NEW GUIDE
APPLICATION OF ENDF/A CROSS SECTION AND UNCERTAINTY FILES
E1018-84 (1)
NEW GUIDE
APPLICATION AND ANALYSIS OF DAMAGE MONITORS FOR REACTOR VESSEL SURVEILLANCE
NEW METHOD (5)
APPLICATION AND ANALYSIS OF TEMPERATURE MONITORS FOR REACTOR VESSEL SURVEILLANCE
NEW METHOD (3)
BENCHMARK TESTING OF REACTOR VESSEL DOSIMETRY
NEW GUIDE (4)
PREDICTING NEUTRON RADIATION DAMAGE TO REACTOR VESSEL MATERIALS
E900-83 (2)
NEW GUIDE
SENSOR SET DESIGN AND IRRADIATION FOR REACTOR SURVEILLANCE
E844-81 (1)
NEW GUIDE
APPLICATION AND ANALYSIS OF RADIOMETRIC MONITORS FOR REACTOR VESSEL SURVEILLANCE
E1005-84 (1)
NEW METHOD
APPLICATION AND ANALYSIS OF SOLID STATE TRACK RECORDER MONITORS FOR REACTOR VESSEL SURVEILLANCE
E854-81 (1)
NEW METHOD
APPLICATION AND ANALYSIS OF HELIUM ACCUMULATION FLUENCE MONITORS FOR REACTOR VESSEL SURVEILLANCE
E910-82 (1)
NEW METHOD

STATUS CODE

(1) ACCEPTED AS ASTM STANDARD; TWO DIGITS AFTER STANDARD NUMBER INDICATE YEAR OF ACCEPTANCE
(2) ACCEPTED AS ASTM STANDARD BUT CURRENTLY UNDERGOING MAJOR REVISION
(3) STANDARD COMPLETED AND IN BALLOT PROCESS
(4) DRAFT COMPLETED AND IN REVIEW PROCESS
(5) DRAFT AND/OR OUTLINE PARTIALLY COMPLETED

HEDL 8407-057

FIGURE 1.0.1. ASTM Standards for Surveillance of LWR Nuclear Reactor Pressure Vessels and Their Support Structures.

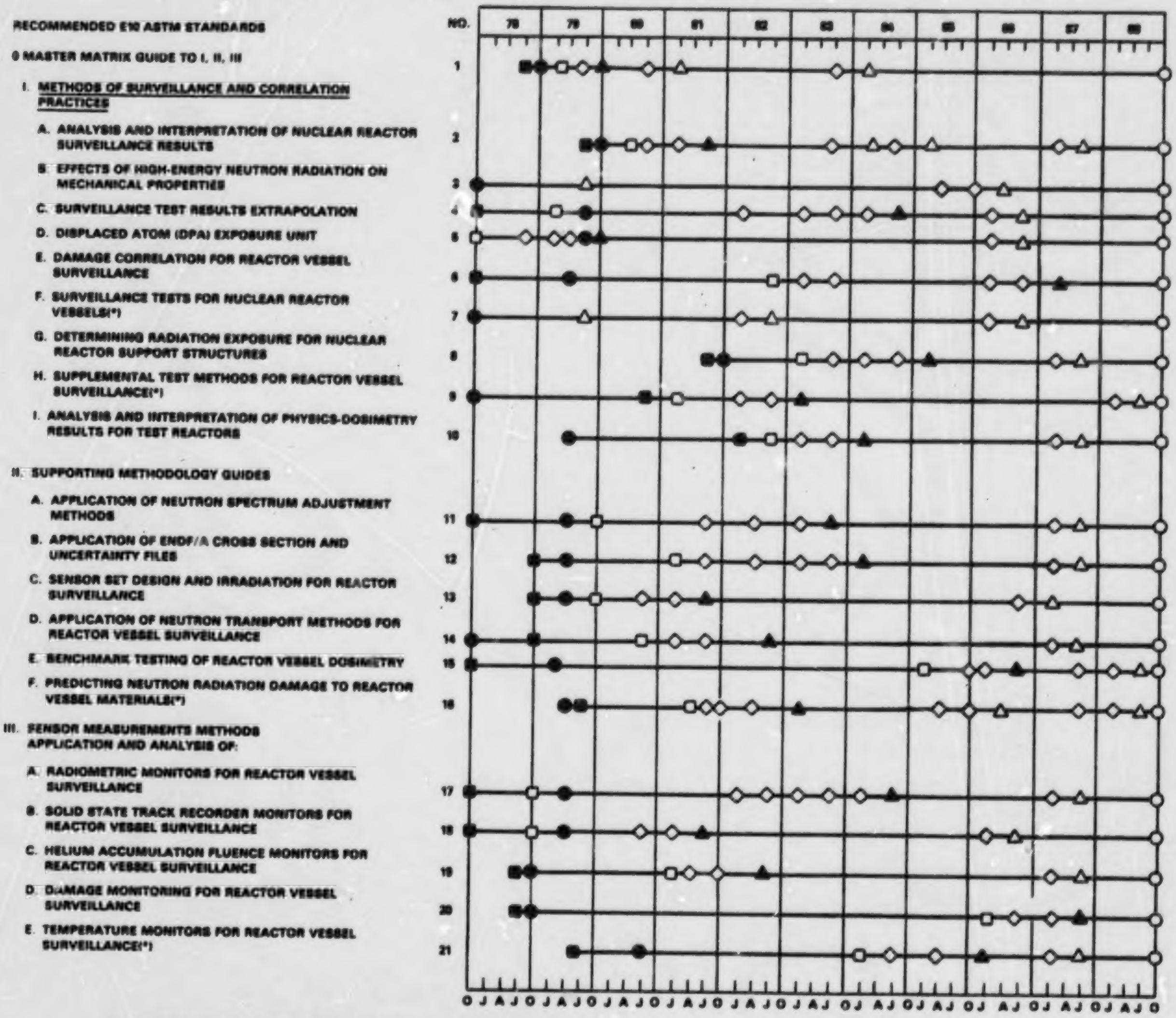

■ DRAFT OUTLINE DUE TO ASTM E10 SUBCOMMITTEE TASK GROUPS
□ 1ST DRAFT TO APPRORIATE ASTM E10 SUBCOMMITTEE TASK GROUPS
◇ REVISED DRAFT FOR ASTM E10 SUBCOMMITTEES, ASTM E10 COMMITTEE, AND/OR ASTM SOCIETY BALLOTING(*)
▲ ACCEPTANCE AS ASTM STANDARD
△ REVISION AND ACCEPTANCE AS ASTM STANDARD
●–○ PRIMARY TIME INTERVAL FOR ROUND ROBIN VALIDATION AND CALIBRATION TESTS

(*)INDICATES THAT THE LEAD RESPONSIBILITY IS WITH SUBCOMMITTEE E10.02 INSTEAD OF WITH SUBCOMMITTEE E10.05.

NOTE: ALL ASTM STANDARDS MUST BE REVIEWED, UPDATED AS REQUIRED, AND REBALLOTED EVERY 5 YEARS.

HEDL 8211-135.17

FIGURE 1.0.2. Preparation, Validation, and Calibration Schedule for LWR-PV and Support Structure Surveillance Standards.

Sections 4 through 7, for more specific and detailed information on the use and application of those standards of the set of 20 ASTM LWR Surveillance Standards that pertain to the physics-dosimetry data and results presented in Section 4.0 and 5.0 of this document.

The following relevant statements about the objectives and requirements of the reactor vessel and support structure surveillance program were taken from ASTM Standard E853-84:

1) The objectives of a reactor vessel surveillance program are twofold. The first requirement of the program is to monitor changes in the fracture toughness properties of ferritic materials in the reactor vessel beltline region resulting from exposure to neutron irradiation and the thermal environment. The second requirement is to make use of the data obtained from the surveillance program to determine the conditions under which the vessel can be operated throughout its service life.

   To satisfy the first requirement, the tasks to be carried out are straightforward. Each of the irradiation capsules that comprise the surveillance program may be treated as a separate experiment. The goal is to define and carry to completion a dosimetry program that will, a posteriori, describe the neutron field to which the materials test specimens were exposed. The resultant information will then become part of a data base applicable in a stricter sense to the specific plant from which the capsule was removed, but also in a broader sense to the industry as a whole.

   To satisfy the second requirement, the tasks to be carried out are somewhat complex. The objective is to describe accurately the neutron field to which the pressure vessel itself will be exposed over its service life. This description of the neutron field must include spatial gradients within the vessel wall. Therefore, heavy emphasis must be placed on the use of neutron transport techniques as well as on the choice of a design basis for the computations. Since a given surveillance capsule measurement, particularly those obtained early in plant life, is not necessarily representative of long-term reactor operation, simple normalization of neutron transport calculations to dosimetry data from a given capsule may not be appropriate.

2) The objectives and requirements of a reactor vessel's support structure's surveillance program are much less stringent and, at present, are limited to physics-dosimetry measurements through ex-vessel cavity monitoring coupled with the use of available test reactor metallurgical data to determine the condition of any support structure steels that might be subject to neutron-induced property changes.

1.1 WESTINGHOUSE (W) REACTORS

1.1.1 Surveillance Programs

Radiation surveillance programs for Westinghouse (W) designed two-, three-, and four-loop Nuclear Steam Supply Systems (NSSS) are identified in Tables 1.1.1 and 1.1.2 for Westinghouse PWRs located in the United States and other countries, respectively. There are 37 surveillance programs in the US (Table 1.1.1) and 23 in foreign countries (Table 1.1.2).

An example of a typical W Surveillance Program for R. E. Ginna Unit No. 1 is provided in Chapter 5 of Reference (St83a).

1.1.1.1 Surveillance Capsules

As a minimum, the Westinghouse reactor vessel surveillance program is based on ASTM E185-73 (As73), "Recommended Practice for Surveillance Tests on Structural Materials in Nuclear Reactors." Currently, six capsules are inserted into each NSSS nuclear reactor between the core and the pressure vessel wall. Previously, six capsules (for two-loop plants) or eight capsules (for three- and four-loop plants) were inserted inside each reactor vessel. (Note: The size and placement of W surveillance capsules compared to those of other US NSSS vendors are shown schematically in Figure S.1.)

A typical capsule is shown in Figure 1.1.1. The capsule consists of mated stainless steel enclosure halves to prevent corrosion and to ensure good thermal conductivity in a carefully welded configuration. In-reactor, the capsules are contained in specimen guide tubes attached to the thermal shield or thermal pads (depending on the year of plant design). Current plants used the thermal pad concept. Thermal pads are segmented thermal shields that are attached to the outside of the vessel core barrel at four locations where the neutron flux impinging on the vessel will be the highest.

Each of the surveillance capsules contains Charpy V-notch impact specimens, tension specimens, and IX-WOL (wedge opening loading) or 1/2-T CT (compact tension) fracture mechanics specimens. Current (since 1973) plants use 1/2-T CT specimens. The specimens are machined from materials representative of that from which the reactor vessel was fabricated. The representative materials include base metal from the core region shell courses and associated weld and heat-affected-zone (HAZ) material. The contents of a typical Westinghouse capsule are given in Table 1.1.3. Dosimeters to measure the integrated neutron flux and thermal monitors to assess temperature limits attained by the capsules are also contained in each test capsule.

11

TABLE 1.1.1

WESTINGHOUSE RADIATION SURVEILLANCE PROGRAMS IN THE UNITED STATES

Owner	Plant	Location
Alabama Power Co.	Joseph M. Farley No. 1	Alabama
	Joseph M. Garley No. 2	Alabama
Carolina Power & Light Co.	H. B. Robinson No. 2	South Carolina
Commonwealth Edison Co.	Zion No. 1	Illinois
	Zion No. 2	Illinois
Connecticut Yankee Atomic Power Co.	Haddam Neck	Connecticut
Consolidated Edison Company of New York, Inc.	Indian Point No. 2	New York
Duke Power Co.	William B. McGuire No. 1	North Carolina
	William B. NcGuire No. 2	North Carolina
Duquesne Light Co, Department of Energy (DOE)	Shippingport	Pennsylvania
Duquesne Light Co; Ohio Edison Co; Pennsylvania Power Co.	Beaver Valley No. 1	Pennsylvania
Florida Power & Light Co.	Turkey Point No. 3	Florida
	Turkey Point No. 4	Florida
Indiana & Michigan Electric Co. (AEP)	Donald C. Cook No. 1	Michigan
	Donald C. Cook No. 2	Michigan
Northern States Power Co.	Prairie Island No. 1	Minnesota
	Prairie Island No. 2	Minnesota
Pacific Gas & Electric Co.	Diablo Canyon No. 1	California
	Diablo Canyon No. 2	California
Portland General Electric Co; Eugene Water & Electric Board; Pacific Power & Light Co.	Trojan	Oregon
Power Authority of the State of New York (PASNY).	Indian Point 3	New York
Public Service Electric & Gas Co. Philadelphia Electric Co; Atlantic Electric Co; Delmarva Power & Light Co.	Salem No. 1	New Jersey
	Salem No. 2	New Jersey
Rochester Gas & Electric Corp.	Robert Emmett Ginna	New York
South Carolina Electric & Gas Co.	Virgil C. Summer	South Carolina
Southern California Edison Co; San Diego Gas & Electric Co.	San Onofre No. 1	California
Tennessee Valley Authority.	Sequoyah No. 1	Tennessee
	Sequoyah No. 2	Tennessee
	Watts Bar No. 1	Tennessee
Virginia Electric & Power Co.	Surry No. 1	Virginia
	Surry No. 2	Virginia
	North Anna No. 1	Virginia
	North Anna No. 2	Virginia
Wisconsin Electric Power Co; Wisconsin Michigan Power Co.	Point Beach No. 1	Wisconsin
	Point Beach No. 2	Wisconsin
Wisconsin Public Service Corp. Wisconsin Power & Light Co; Madison Gas & Electric Co.	Kewaunee	Wisconsin
Yankee Atomic Electric Co.	Yankee-Rowe	Massachusetts

TABLE 1.1.2

WESTINGHOUSE RADIATION SURVEILLANCE PROGRAMS (FOREIGN)

Owner	Plant	Location
Centre d'Etude de l'Energie Nucleaire.	BR-3	Belgium
Ente Nazionale per l'Energie Ellettrica (ENEL).	Trino Vercellese	Italy
Fuerzas Electricas de Cataluna, S.A. (FECSA).	Asco No. 1	Spain
Fuerzas Electricas de Cataluna, S.A. (FECSA), Empresa Nacional Hidroelectrica del Ribagorzana, S.A. (ENHER); Fuerzas Hidroelectricas del Segre S.A; Hidroelectrica de Cataluna, S.A.	Asco No. 2	Spain
Furnas-Centrais Electricas, S.A.	Angra dos Reis No. 1	Brazil
Iberduero, S.A.	Lemoniz No. 1	Spain
	Lemoniz No. 2	Spain
Individion DOEL; Docietes Reunies d'Energie du Bassin de l'Escaut (EBES); Societe Intercommunale Belge de Gaz et d'Electricite (INTERCOM); Societe Intercommunale des Centrales Electriques du Brabant (INTERBRABANT); Societe d'Electricite de Sambre et Meuse, des Ardennes et du Luxembourg (ESMALUX); Union des Centrales Electriques de Liege-Namur-Luxembourg-Hainaut; Union des Centrales Electriques de Campine.	Doel No. 1	Belgium
	Doel No. 2	Belgium
The Kansai Electric Power Company, Inc.	Mihama No. 1	Japan
	Takahama No. 1	Japan
	Ohi No. 1	Japan
	Ohi No. 2	Japan
Korea Electric Power Company, Ltd.	Ko-Ri No. 1	Korea
Nordostschweizerische Kraftwerke AG (NOK).	Beznau No. 1	Switzerland
	Beznau No. 2	Switzerland
Statens Vattenfallsverk (SSPB).	Ringhals No. 2	Sweden
	Ringhals No. 3	Sweden
	Ringhals No. 4	Sweden
Union Electrica, S.A.	Jose Cabrera-Zorita	Spain
Union Electrica, S.A; Compania Sevillana de Electricidad S.A; Hidroelectrica Espanola S.A.	Almaraz No. 1	Spain
	Almaraz No. 2	Spain
Societe d'Energie Nucleaire Franco-Belge des Ardennes.	Chooz	France

13

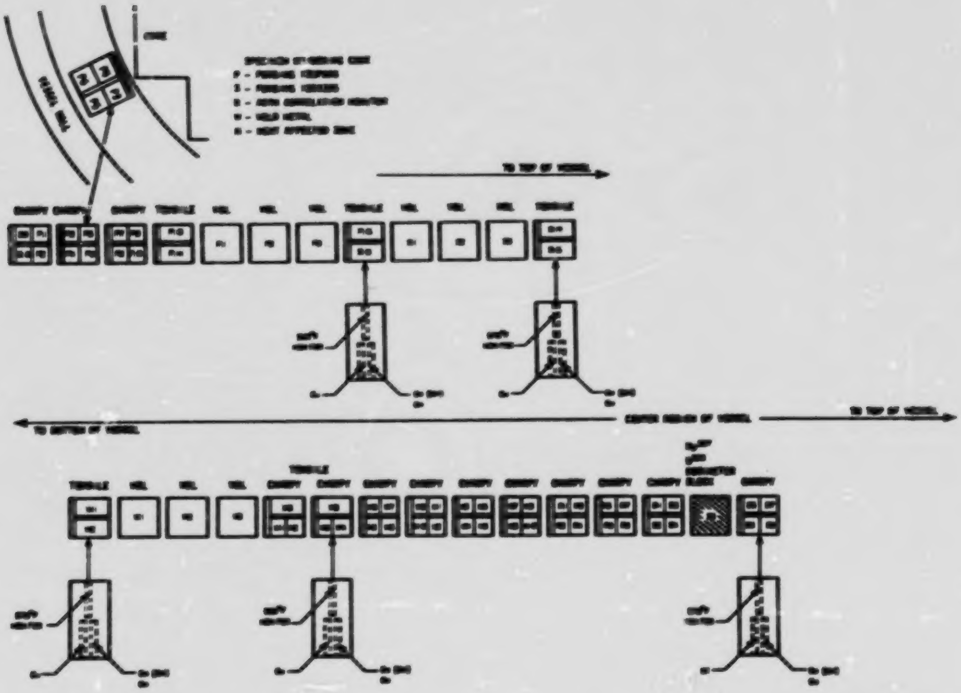
CORE
VESSEL WALL
TO TOP OF VESSEL
CHARPY
TENSILE
WOL
CENTER REGION OF VESSEL
TO TOP OF VESSEL
TO BOTTOM OF VESSEL

FIGURE 1.1.1. Typical Capsule Schematic Showing Specimens, Thermal Monitors, and Dosimeter Placement and Orientation with Respect to the Core and Vessel Wall.

TABLE 1.1.3

CONTENTS OF TYPICAL WESTINGHOUSE CAPSULE

Material	No. of Charpys	No. of Tensiles	No. of 1/2T CT
Shell course (longitudinal)	15	3	4
Shell course (transverse)	15	3	4
Weld metal	15	3	4
Heat-affected zone	15		

14

The capsules contain two low-melting-point eutectic alloys to define more accurately the temperature attained by the test specimens during irradiation. The thermal monitors are sealed in Pyrex tubes and are of the following composition and melting point:

97.5 Pb - 2.5 Ag [304°C (579°F) melting point]
97.5 Pb - 1.75 Ag - 0.75 Sn [310°C (590°F) melting point]

As part of the basic NSSS package, Westinghouse includes preirradiation testing of the materials encapsulated in the test capsules and issues a report to the buying utility documenting the surveillance program. As a rule, the post-irradiation evaluation of the test capsules is not included in the basic package; however, this service is provided upon request.

1.1.1.2 Capsule Removal

Specimen capsules are removed from the reactor only during normal refueling periods. Generally, the first capsule is removed at the end of the first core cycle (usually 1-1/2 years). The second, third, and fourth capsules are removed at approximately maximum exposure levels representative of one quarter, one half, and three quarters of service life. The two remaining capsules are for standby. The removal schedule meets the intent of 10CFR50, Appendix H (Cf83).

1.1.1.3 Neutron Flux Monitors

To effect a correlation between neutron exposure (E > 1 MeV, dpa, etc.) and the radiation-induced property changes observed in the test specimens, a number of neutron flux monitors are included as an integral part of the reactor vessel surveillance program. In particular, the surveillance capsules contain detectors employing the following fast neutron reactions:

$^{54}\mathrm{Fe}(n,p)^{54}\mathrm{Mn}$
$^{58}\mathrm{Ni}(n,p)^{58}\mathrm{Co}$
$^{63}\mathrm{Cu}(n,\alpha)^{60}\mathrm{Co}$
$^{237}\mathrm{Np}(n,f)^{137}\mathrm{Cs}$
$^{238}\mathrm{U}(n,f)^{137}\mathrm{Cs}$

In addition, thermal neutron flux monitors, in the form of bare and cadmium-shielded cobalt-aluminum wire, are included within the capsules to enable an assessment of the effects of thermal neutrons, such as isotopic burnup, on the reponse of the fast neutron detectors (also any contribution to property changes, heating, etc.).

The relative locations of the various monitors within a capsule are shown in Figure 1.1.1, while the radial and azimuthal positions of the capsule with respect to the nuclear core and other reactor internals are illustrated in Figure 1.1.2.

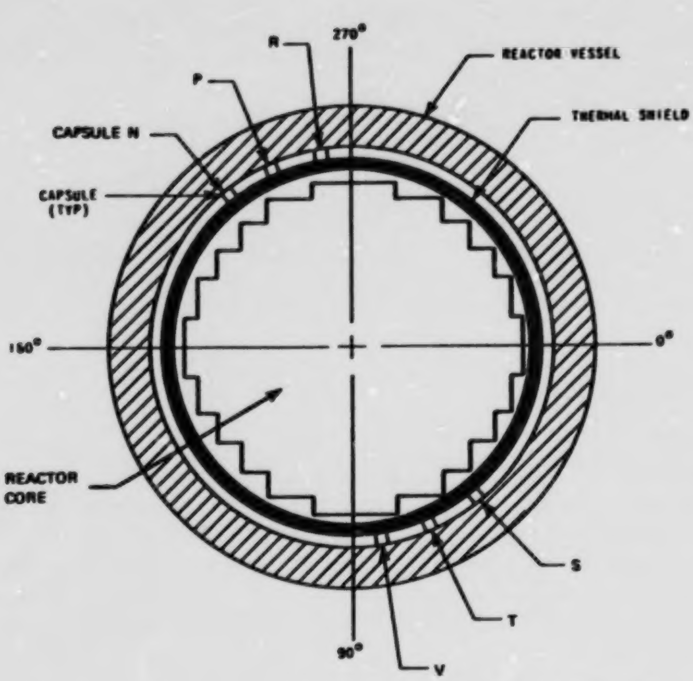

FIGURE 1.1.2. Reactor Vessel Showing Arrangement of Surveillance Capsules.

The iron, nickel, copper, and cobalt-aluminum monitors are in the form of wires placed in holes drilled in spacers at several axial levels within the capsule. Iron dosimetry was obtained by drilling into the Charpy test specimens when iron wires were not included in the capsules.

The cadmium-shielded neptunium and uranium fission detectors are accommodated within the dosimeter block near the center of the capsule.

The use of activation detectors, such as those listed earlier, does not yield a direct measure of the energy-dependent neutron flux level at the point of interest. Rather, the activation process is a measure of the integrated effect that the time and energy-dependent neutron flux has on the target material. An accurate estimate of the average neutron flux level incident on the various detectors may be derived from the activation measurements only if the parameters of the irradiation are well known. In particular, the following variables are of interest:

1) Operating history of the reactor,
2) Energy response of the given detector, and
3) Neutron energy spectrum at the detector location.

The procedures for the derivation of neutron exposure are discussed in subsequent W-NTD sections of this report.

1.2 GENERAL ELECTRIC (GE) REACTORS

1.2.1 Surveillance Programs

In the United States, BWR plants are currently required to have a surveillance program that includes three sets of in-reactor specimens encapsulated and placed adjacent to the vessel wall. A fourth capsule insertion would be required if the projected increase in RT_{NDT} at end of life (EOL) were to exceed 38°C (100°F) but not 93°C (200°F). One capsule is withdrawn and tested after 10 years of operation, a second after 30 years of operation. An in-reactor standby is also required. All GE BWR/6 plants are equipped to meet these mandatory program requirements.

In some countries other than the United States, regulatory authorities have requested additional types and numbers of specimens. These are provided by GE on a case-by-case basis.

General Electric provides each BWR with estimated EOL RPV material properties based on NRC Regulatory Guide 1.99 (Re77), which relates fluence to change in transition temperature for the RPV steel. Sets of mechanical test specimens are also provided to be irradiated in surveillance capsules at the inner wall of the RPV. (Note: In some GE BWRs, surveillance specimen capsules are also located in the region between the core and the shroud; see Section 4.5 and Figure S.1.) These specimens can then be used to verify the projected shift in the RPV material properties at one or more time periods during the nominal 40-year life of the plant.

Examples of the application of the GE Surveillance Program for BWR/4, BWR/5, and BWR/6 reactors are provided in Chapter 4 of Reference (St83a).

1.2.1.1 Surveillance Capsules

Charpy specimens are placed in a thin-walled stainless steel sheet metal capsule. Transverse Charpy V-notch impact specimens in accordance with the ASTM E185-73 specifications for surveillance tests for LWR and Code of Federal Regulations 10CFR50, Appendix H, are provided in quantities in accordance with the minimum requirements of Table 1.2.1 in all BWR/6 plants. In many cases, additional specimens are provided. Copper and phosphorus in the core beltline RPV material are controlled so the EOL RT_{NDT} is $>$38°C (100°F) and the EOL upper shelf is $\geq$68 J (50 ft·lb) for a 102-J (75 ft·lb) unirradiated upper shelf.

TABLE 1.2.1

GE BWR/6 RPV SURVEILLANCE SPECIMENS

Capsule No.	Specimen Type	Specimens		
		Base	Weld	HAZ
In-reactor				
1	Charpy	12	12	12
2	Charpy	12	12	12
3	Charpy	12	12	12
Out-of-reactor				
Baseline:	Charpy	15	15	15
Spare Material:	Sufficient to make following specimens:			
	Charpy	24	24	24

Each capsule contains iron and copper neutron flux monitor wires. Capsules are then placed in a capsule holder that is attached to the RPV wall. General Electric Co. also provides a formal report to plant owners, which gives details of the program and suggests a capsule withdrawal schedule and instructions for specimen testing. (Note: The size and placement of GE surveillance capsules compared to those of other US NSSS vendors are shown schematically in Figure S.1.)

1.2.1.2 Capsule Removal

See Section 1.2.1.

1.2.1.3 Neutron Flux Monitors

As stated in Section 1.2.1.1, GE surveillance capsules only contain iron and copper flux monitors.

1.2.1.4 Potential Surveillance Program Modifications

Potential future changes in the GE surveillance program could result in the following modifications:

1) Temperature monitors may be added.

2) The number and type of neutron flux foils may be increased to better evaluate the specific neutron energy spectrum. This will be accomplished by using one of the following two sets of foils or an additional set yet to be determined: (a) nickel, iron, shielded and unshielded cobalt, and (b) copper, titanium, iron, and aluminum (with ~82 ppm cobalt). Dosimeters will be included in each capsule.

3) The heat of steel used for the surveillance program may be chosen on the basis of the combination of residual elements and location in the pressure vessel to have the largest irradiation-induced changes in properties. In fact, this change has already been incorporated for the BWR/6 standard plant.

1.3 COMBUSTION ENGINEERING (CE) REACTORS

1.3.1 Surveillance Programs

The CE surveillance program described here is applicable to currently operating CE NSSSs sold before 1973. The new program for the 3800-MWt, System 80 design is described in Chapter 3 of Reference (St83a).

The following discussion describes a typical reactor vessel irradiation surveillance program (Ce70) provided by CE for most of the NSSSs already in service or which will be placed in service. This program satisfies the technical intent of both ASTM Standard E185-73 and 10CFR50 Appendix H and, in addition, contains sufficient flexibility, by providing for an adequate number of capsules, to permit monitoring of vessel annealing in the unlikely event that this should become necessary at some point in the life of the vessel.

CE NSSS reactor vessels, with the exception of nozzles and flanges, are fabricated from formed plates and, therefore, contain weldments in the beltline (irradiated) region (Figure 1.3.1). The radiation surveillance program, therefore, includes base metal, deposited weld metal, and the HAZ materials. Sample base metal material is available from each of the six plates that comprise the beltline region after the vessel shell segments are formed (Figure 1.3.2).

The test materials are processed (welded and heat-treated) so that they are representative of the materials in the completed reactor vessel. A record is maintained of chemical analyses, fabrication history, and mechanical properties of the shell plates and welds from which the surveillance test materials are prepared.

In addition to the materials from sections of reactor vessel shell plates, material from a standard heat of ASTM Standard A533 Grade B Class 1 manganese-molybdenum-nickel (designated HSST Plate 01) made available by the Nuclear Regulatory Commission (NRC)-sponsored Heavy Section Steel Technology (HSST) Program is included also. This reference material has been fully processed and characterized and is used for Charpy impact specimen correlation monitors to permit comparisons among irradiation data from operating power reactors and experimental reactors. Compilation of data generated from post-irradiation tests of the correlation monitors is carried out by the HSST Program.

The base-metal material used in the surveillance program is selected from that plate, within the six comprising the "beltline" region (Cf83, Appendix G), that would be most likely to limit the operation of the reactor vessel due to irradiation. Consideration is given to 1) initial reference temperature (RT_{NDT}), 2) chemical composition, and 3) upper-shelf energy. Thus, material in the surveillance capsule is taken directly from the plates actually used in fabricating the vessel.

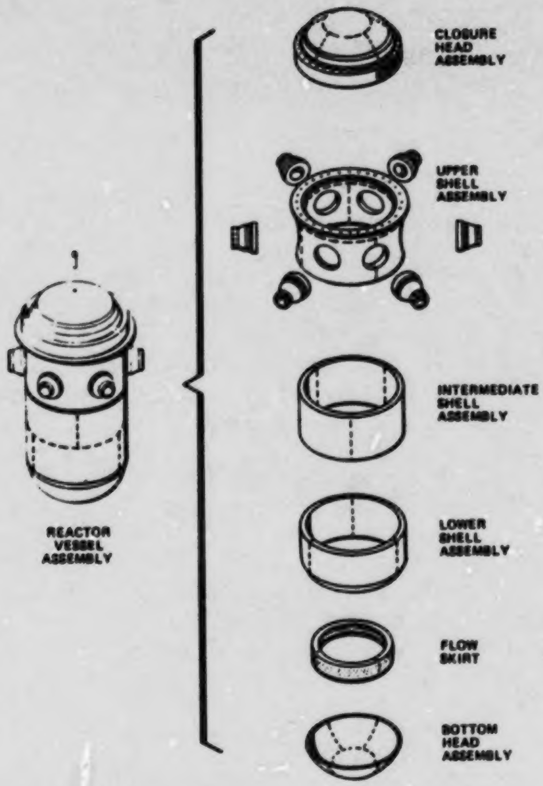
CLOSURE HEAD ASSEMBLY
UPPER SHELL ASSEMBLY
REACTOR VESSEL ASSEMBLY
INTERMEDIATE SHELL ASSEMBLY
LOWER SHELL ASSEMBLY
FLOW SKIRT
BOTTOM HEAD ASSEMBLY

FIGURE 1.3.1. Exploded View of Early Reactor Vessel Assembly Showing Arrangement of Formed Plates, Longitudinal and Circumferential Weld Seams Within Beltline (Irradiated) Region.

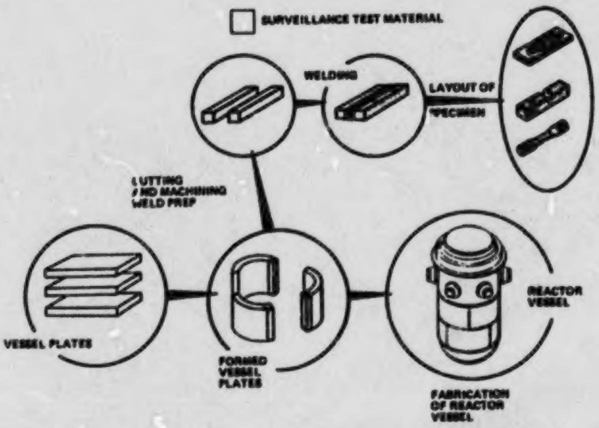
SURVEILLANCE TEST MATERIAL
WELDING
LAYOUT OF SPECIMEN
CUTTING AND MACHINING WELD PREP
VESSEL PLATES
FORMED VESSEL PLATES
REACTOR VESSEL
FABRICATION OF REACTOR VESSEL

FIGURE 1.3.2. Schematic of Operations Included in Preparation of Surveillance Specimens and Fabrication of Reactor Vessel Shell Course. (Note location of surveillance test material on formed shell plate.)

As of September 1978, there are seven operating CE nuclear plants (see Table 1.3.1). They range in size from 480 to 880 MWe and each contains a materials surveillance program. The Palisades and Maine Yankee plants are unique in that they each contain two additional capsules in accelerated exposure locations. The Palisades plant also contains two additional capsules in very-low-flux locations (thermal control capsules) to permit assessment of thermal exposure and cycling in the absence of a neutron radiation environment. Table 1.3.1 presents a summary of the removal schedules for the initial capsules from each of seven operating plants. The original schedule designated the Palisades accelerated capsules and wall capsules for removal in 1973 and 1976, respectively. Operating stretchouts have caused these dates to change. The reader is referred to Chapter 3 of Ref. (St83a) for additional information on these CE reactor surveillance programs.

An example of a typical CE Surveillance Program for the Maine Yankee Nuclear Power Station is provided in Chapter 3 of Reference (St83a).

1.3.1.1 Surveillance Capsules

ASTM Standard A370-77 (As77) drop-weight, Charpy impact, and tension test specimens are provided for unirradiated tests. Charpy impact and tension test specimens are provided for post-irradiation tests. A total of 288 Charpy impact and 54 tension specimens are provided. The type and quantity of test specimens for establishing the properties of the irradiated materials over the lifetime of the vessel are presented in Table 1.3.2.

The test specimens are placed within corrosion-resistant capsule assemblies 1) to prevent corrosion of the carbon steel test specimens by the primary coolant during irradiation 2) to physically locate the test specimens in selected locations within the reactor, 3) to provide a means by which the irradiation conditions (fluence, flux spectrum, temperature) can be determined, and 4) to facilitate the removal of a desired quantity of test specimens from the reactor when a specified fluence has been attained.

A typical capsule assembly (Figure 1.3.3) consists of a series of seven specimen compartments, connected by wedge couplings, and a lock assembly.

Each capsule assembly is made up of four Charpy impact test specimen (Charpy impact) compartments and three tension test specimen-flux/temperature monitor (tensile monitor)-compartments.

Each Charpy impact compartment (Figure 1.3.4 and Table 1.3.2) contains 12 impact test specimens. The specimens are arranged vertically in four 1 x 3 arrays and are oriented with the notch toward the core. The temperature differential between the specimens and the reactor coolant is minimized by using spacers between the specimens and the compartment and by sealing the entire assembly in an atmosphere of helium.

BEST COPY AVAILABLE

TABLE 1.3.1

CE PLANTS AND CAPSULE REMOVAL SCHEDULE BASED ON ORIGINAL (AS-BUILT) REQUIREMENTS

Plant	Commercial Operation Date	Capsule[a]	Original Removal Schedule EFPY[b]	Original Removal Schedule Date	Revised Removal Schedule EFPY	Revised Removal Schedule Date	Status Next Outage EFPY	Status Next Outage Date	Remarks
Palisades	12/71	A-1	2	12/73	2.5	1/78	2.5	1/78	Scheduled 1/78
		A-2	5	12/76	5.5	4/81	3.5	2/79	
		T-1	5	12/76	5.5	4/81	3.5	2/79	
		W-1	5	12/76	5.5	4/81	3.5	2/79	
Maine Yankee	12/72	A-1	1	12/73	---	---	1.2	6/74	Removed 6/74
		A-2	2	12/74	5.8	12/80	4.7	9/79	
		W-1	8	12/80	8.0	6/82	4.7	9/79	
Fort Calhoun	9/73	W-1	5	9/78	4.6	11/79	2.6	10/77	Removed 10/77
Calvert Cliffs No. 1	5/75	W-1	5	5/80	5.4	7/81	3.4	5/79	
Millstone No. 2	12/75	W-1	8	12/83	7.5	12/83	2.2	9/78	
St. Lucie No. 1	12/76	W-1	8	12/84	8.3	5/85	2.3	6/79	
Calvert Cliffs No. 2	4/77	W-1	5	12/82	5.5	9/82	1.5	9/78	

---

[a] A = Accelerated position.
T = Thermal (very low fluence) position.
W = Wall position.

[b] EFPY = Effective full-power years.

TABLE 1.3.2

TYPE AND QUALITY OF SPECIMENS CONTAINED IN EACH IRRADIATION CAPSULE ASSEMBLY

	Target	Base Metal									
	Fluence[a]	Impact			Weld Metal		HAZ		Reference	Total Specimens	
Location	(n/cm²)	L[d]	T[e]	Tensile	Impact	Tensile	Impact	Tensile	Impact[b]	Impact	Tension
Vessel-97[c]	6.0×10^{18}	12	12	3	12	3	12	3	--	48	9
Vessel-104	1.6×10^{19}	--	12	3	12	3	12	3	12	48	9
Vessel-284	2.5×10^{19}	12	12	3	12	3	12	3	--	48	9
Vessel-263	standby	--	12	3	12	3	12	3	12	48	9
Vessel-277	standby	12	12	3	12	3	12	3	--	48	9
Vessel-83	standby	12	12	3	12	3	12	3	--	48	9
Total		48	72	18	72	18	72	18	24	288	54

---

[a] Adjusted to nearest value attainable during scheduled refueling.
[b] Reference material correlation monitors, HSST Plate 01.
[c] Degree location around circumference (see Figure 1.3.6).
[d] L = Longitudinal.
[e] T = Transverse.

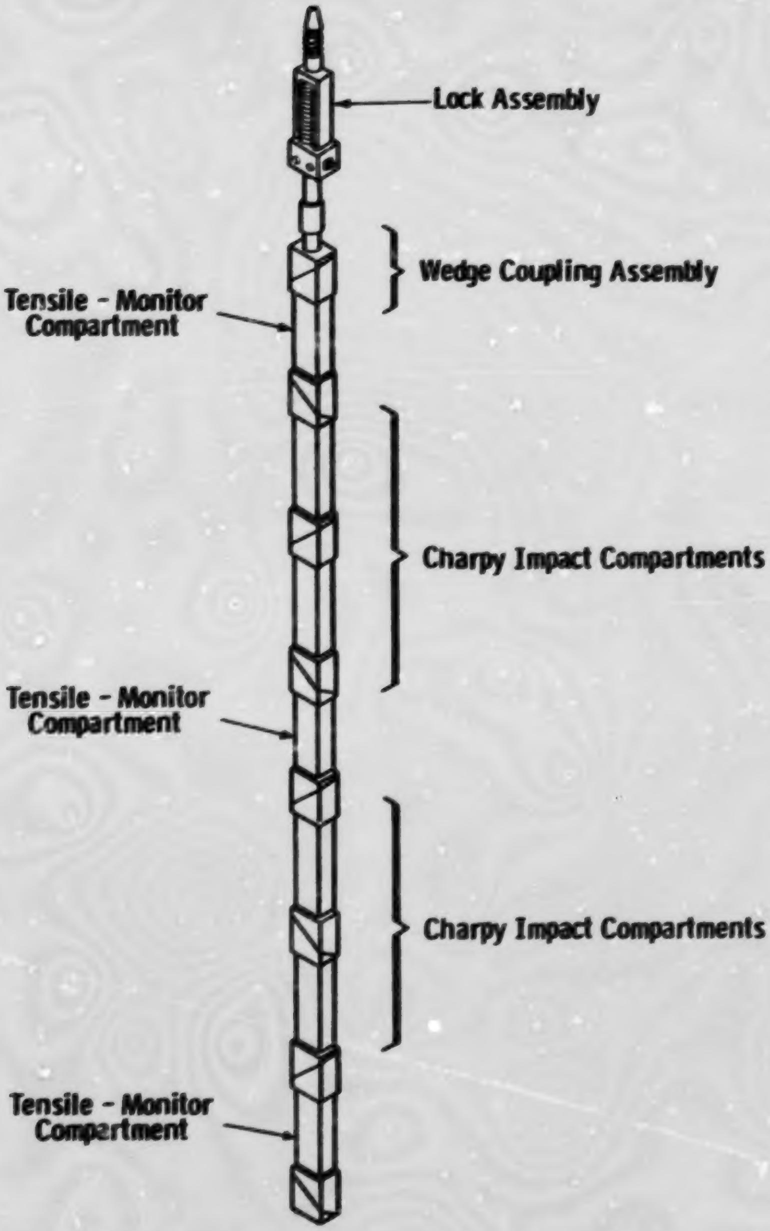
Lock Assembly
Wedge Coupling Assembly
Tensile - Monitor Compartment
Charpy Impact Compartments
Tensile - Monitor Compartment
Charpy Impact Compartments
Tensile - Monitor Compartment

FIGURE 1.3.3. Typical Standard Surveillance Capsule Assembly Used in Operating Plants. (Each assembly consists of three tensile-monitor compartments containing three tension specimens each and four Charpy compartments containing 12 specimens each. The assembly is articulated to permit removal from the holders positioned near the vessel wall without the need for removal of the vessel internals.)

25

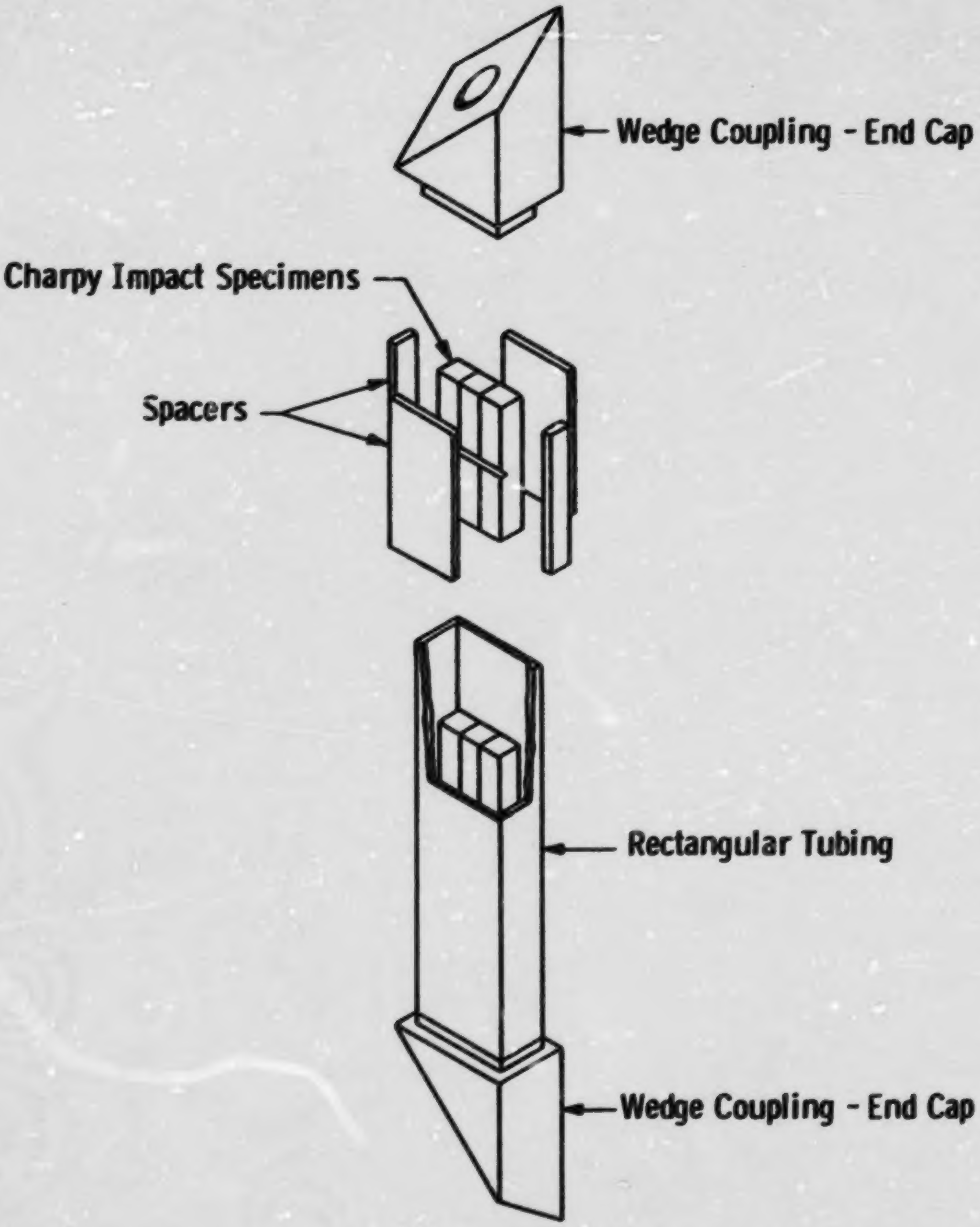
Wedge Coupling - End Cap
Charpy Impact Specimens
Spacers
Rectangular Tubing
Wedge Coupling - End Cap

FIGURE 1.3.4. Typical Charpy Specimen Compartment Containing 12 Charpy Specimens in a 1 x 3 x 4 array. (The notch of each specimen faces the center of the core.)

26

Each tensile-monitor compartment (Figure 1.3.5) contains three tension test specimens, a set of flux spectrum monitors, and a set of temperature monitors for estimating the maximum temperature to which the specimens have been exposed.

The flux monitors are placed in holes drilled in stainless steel housings at three axial locations in each capsule assembly (Figure 1.3.5) to provide an axial profile of the level of fluence that the specimens attain.

A set of temperature monitors (see Table 1.3.3) is included in each tensile-monitor compartment capsule. The temperature monitors are placed in holes drilled in stainless steel housings at three axial locations in each capsule assembly (Figure 1.3.5) to provide an axial profile of the maximum temperature to which the specimens were exposed.

TABLE 1.3.3

COMPOSITION AND MELTING POINTS OF TEMPERATURE MONITOR MATERIALS

Composition (wt%)	Melting Temperature (°C)	Melting Temperature (°F)
80.0 Au - 20.0 Sn	280	536
90.0 Pb - 5.0 Sn - 5.0 Ag	292	558
97.5 Pb - 2.5 Ag	304	580
97.5 Pb - 0.75 Sn - 1.75 Ag	310	590

The capsule assemblies are positioned near the inside wall of the reactor vessel so that the irradiation conditions (fluence, flux spectrum, temperature) of the test specimens resemble as closely as possible the irradiation conditions of the reactor vessel and any differences are minimized. The material property changes resulting from the irradiation of these specimens closely approximate the property changes in the reactor vessel beltline materials.

The encapsulated test specimens are irradiated at approximately identical radial positions about the midplane of the core. The test specimens are enclosed within six capsule assemblies, the axial positions of which are bisected by the midplane of the core. The capsule assemblies are placed in capsule holders positioned circumferentially about the core at locations that include the regions of maximum flux. The exposure locations for the capsule assemblies are illustrated in Figure 1.3.6. The capsule holders are attached to the cladding of the reactor pressure vessel. Details of the holder tube attachment are shown in Figure 1.3.7. (Note: The size and placement of CE surveillance capsules compared to those of other US NSSS vendors are shown schematically in Figure S.1.)

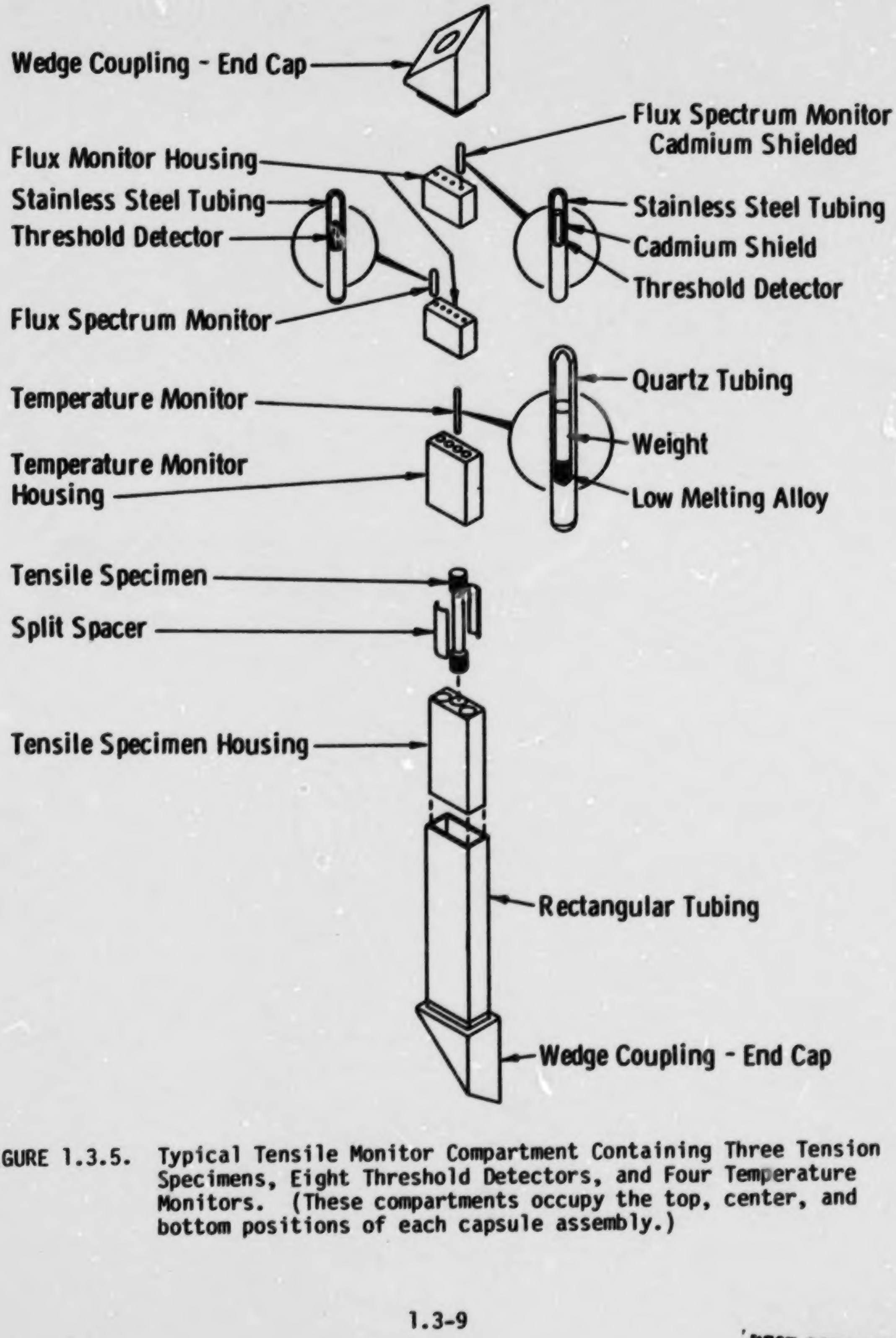
Wedge Coupling - End Cap
Flux Spectrum Monitor Cadmium Shielded
Flux Monitor Housing
Stainless Steel Tubing
Threshold Detector
Stainless Steel Tubing
Cadmium Shield
Threshold Detector
Flux Spectrum Monitor
Quartz Tubing
Temperature Monitor
Weight
Temperature Monitor Housing
Low Melting Alloy
Tensile Specimen
Split Spacer
Tensile Specimen Housing
Rectangular Tubing
Wedge Coupling - End Cap

FIGURE 1.3.5. Typical Tensile Monitor Compartment Containing Three Tension Specimens, Eight Threshold Detectors, and Four Temperature Monitors. (These compartments occupy the top, center, and bottom positions of each capsule assembly.)

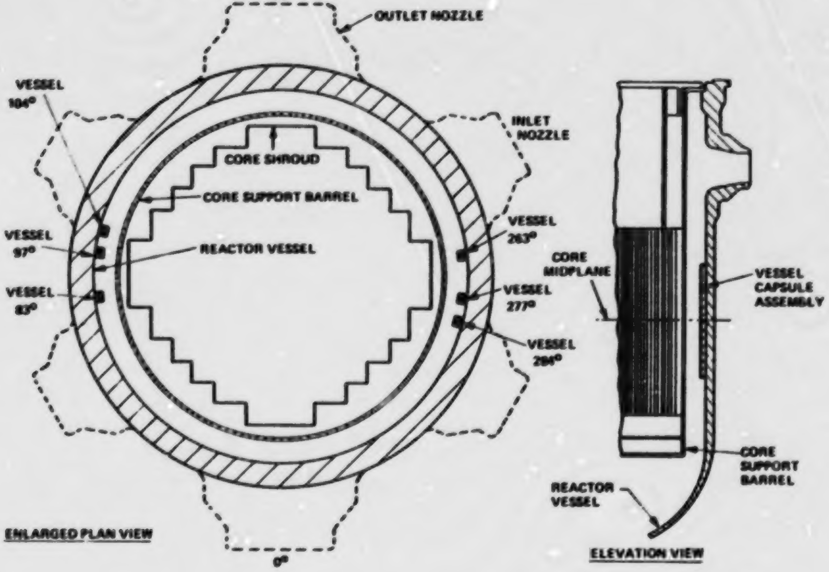
180°
OUTLET NOZZLE
VESSEL
104°
INLET
NOZZLE
CORE SHROUD
CORE SUPPORT BARREL
VESSEL
97°
REACTOR VESSEL
VESSEL
83°
VESSEL
263°
VESSEL
277°
VESSEL
284°
CORE
MIDPLANE
VESSEL
CAPSULE
ASSEMBLY
CORE
SUPPORT
BARREL
REACTOR
VESSEL
ENLARGED PLAN VIEW
0°
ELEVATION VIEW

FIGURE 1.3.6. Location of Capsule Holders with Respect to Peak Fluence of the Vessel, Which Occurs at the 90-deg Location. (Physical constraints prevent use of the 0-deg and 180-deg positions for this purpose. The capsule assembly elevation bisects the core geometric centerline.)

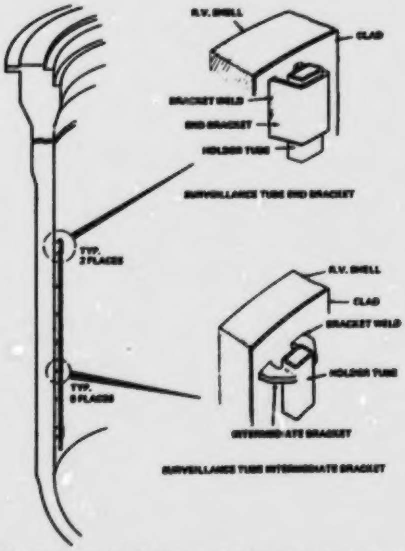
R.V. SHELL
CLAD
BRACKET WELD
END BRACKET
HOLDER TUBE
SURVEILLANCE TUBE END BRACKET
TYP.
2 PLACES
R.V. SHELL
CLAD
BRACKET WELD
HOLDER TUBE
TYP.
8 PLACES
INTERMEDIATE BRACKET
SURVEILLANCE TUBE INTERMEDIATE BRACKET

FIGURE 1.3.7. Details of Surveillance Holder Mounting Scheme. (The end brackets are designed to withstand all anticipated loads. The intermediate brackets are used to stiffen the holder from flow-induced vibrations.)

29

1.3.1.2 Capsule Removal

Surveillance capsules must be placed at locations where the specimens are irradiated to a fluence between one and three times the fluence of the reactor vessel. Capsule positions for a typical CE surveillance program are shown in Figure 1.3.6. The capsule holders are welded to the cladding of the vessel, thereby accurately establishing the location of the specimens with respect to the vessel. A typical removal schedule for the six capsules included in the program is presented in Table 1.3.4. The target fluence levels are determined at the azimuthal locations at the time intervals indicated in the withdrawal schedule in 10CFR50 Appendix H. The fluence values in Table 1.3.4 are accurate within +10%, -40%. The uncertainty is composed of errors in the calculational method and errors in the combined radial and axial power distribution. Withdrawal schedules may be modified to coincide with those refueling outages or plant shutdowns most closely approaching the withdrawal schedule.

TABLE 1.3.4

TYPICAL CAPSULE ASSEMBLY REMOVAL SCHEDULE

Capsule No.	Azimuthal Location (deg)	Removal Time (yr)	Target Fluence (n/cm^2)
1	97	7	6.0×10^{18}
2	104	19	1.6×10^{19}
3	284	30	2.5×10^{19}
4	263	Standby	---
5	277	Standby	---
6	83	Standby	---

Three standby capsules are available for any contingency that might necessitate additional surveillance tests (i.e., to assess the effects of possible annealing and subsequent reirradiation of the reactor vessel).

1.3.1.3 Neutron Flux and Correlation Monitors

The changes in the RT_{NDT} of the reactor vessel materials are determined from specimens irradiated to various fluence levels and in different neutron energy spectra. To permit accurate predictions of the RT_{NDT} of the vessel materials, complete information on the neutron flux and the neutron energy spectra of the surveillance specimens must be available.

Fast neutron flux measurements are obtained from threshold detectors. Such detectors are particularly suited for the proposed application because their effective threshold energies lie in the low-MeV range.

These neutron threshold detectors and the thermal neutron detector, presented in Table 1.3.5 can be used to monitor the thermal and fast neutron spectra incident on the test specimens. These detectors possess reasonably long half-lives and activation cross sections covering the desired neutron energy range.

TABLE 1.3.5

MATERIALS FOR NEUTRON THRESHOLD DETECTORS

Materials	Reaction	Threshold Energy (MeV)	Half-Life
Uranium	$^{238}U(n,f)^{90}Sr$	0.7	28 years
	$^{238}U(n,f)^{137}Cs$	0.7	30.2 years
Sulfur	$^{32}S(n,p)^{32}P$	2.9	14.3 days
Iron	$^{54}Fe(n,p)^{54}Mn$	4.0	314 days
Nickel	$^{58}Ni(n,p)^{58}Co$	5.0	71 days
Copper	$^{63}Cu(n,\alpha)^{60}Co$	7.0	5.3 years
Titanium	$^{46}Ti(n,p)^{46}Sc$	8.0	84 days
Cobalt	$^{59}Co(n,\gamma)^{60}Co$	Thermal	5.3 years

The 5.3-year ^{60}Co formed by the $^{63}Cu(n,\alpha)$ reaction and the 28-year ^{90}Sr and 30.2-year ^{137}Cs formed by fast fission of ^{238}U provide means of automatically integrating the fast neutron flux. The ^{60}Co provides integrated fast neutron flux for the first 10 to 15 years of plant operation while the ^{90}Sr and ^{137}Cs provide integrated flux for the entire life of the plant owing to their 28- and 30.2-year half-lives. All the other reactions become saturated quickly and are useful only in determining the fast neutron flux-spectrum over the desired energy range.

Each detector is placed inside a sheath that identifies the material and facilitates handling. Cadmium covers are used for those materials (i.e., uranium, nickel, copper, and cobalt) that have competing neutron capture reactions.

In addition to these detectors, the CE surveillance capsule also includes correlation monitors (Charpy impact test specimens made from a reference heat, HSST Plate 01, of ASTM Standard A533 Grade B Class 1, manganese-molybdenum-nickel steel) that are irradiated along with the specimens made from reactor vessel materials. The changes in impact properties of the reference material provide a cross-check on the dosimetry and temperature in any given surveillance program. These changes also provide data for correlating results from this surveillance program with results from experimental irradiations and other reactor surveillance programs using specimens of the same reference material.

1.4 BABCOCK AND WILCOX (B&W) REACTORS

1.4.1 Surveillance Programs

All operating 177FA B&W reactors have the same basic configuration and operating characteristics, except for differences in full-power rating and fuel distribution. These reactors are listed in Table 1.4.1. For calculational purposes, a 45° segment of a plane through the reactor at a mid-core elevation is shown in Figure 1.4.1, with corresponding materials and dimensions in Table 1.4.2. Initially, all 177FA reactors contained surveillance capsules that were contained in holder tubes located in the downcomer region. However, excessive vibration of the holder tube assembly was detected during reactor operation. Subsequent examination led to the decision to remove the holder tubes and capsule assemblies from all operating reactors at the next scheduled outage (during Cycle 1 for most plants). A new surveillance program was formulated in which capsules from reactors with failed holder tubes were installed in newly designed holder tubes and mounted in those reactors that were nearly completed. Thus, three extra holder tubes were installed in the host reactors, Crystal River-3 (CR-3) and Davis Besse-1 (DB-1). The Oconee 1, Oconee 2, and Oconee 3 capsules were put in the CR-3 reactor along with CR-3 capsules; and Arkansas One (ANO-1) and Rancho Seco capsules were put in the DB-1 reactor along with DB-1 capsules. This procedure was accepted by the NRC because of structural and operating condition similarities between the reactors.

The surveillance program must comply with the revised version of the ASTM Standard Recommended Practice for Surveillance Tests for Nuclear Reactor Vessels (E185-73)(As73). This version of ASTM E185 requires additional Charpy specimens per material and a minimum of five capsules for the Oconee-class plants.

The objective of the B&W Surveillance Program is to monitor the effects of neutron irradiation on the tensile and impact properties of the reactor pressure vessel materials under actual operating conditions, and to use the data obtained to ensure the continued licensability of the reactor plant. All of this is being done in accordance with the applicable laws, regulations, rules, and standards as set forth by the industry and government. The following describes B&W's approach to these requirements.

Each reactor vessel material surveillance program can obtain data from six B&W surveillance capsule locations. The capsules are inserted into holder tubes inside the reactor vessel as shown in Figures 1.4.1 through 1.4.5. Each capsule is a long stainless steel cylinder. Figures 1.4.1 and 1.4.2 show a typical capsule, its relative locations, and the orientation of the different specimens within each capsule. The Charpy and tension specimens are irradiated in cluster stacks. Any voids in the capsule are filled with aluminum spacers to minimize the movement of specimens in the capsule and improve the heat-transfer characteristics (see Figures 1.4.2 and 1.4.4).

TABLE 1.4.1

OPERATING B&W REACTORS

Utility	Reactor	Full Power Mwt	Operating Time EFPY on 6/1/82	Pressure Vessels	
				Material	Manufacturer
Duke Power Co.	Oconee Unit 1	2568	5.3	SA 302 B	B&W
	Oconee Unit 2	2568	4.8	SA 508 Cl 2	B&W
	Oconee Unit 3	2568	5.1	SA 508 Cl 2	B&W
Arkansas Power & Light	ANO Unit 1	2568	4.7	SA 533 B	B&W
Sacramento Utility District	Rancho Seco	2772	3.9	SA 533 B	B&W
Metropolitan Edison Co.	TMI Unit 1	2535	3.5	SA 302 B	B&W
Toledo Edison Co.	Davis Besse Unit 1	2772	1.8	SA 508 Cl 2	B&W
Florida Power Co.	Crystal River Unit 3	2452	2.9	SA 533 B	B&W

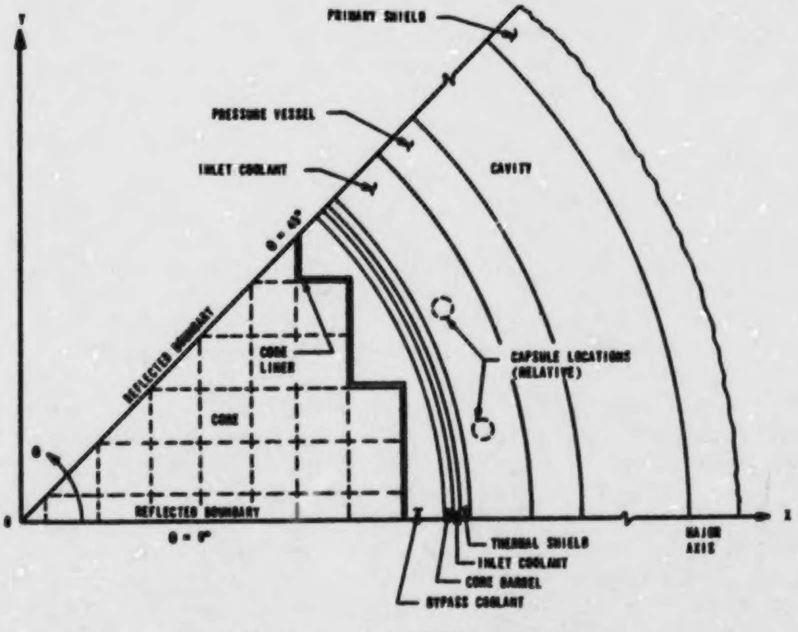
Y
PRIMARY SHIELD
PRESSURE VESSEL
INLET COOLANT
CAVITY
θ = 45°
REFLECTED BOUNDARY
CORE LINER
CORE
CAPSULE LOCATIONS (RELATIVE)
θ
0
REFLECTED BOUNDARY
θ = 0°
X
MAJOR AXIS
THERMAL SHIELD
INLET COOLANT
CORE BARREL
BYPASS COOLANT

FIGURE 1.4.1. Calculational Model of a 177FA Reactor.

TABLE 1.4.2

177FA REACTOR CONFIGURATION MATERIALS AND DIMENSIONS

Region	Material	Outer Boundary (cm)
Core	Homogenized mixture of H_2O, Zr4, UO_2, B, and Inconel 718	163.79
Core Baffle	SS304	165.70
Bypass Coolant	H_2O at 580° F, 2200 psia, 500 ppm B	179.07
Core Barrel	SS304	184.15
Inlet Coolant	H_2O at 555° F, 2200 psia, 500 ppm B	186.69
Thermal Shield	SS304	191.77
Downcomer	H_2O at 555°F, 2200 psia, 500 ppm B	216.69
Pressure Vessel	SA 533 B Carbon Steel	(a)239.08
Cavity	Air at 130° F, 15 psia	350.52
Shield Liner	SA 533 B Carbon Steel	351.15
Primary Shield	Concrete	(b)361.15

(a) Includes .635 cm stainless steel liner on inside surface and stainless steel insulation on outer surface.

(b) Partial depth into shield region.

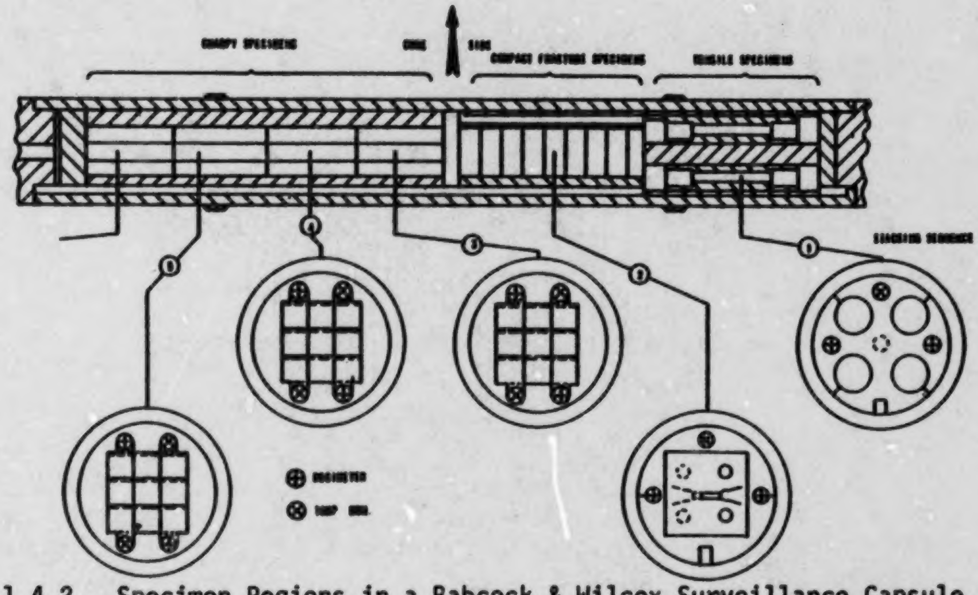
CHARPY SPECIMENS
CORE
SIDE
COMPACT FRACTURE SPECIMENS
TENSILE SPECIMENS
DOSIMETER
TEMP MON.

FIGURE 1.4.2. Specimen Regions in a Babcock & Wilcox Surveillance Capsule.

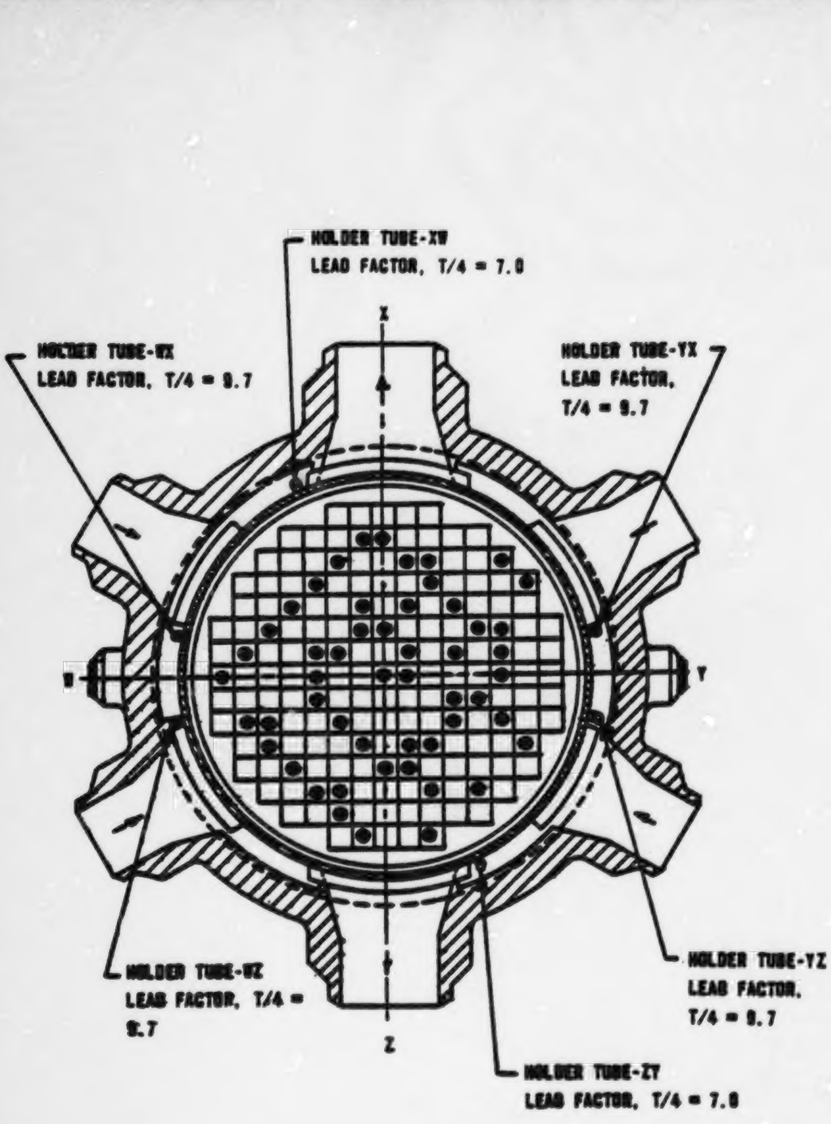
HOLDER TUBE-XW
LEAD FACTOR, T/4 = 7.0
HOLDER TUBE-WX
LEAD FACTOR, T/4 = 9.7
HOLDER TUBE-YX
LEAD FACTOR, T/4 = 9.7
X
W
Y
Z
HOLDER TUBE-WZ
LEAD FACTOR, T/4 = 9.7
HOLDER TUBE-YZ
LEAD FACTOR, T/4 = 9.7
HOLDER TUBE-ZY
LEAD FACTOR, T/4 = 7.0

FIGURE 1.4.3. New Capsule Holder Tube Locations in Host Reactors.

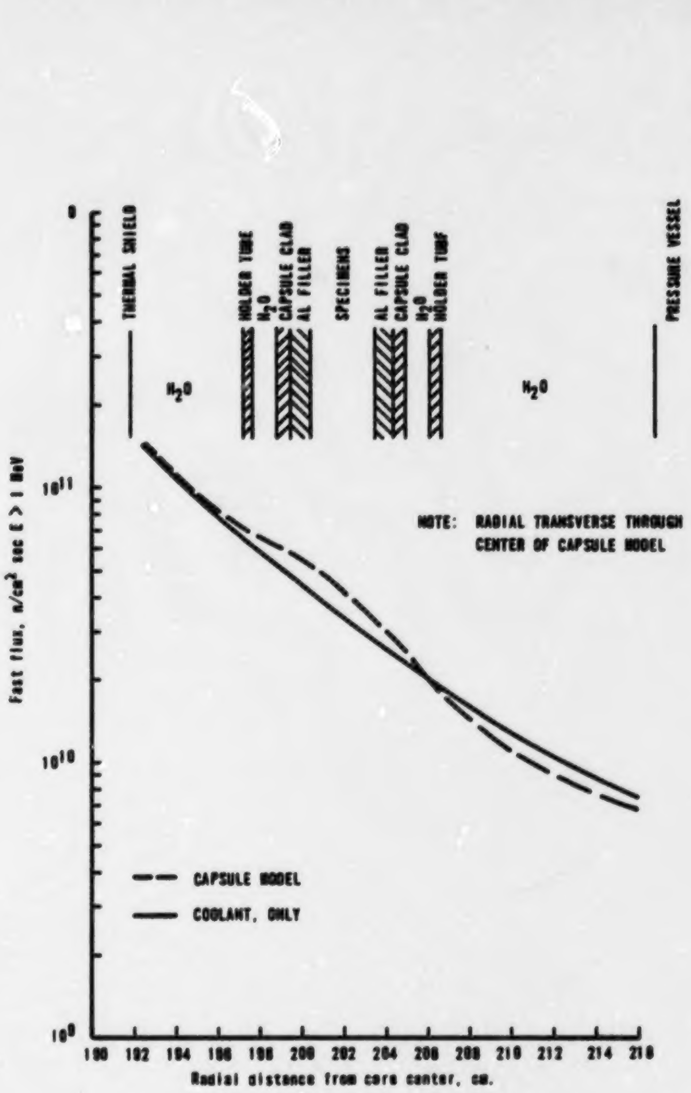

FIGURE 1.4.4. Flux Perturbation Caused by a Surveillance Capsule in a 177FA Reactor.

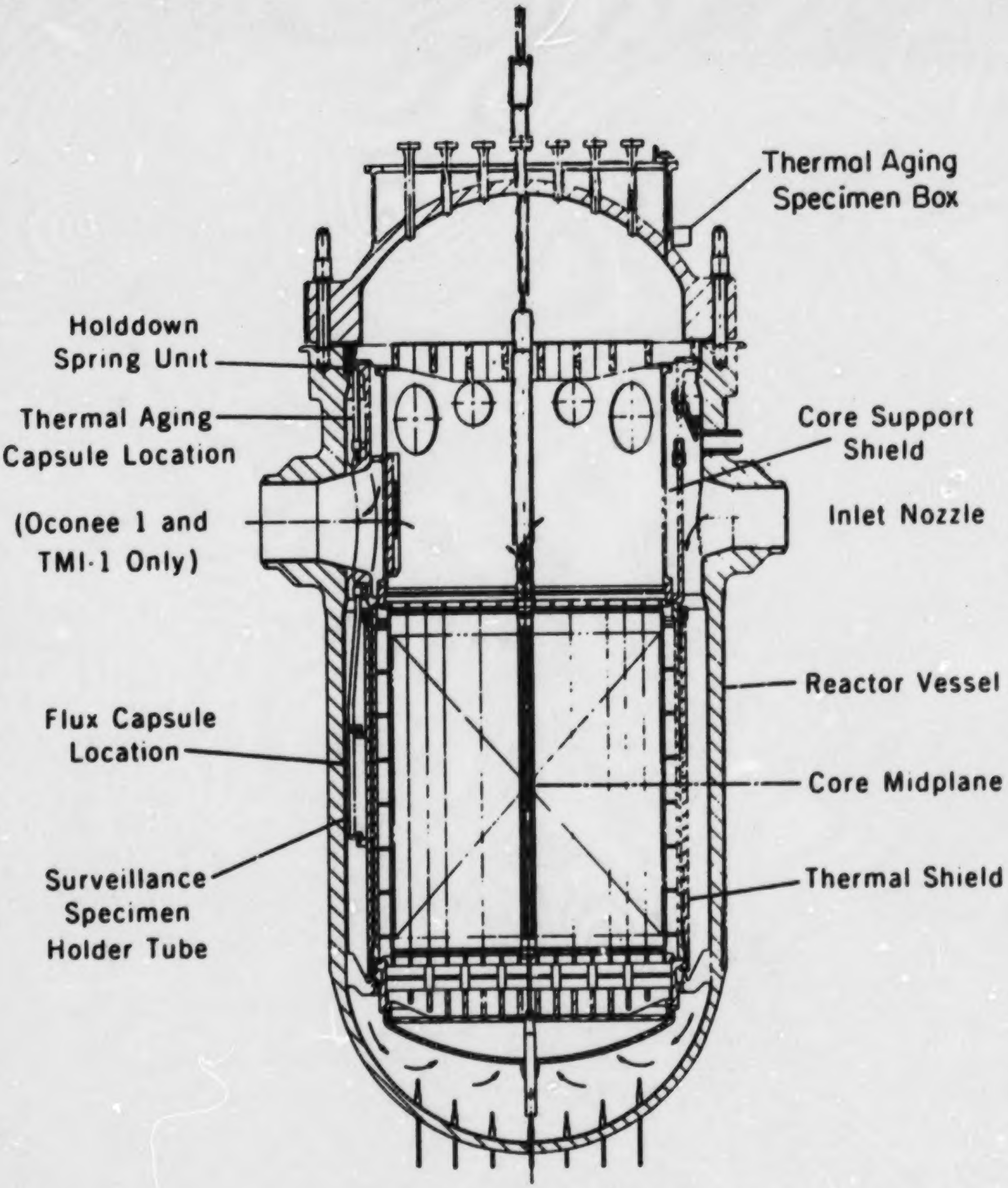
Thermal Aging
Specimen Box
Holddown
Spring Unit
Thermal Aging
Capsule Location
(Oconee 1 and
TMI-1 Only)
Core Support
Shield
Inlet Nozzle
Reactor Vessel
Flux Capsule
Location
Core Midplane
Surveillance
Specimen
Holder Tube
Thermal Shield

FIGURE 1.4.5. Typical Reactor Vessel Arrangement.

After the specimens are positioned in the capsules with the dosimeters, temperature monitors, and spacers, the capsules are purged in an inert atmosphere before the last end cap is welded in place.

Each capsule contains four clusters of Charpy specimens and one stack of tension specimens. Specimens from both heats of base metal surveillance material are included in each capsule.

In addition to the capsules, several Oconee-class reactors have thermal aging capsules or a specimen box as shown in Figure 1.4.5 at a point where the fast neutron fluence is below the threshold value for radiation damage. The material contained in each thermal aging capsule or box can be used to isolate the effects of temperature from those of neutron irradiation. The thermal aging material is selected by the same procedures used to choose surveillance monitoring materials.

As an example of a B&W surveillance program, results for Duke Power Company's Oconee Unit 1 are provided in Chapter 2 of Reference (St83a).

1.4.1.1 Surveillance Capsules

The B&W capsule design is shown in Figure 1.4.2, with pertinent details listed in Table 1.4.3. Two capsules are mounted, end-to-end, in each holder tube. Since several loading schemes are used, a capsule could contain some combination of 36 or 54 Charpy specimens, 4 or 8 tensile specimens, and 0 or 8 compact fracture specimens.

Capsule locations are described in Table 1.4.4. At present all in-reactor capsules are being irradiated at the new locations shown in Figure 1.4.3. Dosimeters are located at four positions around the periphery of the specimens. These positions are symmetric to the capsule center in a radial plane. Axially, two dosimeters are at the elevation of the Charpy specimens and two are in the tensile (or tensile-compact fracture) region. The vertical flux gradient in the capsule is sufficiently flat that all dosimeters are considered to be at the same elevation.

The flux perturbation caused by a capsule and holder tube assembly is indicated in Figure 1.4.4 which shows the fast flux (E > 1 MeV) distribution along a radial traverse through the capsule center. The increased flux, relative to water, reaches a maximum of about 28% near the capsule center and is about 25% averaged over the specimen region.

A number of low-melting fusible alloy temperature monitors are included in each capsule for determining maximum temperature during the irradiation exposure. The temperature monitors and their alloy composition and melting temperature are listed in Table 1.4.5.

TABLE 1.4.3

CAPSULE DESIGN DETAILS

Component	Material	Dimension, cm
Holder tube(1)	SS304	O.D. = 9.525
		I.D. = 8.255
Capsule	-	Length, overall ≅ 76
		Specimens Region ≅ 43
Capsule Cladding	SS304	O.D. = 6.35
		I.D. = 5.08
Charpy Specimens	Low-Alloy Steel	1.51 x 1.51
Filler Material(2)	Al 6061	-

---

(1) Holes in the tube wall represent 25% of the surface area.

(2) Region between specimens and cladding.

TABLE 1.4.4

CAPSULE POSITION

	Old Location	New Location
Radial distance from core center to capsule center	211.0	201.85
Azimuthal position, degrees from a major axis	11 (3)(a)	11 (6)(a) 26.5 (2)
Axial position	lower end of top capsule and upper end of lower capsule near the core midplane.	

(a) Number of holder tube assemblies at symmetric locations.

TABLE 1.4.5

TEMPERATURE MONITOR FUSIBLE ALLOYS

Alloy	Melting Temperature (°C)	(°F)
90 Pb - 5 Ag - 5 Sn	292	558
94.5 Pb - 2.5 Ag - 3 Sn	304	580
97.5 Pb - 1.5 Ag - 1.0 Sn	309	588
Cadmium	321	610
Lead	327	621

38

Calculated flux spectra at the capsule center, vessel surface, and vessel T/4 (Table 1.4.6) indicate that hardening occurs through the water gap from capsule to vessel and softening occurs through the vessel. Typically, about 50% of the flux above 1 MeV occurred in the 1 to 2 MeV region.

TABLE 1.4.6

SPECTRAL DISTRIBUTION OF FLUX IN THE SURVEILLANCE CAPSULE AND THE PRESSURE VESSEL

Upper Energy Boundary (MeV)	Normalized Spectra (a)		
	Capsule Center	Vessel Surface	Vessel T/4
15.0	.0007	.0015	.0012
12.2	.0029	.0061	.0048
10.0	.0088	.0169	.0129
8.18	.0252	.0444	.0320
6.36	.0498	.0771	.0560
4.96	.0500	.0711	.0499
4.06	.0879	.1018	.0774
3.01	.1014	.1073	.0896
2.46	.0338	.0346	.0297
2.35	.1635	.1539	.1537
1.83	.3919	.3206	.3887
1.11 (b)	.0841	.0647	.1042

(a) Normalized to $\sum_{1.0}^{15} \phi\Delta E = 1.0$

(b) Lower limit is 1.0 MeV

(c) Corresponds to new holder tube position

1.4.1.2 Capsule Removal

Surveillance capsule removal schedules for B&W plants are based on 10CFR50 Appendix H and ASTM E185-73 standard requirements but are modified according to the new surveillance program for all 177FA reactors (see Sections 1.4.1 and 1.4.1.3).

1.4.1.3 Neutron Flux Monitors

Each surveillance capsule contains four dosimeter tubes, each holding six dosimeters. They are spaced throughout the capsule to determine the actual neutron fluence levels received by the specimens. The selected dosimeters are listed in Table 1.4.7.

TABLE 1.4.7

SURVEILLANCE CAPSULE DOSIMETERS

Dosimeter	Threshold Energy	Reaction Product Counted
Co-Al	Thermal	5.3 years ^{60}Co
Fe	1.5 MeV	314 days ^{54}Mn
Cd-shielded ^{238}U	0.8 MeV	Appropriate fission products
Cd-shielded ^{237}Np	0.4 MeV	Appropriate fission products
Cd-shielded Co	0.5 eV	5.3 years ^{60}Co
Cd-shielded Ni	1.0 MeV	71 days ^{58}Ni

Initially, the radiation exposure of the reactor vessel wall at the 1/4 T location and of the specimens is calculated as described in Section 3.4.1. For the first surveillance interval, the predicted neutron flux distribution is factored into the prediction of RT_{NDT}. After the first capsule is withdrawn, the actual neutron flux distribution is calculated, taking into account the plant operating history and neutron flux measurements.

Measured neutron flux monitor activities for Cycle 1 exposure have been converted to saturation values and reported in Table 1.4.8 for four reactors: Davis Besse 1, Oconee 3, Oconee 2, and ANO-1. The capsules in Oconee 2 and 3 and in ANO-1 were at the same location and reactor power and, therefore, should exhibit similar activity levels. Relative power density (RPD) distribution is the only pertinent condition that may differ. In Davis Besse 1, however, the capsule was in the newly designed holder tube that was at a different radial and azimuthal location. In addition, reactor power was somewhat higher. Consequently, fast flux was more than twice the fast flux at the old holder tube location. Additional capsule data are listed in

TABLE 1.4.8

CAPSULE DOSIMETER DATA FROM CYCLE 1 EXPOSURE IN SELECTED REACTORS

Reactor	Full Power Mwt	Cycle Time EFPD	Capsule Position	Reaction	(a)Activity, μCi/g End of Irradiation	Saturated
DB-1	2772	374	201.8 cm	^{54}Fe(n,p)^{54}Mn	613	1555
			26.5°	^{58}Ni(n,p)^{58}Co	1109	1969
			lower	^{238}U (n,f)^{137}Cs	2.45	107
				^{237}Np(n,f)^{137}Cs	14.9	651
Oconee 3	2568	345	211 cm	^{54}Fe(n,p)^{54}Mn	363	763
			11°	^{58}Ni(n,p)^{58}Co	719	964
			upper	^{238}U (n,f)^{137}Cs	1.05	48.8
				^{237}Np(n,f)^{137}Cs	5.42	253
Oconee 2	2568	440	211 cm	^{54}Fe(n,p)^{54}Mn	424	776
			11°	^{58}Ni(n,p)^{58}Co	766	946
			upper	^{238}U (n,f)^{137}Cs	1.21	45.0
				^{237}Np(n,f)^{137}Cs	6.70	250
ANO-1	2568	345	211 cm	^{54}Fe(n,p)^{54}Mn	362	796
			11°	^{58}Ni(n,p)^{58}Co	686	951
			upper	^{238}U (n,f)^{137}Cs	0.965	47.4
				^{237}Np(n,f)^{137}Cs	5.15	253

(a) Average of four dosimeter wires; the calculated axial shape factor was 1.15 for DB-1, 1.17 for Oconee 3, 1.14 for Oconee 2, and 1.17 for TMI-1.

Table 1.4.9 for selected capsules that have been irradiated in two reactors. After the holder tube assembly failure, those capsules were removed and then inserted in CR-3 or DB-1. To date, 12 capsules from B&W 177FA reactors have been analyzed and the results reported to the operating utilities (Lo75,Lo77, Lo77a,Lo77b,Lo77c,Lo77d,Lo81,Lo81a,Lo81b,Lo81c,Lo81d,Lo82,Lo82a).

TABLE 1.4.9

CAPSULE DOSIMETER DATA FROM CYCLE 1 EXPOSURE IN ONE REACTOR PLUS EXPOSURE IN A SECOND REACTOR(a)

Reactor	Full Power Mwt	Cycle Time EFPD	Capsule Position	Reaction	Activity µCi/g
CR-3 &	2452	338 &	201.8 cm	$^{54}Fe(n,p)^{54}Mn$	921.
Oconee 3		345	11°	$^{58}Ni(n,p)^{58}Co$	1952.
			upper	$^{238}U\ (n,f)^{137}Cs$	2.99
				$^{237}Np(n,f)^{137}Cs$	18.6
CR-3 &	2452	338 &	201.8 cm	$^{54}Fe(n,p)^{54}Mn$	952.
Oconee 2		440	11°	$^{58}Ni(n,p)^{58}Co$	1940.
			upper	$^{238}U\ (n,f)^{137}Cs$	4.45
				$^{237}Np(n,f)^{137}Cs$	24.2
DB-1 &	2772	374 &	201.8 cm	$^{54}Fe(n,p)^{54}Mn$	966.
ANO-1		345	11°	$^{58}Ni(n,p)^{58}Co$	1672.
			upper	$^{238}U\ (n,f)^{137}Cs$	5.25
				$^{237}Np(n,f)^{137}Cs$	32.2

(a) Data in this table are for the second irradiation period; the first irradiation data are in Table 1.4.6.

(b) Value at end of irradiation period; calculated axial shape factors were 1.1 in CR-3 and 1.15 in DB-1.

2.0 PHYSICS-DOSIMETRY SURVEILLANCE PROGRAMS FOR PWR AND BWR

The surveillance programs, surveillance capsules, capsule removal schedules, temperature monitors, and neutron flux and correlation monitors used for Westinghouse, General Electric, Combustion Engineering, and Babcock & Wilcox reactors are described in Sections 1.1, 1.2, 1.3, and 1.4, respectively. Additional information on 1) the design and placement of surveillance capsules, 2) the modeling and codes used for reactor physics calculations, and 3) the results of reactor physics calculations are described and/or referenced in Sections 2.1, 2.2, 2.3, and 2.4 for Westinghouse, General Electric, Combustion Engineering, and Babcock & Wilcox reactors, respectively. Sections 3.0 and 4.0 provide detailed and summary results, as well as references to documentation, on the benchmarking and the comparison of calculated and measured dosimetry sensor reaction rates and derived neutron exposure parameter values. Surveillance data development, evaluation, applications, and spatial and temporal extrapolations are reviewed and discussed in Section 5.0.

2.1 W-NTD CAPSULE PHYSICS-DOSIMETRY

2.1.1 Surveillance Capsules

A number of different designs has been used for attaching the ~1-in. square x 5-ft long surveillance capsule used in Westinghouse designed PWRs (see Section 4.2). Here only a single generic PWR reactor design will be considered.

A plan view of a generic Westinghouse 2-loop reactor geometry at the core midplane is shown in Figure 2.1.1. Since the reactor exhibits eighth core symmetry, only the 0° - 45° sector is depicted. Six irradiation capsules attached to the thermal shield are included in the design to constitute the reactor vessel surveillance program. Two capsules are located symmetrically at 13°, 23°, and 33° from the cardinal axes. The relative locations of the three pairs of capsules are indicated by points A, B, and C on Figure 2.1.1.

A plan view of a single surveillance capsule attached to the thermal shield is depicted in Figure 2.1.2. The stainless steel specimen container is 1.0 in. square and ~63 in. in length. The containers are positioned axially such that the specimens are centered on the core midplane, thus, spanning the central 5.25 ft of the 12-ft high reactor core.

From a neutronic standpoint, the surveillance capsule structures are significant. These materials introduce marked perturbations in the distributions of neutron flux and energy spectra within the test specimen array. These perturbations, in turn, directly impact the determination of surveillance capsule lead factors as well as the calculation of spectrum-averaged reaction cross sections that are used in dosimetry evaluations. To properly ascertain the neutron environment at the test specimen locations, the capsule induced perturbation effects must be accounted for.

2.1.2 Reactor Physics Calculations

In the analysis of the neutron environment within the reactor geometry, predictions of neutron flux magnitude and energy spectra are made with the DOT two-dimensional discrete ordinates code (So70). The radial and azimuthal distributions are obtained from an R,θ computation wherein the geometry shown in Figures 2.1.1 and 2.1.2 are described in the analytical model. In addition to the R,θ computation, a second calculation in R,Z geometry is also carried out to obtain relative axial variations of neutron flux throughout the geometry of interest. In the R,Z analysis the reactor core is treated as an equivalent volume cylinder and, or course, the surveillance capsules are not included in the model.

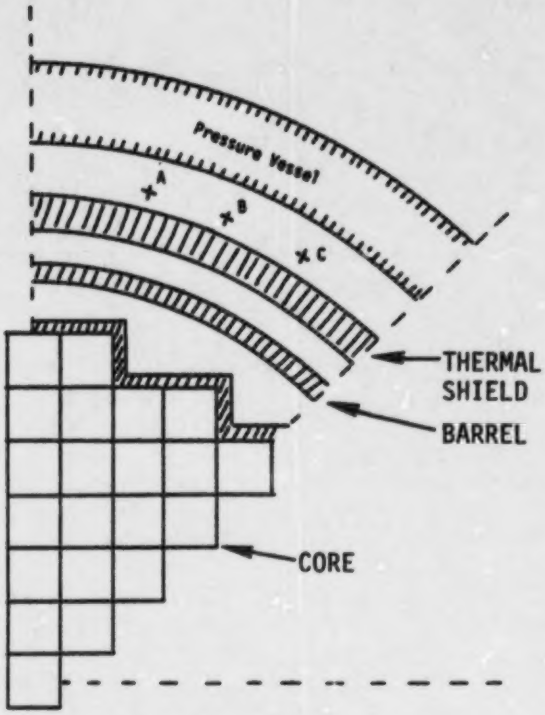
Pressure Vessel
A
B
C
THERMAL SHIELD
BARREL
CORE

FIGURE 2.1.1. 2-Loop Plant Radius, Theta Geometry.

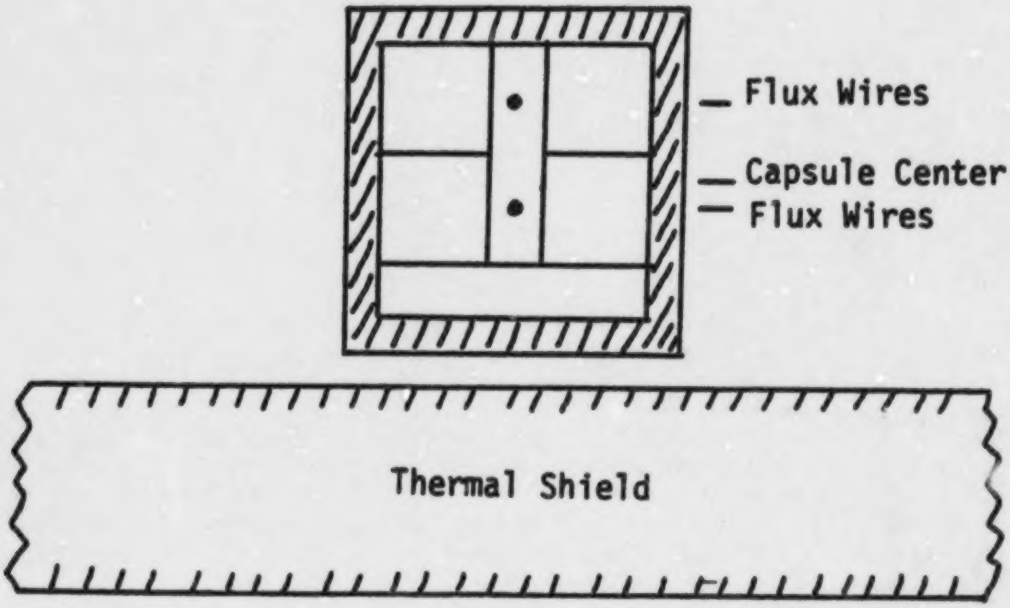
Flux Wires
Capsule Center
Flux Wires
Thermal Shield

FIGURE 2.1.2. Surveillance Capsule Geometry.

BEST COPY AVAILABLE

45

Both the R,θ and RZ analysis employ 47 neutron energy groups and a P_3 expansion of the scattering cross sections. The cross sections used in the analysis are obtained from the SAILOR library (OaSA,SaXX), which was developed specifically for light water reactor applications. The neutron energy group structure used in the analysis is listed in Table 2.1.1.

Once the R,θ and R,Z discrete ordinates calculations are completed, three-dimensional variations of neutron flux are approximated by assuming that the following relation holds for applicable regions of the reactor.

$$\phi(R,Z,\theta,E_G) = \phi(R,\theta,E_G)\ F(Z,E_G)$$

where:

$\phi(R,Z,\theta,E_G)$ = Neutron flux at point R,Z,θ within energy group G

$\phi(R,\theta,E_G)$ = Neutron flux at point R,θ within energy group G obtained from the R,θ calculation

$F(Z,E_G)$ = Relative axial distribution of neutron flux within energy group G obtained from the R,Z calculation

A key input parameter in the analysis of the integrated fast neutron exposure of the reactor vessel is the core power distribution. For this analysis, power distributions representative of time-averaged conditions derived from statistical studies of long-term operation of Westinghouse reactors are used. These input distributions include rod-by-rod spatial variations for all peripheral fuel assemblies.

It should be noted that the generic design basis core power distributions are intended to provide a vehicle for long-term (end-of-life) projection of vessel exposure. Since plant-specific core power distributions reflect only past operation plus possibly one fuel cycle into the future, their use for long-term temporal projections may not be justified; and the use of generic data that reflects long-term operation of similar cores may provide a more suitable approach. It must be added, however, that to achieve the most direct comparison of analytical prediction with measurements from individual surveillance capsules, the use of plant-specific core power distributions is more appropriate. The central question to be addressed in choosing a power distribution for the transport analysis is:

> Are the results of the discrete ordinates analysis expected to provide the best possible comparison with a particular measurement or are they expected to provide a reasonably accurate vehicle for use in predicting the condition of the pressure vessel for some future operating period?

TABLE 2.1.1

47 GROUP ENERGY STRUCTURE

Group	Lower Energy (MeV)	Group	Lower Energy (MeV)
1	14.19*	25	0.183
2	12.21	26	0.111
3	10.00	27	0.0674
4	8.61	28	0.0409
5	7.41	29	0.0318
6	6.07	30	0.0261
7	4.97	31	0.0242
8	3.68	32	0.0219
9	3.01	33	0.0150
10	2.73	34	7.10×10^{-3}
11	2.47	35	3.36×10^{-3}
12	2.37	36	1.59×10^{-3}
13	2.35	37	4.54×10^{-4}
14	2.23	38	2.14×10^{-4}
15	1.92	39	1.01×10^{-4}
16	1.65	40	3.73×10^{-5}
17	1.35	41	1.07×10^{-5}
18	1.00	42	5.04×10^{-6}
19	0.821	43	1.86×10^{-6}
20	0.743	44	8.76×10^{-7}
21	0.608	45	4.14×10^{-7}
22	0.498	46	1.00×10^{-7}
23	0.369	47	0.00
24	0.298		

*The upper energy of Group 1 is 17.33 MeV

For the purposes of this work the emphasis has clearly been placed on the latter goal of the transport calculation. It will be shown in a later section how surveillance dosimetry is used to verify the adequacy of this approach.

One further point should be addressed before leaving the subject of core power distributions. That is, the generic design basis used in this analysis assumes an out-in fuel management strategy (fresh fuel on the periphery). Future commitment to low-leakage loading patterns could significantly reduce the calculated neutron flux levels presented in Section 2.1.3. Furthermore, surveillance capsule lead factors could be changed, thus, impacting the withdrawal schedule of the remaining capsules. Here again, if projections of vessel embrittlement are based on the generic transport results and low-leakage loading patterns are, in fact, implemented the generic projections will turn out to be conservative. If, on the other hand, plant-specific power distributions including low-leakage cores were used to project vessel condition and the fuel management then departed from a low-leakage strategy, those projections could be nonconservative.

2.1.3 Results of Reactor Physics Calculations

Results of the discrete ordinates calculations for the Westinghouse 2-loop reactor design are summarized in Tables 2.1.2 through 2.1.6. All of the analytical results have been normalized to a core power level of 1961 MWt and are representative of the axial midplane of the reactor core.

In Table 2.1.2, calculated exposure rate parameters in terms of $\phi(E > 1.0$ MeV$)$, $\phi(E > 0.1$ Mev$)$, and dpa/s are given for the center of the three pairs of surveillance capsules located at 13°, 23°, and 33°, as well as for the point of maximum exposure on the pressure vessel. In regard to the pressure vessel, data are presented for the vessel inner radius, the 1/4 thickness location, and the 3/4 thickness location.

The data included in Table 2.1.2 may be used to calculate lead factors relating observed embrittlement effects at a surveillance capsule location to the actual condition of the pressure vessel. In Table 2.1.3, calculated lead factors are given based on each of the three exposure parameters listed in Table 2.1.2. Here the lead factor is defined as the ratio of the exposure parameter ($\phi(E > 1.0$ MeV$)$, $\phi(E > 0.1$ MeV$)$, and dpa/s) at the center of the surveillance capsule to the corresponding value of the exposure parameter at the point of interest within the pressure vessel.

In order to derive neutron flux and fluence levels or displacement rates and dpa from measured dosimeter reaction rates it is necessary to employ an adjustment code or to have available suitable spectrum-averaged cross sections for individual dosimeter reactions. In either case, an accurate estimate of the neutron spectrum at the dosimeter location is essential. In Table 2.1.4, the calculated neutron energy spectrum at the center of each

TABLE 2.1.2

CALCULATED FAST NEUTRON EXPOSURE RATE UNITS FOR 2-LOOP PLANT SURVEILLANCE CAPSULES - 1961 MWt

Location	ϕ(E>1.0 MeV) (n/cm^2-sec)	ϕ(E>0.11 MeV) (n/cm^2-sec)	dpa Rate (dpa/sec)
13° Capsule	1.90×10^{11}	7.35×10^{11}	3.55×10^{-10}
23° Capsule	1.15×10^{11}	4.04×10^{11}	2.03×10^{-10}
33° Capsule	1.04×10^{11}	3.72×10^{11}	1.86×10^{-10}
Vessel IR*	6.10×10^{10}	1.62×10^{11}	1.01×10^{-10}
Vessel 1/4 T*	4.00×10^{10}	1.46×10^{11}	7.21×10^{-11}
Vessel 3/4 T*	1.19×10^{10}	7.30×10^{10}	2.98×10^{-11}

---

*Points of maximum exposure on and within the pressure vessel.

TABLE 2.1.3

CALCULATED LEAD FACTORS FOR 2-LOOP PLANT SURVEILLANCE CAPSULES - 1961 MWt

Ratio	ϕ(E>1.0 MeV)	ϕ(E>0.11 MeV)	dpa
13°/IR	3.11	4.54	3.51
13°/ 1/4	4.75	5.03	4.92
13°/ 3/4 T	16.0	10.1	11.9
23°/IR	1.89	2.49	2.01
23°/ 1/4 T	2.88	2.77	2.82
23°/ 3/4 T	9.66	5.53	6.81
33°/IR	1.70	2.30	1.84
33°/ 1/4 T	2.60	2.55	2.58
33°/ 3/4 T	8.74	5.10	6.24

TABLE 2.1.4

CALCULATED NEUTRON SPECTRA WITHIN THE 2-LOOP REACTOR GEOMETRY

	$\phi(n/cm^2\text{-sec})$					
Group	13° Capsule	23° Capsule	33° Capsule	Vessel IR	Vessel 1/4 T	Vessel 3/4 T
1	3.24×10^7	2.62×10^7	2.29×10^7	2.34×10^7	1.22×10^7	3.11×10^6
2	1.18×10^8	9.55×10^7	8.37×10^7	8.47×10^7	4.43×10^7	1.31×10^7
3	4.22×10^8	3.30×10^8	2.88×10^8	2.89×10^8	1.46×10^8	3.46×10^7
4	7.80×10^8	6.02×10^8	5.26×10^8	5.16×10^8	2.59×10^8	5.89×10^7
5	1.32×10^9	9.99×10^8	8.73×10^8	8.41×10^8	4.17×10^8	8.94×10^7
6	2.99×10^9	2.23×10^9	1.95×10^9	1.89×10^9	9.14×10^8	1.82×10^8
7	4.24×10^9	3.06×10^9	2.68×10^9	2.58×10^9	1.21×10^9	2.28×10^8
8	8.89×10^9	6.04×10^9	5.36×10^9	4.84×10^9	2.30×10^9	4.30×10^8
9	8.28×10^9	5.30×10^9	4.77×10^9	3.77×10^9	1.90×10^9	3.93×10^8
10	6.79×10^9	4.31×10^9	3.88×10^9	2.94×10^9	1.60×10^9	3.47×10^8
11	8.09×10^9	5.06×10^9	4.58×10^9	3.39×10^9	1.90×10^9	4.23×10^8
12	4.02×10^9	2.52×10^9	2.28×10^9	1.72×10^9	9.70×10^8	2.18×10^8
13	1.23×10^9	7.72×10^8	6.97×10^8	4.91×10^8	2.92×10^8	7.20×10^7
14	6.08×10^9	3.78×10^9	3.42×10^9	2.31×10^9	1.44×10^9	3.64×10^8
15	1.59×10^{10}	9.76×10^9	8.87×10^9	5.77×10^9	3.67×10^9	9.32×10^8
16	2.13×10^{10}	1.27×10^{10}	1.16×10^{10}	6.45×10^9	4.50×10^9	1.35×10^9
17	3.21×10^{10}	1.89×10^{10}	1.74×10^{10}	9.15×10^9	6.69×10^9	2.11×10^9
18	6.71×10^{10}	3.82×10^{10}	3.51×10^{10}	1.41×10^{10}	1.17×10^{10}	4.65×10^9
19	5.07×10^{10}	2.81×10^{10}	2.59×10^{10}	9.19×10^9	8.16×10^9	3.88×10^9
20	2.42×10^{10}	1.34×10^{10}	1.24×10^{10}	5.11×10^9	4.05×10^9	1.75×10^9
21	8.06×10^{10}	4.33×10^{10}	4.00×10^{10}	1.43×10^{10}	1.59×10^{10}	9.24×10^9

TABLE 2.1.4 (Cont'd)

	$\phi(n/cm^2\text{-sec})$					
Group	13° Capsule	23° Capsule	33° Capsule	Vessel IR	Vessel 1/4 T	Vessel 3/4 T
22	6.35×10^{10}	3.37×10^{10}	3.11×10^{10}	1.10×10^{10}	1.07×10^{10}	6.19×10^{9}
23	7.56×10^{10}	4.01×10^{10}	3.71×10^{10}	1.37×10^{10}	1.52×10^{10}	9.25×10^{9}
24	7.18×10^{10}	3.77×10^{10}	3.48×10^{10}	1.24×10^{10}	1.51×10^{10}	1.06×10^{10}
25	9.03×10^{10}	4.74×10^{10}	4.39×10^{10}	1.72×10^{10}	1.50×10^{10}	9.11×10^{9}
26	8.84×10^{10}	4.59×10^{10}	4.26×10^{10}	1.68×10^{10}	1.78×10^{10}	1.18×10^{10}
27	7.09×10^{10}	3.66×10^{10}	3.40×10^{10}	1.42×10^{10}	1.54×10^{10}	1.04×10^{10}
28	5.29×10^{10}	2.72×10^{10}	2.53×10^{10}	1.06×10^{10}	7.90×10^{9}	4.53×10^{9}
29	1.78×10^{10}	9.21×10^{9}	8.53×10^{9}	4.40×10^{9}	2.10×10^{9}	1.08×10^{9}
30	1.01×10^{10}	5.24×10^{9}	4.86×10^{9}	3.50×10^{9}	1.11×10^{9}	5.64×10^{8}
31	2.04×10^{10}	1.04×10^{10}	9.69×10^{9}	4.00×10^{9}	4.94×10^{9}	3.41×10^{9}
32	1.26×10^{10}	6.39×10^{9}	5.94×10^{9}	2.43×10^{9}	2.61×10^{9}	1.98×10^{9}
33	3.10×10^{10}	1.59×10^{10}	1.48×10^{10}	6.73×10^{9}	5.30×10^{9}	3.51×10^{9}
34	4.66×10^{10}	2.41×10^{10}	2.23×10^{10}	1.19×10^{10}	4.55×10^{9}	1.77×10^{9}
35	6.29×10^{10}	3.24×10^{10}	3.00×10^{10}	1.41×10^{10}	1.00×10^{10}	4.17×10^{9}
36	5.60×10^{10}	2.88×10^{10}	2.67×10^{10}	1.35×10^{10}	8.60×10^{9}	3.45×10^{9}
37	8.60×10^{10}	4.39×10^{10}	4.08×10^{10}	2.20×10^{10}	1.17×10^{10}	3.96×10^{9}
38	4.94×10^{10}	2.53×10^{10}	2.34×10^{10}	1.38×10^{10}	6.73×10^{9}	2.06×10^{9}
39	5.21×10^{10}	2.65×10^{10}	2.46×10^{10}	1.42×10^{10}	7.70×10^{9}	2.21×10^{9}
40	6.98×10^{10}	3.54×10^{10}	3.30×10^{10}	1.97×10^{10}	1.10×10^{10}	3.07×10^{9}
41	8.48×10^{10}	4.29×10^{10}	3.99×10^{10}	2.53×10^{10}	1.37×10^{10}	3.63×10^{9}
42	4.87×10^{10}	2.46×10^{10}	2.29×10^{10}	1.53×10^{10}	7.73×10^{9}	1.94×10^{9}
43	5.93×10^{10}	2.99×10^{10}	2.78×10^{10}	2.05×10^{10}	8.88×10^{9}	1.93×10^{9}
44	3.96×10^{10}	2.00×10^{10}	1.86×10^{10}	1.51×10^{10}	5.50×10^{9}	1.00×10^{9}
45	3.40×10^{10}	1.73×10^{10}	1.60×10^{10}	1.47×10^{10}	4.22×10^{9}	5.94×10^{8}
46	7.18×10^{10}	3.69×10^{10}	3.40×10^{10}	4.70×10^{10}	5.91×10^{9}	3.08×10^{8}
47	1.64×10^{11}	8.67×10^{10}	7.85×10^{10}	2.57×10^{11}	1.07×10^{10}	8.20×10^{7}

TABLE 2.1.5

SPECTRUM-AVERAGED REACTION CROSS SECTIONS AT THE CENTER OF 2-LOOP SURVEILLANCE CAPSULES

Reaction	(barns)		
	13° Capsules	23° Capsules	33° Capsules
$^{63}Cu(n,\alpha)^{60}Co$	0.000517	0.000653	0.000631
$^{54}Fe(n,p)^{54}Mn$	0.0626	0.0712	0.0699
$^{58}Ni(n,p)^{58}Co$	0.0863	0.0965	0.0947
$^{238}U(n,f)FP$	0.330	0.344	0.344
$^{237}Np(n,f)FP$	3.05	2.90	2.92
dpa	1868	1765	1788

surveillance capsule as well as at the pressure vessel inner radius, 1/4 thickness location, and 3/4 thickness location are presented. The surveillance capsule data represent the best available information for use as an a priori spectrum guess for adjustment code analysis and for the determination of individual dosimeter spectrum-averaged reaction cross sections. In Table 2.1.5, typical spectrum-averaged cross sections derived from the ENDFB-IV dosimetry file and the data given in Table 2.1.4 are presented.

Since the neutron dosimeters contained within the surveillance capsules are not all located at the same radial location, it becomes necessary to make gradient corrections to the measured data to provide a consistent set of dosimetry referenced to the capsule center. The use of this gradient corrected dosimeter set permits the evaluation of exposure rates and integrated exposures on a common basis referenced to a common location. In Table 2.1.6, calculated reaction rate gradients are listed for five typical fast neutron dosimetry reactions. These data may be used to radially adjust measured reaction rates to the capsule center (158.10 cm). Axial and azimuthal gradient corrections are negligible for Westinghouse 2-loop plant surveillance capsules.

TABLE 2.1.6

CALCULATED REACTION RATES FOR FLUX MONITOR GRADIENT CORRECTIONS WITHIN 2-LOOP PLANT SURVEILLANCE CAPSULES

	Radial Location (cm)				
Reaction	157.34	157.86	158.10	158.34	158.86
			13° CAPSULES		
^{54}Fe(n,p) ^{54}Mn	8.95×10^{6}	8.10×10^{6}	7.76×10^{6}	7.35×10^{6}	6.65×10^{6}
^{58}Ni(n,p) ^{58}Co	1.32×10^{8}	1.21×10^{8}	1.15×10^{8}	1.09×10^{8}	9.90×10^{7}
^{63}Cu(n,α) ^{60}Co	7.50×10^{5}	6.84×10^{5}	6.49×10^{5}	6.25×10^{5}	5.70×10^{5}
^{237}Np(n,f) ^{137}Cs	1.10×10^{8}	1.00×10^{8}	9.56×10^{7}	9.00×10^{7}	8.00×10^{7}
^{238}U(n,f) ^{137}Cs	1.17×10^{7}	1.05×10^{7}	1.00×10^{7}	9.45×10^{6}	8.40×10^{6}
$\phi(E < 0.414$ eV)	2.20×10^{11}	2.29×10^{11}	2.36×10^{11}	2.50×10^{11}	2.89×10^{11}
			23° CAPSULES		
^{54}Fe(n,p) ^{54}Mn	6.20×10^{6}	5.60×10^{6}	5.34×10^{6}	5.10×10^{6}	4.60×10^{6}
^{58}Ni(n,p) ^{58}Co	9.00×10^{7}	8.15×10^{7}	7.81×10^{7}	7.40×10^{7}	6.70×10^{7}
^{63}Cu(n,α) ^{60}Co	5.75×10^{5}	5.25×10^{5}	4.97×10^{5}	4.80×10^{5}	4.37×10^{5}
^{237}Np(n,f) ^{137}Cs	6.40×10^{7}	5.80×10^{7}	5.50×10^{7}	5.25×10^{7}	4.70×10^{7}
^{238}U(n,f) ^{137}Cs	7.40×10^{6}	6.70×10^{6}	6.31×10^{6}	6.05×10^{6}	5.40×10^{6}
$\phi(E < 0.414$ eV)	1.12×10^{11}	1.20×10^{11}	1.24×10^{11}	1.31×10^{11}	1.52×10^{11}
			33° CAPSULES		
^{54}Fe(n,p) ^{54}Mn	5.55×10^{6}	4.95×10^{6}	4.74×10^{6}	4.50×10^{6}	4.05×10^{6}
^{58}Ni(n,p) ^{58}Co	8.10×10^{7}	7.25×10^{7}	6.93×10^{7}	6.60×10^{7}	5.95×10^{7}
^{63}Cu(n,α) ^{60}Co	5.00×10^{5}	4.56×10^{5}	4.34×10^{5}	4.20×10^{5}	3.82×10^{5}
^{237}Np(n,f) ^{137}Cs	5.85×10^{7}	5.35×10^{7}	5.02×10^{7}	4.80×10^{7}	4.25×10^{7}
^{238}U(n,f) ^{137}Cs	6.75×10^{6}	6.05×10^{6}	5.71×10^{6}	5.46×10^{6}	4.90×10^{6}
$\phi(E < 0.414$ eV)	1.04×10^{11}	1.09×10^{11}	1.13×10^{11}	1.20×10^{11}	1.39×10^{11}

2.2 GENERAL ELECTRIC (GE) CAPSULE PHYSICS-DOSIMETRY

2.2.1 Surveillance Capsules

See Section 1.2 and Reference (St83a).

2.2.2 Reactor Physics Calculations

See Reference (St83a).

2.2.3 Results of Reactor Physics Calculations

See References (St83a).

It is noted that the neutron exposure results presented in Section 4.0 are based primarily on PWR surveillance capsule results. Future additions to this document will involve more information developed from BWR surveillance capsules. The initial BWR power plants that have been selected for study by HEDL, Quad Cities Unit 1 (Ya81c) and Unit 2 (Ya82a) and Dresden Unit 3 (Ya82), have already been analyzed by Anderson et al. of Westinghouse as a part of an existing EPRI "Structural Mechanics Program" (Ma78b,Ma82h,Ma82g, Ma83,Ta82). In regard to the testing and application of BWR physics-dosimetry-metallurgy data, Galliani has reported on recently derived physics-dosimetry exposure parameter values for the Caorso BWR. In his report, he states that available physics calculational predictions of the flux level and fluence (E > 1.0 MeV) appear to be considerably higher than the derived results based on $^{54}Fe(n,p)^{54}Mn$ and $^{63}Cu(n,\alpha)^{60}Co$ measured reaction rates. More specifically he and G. Martin state:

> "The fast neutron flux measurements performed at the end of the first cycle of operation of the Boiling Water Reactor of Caorso, gave a fast neutron flux of about 2 x 10^{8} nv, at about 90% of the nominal thermal power (2410 MW), in the location where the flux monitors were irradiated. Likewise, the fast neutron fluence was about 1 x 10^{16} nvt.
>
> The maximum fast neutron flux and fluence, impinging on the inner vessel wall, were estimated to be of the order of 4 x 10^{8} nv and 2 x 10^{16} nvt, respectively.
>
> The values both predicted for Caorso and measured at similar plants by General Electric were considerably higher. An additional effort should be made to better understand this discrepancy."

To demonstrate the validity of a neutron transport calculation method for determining neutron fluence and neutron spectra at various locations in a BWR pressure vessel containment system, summary results on the analysis of the Browns Ferry Unit 3 irradiation experiment are given by Passell in Ref. (Pa84). He states that, "Using the neutron transport method, analysts performed a series of one- and two-dimensional computations of fast neutron fluence for a particular core source term at the Browns Ferry (Alabama) Unit 3 BWR. For this work they prepared a cross-section library from ORNL data on neutron interaction. They compared the calculations to neutron fluence and neutron spectra data obtained inside the reactor pressure vessel and in the cavity just outside the vessel at the Browns Ferry BWR from November 1976 to August 1979 (Ma81c,Ma81d). The measurements of radiation parameters had been made by activating metal foils sensitive to neutrons above various energy thresholds in the range up to 6 MeV. The calculated in-vessel neutron fluence values demonstrated that this calculation method can effectively predict the measured results, when the calculations include required corrections for photofission and power distributions near the detector. In the ex-vessel cavity, the DOT and ANISN codes predicted values within approximately 50% at the midplane of the core and within a factor of 2 at the plane of the core top. The chief uncertainty in the calculations is the poorly understood distribution of voids (steam bubbles) in and around the core. The 70-group Shielding-and-Application-Independent Libraries for Operating Reactors (SAILOR) cross-section library, developed in this study, is documented in the report."

2.3 COMBUSTION ENGINEERING (CE) CAPSULE PHYSICS-DOSIMETRY

2.3.1 Surveillance Capsules

See Section 1.3 and Reference (St83a).

2.3.2 Reactor Physics Calculations

See References (St83a) and (Mc81).

2.3.3 Results of Reactor Physics Calculations

See References (St83a) and (Mc81).

2.4 BABCOCK AND WILCOX (B&W) CAPSULE PHYSICS-DOSIMETRY

2.4.1 Surveillance Capsules

Each of the surveillance capsules described in Section 1.4.1.1 contains four dosimeter tubes. These are stainless tubes, 1.635-cm OD by 21.4-cm long, each containing six flux wires: Fe, Ni, U-Al, Np-Al, and 2 Co-Al (Figure 2.4.1). The U-Al, Np-Al, and one Co-Al are contained in Cd-Ag tubes with a wall thickness of about 0.1 cm. Selected flux wire data are listed in Table 2.4.1

TABLE 2.4.1

DOSIMETER DETAILS

Material	Reaction	Weight (mg)[a] Total	Weight (mg)[a] Target Material	Purity (%)
Fe	$^{54}\text{Fe}(n,p)^{54}\text{Mn}$	158	9.20	99.999
Ni	$^{58}\text{Ni}(n,p)^{58}\text{Co}$	135	91.2	99.995
U-Al	$^{238}\text{U}(n,f)\text{FP}^{(c)}$	88	9.07	(b) 99.999 Al
Np-Al	$^{237}\text{Np}(n,f)\text{FP}^{(c)}$	70	1.01	99.99 Np 99.999 Al
Co-Al (Bare)	$^{59}\text{Co}(n,\gamma)^{60}\text{Co}$	15	8.4 E-2	99.9
Co-Al (Cd)	$^{59}\text{Co}(n,\gamma)^{60}\text{Co}$	18	1.0 E-1	99.9

(a) Typical values, actual weights vary up to about 30%.

(b) $^{235}\text{U} \leq 380$ ppm is the major impurity.

(c) Although several fission products are counted, ^{137}Cs is used to evaluate fast flux.

2.4.2 Reactor Physics Calculations

See Sections 1.4.1.1 and 3.4.

2.4.3 Results of Reactor Physics Calculations

See Sections 1.4.1.1 and 3.4.

REV No.	DATE	REVISION DESCRIPTION
1	3-15-71	[illegible] DIA WAS [illegible] DIA IN PART No. 4
2	3-29-71	KNURL ADDED TO PART No. 1 | SPOTWELD WAS TACKWELD
3	5-3-71	CORRECTED DATE IN TITLE BLOCK

BILL OF MATERIALS				
ITEM	DWG No.	DESCRIPTION	QUAN	MAT'L.
1	LRC 1803C	END CAP	2	STN STL.
2	LRC 1803C	SPACER - [illegible] DIA × [illegible] LG.	2	ALUM
3	LRC 1803C	CAP - [illegible] DIA × [illegible] LG.	1	CADMIUM SILVER ALLOY
4	LRC 1803C	DOSIMETER WIRE HOLDER	3	CADMIUM SILVER ALLOY
5-A	LRC 1803C	DOSIMETER WIRE	1	^{238}U
5-B	LRC 1803C	DOSIMETER WIRE	1	^{237}Np
5-C	LRC 1803C	DOSIMETER WIRE	1	Ni
5-D	LRC 1803C	DOSIMETER WIRE	1	Co (Cd)
5-E	LRC-1803C	DOSIMETER WIRE	1	Fe
5-F	LRC 1803C	DOSIMETER WIRE	1	Co
6	LRC 1803C	TUBE - .250 O.D. × .218 I.D. × 8[illegible] LG.	1	STN STL.
7	LRC 1803C	SPACER - [illegible] DIA. × [illegible] LG.	1	ALUM
8	LRC 1803C	DOSIMETER WIRE HOLDER	2	ALUM

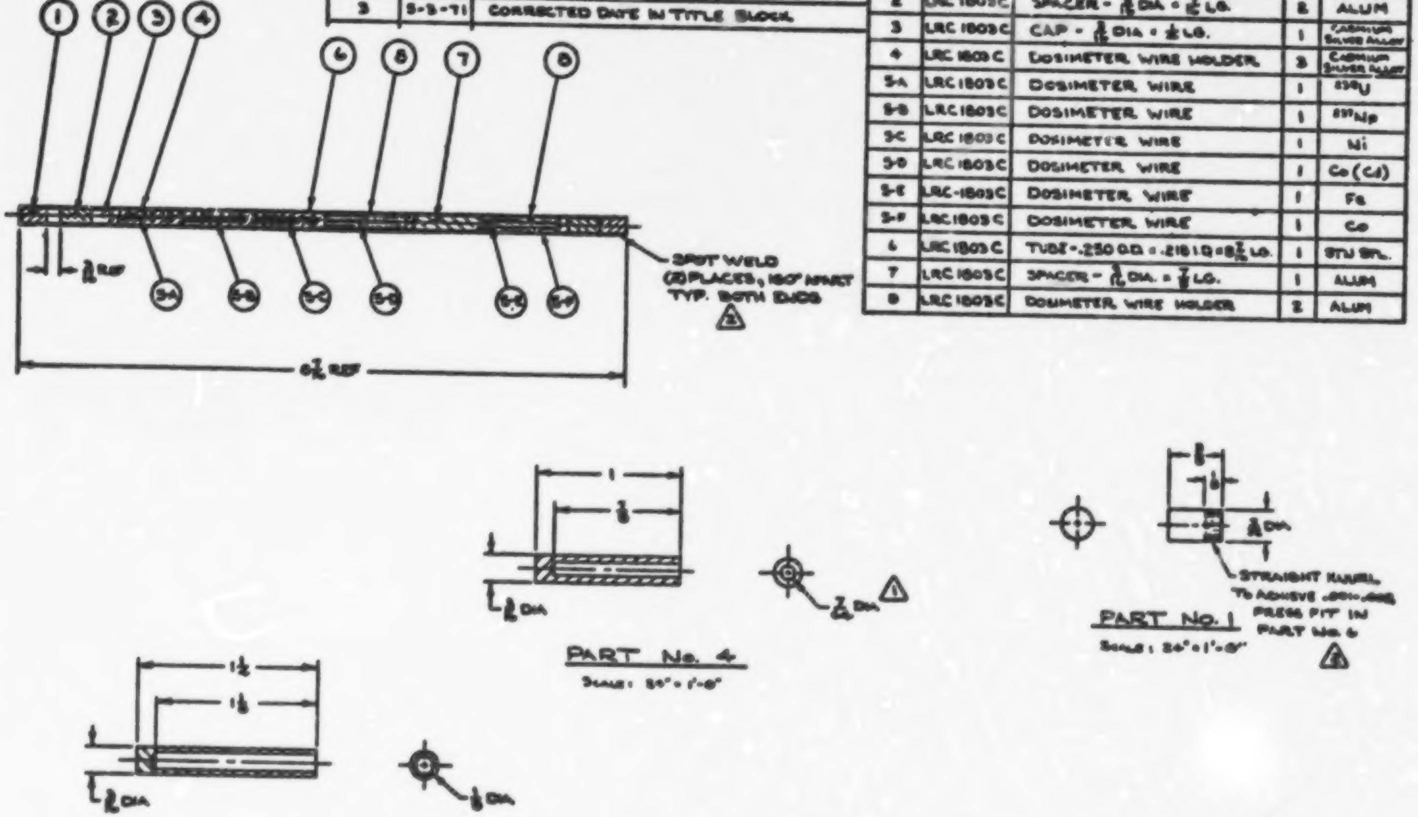

①
②
③
④
⑥
⑤
⑦
⑧
5-A
5-B
5-C
5-D
5-E
5-F
REF
SPOT WELD
(2) PLACES, 180° APART
TYP. BOTH ENDS
2
REF
1
DIA
DIA
1
PART No. 4
Scale: 24" = 1'-0"
DIA
STRAIGHT KNURL
TO ACHIEVE .001-.002
PRESS FIT IN
PART No. 6
PART No. 1
Scale: 24" = 1'-0"
3
DIA
DIA

FIGURE 2.4.1. Dosimeter Design for Capsule Fluence Measurement.

3.0 EVOLUTION OF PWR AND BWR REACTOR SURVEILLANCE DATA PROCESSING

The procedures used for and the evolution of PWR and BWR reactor surveillance capsule physics-dosimetry data processing are described and/or referenced in Sections 3.1, 3.2, 3.3, 3.4, 3.5, and 3.6 for six U.S. service laboratories: Westinghouse, General Electric, Combustion Engineering, Babcock & Wilcox, Battelle Memorial Institute, and Southwest Research Institute, respectively. Summary results and/or appropriate references documenting the comparison of measurements and calculations, the consistency of results, the benchmarking studies, and the observations that justify continued use of specific procedures and data are presented for the six service laboratories. As appropriate, comments on the conservatism and the accuracy of individual laboratory results and practices are provided. The emphasis here is on the need for conservatism in plant operation, for safety, and for meeting NRC licensing and regulatory requirements.

3.1 SURVEILLANCE DOSIMETRY DATA PROCESSING AT W-NTD

3.1.1 Neutron Dosimetry

The passive neutron dosimeters included in Westinghouse 2-loop plant surveillance capsules are listed in Table 3.1.1. The first five reactions in Table 3.1.1 are used as fast neutron monitors to relate neutron fluence and dpa to measured materials properties changes. To properly account for thermal neutron effects induced in the fast neutron dosimeters, bare and cadmium covered cobalt-aluminum monitors are also included to tie down the lower end of the neutron energy spectrum.

Within the 2-loop plant surveillance capsules neutron dosimeters are typically located near the top middle and bottom of the metallurgical test specimen array. Dosimetry using the ^{54}Fe(n,p)^{54}Mn reaction is accomplished in one of two ways. In early capsules, samples of iron were obtained from individual charpy specimens subsequent to testing; while in the later capsule design this approach was abandoned in favor of the use of high-purity iron wire. In all surveillance capsules nickel, copper, and cobalt-aluminum monitors are included in wire form. These wire dosimeters are placed in holes drilled in spacers at two radial locations and from three to five axial elevations within the capsule. A single pair of cadmium-shielded neptunium and uranium fission monitors are accommodated within a dosimeter block located near the geometric center of the surveillance capsule.

As stated in Section 2.1.3, following irradiation the specific activities of individual dosimeters are determined and gradient corrections are applied in order to reference all of the experimental data to the center of the surveillance capsule. The resultant set of gradient corrected activities provides a consistent data package from which exposure rates and integrated exposures may be determined either from analysis of individual reactions or via the use of a suitable adjustment code. The spectrum coverage of the dosimeter set is sufficient to allow determination of both neutron fluence ($E > 1.0$ MeV) and dpa with reasonable accuracy, given that a good estimate of the neutron spectrum is available from the transport calculations.

3.1.2 Comparison of Measurement and Calculations

The most direct comparison of the results of neutron transport calculations with surveillance dosimetry measurements is achieved by examining the measured and calculated specific activities for each dosimeter reaction on an absolute basis. This type of comparison affords the opportunity to evaluate analytical predictions of both neutron flux magnitude and to some extent neutron energy spectra at the surveillance capsule locations.

TABLE 3.1.1

NUCLEAR CONSTANTS FOR NEUTRON FLUX MONITORS CONTAINED IN 2-LOOP PLANT SURVEILLANCE CAPSULES

Monitor Material	Reaction of Interest	Target Weight Fraction	Product Half-Life	Fission Yield(%)
Copper	^{63}Cu(n,α) ^{60}Co	0.6917	5.27 yrs.	
Iron	^{53}Fe(n,p) ^{54}Mn	0.0585	314 days	
Nickel	^{58}(Ni(n,p) ^{58}Co	0.6777	71.4 days	
Uranium-238*	^{238}U(n,f) ^{137}Cs	1.0	30.2 yrs.	6.3
Neptunium-237*	^{237}Np(n,f) ^{137}Cs	1.0	30.2 yrs.	6.5
Cobalt-Aluminum*	^{59}Co(n,γ)^{60}Co	0.0015	5.27 yrs.	
Cobalt-Aluminum	^{59}Co(n,γ) ^{60}Co	0.0015	5.27 yrs.	

---

*Indicates that monitor is cadmium-shielded.

Measured specific activities of fast neutron dosimeters removed from 15 2-loop plant surveillance capsules are summarized in Table 3.1.2. This data base spans six reactors with as many as three capsules removed from a single reactor. The irradiation times associated with the data base range from a low of 1.25 to a high of 6.81 effective full power years (EFPY). Ten of the capsules were extracted from the 13° position, four from the 23° position, and a single capsule from the 33° position.

To facilitate experimental/analytical comparisons, all of the measurements have been normalized to a reactor power of 1961 MWt. In addition, data from the 23° and 33° capsule positions have been normalized to the 13° location using the analytically developed gradient information given in Table 2.1.6. The ^{238}U(n,f)^{137}Cs measurements listed in Table 3.1.2 have been adjusted to account for ^{235}U impurity in the dosimeter and for ^{239}Pu buildup over the course of the irradiation (see Section 4.1.3). However, no adjustment has been made to account for photofission. Preliminary calculations indicate that, for a 2-loop plant, surveillance capsule photofission effects are on the order of 1% to 2%.

The following observations can be extracted from the data listed in Table 3.1.2.

1) For all five fast neutron reactions the data set is remarkably consistent. The bounds on the measured specific activities range from a low of ±9% for the ^{54}Fe(n,p)^{54}Mn reaction to a high of ±22% for the ^{238}U(n,f)^{137}Cs reaction.

2) There appears to be no discernable bias in the experimental data either from reactor to reactor or from year to year for a given reactor. In fact, the variation in the data sets could be attributed to experimental uncertainty.

3) The discrete ordinates calculations using the generic power distribution, generic reactor dimensions, and a P$_3$ neutron scattering approximation produces slightly conservative though reasonable results. The C/E ratios range from a low of 1.07 for the ^{237}Np(n,p)^{137}Cs reaction to a high of 1.22 for the ^{58}Ni(n,p)^{58}Co reaction.

From these observations it can be concluded that the use of generic power distributions and nominal reactor dimensions in neutron transport calculations is justifiable, based on the consistency of the data set and on the good agreement between analysis and measurement. For reactors using a predominantly out-in fuel loading pattern, the generic analysis is shown to be conservative by from 7% to 22%. If low-leakage loading patterns were to be employed, analytical projections of neutron flux could be even more conservative, depending on the specific fuel management scheme employed.

TABLE 3.1.2

SUMMARY OF NEUTRON FLUX MONITOR SATURATED ACTIVITIES AT THE CENTER OF 2-LOOP PLANT SURVEILLANCE CAPSULES - 1961 Mwt - NORMALIZED TO THE 13° LOCATION

Plant/ Capsule	Capsule Location	Operating Time (EFPY)	Monitor Activity (dps/g) ^{54}Fe(n,p)^{54}Mn	^{58}Ni(n,p)^{58}Co	^{63}Cu(n,α)^{60}Co	^{237}Np(n,f)^{137}Cs	^{238}U(n,f)^{137}Cs
A-1	13°	1.49	6.25×10^6	8.35×10^7	--	8.40×10^7	7.19×10^6
A-2	33°	3.60	6.37×10^6	8.65×10^7	5.50×10^5	9.29×10^7	8.60×10^6
A-3	13°	5.08	7.05×10^6	1.06×10^8	5.98×10^5	8.28×10^7	9.24×10^6
B-1	13°	1.52	6.85×10^6	7.96×10^7	5.36×10^5	8.50×10^7	1.05×10^7
B-2	23°	3.45	6.48×10^6	9.63×10^7	5.33×10^5	8.62×10^7	8.78×10^6
B-3	13°	5.10	6.34×10^6	1.02×10^8	5.68×10^5	8.77×10^7	9.82×10^6
C-1	13°	1.64	6.89×10^6	1.12×10^8	5.21×10^5	--	6.88×10^6
C-2	13°	2.55	6.33×10^6	8.08×10^7	5.64×10^5	9.33×10^7	8.16×10^6
C-3	23°	6.81	6.03×10^6	8.33×10^7	6.27×10^5	9.96×10^7	9.21×10^6
D-1	13°	1.25	6.33×10^6	8.85×10^7	5.50×10^5	9.32×10^7	9.33×10^6
D-2	13°	4.50	--	9.98×10^7	5.68×10^5	--	8.37×10^6
E-1	13°	1.34	6.01×10^6	8.69×10^7	5.43×10^5	7.26×10^7	8.24×10^6
E-2	23°	4.59	6.54×10^6	1.10×10^8	6.19×10^5	9.25×10^7	9.24×10^6
F-1	13°	1.28	6.70×10^6	1.03×10^8	5.86×10^5	9.37×10^7	9.59×10^6
F-2	23°	3.99	6.48×10^6	1.01×10^8	5.60×10^5	9.96×10^7	9.18×10^6
Measured	Max/Min		1.17	1.41	1.20	1.37	1.53
Measured	Average		6.48×10^6	9.46×10^7	5.66×10^5	8.95×10^7	8.82×10^6
Calculation			7.76×10^6	1.15×10^8	6.49×10^5	9.56×10^7	1.00×10^7
Calc./Meas. Avg.			1.20	1.22	1.15	1.07	1.13

The fact that the C/E ratios are similar for all five reactions implies that the discrete ordinates calculations are doing an adequate job, not only at predicting neutron flux magnitude but also for fast neutron energy spectra within the surveillance capsules. These comparisons involving long-term irradiations in actual PWR geometries provide an excellent verification of the neutron transport methodology.

3.2 SURVEILLANCE DOSIMETRY DATA PROCESSING AT GE

The reader is referred to Chapter 3 of Reference (St83a) for procedures that were in use as of the late 1970s and early 1980s. Additional and more recent information, including relevant results for GE BWR-type power plants are provided in References (Ke82,Ma80d,Ma81c,Ma81d,Ma82j,Mc82c,Mp79,No78,No79a, No79b,No81a,No81c,No82,Pe84,Sh82,Ti80,Ya82,Ya81c,Ya82a).

3.3 SURVEILLANCE DOSIMETRY DATA PROCESSING AT CE

The reader is referred to Chapter 4 of Reference (St83a) for procedures that were in use as of the late 1970s and early 1980s. Additional and more recent information, including relevant results for CE PWR-type power plants are provided in References (Ar83,By80,Di82,Ke82,Mc81,Mc82c,Mp79,Nr80,Nr82,Pe79b, Pe80,Pe84,Va83).

3.4 SURVEILLANCE DOSIMETRY DATA PROCESSING AT B&W

Dosimeters are removed from surveillance capsules, and then isotopic activities are measured at the Lynchburg Research Center (LRC), a division of Babcock & Wilcox. Fluence calculations are performed by the analytical section and then normalized to fast flux derived from these activities. This normalization is then applied to vessel fluence calculations.

3.4.1 Analytical Fluence Calculations

Flux distribution calculations are performed with the DOT3.5 code which solves the Boltzmann transport equation in two-dimensional geometry using the discrete ordinates method. (Subsequent to 6/30/82, the DOTIV code will be used for this function.) Experience has shown that a $P_3S_8R\theta$ model with a 22 energy group cross-section set is adequate for problems of this type. The P_3 order of scattering is needed to describe the forward scattering of high energy flux in deep penetration problems, and the S_8 quadrature is needed for the large geometries. The $R\theta$ geometric model (Figure 1.4.1) has reflected left, top, and bottom boundary conditions and a vacuum right boundary. Two calculations are required to include the complete model from core to primary concrete because of computer storage limitations. Model A includes the core, baffle, bypass coolant, barrel, inlet coolant, thermal shield, and downcomer regions. Model B, which uses a left boundary source generated by Model A, includes the inlet coolant, thermal shield, downcomer, surveillance capsule, pressure vessel, cavity, and primary concrete (partial) regions. This method is generally known as "bootstrap" calculation. The model overlap is required because the right boundary vacuum condition distorts fluxes within about 10 cm of that boundary. Mesh interval radial dimensions in the steel and water regions are less than 2 cm in most regions and near 1 cm or less in critical regions, such as the capsule and near the vessel inside surface. Similarly, azimuthal interval dimensions are about one or two degrees and are reduced in the critical regions.

For transport calculations, the DLC-23E/CASK microscopic cross-section library was used (OaXX). This is a 22 neutron energy group (Table 3.4.1) set that was developed for deep penetration problems. The broad group flux weighting is based on a calculated spectrum in a uranium-water mixture and resolved resonance data that were generated by the SUPERTOG code. Fundamental data were from ENDF/BII and have been updated to ENDF/BIII for selected materials. Conversion of microscopic cross sections to macroscopic cross sections with the GIP code requires the use of material composition data. For the core region, a homogeneous mixture of fuel, moderator, and structural materials is used. Metal and concrete ex-core regions are based on nominal compositions. The downcomer and inlet coolant regions are based on measured inlet coolant temperature, nominal pressure, and average boron concentration. The bypass coolant region conditions are the same except for temperature, which is assumed to be equivalent to the average core coolant condition.

TABLE 3.4.1

NEUTRON ENERGY GROUP STRUCTURE USED IN CASK 23E LIBRARY

Group	Upper Energy (eV)	Lethargy (Eo=10 MeV)
1	1.5 (+7)	-4.0 (-1)
2	1.22 (+7)	-2.0 (-1)
3	1.0 (+7)	0
4	8.18 (+6)	2.0 (-1)
5	6.36 (+6)	4.5 (-1)
6	4.96 (+6)	7.0 (-1)
7	4.06 (+6)	9.0 (-1)
8	3.01 (+6)	1.20 (+0)
9	2.46 (+6)	1.40 (+0)
10	2.35 (+6)	1.45 (+0)
11	1.83 (+6)	1.70 (+0)
12	1.11 (+6)	2.20 (+0)
13	5.50 (+5)	2.90 (+0)
14	1.11 (+5)	4.50 (+0)
15	3.35 (+3)	8.00 (+0)
16	5.83 (+2)	9.75 (+0)
17	1.01 (+2)	1.15 (+1)
18	2.90 (+1)	1.275 (+1)
19	1.07 (+0)	1.375 (+1)
20	3.06 (+0)	1.50 (+1)
21	1.12 (-1)	1.60 (+1)
22	4.14 (-1)	1.70 (+1)

The source for the transport calculation is a fixed power distribution that is generated in criticality calculations (PDQ code) performed for fuel management analyses. This source is represented by a relative power density (RPD) distribution which is normalized to the average core power in the DOT calculation. Power density is converted to a spectral distribution of neutrons with the Watt fission spectrum for ^{235}U (Table 3.4.2). For capsule fluence calculations, a plant specific RPD distribution is used that represents the average RPD for the capsule irradiation time period. This average RPD is obtained by time weighting all PDQ calculations for the interval of interest. (Generally, a criticality calculation is made for each of 8 to 12 time steps during a fuel cycle.)

Conversion of saturated activiaties (product of DOT-generated flux and dosimeter reaction cross sections) to measured activities requires evaluation of the reactor power-time history. This non-saturation factor is separately calculated with the PRHIST computer code. Hourly power-time data for B&W reactors are available on magnetic tape and are directly input to PRHIST. All calculated activity data are corrected to the reactor shutdown prior to capsule removal.

3.4.2 Dosimeter Activity Calculations and Measurements

Dosimeter reaction cross sections were generated from ENDF/BV data. The broad group flux weighting was based on a ^{235}U fission spectrum at high energies, 1/E spectrum at intermediate energies, and a Maxwellian spectrum at low energies. Fission yields for ^{238}U and ^{237}Np were obtained from a literature evaluation of available data (Mc75c). (These values are a few percent higher than ENDF/BV data.)

Calculated saturation activities are obtained from the product of DOT generated energy dependent fluxes and reaction cross sections. Flux at the radial center of the capsule corresponds to the average of the four dosimeter positions. An axial shape factor is included to account for axial dimension flux gradients which are not included in the DOT calculation. The axial shape factor is the ratio of flux averaged over the capsule length to the average flux over the fuel assembly length. Calculated fuel burnup data in the nearest peripheral fuel assemblies are assumed to represent the axial shape of fast flux in the surveillance capsule. Multiplication by the non-saturation factor (from power-time history data) then converts the saturated activities to values corresponding to reactor shutdown.

Activities of dosimeter flux wires are measured by gamma spectroscopy. A germanium-lithium detector is used to count each sample until adequate counting statistics are obtained. Gamma peaks are processed through a multi-channel analyzer and a minicomputer system to produce specific activity data (μCi/g) that has been corrected to the time of reactor shutdown. The principal reactions of interest are listed in Table 3.4.3.

TABLE 3.4.2

WATT FISSION SPECTRUM

Group	Upper Energy (MeV)	Fractional Source
1	15	1.855 (-4)
2	12.2	1.011 (-3)
3	10	3.787 (-3)
4	8.18	1.469 (-2)
5	6.36	3.539 (-2)
6	4.96	4.863 (-2)
7	4.06	1.070 (-1)
8	3.01	8.811 (-2)
9	2.46	2.325 (-2)
10	2.35	1.183 (-1)
11	1.83	2.146 (-1)
12	1.11	1.953 (-1)
13	0.55	1.336 (-1)
14	0.111	1.607 (-2)
15-22	0.0035	0.0

TABLE 3.4.3

DOSIMETER REACTIONS

Reaction	Product Half Life	Threshhold Energy (Mev)	(a)Effective Energy Range (Mev)
$^{54}Fe(n,p)^{54}Mn$	312.6d	2.4	> 2.5
$^{58}Ni(n,p)^{58}Co$	71.23d	2.0	> 2.3
$^{238}U(n,f)^{137}Cs$	30.03y	1.1	> 1.1
$^{237}Np(n,f)^{137}Cs$	30.03y	0.1	> 0.5
$^{59}Co(n,\gamma)^{60}Co$	5.268y	-	> 0.0

(a) Energy above which 95% of the reactions in a capsule occur.

3.4.3 Normalization of Calculations

For a given reaction, the ratio of measured to calculated activity provides a normalization factor, which is then applied to all calculated fast fluxes throughout the reactor model. Activity and flux are proportional if the calculated relative flux spectrum is correct. The two fission reactions are used for normalization because of the long-lived product isotope and the effective energy range for reactions. In addition, the use of fission reaction normalization factors produced more conservative results (higher flux magnitudes) than were obtained with the Ni and Fe dosimeters.

3.4.4 Calculation Benchmarks

The calculation procedure used for surveillance capsule and vessel flux distributions was benchmarked in the PCA Blind Test. Comparisons of fast flux (E > 1 MeV) and selected dosimeter activities were within 15% at all reported dose points. If the data were normalized to a location corresponding to the capsule position in a B&W 177FA reactor, comparisons would be within 5%. Interpretation of Blind Test results, however, was obscured somewhat by the relatively strong dependence of calculational results on the treatment of flux leakage in the axial dimension. Axial leakage is not significant in surveillance capsule calculations.

The activity measurement facilities and procedures were benchmarked in the "PSF Interlaboratory Comparison" (Ke82) and the "PSF Surveillance Capsule Perturbation" dosimetry tests. Measured values at LRC differed by a few percent or less from benchmark values.

3.5 SURVEILLANCE DOSIMETRY DATA PROCESSING AT BMI

Surveillance dosimetry data analysis can be accomplished either by performing absolute or normalized neutron transport calculations. In the case of power reactor surveillance, normalized calculations are believed to be accurate and cost-effective. In this approach, the transport calculation is used to obtain the flux spectrum at the capsule and the lead factor from the capsule to the peak flux location at the vessel wall. Effective dosimeter cross sections are determined, using the calculated flux spectrum. The fluence experienced by the capsule can then be inferred from the measured foil activity rather than relying on the accuracy of a completely analytical approach. Further, it is not necessary in this approach to perform an axial transport analysis if axial power profile information is available. The procedure used is described in the next section. Recent experience with three-dimensional absolute neutron transport analysis is described in Section 3.5.3 below.

3.5.1 Approach

The flux at full power at the capsule location is determined from the expression:

$$\phi(E > E_c) = \frac{A_i}{N\sigma(E > E_c)C}$$

using the relationships

$$\sigma(E > E_c) = \frac{\int_0^\infty \sigma(E)\phi(E)dE}{\int_{E_c}^\infty \phi(E)dE}$$

and

$$C = \sum_{j=1}^{J} f_j(1 - e^{-\lambda T_j})\, e^{-\lambda(T-t_j)}$$

72

where

A_i = Activation of foil i

$\sigma(E)$ = Differential cross-section for activation reaction

$\phi(E)$ = Neutron differential flux

N = Atom density of target nuclei (atoms/g)

λ = Decay constant of product atom (s^{-1})

J = Number of time intervals of constant flux

f_j = Fractional power level during time interval j

T_j = Time length of interval j

t_j = Elapsed time from beginning of irradiation to end of interval j

T = Time from beginning of irradiation to counting

Thus, from the activity level for each foil, a value of the flux greater than a cutoff level can be inferred. Typically, values for the flux greater than 0.1 MeV and the flux greater than 1.0 MeV have been reported. In some cases, dpa has also been calculated. Since a number of flux values are obtained (a value for each foil), a weighted average of the flux values must be made to obtain the best estimate prediction.

The flux spectrum used in calculating an effective cross section, $\sigma(E > E_c)$, is obtained by means of transport analyses. The progression with time of the methods used in these analyses are described in a later section.

The correction term to account for the time-history of irradiation is calculated using a simple computer code, DECAY, developed for this purpose. The power-history is obtained from the utility. One-month time intervals have been used in describing the time variation. The histories are not provided in the surveillance reports, and it might be necessary to obtain these from utility records if reanalysis of the data was to be undertaken.

The weighting of results obtained with different foils has varied with time as the degree of consistency of results has improved. Initially, the best estimate of the flux was based entirely on the iron foils, using the results obtained for the other foils as a measure of accuracy. Spatial averaging is accounted for in the more recent two-dimensional analyses in which a number of nodes are used to characterize the capsule.

3.5.2 Radiochemistry and Counting Procedures

Techniques have varied to some extent depending on the samples in the capsules and their conditions. After removal from the capsule, the individual samples are placed in vials for transfer to the radiochemistry laboratory. Radiation readings at 1 meter and on contact are recorded. The nickel, copper, and cobalt wires are decontaminated by wiping with dilute acid, distilled water, and reagent-grade acetone. The iron samples and the ^{238}U and ^{237}Np capsules are wiped with dilute acid and distilled water to remove contamination and then are cleaned ultrasonically in a solution of Radiac and water.

The copper, nickel, and Al-0.15 Co wires are weighed to ±0.0001 g, and the activation product intensities are determined directly by gamma-ray spectrometry. In sime cases, iron sample drillings are taken through a complete cross section near the impact area of the designated Charpy impact specimen. The drillings are then mounted on a standard counting ring and gamma counted.

^{238}U and ^{237}Np capsules are opened in an alpha radiation containment box by specially prepared tools used to grip and cut the containers. The ^{238}U and ^{237}Np capsules are often present in the form of oxide powders. Using conventional dissolution techniques, the samples are dissolved and then diluted to known volumes. Radiochemical separations are performed, usually to obtain the ^{137}Cs fraction. This is followed by measurement of the 662-keV gamma ray using a NaI (Tℓ) base detection system.

About seven years ago Battelle-Columbus began using high-resolution solid-state germanium detectors for measurement of gamma-ray emitting radionuclides. This circumvents the need to perform radiochemical separations since the detector can resolve gamma rays from interfering radionuclides. Typical Battelle-Columbus systems are capable of 2-keV resolution or better at the 1332-keV gamma-ray peak of ^{60}Co. American Society for Testing and Materials (ASTM) procedures are used. The references for the procedures are as follows:

ASTM E261-77, "Determining Neutron Flux, Fluence and Spectra by Radioactivation Techniques"

ASTM E262-77, "Determining Thermal Neutron Flux by Radioactive Techniques"

ASTM E263-77, "Determining Fast Neutron Flux by Radioactivation of Iron"

ASTM E264-77, "Determining Fast Neutron Flux by Radioactivation of Nickel"

ASTM E523-76, "Measuring Fast Neutron Flux Density by Radioactivation of Copper"

ASTM E704-79, "Determining Fast Neutron Flux Density by Radioactivation of Uranium-238"

ASTM E705-79, "Determining Fast Neutron Flux Density by Radioactivation of Neptunium-237"

3.5.3 Neutronics Analyses

Over the past eight years the approach to the neutronics analyses has changed substantially. Initially analyses were performed with the ANISN code in one-dimension using the DLC-23 CASK library. An S_8P_3 analysis was performed. Dosimeter cross sections were collapsed into the 22-group spectrum from the fine-group cross sections in the SAND library. A flat spectrum was used to collapse the cross sections. Typically, the equivalent radius of the core was selected in a manner that tended to minimize the hardening of the spectrum at the capsule and to overestimate the flux at the capsule.

Nominal design values were used in characterizing the plant geometry. Different temperatures were selected for water in the downcomer and the core based on normal mid-plane operating conditions. Fixed source calculations were performed using a fission spectrum. The flux at the peak position in the vessel wall was obtained using lead factors provided by the reactor vendors.

In 1979 the computer tool was changed to the two-dimensional DOT3.5 code to account for flux perturbation in the neighborhood of the capsule and to better describe the boundary of the core. Differences in the flux levels in peripheral bundles of the core were accounted for based on power distributions provided by the utility. Calculations were performed in R-θ geometry, using S_8P_3 and the same cross-section set described previously. Lead factors were inferred directly from the analyses.

Most recently R-θ and R-Z analyses have been performed and merged to provide a three-dimensional characterization of the flux. Complete representation of the core is being made in order to obtain an absolute estimate of the flux at the capsule as well as the spectrum. The DOT4.3 code is currently being used with the BUGLE80 cross-section set. Dosimeter cross sections are collapsed from the ENDF/BV cross sections using the DETAN code in a fission spectrum. This approach enables accurate determination of the lead factor since both the azimuthal and axial flux distributions are accounted for.

3.6 SURVEILLANCE DOSIMETRY DATA PROCESSING AT SwRI

3.6.1 Evolution of Processing Procedures

The processing of dosimetry data from power reactor pressure vessel surveillance programs conducted at SwRI currently consists of three steps: (1) measuring the activities of selected isotopes in the dosimeters provided in each capsule and determining their reaction rates; (2) calculating the neutron spectrum and the spectrum-averaged cross sections at the capsule location; and (3) combining these data to determine the full-power fluence rate and the total exposure of the surveillance capsule. The methods by which this is accomplished were developed over a number of years.

When the testing of surveillance specimens was undertaken at SwRI, the dosimetry portion of the programs were subcontracted entirely (No67, No68, No71, No72). The flux determinations for the Elk River Reactor (No67, No68) were based on fission spectrum-averaged cross sections, but those for San Onofre Unit 1 (No71, No72) were calculated using several assumed spectral shapes. The SAND-II code was also employed in the analyses of several capsules (No72, No73, No73a), but its use was discontinued because the sets of dosimeters in many surveillance programs did not cover a wide range of response energies. Neutron spectra and/or cross sections were also obtained from the reactor vendor in several programs (No74, No75, No76, No80a); then SwRI began calculating neutron spectra with the DOT 3.5 discrete ordinates transport code (No76b, No77, No77a, No77b, No78, No79, No79a, No79b, No80, No81, No81a, No81b, No81c).

A scintillation detector system was placed into service during this period, and it was used to measure the isotopic activities of the dosimeter materials from a number of capsules (No73, No73a, No74, No75, No76, No76a, No76b, No77, No77a, No77b, No78, No79, No79b, No80a). The fission monitors contained in a few of these capsules (No76, No76b, No77b, No80a) were analyzed by chemically separating the cesium-137 before counting, but this procedure was discontinued and the fission monitors were counted directly after a Ge(Li) detector system became available (No80, No81, No81a, No81b, No81c).

3.6.2 Evaluation of Dosimeter Activities

The activities of dosimeters are measured using a multichannel analyzer and a Ge(Li) coaxial detector system. The calibration of the equipment is accomplished with ^{54}Mn, ^{60}Co, and ^{137}Cs radioactivity standards obtained from the U.S. Department of Commerce National Bureau of Standards. All activities are corrected to the time-of-removal (TOR) at reactor shutdown. The weight of the target element in each dosimeter is determined and the saturated activities (A_{SAT}) are calculated using the constants given in Table 3.6.1 and the relationship:

$$\frac{A_{TOR}}{A_{SAT}} = \sum_{m=1}^{m=n} P_m \left(1 - e^{-\lambda T_m}\right)\left(e^{-\lambda t_m}\right)$$

where:

A_{TOR} = activity at time-of-removal, dps/mg;
P_m = fraction of full power for the operating period m;
λ = decay constant for the activation product, day^{-1};
T_m = number of operating days for the period m;
t_m = decay time after the operating period m, days.

The plant operating history is broken down either into periods between shutdowns or into monthly periods. The value of P_m is taken as the quotient of the total thermal power generated in the period divided by the corresponding thermal power for full operation.

Reaction rate, R, is defined as the quotient of the saturated activity divided by the number of target atoms, N_0, in the counted sample. The values of N_0 utilized for the common dosimeter materials are included in Table 3.6.1.

3.6.3 Calculation of Spectrum-Averaged Cross Sections

The spatial and spectral distributions of neutrons in the reactor pressure vessel are calculated using a two-dimensional model and the DOT IV discrete ordinates transport code. Calculations are performed using a P_1 expansion of the scattering matrix, an S_8 order of angular quadrature, and R-Θ geometry to determine the radial and azimuthal distributions. In some programs, an R-Z model is also employed to examine the vertical flux distribution at the pressure vessel wall.

The two-dimensional model applied to the LaCrosse Boiling Water Reactor (No77) shown in Figure 3.6.1 is typical of the method used to describe a horizontal plane at midheight in R-Θ geometry. A one-eighth model can be used because of the symmetry involved. The boundary conditions are vacuum on the right side (pressure vessel) and reflected elsewhere. The source input for the transport calculation consists of a Watt fission spectrum and the core power distribution derived from plant records.

BEST COPY AVAILABLE

TABLE 3.6.1

CONSTANTS FOR PROCESSING DOSIMETRY DATA

Reaction	N_0 (atoms/mg)	Half-Life	λ (day^{-1})	X-ray Branching Intensity
$^{46}Ti(n,p)^{46}Sc$	1.018×10^{18}	83.85 d	8.266×10^{-3}	0.9998 @ 889 keV 0.9999 @ 1120 keV
$^{54}Fe(n,p)^{54}Fe$	6.254×10^{17}	312.5 d	2.218×10^{-3}	0.9997 @ 835 keV
$^{58}Ni(n,p)^{58}Co$	7.004×10^{18}	70.85 d	9.783×10^{-3}	0.9944 @ 811 keV
$^{59}Co(n,\gamma)^{60}Co$	1.022×10^{19}	5.271 y	3.600×10^{-4}	0.9990 @ 1173 keV 0.9998 @ 1332 keV
$^{63}Cu(n,\alpha)^{60}Co$	6.555×10^{18}	5.271 y	3.600×10^{-4}	0.9990 @ 1173 keV 0.9998 @ 1332 keV
$^{237}Np(n,f)^{137}Cs$	2.540×10^{18}	30.17 y	6.290×10^{-5}	0.853 @ 662 keV
$^{238}U(n,f)^{137}Cs$	2.530×10^{18}	30.17 y	6.290×10^{-5}	0.853 @ 662 keV

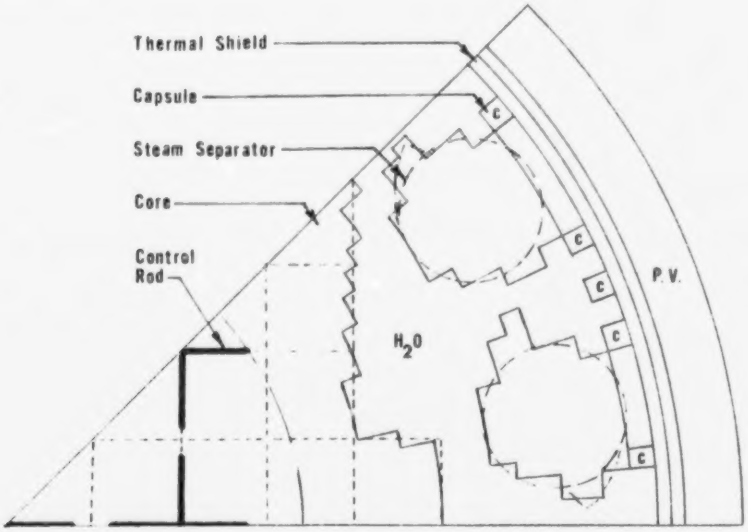

FIGURE 3.6.1. Two-Dimensional (R-Θ) Model of LACBWR Vessel.

The DLC-75/Bugle-80 cross section library for LWR shielding calculations obtained from the Radiation Shielding Information Center at the Oak Ridge National Laboratory is used to provide the cross sections needed for the transport calculations. This library is a 47-neutron energy group set based primarily on ENDF/B-IV. The group structure is given in Table 3.6.2.

The core region materials are homogenized in one or two zones, stainless steel is modeled as an 0.18 Cr/0.08 Ni/0.74 Fe mixture, and ferritic steel is considered as 0.98 Fe. Should the coolant contain voids, as in some BWR applications, this is taken into account. The microscopic cross sections are generated using the GIP code.

The spectrum-averaged reaction cross sections for the dosimeters are calculated as follows:

$$\bar{\sigma} = \frac{\sum \sigma(E)\phi(E)dE}{\sum_{E_L} \phi(E)dE}$$

where $\phi(E)$ is the normalized group fluxes at the capsule location. The group cross sections, $\sigma(E)$, are derived from ENDF/BV. The value of E_L is usually chosen as 1 MeV, but other lower limits for the neutron energies, such as 0.1 MeV, can be selected.

3.6.4 Determination of Surveillance Capsule Fluence

A value for the fast neutron fluence rate (flux) is determined for each dosimeter as the quotient of the reaction rate divided by the appropriate spectrum-averaged cross section. These data are adjusted to the radial centerline of the capsule, if necessary, using the radial dependency of flux generated in the transport calculation; then all credible results are averaged to determine the fast flux at the capsule location. Capsule fluence is calculated as the product of the fluence rate and the equivalent full power operating time covering the exposure period.

In some surveillance capsules, the specimen loading arrangement may be such that one or more of the surveillance materials was confined to a radial layer position other than the capsule centerline. When this is the case, the exposure of each material set is determined by readjusting the capsule fluence to the appropriate radial position.

TABLE 3.6.2

NEUTRON GROUP STRUCTURE FOR BUGLE-80

GROUP	UPPER ENERGY	UPPER LETHARGY
1	1.733299E+07	-5.500267E-01
2	1.419100E+07	-3.500229E-01
3	1.221400E+07	-1.999978E-01
4	1.000000E+07	0.0
5	8.607100E+06	1.499971E-01
6	7.408200E+06	2.999975E-01
7	6.065300E+06	5.000008E-01
8	4.965900E+06	6.999902E-01
9	3.678800E+06	9.999936E-01
10	3.011900E+06	1.200013E+00
11	2.725300E+06	1.300006E+00
12	2.466000E+06	1.399987E+00
13	2.365300E+06	1.441666E+00
14	2.345700E+06	1.450001E+00
15	2.231300E+06	1.500000E+00
16	1.920500E+06	1.649999E+00
17	1.653000E+06	1.799993E+00
18	1.353400E+06	1.999965E+00
19	1.002600E+06	2.299988E+00
20	8.208500E+05	2.500000E+00
21	7.427400E+05	2.599994E+00
22	6.081000E+05	2.800009E+00
23	4.978700E+05	3.000001E+00
24	3.688300E+05	3.300004E+00
25	2.972000E+05	3.515935E+00
26	1.831500E+05	3.999980E+00
27	1.110900E+05	4.499999E+00
28	6.737900E+04	5.000007E+00
29	4.086800E+04	5.499993E+00
30	3.182800E+04	5.749994E+00
31	2.605800E+04	5.950015E+00
32	2.417600E+04	6.024980E+00
33	2.187500E+04	6.124996E+00
34	1.503400E+04	6.500026E+00
35	7.101699E+03	7.250007E+00
36	3.354600E+03	8.000008E+00
37	1.584600E+03	8.750009E+00
38	4.540000E+02	9.999999E+00
39	2.144500E+02	1.075002E+01
40	1.013000E+02	1.150001E+01
41	3.726700E+01	1.249999E+01
42	1.067700E+01	1.375000E+01
43	5.043500E+00	1.450000E+01
44	1.855399E+00	1.550000E+01
45	8.764200E-01	1.625000E+01
46	4.139900E-01	1.700000E+01
47	9.999996E-02	1.842067E+01
48	1.000000E-05	2.763101E+01

3.6.5 Calculation Benchmarks

The procedure used to calculate the neutron distribution in support of reactor vessel surveillance programs was benchmarked in the PCA Blind Test. The DOT 3.5 Code and Cask cross section library were used to calculate reaction rates for sets of foil detectors in two configurations in the PCA Pressure Vessel Wall Benchmark Facility at Oak Ridge. The 8/7 configuration provided approximately an 8-cm water gap between the core face and the thermal shield and a 7-cm water gap between the thermal shield and the PV wall. In the 12/13 configuration, these dimensions were increased to 12 cm and 13 cm, respectively.

X-Y and X-Z calculations were performed instead of the R-Θ/R-Z geometry usually used for power reactor surveillance calculations because the PCA could best be described in rectangular coordinates. The C/E (calculated/experimental) ratios based on equivalent fission fluxes varied from 0.82 to 1.03 (average = 0.92) at the surveillance location.

Recently, SwRI has begun using the DOT-IV Code and the Bugle-80 cross section library for surveillance work. It has not been benchmarked as yet, but the modeling procedures are the same as had been previously benchmarked using the DOT 3.5 Code.

80

4.0 DETERMINATION OF EXPOSURE PARAMETER VALUES AND UNCERTAINTIES FOR OPERATING PWR AND BWR POWER PLANTS

As part of the LWR-PV-SDIP, a number of new ASTM standards have been or will be written for LWR power plant pressure vessel and support structure surveillance (As82). For the routine application of these standards, the recommended procedures and data are being benchmark tested with actual test and power-reactor-derived, physics-dosimetry-metallurgy data (Mc85a). Information and results based on the application and use of the new ASTM procedures and data for the determination of exposure parameter values and uncertainties for operating PWR and BWR power plants are presented in this section. These physics-dosimetry results are needed to support the data development and testing work associated with establishing material property-trend curves and damage analysis studies as discussed in Section 5.0. More specifically, the physics-dosimetry results provided in Section 4.2 through 4.5 are needed for physics-dosimetry-metallurgy data correlation studies that make use of 1) the Metal Properties Council (MPC) data base (Mp79), 2) the NRC MASTSURV data base (St80), and 3) the EPRI data base (Ma78b,Mc82c,Va79,Va81,Va82, Va83).

Over the period in which the physics-dosimetry data for the various LWR power reactor in-vessel surveillance capsules was analyzed for the above and other data bases, the auxillary parameters (such as cross sections, decay constants, neutron spectra, etc. used by vendors and service laboratories) have differed but have progressively improved (Mc82). For example, originally the fission spectrum was used to determine spectrum-averaged cross sections. Over a period of years, the use of one and two-dimensional neutron transport theory calculations was adopted in an effort to improve the physics-dosimetry analysis (An78,Gr81,Mc81). Further, the more recent physics-dosimetry evaluations have included consideration of the capsule perturbation to the flux (An78,As82,Mc81,Mc81a,Mc82,Mc82a). Earlier data correlations of the effects of irradiation on shift (i.e., in ΔNDTT and upper shelf) have not considered these variations in the physics-dosimetry analysis (As79a). Thus, unnecessary errors were oftened included in earlier correlations of irradiation effects data using the available surveillance data bases.

The present analytical effort involves re-evaluating the physics-dosimetry data for all discharged surveillance capsules from operating power plants in order to place all damage exposure values on a common basis. This and future revisions of this compendium will provide results and/or make reference to physics-dosimetry results based on radiometric (RM), solid state track recorder (SSTR), helium accumulation fluence monitors (HAFM), and/or damage monitors (DM) dosimetry measurements obtained from both surveillance capsule and ex-vessel cavity irradiations, as discussed in this and Section 4.1.4.

81

In an evaluation of the safe operation of a reactor pressure vessel, one of the key input parameters is the neutron exposure that the vessel in question has experienced. This neutron exposure is expressed as neutron fluence ($E > 1.0$ MeV) and dpa (displacements per atom). An accurate knowledge of the neutron exposure is desirable whether the information is to be used in vessel integrity evaluations for current issues, such as pressurized thermal shock (PTS) (Di82), or to assess the safety of operating a particular vessel up to or beyond its design lifetime (Ar83,Di82,Ma83b,Mc82,Mc85a).

Determination of the neutron exposure of a reactor pressure vessel and its support structures is best accomplished with a combination of calculation and measurement. To a certain extent, this measurement is achieved by the reactor vessel surveillance program now in place at most operating plants. However, these programs require relatively few (3 to 4) measurements over the plant lifetime; and, as such, they do not provide sufficient data to monitor the effects of various fuel management schemes on neutron exposure of the pressure vessel. Fuel management is one of the methods being considered to reduce this exposure (Ar83,Di82,Gu82,Gu82a,Mc82b,Nr82).

Evaluations of various fuel management schemes can be accomplished with neutron transport calculations. However, the complexity of the problem requires expensive calculations to achieve a satisfactory level of precision and accuracy. The effectiveness of the calculations can be greatly enhanced by providing measured values of neutron exposure to verify and calibrate the calculations (Mc81,Mc85a). Supplementary dosimetry in the reactor cavity is proving to be both beneficial and cost-effective to the safety evaluations of operating plants. In the extreme, a supplementary dosimetry program could provide cycle-to-cycle monitoring of the neutron exposure of a vessel and its support structures.

This section of the compendium report gives results of the re-analysis of dosimetry from 47 LWR surveillance capsules using the HEDL Reactor Dosimetry Center FERRET-SAND II adjustment code procedures and data that were first benchmark tested using differential and integral data from the "PCA Experiments and Blind Test" (Mc81,Mc84i). This re-analysis was a joint effort involving HEDL, NBS, Westinghouse, Babcock & Wilcox, Combustion Engineering, General Electric, South West Research Institute, Battelle Memorial Institute, EPRI and its contractors, and select US Utilities. The work is being accomplished in support of the preparation of the new series of ASTM Committee E10 standards for Light Water Reactor Pressure Vessel Surveillance (As82). These data are urgently needed for 1) verification of the accuracy of LWR power plant final safety analysis reports (FSAR) current and end-of-life projections of changes in the fracture toughness and embrittlement conditions of pressure vessel and support structure steels and 2) establishment of improved trend curves of the shifts in the initial reference nil-ductility temperature and upper-shelf energy versus fluence and dpa derived from test reactor and power reactor surveillance programs (Gr84,Gu80,Gu81,Gu81a,Gu82b, Gu82c,Gu83,Gu83a,Gu83b,Gu83c,Gu84,Gu84a,Gu84c,Gu84d,Gu84e,Gu85,Gu85a,Ma83b, Pe84,Ra79,Ra81b,Ra82a,Ra83,Ra84,Re77,St82a,St82c,St82d,St82e,St84,St84b,Ta82, Va79,Va81,Va82,Va83). The ASTM E706 Master Matrix Standard (As82) provides more detailed information on the status of the preparation of the new ASTM physics-dosimetry-metallurgy-related standards.

4.1 DATA ANALYSIS METHODS

This section provides detailed background and reference information on: 1) dosimetry sensors and their energy response; 2) benchmarking; 3) analysis methods, procedures, and data; 4) reactor surveillance capsule analysis procedures and results; and 5) reactor cavity analysis procedures and results.

This information is provided to help understand the basis and justification for the acceptance of the derived exposure parameter values and uncertainties given in Sections 4.2 through 4.5.

4.1.1 Examination of Individual Detector Responses Using National Bureau of Standards Procedures

Neutron exposure parameters obtained from surveillance capsule measurements depend entirely upon the measurement of neutron reaction rates in a small number of dosimeter types, which until recently have been of the activation type (As82,Gr81,Gr82,Gr83,Mc82a). All of these dosimeters are integral detectors and, as such, do not directly provide neutron exposure parameters. The exposure must be derived from observed reaction rates and a neutron energy spectrum at the surveillance capsule position. The spectrum, generally obtained from a neutron transport calculation, acts as an interpolation function for the otherwise isolated dosimeter results. Some insight regarding the derivation of exposure parameters and associated error bounds can be obtained by deriving exposure parameters from individual detector results. A typical examination procedure will be described in this section and applied to one set of radiometric dosimeters and in-vessel surveillance capsule data, that of a Westinghouse 2-Loop Plant, designated here as West2LP (Si82).

Five threshold detectors and one low-energy detector were employed in the measurement, and a neutron transport calculation of the spectrum was provided in 20 energy groups. A generic set of detector activation rates, the associated spectral indexes, and a comparison with calculation are given in Table 4.1.1.1. The activation rates are typical of those obtained from a surveillance capsule that has been removed after one effective-full-power-year of the plant operation (Mc82a).

Three detector responses parameters, each of which is spectrum-dependent, are essential for this analysis. They are:

- Energy Response Threshold, E_{95} -- Neutron energy above which 95% of the detector response occurs.
- Spectrum Fraction, $\Psi(>E_{95})$ -- Fraction of the neutron spectrum that is above the energy response threshold. (All spectra are assumed normalized to unity for $0.4\ \text{eV} < E < 10\ \text{MeV}$.)
- E_{95}-Truncated Cross Section, $\sigma(>E_{95})$ -- Reaction cross section truncated at E_{95}. [By definition the conventional full-spectrum cross section, $\sigma(>0.4\ \text{eV})$ is equal to $\sigma(>E_{95}) \times \Psi(>E_{95}) \div 0.95$.]

Values of these response parameters for the West2LP spectra and for the ^{235}U fission spectrum are given in Table 4.1.1.2. Also included is the median response energy above which 1/2 of the detector response occurs. All of these parameters have been generated with the NBS DETAN code that interpolates the 20-group transport code spectrum into 620 groups and then performs the necessary integrations using ENDF/BV dosimetry cross sections. For this particular calculated spectrum, which has only two groups above 6 MeV, the code attaches a ^{235}U fission spectrum tail.

TABLE 4.1.1.1

SURVEILLANCE CAPSULE DETECTOR REACTION RATES AND COMPARISON WITH CALCULATION

Detectors	Activation Rate (R/NG) (dps/nucl)	Spectral Index, S (α/28) Meas	Calc/Meas
^{237}Np(n,f)	4.26 E-13	9.88	0.934
^{238}U(n,f)	4.31 E-14	1.000	---
^{58}Ni(n,p)	9.52 E-15	0.221	1.05
^{54}Fe(n,p)	7.67 E-15	0.178	0.961
^{63}Cu(n,α)	6.43 E-17	0.00149	0.965
^{59}Co(n,γ)	3.92 E-12	91	(0.90)

TABLE 4.1.1.2

DETECTOR RESPONSE PARAMETERS

Detector	Response Range: Threshold E_{95} (MeV)	Response Range: Median E_{50} (MeV)	Truncated Cross-Section $\sigma(>E_{95})$ [barn]	Spectrum Fraction $\Psi(>E_{95})$
Spectrum: Westinghouse 2-Loop Plant (West2LP)				
^{237}Np(n,f)	0.24	1.1	0.950	0.347
^{238}U(n,f)	1.3	2.1	0.442	0.0810
^{58}Ni(n,p)	1.66	3.9	0.1584	0.05262
^{54}Fe(n,p)	2.1	4.1	0.1785	0.0342
^{63}Cu(n,α)	5.0	7.5	0.01011	0.00505
^{59}Co(n,γ)	0.4 eV	0.129 keV	2.98	1.0
Spectrum: ^{235}U Fission Neutrons (NBS Evaluation)				
^{237}Np(n,f)	0.67	2.0	1.578	0.796
^{238}U(n,f)	1.5	2.7	0.532	0.527
^{58}Ni(n,p)	2.1	4.1	0.265	0.362
^{54}Fe(n,p)	2.3	4.2	0.233	0.317
^{63}Cu(n,α)	4.7	7.3	0.00780	0.0658

Full-spectrum cross section: $\sigma(>0.4\ \text{eV}) = \Psi(>E_{95}) \times \sigma(>E_{95})/0.95$

Three neutron exposure parameters will be derived: 1) neutron fluence above 1 MeV; 2) neutron fluence above 0.1 MeV; and 3) dpa, the atom displacement probability based upon the atom displacement cross section given in ASTM Standard E693-79. Each detector result, with the aid of the calculated spectrum, may be used to derive an experimental value for the three exposure parameters. The quality of this set of values depends upon the following characteristics of the detectors in addition to specific errors of the experiment:

- Cross-Section Accuracy -- A matter of both the shape and the scale of the reaction cross section.
- Spectral Index Match -- The extent to which the calculated and observed spectral indexes agree.
- Energy Response Overlap -- The energy-response overlap of a detector with the one of next higher threshold. This response separation of two detectors is described by the "Non-overlap Interval," defined as the energy interval between thresholds (E_{95}) for the two detectors (see Table 4.1.1.2).
- Spectrum Coverage (SC) Factor -- Fraction of a given exposure parameter to which a detector is sensitive. For truncated fluence parameters, a spectral coverage factor is defined in percent as the spectrum fraction for the detector, $\Psi(>E_{95})$, divided by the spectrum fraction of the fluence parameter, i.e., $\Psi(>1\text{ MeV}) = 0.118$, and $\Psi(>0.1\text{ MeV}) = 0.446$ for West2LP.

$$SC = \int_{E_{95}}^{\infty} K(E)\,\phi(E)dE \Big/ \int_{0.4\text{ eV}}^{\infty} K(E)\,\phi(E)dE$$

where K(E) = Energy dependence of the exposure parameter.

Spectrum coverage is the most important detector response feature for this analysis because it provides a weighting scheme for averaging the set of exposure parameters from the individual detectors. Such a weighted average represents an implicit adjustment for any mismatch of observed and calculated spectral indexes.

The necessary tools for analyzing the individual detector results are now in hand. The analysis begins with a detector reaction rates, designated R/NG. It is equal to the product of the full-spectrum cross section, σ, and neutron fluence, $(nvt)_0$:

$$R/NG = \sigma \cdot (nvt)_0$$

The fluence exposure parameters, then, are given by

Fluence Above 1 MeV:

$$[\Psi\ (>1\ \text{MeV})\cdot(nvt)_o] = \frac{R}{NG}\cdot\frac{0.95}{\sigma(>E_{95})}\cdot\frac{\Psi\ (>1\ \text{MeV})}{\Psi\ (>E_{95})}$$

Fluence Above 0.1 MeV:

$$[\Psi\ (>0.1\ \text{MeV})\cdot(nvt)_o] = \frac{R}{NG}\cdot\frac{0.95}{\sigma(>E_{95})}\cdot\frac{\Psi\ (>0.1\ \text{MeV})}{\Psi\ (>E_{95})}$$

Displaced Atom Fraction:

$$\text{dpa} \equiv \sigma_d\cdot(nvt)_o = \sigma_d\cdot\frac{R}{NG}\cdot\frac{0.95}{\sigma(>E_{95})\ \Psi\ (>E_{95})}$$

where:

$\sigma = \sigma(>E_{95})\ \Psi\ (>E_{95})/0.95$

$(nvt)_o$ = Total fluence above 0.4 eV for T = 1 second

= 1.193×10^{12} n/cm^2

$$\left.\begin{aligned}\Psi(>1\ \text{MeV}) &= 0.118\\ \Psi(>0.1\ \text{MeV}) &= 0.118\\ \sigma_d &= 208\ \text{b}\end{aligned}\right\}\quad \text{From West2LP calculation}$$

4.1.1.1 Exposure Parameters from Individual Detectors
(All results are given as fluence for a one-second exposure.)

Fission Detector: Uranium-238: The truncated fluences are obtained with the expression just given and detector response parameters from Table 4.1.1.2 and reaction rates from Table 4.1.1.1.

	>1 MeV	>0.1 MeV
Spectrum Coverage Factor:	69%	18%
R/NG = 4.31 E-14		
$\sigma(>E_{95})$ = 0.442 b		
Fluence (n/cm^2):	1.34 E+11	5.1 E+11

For an ideal threshold detector with a step-function response and E_{95} = 1 MeV, the coverage factor would be unity for any spectrum shape. The derived fluence on such a case would not depend upon the result of transport calculation. For uranium in the West2LP spectrum, the coverage factor for the fluence above 1 MeV is 0.081/0.118 or 69%, which may be compared to a uranium coverage factor of 75% for the fission spectrum, the driving source for the neutron flux. The contribution of the calculation, then, is to provide the change in coverage factor from its fission spectrum value to the West2LP spectrum value. Since the coverage factor in the fission spectrum is known to within a few percent, it is the 9% shift, which the calculation must supply, that is the focus of the error estimate.

Analogously, the truncated cross section of 0.44 barns in Table 4.1.1.2 may be compared with corresponding values in the fission spectrum and with other standard neutron fields that serve neutron dosimetry. Results for the fission spectrum and the ISNF Standard Neutron Field from the NBS Compendium of Benchmark Neutron Fields for Reactor Dosimetry are as follows:

		$\sigma(>E_{95})$	
	E_{95} (MeV)	Calc	Calc/Meas
Fission Spectrum	1.5	0.53	0.960 ± 2.2%
ISNF	1.4	0.51	0.950 ± 3.1%
West2LP	1.3	0.44	

Again, the purpose of the transport calculation is to establish the shift in truncated cross sections from 0.53 b in the fission spectrum to 0.44 b in the surveillance capsule. The shift is 17% with an estimated error bound of no more than ±6% (i.e., 17% ± 6%), based on the agreement of measured and calculated spectral indexes shown in the last column of Table 4.1.1.1 and on the generic analysis of errors to be found in (Gr83) (see next section). The dpa exposure is obtained with parameters from Tables 4.1.1.1 and 4.1.1.2 and the dpa cross section, σ_d = 208 b:

$$\text{dpa} = 208 \cdot (4.31\ \text{E-14}) \cdot \frac{0.95}{0.442\ (0.081)} = 2.38\ \text{E-10}$$

The equivalent of the spectrum coverage factor in this case is the spectrum fraction for the spectrum shape weighted by the dpa cross section. For the uranium detector, the dpa coverage factor is 37%. Clearly, the calculation is more important for establishing the dpa exposure than it is for fluence above 1 MeV. This reflects the sensitivity of the dpa exposure unit to sub-MeV portions of the spectrum.

Fission Detector: Neptunium -- The truncated fluence and dpa are obtained in the same manner as with the uranium fission detector:

	Fluence >1 MeV	Fluence >0.1 MeV	dpa
Spectrum Coverage Factor	>100%	78%	68%
Value	1.45 E+11	5.5 E+11	2.55 E-10

The neptunium detector, with a threshold lower than uranium, samples all the fluence above 1 MeV and even provides respectable coverage for the dpa exposure parameter. The coverage factor of 78% for the fluence above 0.1 MeV is down to ~0.6 of its fission spectrum value, indicating that reliance upon calculation is still important though not to the extent required for the uranium detector where the coverage factor is one third of its fission spectrum value.

Truncated cross sections for this detector in the fission spectrum and in ISNF show good agreement between measurement and calculation.

		$\sigma(>E95)$	
	E_{95} (MeV)	Calc	Calc/Meas
Fission Spectrum	0.67	1.58	0.990 ± 2.1%
ISNF	0.53	1.46	0.969 ± 3.0%
West2LP	0.24	0.950	

The shift in truncated cross section from the fission spectrum to the West2LP spectrum is 40%. It is estimated that this shift is known to one sixth of its value (~7%) as an upper bound of error. This estimate is guided by the generic analysis of (As82) and by the agreement of measured and calculated spectral indexes shown in Table 4.1.1.1. The worst discrepancy there is about 12% for the Np/Ni index.

Higher-Energy Threshold Detectors: ^{58}Ni(n,p), ^{54}Fe(n,p), ^{63}Cu(n,α) -- Exposure parameters derived from these three threshold detectors, which sample successively higher portions of the spectrum, are given in Table 4.1.1.3 along with their correspondng spectrum coverage factors. The detectors give rather consistent results, including the copper detector that samples only about one tenth as much of the spectrum as does the nickel detector. The 10% discrepancy between the nickel and iron results is notable because of their large energy-response overlap.

89

TABLE 4.1.1.3

SURVEILLANCE CAPSULE NEUTRON EXPOSURE PARAMETERS FROM INDIVIDUAL DETECTORS (1-SECOND EXPOSURE)

Detector	E_{95} (MeV)	Fluence > 1 MeV		Fluence > 0.1 MeV		dpa/s	
		Spectrum Coverage (%)	Value (x 10^{11} n/cm^2)	Spectrum Coverage (%)	Value (x 10^{11} n/cm^2)	Spectrum Coverage (%)	Value (x 10^{-10})
^{237}Np(n,f)	0.24	>100	1.45	78	5.48	86	2.55
^{238}U(n,f)	1.3	69	1.35	18	5.10	39	2.38
^{58}Ni(n,p)	1.66	45	1.28	11.8	4.84	30	2.26
^{54}Fe(n,p)	2.1	29	1.41	7.7	5.32	25	2.48
^{63}Cu(n,α)	5.0	4.3	1.41	1.1	5.34	4.8	2.48
Average Values							
Equal Weight*:			1.38 ± 0.07		5.22 ± 0.25		2.43 ± 0.11
Weighted by Spectrum Coverage Factor:			1.38		5.34		2.46

---

*Includes standard deviation of the mean for the five values given.

The shifts in coverage factor from the fission spectrum for fluence >1 MeV are:

Fission Spectrum	Ni	Fe	Cu
Spectrum Coverage Ratio: $\left[\frac{\text{West2LP}}{\text{fiss spec}}\right]$	0.87	0.64	0.46

The truncated cross sections in the fission spectrum are as follows:

Fission Spectrum	Ni	Fe	Cu
Calculated:	0.265	0.233	0.0078
Calculated/Measured:	0.93 ± 3.8%	0.97 ± 4.5%	0.93 ± 7.8%

Measurement and calculation (i.e, using ENDF/BV cross sections and the NBS evaluated fission spectrum) disagree by less than 10% but are notably close to 10% for nickel. These discrepancies must be entered as an error with full weight since the West2LP measurement was not calibrated in a fission spectrum. [If it had been so calibrated, it is possible that the Ni/Np disagreement in Table 4.1.1.1 (i.e., 0.934 vs 1.05) would be half again as large and at the same time less ambiguous.]

The calculated shape changes in the high-energy component of the West2LP spectrum results in truncated cross-section shifts of up to 40%. Error bounds are set at one fifth of the calculated shift based on the spectral index measurement results and the generic analysis of (Gr83).

Average Values of Exposure Parameters -- The exposure parameters from individual detectors can be averaged to give final recommended values. For equal weighting the five detectors give average values with a standard deviation (1 σ) of near ±4% (see Table 4.1.1.3). A more appropriate set of average values are those for which the detector results are weighted by the corresponding spectrum coverage factor. Results are as follows:

Fluence >1 MeV: $(1.38 \pm 0.18) \times 10^{11}$ n/cm^2
Fluence >0.1 MeV: $(5.34 \pm 0.9) \times 10^{11}$ n/cm^2
dpa: $(2.46 \pm 0.4) \times 10^{-10}$

and they are the recommended exposure parameters with (1 σ) uncertainties from this single-detector analysis without spectrum adjustment. The uncertainty assignments, which do not include errors in measured reaction rates since they were not available for this analysis, are discussed and estimated in the next section.

4.1.1.2 Consideration of Errors

Activation detectors do not measure neutron fluence directly, and sources of error are numerous. On the side of reaction rate measurement, there are errors associated with gamma counting (e.g., photopeak integration, coincidence corrections, and competing activations), with gamma detection efficiencies (e.g., interpolation of efficiency curves, detector distance), and with reaction parameters (e.g., decay constants, branching ratios, fission yields). Additional discussion of these matters, including the value of performing detector calibrations in standard neutron fields to reduce errors (the so-called neutron fluence transfer procedure) can be found in (Gr83). The estimate of reaction rate measurement errors is not a part of this exercise since they were not available. In a properly benchmarked measurement, they would be small compared to the cross-section and spectrum calculation uncertainties considered in this exercise.

Errors in truncated cross sections and spectrum coverage factors are associated with the accuracy of each detector cross section (both its scale and its energy dependence), and that of the spectrum calculation. The cross-section scale error, and to a lesser extend the shape error, for a cross section can be judged from C/E ratios in standard neutron fields. Regarding the more important influence of the spectrum calculation, one way to proceed is to set up a few-group descriptions of the spectrum and of the detector cross sections (e.g., less than six above 1 MeV) and to examine changes in spectrum-averaged cross sections associated with credibly large cross-section and spectrum errors assigned to each energy group. The choice of "credibly large" is guided by the agreement of observed spectral indexes with calculation (i.e., Table 4.1.1.1) and by an error band that encompasses the spread of the cross-section data used for the ENDF/BV dosimetry file evaluation. This ad hoc procedure has been carried out for a pressure vessel cavity spectrum in (Gr83). The results (obtained as 2σ error bounds) may be summarized as follows:

- Cross-section shape errors of between 10% and 40% contribute less than 2% to the error in the shift of the truncated cross section from its fission spectrum value. (Copper is an exception with an error contribution of 26%.)
- Spectrum errors (taken as the larger of 5% or 1/3 of the departure of each group flux from its fission spectrum value) contribute between 7% and 14% to the error in the shift of the truncated cross sections from their fission spectrum value. (Again, copper is an exception with an error contributions of 27%.)
- Spectrum errors as above contribute between 9% and 24% to errors in spectrum coverage factors.

In (Gr83) the agreement between measured and calculated spectral indexes is not worse than 7%. Using detector non-overlap intervals as a spectrum adjustment indicator, it is estimated that this agreement is consistent with

92

a spectrum error of about 1/5 (rather than 1/3) of the departure from fission spectrum; and this conclusion is made without benefit of a Np detector response. In the present study of West2LP, the agreement with calculation of the spectral indexes is about the same as in (Gr83) but, in addition, the crucial Np response was obtained and it agrees with calculation to within 7% (see Table 4.1.1.1).

Taking all this into account, an inventory of errors sources and error ranges within which individual detector errors are estimated to fall is as follows:

	2 σ Error Bounds (%)		
	Fluence >1 MeV	Fluence >0.1 MeV	dpa
Measured Reaction Rates: (gamma counting, detection eff., reaction parameters, perturbations)	(not available for this analysis)		
Truncated Cross Sections:	6 - 8	6 - 8	6 - 8
Spectrum Coverage Factor: (copper excluded)	5 - 10	10 - 15	10 - 15
Total:	8 - 13	12 - 17	12 - 17

The range of errors shown represents primarily the differing match of the detectors response to the fission spectrum, to the West2LP spectrum, and to the characteristics of the exposure parameter. The final composite error bound for average values will be somewhere between the limits of the total error. In lieu of some additional examination of the West2LP calculated spectrum and its relation to deep-penetration spectra in water and iron, it is reasonable to choose the high end of the error range. It is this error that is assigned to the recommended exposure parameters listed at the end of Section 4.1.1.

Clearly, this error assessment, though complete, is imprecise. It is simply an ad hoc procedure that puts forth all the error sources (i.e., truncated cross sections and spectrum coverage factors) appropriate for estimating the error enhancement in a neutron field measurement that is tied to a calculation (i.e., West21P) of unknown accuracy relative to errors in measurements and detector response data associated with a standard neutron field (i.e., the fission spectrum). Nevertheless, if the C/E ratios of Table 4.1.1.1 were confirmed by standard neutron field calibration, and if the errors in the measured reaction rate were known to be small, it would be difficult to show that the errors estimated above could be half again as large.

4.1.2 HEDL National Reactor Dosimetry Center Procedures

4.1.2.1 Introduction

As part of the process of determining the neutron flux-spectra, exposure and their accuracies, analytical studies are performed with the FERRET and SAND-II codes (Mc67,Sc79). The FERRET code compares integral measurements and calculated group fluxes, using covariance information. At this time, the SAND-II code has been used primarily to process data that was input to the FERRET code.

4.1.2.2 Description of the FERRET-SAND II Analysis and Input Data

The FERRET code uses both integral and differential data to adjust a priori fluxes ϕ_0, which are typically obtained from calculations. A lognormal least-squares algorithm weights both the a priori values and the measured data in accordance with assigned uncertainties and correlations. In general, the measured values f are linearly related to the flux ϕ by some response matrix A:

$$f_i^{(s,\alpha)} = \sum_g A_{ig}^{(s)} \phi_g^{(\alpha)} \tag{1}$$

where i indexes the measured values belonging to a single data set s, g designates the energy group, and α delineates separate spectra that may be simultaneously adjusted. For example,

$$R_i = \sum_g \sigma_{ig} \phi_g \tag{2}$$

relates a set of measured reaction rates R_i to a single spectrum ϕ_g by the multigroup cross sections σ_{ig}. (In this case, FERRET also adjusts the cross sections.) Differential flux measurements have the particularly simple response, $A_{gg'} = \delta_{gg'}$, where $\delta_{gg'}$ is the Kronecker delta. The lognormal approach automatically accounts for the physical constraint of positive fluxes, even with large assigned uncertainties.

For the analysis of dosimetry data, the continuous quantities (i.e., fluxes and cross sections) were approximated in 53 groups. The group structure is given in Table 4.1.2.1. The calculated flux-spectra were expanded or contracted into this group structure using the SAND II code. This procedure is carried out by first expanding the spectrum into the SAND II 620-group structure using a SPLINE interpolation procedure for interpolation in

TABLE 4.1.2.1

NEUTRON ENERGY GROUP STRUCTURE

	Group Upper Bound (UB) (MeV)
1	.16905+002
2	.14918+002
3	.13499+002
4	.11618+002
5	.10000+002
6	.86071+001
7	.74082+001
8	.60653+001
9	.49659+001
10	.36788+001
11	.28650+001
12	.22313+001
13	.17377+001
14	.13534+001
15	.11080+001
16	.82085+000
17	.63928+000
18	.49787+000
19	.38774+000
20	.30197+000
21	.18316+000
22	.11109+000
23	.67379-001
24	.40868-001
25	.25540-001
26	.19890-001
27	.15034-001
28	.91188-002
29	.55308-002
30	.33546-002
31	.28395-002
32	.24038-002
33	.20347-002
34	.12341-002
35	.74852-003
36	.45400-003
37	.27536-003
38	.16702-003
39	.10130-003
40	.61442-004
41	.37267-004
42	.22603-004
43	.13710-004
44	.83153-005
45	.50435-005
46	.30590-005
47	.18554-005
48	.11254-005
49	.68256-006
50	.41399-006
51	.25110-006
52	.15230-006
53	.92370-007
E_{LB}	10000-009*

---

*Group 53 Lower Bound (LB)

regions where group boundaries do not coincide. The high end of the spectrum is extrapolated using a fission spectrum form. The 620-point spectrum is then easily collapsed to 53 groups. This procedure is, in some cases, sensitive to differences in group boundaries; and energy groups must be chosen to minimize variations in results. For the present work, the boundary effects were ignored.

The cross sections were also collapsed into the 53 energy-group structure using SAND II with calculated spectra (as expanded to 620 groups) as weighting functions. The cross sections were taken from the ENDF/B-V dosimetry file. Uncertainty estimates and 53 x 53 covariance matrices were constructed for each cross section. Correlations between cross sections were neglected due to data and code limitations, but are expected to be unimportant.

For each set of data or a priori values, the inverse of the corresponding relative covariance matrix M is used as a statistical weight. In some cases, as for the cross sections, a multigroup covariance matrix is used. More often, a simple parameterized form is used:

$$M_{gg'} = R_N^2 + R_g R_{g'} \rho_{gg'}$$

where R_N specifies an overall fractional normalization uncertainty (i.e., complete correlation) for the corresponding set of values. The fractional uncertainties R_g specify additional random uncertainties for group g that are correlated with a correlation matrix:

$$\rho_{gg'} = (1 - \theta)\, \delta_{gg'} + \theta \exp \left(- \frac{(g - g')^2}{2\gamma^2} \right)$$

The first term specifies purely random uncertainties while the second term describes short-range correlations over a range γ (θ specifies the strength of the latter term).

For the a priori calculated fluxes, a short-range correlation of $\gamma = 6$ groups was used. This choice implies that neighboring groups are strongly correlated. Strong long-range correlations (or anticorrelations) were justified based on information presented by R. A. Maerker (St82). Maerker's results are closely duplicated when $\gamma = 6$. For the integral reaction rate covariances, simple normalization and random uncertainties were combined as deduced from experimental uncertainties. Specific assignments of uncertainty values were made, as described in the following sections.

4.1.2.3 Calculated Flux-Spectral Data

The FERRET adjusted spectra were found to be only slightly dependent on the input calculated spectra. No estimates on calculational uncertainties and covariances were supplied in the surveillance reports. Therefore reasonable assumptions about these uncertainties were made for input to the FERRET code. The calculated spectra were assumed to have a normalization uncertainty of 100%. This estimate was assumed so that the reaction ratio would estabish the flux magnitude. The value of group uncertainties was chosen to be 50% for all groups correlated as detailed in Table 4.1.2.2.

4.1.2.4 Cross-Section Data

The cross-section uncertainties and errors associated with the ENDF-V and other values are included in the cross-section covariance matrices. The uncertainties and errors reflected in these matrices appear to be conservative.

Intercorrelations between sets of data (i.e., between spectra at different positions, etc.) are not included in the FERRET analysis at this time. These neglected correlations are not expected to significantly affect the adjusted flux-spectra.

4.1.2.5 Comparison of FERRET-SAND II Analysis and Individual Detectors

In Section 4.1.1 the NBS method of examining individual detector responses was used to predict the flux for a generic two-loop Westinghouse pressurized water reactor. That method did not include uncertainties in the measured reaction rates because explicit estimates were not available. For comparison with the NBS results, the FERRET code exposure parameter derived values used a generic set of estimated certainties. Using the same reactions from Table 4.1.1.1 and the reaction rate standard deviations from (Si82a), multiple-foil adjusted values of flux-spectrum were determined with the FERRET code. Results are shown in Table 4.1.2.3 along with results derived from single-foil response analysis. In general, the two methods yield similar results.

TABLE 4.1.2.2

FERRET INPUT UNCERTAINTIES AND CORRELATION PARAMETER VALUES*

Data Set	Normalization Uncertainty R_N	Random Uncertainty R_g	Correlation Strength θ	Correlation Width γ
Calculated Flux				
$E = 10^{-10}$ - 18 MeV	1.00	0.50	0.8	6.0
Cross Sections				
(Input as full covariance matrix)				
Reaction Rates				
(Values were taken from Sections 4.2.)				

Correlation Matrix Format

$$M_{ij} = (R_N)^2 + (R_g)_i \cdot (R_g)_j \cdot P_{ij}$$

$$P_{ij} = (1 - \theta) \cdot \delta_{ij} + \theta \cdot \exp\left[-(i - j)^2/2\gamma^2\right]$$

(i and j denote energy groups)

---

*Uncertainty expressed as a fraction (e.g., 0.25 = 25%).

TABLE 4.1.2.3

COMPARISON OF SURVEILLANCE CAPSULE MULTIPLE- AND SINGLE-FOIL INTEGRAL FLUX/s AND dpa/s

Integral Value	Multiple-Foil	Single-Foil
Flux, E > 0.1 MeV (n/cm^2-s)	$(5.6 \pm 0.85) \times 10^{11}$	$(5.34 \pm 0.9) \times 10^{11}$
Flux, E > 1.0 MeV (n/cm^2-s)	$(1.44 \pm 0.13) \times 10^{11}$	$(1.38 \pm 0.18) \times 10^{11}$
dpa/s	$(2.53 \pm 0.25) \times 10^{-10}$	$(2.46 \pm 0.4) \times 10^{-10}$

4.1.3 REACTOR SURVEILLANCE CAPSULE ANALYSIS PROCEDURES AND RESULTS

4.1.3.1 Introduction

The basic analysis method used in this work is the adjustment of the a priori calculated neutron spectrum by a generalized least-squares analysis method using measured reaction rates. The FERRET computer code (Sc79) is used in this work. The SAND II code (Be67b) has been used primarily to process data that were input to the FERRET code (Mc81). The main focus of the present analysis effort is to determine the correct reaction rates and their uncertainties. This involves evaluation of the power-time history, corrections for dosimeter position, corrections for competing reactions due to impurities, and the initiation of necessary HEDL and NBS overchecks on measured reaction rates and isotopic mass assay of dosimeters (Mc82). As a result of the "PCA Experiments and Blind Test" studies, the limiting accuracy of the FERRET-SAND (or any other such code system) derived values of exposure parameters (flux-fluence greater than 1 MeV and dpa) is estimated to be in the range of ±5% to 15% (1σ) (Mc81,Mc84i).

4.1.3.2 Analysis Procedure

The effective time at full power and the extrapolation of reaction rates at the time of shutdown to the reaction rates at full power were determined from the power history for each reactor and the TIMWH computer code (Bo70). The decay constants (λ) currently used by the HEDL Reactor Dosimetry Center were used in this analysis (Li75) and are tabulated in Table 4.1.2.1 along with K factors used to convert the reaction rate data from dps/mg of target material to dps/nucleus. Saturated reaction rates reported in the surveillance reports and the rates found in this work differed at most by 1% to 2%. This was generally attributed to slight differences in the decay constants used. The power-time history analysis assumes a constant flux level per megawatt of power. For most capsules, this is a fair assumption. However, in some cases, reaction rate variations of 10% to 20% were noted due to differences in fuel loading for each fuel cycle. In these circumstances long half-lived dosimeters integrate over the irradiation period to give the average effective flux level, while short half-lived dosimeters are sensitive to the flux level at the end of the irradiation.

Fission yield and nuclear cross-section data (Table 4.1.3.1) used in this work were based on the ENDF/B-V data file. The cross-section covariance files were based on the ENDF/B-V data for most cross sections (Pe77). However, some are due to recent HEDL evaluations by Schmittroth, Schenter, and Mann.

TABLE 4.1.3.1

NUCLEAR DATA USED TO ANALYZE REACTION RATE DATA

Reaction Name	λ (s^{-1})	Fission Yield	K Factor (x 10^{19})
Fe54(n,p)Mn54	2.566-008	---	1.588+001
Ni58(n,p)Co58	1.126-007	---	1.436+000
Cu63(n,α)Co60	4.170-009	---	1.527+000
Ti46(n,p)Ti46	9.568-008	---	9.955+000
Co59(n,γ)Co60	4.170-009	---	9.786+001
Fe58(n,q)Fe59	1.799-007	---	2.810+002
U238(n,f)Cs137	7.279-010	6.000-002	3.953+000
U238(n,f)Zr95	1.246-007	5.105-002	3.953+000
U238(n,f)Ru103	2.035-007	6.229-002	3.953+000
U238(n,f)Ce141	2.468-007	5.456-002	3.953+000
U238(n,f)Ru106	2.180-008	2.513-002	3.953+000
U238(n,f)Ce144	2.821-008	4.543-002	3.953+000
Np237(n,f)Cs137	7.279-010	6.267-002	3.936+000
Np237(n,f)Zr95	1.246-007	5.699-002	3.936+000
Np237(n,f)Ru103	2.035-007	5.584-002	3.936+000
Np237(n,f)Ce141	2.468-007	5.439-002	3.936+000
Np237(n,f)Ru106	2.180-008	2.240-002	3.936+000
Np237(n,f)Ce144	2.821-008	4.198-002	3.936+000

The reader is referred to Sections 1.0, 2.0, 3.0, and 5.0 for more detailed information on 1) specific types of LWR power plants and gross features, 2) existing physics-dosimetry surveillance programs, 3) evolution of surveillance data processing, and 4) extrapolation and interpolation techniques as well as the determination and verification of peak fluxes, fluences, dpa, and lead factors with their associated uncertainties, including perturbation treatments, respectively.

Significant geometry corrections were necessary in the Westinghouse and Babcock & Wilcox (B&W) capsules in order to determine the reaction rate at the center of the surveillance capsule. For Westinghouse plants these corrections were in the 0% to 20% range. No corrections were necessary for the fission foils located at the capsule center. Westinghouse transport calculations show about a 10% variation in flux from the top to the bottom of the capsule. This could introduce a maximum bias in the fluence for any particular metallurgical specimen of about ±5%. The determination of the charpy transition temperature shift is not expected to be sensitive to this level of flux difference. For B&W plants the front and rear dosimeters were logarithmically averaged to account for flux gradients. This value was then linearly averaged with the side dosimeters.

Corrections for impurity fissile atoms were found to be significant in some cases. In all cases, cadmium covers were used to reduce competing reactions. Babcock & Wilcox indicate < 375 appm ^{235}U impurity in their ^{238}U dosimeters. For old capsules located adjacent to the vessel wall this amounts to < 3.4% correction for ^{235}U fission. The Westinghouse ^{238}U dosimeters have 320 appm ^{235}U. This level of impurity in the accelerated capsules requires about a 9% correction for ^{235}U fission in two-loop shield plants. For Combustion Engineering ^{238}U dosimeters, the impurity level is about 400 appm. This requires about a 9% correction for both wall capsules and accelerated surveillance capsules. Preliminary results of HEDL overchecks on the purity and/or isotopic content of a number of the Point Beach 2 Capsule R dosimeters are discussed in Ref. (Mc82). Good agreement was found between HEDL and ORNL results for the ^{238}U dosimetry material.

Burnin of ^{239}Pu in the high-fluence accelerated surveillance location was found to contribute up to 29% to the measured fission rate. For low fluxes ($< 10^{13}$ n/cm^2·s, E > 1 MeV) and irradiation times on the order of a year or longer, the ^{239}Pu contribution to the reaction rate can accurately be approximated by a second-order function of flux. The corrected fission rate (R^F_{238}) is then given by:

$$R^F_{238} = R^F_{meas}\left(1 + N_{235}\,\frac{Y_{235}}{Y_{238}}\,\frac{\sigma^f_{235}}{\sigma^f_{238}} + \frac{1}{2}\,\bar{S}\,\sigma^Y_{238}\,\frac{\sigma^f_{239}}{\sigma^f_{238}}\,\frac{Y_{239}}{Y_{238}}\,\phi t\right)^{-1}$$

where the subscripts 235, 238, and 239 refer to the isotopes ^{235}U, ^{238}U, and ^{239}Pu, the superscripts f and γ refer to (n,f) and (n,γ) reactions, σ is an infinitely dilute spectrum-averaged cross section (using 40-mil cadmium covers), ^{235}N is the initial atomic fraction of ^{235}U, ϕ is the total neutron flux (E > 0 MeV) at full power, t is the effective full power irradiation time, Y is the fission yield, and S is the average neutron self-shielding factor for the $^{238}U(n,\gamma)^{239}U$ reaction.

An estimate of S was obtained from simplified calculations. (A precise self-shielding correction for the ^{238}U dosimeter may be difficult to calculate because the density and geometry of individual dosimeters are not well known). Furthermore, it was necessary to assume an isotropic flux that is not entirely representive of the neutron environment outside the core and at the surveillance capsule location.

The self-shielding correction was determined by calculating the reduction in reaction rate in a slab of ^{238}U with reduced density equal to ρx (b^{-1} units), where ρ is the density of the material and x is the thickness of the slab. The flux was proportional to 1/E above the cadmium cutoff energy of 0.5 eV. The calculated self-shielding factor is represented by the equation:

$$f = \frac{1.0}{\sqrt{1.0 + 1.2 \times 10^4 \ (\rho x)}} \qquad \rho x < 3.65 \times 10^{-2} \ b^{-1}$$

$$f = 0.047 \qquad \rho x \geq 3.65 \times 10^{-2} \ b^{-1}$$

The latter value is the self-shielding factor for an infinitely thick slab. The self-shielding factor for the geometry of the dosimeter was determined by numerical integration:

$$\overline{S} = \frac{\sum_i f(\rho x_i) \ W_i}{\sum_i \ W_i}$$

where W_i is a slab of incremental volume for which the f factor was calculated.

Figure 4.1.3.1 shows the three geometries of the three types of dosimeters. The Westinghouse ^{238}U dosimeter is in the form of a U_3O_8 powder. The capsule is filled 1/4 to 1/3 full, sealed and irradiated on its side. It is assumed that the powder fills the bottom third of the cylinderical container as shown in Figure 4.1.3.1a. The Combustion Engineering dosimeters (Figure 4.1.3.1b) are in the form of a solid rectangular piece of pure ^{238}U. The Babcock & Wilcox dosimeter (Figure 4.1.3.1c) is in the form of a 50-mil

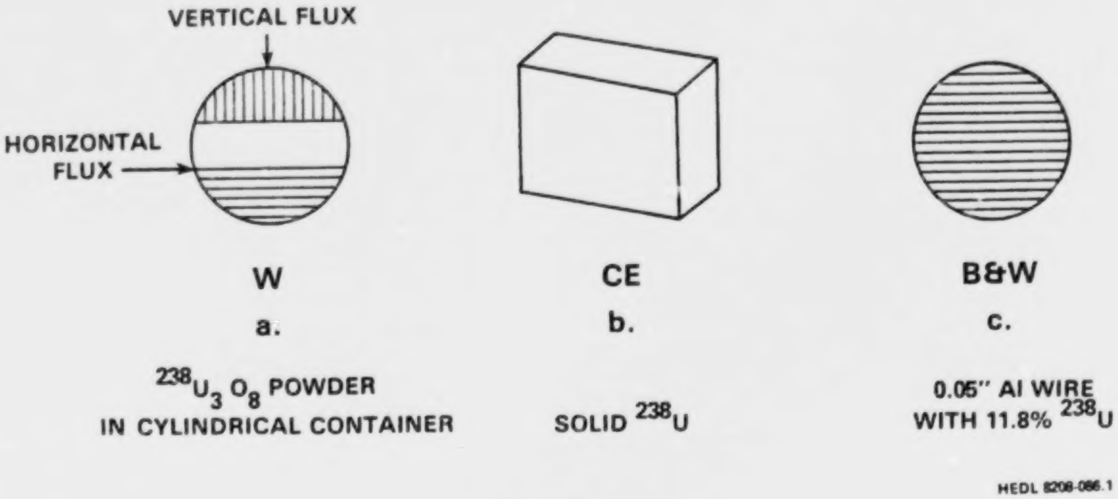
VERTICAL FLUX
HORIZONTAL FLUX
W
a.
$^{238}U_3O_8$ POWDER IN CYLINDRICAL CONTAINER
CE
b.
SOLID ^{238}U
B&W
c.
0.05" Al WIRE WITH 11.8% ^{238}U
HEDL 8208-086.1

FIGURE 4.1.3.1. Geometries of U Dosimeters.

diameter wire of 11.8% ^{238}U alloyed in aluminum. For the Westinghouse dosimeter, two flux orientations were assumed: 1) vertical and 2) horizontal. The two S values were then averaged using projected areas with normals parallel to the incident flux direction as the weighting values. Similarly, the S value for the Combustion Engineering dosimeter was the average value using the surface area of each side as the weighting value. The results of S values averaged over the dosimeters are shown in Table 4.1.3.2.

Figure 4.1.3.2 shows the measured ^{238}U fission rate as a function of fluence (E > 1 MeV) for eight Westinghouse surveillance capsules from similar two-loop plants. The dashed curve is the calculated fission rate with Pu buildup and 320 appm ^{235}U for operation at full power, and with S set equal to 1.00.

The similarity between the slope of the calculated and measured data is apparent. The lower two points are from the R. E. Ginna plant. Even though the slope is about 1/2 that for the other capsules, the two Ginna data points extrapolate back to a common initial fission rate of about 4.5×10^{-14} fps/nucleus. One explanation for the high fission rate datum point at low fluence obtained for the Point Beach Unit 2 Capsule V is the thermal neutron leakage of the cadmium cover. Seven of the eight measured fission rates extrapolate back to an initial fission rate (corrected for ^{235}U) in good agreement with the calculated value of 4.4×10^{-14} fps/nucleus.

TABLE 4.1.3.2

AVERAGE SELF-SHIELDING CORRECTION FACTORS FOR THE $^{238}U(n,\gamma)^{239}U$ REACTION

Vendor	Flux Direction	S	Weight (cm^2)	$\overline{S}$
Westinghouse	Horizontal	0.57	0.20	0.70
	Vertical	0.75	0.53	
Combustion Engineering	Perpend. to A_x	0.12	0.0025	0.36
	Perpend. to A_y	0.38	0.03	
	Perpend. to A_z	0.047	0.00019	
Babcock & Wilcox	Parallel to r	0.36	1.0	0.36

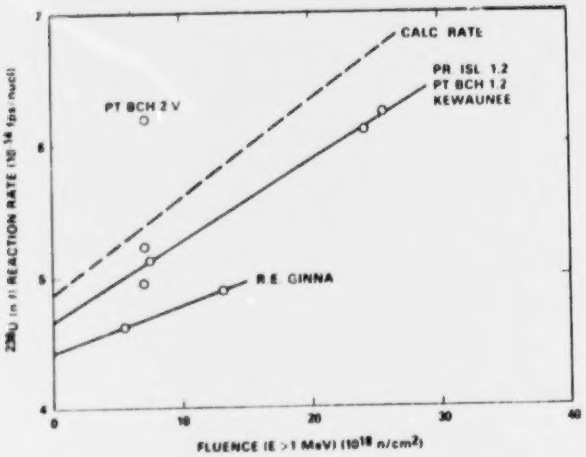

FIGURE 4.1.3.2. ^{238}U Fission Rate with Burnin of ^{239}Pu as a Function of Fluence (E > 1 MeV) in Two-Loop Westinghouse Plants.

Since the low-energy spectrum is nearly proportioned to 1/E, the spectrum-averaged cross sections σ^f_{239} and σ^f_{238} are approximately the same for all spectra. Thus the relative ^{239}Pu correction to the measured fission rate in a ^{238}U dosimeter is most sensitive to the relative number of fissions from the ^{238}U. For example, the ^{238}U fission cross section in a two-loop Westinghouse plant is ~30 mb compared to ~46 mb in a four-loop plant; thus the two-loop plant requires a larger correction than the four-loop plant.

Other corrections that have not yet been made in all cases but may be important are for photo fission and variation in the flux per megawatt from differences in cycle-to-cycle fuel loadings. The photo fission correction was estimated by Anderson of Westinghouse to be < 3% for the Point Beach Unit 2 Capsule R and similar capsules*. For Westinghouse capsule locations, this would be a marginally important correction. Flux level variation would only be important when mixing the use of short and long half-lived dosimeter reactions. The long half-lived dosimeters give an average flux value while the short half-lived ones give an end-of-cycle flux value.

The reaction rate uncertainties were generally set at 10% for a specific capsule. In some cases, larger uncertainties were assigned to account for anomalous reaction rate values or larger variations across the length of the capsule.

4.1.3.3 Results

The desired exposures resulting from this analysis are the traditional fluence (E > 1 MeV) and the new ASTM recommended displacements per atom (dpa) in iron[32] and their uncertainties. Table 4.1.3.3 summarizes the exposures, their uncertainties, and the exposure rates that are tabulated for each capsule in Section 4.2 through 4.5. The following discussion is a generic description of the dosimetry information for each capsule reported in Sections 4.2 through 4.5. The dosimetry information used to determine these exposures is summarized in one figure and four tables for each capsule reported. A general note explaining the number designation is in order. All tables are reported in Section 4 of this NUREG report. The second number designates the reactor plant vendor (W=2, CE=3, B&W=4, and GE=5). The third number delineates between generic designs of the vendor. For further discussion of specific vendor generic plants see Sections 1 through 3. The fourth number designates tabulated information for a specific plant, and the fifth number designates the specific capsule. The last number refers to the table or figure number for the specific capsule information.

Figure 4.2.1.1.1.1 shows the orientation of the capsule relative to the core and vessel wall. This is particularly important for Westinghouse capsules when the capsule was inserted 180° from the correct orientation.

---

*At present, there is no direct experimental method to determine photo-fission correction factors; however, Gold et al. have recently proposed a method that has yet to be tested (Go82c).

TABLE 4.1.3.3

RE-EVALUATED EXPOSURE VALUES AND THEIR UNCERTAINTY FOR LWR PRESSURE VESSEL SURVEILLANCE CAPSULES

Plant	Unit	Capsule	Service Lab*	Biblio Ref	Fluence (ϕt > 1 MeV) (n/cm^2) Old	New [% (1σ)]	New/Old	Fluence (E < 0.414 eV) (n/cm^2)	dpa [% (1σ)]	New dpa/ϕt	dpa/s	hpa (appb)†	Exposure** Time (s)
Westinghouse													
Conn. Yankee		A	BMI	(Ir70)	2.08 E+18	3.16 E+18 (12)***	1.53	2.54 E+18 (18)	0.00482 (12)	1.52 E-21	9.06 E-11	6	5.233 E+07
Conn. Yankee		F	BMI	(Pe72)	4.04 E+18	6.06 E+18 (24)	1.50	5.43 E+18 (32)	0.00949 (27)	1.56 E-21	1.24 E-10	13	7.651 E+07
Conn. Yankee		H	W	(Ya67)	1.79 E+19	2.00 E+19 (24)	1.12	2.33 E+19 (19)	0.0324 (27)	1.62 E-21	1.36 E-10	52	2.390 E+08
San Onofre		A	SwRI	(No71)	1.20 E+19	2.86 E+19 (22)	2.38	2.05 E+19 (23)	0.0486 (27)	1.70 E-21	8.35 E-10	43	5.824 E+07
San Onofre		D	SwRI	(No72)	2.36 E+19	5.62 E+19 (26)	2.38	3.76 E+19 (23)	0.0944 (29)	1.68 E-21	1.06 E-09	80	8.881 E+07
San Onofre		F	W	(Ya79)	5.14 E+19	5.73 E+19 (14)	1.11	2.99 E+19 (28)	0.0955 (20)	1.67 E-21	3.92 E-10	73	2.438 E+08
Turkey Point	3	S	SwRI	(No79)	1.41 E+19	1.62 E+19 (24)	1.15	1.34 E+19 (24)	0.0255 (27)	1.57 E-21	2.33 E-10	33	1.095 E+08
Turkey Point	3	T	W	(Ya75)	5.68 E+18	7.01 E+18 (10)	1.23	5.12 E+18 (58)	0.0109 (12)	1.55 E-21	4.73 E-10	14	2.302 E+07
Turkey Point	4	S	SwRI	(No79)	1.25 E+19	1.31 E+19 (25)	1.05	1.31 E+19 (25)	0.0213 (27)	1.63 E-21	1.97 E-10	37	1.079 E+08
Turkey Point	4	T	SwRI	(No76)	6.05 E+18	7.54 E+18 (13)	1.25	8.40 E+18 (21)	0.0130 (13)	1.72 E-21	3.48 E-10	20	3.728 E+07
H. B. Robinson	2	V	W	(Ya73)	3.02 E+18	3.91 E+18 (24)	1.29	8.81 E+18 (18)	0.00615 (27)	1.57 E-21	1.06 E-10	19	4.209 E+07
H. B. Robinson	2	S	SwRI	(No76b)	4.51 E+18	7.42 E+18 (22)	1.61	8.96 E+18 (20)	0.0119 (25)	1.59 E-21	1.09 E-10	21	1.050 E+08
Surry	1	T	BMI	(Pe75)	2.50 E+18	2.86 E+18 (9)	1.14	3.57 E+18 (20)	0.00449 (12)	1.57 E-21	1.33 E-10	8	3.378 E+07
Surry	2	X	BMI	(Pe75a)	3.02 E+18	3.03 E+18 (11)	1.00	3.64 E+18 (20)	0.00473 (13)	1.56 E-21	1.28 E-10	9	3.687 E+07
North Anna	1	V	B&W	(Lo81d)	2.49 E+18	2.72 E+18 (9)	1.09	5.80 E+18 (14)	0.00411 (11)	1.51 E-21	1.15 E-10	11	3.570 E+07
Beznau	2	R	EIR	( )	1.70 E+19	1.34 E+19 (9)	1.27	2.27 E+19 (21)	0.0198 (11)	1.48 E-21	1.16 E-10	49	1.714 E+08
Pr. Island	1	V	W	(Da77)	5.21 E+18	6.03 E+18 (11)	1.16	9.21 E+18 (21)	0.0102 (16)	1.69 E-21	2.41 E-10	20	4.248 E+07
Pr. Island	2	V	W	(Ya81)	5.49 E+18	6.74 E+18 (10)	1.23	9.75 E+18 (26)	0.0117 (13)	1.74 E-21	2.67 E-10	21	4.394 E+07
R. E. Ginna	1	R	W	(Ya74)	7.60 E+18	1.17 E+19 (10)	1.54	1.84 E+19 (25)	0.0215 (14)	1.83 E-21	2.59 E-10	38	8.328 E+07
R. E. Ginna	1	V	W	(Ma73a)	4.90 E+18	5.93 E+18 (14)	1.21	1.37 E+19 (59)	0.0102 (22)	1.72 E-21	2.20 E-10	29	4.612 E+07
Kewaunee		V	W	(Ya77)	5.59 E+18	6.41 E+18 (10)	1.15	1.23 E+19 (23)	0.0114 (13)	1.78 E-21	2.82 E-10	26	4.057 E+07
Point Beach	1	S	W	(Ya76)	7.05 E+18	8.45 E+18 (10)	1.20	1.20 E+19 (19)	0.0146 (13)	1.73 E-21	1.25 E-10	27	1.163 E+08
Point Beach	1	R	W	(Ya78)	2.22 E+19	2.29 E+19 (10)	1.37	2.85 E+19 (22)	0.0408 (13)	1.78 E-21	2.50 E-10	61	1.632 E+08
Point Beach	2	V	BMI	(Pe75b)	4.74 E+18	7.28 E+18 (11)	1.54	1.09 E+19 (18)	0.0121 (13)	1.66 E-21	2.52 E-10	23	4.805 E+07
Point Beach	2	T	W	(Da78a)	9.45 E+18	9.40 E+18 (10)	0.99	1.48 E+19 (21)	0.0157 (12)	1.67 E-21	1.44 E-10	32	1.087 E+08
Point Beach	2	R	W	(Ya79a)	2.01 E+19	2.52 E+19 (10)	1.25	4.71 E+19 (26)	0.0460 (14)	1.83 E-21	2.81 E-10	93	1.640 E+08
D. C. Cook	1	T	SwRI	(No77b)	1.80 E+18	2.71 E+18 (22)	1.51	3.26 E+19 (19)	0.00445 (25)	1.64 E-21	1.12 E-10	77	3.991 E+07
Indian Point	2	T	SwRI	(No77a)	2.02 E+18	3.28 E+18 (22)	1.62	4.01 E+18 (44)	0.00537 (27)	1.64 E-21	1.20 E-10	91	4.473 E+07
Indian Point	3	T	W	(Da79)	2.92 E+18	3.23 E+18 (22)	1.11	3.13 E+18 (21)	0.00520 (25)	1.61 E-21	1.23 E-10	74	4.211 E+07
Zion	1	T	BMI	(Pe78)	1.80 E+18	3.04 E+18 (10)	1.69	3.17 E+18 (21)	0.00488 (12)	1.61 E-21	1.29 E-10	82	3.789 E+07
Zion	1	U	W	(Ya81a)	8.92 E+18	1.01 E+19 (10)	1.13	8.87 E+18 (24)	0.0166 (13)	1.64 E-21	1.47 E-10	21	1.123 E+08
Zion	2	U	BMI	(Pe78)	2.00 E+18	2.80 E+18 (9)	1.40	3.80 E+18 (15)	0.00446 (12)	1.59 E-21	1.11 E-10	10	4.007 E+07
Salem	1	T	W	(Ya80)	2.56 E+18	2.84 E+18 (22)	1.11	3.26 E+18 (19)	0.00460 (25)	1.62 E-21	1.34 E-10	7	3.426 E+07

---

*BMI = Battelle Memorial Institute; W = Westinghouse; SwRI = Southwest Research Institute; CE = Combustion Engineering; ET = Effects Technology; B&W = Babcock and Wilcox; EIR = Eidg. Institute für Reaktorforschung.

**Equivalent constant power level exposure time.

***3.16 E+18 (12) means 3.16 x 10^{18} with a 12% (1σ) uncertainty.

†Calculated for A302B steel with a nominal concentration of 0.55 appm boron present.

TABLE 4.1.3.3 (Cont'd)

Plant	Unit	Capsule	Service Lab*	Biblio Ref	Fluence (φt > 1 MeV) (n/cm^2)			Fluence (E < 0.414 eV) (n/cm^2)	dpa [% (1σ)]	New dpa/φt	dpa/s	hpa (appb)†	Exposure** Time (s)
					Old	New [% (1σ)]	New/Old						
Combustion Engineering													
Palisades		A240	BMI	(Pe79b)	4.40 E+19	6.06 E+19 (23)	1.38	7.26 E+19 (61)	0.0972 (28)	1.60 E-21	1.36 E-09	170	7.130 E+07
Fort Calhoun		W225	CE	(By80)	5.10 E+18	5.83 E+18 (14)	1.14	3.09 E+19 (60)	0.00879 (18)	1.51 E-21	1.07 E-10	63	8.191 E+07
Maine Yankee		1	ET	(Wu75)	1.30 E+19	1.76 E+19 (19)	1.35	3.00 E+19 (29)	0.0285 (23)	1.62 E-21	1.03 E-09	62	2.777 E+07
Maine Yankee		2	W	(Ya81b)	8.84 E+19	7.73 E+19 (13)	0.87	1.20 E+20 (23)	0.121 (18)	1.57 E-21	8.38 E-10	230	1.446 E+08
Maine Yankee		W263	BMI	(Pe80)	7.10 E+18	5.67 E+18 ([illegible]2)	0.82	2.67 E+19 (21)	0.00843 (14)	1.49 E-21	5.83 E-11	55	1.446 E+08
Babcock & Wilcox													
Oconee	1	F	B&W	(Lo75)	8.70 E+17	6.98 E+17 (21)	0.80	1.00 E+18 (13)	0.000959 (19)	1.37 E-21	3.65 E-11	3	2.629 E+07
Oconee	1	E	B&W	(Lo77)	1.50 E+18	1.50 E+18 (10)	1.00	2.61 E+18 (15)	0.00208 (10)	1.39 E-21	4.01 E-11	7	5.186 E+07
Oconee	2	C	B&W	(Lo77a)	9.43 E+17	1.01 E+18 (10)	1.07	1.55 E+18 (15)	0.00148 (11)	1.47 E-21	3.88 E-11	4	3.802 E+07
Oconee	3	A	B&W	(Lo77b)	7.39 E+17	8.05 E+17 (10)	1.09	1.34 E+18 (11)	0.00113 (11)	1.40 E-21	3.79 E-11	3	2.983 E+07
Three Mile Is.	1	E	B&W	(Lo77c)	1.07 E+18	1.09 E+18 (9)	1.02	1.90 E+18 (11)	0.00151 (9)	1.39 E-21	3.75 E-11	5	4.036 E+07
Arkansas Nuclear	1	E	B&W	(Lo77d)	7.27 E+17	8.18 E+17 (8)	1.13	6.32 E+17 (9)	0.00117 (8)	1.43 E-21	3.92 E-11	2	2.981 E+07
General Electric													
Dresden	3	4G14	W	(Ya82)	2.06 E+19	1.86 E+19 (17)	0.89	1.51 E+20 (62)	0.0285 (17)	1.53 E-21	3.35 E-10	290	8.483 E+07
Dresden	3	4G15	W	(Ya82)	1.50 E+19	1.35 E+19 (17)		1.19 E+20 (62)	0.0209 (17)	1.55 E-21	2.46 E-10	240	8.483 E+07
Dresden	3	4G16	W	(Ya82)	1.20 E+19	1.08 E+19 (17)		9.70 E+19 (62)	0.0168 (17)	1.55 E-21	1.98 E-10	200	8.483 E-07
Dresden	3	4G17	W	(Ya82)	5.16 E+18	4.51 E+18 (17)		5.20 E+19 (62)	0.00733 (18)	1.63 E-21	8.64 E-11	120	8.438 E+07
Quad Cities	1	3G5	W	(Ya81c)	4.04 E+19	4.23 E+19 (17)	1.01	2.41 E+20 (62)	0.0604 (17)	1.43 E-21	4.85 E-10	400	1.243 E+08
Quad Cities	1	3G6	W	(Ya81c)	3.08 E+19	3.12 E+19 (17)		1.92 E+20 (62)	0.0450 (17)	1.44 E-21	3.62 E-10	340	1.243 E+08
Quad Cities	1	3G7	W	(Ya81c)	2.37 E+19	2.47 E+19 (17)		1.54 E+20 (62)	0.0356 (17)	1.44 E-21	2.86 E-10	290	1.253 E+08
Quad Cities	1	3G8	W	(Ya81c)	1.24 E+19	1.17 E+19 (17)		1.03 E+20 (62)	0.0180 (17)	1.54 E-21	1.45 E-10	210	1.243 E+08
Quad Cities	2	3G14	W	(Ya82a)	4.14 E+19	4.28 E+19 (16)	1.03	2.45 E+20 (62)	0.0611 (17)	1.43 E-21	4.29 E-10	400	1.422 E+08
Quad Cities	2	3G15	W	(Ya82a)	3.48 E+19	3.60 E+19 (16)		2.13 E+20 (62)	0.0516 (17)	1.43 E-21	3.63 E-10	370	1.422 E+08
Quad Cities	2	3G16	W	(Ya82a)	2.43 E+19	2.52 E+19 (16)		1.55 E+20 (62)	0.0362 (17)	1.44 E-21	2.54 E-10	290	1.422 E+08
Quad Cities	2	3G17	W	(Ya82a)	2.32 E+19	2.37 E+19 (17)		1.49 E+20 (62)	0.0342 (17)	1.44 E-21	2.41 E-10	290	1.422 E+08
							Avg 1.25						

---

*BMI = Battelle Memorial Institute; W = Westinghouse; SwRI = Southwest Research Institute; CE = Combustion Engineering; ET = Effects Technology; B&W = Babcock and Wilcox; EIR = Eidg. Institute für Reaktorforschung.

**Equivalent constant power level exposure time.

***3.16 E+18 (12) means 3.16 x 10^{18} with a 12% (1σ) uncertainty.

†Calculated for A302B steel with a nominal concentration of 0.55 appm boron present.

Table 4.2.1.1.1.1 shows the time-history data used in this analysis. Included in the table are the starting date for each time interval, the length of the time interval in days, the average global power level for the time interval, and the local power factor for the capsule during the time interval. The local power factor accounts for local power variations that do not follow the global power-time history. This power factor is not used in the present analysis. However, it could have a significant effect on short half-lived dosimeters irradiated over several fuel cycle loadings in which the adjacent fuel assembly's relative power level varies between fuel cycles; i.e., ongoing from past to present to new low-leakage core fuel management schemes (Ar83,Gu82,Gu82a,Mc82a,Mc82b,Nr82). The footnote shows the reference full-power level and the effective full-power seconds of operation.

Table 4.2.1.1.1.2 shows the measured reaction rates and correction factors applied to the reaction rates. The table shows the reaction name, the dosimeter identity, the activity at reactor shutdown (TOR), correction factors for saturation, gradients from the dosimeter location to the center of the capsule, and initial or buildup impurities in the dosimeter. The saturated reaction rate is the TOR rate times the three correction factors. A 10% (1σ) uncertainty was assigned to all reaction rates (or the standard deviation of multiple measurements if it exceeded 10%).

Table 4.2.1.1.1.3 shows the flux group lower bound energy, the group flux for the a priori spectrum and adjusted spectrum, and the percent (one standard deviation) uncertainty in the adjusted group integral flux. The a priori flux is either an absolute calculated value or it has been normalized to the ^{54}Fe(n,p)^{54}Mn reaction rate. The bottom of Table 4.2.1.1.1.2 gives selected integral fluxes (>E or <E*), the displacement rate in iron, and their uncertainties. The uncertainties were calculated from the full covariance matrix of the adjusted neutron spectrum. The last values are the fluence (E > 1 MeV) and iron dpa exposure for the capsule.

Table 4.2.1.1.1.4 shows a comparison of the measured and calculated reaction rates. The table includes the reaction name, measured reaction rate, a priori calculated reaction rate, adjusted calculated reaction rate, ratio of measured/a priori-calculated reaction rate, and the ratio of measured/adjusted-calculated reaction rates. A ratio of measured/a priori-calculated ^{54}Fe(n,p)^{54}Mn reaction rate of 1.00 generally indicates the a priori spectrum was normalized to that reaction rate. Reactions whose ratios deviate substantially from 1.0 were not used in the final flux adjustment procedure because the reaction rates deviated anomalously from the expected values. This behavior was not reflected in the assigned uncertainties shown in Table 4.2.1.1.1.2. The asterisked entries in some of the Table 4's show measured and calculated reaction rates and ratios for reactions not used in the analysis. Those reactions are provided for future reference and help in identifying any systematic trends and the possible subsequent determination of the cause or causes of the anomalous behavior.

---

*The thermal flux was defined as the sum of the group fluxes below 0.414 eV. The thermal maxwellian temperature for the a priori spectrum was 288°C.

4.1.4 Reactor Cavity Analysis Procedures and Results

4.1.4.1 Introduction*

As discussed in Section 1.0, Federal codes (Cf83,Re77) require that reactor coolant pressure boundaries have sufficient margin to ensure that the boundary behaves in a nonbrittle manner when stressed under operating, maintenance, testing, and postulated accident conditions and that the probability of rapidly propagating fracture is minimized. These requirements necessitate the prediction of the amount of radiation damage to the reactor vessel throughout its service life, which in turn requires that the neutron exposure to the PV be monitored. Both in-vessel surveillance capsule and ex-vessel cavity physics-dosimetry monitoring studies are being implemented by U.S. Utilities.

As previously stated, a matrix of ASTM Standard Practices, Guides, and Methods is being established to document the physics-dosimetry procedures to be followed for LWR in-vessel and cavity surveillance programs. These standards are in turn being validated by data development and testing of the dosimetry in reference neutron fields, such as SDMF, ANO-1, H. B. Robinson, and Maine Yankee. Physics-dosimetry results for in-vessel surveillance capsules are presented in this document in Section 4.1.3. The purpose of Section 4.1.4 is only to discuss and make reference to the analysis procedures and available results for ex-vessel cavity measurements. It is important to understand, however, that the cavity physics-dosimetry results referenced herein will be combined with those obtained from surveillance capsules to provide a more accurate and complete determination of neutron exposure parameter values for both the PV and its support structures.

The LWR-PV-SDIP (Mc85a) is in the process of establishing a series of 21 ASTM Standard Practices, Guides, and Methods as discussed and referenced in Section 1.0.2.2. The application of standardized physics-dosimetry for PV cavity surveillance programs will rely on these standards for: 1) selection and deployment of recommended dosimetry sets [made up of an appropriate balance of advanced Radiometric Monitors (RM), Solid State Track Recorders (SSTR), Helium Accumulation Fluence Monitors (HAFM), and Damage Monitors (DM)]; 2) selection of dosimetry capsules and thermal neutron shields; 3) placement of dosimetry; 4) methods of measurement of dosimetry sensor reaction products; 5) data analysis procedures; and 6) uncertainty evaluation procedures. The reader is referred to ASTM E853 [E706-(IA)] (As84), "Standard Practice for Analysis and Interpretation of Light-Water Reactor Surveillance Results," for a discussion of current recommendations for reactor cavity dosimetry for verification of reactor physics computations for surveillance programs.

---

*Ref (Ru84a) is the basis for the information presented in Section 4.1.4.

109

The status of data development and testing work for the application of advanced standardized PV physics-dosimetry for cavity surveillance are discussed and summarized in subsequent sections. The use of individual ASTM standards to guide in the selection and deployment of advanced cavity dosimetry sets for operating LWRs is also reviewed.

4.1.4.2 Recommended Dosimetry Sets

ASTM E844 [E706-(IIC)] (As83b), "Standard Guide for Sensor Set Design and Irradiation for Reactor Surveillance," deals with the overall selection, design, irradiation, and post-irradiation handling of RMs, SSTRs, HAFMs, DMs and temperature monitor (TM) sensors and sensor sets. Specific information on TM sensors is not, as yet, provided in ASTM E844.

Radiometric Monitors -- ASTM E1005 [E706-(IIIA)] (As85c), "Standard Method for Application and Analysis of Radiometric Monitors for Reactor Vessel Surveillance," describes the use of RMs for neutron dosimetry in LWR applications. The useful flux-fluence range and limitations for the application of RMs for time-integrated LWR reaction rate measurements are specified. This standard contains a list of proposed RMs for reactor surveillance along with the neutron response and decay characteristics of each RM. This method should be used in conjunction with Standard Guide E844 for selection of appropriate fission and nonfission RMs for reactor surveillance. In the case of cavity surveillance, primary concerns are lower neutron fluence and the high degree of thermalization of the neutron spectrum.

Solid State Track Recorders -- ASTM E854 [E706-(IIIB)] (As82b), "Standard Method for Application and Analysis of Solid State Track Recorder Monitors for Reactor Vessel Surveillance," describes the use of SSTRs in LWR applications. The useful flux-fluence range and limitations for the application of SSTRs for time-integrated LWR reaction and reaction rate measurements are specified. The uses of both fission and nonfission [(n,α),(n,p)] reactions are described. The production of ultra low-mass fissionable deposits for surveillance applications is summarized. This standard is also used in conjunction with ASTM E844 for selection of appropriate monitor sets.

Helium Accumulation Fluence Monitors -- ASTM E910 [E706-(IIC)] (As83a), "Standard Method for Application and Analysis of Helium Accumulation Fluence Monitors for Reactor Vessel Surveillance," describes the use of HAFMs in LWR applications. The useful flux-fluence range and limitations for the application of HAFMs for time-integrated LWR reaction and reaction rate measurements are specified. Proposed HAFM sensors for LWR applications are given. This method uses high-sensitivity helium gas mass spectrometry coupled with isotope dilution methods to accurately measure helium produced by selected (n,α) reactions. Selection of appropriate (n,α) reaction dosimeters is made using this method in conjunction with ASTM E844.

110

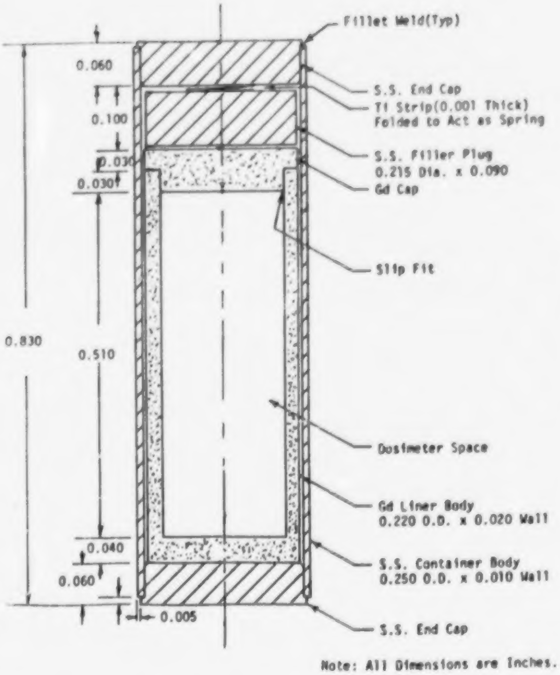
Fillet Weld(Typ)
S.S. End Cap
Ti Strip(0.001 Thick)
Folded to Act as Spring
S.S. Filler Plug
0.215 Dia. x 0.090
Gd Cap
Slip Fit
Dosimeter Space
Gd Liner Body
0.220 O.D. x 0.020 Wall
S.S. Container Body
0.250 O.D. x 0.010 Wall
S.S. End Cap
0.060
0.100
0.030
0.030
0.830
0.510
0.040
0.060
0.005
Note: All Dimensions are Inches.

FIGURE 4.1.4.1. Typical Dosimetry Capsule for Light Water Reactor Pressure Vessel Surveillance Applications.

Damage Monitors -- ASTM E706-(IIID) (As85a), "Standard Method for Application and Analysis of Damage Monitors for Reactor Vessel Surveillance," will describe the use of DMs for LWR applications. Emphasis is placed on the use of sapphire, which has great potential as a direct monitor of neutron damage because of its increase in optical absorbance with increased neutron bombardment. The uses of quartz, graphite, iron, and tungston sensors, as well as the development of new DMs, are referenced and/or described (Mc85a).

4.1.4.3 Dosimetry Capsules and Thermal Neutron Shields

ASTM E844 also provides information on design of dosimetry capsules and thermal neutron shields. Figure 4.1.4.1 shows a typical dosimetry capsule fabricated of stainless steel with a gadolinium liner for thermal neutron absorption for higher fluence LWR applications. The space inside the shield is used for the placement of an appropriate mix of RM, SSTR, HAFM, and DM. The mix of sensors is chosen to give spectral sensitivity over the desired range of neutron energies as well as time-history (exposure time and time-integration) information. When thermal neutron-induced reactions are to be monitored, selected broad energy range sensors [(n,γ) and/or (n,f)] are also included, but in a separate capsule with the gadolinium shield omitted.

111

4.1.4.4 Placement of Dosimeters

ASTM Standard Practices: E185 [E706-(IB)], "Surveillance Tests for Nuclear Reactor Vessels" (As79c); E706-(IG), "Determining Radiation Exposure for Nuclear Reactor Support Structures" (As85f); and E853-(IA), "Analysis and Interpretation of LWR Surveillance Results" (As84) should be used in conjunction with ASTM E844 to guide the selection, number, and placement of the dosimetry sets. The primary concerns are that in-vessel surveillance and cavity dosimetry capsule exposures can be related to the exposures of the beltline welds and that the dosimetry data provide results useful for evaluation of the radiation effects on the reactor vessel and its support structures.

4.1.4.5 Measurement of Dosimetry Sensor Reaction Products

Radiometric Monitors -- Methods for absolute high-resolution gamma-ray spectrometric analysis of RM reaction products for fission and nonfission sensors are described and referenced in ASTM Standard Method E1005. General procedures for measuring the amounts of radioactive nuclides produced in RMs by nuclear reactions induced during surveillance exposures are outlined with emphasis on the use of high-resolution gamma-ray spectrometry. Primary concerns include the presence of interfering reactions or radionuclide activities, sample size effects, and absolute counter efficiency calibrations.

Solid State Track Recorders -- Methods for high-accuracy SSTR track counting are detailed in ASTM Standard Method E854. Primary concerns include standardizing etching procedures and calibrating scanning equipment and scanning techniques.

Helium Accumulation Fluence Monitors -- Methods for high-accuracy HAFM analysis are detailed in ASTM Standard Method E910. Primary concerns include ensuring that no helium is lost from the HAFM (encapsulation is usually used) and uniformity of the HAFM dosimetry material (when alloys and compounds are used). The presence of small amounts of boron and/or lithium is a concern in highly thermalized neutron fields except when the HAFMs are being used to determine thermal neutron fluences.

Damage Monitors -- Methods for observing neutron-induced damage in DMs will be described in ASTM Standard Method E706-(IIID). Primary concerns include the usable range of fluences for DM sensitivity and the temperature and rate effects on the response of the DM.

4.1.4.6 Data Analysis

Neutron Transport -- ASTM E482 [E706-(IID)], "Standard Guide for Application of Neutron Transport Methods for Reactor Vessel Surveillance," (As82a) describes the methodology for performing radiation transport calculations to determine the neutron and gamma flux spectra at in- and ex-vessel surveillance positions and within the PV. These procedures are applicable for the evaluation and extrapolation of both research and surveillance program measurement results obtained in operating reactors. The reader is referred to ASTM E1006 [E706-(II)], "Standard Practice for Analysis and Interpretation of Physics-Dosimetry Results for Test Reactors" (As85d) for additional and supplementary information.

Spectral Adjustment -- ASTM E944 [E706-(IIA)], "Standard Guide for Application of Neutron Spectrum Adjustment Methods," (As85b) describes the procedures and codes recommended for use in determining neutron flux-fluence spectra from multiple sensor dosimetry measurements. ASTM E706-(IIB), "Standard Guide for Application of ENDF/A Cross-Section and Uncertainty Files," (As85e) is directly related to and should be used in conjunction with ASTM E944. This guide covers the establishment and use of an ASTM ENDF/A cross-section and uncertainty tape file for analysis of multiple sensor measurements in LWR neutron fields. Also included are calculations of spectral-averaged damage cross sections for iron, quartz, and other sensors that might be used as DMs.

Documentation -- Documentation in the form of as-built reports should be provided with each dosimetry set. The as-built report should document the type and number of dosimeters, dosimeter materials (supplier, batch number, isotopic composition, chemical form, weight, dimensions, impurity content, etc.), dosimeter capsules (materials, dimensions, characteristics of thermal neutron shields, etc), capsule support structure (materials, dimensions, etc), location of dosimetry in the reactor, and any other pertinent information. Following the exposure, the reactor power and sensor set flux time history should be documented along with analysis results and interpretation (including spectral adjustment calculations and damage calculations).

4.1.4.7 Benchmarking and Uncertainty Evaluation

Benchmark Referencing -- ASTM E706-(IIE), "Standard Guide for Benchmark Testing of Reactor Vessel Dosimetry," (As85) will describe the methodology for using the known characteristics of selected neutron fields to calibrate neutron sensors or to validate procedures used to derive neutron field information from measurements of their response. Of particular interest to cavity surveillance measurements are the calibration measurements performed at the Surveillance Dosimetry Measurements Facility (SDMF) at Oak Ridge (Ma82e,To82), in the ANO-1 (Arkansas) reactor cavity (Br82a,Pe82b), and in other related benchmark fields (Mc85a).

113

The SDMF serves as a realistic mockup of operating power reactors. This facility has been used for a series of dosimetry tests, some of which were designed to replicate some details of cavity dosimetry. ANO-1, ANO-2, Browns Ferry 3, H. B. Robinson, Maine Yankee, and BR-3 (Belgium), on the other hand, are operating commercial power reactors that have been the sites of numerous cavity dosimetry measurements and related neutronic calculations (Br82a,Mc85a,Pe82b).

Experimental Uncertainties -- The maximum uncertainties desirable for LWR-PV steel exposure definition are in the range of ±10% to 15%. In order to achieve these accuracy goals, the dosimeter reaction and reaction rates must, in general, be measurable to within ±5% (1σ). Experimental design and analysis should provide a margin such that overall errors (response uncertainty, extrapolation, interpolation, etc.) are within these bounds.

4.1.4.8 Status of Work and Results for Cavity Surveillance Dosimetry

Advanced surveillance dosimetry sets have been chosen, assembled, and deployed by LWR-PV-SDIP participants and US utilities in the cavities of operating commercial reactors (see Table 4.1.4.1). (Br82a,Ma81d,Mc85a,Pe82b). These sets contain a mix of RMs, SSTRs, and HAFMs. The layout of a typical set is shown in Figure 4.1.4.2. RMs consisting of silver (in the form of Ag-Al alloy wires), cobalt (in the form of Co-Al alloy wires), and iron are deployed as thermal neutron monitors. Included in this so-called bare (aluminum-wrapped) set are ultra-low-mass fissionable deposits of ^{235}U and ^{239}Pu with mica SSTRs to measure the integral neutron-induced fission rates. After radiometric analysis of the Ag and Co dosimeters for their (n,γ) reaction products, they may be subjected to analysis as HAFMs for their helium content [Al(n,α) integral reaction rates]. The thermal-neutron-shielded (cadmium-covered) dosimeter set contains Co, Ti, Ni, Cu, and Fe RMs. The Co, Ti, Fe, Ni, and Cu dosimeters can also serve as HAFMs. ^{235}U, ^{239}Pu, ^{237}Np, and ^{238}U ultra-low-mass fissionable deposits and mica SSTRs are also included. The former two isotopes provide epithermal neutron response, whereas the latter provide threshold neutron response. Additional HAFM sensors are currently being developed to supplement existing RMs and SSTRs and are discussed in ASTM Standard Method E910 (As83a). HAFMs have a particular advantage for those LWR applications where long durations are involved.

Figure 4.1.4.3 shows a typical dosimetry holder for emplacement of the assembled dosimetry capsules in the reactor cavity. Capsules are typically located at three locations (above midplane, midplane, and below midplane) at several azimuthal positions around the PV. Dosimetry sets of the type shown in Figure 4.1.4.2 that have been deployed (or have been planned for deployment) in commercial power reactors are as shown in Table 4.1.4.2. In the case of SSTRs, replicate sets of SSTR fissionable deposits are made to facilitate replacement of the dosimetry at the end of an operating cycle. The pairs of SSTR dosimetry sets are exchanged with the ex-reactor set being subjected to mass calibration overchecks before re-insertion with new mica SSTRs in the following cycle.

TABLE 4.1.4.1

POWER REACTORS BEING USED BY LWR-PV-SDIP PARTICIPANTS TO BENCHMARK PHYSICS-DOSIMETRY METHODS, PROCEDURES AND DATA FOR PRESSURE VESSEL AND SUPPORT STRUCTURE SURVEILLANCE*

(Plant name; reactor type/supplier; reactor operator; ex-vessel cavity (C) and in-vessel (V) surveillance positions available;

Energy Range (MeV)	Type of Dosimeter	Dosimetry Reaction	Nuclear One-1 PWR/B&W Arkansas Power & Light		Nuclear One-2 PWR/CE Arkansas Power & Light		Brown's Ferry-3 BWR/GE Tennessee Valley Authority		H.B. Robinson PWR/WEC Carolina Power & Light		Maine Yankee PWR/CE Maine Yankee Atomic Power		Point Beach-2 PWR/WEC Wisconsin Electric Power		McGuire PWR/WEC Duke Power		CR or DB[1] PWR/B&W		Oconee 1,2&3 PWR/B&W Duke Power[1]		BR-3 PWR/WEC Belgium	
			C	V	C	V	C	V	C	V	C	V	C	V	C	V	C	V	C	V	C	V
>1.5	RMs	^{63}Cu(n,α)^{60}Co[f]	Y		Y	Y	Y	Y	Y	Y	Y	Y		Y	Y	Y	P	Y	P		Y	Y
		^{46}Ti(n,p)^{46}Sc[f]	Y		Y	Y	Y	Y	Y	Y	Y	Y			Y		P	P	PY[j]		Y	Y
		^{54}Fe(n,p)^{54}Mn[f]	Y	Y	Y	Y	Y	Y	Y	Y	Y	Y		Y	Y	Y	P	Y	PY	Y	Y	Y
		^{58}Ni(n,p)^{58}Co[f]	Y	Y	Y	Y	Y	Y	Y	Y	Y	Y		Y	Y	Y	P	Y	PY	Y	Y	Y
		^{238}U(n,f)^{140}Ba-La	Y	(N)	Y	(N)	Y	Y	(N)	(N)	(N)	(N)	(N)	(N)	(N)	(N)	(N)	(N)	(N)	(N)	(N)	(N)
		^{238}U(n,f)^{103}Ru	(Y)	Y	(Y)	(Y)	Y	Y	Y	Y	Y	Y			Y	Y	P	Y	P	Y	Y	Y
		^{238}U(n,f)^{95}Zr-Nb	(Y)	Y	(Y)	(Y)	Y	Y	Y	Y	Y	Y			Y	Y	P	Y	P	Y	Y	Y
		^{238}U(n,f)^{137}Cs	(Y)	Y	(Y)	Y	Y	Y	Y	Y	Y	Y			Y	Y	P	Y	P	Y	Y	Y
>0.4		^{232}Th(n,f)^{140}Ba-La		(N)		(N)	(N)	(N)	(N)	(N)	(N)	(N)	(N)	(N)	(N)	(N)	(N)	(N)	(N)	(N)	(N)	
		^{232}Th(n,f)^{95}Zr-Nb					Y	Y									P	P				
		^{232}Th(n,f)^{137}Cs					Y	Y									P	P				
		^{237}Np(n,f^{140}Ba-La	Y	(N)	Y	(N)	Y	Y	(N)	(N)	(N)	(N)	(N)	(N)	(N)	(N)	P	(N)	(N)	(N)		(N)
		^{237}Np(n,f)^{103}Ru	(Y)	Y	(Y)	(Y)	Y	Y	Y	Y	Y	Y			Y	Y	P	Y	P	Y		Y
		^{237}Np(n,f)^{95}Zr-Nb	(Y)	Y	(Y)	(Y)	Y	Y	Y	Y	Y	Y			Y	Y	P	Y	P	Y		Y
		^{237}Np(n,f)^{137}Cs	(Y)	Y	(Y)	Y	Y	Y	Y	Y	Y	Y		Y	Y	Y	P	Y	P	Y		Y
		^{93}Nb(n,n')^{93m}Nb								Y	Y	Y					P	P	P			Y
5 x 10^{-7} to 0.5^{b}		^{59}Co(n,γ)^{60}Co[e]	Y	Y	Y	Y	Y	Y	Y	Y	Y	Y		Y	Y	Y	P	Y	PY	Y	Y	Y
		^{109}Ag(n,γ)^{110m}Ag[e]	Y		Y	Y	Y	Y	Y	Y	Y	Y			Y		P	P	P		Y	Y
		^{58}Fe(n,γ)^{59}Fe	Y	Y	Y	Y	Y	Y	Y	Y	Y	Y			Y		P	Y	PY	Y	Y	Y
		^{45}Sc(n,γ)^{46}Sc[e]	Y		Y	Y	Y	Y	Y		Y	Y			Y		P	P	PY		Y	Y
		^{235}U(n,f)^{140}Ba-La	Y	(N)	Y	(N)	Y	Y	(N)	(N)	(N)	(N)	(N)	(N)	(N)		(N)	(N)	(N)	(N)		(N)
		^{235}U(n,f)^{103}Ru	(Y)		(Y)		Y	Y	Y	Y	Y	Y			Y		P	P	P			Y
		^{235}U(n,f)^{95}Zr-Nb	(Y)		(Y)		Y	Y	Y	Y	Y	Y			Y		P	P	P			Y
		^{235}U(n,f)^{137}Cs	(Y)		(Y)		Y	Y	Y	Y	Y	Y			Y		P	P	P			Y
As Above[a]	SSTRs[h]	^{238}U(n,f)FP					Y		Y	Y	Y	Y			Y		P	P	P			
		^{232}Th(n,f)FP					Y								Y		P	P	P			
		^{237}Np(n,f)FP					Y		Y	Y	Y	Y			Y		P	P	P			
		^{235}U(n,f)FP					Y		Y	Y	Y	Y			Y		P	P	P		Y	
		^{239}Pu(n,f)FP					Y										P	P	P			
<0.1		^{6}Li(n,α)															P	P	P			
		^{10}B(n,α)															P	P	P			
>0.3		H(n,p) as CR-39		N		N		N		N		N	(N)	N		N	(P)	N	(P)			N
>4	HAFMs[d]	Ni(n,He) as metal[f]							(Y)	Y	(Y)	Y		Y	(Y)	Y	(P)	P	(Y)		(Y)	(Y)
		Al(n,He) as metal[f]	N		N		N		N	Y	(N)	Y		Y	N	Y	N	P	N		N	(Y)
		Cu(n,He) as metal[f]	N		N		N		N	Y	(N)	Y		Y	N	Y	N	P	N		N	(Y)
		Fe(n,He) as metal[f,h]	N		N		N		N	Y	(N)	Y		Y	N	Y	N	P	N		N	(Y)
>0.1[b]		^{7}Li(n,He) as LiF															P	P				
		Be(n,He) as metal								Y	Y						P	P				(Y)
		S(n,He) as PbS									Y						P	P				
		F(n,He) as PbF_2									Y						P	P				
		Ca(n,He) as CaF_2									Y						P	P				
		N(n,He) as NbN or TiN									Y						P	P				(Y)
		Cl(n,He) as $PbCl_2$									Y						P	P				
		O(n,He) as GeO_2															P	P				
<0.1		^{6}Li(n,He) as LiF or alloy								Y	Y						P	P				(Y)
		^{10}B(n,He) nat. or alloy								Y	Y						P	P				(Y)
>0.1	DMs[c]	Quartz															P	P				
		Sapphire								Y							P	P				
		A302B[f,k]								Y				Y			P	P				
		A533B[f,k]								Y				(Y)		Y	P	P				
		Other Steel[f]								Y		Y				Y	P	P				P

*See footnotes for this table on next page. B & W, CE, GE, and WEC are Babcock and Wilcox, Combustion Engineering, General Electric, and Westinghouse Electric Company, respectively.

TABLE 4.1.4.1 FOOTNOTES*

[a] Energy ranges for the solid state track recorders (SSTRs) are the same as those given for the fissionable radiometric sensors.

[b] Generally these reactions are used with cadmium, cadmium-oxide or gadolinium filters to eliminate their sensitivity to neutrons having energies less than 0.5 eV. The cavity measurements in the Arkansas Power & Light reactors have also included intermediate-energy measurements using thick (1.65 g/cm^2) ^{10}B filters (shells) for the ^{235}U, ^{238}U and ^{237}P fission sensors.

[c] DM means damage monitors (damage to the sensor crystal lattice, such as sapphire, A302B and A533B or other steels with high copper and nickel content and high sensitivity to damage).

[d] HAFM means helium accumulation fluence monitors.

[e] Generally cobalt and silver are included as dilute alloys with aluminum. Scandium is normally Sc_2O_3, and more recently is included as a ∿0.1% Sc_2O_3-MgO ceramic wire.

[f] Frequently when there is no specific HAFM dosimetry package, some radiometric sensors and some steel damage monitors serve as HAFMs after they have been analyzed for their principal function.

[g] Ni and/or Fe gradient disks were also included in the SSTR capsule, as required.

[h] Iron from RM sensors or Charpy specimens. Postirradiation determination of the boron content of these sensors has been noted to permit direct measurement of the thermal fluence.

[i] CR means power plant Crystal River-3 (Florida Power Corp.) and DB means Davis Besse-1 (Toledo Edison Co.).

[j] The Y following the P refers to a previous Oconee 2 test.

[k] Surveillance capsule reference correlation material (ASTM reference steel plates).

[l] The determination (or feasibility) of using any of the Oconee plants for future bench mark studies has yet to be made.

GE - General Electric
WEC - Westinghouse Electric Company
B&W - Babcock and Wilcox
CE - Combustion Engineering

Y - Yes, this type of dosimetry has been used.
P - This type is planned for use.
N - This type is not desired or cannot be used.
() - There is some doubt about any of the letters enclosed in parentheses.

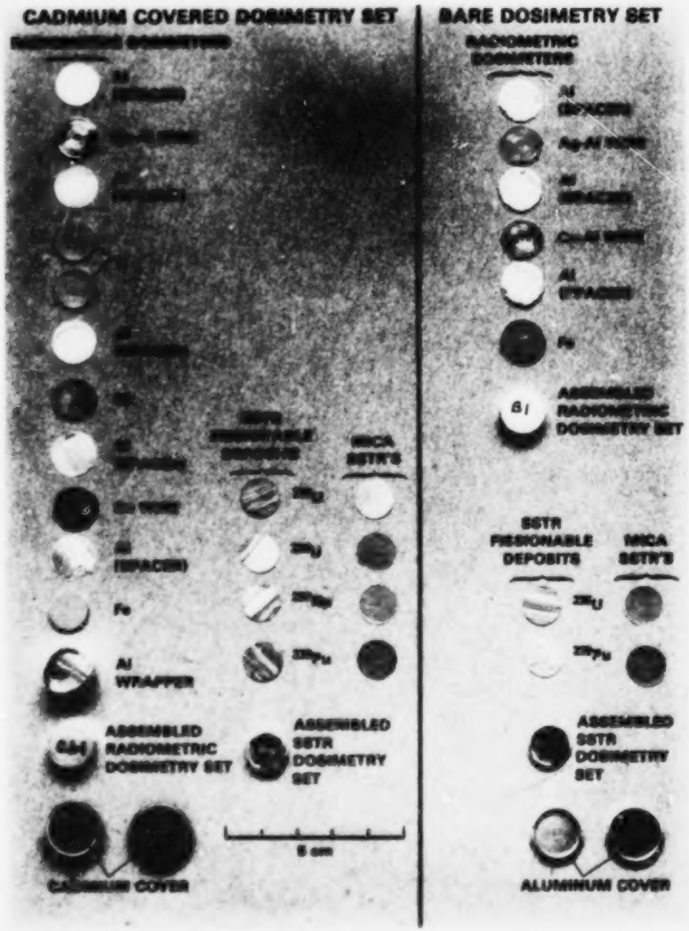
CADMIUM COVERED DOSIMETRY SET
RADIOMETRIC DOSIMETERS
Al (SPACER)
Al (SPACER)
Fe
Al (SPACER)
Al (SPACER)
Fe
Al WRAPPER
ASSEMBLED RADIOMETRIC DOSIMETRY SET
SSTR FISSIONABLE DEPOSITS
MICA SSTR'S
^{235}U
^{238}U
^{237}Np
^{239}Pu
ASSEMBLED SSTR DOSIMETRY SET
5 cm
CADMIUM COVER
BARE DOSIMETRY SET
RADIOMETRIC DOSIMETERS
Al (SPACER)
Ag-Al WIRE
Al (SPACER)
Co-Al WIRE
Al (SPACER)
Fe
ASSEMBLED RADIOMETRIC DOSIMETRY SET
SSTR FISSIONABLE DEPOSITS
MICA SSTR'S
^{235}U
^{239}Pu
ASSEMBLED SSTR DOSIMETRY SET
ALUMINUM COVER

FIGURE 4.1.4.2. Advanced Cavity Dosimetry Set for Light Water Reactor Pressure Vessel Surveillance.

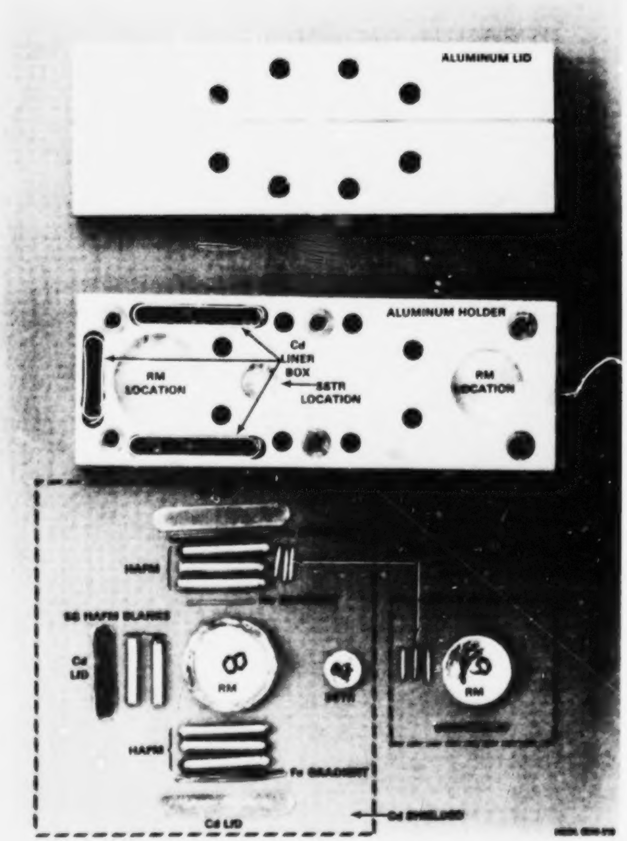
ALUMINUM LID
ALUMINUM HOLDER
Cd LINER BOX
RM LOCATION
SSTR LOCATION
RM LOCATION
HAFM
SS HAFM BLANKS
Cd LID
RM
SSTR
RM
HAFM
Fe GRADIENT
Cd LID
Cd SHIELDED

FIGURE 4.1.4.3. Cavity Dosimetry Holder for Light Water Reactor Pressure Vessel Surveillance.

TABLE 4.1.4.2

ADVANCED CAVITY SURVEILLANCE DOSIMETRY IN OPERATING LWRs

Location	Number of Sets RM	 SSTR	 HAFM
Maine Yankee	6	5	3
H. B. Robinson	6	6	*
Turkey Point 3	6	6	*
Diablo Canyon 1	6	6	*
Diablo Canyon 2	6	6	*
Zion 1 (planned)	(6)	(6)	*
Zion 2 (planned)	(6)	(6)	*
Brunswick (BWR) (planned)	(2)	(2)	*
B&W Reactors (planned)	TBD	TBD	*

---

*No separate HAFM sets are included. However, after radiometric analysis, selected RMs can be analyzed for helium (see text).

118

4.2 WESTINGHOUSE SURVEILLANCE CAPSULES: SPECIFIC DETAILS

At present capsules from Westinghouse plants have been reanalyzed. All a priori neutron spectra were supplied by Stan Anderson of Westinghouse. The calculated spectra were determined with two-dimensional transport calculations. For this report issue, the three-loop plants (Turkey Point, H. B. Robinson, and Surry) used spectra calculated for four-loop shield plants as the a priori spectrum input to the FERRET code. Consequently, as correct spectra are available and dosimetry for these plants are reanalyzed, the exposure values will change. However, the change is expected to be within the specified uncertainties for each capsule.

The dosimetry information used to determine the exposures is summarized in one figure and four tables for each capsule reported. A general note explaining the number designation is in order. All tables are identified with Section 4 of this NUREG report. The second number designates the reactor plant vendor (W=2, CE=3, B&W=4, and GE=5). The third number delineates between generic designs of the vendor. For further discussion of specific vendor generic plants see Sections 1 through 3. The fourth number designates tabulated information for a specific plant, and the fifth number designates the specific capsule. The last number refers to the table or figure number for the specific capsule information.

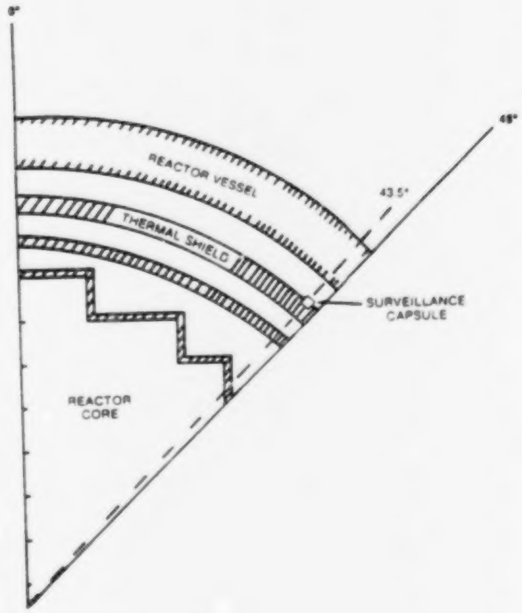
0°
45°
43.5°
REACTOR VESSEL
THERMAL SHIELD
SURVEILLANCE CAPSULE
REACTOR CORE

(a) Reactor Geometry.

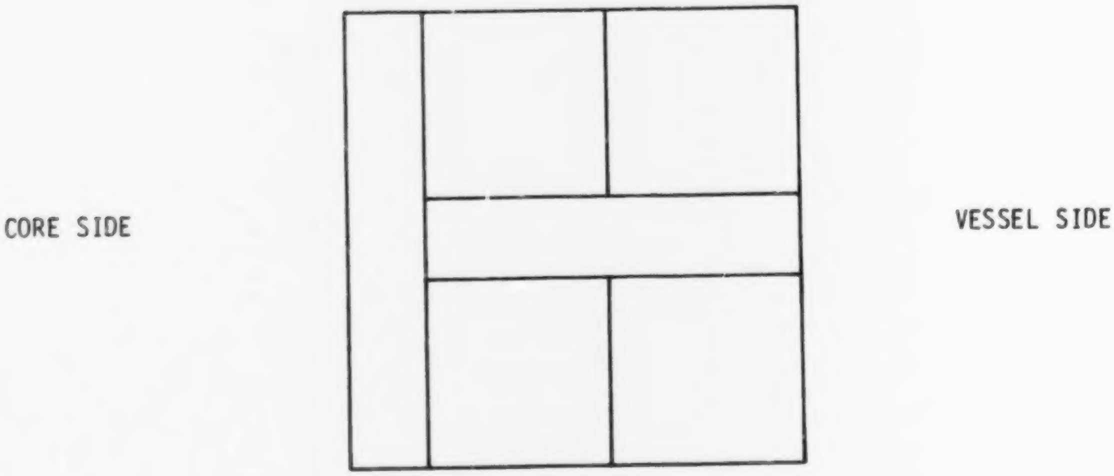
CORE SIDE
VESSEL SIDE

(b) Plan View of Surveillance Capsule

FIGURE 4.2.1.1.1.1. Orientation of the Capsule Relative to the Core and Vessel Wall - Connecticut Yankee Capsule A.

TABLE 4.2.1.1.1.1

SUMMARY OF REACTOR OPERATIONS
CONNECTICUT YANKEE CAPSULE A

TIME PERIOD	START DATE	TIME INTERVAL	AVERAGE POWER LEVEL (MWt)	LOCAL POWER FACTOR
1	10/ 1/67	31.	246.	1.00
2	11/ 1/67	30.	635.	1.00
3	12/ 1/67	31.	1434.	1.00
4	1/ 1/68	31.	982.	1.00
5	2/ 1/68	29.	1467.	1.00
6	3/ 1/68	31.	82.	1.00
7	4/ 1/68	30.	516.	1.00
8	5/ 1/68	31.	1456.	1.00
9	6/ 1/68	30.	1204.	1.00
10	7/ 1/68	31.	1245.	1.00
11	8/ 1/68	31.	967.	1.00
12	9/ 1/68	30.	1210.	1.00
13	10/ 1/68	31.	1496.	1.00
14	11/ 1/68	30.	1279.	1.00
15	12/ 1/68	31.	1279.	1.00
16	1/ 1/69	31.	1465.	1.00
17	2/ 1/69	28.	1447.	1.00
18	3/ 1/69	31.	1619.	1.00
19	4/ 1/69	30.	662.	1.00
20	5/ 1/69	31.	785.	1.00
21	6/ 1/69	30.	1148.	1.00
22	7/ 1/69	31.	1259.	1.00
23	8/ 1/69	31.	1299.	1.00
24	9/ 1/69	30.	1467.	1.00
25	10/ 1/69	31.	1611.	1.00
26	11/ 1/69	30.	1456.	1.00
27	12/ 1/69	31.	1776.	1.00
28	1/ 1/70	31.	1812.	1.00
29	2/ 1/70	28.	1659.	1.00
30	3/ 1/70	31.	1318.	1.00
31	4/ 1/70	30.	714.	1.00
	5/ 1/70	DISCHARGED*		

---

*EFFECTIVE FULL POWER OPERATION TIME WAS 5.323+007 SECONDS AT A FULL POWER LEVEL OF 1825. MWt.

TABLE 4.2.1.1.1.2

REACTION RATE DATA AND CORRECTION FACTORS FOR CONNECTICUT YANKEE CAPSULE A

REACTION NAME	IDENT	TOR RATE (DPS/NUCL)	SATURATION FACTOR	GRADIENT FACTOR	IMPURITY FACTOR	AVG REACTION RATE (RPS/NUCL)	% UNCERT (1σ)
$^{54}Fe(n,p)^{54}Mn$	Fe-41	2.16-015	1.613+000	1.100	1.000	3.79-015	10.
	Fe-44	2.30-015	1.613+000	1.100	1.000		
	Fe-48	1.95-015	1.613+000	1.100	1.000		
$^{58}Ni(n,p)^{58}Co$	MID	4.20-015	1.388+000	0.950	1.000	5.54-015	10.
$^{238}U(n,f)^{137}Cs$	MID	2.57-017	2.650+001	1.000	0.901	1.02-014	10.
$^{237}Np(n,f)^{137}Cs$	MID	3.49-016	2.650+001	1.000	1.000	1.48-013	10.
$^{59}Co(n,\gamma)^{60}Co$	MID (Cd)	1.52-013	5.230+000	0.880	1.000	7.00-013	10.
$^{59}Co(n,\gamma)^{60}Co$	MID (B)	3.25-013	5.230+000	1.000	1.000	1.70-012	10.

CD = Cadmium-Covered Dosimeter.
B = Bare Dosimeter.

122

TABLE 4.2.1.1.1.3

FERRET-SAND II RESULTS FOR CONNECTICUT YANKEE CAPSULE A (AVERAGE FOR CAPSULE)

GROUP	ENERGY (MeV)	A PRIORI FLUX* (n/cm^2•s)	ADJUSTED FLUX (n/cm^2•s)	% UNCERTAIN (1 σ)
1	1.492+001	1.884+006	1.727+006	48.
2	1.350+001	3.917+006	3.676+006	46.
3	1.162+001	1.816+007	1.745+007	42.
4	1.000+001	5.512+007	5.420+007	39.
5	8.607+000	1.394+008	1.400+008	35.
6	7.408+000	3.285+008	3.356+008	31.
7	6.065+000	1.167+009	1.213+009	25.
8	4.966+000	1.635+009	1.709+009	22.
9	3.679+000	2.599+009	2.717+009	21.
10	2.865+000	3.711+009	3.819+009	22.
11	2.231+000	7.094+009	7.187+009	23.
12	1.738+000	1.026+010	1.009+010	25.
13	1.353+000	1.363+010	1.299+010	25.
14	1.108+000	1.358+010	1.254+010	26.
15	8.208-001	2.146+010	1.920+010	25.
16	6.393-001	1.861+010	1.624+010	28.
17	4.979-001	1.909+010	1.628+010	32.
18	3.877-001	1.882+010	1.575+010	35.
19	3.020-001	1.714+010	1.412+010	39.
20	1.832-001	2.842+010	2.313+010	42.
21	1.111-001	2.104+010	1.698+010	45.
22	6.738-002	1.485+010	1.191+010	48.
23	4.087-002	1.236+010	9.884+009	50.
24	2.554-002	1.036+010	8.269+009	51.
25	1.989-002	4.912+009	3.917+009	52.
26	1.503-002	4.956+009	3.946+009	53.
27	9.119-003	7.648+009	6.078+009	53.
28	5.531-003	7.511+009	5.950+009	53.
29	3.355-003	8.094+009	6.384+009	52.
30	2.839-003	2.798+009	2.194+009	51.
31	2.404-003	2.823+009	2.199+009	49.
32	2.035-003	2.841+009	2.195+009	47.
33	1.234-003	8.485+009	6.501+009	44.
34	7.485-004	8.162+009	6.200+009	41.
35	4.540-004	7.508+009	5.656+009	38.
36	2.754-004	6.882+009	5.145+009	35.
37	1.670-004	6.641+009	4.930+009	33.
38	1.013-004	6.801+009	4.930+009	15.
39	6.144-005	7.344+009	5.395+009	30.
40	3.727-005	7.859+009	5.752+009	31.

TABLE 4.2.1.1.1.3 (Cont'd)

FERRET-SAND II RESULTS FOR CONNECTICUT YANKEE CAPSULE A (AVERAGE FOR CAPSULE)

GROUP	ENERGY (MeV)	A PRIORI FLUX* ($n/cm^2 \cdot s$)	ADJUSTED FLUX ($n/cm^2 \cdot s$)	% UNCERTAIN ($1\ \sigma$)
41	2.260-005	7.939+009	5.792+009	33.
42	1.371-005	7.561+009	5.498+009	35.
43	8.315-006	6.858+009	4.968+009	37.
44	5.043-006	6.717+009	4.842+009	39.
45	3.059-006	6.718+009	4.816+009	39.
46	1.855-006	6.720+009	4.785+009	40.
47	1.125-006	6.722+009	4.753+009	39.
48	6.826-007	6.725+009	4.721+009	38.
49	4.140-007	6.726+009	4.692+009	36.
50	2.511-007	6.641+009	4.609+009	33.
51	1.523-007	8.990+009	6.217+009	31.
52	9.237-008	1.484+010	1.023+010	29.
53	1.000-010	3.221+010	2.191+010	21.
FLUX, E > 0.0 MeV		4.715+011	3.698+011	16.
FLUX, E < 0.414 eV		7.067+010	4.766+010	18.
FLUX, E > 0.1 MeV		2.056+011	1.770+011	19.
FLUX, E > 1.0 MeV		6.269+010	5.938+010	12.
dpa/s		1.001-010	9.056-011	12.
FLUENCE+, E > 1.0 MeV		3.337+018	3.161+018	12.
dpa+		5.329-003	4.821-003	12.

---

* ABSOLUTE CALCULATED FLUX (OR NORMALIZED TO Fe54(n,p)Mn54 REACTION RATE).

+ BASED ON 5.323+007 EFFECTIVE FULL POWER SECONDS OF EXPOSURE; UNITS OF n/cm^2 FOR FLUENCE AND TOTAL NUMBER OF DISPLACED ATOMS OF IRON PER TARGET ATOM OF IRON FOR dpa.

TABLE 4.2.1.1.1.4

COMPARISON OF MEASURED AND CALCULATED REACTION RATES USED IN THE ANALYSIS OF CONNECTICUT YANKEE CAPSULE A

	REACTION RATE (DPS/NUCLEUS)			RATIO MEAS/CALC	
REACTION	MEAS	A PRIORI CALC	ADJ CALC	A PRIORI	ADJ CALC
Fe54(n,p)Mn54	3.79-015	3.78-015	3.88-015	1.00	.98
Ni58(n,p)Co58	5.54-015	5.11-015	5.32-015	1.09	1.04
Np237(n,f)Cs137	1.48-013	1.63-013	1.49-013	.91	.99
Co59(n,γ)Co60	1.70-012	2.46-012	1.72-012	.69	.99
Co59(n,γ)Co60 (Cd)	7.00-013	9.69-013	7.00-013	.72	1.00
*U238(n,f)Fp Cd	1.02-014	2.07-014	2.06-014	.49	.50

---

* REACTION NOT USED TO ADJUST SPECTRUM

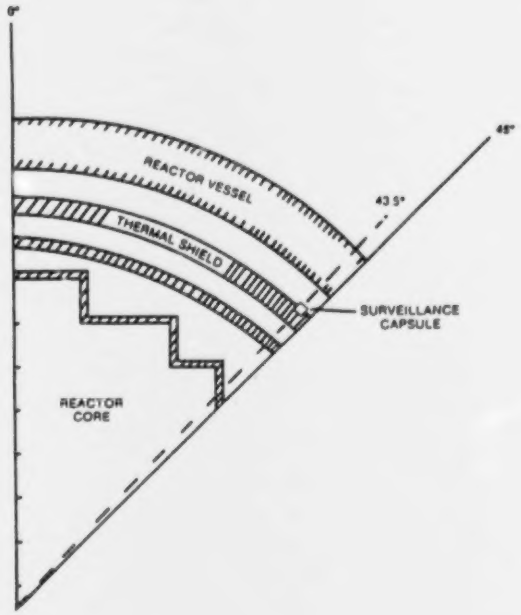
0°
45°
43.5°
REACTOR VESSEL
THERMAL SHIELD
SURVEILLANCE CAPSULE
REACTOR CORE

(a) Reactor Geometry.

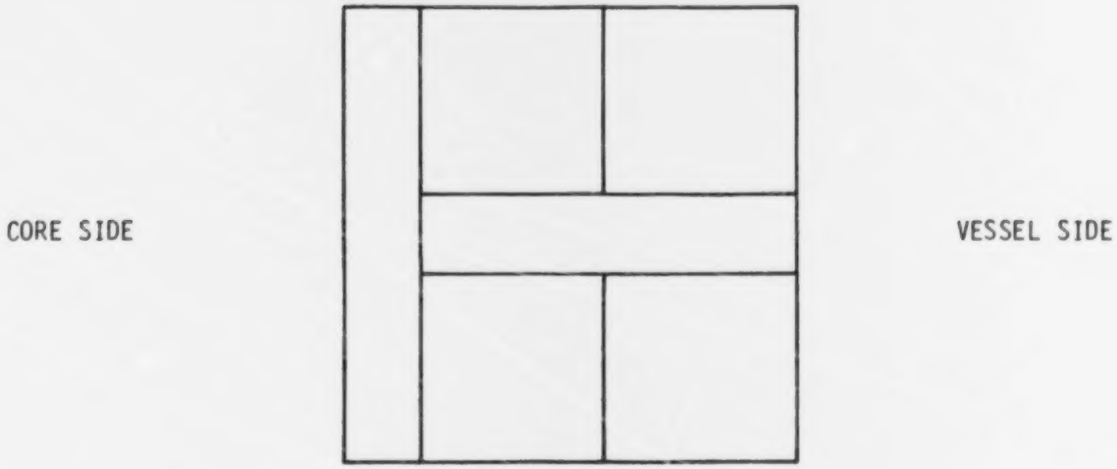
CORE SIDE
VESSEL SIDE

(b) Plan View of Surveillance Capsule

FIGURE 4.2.1.1.2.1. Orientation of the Capsule Relative to the Core and Vessel Wall - Connecticut Yankee Capsule F.

TABLE 4.2.1.1.2.1

SUMMARY OF REACTOR OPERATIONS
CONNECTICUT YANKEE CAPSULE F

TIME PERIOD	START DATE	TIME INTERVAL	AVERAGE POWER LEVEL (MWt)	LOCAL POWER FACTOR
1	10/ 1/67	31.	246.	1.00
2	11/ 1/67	30.	635.	1.00
3	12/ 1/67	31.	1434.	1.00
4	1/ 1/68	31.	982.	1.00
5	2/ 1/68	29.	1467.	1.00
6	3/ 1/68	31.	82.	1.00
7	4/ 1/68	30.	516.	1.00
8	5/ 1/68	31.	1456.	1.00
9	6/ 1/68	30.	1204.	1.00
10	7/ 1/68	31.	1245.	1.00
11	8/ 1/68	31.	967.	1.00
12	9/ 1/68	30.	1210.	1.00
13	10/ 1/68	31.	1496.	1.00
14	11/ 1/68	30.	1279.	1.00
15	12/ 1/68	31.	1279.	1.00
16	1/ 1/69	31.	1465.	1.00
17	2/ 1/69	28.	1447.	1.00
18	3/ 1/69	31.	1619.	1.00
19	4/ 1/69	30.	662.	1.00
20	5/ 1/69	31.	785.	1.00
21	6/ 1/69	30.	1148.	1.00
22	7/ 1/69	31.	1259.	1.00
23	8/ 1/69	31.	1299.	1.00
24	9/ 1/69	30.	1467.	1.00
25	10/ 1/69	31.	1611.	1.00
26	11/ 1/69	30.	1456.	1.00
27	12/ 1/69	31.	1776.	1.00
28	1/ 1/70	31.	1812.	1.00
29	2/ 1/70	28.	1659.	1.00
30	3/ 1/70	31.	1318.	1.00
31	4/ 1/70	30.	714.	1.00
32	5/ 1/70	31.	0.	1.00
33	6/ 1/70	30.	69.	1.00
34	7/ 1/70	31.	1675.	1.00
35	8/ 1/70	31.	1520.	1.00
36	9/ 1/70	30.	1462.	1.00
37	10/ 1/70	31.	1728.	1.00
38	11/ 1/70	30.	1781.	1.00
39	12/ 1/70	31.	1761.	1.00
40	1/ 1/71	31.	1810.	1.00
41	2/ 1/71	28.	1787.	1.00
42	3/ 1/71	31.	1736.	1.00
43	4/ 1/71	17.	1478.	1.00
	4/18/71	DISCHARGED*		

---

*EFFECTIVE FULL POWER OPERATION TIME WAS 7.651+007 SECONDS AT A FULL POWER LEVEL OF 1825. MWt.

TABLE 4.2.1.1.2.2

REACTION RATE DATA AND CORRECTION FACTORS FOR CONNECTICUT YANKEE CAPSULE F

REACTION NAME	IDENT	TOR RATE (DPS/NUCL)	SATURATION FACTOR	GRADIENT FACTOR	IMPURITY FACTOR	AVG REACTION RATE (RPS/NUCL)	% UNCERT (1σ)
^{54}Fe(n,p)^{54}Mn	C-24	3.32-015	1.378+000	1.100	1.000	5.11-015	10.
	C-20	3.47-015	1.378+000	1.100	1.000		
	C-17	3.32-015	1.378+000	1.100	1.000		
^{63}Cu(n,α)^{60}Co	TOP	1.08-017	3.837+000	1.080	1.000	4.68-017	10.
	MID	1.19-017	3.837+000	1.080	1.000		
	BOT	1.12-017	3.837+000	1.080	1.000		
^{59}Co(n,γ)^{60}Co	TOP (B)	4.88-013	3.837+000	0.930	1.000	2.41-012	24.
	MID (B)	7.78-013	3.837+000	0.930	1.000		
	BOT (B)	7.62-013	3.837+000	0.930	1.000		
^{59}Co(n,γ)^{60}Co	TOP (Cd)	2.36-013	3.837+000	1.190	1.000	1.06-012	10.
	BOT (Cd)	2.29-013	3.837+000	1.190	1.000		

CD = Cadmium-Covered Dosimeter.
B = Bare Dosimeter.

TABLE 4.2.1.1.2.3

FERRET-SAND II RESULTS FOR CONNECTICUT YANKEE CAPSULE F (AVERAGE FOR CAPSULE)

GROUP	ENERGY (MeV)	A PRIORI FLUX* ($n/cm^2 \cdot s$)	ADJUSTED FLUX ($n/cm^2 \cdot s$)	% UNCERTAIN (1 σ)
1	1.492+001	2.535+006	2.518+006	41.
2	1.350+001	5.271+006	5.309+006	38.
3	1.162+001	2.444+007	2.493+007	34.
4	1.000+001	7.417+007	7.657+007	30.
5	8.607+000	1.876+008	1.954+008	26.
6	7.408+000	4.420+008	4.608+008	24.
7	6.065+000	1.570+009	1.641+009	20.
8	4.966+000	2.200+009	2.256+009	22.
9	3.679+000	3.497+009	3.523+009	22.
10	2.865+000	4.993+009	4.952+009	24.
11	2.231+000	9.546+009	9.322+009	27.
12	1.738+000	1.381+010	1.328+010	31.
13	1.353+000	1.834+010	1.737+010	35.
14	1.108+000	1.828+010	1.705+010	39.
15	8.208-001	2.888+010	2.659+010	42.
16	6.393-001	2.505+010	2.280+010	46.
17	4.979-001	2.569+010	2.317+010	48.
18	3.877-001	2.533+010	2.268+010	51.
19	3.020-001	2.306+010	2.054+010	52.
20	1.832-001	3.825+010	3.393+010	54.
21	1.111-001	2.832+010	2.505+010	55.
22	6.738-002	1.998+010	1.763+010	55.
23	4.087-002	1.663+010	1.465+010	56.
24	2.554-002	1.394+010	1.226+010	56.
25	1.989-002	6.610+009	5.802+009	56.
26	1.503-002	6.669+009	5.841+009	55.
27	9.119-003	1.029+010	8.990+009	55.
28	5.531-003	1.011+010	8.799+009	54.
29	3.355-003	1.089+010	9.444+009	53.
30	2.839-003	3.764+009	3.249+009	51.
31	2.404-003	3.799+009	3.262+009	49.
32	2.035-003	3.823+009	3.264+009	47.
33	1.234-003	1.142+010	9.690+009	44.
34	7.485-004	1.098+010	9.266+009	41.
35	4.540-004	1.010+010	8.476+009	38.
36	2.754-004	9.261+009	7.728+009	35.
37	1.670-004	8.936+009	7.419+009	33.
38	1.013-004	9.152+009	7.476+009	16.
39	6.144-005	9.882+009	8.134+009	30.
40	3.727-005	1.058+010	8.674+009	31.

129

TABLE 4.2.1.1.2.3 (Cont'd)

FERRET-SAND II RESULTS FOR
CONNECTICUT YANKEE CAPSULE F
(AVERAGE FOR CAPSULE)

GROUP	ENERGY (MeV)	A PRIORI FLUX* ($n/cm^2 \cdot s$)	ADJUSTED FLUX ($n/cm^2 \cdot s$)	% UNCERTAIN (1 σ)
41	2.260-005	1.068+010	8.728+009	33.
42	1.371-005	1.017+010	8.276+009	35.
43	8.315-006	9.229+009	7.468+009	37.
44	5.043-006	9.038+009	7.269+009	39.
45	3.059-006	9.040+009	7.219+009	41.
46	1.855-006	9.043+009	7.164+009	42.
47	1.125-006	9.046+009	7.107+009	42.
48	6.826-007	9.050+009	7.052+009	42.
49	4.140-007	9.051+009	7.001+009	41.
50	2.511-007	8.937+009	6.870+009	41.
51	1.523-007	1.210+010	9.257+009	40.
52	9.237-008	1.996+010	1.522+010	39.
53	1.000-010	4.334+010	3.260+010	36.
FLUX, E > 0.0 MeV		6.736+011	5.362+011	25.
FLUX, E < 0.414 eV		1.010+011	7.095+010	32.
FLUX, E > 0.1 MeV		2.938+011	2.486+011	36.
FLUX, E > 1.0 MeV		8.956+010	7.925+010	24.
dpa/s		1.430-010	1.240-010	27.
FLUENCE+, E > 1.0 MeV		6.853+018	6.064+018	24.
dpa+		1.094-002	9.491-003	27.

---

* ABSOLUTE CALCULATED FLUX (OR NORMALIZED TO Fe54(n,p)Mn54 REACTION RATE).

+ BASED ON 7.651+007 EFFECTIVE FULL POWER SECONDS OF EXPOSURE; UNITS OF n/cm^2 FOR FLUENCE AND TOTAL NUMBER OF DISPLACED ATOMS OF IRON PER TARGET ATOM OF IRON FOR dpa.

BEST COPY AVAILABLE

TABLE 4.2.1.1.2.4

COMPARISON OF MEASURED AND CALCULATED REACTION RATES USED IN THE ANALYSIS OF CONNECTICUT YANKEE CAPSULE F

	REACTION RATE (DPS/NUCLEUS)			RATIO MEAS/CALC	
REACTION	MEAS	A PRIORI CALC	ADJ CALC	A PRIORI	ADJ CALC
Fe54(n,p)Mn54	5.11-015	5.09-015	5.12-015	1.00	1.00
Cu63(n,α)Co60	4.68-017	4.44-017	4.63-017	1.05	1.01
Co59(n,γ)Co60	2.41-012	3.31-012	2.58-012	.73	.93
Co59(n,γ)Co60 (Cd)	1.06-012	1.30-012	1.06-012	.81	1.00

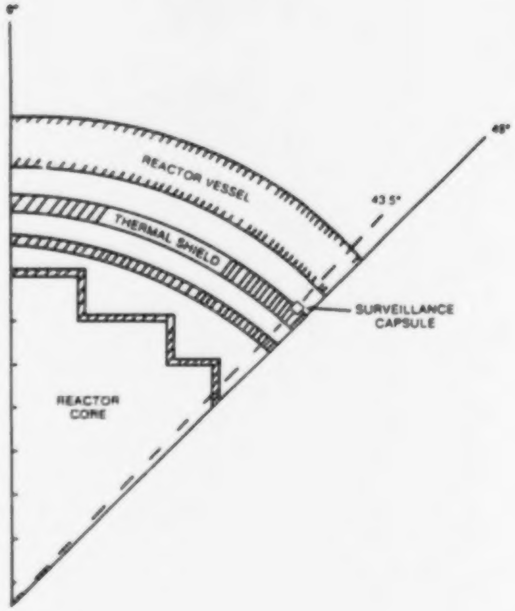
0°
45°
43.5°
REACTOR VESSEL
THERMAL SHIELD
SURVEILLANCE CAPSULE
REACTOR CORE

(a) Reactor Geometry.

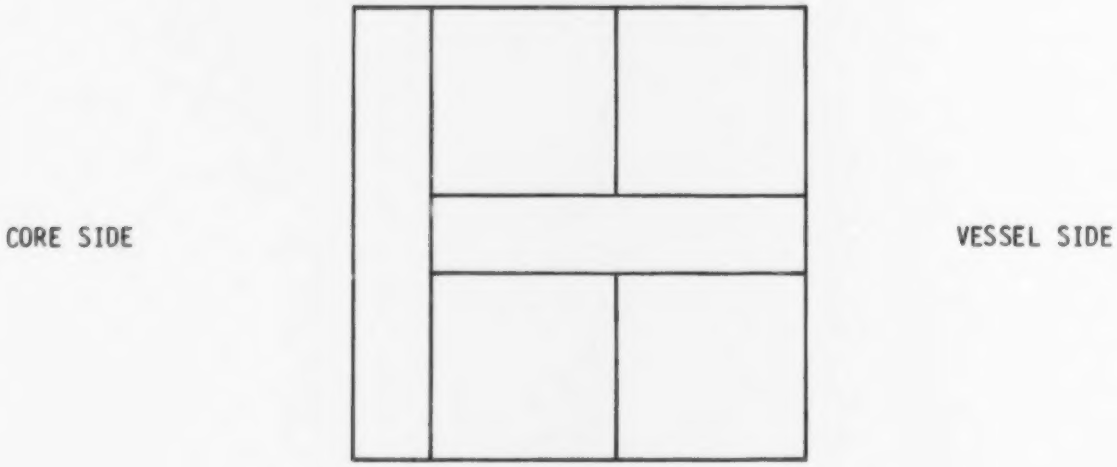
CORE SIDE
VESSEL SIDE

(b) Plan View of Surveillance Capsule

FIGURE 4.2.1.1.3.1. Orientation of the Capsule Relative to the Core and Vessel Wall - Connecticut Yankee Capsule H.

TABLE 4.2.1.1.3.1

SUMMARY OF REACTOR OPERATIONS
CONNECTICUT YANKEE CAPSULE H

TIME PERIOD	START DATE	TIME INTERVAL	AVERAGE POWER LEVEL (MWt)	LOCAL POWER FACTOR
1	10/ 1/67	31.	246.	1.00
2	11/ 1/67	30.	635.	1.00
3	12/ 1/67	31.	1434.	1.00
4	1/ 1/68	31.	982.	1.00
5	2/ 1/68	29.	1467.	1.00
6	3/ 1/68	31.	82.	1.00
7	4/ 1/68	30.	516.	1.00
8	5/ 1/68	31.	1456.	1.00
9	6/ 1/68	30.	1204.	1.00
10	7/ 1/68	31.	1245.	1.00
11	8/ 1/68	31.	967.	1.00
12	9/ 1/68	30.	1210.	1.00
13	10/ 1/68	31.	1496.	1.00
14	11/ 1/68	30.	1279.	1.00
15	12/ 1/68	31.	1279.	1.00
16	1/ 1/69	31.	1465.	1.00
17	2/ 1/69	28.	1447.	1.00
18	3/ 1/69	31.	1619.	1.00
19	4/ 1/69	30.	662.	1.00
20	5/ 1/69	31.	785.	1.00
21	6/ 1/69	30.	1148.	1.00
22	7/ 1/69	31.	1259.	1.00
23	8/ 1/69	31.	1299.	1.00
24	9/ 1/69	30.	1467.	1.00
25	10/ 1/69	31.	1611.	1.00
26	11/ 1/69	30.	1456.	1.00
27	12/ 1/69	31.	1776.	1.00
28	1/ 1/70	31.	1812.	1.00
29	2/ 1/70	28.	1659.	1.00
30	3/ 1/70	31.	1318.	1.00
31	4/ 1/70	30.	714.	1.00
32	5/ 1/70	31.	0.	1.00
33	6/ 1/70	30.	69.	1.00
34	7/ 1/70	31.	1675.	1.00
35	8/ 1/70	31.	1520.	1.00
36	9/ 1/70	30.	1462.	1.00
37	10/ 1/70	31.	1728.	1.00
38	11/ 1/70	30.	1781.	1.00
39	12/ 1/70	31.	1761.	1.00
40	1/ 1/71	31.	1810.	1.00
41	2/ 1/71	28.	1787.	1.00
42	3/ 1/71	31.	1736.	1.00
43	4/ 1/71	30.	838.	1.00

TABLE 4.2.1.1.3.1 (Cont'd)

SUMMARY OF REACTOR OPERATIONS
CONNECTICUT YANKEE CAPSULE H

TIME PERIOD	START DATE	TIME INTERVAL	AVERAGE POWER LEVEL (MWt)	LOCAL POWER FACTOR
44	5/ 1/71	31.	237.	1.00
45	6/ 1/71	61.	1621.	1.00
46	8/ 1/71	31.	1686.	1.00
47	9/ 1/71	30.	1745.	1.00
48	10/ 1/71	31.	1692.	1.00
49	11/ 1/71	30.	1825.	1.00
50	12/ 1/71	31.	1748.	1.00
51	1/ 1/72	31.	1772.	1.00
52	2/ 1/72	29.	1754.	1.00
53	3/ 1/72	31.	1810.	1.00
54	4/ 1/72	30.	1803.	1.00
55	5/ 1/72	31.	1747.	1.00
56	6/ 1/72	30.	516.	1.00
57	7/ 1/72	31.	794.	1.00
58	8/ 1/72	31.	1763.	1.00
59	9/ 1/72	30.	1555.	1.00
60	10/ 1/72	31.	1812.	1.00
61	11/ 1/72	30.	1619.	1.00
62	12/ 1/72	31.	1812.	1.00
63	1/ 1/73	181.	1606.	1.00
64	7/ 1/73	184.	175.	1.00
65	1/ 1/74	31.	1721.	1.00
66	2/ 1/74	28.	1736.	1.00
67	3/ 1/74	31.	1288.	1.00
68	4/ 1/74	30.	535.	1.00
69	5/ 1/74	31.	1748.	1.00
70	6/ 1/74	30.	1664.	1.00
71	7/ 1/74	31.	1703.	1.00
72	8/ 1/74	31.	1701.	1.00
73	9/ 1/74	30.	1719.	1.00
74	10/ 1/74	31.	1672.	1.00
75	11/ 1/74	30.	1794.	1.00
76	12/ 1/74	31.	1743.	1.00
77	1/ 1/75	31.	1803.	1.00
78	2/ 1/75	28.	1703.	1.00
79	3/ 1/75	31.	1675.	1.00
80	4/ 1/75	30.	1796.	1.00

TABLE 4.2.1.1.3.1 (Cont'd)

SUMMARY OF REACTOR OPERATIONS
CONNECTICUT YANKEE CAPSULE H

TIME PERIOD	START DATE	TIME INTERVAL	AVERAGE POWER LEVEL (MWt)	LOCAL POWER FACTOR
81	5/ 1/75	31.	872.	1.00
82	6/ 1/75	30.	2.	1.00
83	7/ 1/75	31.	1712.	1.00
84	8/ 1/75	31.	1728.	1.00
85	9/ 1/75	30.	1747.	1.00
86	10/ 1/75	31.	1803.	1.00
87	11/ 1/75	30.	1801.	1.00
88	12/ 1/75	31.	1579.	1.00
89	1/ 1/76	31.	1737.	1.00
90	2/ 1/76	29.	1796.	1.00
91	3/ 1/76	31.	1792.	1.00
92	4/ 1/76	30.	1622.	1.00
93	5/ 1/76	31.	1031.	1.00
94	6/ 1/76	30.	0.	1.00
95	7/ 1/76	31.	673.	1.00
96	8/ 1/76	31.	1726.	1.00
97	9/ 1/76	30.	1748.	1.00
98	10/ 1/76	31.	1823.	1.00
99	11/ 1/76	30.	1821.	1.00
100	12/ 1/76	31.	1807.	1.00
101	1/ 1/77	31.	1821.	1.00
102	2/ 1/77	28.	1818.	1.00
103	3/ 1/77	31.	1823.	1.00
104	4/ 1/77	30.	1821.	1.00
105	5/ 1/77	31.	1805.	1.00
106	6/ 1/77	30.	1779.	1.00
107	7/ 1/77	31.	1739.	1.00
108	8/ 1/77	31.	1223.	1.00
109	9/ 1/77	30.	1725.	1.00
110	10/ 1/77	31.	779.	1.00
	11/ 1/77	DISCHARGED*		

---

*EFFECTIVE FULL POWER OPERATION TIME WAS 2.390+008 SECONDS AT A FULL POWER LEVEL OF 1825. MWt.

135

TABLE 4.2.1.1.3.2

REACTION RATE DATA AND CORRECTION FACTORS FOR CONNECTICUT YANKEE CAPSULE H

REACTION NAME	IDENT	TOR RATE (DPS/NUCL)	SATURATION FACTOR	GRADIENT FACTOR	IMPURITY FACTOR	AVG REACTION RATE (RPS/NUCL)	% UNCERT (1σ)
$^{54}\mathrm{Fe}(n,p)^{54}\mathrm{Mn}$	R-33	4.24-015	1.194+000	0.960	1.000	5.13-015	10.
	C-33	3.92-015	1.194+000	1.100	1.000		
	R-40	4.40-015	1.194+000	0.960	1.000		
	C-40	3.64-015	1.194+000	1.100	1.000		
	R-37	4.86-015	1.194+000	0.960	1.000		
	C-37	4.11-015	1.194+000	1.100	1.000		
$^{63}\mathrm{Cu}(n,\alpha)^{60}\mathrm{Co}$	TOP	2.55-017	1.754+000	1.080	1.000	4.96-017	10.
	MID	2.69-017	1.754+000	1.080	1.000		
$^{59}\mathrm{Co}(n,\gamma)^{60}\mathrm{Co}$	TOP (CD)	7.96-013	1.754+000	1.190	1.000	1.66-012	10.
	MID (CD)	7.96-013	1.754+000	1.190	1.000		
	BOT (CD)	7.90-013	1.754+000	1.190	1.000		
$^{59}\mathrm{Co}(n,\gamma)^{60}\mathrm{Co}$	TOP (B)	2.29-012	1.754+000	0.930	1.000	3.71-012	10.
	MID (B)	2.28-012	1.754+000	0.930	1.000		
	BOT (B)	2.26-012	1.754+000	0.930	1.000		

CD = Cadmium-Covered Dosimeter.
B = Bare Dosimeter.

TABLE 4.2.1.1.3.3

FERRET-SAND II RESULTS FOR CONNECTICUT YANKEE CAPSULE H (AVERAGE FOR CAPSULE)

GROUP	ENERGY (MeV)	A PRIORI FLUX* ($n/cm^2 \cdot s$)	ADJUSTED FLUX ($n/cm^2 \cdot s$)	% UNCERTAIN (1 σ)
1	1.492+001	2.609+006	2.959+006	41.
2	1.350+001	5.425+006	6.144+006	38.
3	1.162+001	2.515+007	2.837+007	34.
4	1.000+001	7.633+007	8.568+007	30.
5	8.607+000	1.931+008	2.148+008	26.
6	7.408+000	4.549+008	4.974+008	24.
7	6.065+000	1.616+009	1.737+009	20.
8	4.966+000	2.264+009	2.344+009	22.
9	3.679+000	3.599+009	3.619+009	22.
10	2.865+000	5.139+009	5.079+009	24.
11	2.231+000	9.824+009	9.609+009	27.
12	1.738+000	1.421+010	1.386+010	31.
13	1.353+000	1.888+010	1.837+010	35.
14	1.108+000	1.881+010	1.830+010	39.
15	8.208-001	2.972+010	2.901+010	42.
16	6.393-001	2.578+010	2.532+010	45.
17	4.979-001	2.644+010	2.619+010	48.
18	3.877-001	2.607+010	2.608+010	50.
19	3.020-001	2.373+010	2.399+010	52.
20	1.832-001	3.937+010	4.021+010	53.
21	1.111-001	2.914+010	3.005+010	54.
22	6.738-002	2.056+010	2.139+010	55.
23	4.087-002	1.711+010	1.795+010	55.
24	2.554-002	1.434+010	1.516+010	55.
25	1.989-002	6.802+009	7.247+009	55.
26	1.503-002	6.863+009	7.370+009	55.
27	9.119-003	1.059+010	1.147+010	54.
28	5.531-003	1.040+010	1.138+010	54.
29	3.355-003	1.121+010	1.239+010	52.
30	2.839-003	3.874+009	4.335+009	51.
31	2.404-003	3.910+009	4.433+009	49.
32	2.035-003	3.935+009	4.523+009	47.
33	1.234-003	1.175+010	1.370+010	44.
34	7.485-004	1.130+010	1.335+010	41.
35	4.540-004	1.040+010	1.243+010	38.
36	2.754-004	9.531+009	1.150+010	35.
37	1.670-004	9.197+009	1.117+010	33.
38	1.013-004	9.419+009	1.183+010	15.
39	6.144-005	1.017+010	1.239+010	30.
40	3.727-005	1.088+010	1.318+010	31.

TABLE 4.2.1.1.3.3 (Cont'd)

FERRET-SAND II RESULTS FOR
CONNECTICUT YANKEE CAPSULE H
(AVERAGE FOR CAPSULE)

GROUP	ENERGY (MeV)	A PRIORI FLUX* (n/cm^2•s)	ADJUSTED FLUX (n/cm^2•s)	% UNCERTAIN (1 σ)
41	2.260-005	1.099+010	1.320+010	33.
42	1.371-005	1.047+010	1.242+010	35.
43	8.315-006	9.498+009	1.110+010	37.
44	5.043-006	9.302+009	1.068+010	39.
45	3.059-006	9.304+009	1.049+010	40.
46	1.855-006	9.306+009	1.030+010	40.
47	1.125-006	9.310+009	1.012+010	39.
48	6.826-007	9.314+009	9.947+009	38.
49	4.140-007	9.315+009	9.787+009	36.
50	2.511-007	9.198+009	9.518+009	34.
51	1.523-007	1.245+010	1.273+010	32.
52	9.237-008	2.055+010	2.080+010	30.
53	1.000-010	4.461+010	4.452+010	22.
FLUX, E > 0.0 MeV		4.715+011	6.774+011	23.
FLUX, E < 0.414 eV		7.067+010	9.735+010	19.
FLUX, E > 0.1 MeV		2.056+011	2.791+011	36.
FLUX, E > 1.0 MeV		6.269+010	8.366+010	24.
dpa/s		1.001-010	1.355-010	27.
FLUENCE+, E > 1.0 MeV		1.498+019	2.000+019	24.
dpa+		2.393-002	3.238-002	27.

---

* ABSOLUTE CALCULATED FLUX (OR NORMALIZED TO Fe54(n,p)Mn54 REACTION RATE).

+ BASED ON 2.390+008 EFFECTIVE FULL POWER SECONDS OF EXPOSURE; UNITS OF n/cm^2 FOR FLUENCE AND TOTAL NUMBER OF DISPLACED ATOMS OF IRON PER TARGET ATOM OF IRON FOR dpa.

TABLE 4.2.1.1.3.4

COMPARISON OF MEASURED AND CALCULATED REACTION RATES USED IN THE ANALYSIS OF CONNECTICUT YANKEE CAPSULE H.

	REACTION RATE (DPS/NUCLEUS)			RATIO MEAS/CALC	
REACTION	MEAS	A PRIORI CALC	ADJ CALC	A PRIORI	ADJ CALC
Fe54(n,p)Mn54	5.13-015	5.13-015	5.21-015	1.00	.98
Cu63(n,α)Co60	4.96-017	4.48-017	4.88-017	1.11	1.02
Co59(n,γ)Co60 (Cd)	1.66-012	1.34-012	1.64-012	1.24	1.01
Co59(n,γ)Co60	3.71-012	3.41-012	3.73-012	1.09	.99

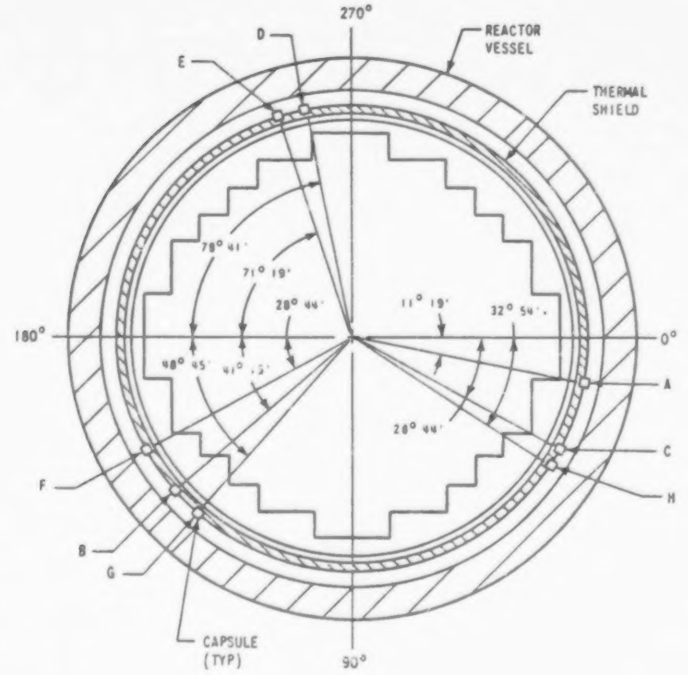
270°
D
E
REACTOR VESSEL
THERMAL SHIELD
78° 41'
71° 19'
28° 44'
11° 19'
32° 54'
180°
0°
48° 45'
41° 15'
A
28° 44'
C
F
H
B
G
CAPSULE (TYP)
90°

(a) Reactor Geometry.

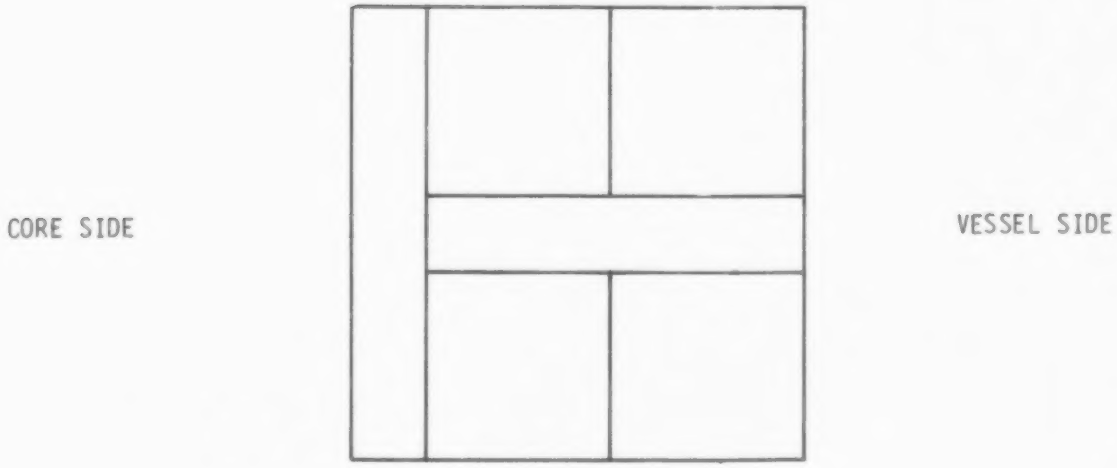
CORE SIDE
VESSEL SIDE

(b) Plan View of Surveillance Capsule

FIGURE 4.2.2.1.1.1. Orientation of the Capsule Relative to the Core and Vessel Wall - San Onofre Capsule A.

TABLE 4.2.2.1.1.1

SUMMARY OF REACTOR OPERATIONS
SAN ONOFRE UNIT 1 CAPSULE A

TIME PERIOD	START DATE	TIME INTERVAL	AVERAGE POWER LEVEL (MWt)	LOCAL POWER FACTOR
1	6/14/67	201.	240.	1.00
2	1/ 1/68	31.	944.	1.00
3	2/ 1/68	29.	700.	1.00
4	3/ 1/68	31.	277.	1.00
5	4/ 1/68	153.	0.	1.00
6	9/ 1/68	30.	254.	1.00
7	10/ 1/68	31.	1135.	1.00
8	11/ 1/68	30.	1182.	1.00
9	12/ 1/68	31.	1077.	1.00
10	1/ 1/69	31.	852.	1.00
11	2/ 1/69	28.	1150.	1.00
12	3/ 1/69	31.	773.	1.00
13	4/ 1/69	30.	1034.	1.00
14	5/ 1/69	31.	1210.	1.00
15	6/ 1/69	30.	798.	1.00
16	7/ 1/69	31.	0.	1.00
17	8/ 1/69	31.	587.	1.00
18	9/ 1/69	30.	1342.	1.00
19	10/ 1/69	31.	919.	1.00
20	11/ 1/69	30.	1331.	1.00
21	12/ 1/69	31.	1329.	1.00
22	1/ 1/70	212.	1253.	1.00
23	8/ 1/70	31.	1325.	1.00
24	9/ 1/70	30.	1337.	1.00
	10/ 1/70	DISCHARGED*		

---

*EFFECTIVE FULL POWER OPERATION TIME WAS 5.824+007 SECONDS AT A FULL POWER LEVEL OF 1347. MWt.

TABLE 4.2.2.1.1.2

REACTION RATE DATA AND CORRECTION FACTORS FOR SAN ONOFRE UNIT 1 CAPSULE A

REACTION NAME	IDENT	TOR RATE (DPS/NUCL)	SATURATION FACTOR	GRADIENT FACTOR	IMPURITY FACTOR	AVG REACTION RATE (RPS/NUCL)	% UNCERT (1σ)
^{54}Fe(n,p)^{54}Mn	R-48	1.47-014	1.419+000	1.230	1.000	2.42-014	10.
	R-47	1.43-014	1.419+000	1.120	1.000		
	R-45	1.49-014	1.419+000	1.230	1.000		
	R-42	1.33-014	1.419+000	1.120	1.000		
	R-41	1.46-014	1.419+000	1.230	1.000		
^{58}Fe(n,γ)^{59}Fe	R-48	5.43-013	1.036+000	0.820	1.000	4.86-013	10.
	R-47	5.72-013	1.036+000	0.950	1.000		
	R-45	5.06-013	1.036+000	0.820	1.000		
	R-42	4.92-013	1.036+000	0.950	1.000		
	R-41	5.76-013	1.036+000	0.820	1.000		
^{63}Cu(n,α)^{60}Co	TOP	2.83-017	4.773+000	1.200	1.000	1.60-016	10.
	MID	2.93-017	4.773+000	1.200	1.000		
	BOT	2.65-017	4.773+000	1.200	1.000		
^{58}Ni(n,p)^{58}Co	MID	2.66-014	1.056+000	1.220	1.000	3.42-014	10.
^{237}Np(n,f)^{137}Cs	MID	1.41-015	2.422+001	1.000	1.000	5.45-013	10.
^{238}U(n,f)^{137}Cs	MID	2.26-016	2.422+001	1.000	0.813	7.42-014	10.
^{59}Co(n,γ)^{60}Co	TOP (CD)	1.46-012	4.773+000	1.190	1.000	8.00-012	10.
	MID (CD)	1.35-012	4.773+000	1.190	1.000		
	BOT (CD)	1.41-012	4.773+000	1.190	1.000		
^{59}Co(n,γ)^{60}Co	BOT (B)	3.34-012	4.773+000	0.940	1.000	1.50-011	10.

CD = Cadmium-Covered Dosimeter.
B = Bare Dosimeter.

TABLE 4.2.2.1.1.3

FERRET-SAND II RESULTS FOR SAN ONOFRE CAPSULE A (AVERAGE FOR CAPSULE)

GROUP	ENERGY (MeV)	A PRIORI FLUX* ($n/cm^2 \cdot s$)	ADJUSTED FLUX ($n/cm^2 \cdot s$)	% UNCERTAIN ($1\ \sigma$)
1	1.492+001	1.261+007	8.979+006	41.
2	1.350+001	2.621+007	1.855+007	38.
3	1.162+001	1.215+008	8.577+007	34.
4	1.000+001	3.688+008	2.603+008	30.
5	8.607+000	9.330+008	6.622+008	26.
6	7.408+000	2.184+009	1.576+009	24.
7	6.065+000	7.768+009	5.686+009	20.
8	4.966+000	1.200+010	9.175+009	22.
9	3.679+000	2.230+010	1.780+010	21.
10	2.865+000	3.315+010	2.724+010	21.
11	2.231+000	6.212+010	5.230+010	23.
12	1.738+000	9.165+010	7.823+010	28.
13	1.353+000	1.283+011	1.109+011	32.
14	1.108+000	1.372+011	1.194+011	36.
15	8.208-001	2.299+011	2.008+011	40.
16	6.393-001	2.086+011	1.820+011	43.
17	4.979-001	2.174+011	1.889+011	46.
18	3.877-001	2.123+011	1.831+011	49.
19	3.020-001	1.952+011	1.670+011	51.
20	1.832-001	3.310+011	2.805+011	53.
21	1.111-001	2.509+011	2.107+011	54.
22	6.738-002	1.771+011	1.476+011	54.
23	4.087-002	1.395+011	1.154+011	55.
24	2.554-002	1.125+011	9.263+010	55.
25	1.989-002	5.234+010	4.297+010	55.
26	1.503-002	5.261+010	4.313+010	55.
27	9.119-003	8.155+010	6.688+010	54.
28	5.531-003	7.983+010	6.558+010	54.
29	3.355-003	8.742+010	7.205+010	52.
30	2.839-003	3.060+010	2.532+010	51.
31	2.404-003	3.099+010	2.578+010	49.
32	2.035-003	3.125+010	2.615+010	47.
33	1.234-003	9.311+010	7.838+010	44.
34	7.485-004	8.812+010	7.460+010	41.
35	4.540-004	7.809+010	6.644+010	38.
36	2.754-004	6.866+010	5.864+010	35.
37	1.670-004	6.543+010	5.601+010	32.
38	1.013-004	6.738+010	5.851+010	14.
39	6.144-005	7.099+010	6.070+010	30.
40	3.727-005	7.443+010	6.338+010	31.

TABLE 4.2.2.1.1.3 (Cont'd)

FERRET-SAND II RESULTS FOR
SAN ONOFRE CAPSULE A
(AVERAGE FOR CAPSULE)

GROUP	ENERGY (MeV)	A PRIORI FLUX* ($n/cm^2 \cdot s$)	ADJUSTED FLUX ($n/cm^2 \cdot s$)	% UNCERTAI (1 σ)
41	2.260-005	7.557+010	6.395+010	33.
42	1.371-005	7.386+010	6.199+010	35.
43	8.315-006	6.941+010	5.768+010	37.
44	5.043-006	6.383+010	5.245+010	39.
45	3.059-006	5.879+010	4.772+010	40.
46	1.855-006	5.434+010	4.357+010	40.
47	1.125-006	5.053+010	4.002+010	40.
48	6.826-007	4.781+010	3.743+010	39.
49	4.140-007	4.957+010	3.839+010	37.
50	2.511-007	7.717+010	5.916+010	35.
51	1.523-007	8.027+010	6.109+010	33.
52	9.237-008	7.550+010	5.719+010	32.
53	1.000-010	1.824+011	1.367+011	26.
FLUX, E > 0.0 MeV		4.584+012	3.834+012	25.
FLUX, E < 0.414 eV		4.649+011	3.525+011	23.
FLUX, E > 0.1 MeV		2.181+012	1.867+012	36.
FLUX, E > 1.0 MeV		5.768+011	4.919+011	22.
dpa/s		9.827-010	8.351-010	27.
FLUENCE+, E > 1.0 MeV		3.359+019	2.865+019	22.
dpa+		5.723-002	4.864-002	27.

---

* ABSOLUTE CALCULATED FLUX (OR NORMALIZED TO Fe54(n,p)Mn54 REACTION RATE).

+ BASED ON 5.824+007 EFFECTIVE FULL POWER SECONDS OF EXPOSURE; UNITS OF n/cm^2 FOR FLUENCE AND TOTAL NUMBER OF DISPLACED ATOMS OF IRON PER TARGET ATOM OF IRON FOR dpa.

TABLE 4.2.2.1.1.4

COMPARISON OF MEASURED AND CALCULATED REACTION RATES USED IN THE ANALYSIS OF SAN ONOFRE CAPSULE A

	REACTION RATE (DPS/NUCLEUS)			RATIO MEAS/CALC	
REACTION	MEAS	A PRIORI CALC	ADJ CALC	A PRIORI	ADJ CALC
Co59(n,γ)Co60	8.00-012	9.27-012	7.94-012	.86	1.01
Co59(n,γ)Co60	1.50-011	1.87-011	1.51-011	.80	.99
Fe54(n,p)Mn54	2.41-014	3.04-014	2.42-014	.79	1.00
Ni58(n,P)Co58	3.43-014	4.16-014	3.36-014	.82	1.02
Cu63(n,α)Co60	1.60-016	2.25-016	1.63-016	.71	.98

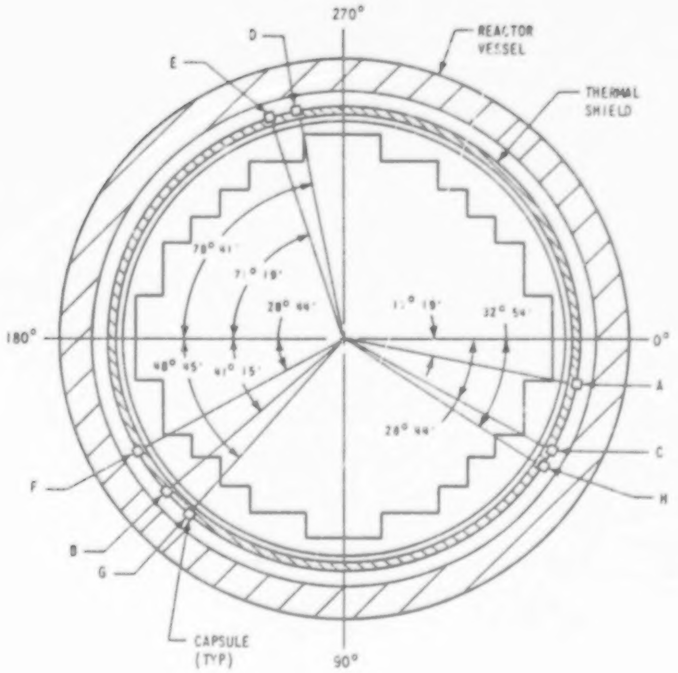
270°
D
E
REACTOR VESSEL
THERMAL SHIELD
78° 41'
71° 19'
28° 44'
11° 19'
32° 54'
180°
0°
48° 45'
41° 15'
A
28° 44'
C
F
H
B
G
CAPSULE (TYP)
90°

(a) Reactor Geometry.

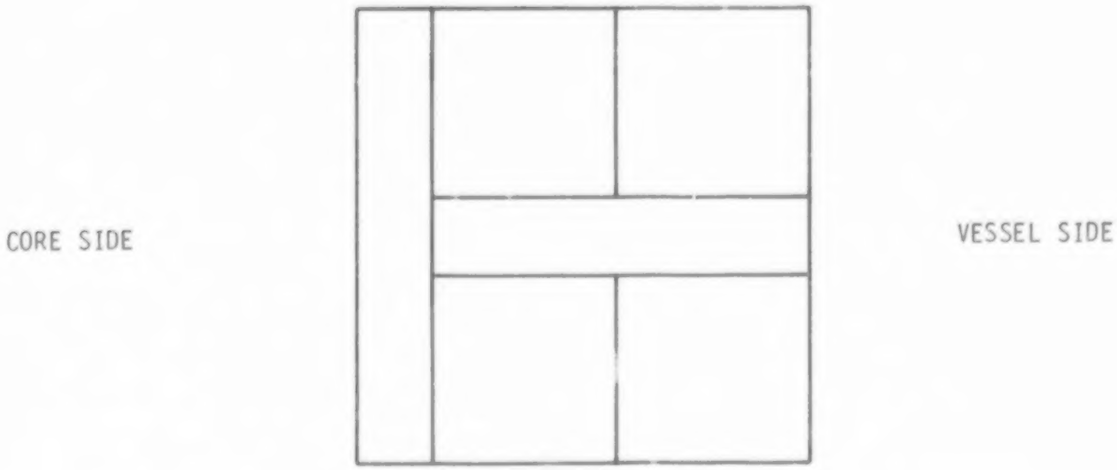
CORE SIDE
VESSEL SIDE

(b) Plan View of Surveillance Capsule

FIGURE 4.2.2.1.2.1. Orientation of the Capsule Relative to the Core and Vessel Wall - San Onofre Capsule D.

TABLE 4.2.2.1.2.1

SUMMARY OF REACTOR OPERATIONS
SAN ONOFRE CAPSULE D

TIME PERIOD	START DATE	TIME INTERVAL	AVERAGE POWER LEVEL (MWt)	LOCAL POWER FACTOR
1	6/14/67	201.	240.	1.00
2	1/ 1/68	31.	944.	1.00
3	2/ 1/68	29.	700.	1.00
4	3/ 1/68	31.	277.	1.00
5	4/ 1/68	153.	0.	1.00
6	9/ 1/68	30.	254.	1.00
7	10/ 1/68	31.	1135.	1.00
8	11/ 1/68	30.	1182.	1.00
9	12/ 1/68	31.	1077.	1.00
10	1/ 1/69	31.	852.	1.00
11	2/ 1/69	28.	1150.	1.00
12	3/ 1/69	31.	773.	1.00
13	4/ 1/69	30.	1034.	1.00
14	5/ 1/69	31.	1210.	1.00
15	6/ 1/69	30.	798.	1.00
16	7/ 1/69	31.	0.	1.00
17	8/ 1/69	31.	587.	1.00
18	9/ 1/69	30.	1342.	1.00
19	10/ 1/69	31.	919.	1.00
20	11/ 1/69	30.	1331.	1.00
21	12/ 1/69	31.	1329.	1.00
22	1/ 1/70	212.	1253.	1.00
23	8/ 1/70	31.	1325.	1.00
24	9/ 1/70	30.	1337.	1.00
25	10/ 1/70	31.	80.	1.00
26	11/ 1/70	30.	299.	1.00
27	12/ 1/70	31.	1342.	1.00
28	1/ 1/71	31.	1328.	1.00
29	2/ 1/71	28.	1328.	1.00
30	3/ 1/71	31.	1330.	1.00
31	4/ 1/71	30.	1317.	1.00
32	5/ 1/71	31.	934.	1.00
33	6/ 1/71	30.	1138.	1.00
34	7/ 1/71	31.	980.	1.00
35	8/ 1/71	31.	1124.	1.00
36	9/ 1/71	30.	1252.	1.00
37	10/ 1/71	31.	1079.	1.00
38	11/ 1/71	30.	1115.	1.00
39	12/ 1/71	31.	1024.	1.00
	1/ 1/72	DISCHARGED*		

---

*EFFECTIVE FULL POWER OPERATION TIME WAS 8.881+007 SECONDS AT A FULL POWER LEVEL OF 1347. MWt.

TABLE 4.2.2.1.2.2

REACTION RATE DATA AND CORRECTION FACTORS FOR SAN ONOFRE CAPSULE D

REACTION NAME	REACTION IDENT	TOR RATE (DPS/NUCL)	SATURATION FACTOR	GRADIENT FACTOR	IMPURITY FACTOR	AVG REACTION RATE (RPS/NUCL)	% UNCERT (1σ)
$^{54}Fe(n,p)^{54}Mn$	TOP	2.10-014	1.310+000	1.230	1.000	3.41-014	10.
	TOP MID	1.81-014	1.310+000	1.230	1.000		
	MID	2.19-014	1.310+000	1.230	1.000		
	BOT MID	2.22-014	1.310+000	1.230	1.000		
	BOT	2.25-014	1.310+000	1.230	1.000		
$^{58}Fe(n,\gamma)^{59}FE$	TOP	7.36-013	1.243+000	0.820	1.000	7.68-013	11.
	TOP MID	8.95-013	1.243+000	0.820	1.000		
	MID	6.78-013	1.243+000	0.820	1.000		
	BOT MID	7.66-013	1.243+000	0.820	1.000		
	BOT	6.96-013	1.243+000	0.820	1.000		
$^{63}Cu(n,\alpha)^{60}Co$	TOP	3.19-017	3.379+000	1.200	1.000	1.44-016	11.
	MID	3.68-017	3.379+000	1.200	1.000		
	BOT	3.78-017	3.379+000	1.200	1.000		
$^{59}Co(n,\gamma)^{60}Co$	TOP (B)	5.77-012	3.379+000	0.940	1.000	1.84-011	10.
	MID (B)	5.72-012	3.379+000	0.940	1.000		
	BOT (B)	5.87-012	3.379+000	0.940	1.000		
$^{59}Co(n,\gamma)^{60}Co$	TOP (CD)	2.66-012	3.379+000	1.190	1.000	1.03-011	10.
	MID (CD)	2.54-012	3.379+000	1.190	1.000		
	BOT (CD)	2.46-012	3.379+000	1.190	1.000		

CD = Cadmium-Covered Dosimeter.
B = Bare Dosimeter.

TABLE 4.2.2.1.2.3

FERRET-SAND II RESULTS FOR SAN ONOFRE CAPSULE D (AVERAGE FOR CAPSULE)

GROUP	ENERGY (MeV)	A PRIORI FLUX* $(n/cm^2 \cdot s)$	ADJUSTED FLUX $(n/cm^2 \cdot s)$	% UNCERTAIN $(1\ \sigma)$
1	1.492+001	1.412+007	1.344+007	49.
2	1.350+001	2.935+007	2.811+007	47.
3	1.162+001	1.361+008	1.312+008	44.
4	1.000+001	4.130+008	4.010+008	41.
5	8.607+000	1.045+009	1.021+009	37.
6	7.408+000	2.446+009	2.405+009	33.
7	6.065+000	8.700+009	8.602+009	28.
8	4.966+000	1.344+010	1.334+010	24.
9	3.679+000	2.497+010	2.484+010	22.
10	2.865+000	3.713+010	3.690+010	23.
11	2.231+000	6.957+010	6.891+010	27.
12	1.738+000	1.026+011	1.011+011	32.
13	1.353+000	1.437+011	1.407+011	36.
14	1.108+000	1.537+011	1.495+011	40.
15	8.208-001	2.575+011	2.489+011	43.
16	6.393-001	2.336+011	2.243+011	46.
17	4.979-001	2.435+011	2.322+011	49.
18	3.877-001	2.377+011	2.254+011	51.
19	3.020-001	2.187+011	2.062+011	52.
20	1.832-001	3.707+011	3.481+011	53.
21	1.111-001	2.810+011	2.629+011	54.
22	6.738-002	1.984+011	1.851+011	55.
23	4.087-002	1.562+011	1.456+011	55.
24	2.554-002	1.260+011	1.173+011	55.
25	1.989-002	5.862+010	5.462+010	55.
26	1.503-002	5.892+010	5.498+010	55.
27	9.119-003	9.134+010	8.543+010	54.
28	5.531-003	8.941+010	8.390+010	54.
29	3.355-003	9.791+010	9.226+010	53.
30	2.839-003	3.427+010	3.245+010	51.
31	2.404-003	3.471+010	3.305+010	49.
32	2.035-003	3.499+010	3.352+010	47.
33	1.234-003	1.043+011	1.005+011	44.
34	7.485-004	9.869+010	9.559+010	41.
35	4.540-004	8.746+010	8.510+010	38.
36	2.754-004	7.690+010	7.504+010	35.
37	1.670-004	7.328+010	7.161+010	32.
38	1.013-004	7.546+010	7.468+010	14.
39	6.144-005	7.951+010	7.734+010	30.
40	3.727-005	8.336+010	8.056+010	31.

TABLE 4.2.2.1.2.3 (Cont'd)

FERRET-SAND II RESULTS FOR
SAN ONOFRE CAPSULE D
(AVERAGE FOR CAPSULE)

GROUP	ENERGY (MeV)	A PRIORI FLUX* ($n/cm^2 \cdot s$)	ADJUSTED FLUX ($n/cm^2 \cdot s$)	% UNCERTAIN ($1\ \sigma$)
41	2.260-005	8.464+010	8.102+010	33.
42	1.371-005	8.272+010	7.824+010	35.
43	8.315-006	7.774+010	7.247+010	37.
44	5.043-006	7.149+010	6.555+010	39.
45	3.059-006	6.584+010	5.929+010	40.
46	1.855-006	6.086+010	5.379+010	40.
47	1.125-006	5.660+010	4.910+010	40.
48	6.826-007	5.355+010	4.565+010	39.
49	4.140-007	5.552+010	4.656+010	37.
50	2.511-007	8.643+010	7.137+010	35.
51	1.523-007	8.990+010	7.345+010	33.
52	9.237-008	8.456+010	6.865+010	33.
53	1.000-010	2.043+011	1.629+011	27.
FLUX, E > 0.0 MeV		4.584+012	4.803+012	26.
FLUX, E < 0.414 eV		4.649+011	4.230+011	23.
FLUX, E > 0.1 MeV		2.181+012	2.335+012	38.
FLUX, E > 1.0 MeV		5.768+011	6.330+011	26.
dpa/s		9.827-010	1.063-009	29.
FLUENCE+, E > 1.0 MeV		5.122+019	5.622+019	26.
dpa+		8.728-002	9.444-002	29.

---

* ABSOLUTE CALCULATED FLUX (OR NORMALIZED TO Fe54(n,p)Mn54 REACTION RATE).

+ BASED ON 8.881+007 EFFECTIVE FULL POWER SECONDS OF EXPOSURE; UNITS OF n/cm^2 FOR FLUENCE AND TOTAL NUMBER OF DISPLACED ATOMS OF IRON PER TARGET ATOM OF IRON FOR dpa.

TABLE 4.2.2.1.2.4

COMPARISON OF MEASURED AND CALCULATED REACTION RATES USED IN THE ANALYSIS OF SAN ONOFRE CAPSULE D

REACTION	REACTION RATE (DPS/NUCLEUS) MEAS	A PRIORI CALC	ADJ CALC	RATIO MEAS/CALC A PRIORI	ADJ CALC
Co59(n,γ)Co60 (Cd)	1.02-011	1.04-011	1.01-011	.98	1.01
Co59(n,γ)Co60	1.84-011	2.10-011	1.87-011	.88	.98
Fe54(n,p)Mn54	3.39-014	3.41-014	3.38-014	1.00	1.00
*Fe58(n,γ)Fe59	7.68-013	5.34-013	4.56-013	1.44	1.68
*Cu63(n,α)Co60	1.44-016	2.50-016	2.46-016	.58	.59

---

* REACTION NOT USED TO ADJUST SPECTRUM

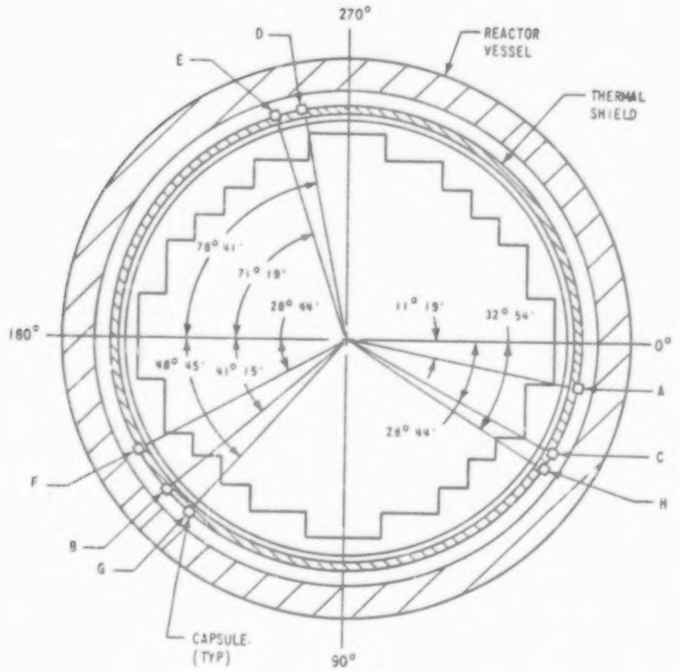
270°
D
E
REACTOR VESSEL
THERMAL SHIELD
78° 41'
71° 19'
28° 44'
11° 19'
32° 54'
180°
0°
48° 45'
41° 15'
A
28° 44'
C
H
F
B
G
CAPSULE (TYP)
90°

(a) Reactor Geometry.

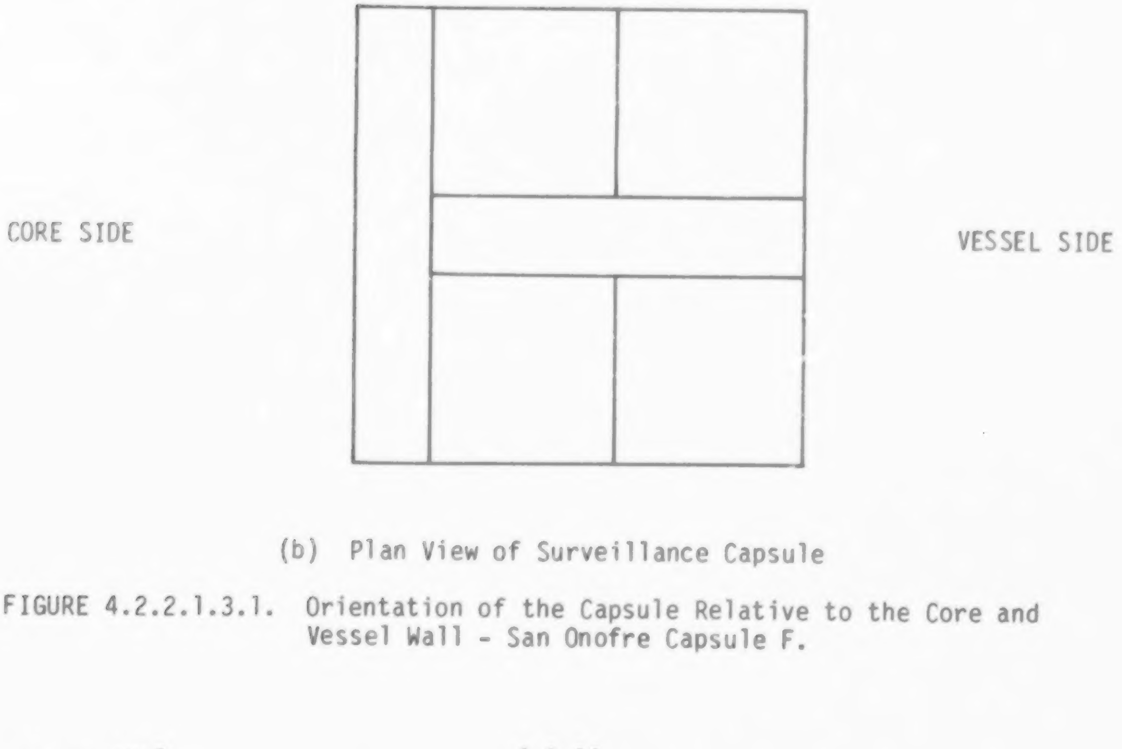
CORE SIDE
VESSEL SIDE

(b) Plan View of Surveillance Capsule

FIGURE 4.2.2.1.3.1. Orientation of the Capsule Relative to the Core and Vessel Wall - San Onofre Capsule F.

152

TABLE 4.2.2.1.3.1

SUMMARY OF REACTOR OPERATIONS
SAN ONOFRE CAPSULE F

TIME PERIOD	START DATE	TIME INTERVAL	AVERAGE POWER LEVEL (MWt)	LOCAL POWER FACTOR
1	6/14/67	201.	240.	1.00
2	1/ 1/68	31.	944.	1.00
3	2/ 1/68	29.	700.	1.00
4	3/ 1/68	31.	277.	1.00
5	4/ 1/68	153.	0.	1.00
6	9/ 1/68	30.	254.	1.00
7	10/ 1/68	31.	1135.	1.00
8	11/ 1/68	30.	1182.	1.00
9	12/ 1/68	31.	1077.	1.00
10	1/ 1/69	31.	852.	1.00
11	2/ 1/69	28.	1150.	1.00
12	3/ 1/69	31.	773.	1.00
13	4/ 1/69	30.	1034.	1.00
14	5/ 1/69	31.	1210.	1.00
15	6/ 1/69	30.	798.	1.00
16	7/ 1/69	31.	0.	1.00
17	8/ 1/69	31.	587.	1.00
18	9/ 1/69	30.	1342.	1.00
19	10/ 1/69	31.	919.	1.00
20	11/ 1/69	30.	1331.	1.00
21	12/ 1/69	31.	1329.	1.00
22	1/ 1/70	212.	1253.	1.00
23	8/ 1/70	31.	1325.	1.00
24	9/ 1/70	30.	1337.	1.00
25	10/ 1/70	31.	80.	1.00
26	11/ 1/70	30.	299.	1.00
27	12/ 1/70	31.	1342.	1.00
28	1/ 1/71	31.	1328.	1.00
29	2/ 1/71	28.	1328.	1.00
30	3/ 1/71	31.	1330.	1.00
31	4/ 1/71	30.	1317.	1.00
32	5/ 1/71	31.	934.	1.00
33	6/ 1/71	30.	1138.	1.00
34	7/ 1/71	31.	980.	1.00
35	8/ 1/71	31.	1124.	1.00
36	9/ 1/71	30.	1252.	1.00
37	10/ 1/71	31.	1079.	1.00
38	11/ 1/71	30.	1115.	1.00
39	12/ 1/71	31.	1024.	1.00
40	1/ 1/72	31.	0.	1.00

TABLE 4.2.2.1.3.1 (Cont'd)

SUMMARY OF REACTOR OPERATIONS
SAN ONOFRE CAPSULE F

TIME PERIOD	START DATE	TIME INTERVAL	AVERAGE POWER LEVEL (MWt)	LOCAL POWER FACTOR
41	2/ 1/72	29.	181.	1.00
42	3/ 1/72	31.	1272.	1.00
43	4/ 1/72	30.	1237.	1.00
44	5/ 1/72	31.	1019.	1.00
45	6/ 1/72	30.	1307.	1.00
46	7/ 1/72	31.	910.	1.00
47	8/ 1/72	31.	1190.	1.00
48	9/ 1/72	30.	1165.	1.00
49	10/ 1/72	31.	1051.	1.00
50	11/ 1/72	30.	1327.	1.00
51	12/ 1/72	31.	1342.	1.00
52	1/ 1/73	31.	1115.	1.00
53	2/ 1/73	28.	1326.	1.00
54	3/ 1/73	31.	1340.	1.00
55	4/ 1/73	30.	1322.	1.00
56	5/ 1/73	31.	1333.	1.00
57	6/ 1/73	30.	43.	1.00
58	7/ 1/73	31.	121.	1.00
59	8/ 1/73	31.	1103.	1.00
60	9/ 1/73	30.	1312.	1.00
61	10/ 1/73	31.	845.	1.00
62	11/ 1/73	61.	0.	1.00
63	1/ 1/74	31.	369.	1.00
64	2/ 1/74	28.	1347.	1.00
65	3/ 1/74	31.	1306.	1.00
66	4/ 1/74	30.	1182.	1.00
67	5/ 1/74	31.	471.	1.00
68	6/ 1/74	30.	1315.	1.00
69	7/ 1/74	31.	1180.	1.00
70	8/ 1/74	31.	1330.	1.00
71	9/ 1/74	30.	1237.	1.00
72	10/ 1/74	31.	1193.	1.00
73	11/ 1/74	30.	1330.	1.00
74	12/ 1/74	31.	1347.	1.00
75	1/ 1/75	31.	1330.	1.00
76	2/ 1/75	28.	1334.	1.00
77	3/ 1/75	31.	579.	1.00
78	4/ 1/75	30.	277.	1.00
79	5/ 1/75	31.	1304.	1.00
80	6/ 1/75	30.	1090.	1.00

TABLE 4.2.2.1.3.1 (Cont'd)

SUMMARY OF REACTOR OPERATIONS
SAN ONOFRE CAPSULE F

TIME PERIOD	START DATE	TIME INTERVAL	AVERAGE POWER LEVEL (MWt)	LOCAL POWER FACTOR
81	7/ 1/75	31.	1347.	1.00
82	8/ 1/75	31.	1337.	1.00
83	9/ 1/75	30.	1347.	1.00
84	10/ 1/75	31.	1320.	1.00
85	11/ 1/75	30.	1347.	1.00
86	12/ 1/75	31.	1347.	1.00
87	1/ 1/76	31.	1311.	1.00
88	2/ 1/76	29.	1306.	1.00
89	3/ 1/76	31.	1337.	1.00
90	4/ 1/76	30.	913.	1.00
91	5/ 1/76	31.	1342.	1.00
92	6/ 1/76	30.	1315.	1.00
93	7/ 1/76	31.	1144.	1.00
94	8/ 1/76	31.	1089.	1.00
95	9/ 1/76	30.	930.	1.00
96	10/ 1/76	92.	0.	1.00
97	1/ 1/77	90.	0.	1.00
98	4/ 1/77	30.	669.	1.00
99	5/ 1/77	31.	1340.	1.00
100	6/ 1/77	30.	1332.	1.00
101	7/ 1/77	31.	1335.	1.00
102	8/ 1/77	31.	1313.	1.00
103	9/ 1/77	30.	374.	1.00
104	10/ 1/77	31.	1040.	1.00
105	11/ 1/77	30.	1285.	1.00
106	12/ 1/77	31.	1340.	1.00
107	1/ 1/78	31.	1347.	1.00
108	2/ 1/78	28.	1347.	1.00
109	3/ 1/78	31.	1337.	1.00
110	4/ 1/78	30.	459.	1.00
111	5/ 1/78	31.	920.	1.00
112	6/ 1/78	30.	896.	1.00
113	7/ 1/78	31.	1164.	1.00
114	8/ 1/78	31.	1238.	1.00
115	9/ 1/78	15.	1033.	1.00
	9/16/78	DISCHARGED*		

---

*EFFECTIVE FULL POWER OPERATION TIME WAS 2.438+008 SECONDS AT A FULL POWER LEVEL OF 1347. MWt.

TABLE 4.2.2.1.3.2

REACTION RATE DATA AND CORRECTION FACTORS FOR SAN ONOFRE CAPSULE F

REACTION NAME	IDENT	TOR RATE (DPS/NUCL)	SATURATION FACTOR	GRADIENT FACTOR	IMPURITY FACTOR	AVG REACTION RATE (RPS/NUCL)	% UNCERT (1σ)
^{54}Fe(n,p)^{54}Mn	D-17	1.21-014	1.356+000	0.890	1.000	1.48-014	10.
	D-20	1.28-014	1.356+000	0.890	1.000		
	D-24	1.09-014	1.356+000	0.890	1.000		
	R-57	9.41-015	1.356+000	1.190	1.000		
	R-60	9.98-015	1.356+000	1.190	1.000		
	R-64	8.85-015	1.356+000	1.190	1.000		
^{58}Ni(n,p)^{58}Co	MID	9.78-015	1.252+000	1.200	1.000	1.47-014	10.
^{63}Cu(n,α)^{60}Co	TOP	5.42-017	1.814+000	1.170	1.000	1.21-016	10.
	MID	5.80-017	1.814+000	1.170	1.000		
	BOT	5.88-017	1.814+000	1.170	1.000		
^{237}Np(n,f)^{137}Cs	MID	3.30-016	6.339+000	1.000	1.000	3.34-014	10.
^{238}U(n,f)^{137}Cs	MID	7.81-016	6.339+000	1.000	0.901	7.43-014	10.
^{59}Co(n,γ)^{60}Co	MID (B)	3.76-012	1.814+000	0.950	1.000	6.47-012	10.
^{59}Co(n,γ)^{60}Co	MID (CD)	2.11-012	1.814+000	1.200	1.000	4.60-012	10.

CD = Cadmium-Covered Dosimeter.
B = Bare Dosimeter.

156

TABLE 4.2.2.1.3.3

FERRET-SAND II RESULTS FOR
SAN ONOFRE CAPSULE F
(AVERAGE FOR CAPSULE)

GROUP	ENERGY (MeV)	A PRIORI FLUX* ($n/cm^2 \cdot s$)	ADJUSTED FLUX ($n/cm^2 \cdot s$)	% UNCERTAIN ($1\ \sigma$)
1	1.492+001	6.177+006	6.509+006	41.
2	1.350+001	1.284+007	1.386+007	38.
3	1.162+001	5.954+007	6.549+007	34.
4	1.000+001	1.807+008	2.016+008	30.
5	8.607+000	4.572+008	5.122+008	26.
6	7.408+000	1.070+009	1.183+009	24.
7	6.065+000	3.806+009	4.156+009	20.
8	4.966+000	5.882+009	6.071+009	22.
9	3.679+000	1.093+010	1.062+010	21.
10	2.865+000	1.624+010	1.500+010	22.
11	2.231+000	3.044+010	2.657+010	22.
12	1.738+000	4.491+010	3.736+010	22.
13	1.353+000	6.288+010	5.045+010	24.
14	1.108+000	6.723+010	5.293+010	30.
15	8.208-001	1.127+011	8.686+010	34.
16	6.393-001	1.022+011	7.778+010	38.
17	4.979-001	1.065+011	8.056+010	41.
18	3.877-001	1.040+011	7.868+010	44.
19	3.020-001	9.566+010	7.275+010	47.
20	1.832-001	1.622+011	1.245+011	50.
21	1.111-001	1.229+011	9.541+010	52.
22	6.738-002	8.679+010	6.818+010	53.
23	4.087-002	6.833+010	5.437+010	54.
24	2.554-002	5.511+010	4.442+010	54.
25	1.989-002	2.565+010	2.094+010	55.
26	1.503-002	2.578+010	2.133+010	54.
27	9.119-003	3.996+010	3.353+010	54.
28	5.531-003	3.912+010	3.331+010	53.
29	3.355-003	4.284+010	3.707+010	52.
30	2.839-003	1.499+010	1.320+010	51.
31	2.404-003	1.519+010	1.361+010	49.
32	2.035-003	1.531+010	1.399+010	46.
33	1.234-003	4.563+010	4.244+010	44.
34	7.485-004	4.318+010	4.083+010	41.
35	4.540-004	3.827+010	3.667+010	38.
36	2.754-004	3.364+010	3.253+010	35.
37	1.670-004	3.206+010	3.110+010	32.
38	1.013-004	3.302+010	3.326+010	14.
39	6.144-005	3.479+010	3.318+010	30.
40	3.727-005	3.647+010	3.405+010	32.

TABLE 4.2.2.1.3.3 (Cont'd)

FERRET-SAND II RESULTS FOR
SAN ONOFRE CAPSULE F
(AVERAGE FOR CAPSULE)

GROUP	ENERGY (MeV)	A PRIORI FLUX* ($n/cm^2 \cdot s$)	ADJUSTED FLUX ($n/cm^2 \cdot s$)	% UNCERTAIN ($1\ \sigma$)
41	2.260-005	3.703+010	3.352+010	34.
42	1.371-005	3.619+010	3.151+010	36.
43	8.315-006	3.401+010	2.825+010	38.
44	5.043-006	3.128+010	2.464+010	40.
45	3.059-006	2.881+010	2.142+010	41.
46	1.855-006	2.663+010	1.865+010	42.
47	1.125-006	2.476+010	1.635+010	41.
48	6.826-007	2.343+010	1.463+010	41.
49	4.140-007	2.429+010	1.441+010	40.
50	2.511-007	3.781+010	2.137+010	38.
51	1.523-007	3.933+010	2.151+010	37.
52	9.237-008	3.700+010	1.985+010	36.
53	1.000-010	8.939+010	4.542+010	32.
FLUX, E > 0.0 MeV		2.246+012	1.771+012	23.
FLUX, E < 0.414 eV		2.278+011	1.225+011	28.
FLUX, E > 0.1 MeV		1.069+012	8.360+011	30.
FLUX, E > 1.0 MeV		2.826+011	2.348+011	14.
dpa/s		4.815-010	3.915-010	20.
FLUENCE+, E > 1.0 MeV		6.890+019	5.725+019	14.
dpa+		1.174-001	9.545-002	20.

---

* ABSOLUTE CALCULATED FLUX (OR NORMALIZED TO Fe54(n,p)Mn54 REACTION RATE).

+ BASED ON 2.438+008 EFFECTIVE FULL POWER SECONDS OF EXPOSURE; UNITS OF n/cm^2 FOR FLUENCE AND TOTAL NUMBER OF DISPLACED ATOMS OF IRON PER TARGET ATOM OF IRON FOR dpa.

TABLE 4.2.2.1.3.4

COMPARISON OF MEASURED AND CALCULATED REACTION RATES USED IN THE ANALYSIS OF SAN ONOFRE CAPSULE F

	REACTION RATE (DPS/NUCLEUS)			RATIO MEAS/CALC	
REACTION	MEAS	A PRIORI CALC	ADJ CALC	A PRIORI	ADJ CALC
U238(n,f)Cs137	7.43-014	8.66-014	7.52-014	.86	.99
Co59(n,γ)Co60 (Cd)	4.56-012	4.54-012	4.33-012	1.00	1.05
Co59(n,γ)Co60	6.40-012	9.18-012	6.85-012	.70	.93
Fe54(n,p)Mn54	1.48-014	1.49-014	1.45-014	.99	1.02
Ni58(n,P)Co58	1.49-014	2.04-014	1.93-014	.73	.77
Cu63(n,α)Co60	1.24-016	1.10-016	1.21-016	1.13	1.02
*Np237(n,γ)Fp Cd	3.34-014	8.24-013	6.64-013	.04	.05

---

* REACTION NOT USED TO ADJUST SPECTRUM

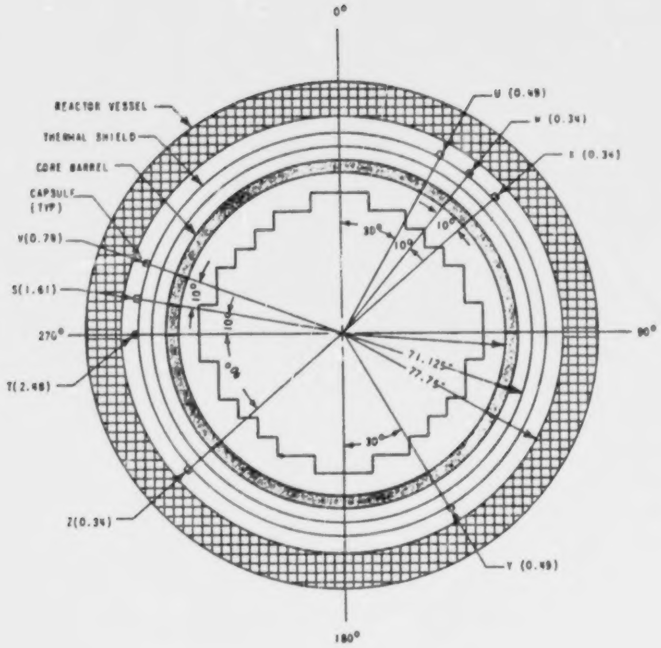
0°
REACTOR VESSEL
THERMAL SHIELD
CORE BARREL
CAPSULE (TYP)
V(0.78)
S(1.61)
270°
T(2.48)
Z(0.34)
U (0.48)
W (0.34)
X (0.34)
90°
Y (0.48)
180°
30°
10°
10°
10°
10°
8°
71.125°
77.75°
30°

(a) Reactor Geometry.

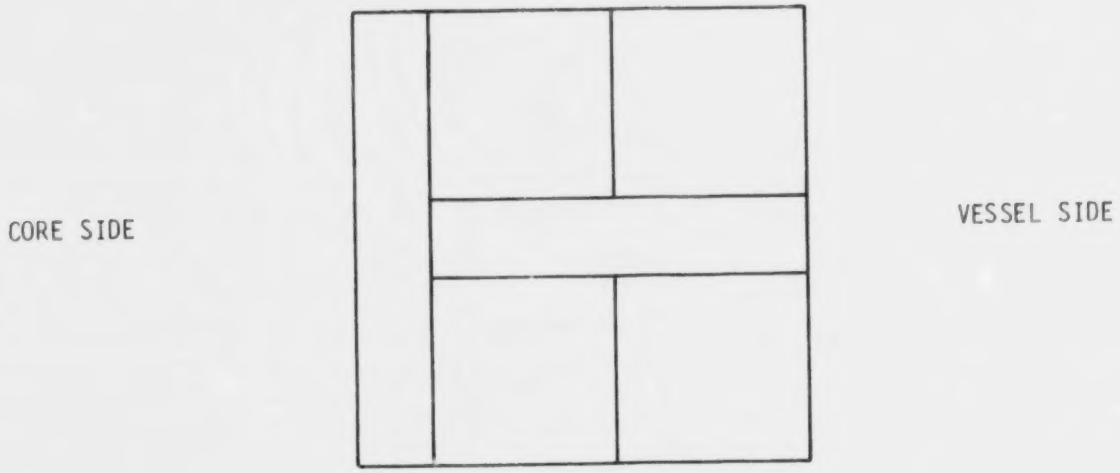
CORE SIDE
VESSEL SIDE

(b) Plan View of Surveillance Capsule

FIGURE 4.2.3.1.1.1. Orientation of the Capsule Relative to the Core and Vessel Wall - Turkey Point Unit 3 Capsule S.

TABLE 4.2.3.1.1.1

SUMMARY OF REACTOR OPERATIONS
TURKEY POINT UNIT 3 CAPSULE S

TIME PERIOD	START DATE	TIME INTERVAL	AVERAGE POWER LEVEL (MWt)	LOCAL POWER FACTOR
1	11/ 2/72	2.	7.	1.00
2	11/ 4/72	1.	0.	1.00
3	11/ 5/72	8.	438.	1.00
4	11/13/72	5.	0.	1.00
5	11/18/72	3.	192.	1.00
6	11/21/72	13.	0.	1.00
7	12/ 4/72	5.	607.	1.00
8	12/ 9/72	13.	0.	1.00
9	12/22/72	25.	849.	1.00
10	1/16/73	7.	0.	1.00
11	1/23/73	42.	1189.	1.00
12	3/ 6/73	7.	0.	1.00
13	3/13/73	24.	1285.	1.00
14	4/ 6/73	10.	0.	1.00
15	4/16/73	102.	1623.	1.00
16	7/27/73	13.	0.	1.00
17	8/ 9/73	73.	1542.	1.00
18	10/21/73	8.	0.	1.00
19	10/29/73	39.	1553.	1.00
20	12/ 7/73	14.	0.	1.00
21	12/21/73	6.	1520.	1.00
22	12/27/73	3.	0.	1.00
23	12/30/73	79.	1637.	1.00
24	3/19/74	12.	0.	1.00
25	3/31/74	42.	1987.	1.00
26	5/12/74	1.	0.	1.00
27	5/13/74	26.	2069.	1.00
28	6/ 8/74	6.	0.	1.00
29	6/14/74	92.	1967.	1.00
30	9/14/74	9.	0.	1.00
31	9/23/74	12.	1675.	1.00
32	10/ 5/74	71.	0.	1.00
33	12/15/74	79.	1935.	1.00
34	3/ 4/75	5.	0.	1.00
35	3/ 9/75	129.	2096.	1.00
36	7/16/75	4.	0.	1.00
37	7/20/75	98.	2050.	1.00
38	10/26/75	60.	0.	1.00
39	12/25/75	8.	1629.	1.00
40	1/ 2/76	1.	0.	1.00

161

TABLE 4.2.3.1.1.1 (Cont'd)

SUMMARY OF REACTOR OPERATIONS
TURKEY POINT UNIT 3 CAPSULE S

TIME PERIOD	START DATE	TIME INTERVAL	AVERAGE POWER LEVEL (MWt)	LOCAL POWER FACTOR
41	1/ 3/76	50.	2148.	1.00
42	2/22/76	6.	0.	1.00
43	2/28/76	8.	2113.	1.00
44	3/ 7/76	5.	0.	1.00
45	3/12/76	50.	2131.	1.00
46	5/ 1/76	2.	0.	1.00
47	5/ 3/76	25.	2130.	1.00
48	5/28/76	6.	0.	1.00
49	6/ 3/76	17.	2059.	1.00
50	6/20/76	6.	0.	1.00
51	6/26/76	48.	2161.	1.00
52	8/13/76	4.	0.	1.00
53	8/17/76	8.	2070.	1.00
54	8/25/76	7.	0.	1.00
55	9/ 1/76	74.	2153.	1.00
56	11/14/76	66.	0.	1.00
57	1/19/77	95.	2073.	1.00
58	4/24/77	5.	0.	1.00
59	4/29/77	82.	2110.	1.00
60	7/20/77	2.	0.	1.00
61	7/22/77	125.	2055.	1.00
	11/24/77	DISCHARGED*		

---

*EFFECTIVE FULL POWER OPERATION TIME WAS 1.095+008 SECONDS AT A FULL POWER LEVEL OF 2200. MWt.

162

TABLE 4.2.3.1.1.2

REACTION RATE DATA AND CORRECTION FACTORS FOR
TURKEY POINT UNIT 3 CAPSULE S

REACTION		TOR RATE	SATURATION	GRADIENT	IMPURITY	AVG REACTION	% UNCERT
NAME	IDENT	(DPS/NUCL)	FACTOR	FACTOR	FACTOR	RATE (RPS/NUCL)	(1σ)
$^{54}Fe(n,p)^{54}Mn$	S9	9.39-015	1.289+000	0.950	1.000	1.05-014	10.
	S7	8.27-015	1.289+000	0.950	1.000		
	R8	7.53-015	1.289+000	0.950	1.000		
	S5	8.62-015	1.289+000	0.950	1.000		
	S1	8.38-015	1.289+000	0.950	1.000		
	P9	7.29-015	1.289+000	1.170	1.000		
	P7	7.11-015	1.289+000	1.170	1.000		
	R6	6.72-015	1.289+000	1.170	1.000		
	P5	7.40-015	1.289+000	1.170	1.000		
	P1	6.89-015	1.289+000	1.170	1.000		
$^{63}Cu(n,\alpha)^{60}Co$	TOP	3.44-017	2.911+000	0.950	1.000	9.48-017	10.
	MID	3.42-017	2.911+000	0.950	1.000		
$^{59}Co(n,\gamma)^{60}Co$	TOP (B)	2.29-012	2.911+000	0.940	1.000	5.73-012	10.
	MID (B)	2.03-012	2.911+000	0.940	1.000		
	BOT (B)	1.97-012	2.911+000	0.940	1.000		
$^{59}Co(n,\gamma)^{60}Co$	TOP (CD)	1.09-012	2.911+000	1.180	1.000	3.45-012	12.
	BOT (CD)	9.20-013	2.911+000	1.180	1.000		

CD = Cadmium-Covered Dosimeter.
B = Bare Dosimeter.

TABLE 4.2.3.1.1.3

FERRET-SAND II RESULTS FOR TURKEY POINT UNIT 3 CAPSULE S (AVERAGE FOR CAPSULE)

GROUP	ENERGY (MeV)	A PRIORI FLUX* ($n/cm^2 \cdot s$)	ADJUSTED FLUX ($n/cm^2 \cdot s$)	% UNCERTAIN ($1\ \sigma$)
1	1.492+001	6.569+006	5.960+006	41.
2	1.350+001	1.366+007	1.210+007	38.
3	1.162+001	6.331+007	5.510+007	34.
4	1.000+001	1.921+008	1.647+008	30.
5	8.607+000	4.861+008	4.145+008	26.
6	7.408+000	1.172+009	1.013+009	24.
7	6.065+000	4.130+009	3.617+009	20.
8	4.966+000	5.036+009	4.733+009	22.
9	3.679+000	6.909+009	6.892+009	22.
10	2.865+000	8.799+009	9.159+009	24.
11	2.231+000	1.599+010	1.727+010	27.
12	1.738+000	2.172+010	2.417+010	32.
13	1.353+000	2.770+010	3.172+010	36.
14	1.108+000	2.688+010	3.158+010	39.
15	8.208-001	4.174+010	5.002+010	43.
16	6.393-001	3.514+010	4.268+010	46.
17	4.979-001	3.527+010	4.319+010	48.
18	3.877-001	3.525+010	4.333+010	51.
19	3.020-001	3.215+010	3.954+010	52.
20	1.832-001	5.072+010	6.235+010	54.
21	1.111-001	3.602+010	4.424+010	55.
22	6.738-002	2.587+010	3.179+010	55.
23	4.087-002	2.187+010	2.696+010	55.
24	2.554-002	1.822+010	2.260+010	56.
25	1.989-002	8.580+009	1.076+010	55.
26	1.503-002	8.604+009	1.096+010	55.
27	9.119-003	1.324+010	1.723+010	54.
28	5.531-003	1.310+010	1.752+010	54.
29	3.355-003	1.389+010	1.923+010	53.
30	2.839-003	4.782+009	6.884+009	51.
31	2.404-003	4.822+009	7.254+009	49.
32	2.035-003	4.849+009	7.645+009	47.
33	1.234-003	1.448+010	2.393+010	44.
34	7.485-004	1.395+010	2.412+010	41.
35	4.540-004	1.289+010	2.319+010	38.
36	2.754-004	1.186+010	2.203+010	35.
37	1.670-004	1.144+010	2.171+010	33.
38	1.013-004	1.166+010	2.478+010	15.
39	6.144-005	1.244+010	2.367+010	31.
40	3.727-005	1.314+010	2.446+010	32.

TABLE 4.2.3.1.1.3 (Cont'd)

FERRET-SAND II RESULTS FOR TURKEY POINT UNIT 3 CAPSULE S (AVERAGE FOR CAPSULE)

GROUP	ENERGY (MeV)	A PRIORI FLUX* (n/cm^2•s)	ADJUSTED FLUX (n/cm^2•s)	% UNCERTAIN (1 σ)
41	2.260-005	1.324+010	2.379+010	34.
42	1.371-005	1.269+010	2.177+010	36.
43	8.315-006	1.161+010	1.882+010	38.
44	5.043-006	1.122+010	1.708+010	40.
45	3.059-006	1.123+010	1.599+010	41.
46	1.855-006	1.126+010	1.497+010	41.
47	1.125-006	1.129+010	1.405+010	41.
48	6.826-007	1.131+010	1.323+010	40.
49	4.140-007	1.133+010	1.251+010	38.
50	2.511-007	1.135+010	1.192+010	36.
51	1.523-007	1.635+010	1.648+010	35.
52	9.237-008	2.720+010	2.653+010	33.
53	1.000-010	5.905+010	5.493+010	28.
FLUX, E > 0.0 MeV		9.176+011	1.085+012	23.
FLUX, E < 0.414 eV		1.362+011	1.224+011	24.
FLUX, E > 0.1 MeV		4.248+011	4.628+011	36.
FLUX, E > 1.0 MeV		1.450+011	1.479+011	24.
dpa/s		2.243-010	2.332-010	27.
FLUENCE+, E > 1.0 MeV		1.587+019	1.619+019	24.
dpa+		2.456-002	2.553-002	27.

---

* ABSOLUTE CALCULATED FLUX (OR NORMALIZED TO Fe54(n,p)Mn54 REACTION RATE).

+ BASED ON 1.095+008 EFFECTIVE FULL POWER SECONDS OF EXPOSURE; UNITS OF n/cm^2 FOR FLUENCE AND TOTAL NUMBER OF DISPLACED ATOMS OF IRON PER TARGET ATOM OF IRON FOR dpa.

TABLE 4.2.3.1.1.4

COMPARISON OF MEASURED AND CALCULATED REACTION RATES USED IN THE ANALYSIS OF TURKEY POINT UNIT 3 CAPSULE S

REACTION	REACTION RATE (DPS/NUCLEUS) MEAS	A PRIORI CALC	ADJ CALC	RATIO MEAS/CALC A PRIORI	ADJ CALC
Fe54(n,p)Mn54	1.05-014	1.05-014	1.03-014	1.00	1.02
Cu63(n,α)Co60	9.48-017	1.13-016	9.82-017	.84	.97
Co59(n,γ)Co60	5.73-012	4.37-012	5.91-012	1.31	.97
Co59(n,γ)Co60 (Cd)	3.45-012	1.65-012	3.24-012	2.09	1.06

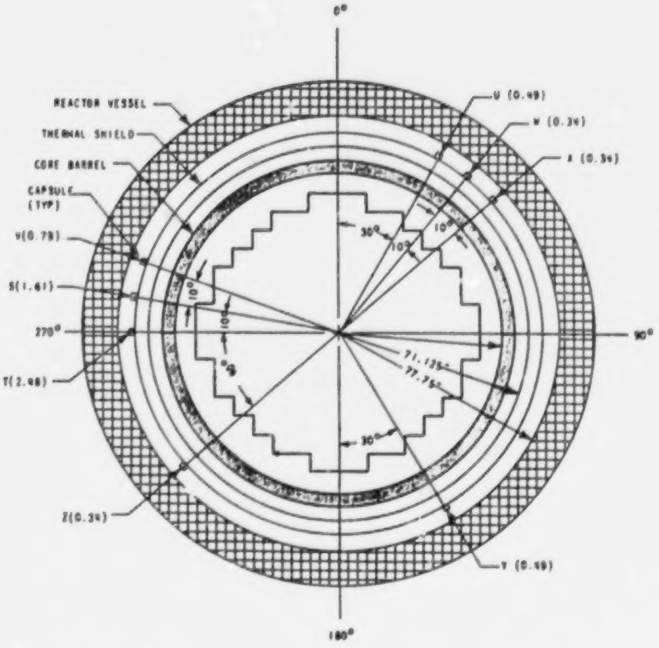
0°
REACTOR VESSEL
THERMAL SHIELD
CORE BARREL
CAPSULE (TYP)
V(0.79)
S(1.61)
270°
T(2.48)
Z(0.34)
U (0.49)
W (0.34)
X (0.34)
30°
10°
10°
10°
10°
90°
71.125°
77.75°
30°
Y (0.49)
180°

(a) Reactor Geometry.

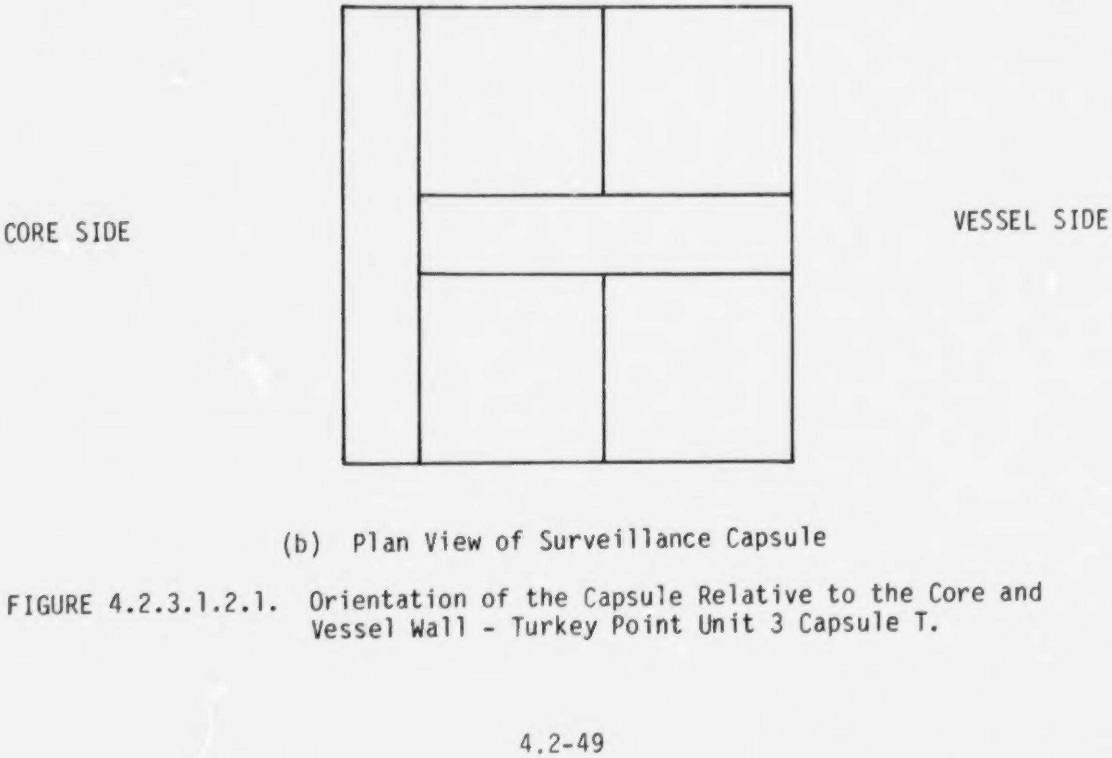
CORE SIDE
VESSEL SIDE

(b) Plan View of Surveillance Capsule

FIGURE 4.2.3.1.2.1. Orientation of the Capsule Relative to the Core and Vessel Wall - Turkey Point Unit 3 Capsule T.

167

TABLE 4.2.3.1.2.1

SUMMARY OF REACTOR OPERATIONS
TURKEY POINT UNIT 3 CAPSULE T

TIME PERIOD	START DATE	TIME INTERVAL	AVERAGE POWER LEVEL (MWt)	LOCAL POWER FACTOR
1	11/ 2/72	2.	7.	1.00
2	11/ 4/72	1.	0.	1.00
3	11/ 5/72	8.	438.	1.00
4	11/13/72	5.	0.	1.00
5	11/18/72	3.	192.	1.00
6	11/21/72	13.	0.	1.00
7	12/ 4/72	5.	607.	1.00
8	12/ 9/72	13.	0.	1.00
9	12/22/72	25.	849.	1.00
10	1/16/73	7.	0.	1.00
11	1/23/73	42.	1189.	1.00
12	3/ 6/73	7.	0.	1.00
13	3/13/73	24.	1285.	1.00
14	4/ 6/73	10.	0.	1.00
15	4/16/73	102.	1623.	1.00
16	7/27/73	13.	0.	1.00
17	8/ 9/73	73.	1542.	1.00
18	10/21/73	8.	0.	1.00
19	10/29/73	39.	1553.	1.00
20	12/ 7/73	14.	0.	1.00
21	12/21/73	6.	1520.	1.00
22	12/27/73	3.	0.	1.00
23	12/30/73	79.	1637.	1.00
	3/19/74	DISCHARGED*		

---

*EFFECTIVE FULL POWER OPERATION TIME WAS 2.302+007 SECONDS AT A FULL POWER LEVEL OF 2200. MWt.

TABLE 4.2.3.1.2.2

REACTION RATE DATA AND CORRECTION FACTORS FOR TURKEY POINT UNIT 3 CAPSULE T

REACTION NAME	IDENT	TOR RATE (DPS/NUCL)	SATURATION FACTOR	GRADIENT FACTOR	IMPURITY FACTOR	AVG REACTION RATE (RPS/NUCL)	% UNCERT (1σ)
^{54}Fe(n,p)^{54}Mn	R-63	4.61-015	2.610+000	1.170	1.000	1.47-014	10.
	H-23	5.13-015	2.610+000	1.170	1.000		
	H-17	5.34-015	2.610+000	1.170	1.000		
	P-58	5.57-015	2.610+000	0.950	1.000		
	W-24	5.89-015	2.610+000	0.950	1.000		
	W-18	5.57-015	2.610+000	0.950	1.000		
^{58}Ni(n,p)^{58}Co	MID	3.68-015	1.561+000	0.930	1.000	5.34-015	10.
^{63}Cu(n,α)^{60}Co	TOP	1.45-017	1.124+001	0.950	1.000	1.53-016	10.
	BOT	1.40-017	1.124+001	0.950	1.000		
^{237}Np(n,f)^{137}Cs	MID	8.50-016	6.047+001	1.000	1.000	8.20-013	10.
^{238}U(n,f)^{137}Cs	MID	1.15-016	6.047+001	1.000	0.901	1.05-013	10.

TABLE 4.2.3.1.2.3

FERRET-SAND II RESULTS FOR TURKEY POINT UNIT 3 CAPSULE T (AVERAGE FOR CAPSULE)

GROUP	ENERGY (MeV)	A PRIORI FLUX* (n/cm^2•s)	ADJUSTED FLUX (n/cm^2•s)	% UNCERTAIN (1 σ)
1	1.492+001	9.282+006	8.978+006	43.
2	1.350+001	1.930+007	1.805+007	39.
3	1.162+001	8.947+007	8.169+007	35.
4	1.000+001	2.715+008	2.456+008	30.
5	8.607+000	6.869+008	6.255+008	26.
6	7.408+000	1.656+009	1.539+009	24.
7	6.065+000	5.836+009	5.511+009	20.
8	4.966+000	7.116+009	7.034+009	22.
9	3.679+000	9.763+009	1.048+010	22.
10	2.865+000	1.243+010	1.501+010	22.
11	2.231+000	2.260+010	3.183+010	22.
12	1.738+000	3.069+010	5.146+010	21.
13	1.353+000	3.914+010	7.242+010	21.
14	1.108+000	3.798+010	6.963+010	24.
15	8.208-001	5.898+010	1.128+011	25.
16	6.393-001	4.965+010	9.654+010	28.
17	4.979-001	4.984+010	9.697+010	31.
18	3.877-001	4.981+010	9.518+010	35.
19	3.020-001	4.543+010	8.404+010	39.
20	1.832-001	7.167+010	1.271+011	43.
21	1.111-001	5.089+010	8.600+010	46.
22	6.738-002	3.655+010	5.877+010	49.
23	4.087-002	3.091+010	4.739+010	52.
24	2.554-002	2.574+010	3.781+010	54.
25	1.989-002	1.212+010	1.715+010	56.
26	1.503-002	1.216+010	1.668+010	57.
27	9.119-003	1.871+010	2.505+010	59.
28	5.531-003	1.850+010	2.432+010	59.
29	3.355-003	1.963+010	2.544+010	60.
30	2.839-003	6.757+009	8.673+009	60.
31	2.404-003	6.813+009	8.686+009	61.
32	2.035-003	6.852+009	8.697+009	61.
33	1.234-003	2.046+010	2.589+010	61.
34	7.485-004	1.971+010	2.490+010	61.
35	4.540-004	1.821+010	2.298+010	61.
36	2.754-004	1.676+010	2.114+010	61.
37	1.670-004	1.617+010	2.038+010	61.
38	1.013-004	1.647+010	2.076+010	61.
39	6.144-005	1.758+010	2.215+010	61.
40	3.727-005	1.857+010	2.340+010	61.

TABLE 4.2.3.1.2.3 (Cont'd)

FERRET-SAND II RESULTS FOR
TURKEY POINT UNIT 3 CAPSULE T
(AVERAGE FOR CAPSULE)

GROUP	ENERGY (MeV)	A PRIORI FLUX* (n/cm^2•s)	ADJUSTED FLUX (n/cm^2•s)	% UNCERTAIN (1 σ)
41	2.260-005	1.870+010	2.355+010	61.
42	1.371-005	1.794+010	2.258+010	61.
43	8.315-006	1.640+010	2.064+010	61.
44	5.043-006	1.585+010	1.995+010	61.
45	3.059-006	1.587+010	1.997+010	61.
46	1.855-006	1.591+010	2.001+010	61.
47	1.125-006	1.595+010	2.005+010	61.
48	6.826-007	1.598+010	2.009+010	61.
49	4.140-007	1.600+010	2.012+010	61.
50	2.511-007	1.640+010	2.061+010	61.
51	1.523-007	1.659+010	2.085+010	61.
52	9.237-008	1.791+010	2.250+010	61.
53	1.000-010	1.102+011	1.385+011	61.
FLUX, E > 0.0 MeV		9.177+011	1.814+012	26.
FLUX, E < 0.414 eV		1.363+011	2.225+011	58.
FLUX, E > 0.1 MeV		4.248+011	9.769+011	20.
FLUX, E > 1.0 MeV		1.450+011	3.045+011	10.
dpa/s		2.244-010	4.729-010	12.
FLUENCE+, E > 1.0 MeV		3.337+018	7.009+018	10.
dpa+		5.167-003	1.089-002	12.

---

* ABSOLUTE CALCULATED FLUX (OR NORMALIZED TO Fe54(n,p)Mn54 REACTION RATE).

+ BASED ON 2.302+007 EFFECTIVE FULL POWER SECONDS OF EXPOSURE; UNITS OF n/cm^2 FOR FLUENCE AND TOTAL NUMBER OF DISPLACED ATOMS OF IRON PER TARGET ATOM OF IRON FOR dpa.

TABLE 4.2.3.1.2.4

COMPARISON OF MEASURED AND CALCULATED REACTION RATES USED IN THE ANALYSIS OF TURKEY POINT UNIT 3 CAPSULE T

REACTION	REACTION RATE (DPS/NUCLEUS) MEAS	A PRIORI CALC	ADJ CALC	RATIO MEAS/CALC A PRIORI	ADJ CALC
Fe54(n,p)Mn54	1.48-014	1.49-014	1.63-014	1.00	.91
Cu63(n,α)Co60	1.53-016	1.60-016	1.52-016	.95	1.01
Np237(n,f)Cs137	8.20-013	4.73-013	8.13-013	1.73	1.01
U238(n,f)Cs137	1.05-013	6.60-014	9.70-014	1.59	1.08
*Ni58(n,p)Co58	5.34-015	1.97-014	2.27-014	.27	.23

---

* REACTION NOT USED TO ADJUST SPECTRUM

172

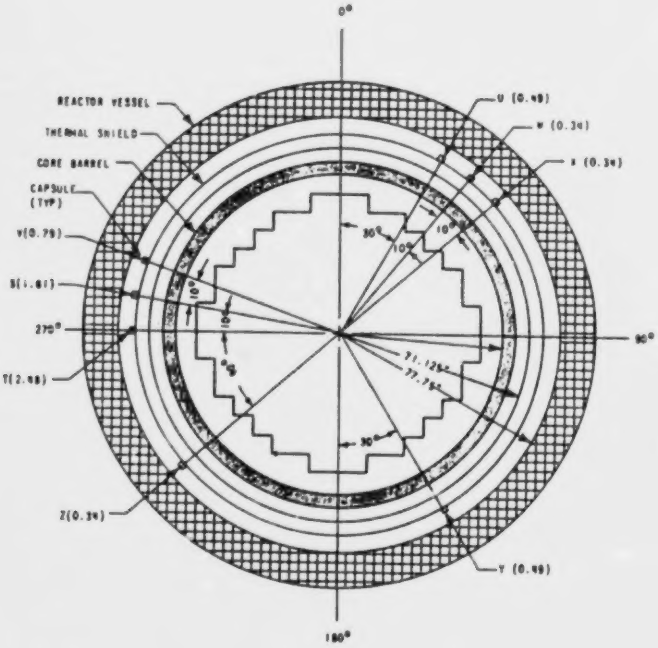
0°
REACTOR VESSEL
THERMAL SHIELD
CORE BARREL
CAPSULE (TYP)
V(0.79)
S(1.61)
270°
T(2.98)
Z(0.34)
U (0.49)
W (0.34)
X (0.34)
30°
10°
10°
10°
10°
10°
90°
71.125°
77.75°
30°
Y (0.49)
180°

(a) Reactor Geometry.

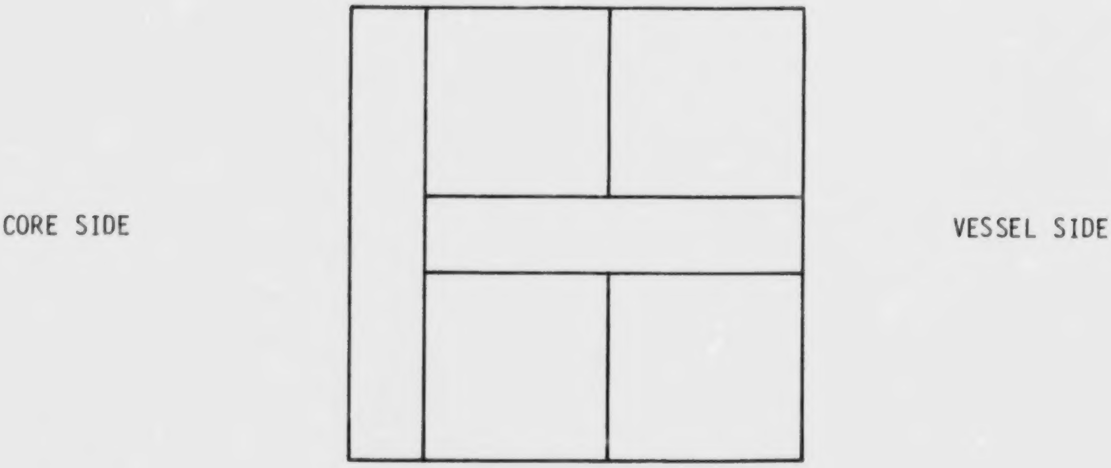
CORE SIDE
VESSEL SIDE

(b) Plan View of Surveillance Capsule

FIGURE 4.2.3.2.1.1. Orientation of the Capsule Relative to the Core and Vessel Wall - Turkey Point Unit 4 Capsule S.

173

TABLE 4.2.3.2.1.1

SUMMARY OF REACTOR OPERATIONS
TURKEY POINT UNIT 4 CAPSULE S

TIME PERIOD	START DATE	TIME INTERVAL	AVERAGE POWER LEVEL (MWt)	LOCAL POWER FACTOR
1	6/19/73	12.	272.	1.00
2	7/ 1/73	1.	0.	1.00
3	7/ 2/73	5.	519.	1.00
4	7/ 7/73	2.	0.	1.00
5	7/ 9/73	5.	607.	1.00
6	7/14/73	4.	0.	1.00
7	7/18/73	11.	641.	1.00
8	7/29/73	7.	0.	1.00
9	8/ 5/73	27.	793.	1.00
10	9/ 1/73	1.	0.	1.00
11	9/ 2/73	21.	1353.	1.00
12	9/23/73	1.	0.	1.00
13	9/24/73	41.	1490.	1.00
14	11/ 4/73	12.	0.	1.00
15	11/16/73	48.	1519.	1.00
16	1/ 3/74	31.	0.	1.00
17	2/ 3/74	59.	1747.	1.00
18	4/ 3/74	2.	0.	1.00
19	4/ 5/74	12.	1862.	1.00
20	4/17/74	1.	0.	1.00
21	4/18/74	37.	2030.	1.00
22	5/25/74	6.	0.	1.00
23	5/31/74	79.	2019.	1.00
24	8/18/74	23.	0.	1.00
25	9/10/74	47.	2092.	1.00
26	10/27/74	6.	0.	1.00
27	11/ 2/74	32.	1829.	1.00
28	12/ 4/74	3.	0.	1.00
29	12/ 7/74	30.	2128.	1.00
30	1/ 6/75	4.	0.	1.00
31	1/10/75	79.	2136.	1.00
32	3/30/75	83.	0.	1.00
33	6/21/75	43.	2005.	1.00
34	8/ 3/75	6.	0.	1.00
35	8/ 9/75	43.	2100.	1.00
36	9/21/75	10.	0.	1.00
37	10/ 1/75	11.	2041.	1.00
38	10/12/75	1.	0.	1.00
39	10/13/75	89.	2142.	1.00
40	1/10/76	7.	0.	1.00

TABLE 4.2.3.2.1.1 (Cont'd)

SUMMARY OF REACTOR OPERATIONS
TURKEY POINT UNIT 4 CAPSULE S

TIME PERIOD	START DATE	TIME INTERVAL	AVERAGE POWER LEVEL (MWt)	LOCAL POWER FACTOR
41	1/17/76	92.	2106.	1.00
42	4/18/76	53.	0.	1.00
43	6/10/76	2.	1145.	1.00
44	6/12/76	4.	0.	1.00
45	6/16/76	1.	480.	1.00
46	6/17/76	2.	0.	1.00
47	6/19/76	83.	2101.	1.00
48	9/10/76	6.	0.	1.00
49	9/16/76	8.	1770.	1.00
50	9/24/76	5.	0.	1.00
51	9/29/76	11.	2141.	1.00
52	10/10/76	4.	0.	1.00
53	10/14/76	14.	1978.	1.00
54	10/28/76	36.	0.	1.00
55	12/ 3/76	34.	2101.	1.00
56	1/ 6/77	5.	0.	1.00
57	1/11/77	14.	2190.	1.00
58	1/25/77	5.	0.	1.00
59	1/30/77	49.	2188.	1.00
60	3/20/77	6.	0.	1.00
61	3/26/77	31.	2143.	1.00
62	4/26/77	8.	0.	1.00
63	5/ 4/77	5.	2165.	1.00
64	5/ 9/77	86.	0.	1.00
65	8/ 3/77	8.	1575.	1.00
66	8/11/77	4.	0.	1.00
67	8/15/77	75.	2094.	1.00
68	10/29/77	13.	0.	1.00
69	11/11/77	95.	2127.	1.00
70	2/14/78	23.	0.	1.00
71	3/ 9/78	157.	2004.	1.00
	8/13/78	DISCHARGED*		

---

*EFFECTIVE FULL POWER OPERATION TIME WAS 1.079+008 SECONDS AT A FULL POWER LEVEL OF 2200. MWt.

175

TABLE 4.2.3.2.1.2

REACTION RATE DATA AND CORRECTION FACTORS FOR TURKEY POINT UNIT 4 CAPSULE S

REACTION NAME	REACTION IDENT	TOR RATE (DPS/NUCL)	SATURATION FACTOR	GRADIENT FACTOR	IMPURITY FACTOR	AVG REACTION RATE (RPS/NUCL)	% UNCERT (1σ)
$^{54}Fe(n,p)^{54}Mn$	P9	6.89-015	1.403+000	0.950	1.000	9.25-015	10.
	R5	6.67-015	1.403+000	0.950	1.000		
	P1	6.83-015	1.403+000	0.950	1.000		
	S9	5.95-015	1.403+000	1.170	1.000		
	R7	5.46-015	1.403+000	1.170	1,000		
	S1	5.83-015	1.403+000	1.170	1.000		
$^{63}Cu(n,\alpha)^{60}Co$	TOP	3.51-017	3.014+000	1.100	1.000	1.15-016	10.
	BOT	3.41-017	3.014+000	1.100	1.000		
$^{59}Co(n,\gamma)^{60}Co$	TOP (B)	2.45-012	3.014+000	0.940	1.000	6.16-012	13.
	MID (B)	1.87-012	3.014+000	0.940	1.000		
	BOT (B)	2.21-012	3.014+000	0.940	1.000		
$^{59}Co(n,\gamma)^{60}Co$	TOP (CD)	9.16-013	3.014+000	1.180	1.000	3.40-012	10.
	BOT (CD)	9.98-013	3.014+000	1.180	1.000		

CD = Cadmium-Covered Dosimeter.
B = Bare Dosimeter.

TABLE 4.2.3.2.1.3

FERRET-SAND II RESULTS FOR
TURKEY POINT UNIT 4 CAPSULE S
(AVERAGE FOR CAPSULE)

GROUP	ENERGY (MeV)	A PRIORI FLUX* (n/cm^2•s)	ADJUSTED FLUX (n/cm^2•s)	% UNCERTAIN (1 σ)
1	1.492+001	5.783+006	7.592+006	41.
2	1.350+001	1.202+007	1.542+007	38.
3	1.162+001	5.574+007	6.960+007	34.
4	1.000+001	1.692+008	2.055+008	29.
5	8.607+000	4.280+008	5.043+008	26.
6	7.408+000	1.032+009	1.169+009	23.
7	6.065+000	3.636+009	3.952+009	20.
8	4.966+000	4.434+009	4.577+009	22.
9	3.679+000	6.083+009	6.087+009	23.
10	2.865+000	7.747+009	7.680+009	25.
11	2.231+000	1.408+010	1.398+010	28.
12	1.738+000	1.913+010	1.928+010	33.
13	1.353+000	2.439+010	2.504+010	37.
14	1.108+000	2.366+010	2.482+010	40.
15	8.208-001	3.675+010	3.958+010	43.
16	6.393-001	3.094+010	3.432+010	46.
17	4.979-001	3.105+010	3.553+010	49.
18	3.877-001	3.104+010	3.662+010	51.
19	3.020-001	2.830+010	3.438+010	53.
20	1.832-001	4.466+010	5.572+010	54.
21	1.111-001	3.171+010	4.054+010	55.
22	6.738-002	2.277+010	2.977+010	55.
23	4.087-002	1.926+010	2.571+010	56.
24	2.554-002	1.604+010	2.186+010	56.
25	1.989-002	7.555+009	1.052+010	56.
26	1.503-002	7.576+009	1.080+010	55.
27	9.119-003	1.166+010	1.709+010	55.
28	5.531-003	1.153+010	1.745+010	54.
29	3.355-003	1.223+010	1.920+010	53.
30	2.839-003	4.210+009	6.888+009	51.
31	2.404-003	4.245+009	7.268+009	49.
32	2.035-003	4.270+009	7.667+009	47.
33	1.234-003	1.275+010	2.402+010	44.
34	7.485-004	1.228+010	2.422+010	41.
35	4.540-004	1.135+010	2.330+010	38.
36	2.754-004	1.045+010	2.214+010	35.
37	1.670-004	1.008+010	2.183+010	32.
38	1.013-004	1.026+010	2.495+010	14.
39	6.144-005	1.095+010	2.383+010	31.
40	3.727-005	1.157+010	2.463+010	32.

TABLE 4.2.3.2.1.3 (Cont'd)

FERRET-SAND II RESULTS FOR
TURKEY POINT UNIT 4 CAPSULE S
(AVERAGE FOR CAPSULE)

GROUP	ENERGY (MeV)	A PRIORI FLUX* ($n/cm^2 \cdot s$)	ADJUSTED FLUX ($n/cm^2 \cdot s$)	% UNCERTAIN (1 σ)
41	2.260-005	1.165+010	2.397+010	34.
42	1.371-005	1.118+010	2.195+010	36.
43	8.315-006	1.022+010	1.898+010	38.
44	5.043-006	9.878+009	1.723+010	40.
45	3.059-006	9.891+009	1.613+010	42.
46	1.855-006	9.911+009	1.510+010	42.
47	1.125-006	9.936+009	1.416+010	42.
48	6.826-007	9.959+009	1.333+010	41.
49	4.140-007	9.972+009	1.259+010	40.
50	2.511-007	1.022+010	1.225+010	38.
51	1.523-007	1.034+010	1.190+010	37.
52	9.237-008	1.116+010	1.247+010	36.
53	1.000-010	6.868+010	7.175+010	27.
FLUX, E > 0.0 MeV		9.177+011	1.009+012	23.
FLUX, E < 0.414 eV		1.363+011	1.210+011	25.
FLUX, E > 0.1 MeV		4.248+011	3.903+011	37.
FLUX, E > 1.0 MeV		1.450+011	1.209+011	25.
dpa/s		2.244-010	1.974-010	27.
FLUENCE+, E > 1.0 MeV		1.564+019	1.305+019	25.
dpa+		2.422-002	2.130-002	27.

---

* ABSOLUTE CALCULATED FLUX (OR NORMALIZED TO Fe54(n,p)Mn54 REACTION RATE).

+ BASED ON 1.079+008 EFFECTIVE FULL POWER SECONDS OF EXPOSURE; UNITS OF n/cm^2 FOR FLUENCE AND TOTAL NUMBER OF DISPLACED ATOMS OF IRON PER TARGET ATOM OF IRON FOR dpa.

TABLE 4.2.3.2.1.4

COMPARISON OF MEASURED AND CALCULATED REACTION RATES USED IN THE ANALYSIS OF TURKEY POINT UNIT 4 CAPSULE S

	REACTION RATE (DPS/NUCLEUS)			RATIO MEAS/CALC	
REACTION	MEAS	A PRIORI CALC	ADJ CALC	A PRIORI	ADJ CALC
Fe54(n,p)Mn54	9.25-015	9.27-015	9.56-015	1.00	.97
Cu63(n,α)Co60	1.15-016	9.99-017	1.13-016	1.15	1.02
Co59(n,γ)Co60	6.16-012	4.39-012	6.47-012	1.40	.95
Co59(n,γ)Co60 (Cd)	3.40-012	1.46-012	3.26-012	2.34	1.04

179

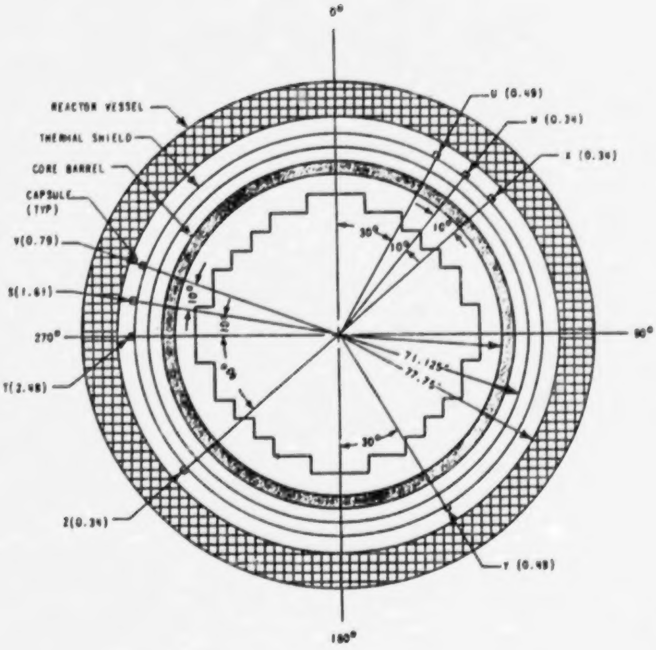
0°
REACTOR VESSEL
THERMAL SHIELD
CORE BARREL
CAPSULE (TYP)
V(0.79)
S(1.61)
270°
T(2.48)
Z(0.34)
U (0.49)
W (0.34)
X (0.34)
30°
10°
10°
10°
10°
90°
71.125°
77.75°
30°
Y (0.49)
180°

(a) Reactor Geometry.

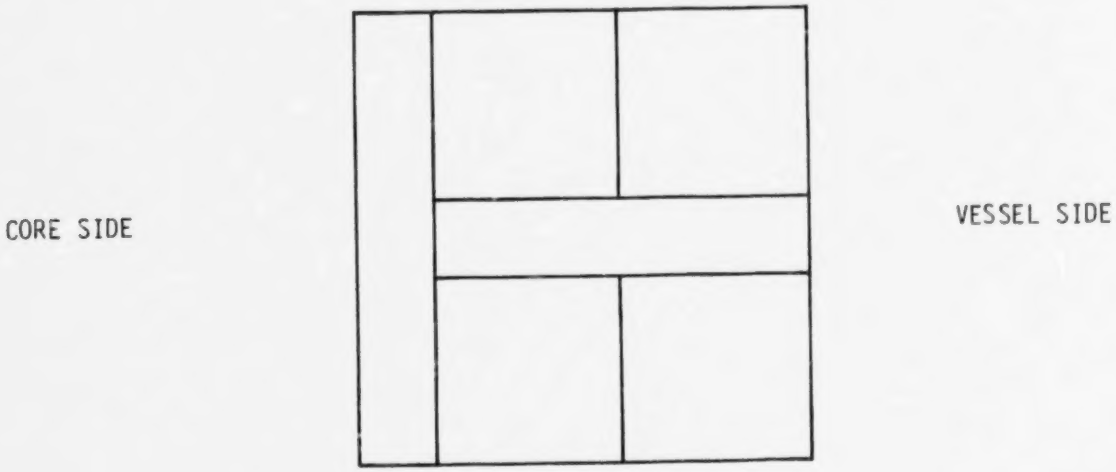
CORE SIDE
VESSEL SIDE

(b) Plan View of Surveillance Capsule

FIGURE 4.2.3.2.2.1. Orientation of the Capsule Relative to the Core and Vessel Wall - Turkey Point Unit 4 Capsule T.

TABLE 4.2.3.2.2.1

SUMMARY OF REACTOR OPERATIONS
TURKEY POINT UNIT 4 CAPSULE T

TIME PERIOD	START DATE	TIME INTERVAL	AVERAGE POWER LEVEL (MWt)	LOCAL POWER FACTOR
1	6/19/73	12.	272.	1.00
2	7/ 1/73	1.	0.	1.00
3	7/ 2/73	5.	519.	1.00
4	7/ 7/73	2.	0.	1.00
5	7/ 9/73	5.	607.	1.00
6	7/14/73	4.	0.	1.00
7	7/18/73	11.	641.	1.00
8	7/29/73	7.	0.	1.00
9	8/ 5/73	27.	793.	1.00
10	9/ 1/73	1.	0.	1.00
11	9/ 2/73	21.	1353.	1.00
12	9/23/73	1.	0.	1.00
13	9/24/73	41.	1490.	1.00
14	11/ 4/73	12.	0.	1.00
15	11/16/73	48.	1519.	1.00
16	1/ 3/74	31.	0.	1.00
17	2/ 3/74	59.	1747.	1.00
18	4/ 3/74	2.	0.	1.00
19	4/ 5/74	12.	1862.	1.00
20	4/17/74	1.	0.	1.00
21	4/18/74	37.	2030.	1.00
22	5/25/74	6.	0.	1.00
23	5/31/74	79.	2019.	1.00
24	8/18/74	23.	0.	1.00
25	9/10/74	47.	2092.	1.00
26	10/27/74	6.	0.	1.00
27	11/ 2/74	32.	1829.	1.00
28	12/ 4/74	3.	0.	1.00
29	12/ 7/74	30.	2128.	1.00
30	1/ 6/75	4.	0.	1.00
31	1/10/75	79.	2136.	1.00
	3/30/75	DISCHARGED*		

---

*EFFECTIVE FULL POWER OPERATION TIME WAS 3.728+007 SECONDS AT A FULL POWER LEVEL OF 2200. MWt.

TABLE 4.2.3.2.2.2

REACTION RATE DATA AND CORRECTION FACTORS FOR TURKEY POINT UNIT 4 CAPSULE T

REACTION NAME	REACTION IDENT	TOR RATE (DPS/NUCL)	SATURATION FACTOR	GRADIENT FACTOR	IMPURITY FACTOR	AVG REACTION RATE (RPS/NUCL)	% UNCERT (1σ)
^{54}Fe(n,p)^{54}Mn	W17	5.56-015	1.780+000	1.170	1.000	1.15-014	10.
	W21	6.18-015	1.780+000	0.950	1.000		
	S67	6.37-015	1.780+000	0.950	1.000		
	S69	6.53-015	1.780+000	0.950	1.000		
	S73	7.96-015	1.780+000	0.950	1.000		
^{63}Cu(n,α)^{60}Co	TOP	1.99-017	7.083+000	0.950	1.000	1.29-016	10.
	MID	1.85-017	7.083+000	0.950	1.000		
^{59}Co(n,γ)^{60}Co	TOP (B)	1.30-012	7.083+000	0.940	1.000	9.21-012	10.
	MID (B)	1.44-012	7.083+000	0.940	1.000		
	BOT (B)	1.41-012	7.083+000	0.940	1.000		
^{59}Co(n,γ)^{60}Co	TOP (CD)	4.97-013	7.083+000	1.180	1.000	4.59-012	15.
	MID (CD)	6.46-013	7.083+000	1.180	1.000		
	BOT (CD)	5.05-013	7.083+000	1.180	1.000		
^{237}Np(n,f)^{137}Cs	MID	1.02-015	3.748+001	1.000	1.000	6.12-013	10.
^{238}U(n,f)^{137}Cs	MID	8.66-014	3.748+001	1.000	0.901	4.87-011	10.

CD = Cadmium-Covered Dosimeter.
B = Bare Dosimeter.

TABLE 4.2.3.2.2.3

FERRET-SAND II RESULTS FOR
TURKEY POINT UNIT 4 CAPSULE T
(AVERAGE FOR CAPSULE)

GROUP	ENERGY (MeV)	A PRIORI FLUX* ($n/cm^2 \cdot s$)	ADJUSTED FLUX ($n/cm^2 \cdot s$)	% UNCERTAIN (1 σ)
1	1.492+001	7.211+006	9.089+006	41.
2	1.350+001	1.499+007	1.792+007	38.
3	1.162+001	6.951+007	7.895+007	34.
4	1.000+001	2.109+008	2.292+008	29.
5	8.607+000	5.337+008	5.594+008	26.
6	7.408+000	1.286+009	1.311+009	23.
7	6.065+000	4.534+009	4.490+009	20.
8	4.966+000	5.528+009	5.479+009	22.
9	3.679+000	7.585+009	7.756+009	22.
10	2.865+000	9.660+009	1.054+010	23.
11	2.231+000	1.756+010	2.087+010	24.
12	1.738+000	2.385+010	3.151+010	25.
13	1.353+000	3.041+010	4.456+010	25.
14	1.108+000	2.951+010	4.723+010	25.
15	8.208-001	4.582+010	8.037+010	25.
16	6.393-001	3.857+010	7.167+010	27.
17	4.979-001	3.872+010	7.529+010	30.
18	3.877-001	3.870+010	7.747+010	34.
19	3.020-001	3.529+010	7.190+010	38.
20	1.832-001	5.568+010	1.142+011	41.
21	1.111-001	3.954+010	8.065+010	44.
22	6.738-002	2.840+010	5.721+010	47.
23	4.087-002	2.401+010	4.760+010	49.
24	2.554-002	2.000+010	3.897+010	50.
25	1.989-002	9.420+009	1.808+010	52.
26	1.503-002	9.446+009	1.794+010	52.
27	9.119-003	1.454+010	2.750+010	52.
28	5.531-003	1.438+010	2.728+010	52.
29	3.355-003	1.525+010	2.924+010	51.
30	2.839-003	5.250+009	1.024+010	50.
31	2.404-003	5.293+009	1.057+010	49.
32	2.035-003	5.324+009	1.093+010	47.
33	1.234-003	1.590+010	3.365+010	44.
34	7.485-004	1.531+010	3.341+010	42.
35	4.540-004	1.415+010	3.173+010	39.
36	2.754-004	1.302+010	2.989+010	36.
37	1.670-004	1.256+010	2.934+010	34.
38	1.013-004	1.280+010	3.240+010	18.
39	6.144-005	1.366+010	3.214+010	32.
40	3.727-005	1.443+010	3.365+010	33.

TABLE 4.2.3.2.2.3 (Cont'd)

FERRET-SAND II RESULTS FOR TURKEY POINT UNIT 4 CAPSULE T (AVERAGE FOR CAPSULE)

GROUP	ENERGY (MeV)	A PRIORI FLUX* (n/cm^2•s)	ADJUSTED FLUX (n/cm^2•s)	% UNCERTAIN (1 σ)
41	2.260-005	1.453+010	3.323+010	34.
42	1.371-005	1.393+010	3.104+010	36.
43	8.315-006	1.274+010	2.752+010	38.
44	5.043-006	1.232+010	2.569+010	39.
45	3.059-006	1.233+010	2.479+010	40.
46	1.855-006	1.236+010	2.394+010	40.
47	1.125-006	1.239+010	2.316+010	40.
48	6.826-007	1.242+010	2.245+010	39.
49	4.140-007	1.243+010	2.179+010	37.
50	2.511-007	1.246+010	2.123+010	35.
51	1.523-007	1.795+010	2.989+010	33.
52	9.237-008	2.986+010	4.879+010	31.
53	1.000-010	6.483+010	1.037+011	25.
FLUX, E > 0.0 MeV		9.176+011	1.735+012	16.
FLUX, E < 0.414 eV		1.362+011	2.254+011	21.
FLUX, E > 0.1 MeV		4.248+011	7.582+011	20.
FLUX, E > 1.0 MeV		1.450+011	2.021+011	13.
dpa/s		2.243-010	3.477-010	13.
FLUENCE+, E > 1.0 MeV		5.404+018	7.535+018	13.
dpa+		8.363-003	1.296-002	13.

---

* ABSOLUTE CALCULATED FLUX (OR NORMALIZED TO Fe54(n,p)Mn54 REACTION RATE).

+ BASED ON 3.728+007 EFFECTIVE FULL POWER SECONDS OF EXPOSURE; UNITS OF n/cm^2 FOR FLUENCE AND TOTAL NUMBER OF DISPLACED ATOMS OF IRON PER TARGET ATOM OF IRON FOR dpa.

TABLE 4.2.3.2.2.4

COMPARISON OF MEASURED AND CALCULATED REACTION RATES USED IN THE ANALYSIS OF TURKEY POINT UNIT 4 CAPSULE T

REACTION	REACTION RATE (DPS/NUCLEUS) MEAS	A PRIORI CALC	ADJ CALC	RATIO MEAS/CALC A PRIORI	ADJ CALC
Fe54(n,p)Mn54	1.15-014	1.16-014	1.22-014	1.00	.95
Cu63(n,α)Co60	1.29-016	1.25-016	1.28-016	1.04	1.01
Np237(n,f)Cs137	6.12-013	3.68-013	5.92-013	1.66	1.03
Co59(n,γ)Co60	9.21-012	4.80-012	9.27-012	1.92	.99
Co59(n,γ)Co60 (Cd)	4.59-012	1.82-012	4.37-012	2.53	1.05
*U238(n,f)FP Cd	4.87-011	5.28-014	6.57-014	922.27	741.74

----

* REACTION NOT USED TO ADJUST SPECTRUM

185

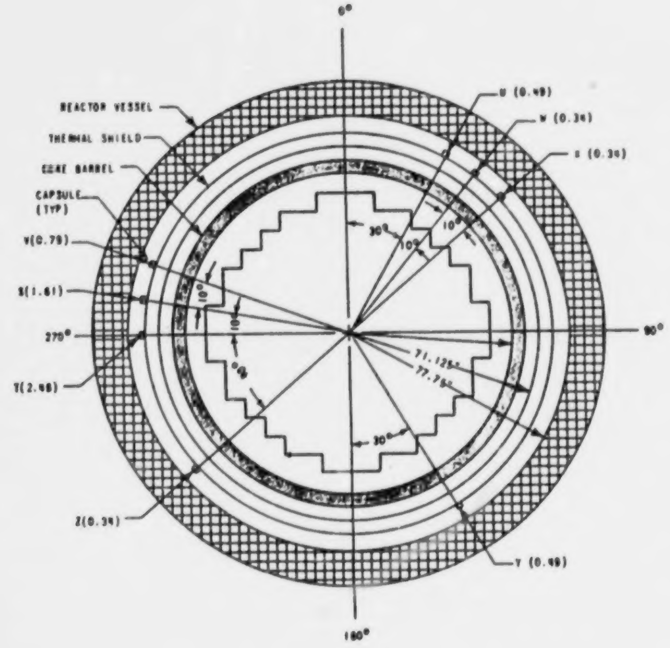
0°
REACTOR VESSEL
THERMAL SHIELD
CORE BARREL
CAPSULE (TYP)
V(0.79)
S(1.61)
270°
T(2.48)
Z(0.34)
U (0.49)
W (0.34)
X (0.34)
90°
Y (0.49)
180°
30°
10°
10°
10°
10°
10°
30°
71.125°
77.75°

(a) Reactor Geometry.

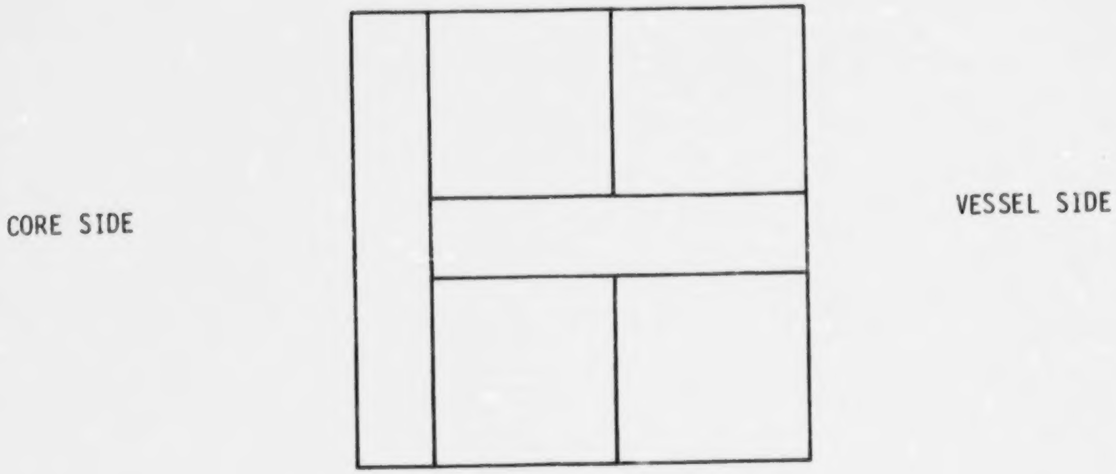
CORE SIDE
VESSEL SIDE

(b) Plan View of Surveillance Capsule

FIGURE 4.2.3.3.1.1. Orientation of the Capsule Relative to the Core and Vessel Wall - H. B. Robinson Unit 2 Capsule V.

TABLE 4.2.3.3.1.1

SUMMARY OF REACTOR OPERATIONS
H. B. ROBINSON UNIT 2 CAPSULE V

TIME PERIOD	START DATE	TIME INTERVAL	AVERAGE POWER LEVEL (MWt)	LOCAL POWER FACTOR
1	9/26/70	6.	106.	1.00
2	10/ 2/70	28.	0.	1.00
3	10/30/70	5.	308.	1.00
4	11/ 4/70	70.	0.	1.00
5	1/13/71	17.	778.	1.00
6	1/30/71	20.	0.	1.00
7	2/19/71	10.	1195.	1.00
8	3/ 1/71	1.	0.	1.00
9	3/ 2/71	2.	1144.	1.00
10	3/ 4/71	2.	0.	1.00
11	3/ 6/71	9.	1721.	1.00
12	3/15/71	54.	0.	1.00
13	5/ 8/71	14.	1557.	1.00
14	5/22/71	2.	0.	1.00
15	5/24/71	5.	651.	1.00
16	5/29/71	83.	0.	1.00
17	8/20/71	35.	1960.	1.00
18	9/24/71	2.	0.	1.00
19	9/26/71	27.	1947.	1.00
20	10/23/71	1.	0.	1.00
21	10/24/71	20.	1885.	1.00
22	11/13/71	1.	0.	1.00
23	11/14/71	62.	2084.	1.00
24	1/15/72	2.	0.	1.00
25	1/17/72	112.	2118.	1.00
26	5/ 8/72	32.	0.	1.00
27	6/ 9/72	59.	1787.	1.00
28	8/ 7/72	2.	0.	1.00
29	8/ 9/72	89.	2076.	1.00
30	11/ 6/72	3.	0.	1.00
31	11/ 9/72	43.	1947.	1.00
32	12/22/72	1.	0.	1.00
33	12/23/72	13.	812.	1.00
34	1/ 5/73	5.	0.	1.00
35	1/10/73	34.	1485.	1.00
36	2/13/73	4.	0.	1.00
37	2/17/73	28.	1476.	1.00
38	3/17/73	58.	0.	1.00
39	5/14/73	12.	695.	1.00
40	5/26/73	2.	0.	1.00

TABLE 4.2.3.3.1.1 (Cont'd)

SUMMARY OF REACTOR OPERATIONS
H. B. ROBINSON UNIT 2 CAPSULE V

TIME PERIOD	START DATE	TIME INTERVAL	AVERAGE POWER LEVEL (MWt)	LOCAL POWER FACTOR
41	5/28/73	145.	1987.	1.00
42	10/20/73	1.	0.	1.00
43	10/21/73	33.	2095.	1.00
44	11/23/73	10.	0.	1.00
45	12/ 3/73	155.	2067.	1.00
46	5/ 7/74	49.	0.	1.00
47	6/25/74	67.	1973.	1.00
48	8/31/74	2.	0.	1.00
49	9/ 2/74	40.	2054.	1.00
50	10/12/74	2.	0.	1.00
51	10/14/74	82.	2171.	1.00
52	1/ 4/75	2.	0.	1.00
53	1/ 6/75	96.	2132.	1.00
54	4/12/75	18.	0.	1.00
55	4/30/75	2.	1452.	1.00
56	5/ 2/75	25.	0.	1.00
57	5/27/75	6.	1364.	1.00
58	6/ 2/75	5.	0.	1.00
59	6/ 7/75	35.	2152.	1.00
60	7/12/75	2.	0.	1.00
61	7/14/75	110.	2121.	1.00
	11/ 1/75	DISCHARGED*		

---

*EFFECTIVE FULL POWER OPERATION TIME WAS 1.050+008 SECONDS AT A FULL POWER LEVEL OF 2200. MWt.

TABLE 4.2.3.3.1.2

REACTION RATE DATA AND CORRECTION FACTORS FOR H. B. ROBINSON UNIT 2 CAPSULE V

REACTION NAME	REACTION IDENT	TOR RATE (DPS/NUCL)	SATURATION FACTOR	GRADIENT FACTOR	IMPURITY FACTOR	AVG REACTION RATE (RPS/NUCL)	% UNCERT (1σ)
$^{54}\mathrm{Fe}(n,p)^{54}\mathrm{Mn}$	H-9	3.08-015	1.298+000	1.050	1.000	4.92-015	14.
	H-13	3.56-015	1.298+000	1.200	1.000		
	R-49	3.37-015	1.298+000	1.050	1.000		
	R-51	3.30-015	1.298+000	1.050	1.000		
	R-55	3.72-015	1.298+000	1.200	1.000		
$^{58}\mathrm{Ni}(n,p)^{58}\mathrm{Co}$	MID	6.02-015	1.153+000	0.900	1.000	6.24-015	10.
$^{63}\mathrm{Cu}(n,\alpha)^{60}\mathrm{Co}$	TOP	1.80-017	2.988+000	0.900	1.000	4.72-017	10.
	BOT	1.71-017	2.988+000	0.900	1.000		
$^{237}\mathrm{Np}(n,f)^{137}\mathrm{Cs}$	MID	7.20-015	1.374+001	1.000	1.000	1.58-012	10.
$^{238}\mathrm{U}(n,f)^{137}\mathrm{Cs}$	MID	1.09-014	1.374+001	1.000	0.909	2.26-012	10.
$^{59}\mathrm{Co}(n,\gamma)^{60}\mathrm{Co}$	TOP (B)	1.10-012	2.988+000	0.940	1.000	3.00-012	10.
	MID (B)	1.05-012	2.988+000	0.940	1.000		
	BOT (B)	1.06-012	2.988+000	0.940	1.000		
$^{59}\mathrm{Co}(n,\gamma)^{60}\mathrm{Co}$	TOP (CD)	2.10-013	2.988+000	1.100	1.000	1.07-012	37.
	MID (CD)	3.15-013	2.988+000	1.100	1.000		
	BOT (CD)	4.50-013	2.988+000	1.100	1.000		

CD = Cadmium-Covered Dosimeter.
B = Bare Dosimeter.

TABLE 4.2.3.3.1.3

FERRET-SAND II RESULTS FOR
H. B. ROBINSON UNIT 2 CAPSULE V
(AVERAGE FOR CAPSULE)

GROUP	ENERGY (MeV)	A PRIORI FLUX* ($n/cm^2 \cdot s$)	ADJUSTED FLUX ($n/cm^2 \cdot s$)	% UNCERTAIN ($1\ \sigma$)
1	1.492+001	3.277+006	3.146+006	41.
2	1.350+001	6.812+006	6.408+006	38.
3	1.162+001	3.158+007	2.919+007	34.
4	1.000+001	9.585+007	8.714+007	30.
5	8.607+000	2.425+008	2.182+008	26.
6	7.408+000	5.845+008	5.269+008	24.
7	6.065+000	2.060+009	1.859+009	20.
8	4.966+000	2.512+009	2.357+009	21.
9	3.679+000	3.447+009	3.335+009	21.
10	2.865+000	4.389+009	4.357+009	23.
11	2.231+000	7.979+009	8.072+009	25.
12	1.738+000	1.084+010	1.120+010	30.
13	1.353+000	1.382+010	1.458+010	34.
14	1.108+000	1.341+010	1.447+010	38.
15	8.208-001	2.082+010	2.288+010	41.
16	6.393-001	1.753+010	1.956+010	45.
17	4.979-001	1.759+010	1.987+010	47.
18	3.877-001	1.758+010	2.003+010	50.
19	3.020-001	1.604+010	1.839+010	52.
20	1.832-001	2.530+010	2.917+010	53.
21	1.111-001	1.797+010	2.079+010	54.
22	6.738-002	1.290+010	1.498+010	55.
23	4.087-002	1.091+010	1.270+010	55.
24	2.554-002	9.088+009	1.061+010	56.
25	1.989-002	4.280+009	5.018+009	55.
26	1.503-002	4.292+009	5.055+009	55.
27	9.119-003	6.606+009	7.825+009	55.
28	5.531-003	6.533+009	7.793+009	54.
29	3.355-003	6.929+009	8.335+009	54.
30	2.839-003	2.385+009	2.897+009	53.
31	2.404-003	2.405+009	2.953+009	51.
32	2.035-003	2.419+009	3.004+009	50.
33	1.234-003	7.223+009	9.075+009	48.
34	7.485-004	6.958+009	8.846+009	46.
35	4.540-004	6.429+009	8.262+009	44.
36	2.754-004	5.918+009	7.680+009	42.
37	1.670-004	5.708+009	7.470+009	41.
38	1.013-004	5.814+009	7.846+009	33.
39	6.144-005	6.205+009	8.212+009	39.
40	3.727-005	6.556+009	8.697+009	39.

TABLE 4.2.3.3.1.3 (Cont'd)

FERRET-SAND II RESULTS FOR
H. B. ROBINSON UNIT 2 CAPSULE V
(AVERAGE FOR CAPSULE)

GROUP	ENERGY (MeV)	A PRIORI FLUX* ($n/cm^2 \cdot s$)	ADJUSTED FLUX ($n/cm^2 \cdot s$)	% UNCERTAIN ($1\ \sigma$)
41	2.260-005	6.603+009	8.773+009	39.
42	1.371-005	6.332+009	8.422+009	40.
43	8.315-006	5.790+009	7.709+009	40.
44	5.043-006	5.597+009	7.462+009	41.
45	3.059-006	5.604+009	7.488+009	41.
46	1.855-006	5.615+009	7.525+009	40.
47	1.125-006	5.630+009	7.572+009	39.
48	6.826-007	5.643+009	7.618+009	38.
49	4.140-007	5.650+009	7.652+009	36.
50	2.511-007	5.662+009	7.683+009	34.
51	1.523-007	8.157+009	1.108+010	32.
52	9.237-008	1.357+010	1.845+010	31.
53	1.000-010	2.946+010	4.051+010	24.
FLUX, E > 0.0 MeV		4.211+011	5.070+011	22.
FLUX, E < 0.414 eV		6.250+010	8.538+010	20.
FLUX, E > 0.1 MeV		1.950+011	2.149+011	35.
FLUX, E > 1.0 MeV		6.653+010	6.892+010	22.
dpa/s		1.030-010	1.093-010	25.
FLUENCE+, E > 1.0 MeV		6.986+018	7.237+018	22.
dpa+		1.081-002	1.147-002	25.

---

* ABSOLUTE CALCULATED FLUX (OR NORMALIZED TO Fe54(n,p)Mn54 REACTION RATE).

+ BASED ON 1.050+008 EFFECTIVE FULL POWER SECONDS OF EXPOSURE; UNITS OF n/cm^2 FOR FLUENCE AND TOTAL NUMBER OF DISPLACED ATOMS OF IRON PER TARGET ATOM OF IRON FOR dpa.

TABLE 4.2.3.3.1.4

COMPARISON OF MEASURED AND CALCULATED REACTION RATES USED IN THE ANALYSIS OF H. B. ROBINSON UNIT 2 CAPSULE V

	REACTION RATE (DPS/NUCLEUS)			RATIO MEAS/CALC	
REACTION	MEAS	A PRIORI CALC	ADJ CALC	A PRIORI	ADJ CALC
Fe54(n,p)Mn54	5.22-015	5.25-015	5.04-015	0.99	1.04
Ni58(n,p)Co58	6.45-015	6.95-015	6.62-015	0.93	0.97
Cu63(n,α)Co60	4.99-017	5.66-017	5.10-017	0.88	0.98
Co59(n,γ)Co60	3.00-012	2.18-012	2.97-012	1.38	1.01
Co59(n,γ)Co60(Cd)	1.07-012	8.25-013	1.11-012	1.30	0.96
*U238(n,f)FP Cd	2.26-012	2.40-014	2.42-014	94.19	93.49
*Np237(n,f)FP Cd	1.58-012	1.72-013	1.84-013	9.19	8.59

---

*REACTION NOT USED TO ADJUST SPECTRUM

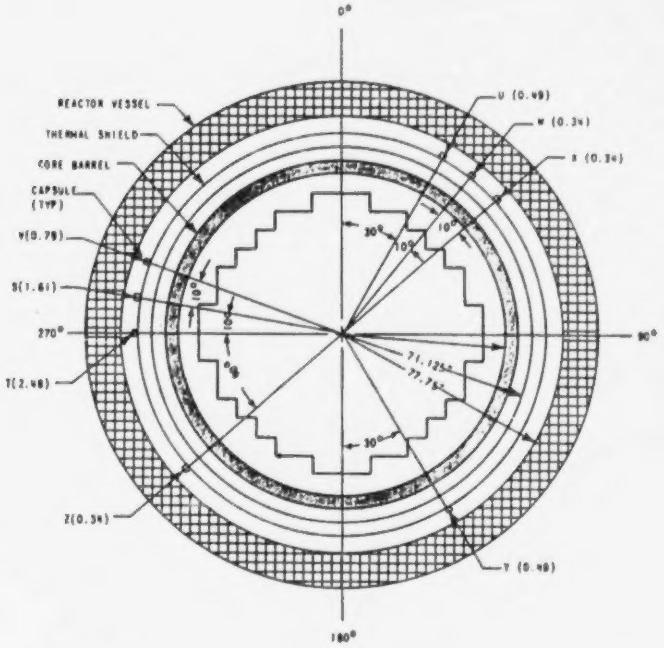
0°
REACTOR VESSEL
THERMAL SHIELD
CORE BARREL
CAPSULE (TYP)
V(0.79)
S(1.61)
270°
T(2.48)
Z(0.34)
U (0.48)
W (0.34)
X (0.34)
90°
Y (0.48)
180°
30°
10°
10°
10°
10°
6°
71.125°
77.75°
30°

(a) Reactor Geometry.

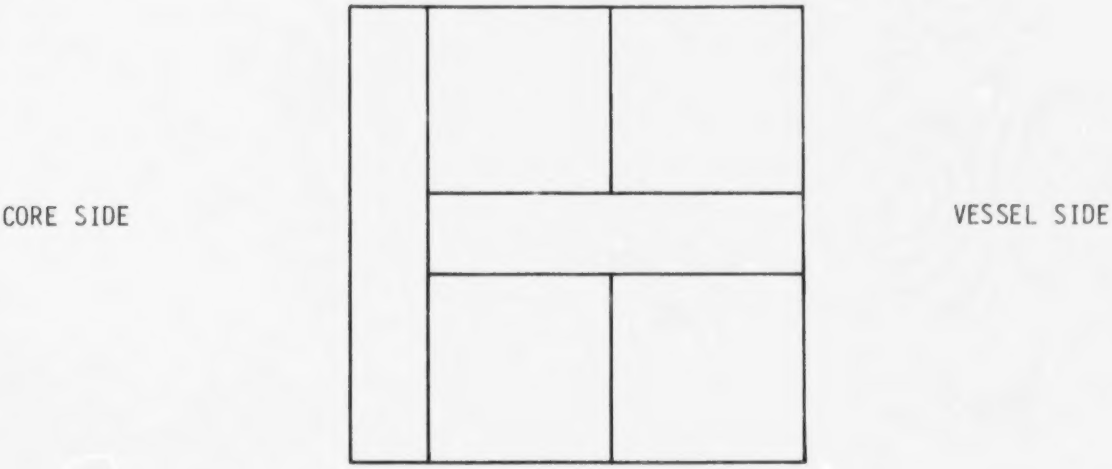
CORE SIDE
VESSEL SIDE

(b) Plan View of Surveillance Capsule

FIGURE 4.2.3.3.2.1. Orientation of the Capsule Relative to the Core and Vessel Wall - H. B. Robinson Unit 2 Capsule S.

TABLE 4.2.3.3.2.1

SUMMARY OF REACTOR OPERATIONS
H. B. ROBINSON UNIT 2 CAPSULE S

TIME PERIOD	START DATE	TIME INTERVAL	AVERAGE POWER LEVEL (MWt)	LOCAL POWER FACTOR
1	9/26/70	6.	106.	1.00
2	10/ 2/70	28.	0.	1.00
3	10/30/70	5.	308.	1.00
4	11/ 4/70	70.	0.	1.00
5	1/13/71	17.	778.	1.00
6	1/30/71	20.	0.	1.00
7	2/19/71	10.	1195.	1.00
8	3/ 1/71	1.	0.	1.00
9	3/ 2/71	2.	1144.	1.00
10	3/ 4/71	2.	0.	1.00
11	3/ 6/71	9.	1721.	1.00
12	3/15/71	54.	0.	1.00
13	5/ 8/71	14.	1557.	1.00
14	5/22/71	2.	0.	1.00
15	5/24/71	5.	651.	1.00
16	5/29/71	83.	0.	1.00
17	8/20/71	35.	1960.	1.00
18	9/24/71	2.	0.	1.00
19	9/26/71	27.	1947.	1.00
20	10/23/71	1.	0.	1.00
21	10/24/71	20.	1885.	1.00
22	11/13/71	1.	0.	1.00
23	11/14/71	62.	2084.	1.00
24	1/15/72	2.	0.	1.00
25	1/17/72	112.	2118.	1.00
26	5/ 8/72	32.	0.	1.00
27	6/ 9/72	59.	1787.	1.00
28	8/ 7/72	2.	0.	1.00
29	8/ 9/72	89.	2076.	1.00
30	11/ 6/72	3.	0.	1.00
31	11/ 9/72	43.	1947.	1.00
32	12/22/72	1.	0.	1.00
33	12/23/72	13.	812.	1.00
34	1/ 5/73	5.	0.	1.00
35	1/10/73	34.	1485.	1.00
36	2/13/73	4.	0.	1.00
37	2/17/73	28.	1476.	1.00
	3/17/73	DISCHARGED*		

---

*EFFECTIVE FULL POWER OPERATION TIME WAS 4.209+007 SECONDS AT A FULL POWER LEVEL OF 2200. MWt.

BLANK PAGE

BLANK PAGE

BLANK PAGE

TABLE 4.2.3.3.2.2

REACTION RATE DATA AND CORRECTION FACTORS FOR H. B. ROBINSON UNIT 2 CAPSULE S

REACTION		TOR RATE	SATURATION	GRADIENT	IMPURITY	AVG REACTION	% UNCERT
NAME	IDENT	(DPS/NUCL)	FACTOR	FACTOR	FACTOR	RATE (RPS/NUCL)	(1σ)
$^{54}Fe(n,p)^{54}Mn$	TOP	3.59-015	1.769+000	1.050	1.000	6.90-015	10.
	TOP MID	3.73-015	1.769+000	1.050	1.000		
	MID	3.62-015	1.769+000	1.050	1.000		
	BOT MID	4.14-015	1.769+000	0.960	1.000		
	BOT	3.45-015	1.769+000	1.170	1.000		
$^{58}Ni(n,p)^{58}Co$	MID	6.81-015	1.452+000	0.900	1.000	8.89-015	10.
$^{63}Cu(n,\alpha)^{60}Co$	TOP	2.54-017	6.403+000	0.900	1.000	1.10-016	47.
	BOT	1.27-017	6.403+000	0.900	1.000		
$^{59}Co(n,\gamma)^{60}Co$	TOP (B)	1.19-012	6.403+000	0.940	1.000	7.63-012	10.
	BOT (B)	1.34-012	6.403+000	0.940	1.000		
$^{59}Co(n,\gamma)^{60}Co$	TOP (CD)	3.81-013	6.403+000	1.100	1.000	2.94-012	14.
	MID (CD)	3.85-013	6.403+000	1.100	1.000		
	BOT (CD)	4.85-013	6.403+000	1.100	1.000		

CD = Cadmium-Covered Dosimeter.
B = Bare Dosimeter.

TABLE 4.2.3.3.2.3

FERRET-SAND II RESULTS FOR
H. B. ROBINSON UNIT 2 CAPSULE S
(AVERAGE FOR CAPSULE)

GROUP	ENERGY (MeV)	A PRIORI FLUX* ($n/cm^2 \cdot s$)	ADJUSTED FLUX ($n/cm^2 \cdot s$)	% UNCERTAIN ($1\ \sigma$)
1	1.492+001	4.335+006	6.366+006	46.
2	1.350+001	9.012+006	1.258+007	44.
3	1.162+001	4.178+007	5.522+007	40.
4	1.000+001	1.268+008	1.587+008	37.
5	8.607+000	3.208+008	3.797+008	33.
6	7.408+000	7.733+008	8.628+008	29.
7	6.065+000	2.726+009	2.853+009	24.
8	4.966+000	3.323+009	3.304+009	22.
9	3.679+000	4.560+009	4.406+009	21.
10	2.865+000	5.807+009	5.623+009	24.
11	2.231+000	1.056+010	1.036+010	27.
12	1.738+000	1.434+010	1.460+010	32.
13	1.353+000	1.828+010	1.943+010	36.
14	1.108+000	1.774+010	1.981+010	40.
15	8.208-001	2.754+010	3.246+010	43.
16	6.393-001	2.319+010	2.893+010	46.
17	4.979-001	2.328+010	3.072+010	49.
18	3.877-001	2.326+010	3.240+010	51.
19	3.020-001	2.122+010	3.105+010	52.
20	1.832-001	3.347+010	5.119+010	53.
21	1.111-001	2.377+010	3.776+010	54.
22	6.738-002	1.707+010	2.802+010	55.
23	4.087-002	1.444+010	2.436+010	55.
24	2.554-002	1.202+010	2.079+010	55.
25	1.989-002	5.663+009	1.001+010	55.
26	1.503-002	5.678+009	1.026+010	55.
27	9.119-003	8.739+009	1.614+010	54.
28	5.531-003	8.642+009	1.635+010	54.
29	3.355-003	9.167+009	1.780+010	53.
30	2.839-003	3.156+009	6.308+009	51.
31	2.404-003	3.182+009	6.562+009	50.
32	2.035-003	3.200+009	6.821+009	47.
33	1.234-003	9.555+009	2.106+010	45.
34	7.485-004	9.205+009	2.096+010	42.
35	4.540-004	8.505+009	1.996+010	39.
36	2.754-004	7.829+009	1.887+010	36.
37	1.670-004	7.552+009	1.860+010	34.
38	1.013-004	7.692+009	2.064+010	18.
39	6.144-005	8.209+009	2.077+010	32.
40	3.727-005	8.673+009	2.202+010	33.

TABLE 4.2.3.3.2.3 (Cont'd)

FERRET-SAND II RESULTS FOR
H. B. ROBINSON UNIT 2 CAPSULE S
(AVERAGE FOR CAPSULE)

GROUP	ENERGY (MeV)	A PRIORI FLUX* (n/cm^2•s)	ADJUSTED FLUX (n/cm^2•s)	% UNCERTAIN (1 σ)
41	2.260-005	8.735+009	2.218+010	34.
42	1.371-005	8.377+009	2.121+010	36.
43	8.315-006	7.660+009	1.932+010	38.
44	5.043-006	7.404+009	1.861+010	39.
45	3.059-006	7.414+009	1.859+010	40.
46	1.855-006	7.429+009	1.862+010	40.
47	1.125-006	7.448+009	1.868+010	39.
48	6.826-007	7.465+009	1.876+010	38.
49	4.140-007	7.475+009	1.881+010	36.
50	2.511-007	7.491+009	1.883+010	34.
51	1.523-007	1.079+010	2.708+010	31.
52	9.237-008	1.795+010	4.496+010	29.
53	1.000-010	3.897+010	9.973+010	21.
FLUX, E > 0.0 MeV		?????????	1.018+012	20.
FLUX, E < 0.414 eV		9.727+010	2.094+011	18.
FLUX, E > 0.1 MeV		3.034+011	3.323+011	37.
FLUX, E > 1.0 MeV		1.035+011	9.295+010	24.
dpa/s		1.602-010	1.604-010	27.
FLUENCE+, E > 1.0 MeV		4.358+018	3.912+018	24.
dpa+		6.744-003	6.750-003	27.

---

* ABSOLUTE CALCULATED FLUX (OR NORMALIZED TO Fe54(n,p)Mn54 REACTION RATE).

+ BASED ON 4.209+007 EFFECTIVE FULL POWER SECONDS OF EXPOSURE; UNITS OF n/cm^2 FOR FLUENCE AND TOTAL NUMBER OF DISPLACED ATOMS OF IRON PER TARGET ATOM OF IRON FOR dpa.

TABLE 4.2.3.3.2.4

COMPARISON OF MEASURED AND CALCULATED REACTION RATES USED IN THE ANALYSIS OF H. B. ROBINSON UNIT 2 CAPSULE S

REACTION	REACTION RATE (DPS/NUCLEUS) MEAS	A PRIORI CALC	ADJ CALC	RATIO MEAS/CALC A PRIORI	ADJ CALC
Fe54(n,p)Mn54	6.92-015	6.95-015	7.00-015	1.00	.99
Ni58(n,p)Co58	8.89-015	9.19-015	9.19-015	.97	.97
Cu63(n,α)Co60	1.10-016	7.49-017	8.31-017	1.47	1.32
Co59(n,γ)Co60	7.63-012	2.88-012	7.46-012	2.65	1.02
Co59(n,γ)Co60 (Cd)	2.94-012	1.09-012	2.89-012	2.69	1.02

BEST COPY AVAILABLE

198

TO BE PROVIDED

(a) Reactor Geometry.

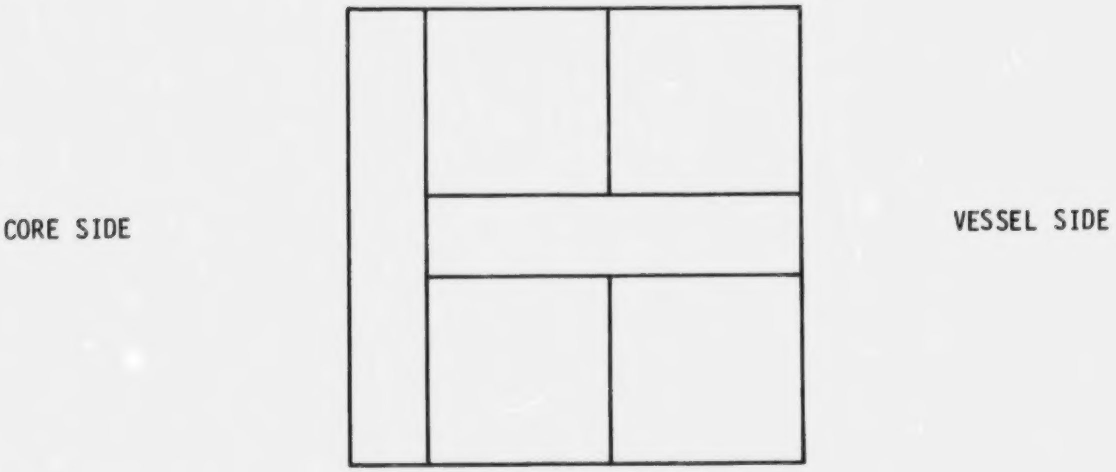
CORE SIDE
VESSEL SIDE

(b) Plan View of Surveillance Capsule

FIGURE 4.2.3.4.1.1. Orientation of the Capsule Relative to the Core and Vessel Wall - Surry Unit 1 Capsule T.

TABLE 4.2.3.4.1.1

SUMMARY OF REACTOR OPERATIONS
SURRY UNIT 1 CAPSULE T

TIME PERIOD	START DATE	TIME INTERVAL	AVERAGE POWER LEVEL (MWt)	LOCAL POWER FACTOR
1	6/20/72	194.	1032.	1.00
2	12/31/72	365.	1032.	1.00
3	12/31/73	365.	1032.	1.00
	12/31/74	DISCHARGED*		

---

*EFFECTIVE FULL POWER OPERATION TIME WAS 3.377+007 SECONDS AT A FULL POWER LEVEL OF 2441. MWt.

200

TABLE 4.2.3.4.1.2

REACTION RATE DATA AND CORRECTION FACTORS FOR SURRY UNIT 1 CAPSULE T

REACTION NAME	REACTION IDENT	TOR RATE (DPS/NUCL)	SATURATION FACTOR	GRADIENT FACTOR	IMPURITY FACTOR	AVG REACTION RATE (RPS/NUCL)	% UNCERT (1σ)
^{54}Fe(n,p)^{54}Mn	TOP			0.950	1.000	5.86-015	10.
	MID			0.950	1.000		
	BOT			0.950	1.000		
^{58}Ni(n,p)^{58}Co	MID			0.930	1.000	8.03-015	10.
^{63}Cu(n,α)^{60}Co	TOP			0.950	1.000	6.02-017	10.
	BOT			0.950	1.000		
^{238}U(n,f)^{137}Cs	MID			1.000	0.935	3.03-014	10.
^{237}Np(n,f)^{137}Cs	MID			1.000	1.000	2.03-013	10.
^{59}Co(n,γ)^{60}Co	TOP (B)			0.930	1.000	4.16-012	10.
	MID (B)			0.930	1.000		
	BOT (B)			0.930	1.000		
^{59}Co(n,γ)^{60}Co	TOP (CD)			1.190	1.000	1.96-012	10.
	MID (CD)			1.190	1.000		
	BOT (CD)			1.190	1.000		

CD = Cadmium-Covered Dosimeter.
B = Bare Dosimeter.

201

TABLE 4.2.3.4.1.3

FERRET-SAND II RESULTS FOR SURRY UNIT 1 CAPSULE T (AVERAGE FOR CAPSULE)

GROUP	ENERGY (MeV)	A PRIORI FLUX* (n/cm^2•s)	ADJUSTED FLUX (n/cm^2•s)	% UNCERTAIN (1 σ)
1	1.492+001	2.988+006	3.515+006	41.
2	1.350+001	6.211+006	7.385+006	37.
3	1.162+001	2.880+007	3.444+007	34.
4	1.000+001	8.740+007	1.047+008	29.
5	8.607+000	2.211+008	2.632+008	26.
6	7.408+000	5.209+008	6.070+008	24.
7	6.065+000	1.850+009	2.103+009	20.
8	4.966+000	2.592+009	2.777+009	21.
9	3.679+000	4.121+009	4.176+009	21.
10	2.865+000	5.884+009	5.672+009	22.
11	2.231+000	1.125+010	1.038+010	22.
12	1.738+000	1.628+010	1.441+010	21.
13	1.353+000	2.161+010	1.816+010	22.
14	1.108+000	2.154+010	1.712+010	25.
15	8.208-001	3.403+010	2.603+010	25.
16	6.393-001	2.952+010	2.238+010	28.
17	4.979-001	3.027+010	2.296+010	32.
18	3.877-001	2.985+010	2.288+010	35.
19	3.020-001	2.718+010	2.118+010	39.
20	1.832-001	4.507+010	3.588+010	42.
21	1.111-001	3.337+010	2.729+010	45.
22	6.738-002	2.354+010	1.985+010	47.
23	4.087-002	1.959+010	1.705+010	49.
24	2.554-002	1.642+010	1.476+010	51.
25	1.989-002	7.789+009	7.225+009	52.
26	1.503-002	7.858+009	7.516+009	52.
27	9.119-003	1.213+010	1.194+010	52.
28	5.531-003	1.191+010	1.207+010	52.
29	3.355-003	1.283+010	1.337+010	51.
30	2.839-003	4.436+009	4.745+009	50.
31	2.404-003	4.477+009	4.916+009	49.
32	2.035-003	4.505+009	5.075+009	46.
33	1.234-003	1.345+010	1.552+010	44.
34	7.485-004	1.294+010	1.526+010	41.
35	4.540-004	1.191+010	1.431+010	38.
36	2.754-004	1.091+010	1.332+010	35.
37	1.670-004	1.053+010	1.299+010	32.
38	1.013-004	1.078+010	1.403+010	15.
39	6.144-005	1.164+010	1.445+010	30.
40	3.727-005	1.246+010	1.531+010	31.

TABLE 4.2.3.4.1.3 (Cont'd)

FERRET-SAND II RESULTS FOR SURRY UNIT 1 CAPSULE T (AVERAGE FOR CAPSULE)

GROUP	ENERGY (MeV)	A PRIORI FLUX* ($n/cm^2 \cdot s$)	ADJUSTED FLUX ($n/cm^2 \cdot s$)	% UNCERTAIN ($1\ \sigma$)
41	2.260-005	1.259+010	1.530+010	33.
42	1.371-005	1.199+010	1.433+010	35.
43	8.315-006	1.088+010	1.272+010	37.
44	5.043-006	1.065+010	1.217+010	39.
45	3.059-006	1.065+010	1.186+010	40.
46	1.855-006	1.066+010	1.156+010	40.
47	1.125-006	1.066+010	1.127+010	40.
48	6.826-007	1.066+010	1.101+010	38.
49	4.140-007	1.067+010	1.076+010	36.
50	2.511-007	1.053+010	1.040+010	34.
51	1.523-007	1.426+010	1.385+010	32.
52	9.237-008	2.352+010	2.255+010	30.
53	1.000-010	5.107+010	4.802+010	23.
FLUX, E > 0.0 MeV		6.736+011	6.939+011	15.
FLUX, E < 0.414 eV		1.010+011	1.056+011	20.
FLUX, E > 0.1 MeV		2.938+011	2.586+011	20.
FLUX, E > 1.0 MeV		8.956+010	8.472+010	9.
dpa/s		1.430-010	1.330-010	12.
FLUENCE+, E > 1.0 MeV		3.025+018	2.862+018	9.
dpa+		4.831-003	4.492-003	12.

---

* ABSOLUTE CALCULATED FLUX (OR NORMALIZED TO Fe54(n,p)Mn54 REACTION RATE).

+ BASED ON 3.378+007 EFFECTIVE FULL POWER SECONDS OF EXPOSURE; UNITS OF n/cm^2 FOR FLUENCE AND TOTAL NUMBER OF DISPLACED ATOMS OF IRON PER TARGET ATOM OF IRON FOR dpa.

TABLE 4.2.3.4.1.4

COMPARISON OF MEASURED AND CALCULATED REACTION RATES USED IN THE ANALYSIS OF SURRY UNIT 1 CAPSULE T

	REACTION RATE (DPS/NUCLEUS)			RATIO MEAS/CALC	
REACTION	MEAS	A PRIORI CALC	ADJ CALC	A PRIORI	ADJ CALC
Fe54(n,p)Mn54	5.86-015	5.87-015	5.99-015	1.00	.98
Ni58(n,p)Co58	8.08-015	7.93-015	8.02-015	1.02	1.01
Cu63(n,α)Co60	6.02-017	5.13-017	5.92-017	1.17	1.02
Np237(n,f)Cs137	2.03-013	2.58-013	2.10-013	.79	.96
Co59(n,γ)Co60	4.16-012	3.90-012	4.20-012	1.07	.99
Co59(n,γ)Co60 (Cd)	1.96-012	1.54-012	1.93-012	1.28	1.02
U238(n,f)Cs137	3.03-014	3.20-014	2.96-014	.95	1.02

TO BE PROVIDED

(a) Reactor Geometry.

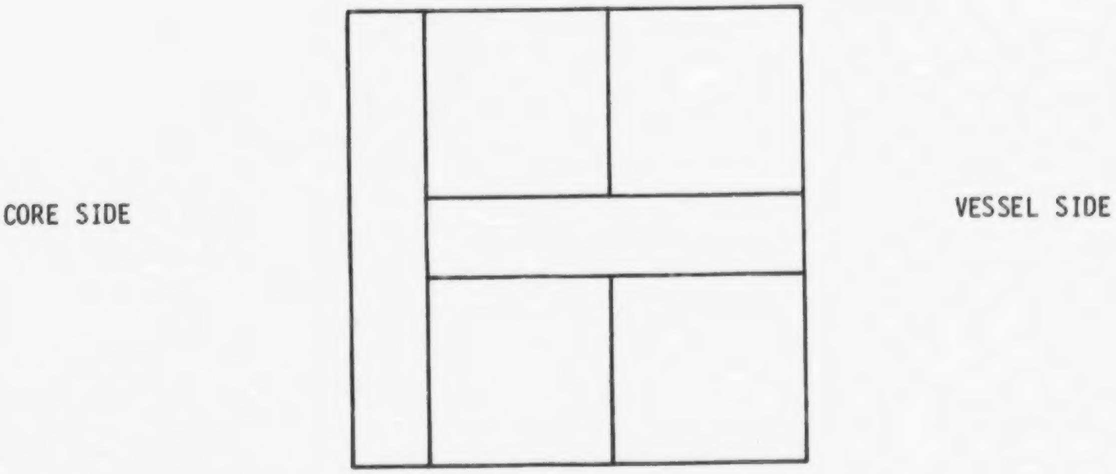
CORE SIDE
VESSEL SIDE

(b) Plan View of Surveillance Capsule

FIGURE 4.2.3.5.1.1. Orientation of the Capsule Relative to the Core and Vessel Wall - Surry Unit 2 Capsule X.

TABLE 4.2.3.5.1.1

SUMMARY OF REACTOR OPERATIONS
SURRY UNIT 2 CAPSULE X

TIME PERIOD	START DATE	TIME INTERVAL	AVERAGE POWER LEVEL (MWt)	LOCAL POWER FACTOR
1	9/ 1/74	427.	2441.	1.00
	11/ 2/75	DISCHARGED*		

---

*EFFECTIVE FULL POWER OPERATION TIME WAS 3.689+007 SECONDS AT A FULL POWER LEVEL OF 2441. MWt.

TABLE 4.2.3.5.1.2

REACTION RATE DATA AND CORRECTION FACTORS FOR SURRY UNIT 2 CAPSULE X

REACTION		TOR RATE	SATURATION	GRADIENT	IMPURITY	AVG REACTION	% UNCERT
NAME	IDENT	(DPS/NUCL)	FACTOR	FACTOR	FACTOR	RATE (RPS/NUCL)	(1σ)
$^{54}\mathrm{Fe}(n,p)^{54}\mathrm{Mn}$	TOP			0.950	1.000	5.97-015	10.
	TOP MID			0.950	1.000		
	MID			0.950	1.000		
	BOT MID			0.950	1.000		
	MID			0.950	1.000		
$^{58}\mathrm{Ni}(n,p)^{58}\mathrm{Co}$	TOP MID			0.930	1.000	6.66-015	10.
	MID			0.930	1.000		
	BOT MID			0.930	1.000		
$^{63}\mathrm{Cu}(n,\alpha)^{60}\mathrm{Co}$	TOP MID			0.950	1.000	5.82-017	10.
	MID			0.950	1.000		
	BOT MID			0.950	1.000		
$^{238}\mathrm{U}(n,f)^{137}\mathrm{Cs}$	MID			1.000	0.926	3.00-014	10.
$^{237}\mathrm{Np}(n,f)^{137}\mathrm{Cs}$	MID			1.000	1.000	1.90-013	10.
$^{59}\mathrm{Co}(n,\gamma)^{60}\mathrm{Co}$	TOP (B)			0.930	1.000	3.85-012	10.
	BOT (B)			0.930	1.000		
$^{59}\mathrm{Co}(n,\gamma)^{60}\mathrm{Co}$	TOP (CD)			1.00	1.000	1.80-012	10.

CD = Cadmium-Covered Dosimeter.
B = Bare Dosimeter.

TABLE 4.2.3.5.1.3

FERRET-SAND II RESULTS FOR
SURRY UNIT 2 CAPSULE X
(AVERAGE FOR CAPSULE)

GROUP	ENERGY (MeV)	A PRIORI FLUX* ($n/cm^2 \cdot s$)	ADJUSTED FLUX ($n/cm^2 \cdot s$)	% UNCERTAIN ($1\ \sigma$)
1	1.492+001	3.059+006	3.369+006	41.
2	1.350+001	6.360+006	7.091+006	37.
3	1.162+001	2.948+007	3.314+007	34.
4	1.000+001	8.948+007	1.010+008	30.
5	8.607+000	2.264+008	2.542+008	26.
6	7.408+000	5.333+008	5.879+008	24.
7	6.065+000	1.894+009	2.043+009	20.
8	4.966+000	2.654+009	2.709+009	21.
9	3.679+000	4.219+009	4.077+009	22.
10	2.865+000	6.025+009	5.549+009	22.
11	2.231+000	1.152+010	1.010+010	22.
12	1.738+000	1.666+010	1.399+010	22.
13	1.353+000	2.213+010	1.756+010	23.
14	1.108+000	2.205+010	1.650+010	26.
15	8.208-001	3.484+010	2.501+010	27.
16	6.393-001	3.022+010	2.145+010	30.
17	4.979-001	3.099+010	2.196+010	33.
18	3.877-001	3.056+010	2.185+010	37.
19	3.020-001	2.782+010	2.019+010	40.
20	1.832-001	4.615+010	3.417+010	43.
21	1.111-001	3.416+010	2.598+010	46.
22	6.738-002	2.410+010	1.888+010	48.
23	4.087-002	2.006+010	1.622+010	50.
24	2.554-002	1.681+010	1.403+010	51.
25	1.989-002	7.974+009	6.867+009	52.
26	1.503-002	8.046+009	7.139+009	53.
27	9.119-003	1.242+010	1.133+010	53.
28	5.531-003	1.219+010	1.143+010	52.
29	3.355-003	1.314+010	1.264+010	52.
30	2.839-003	4.542+009	4.476+009	50.
31	2.404-003	4.583+009	4.624+009	49.
32	2.035-003	4.612+009	4.759+009	47.
33	1.234-003	1.377+010	1.451+010	44.
34	7.485-004	1.325+010	1.422+010	41.
35	4.540-004	1.219+010	1.330+010	38.
36	2.754-004	1.117+010	1.235+010	35.
37	1.670-004	1.078+010	1.201+010	32.
38	1.013-004	1.104+010	1.287+010	15.
39	6.144-005	1.192+010	1.333+010	30.
40	3.727-005	1.276+010	1.413+010	31.

TABLE 4.2.3.5.1.3 (Cont'd)

FERRET-SAND II RESULTS FOR
SURRY UNIT 2 CAPSULE X
(AVERAGE FOR CAPSULE)

GROUP	ENERGY (MeV)	A PRIORI FLUX* ($n/cm^2 \cdot s$)	ADJUSTED FLUX ($n/cm^2 \cdot s$)	% UNCERTAIN ($1\ \sigma$)
41	2.260-005	1.289+010	1.413+010	33.
42	1.371-005	1.228+010	1.325+010	35.
43	8.315-006	1.113+010	1.178+010	37.
44	5.043-006	1.090+010	1.128+010	39.
45	3.059-006	1.091+010	1.101+010	40.
46	1.855-006	1.091+010	1.075+010	40.
47	1.125-006	1.091+010	1.049+010	39.
48	6.826-007	1.092+010	1.025+010	38.
49	4.140-007	1.092+010	1.003+010	36.
50	2.511-007	1.078+010	9.710+009	34.
51	1.523-007	1.460+010	1.294+010	32.
52	9.237-008	2.409+010	2.107+010	30.
53	1.000-010	5.229+010	4.484+010	23.
FLUX, E > 0.0 MeV		8.083+011	6.548+011	16.
FLUX, E < 0.414 eV		1.212+011	9.860+010	20.
FLUX, E > 0.1 MeV		3.525+011	2.481+011	21.
FLUX, E > 1.0 MeV		1.075+011	8.207+010	11.
dpa/s		1.716-010	1.282-010	13.
FLUENCE+, E > 1.0 MeV		3.963+018	3.026+018	11.
dpa+		6.328-003	4.728-003	13.

---

* ABSOLUTE CALCULATED FLUX (OR NORMALIZED TO Fe54(n,p)Mn54 REACTION RATE).

+ BASED ON 3.687+007 EFFECTIVE FULL POWER SECONDS OF EXPOSURE; UNITS OF n/cm^2 FOR FLUENCE AND TOTAL NUMBER OF DISPLACED ATOMS OF IRON PER TARGET ATOM OF IRON FOR dpa.

TABLE 4.2.3.5.1.4

COMPARISON OF MEASURED AND CALCULATED REACTION RATES USED IN THE ANALYSIS OF SURRY UNIT 2 CAPSULE X

REACTION	REACTION RATE (DPS/NUCLEUS) MEAS	A PRIORI CALC	ADJ CALC	RATIO MEAS/CALC A PRIORI	ADJ CALC
Fe54(n,p)Mn54	5.97-015	6.01-015	5.86-015	.99	1.02
Ni58(n,p)Co58	6.66-015	8.12-015	7.69-015	.82	.87
Cu63(n,α)Co60	5.82-017	5.25-017	5.73-017	1.11	1.02
U238(n,f)Cs137	3.00-014	3.26-014	2.86-014	.92	1.05
Np237(n,f)Cs137	1.90-013	2.64-013	2.03-013	.72	.94
Co59(n,γ)Co60	3.85-012	4.00-012	3.89-012	.96	.99
Co59(n,γ)Co60 (Cd)	1.80-012	1.57-012	1.77-012	1.14	1.02

TO BE PROVIDED

(a) Reactor Geometry.

CORE SIDE

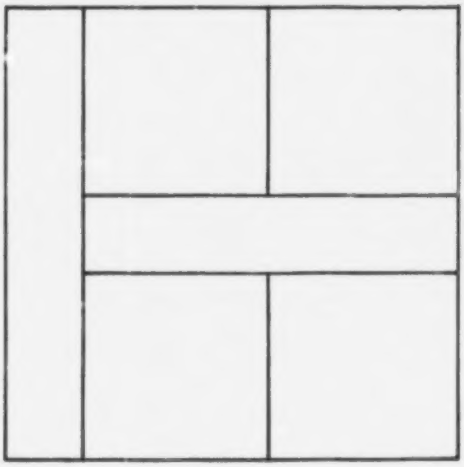

VESSEL SIDE

(b) Plan View of Surveillance Capsule

FIGURE 4.2.3.6.1.1. Orientation of the Capsule Relative to the Core and Vessel Wall - North Anna Unit 1 Capsule V.

211

TABLE 4.2.3.6.1.1

SUMMARY OF REACTOR OPERATIONS
NORTH ANNA UNIT 1 CAPSULE V

TIME PERIOD	START DATE	TIME INTERVAL	AVERAGE POWER LEVEL (MWt)	LOCAL POWER FACTOR
1	4/ 9/78	22.	405.	1.00
2	5/ 1/78	31.	1141.	1.00
3	6/ 1/78	30.	2304.	1.00
4	7/ 1/78	31.	2354.	1.00
5	8/ 1/78	31.	2633.	1.00
6	9/ 1/78	30.	1995.	1.00
7	10/ 1/78	31.	2353.	1.00
8	11/ 1/78	30.	2631.	1.00
9	12/ 1/78	31.	2583.	1.00
10	1/ 1/79	31.	2299.	1.00
11	2/ 1/79	28.	2383.	1.00
12	3/ 1/79	31.	2482.	1.00
13	4/ 1/79	30.	0.	1.00
14	5/ 1/79	31.	2438.	1.00
15	6/ 1/79	30.	2703.	1.00
16	7/ 1/79	31.	2671.	1.00
17	8/ 1/79	31.	2747.	1.00
18	9/ 1/79	25.	1891.	1.00
	9/26/79	DISCHARGED*		

---

*EFFECTIVE FULL POWER OPERATION TIME WAS 3.570+007 SECONDS AT A FULL POWER LEVEL OF 2775. MWt.

TABLE 4.2.3.6.1.2

REACTION RATE DATA AND CORRECTION FACTORS FOR NORTH ANNA UNIT 1 CAPSULE V

REACTION NAME	IDENT	TOR RATE (DPS/NUCL)	SATURATION FACTOR	GRADIENT FACTOR	IMPURITY FACTOR	AVG REACTION RATE (RPS/NUCL)	% UNCERT (1σ)
^{54}Fe(n,p)^{54}Mn	TOP	3.13-015	1.816+000	0.950	1.000	5.26-015	10.
	TOP MID	2.98-015	1.816+000	0.950	1.000		
	MID	3.12-015	1.816+000	0.950	1.000		
	BOT MID	2.95-015	1.816+000	0.950	1.000		
	BOT	3.06-015	1.816+000	0.950	1.000		
^{58}Fe(n,γ)^{59}Fe	TOP	1.20-013	1.200+000	1.000	1.000	1.45-013	10.
	TOP MID	1.26-013	1.200+000	1.000	1.000		
	MID	1.21-013	1.200+000	1.000	1.000		
	BOT MID	1.16-013	1.200+000	1.000	1.000		
	BOT	1.23-013	1.200+000	1.000	1.000		
^{58}Ni(n,p)^{58}Co	TOP MID	5.58-015	1.217+000	0.930	1.000	6.34-015	10.
	MID	5.74-015	1.217+000	0.930	1.000		
	BOT MID	5.47-015	1.217+000	0.930	1.000		
^{63}Cu(n,α)^{60}Co	TOP MID	7.91-018	7.350+000	0.950	1.000	5.63-017	10.
	MID	8.36-018	7.350+000	0.950	1.000		
	BOT MID	7.91-018	7.350+000	0.950	1.000		
^{59}Co(n,γ)^{60}Co	TOP (B)	5.90-013	7.350+000	1.000	1.000	4.46-012	10.
	BOT (B)	6.23-013	7.350+000	1.000	1.000		
^{59}Co(n,γ)^{60}Co	TOP (CD)	2.14-013	7.350+000	1.180	1.000	1.85-012	10.
	BOT (CD)	2.13-013	7.350+000	1.180	1.000		
^{238}U(n,f)^{137}Cs	MID	4.80-017	3.910+001	1.000	0.926	2.89-014	10.
^{238}U(n,f)^{95}Zr	MID	1.23-015	1.211+000	1.000	0.926	2.71-014	10.

TABLE 4.2.3.6.1.2 (Cont'd)

REACTION RATE DATA AND CORRECTION FACTORS FOR NORTH ANNA UNIT 1 CAPSULE V

REACTION NAME	REACTION IDENT	TOR RATE (DPS/NUCL)	SATURATION FACTOR	GRADIENT FACTOR	IMPURITY FACTOR	AVG REACTION RATE (RPS/NUCL)	% UNCERT (1σ)
$^{238}U(n,f)^{103}Ru$	MID	1.58-015	1.200+000	1.000	0.926	2.82-014	10.
$^{238}U(n,f)^{106}Ru$	MID	4.02-016	1.993+000	1.000	0.926	2.95-014	10.
$^{238}U(n,f)^{141}Ce$	MID	9.43-016	1.204+000	1.000	0.926	1.93-014	10.
$^{238}U(n,f)^{144}Ce$	MID	7.47-016	1.728+000	1.000	0.926	2.63-014	10.
$^{237}Np(n,f)^{137}Cs$	MID	3.10-016	3.910+001	1.000	1.000	1.94-013	10.
$^{237}Np(n,p)^{95}Zr$	MID	8.86-015	1.211+000	1.000	1.000	1.88-013	10.
$^{237}Np(n,f)^{103}Ru$	MID	9.04-015	1.200+000	1.000	1.000	1.94-013	10.
$^{237}Np(n,f)^{106}Ce$	MID	1.98-015	1.993+000	1.000	1.000	1.76-013	10.
$^{237}Np(n,f)^{141}Ce$	MID	1.46-014	1.204+000	1.000	1.000	3.22-013	10.
$^{237}Np(n,f)^{144}Ce$	MID	4.40-015	1.728+000	1.000	1.000	1.81-013	10.

CD = Cadmium-Covered Dosimeter.
B = Bare Dosimeter.

TABLE 4.2.3.6.1.3

FERRET-SAND II RESULTS FOR
NORTH ANNA UNIT 1 CAPSULE V
(AVERAGE FOR CAPSULE)

GROUP	ENERGY (MeV)	A PRIORI FLUX* (n/cm^2•s)	ADJUSTED FLUX (n/cm^2•s)	% UNCERTAIN (1 σ)
1	1.492+001	6.120+006	4.914+006	38.
2	1.350+001	1.272+007	9.823+006	35.
3	1.162+001	9.544+007	7.138+007	31.
4	1.000+001	3.272+008	2.393+008	25.
5	8.607+000	3.289+008	2.410+008	24.
6	7.408+000	5.976+008	4.454+008	24.
7	6.065+000	1.789+009	1.357+009	21.
8	4.966+000	2.733+009	2.166+009	22.
9	3.679+000	4.906+009	4.142+009	20.
10	2.865+000	4.984+009	4.758+009	22.
11	2.231+000	9.435+009	1.029+010	21.
12	1.738+000	1.018+010	1.276+010	21.
13	1.353+000	1.251+010	1.704+010	22.
14	1.108+000	1.071+010	1.470+010	25.
15	8.208-001	1.627+010	2.339+010	26.
16	6.393-001	1.361+010	2.009+010	29.
17	4.979-001	1.293+010	1.931+010	32.
18	3.877-001	1.167+010	1.737+010	36.
19	3.020-001	1.049+010	1.540+010	39.
20	1.832-001	1.788+010	2.567+010	42.
21	1.111-001	1.453+010	2.033+010	45.
22	6.738-002	1.206+010	1.645+010	47.
23	4.087-002	1.039+010	1.386+010	49.
24	2.554-002	8.920+009	1.171+010	50.
25	1.989-002	4.622+009	6.020+009	51.
26	1.503-002	5.135+009	6.695+009	52.
27	9.119-003	9.050+009	1.195+010	52.
28	5.531-003	8.868+009	1.194+010	52.
29	3.355-003	8.654+009	1.197+010	51.
30	2.839-003	2.833+009	4.060+009	50.
31	2.404-003	2.804+009	4.185+009	48.
32	2.035-003	2.777+009	4.330+009	46.
33	1.234-003	8.161+009	1.328+010	43.
34	7.485-004	7.900+009	1.338+010	40.
35	4.540-004	7.631+009	1.335+010	37.
36	2.754-004	7.368+009	1.359+010	34.
37	1.670-004	7.123+009	1.299+010	32.
38	1.013-004	6.899+009	1.341+010	13.
39	6.144-005	6.694+009	1.186+010	31.
40	3.727-005	6.509+009	1.114+010	32.

TABLE 4.2.3.6.1.3 (Cont'd)

FERRET-SAND II RESULTS FOR
NORTH ANNA UNIT 1 CAPSULE V
(AVERAGE FOR CAPSULE)

GROUP	ENERGY (MeV)	A PRIORI FLUX* ($n/cm^2 \cdot s$)	ADJUSTED FLUX ($n/cm^2 \cdot s$)	% UNCERTAIN (1 σ)
41	2.260-005	6.344+009	1.034+010	34.
42	1.371-005	6.198+009	9.505+009	36.
43	8.315-006	6.073+009	8.668+009	38.
44	5.043-006	5.967+009	7.864+009	39.
45	3.059-006	5.881+009	7.122+009	40.
46	1.855-006	5.814+009	6.460+009	40.
47	1.125-006	5.767+009	5.890+009	39.
48	6.826-007	5.741+009	5.416+009	37.
49	4.140-007	1.746+010	1.536+010	34.
50	2.511-007	3.642+010	2.976+010	31.
51	1.523-007	3.580+010	2.778+010	28.
52	9.237-008	3.521+010	2.640+010	27.
53	1.000-010	9.064+010	6.316+010	17.
FLUX, E > 0.0 MeV		5.537+011	6.397+011	14.
FLUX, E < 0.414 eV		2.155+011	1.625+011	14.
FLUX, E > 0.1 MeV		1.585+011	2.132+011	19.
FLUX, E > 1.0 MeV		6.417+010	7.622+010	9.
dpa/s		9.599-011	1.151-010	11.
FLUENCE+, E > 1.0 MeV		2.291+018	2.721+018	9.
dpa+		3.427-003	4.108-003	11.

---

* ABSOLUTE CALCULATED FLUX (OR NORMALIZED TO Fe54(n,p)Mn54 REACTION RATE).

+ BASED ON 3.570+007 EFFECTIVE FULL POWER SECONDS OF EXPOSURE; UNITS OF n/cm^2 FOR FLUENCE AND TOTAL NUMBER OF DISPLACED ATOMS OF IRON PER TARGET ATOM OF IRON FOR dpa.

TABLE 4.2.3.6.1.4

COMPARISON OF MEASURED AND CALCULATED REACTION RATES USED IN THE ANALYSIS OF NORTH ANNA UNIT 1 CAPSULE V

REACTION	REACTION RATE (DPS/NUCLEUS) MEAS	A PRIORI CALC	ADJ CALC	RATIO MEAS/CALC A PRIORI	ADJ CALC
Fe54(n,p)Mn54	5.26-015	6.04-015	5.29-015	.87	1.00
Fe58(n,γ)Fe59	1.45-013	1.54-013	1.38-013	.94	1.05
Ni58(n,p)Co58	6.34-015	7.93-015	6.89-015	.80	.92
Cu63(n,α)Co60	5.63-017	7.52-017	5.65-017	.75	1.00
Co59(n,γ)Co60	4.46-012	5.40-012	4.98-012	.83	.90
Co59(n,γ)Co60 (Cd)	1.85-012	1.01-012	1.75-012	1.83	1.06
U235(n,f)Cs137	2.89-014	2.45-014	2.68-014	1.18	1.08
Np237(n,f)Cs137	1.94-013	1.50-013	1.93-013	1.29	1.01

TO BE PROVIDED

(a) Reactor Geometry.

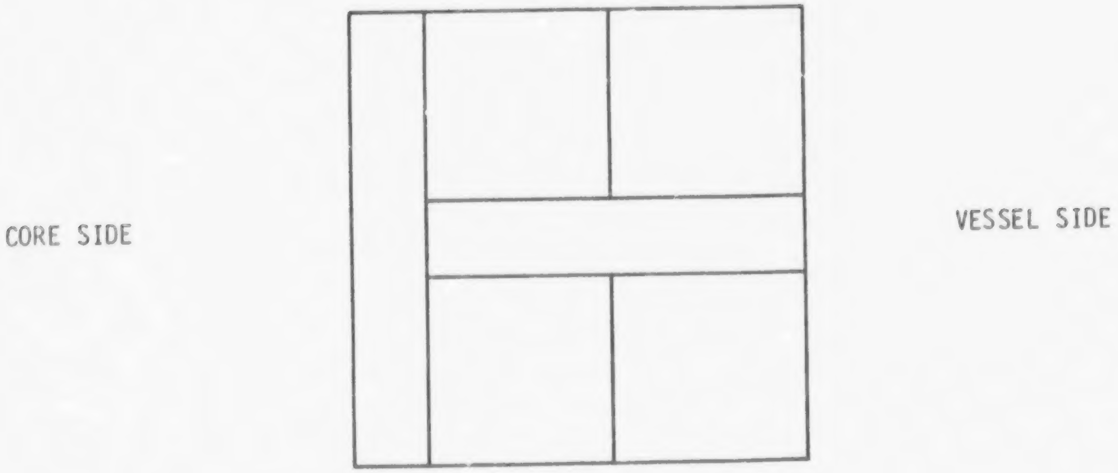
CORE SIDE
VESSEL SIDE

(b) Plan View of Surveillance Capsule

FIGURE 4.2.3.7.1.1. Orientation of the Capsule Relative to the Core and Vessel Wall - Beznau Unit 2 Capsule R.

TABLE 4.2.3.7.1.1

SUMMARY OF REACTOR OPERATIONS
BEZNAU UNIT 2 CAPSULE R

TIME PERIOD	START DATE	TIME INTERVAL	AVERAGE POWER LEVEL (MWt)	LOCAL POWER FACTOR
1	4/23/71	1984	Not Available	1.00
	7/15/78	DISCHARGED*		

---

*EFFECTIVE FULL POWER OPERATION TIME WAS 1.714+008 SECONDS.

219

TABLE 4.2.3.7.1.2

REACTION RATE DATA AND CORRECTION FACTORS FOR BEZNAU UNIT 2 CAPSULE R

REACTION NAME	REACTION IDENT	TOR RATE (DPS/NUCL)	SATURATION FACTOR	GRADIENT FACTOR	IMPURITY FACTOR	AVG REACTION RATE (RPS/NUCL)	% UNCERTAIN (1σ)
^{54}Fe(n,p)^{54}Mn	C-15 C-18			0.950	1.000	6.21-015	10.
^{63}Cu(n,α)^{60}Co	TOP MID-TOP MID-BOT BOT			1.050	1.000	5.29-017	10.
^{58}N(n,p)^{58}Co	MID			0.860	1.000	7.07-015	10.
^{237}Np(n,f)F.P.	MID			1.000	1.000	1.92-013	10.
^{238}U(n,f)F.P.	MID			1.000	0.550	2.93-014	10.
^{59}Co(n,γ)^{60}Co (Cd)	TOP MID-TOP MID MID-BOT BOT			1.170	1.000	4.35-012	10.
^{59}Co(n,γ)^{60}Co (Bare)	TOP MID-TOP MID MID-BOT BOT			0.950	1.000	6.87-012	10.

TABLE 4.2.3.7.1.3

FERRET-SAND II RESULTS FOR
BEZNAU UNIT 2 CAPSULE R
(AVERAGE FOR CAPSULE)

GROUP	ENERGY (MeV)	A PRIORI FLUX* (n/cm^2•s)	ADJUSTED FLUX (n/cm^2•s)	% UNCERTAIN (1σ)
1	1.492+001	6.120+006	4.646+006	39.
2	1.350+001	1.272+007	9.331+006	35.
3	1.162+001	9.544+007	6.801+007	31.
4	1.000+001	3.272+008	2.253+008	25.
5	8.607+000	3.289+008	2.352+008	24.
6	7.408+000	5.976+008	4.498+008	24.
7	6.065+000	1.789+009	1.413+009	21.
8	4.966+000	2.733+009	2.399+009	22.
9	3.679+000	4.906+009	4.818+009	20.
10	2.865+000	4.984+009	5.389+009	22.
11	2.231+000	9.435+009	1.114+010	21.
12	1.738+000	1.018+010	1.292+010	21.
13	1.353+000	1.251+010	1.658+010	22.
14	1.108+000	1.071+010	1.434+010	25.
15	8.208-001	1.627+010	2.219+010	26.
16	6.393-001	1.361+010	1.881+010	29.
17	4.979-001	1.293+010	1.794+010	33.
18	3.877-001	1.167+010	1.612+010	36.
19	3.020-001	1.049+010	1.435+010	39.
20	1.832-001	1.788+010	2.420+010	42.
21	1.111-001	1.453+010	1.951+010	45.
22	6.738-002	1.206+010	1.616+010	48.
23	4.087-002	1.039+010	1.398+010	49.
24	2.554-002	8.920+009	1.218+010	51.
25	1.989-002	4.622+009	6.474+009	52.
26	1.503-002	5.135+009	7.468+009	52.
27	9.119-003	9.050+009	1.386+010	52.
28	5.531-003	8.868+009	1.450+010	52.
29	3.355-003	8.654+009	1.531+010	51.
30	2.839-003	2.833+009	5.490+009	50.
31	2.404-003	2.804+009	6.010+009	48.
32	2.035-003	2.777+009	6.622+009	46.
33	1.234-003	8.161+009	2.164+010	43.
34	7.485-004	7.900+009	2.315+010	40.
35	4.540-004	7.631+009	2.439+010	37.
36	2.754-004	7.368+009	2.516+010	34.
37	1.670-004	7.123+009	2.535+010	32.
38	1.013-004	6.899+009	3.183+010	13.
39	6.144-005	6.694+009	2.356+010	31.
40	3.727-005	6.509+009	2.153+010	32.

TABLE 4.2.3.7.1.3 (Cont'd)

FERRET-SAND II RESULTS FOR
BEZNAU UNIT 2 CAPSULE R
(AVERAGE FOR CAPSULE)

GROUP	ENERGY (MeV)	A PRIORI FLUX* (n/cm^2•s)	ADJUSTED FLUX (n/cm^2•s)	% UNCERTAIN (1σ)
41	2.260-005	6.344+009	1.919+010	35.
42	1.371-005	6.198+009	1.668+010	37.
43	8.315-006	6.073+009	1.422+010	39.
44	5.043-006	5.967+009	1.197+010	41.
45	3.059-006	5.881+009	1.002+010	42.
46	1.855-006	5.814+009	8.416+009	42.
47	1.125-006	5.767+009	7.132+009	41.
48	6.826-007	5.741+009	6.139+009	40.
49	4.140-007	1.729+010	1.627+010	38.
50	2.511-007	3.442+010	2.872+010	36.
51	1.523-007	3.219+010	2.463+010	34.
52	9.237-008	3.012+010	2.176+010	33.
53	1.000-010	1.014+011	6.448+010	25.
FLUX, E > 0.0 MeV		5.536+011	7.674+011	15.
FLUX, E < 0.414 eV		2.154+011	1.558+011	23.
FLUX, E > 0.1 MeV		1.585+011	2.065+011	19.
FLUX, E > 1.0 MeV		6.417+010	7.757+010	9.
dpa/s		9.605-011	1.157-010	11.
FLUENCE+, E > 1.0 MeV		1.100+019	1.330+019	9.
dpa+		1.646-002	1.983-002	11.

---

*ABSOLUTE CALCULATED FLUX (OR NORMALIZED TO Fe54(n,p)Mn54 REACTION RATE).

+BASED ON 1.714+008 EFFECTIVE FULL POWER SECONDS OF EXPOSURE; UNITS OF n/cm^2 FOR FLUENCE AND TOTAL NUMBER OF DISPLACED ATOMS OF IRON PER TARGET ATOM OF IRON FOR dpa.

TABLE 4.2.3.7.1.4

COMPARISON OF MEASURED AND CALCULATED REACTION RATES USED IN THE ANALYSIS OF BEZNAU UNIT 2 CAPSULE R

	REACTION RATE (DPS/NUCLEUS)			RATIO MEAS/CALC	
REACTION	MEAS	A PRIORI CALC	ADJ CALC	A PRIORI	ADJ CALC
Co59(n,γ)Co60 (Bare)	6.87-012	6.03-012	7.44-012	1.14	0.92
Co59(n,γ)Co60 (Cd)	4.35-012	1.04-012	3.95-012	4.17	1.10
Cu63(n,α)Co60	5.29-017	7.52-017	5.57-017	0.70	0.95
Ni58(n,p)Co58	7.07-015	7.93-015	7.55-015	0.89	0.94
U238(n,f)Cs137	2.93-014	2.46-014	2.81-014	1.19	1.04
Np237(n,f)Cs137	1.92-013	1.51-013	1.95-013	1.27	0.99
Fe54(n,p)Mn54	6.21-015	6.04-015	5.84-015	1.03	1.06

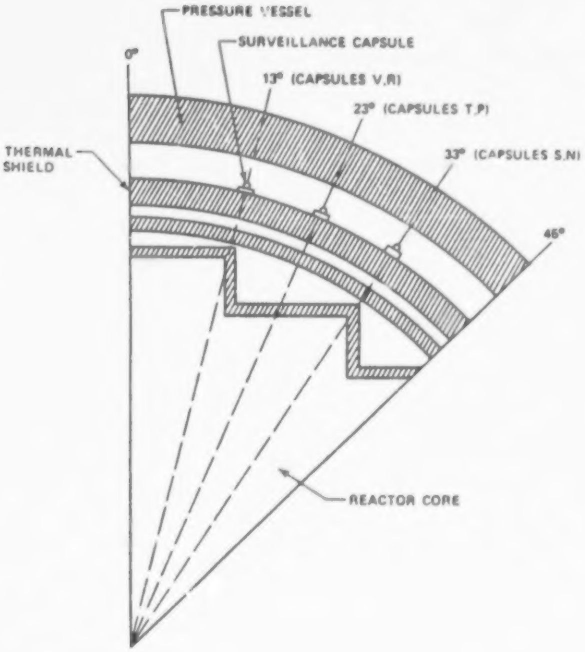
PRESSURE VESSEL
SURVEILLANCE CAPSULE
0°
13° (CAPSULES V,R)
23° (CAPSULES T,P)
33° (CAPSULES S,N)
THERMAL SHIELD
45°
REACTOR CORE

(a) Reactor Geometry.

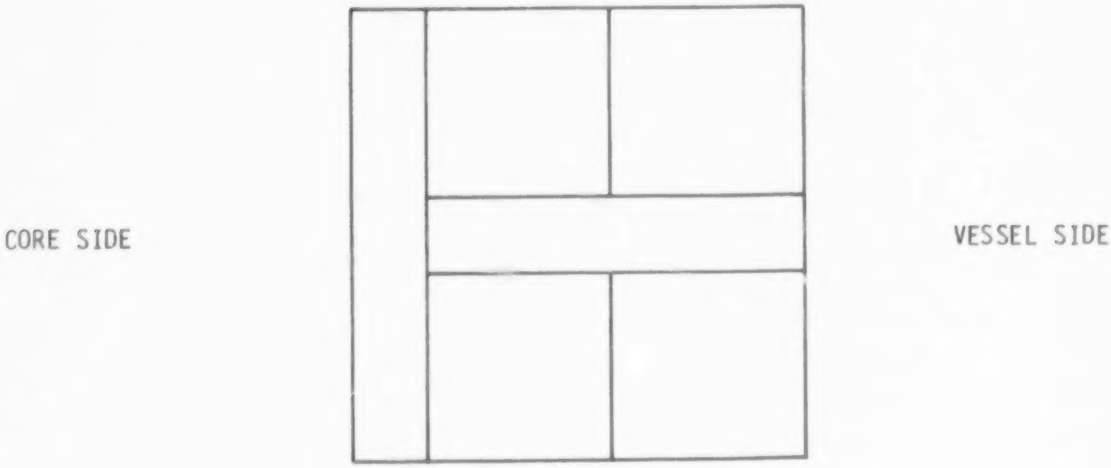
CORE SIDE
VESSEL SIDE

(b) Plan View of Surveillance Capsule

FIGURE 4.2.4.1.1.1. Orientation of the Capsule Relative to the Core and Vessel Wall - Prairie Island Unit 1 Capsule V.

TABLE 4.2.4.1.1.1

SUMMARY OF REACTOR OPERATIONS
PRAIRIE ISLAND UNIT 1 CAPSULE V

TIME PERIOD	START DATE	TIME INTERVAL	AVERAGE POWER LEVEL (MWt)	LOCAL POWER FACTOR
1	12/ 2/73	30.	178.	1.00
2	1/ 1/74	31.	0.	1.00
3	2/ 1/74	28.	574.	1.00
4	3/ 1/74	31.	140.	1.00
5	4/ 1/74	30.	527.	1.00
6	5/ 1/74	31.	0.	1.00
7	6/ 1/74	30.	0.	1.00
8	7/ 1/74	31.	1048.	1.00
9	8/ 1/74	31.	1255.	1.00
10	9/ 1/74	30.	203.	1.00
11	10/ 1/74	31.	259.	1.00
12	11/ 1/74	30.	1547.	1.00
13	12/ 1/74	31.	1593.	1.00
14	1/ 1/75	31.	1329.	1.00
15	2/ 1/75	28.	1319.	1.00
16	3/ 1/75	31.	1606.	1.00
17	4/ 1/75	30.	1274.	1.00
18	5/ 1/75	31.	934.	1.00
19	6/ 1/75	30.	1343.	1.00
20	7/ 1/75	31.	1299.	1.00
21	8/ 1/75	31.	1102.	1.00
22	9/ 1/75	30.	1577.	1.00
23	10/ 1/75	31.	1418.	1.00
24	11/ 1/75	30.	1574.	1.00
25	12/ 1/75	31.	1593.	1.00
26	1/ 1/76	31.	1602.	1.00
27	2/ 1/76	29.	1194.	1.00
28	3/ 1/76	4.	945.	1.00
	3/ 5/76	DISCHARGED*		

---

*EFFECTIVE FULL POWER OPERATION TIME WAS 4.234+007 SECONDS AT A FULL POWER LEVEL OF 1650. MWt.

TABLE 4.2.4.1.1.2

REACTION RATE DATA AND CORRECTION FACTORS FOR PRAIRIE ISLAND UNIT 1 CAPSULE V

REACTION NAME	IDENT	TOR RATE (DPS/NUCL)	SATURATION FACTOR	GRADIENT FACTOR	IMPURITY FACTOR	AVG REACTION RATE (RPS/NUCL)	% UNCERT (1σ)
^{54}Fe(n,p)^{54}Mn	BOT	5.39-015	1.658+000	0.950	1.000	7.96-015	10.
	BOT MID	5.05-015	1.658+000	0.950	1.000		
	MID	4.86-015	1.658+000	0.950	1.000		
	TOP MID	4.77-015	1.658+000	0.950	1.000		
	TOP	5.19-015	1.658+000	0.950	1.000		
^{58}Ni(n,p)^{58}Co	MID	7.66-015	1.183+000	1.130	1.000	1.02-014	10.
^{63}Cu(n,α)^{60}Co	BOT MID	1.03-017	6.306+000	1.100	1.000	6.74-017	10.
	TOP MID	9.12-018	6.306+000	1.100	1.000		
^{237}Np(n,f)^{137}Cs	MID	7.48-016	3.307+001	1.000	1.000	3.95-013	10.
^{238}U(n,f)^{137}Cs	MID	9.75-017	3.307+001	1.000	0.847	4.55-014	10.
^{59}Co(n,γ)^{60}Co	BOT (B)	1.55-012	6.306+000	0.940	1.000	8.52-012	11.
	TOP (B)	1.32-012	6.306+000	0.940	1.000		
^{59}Co(n,γ)^{60}Co	BOT (CD)	5.33-013	6.306+000	1.180	1.000	4.11-012	10.
	TOP (CD)	5.73-013	6.306+000	1.180	1.000		

CD = Cadmium-Covered Dosimeter.
B = Bare Dosimeter.

TABLE 4.2.4.1.1.3

FERRET-SAND II RESULTS FOR PRAIRIE ISLAND UNIT 1 CAPSULE V (AVERAGE FOR CAPSULE)

GROUP	ENERGY (MeV)	A PRIORI FLUX* (n/cm^2•s)	ADJUSTED FLUX (n/cm^2•s)	% UNCERTAIN (1 σ)
1	1.492+001	3.914+006	3.741+006	41.
2	1.350+001	8.138+006	7.817+006	38.
3	1.162+001	3.773+007	3.638+007	34.
4	1.000+001	1.145+008	1.109+008	30.
5	8.607+000	2.897+008	2.810+008	26.
6	7.408+000	6.805+008	6.567+008	24.
7	6.065+000	2.391+009	2.294+009	20.
8	4.966+000	3.481+009	3.255+009	21.
9	3.679+000	5.958+009	5.458+009	21.
10	2.865+000	8.783+009	8.012+009	21.
11	2.231+000	1.687+010	1.538+010	21.
12	1.738+000	2.487+010	2.289+010	21.
13	1.353+000	3.495+010	3.201+010	22.
14	1.108+000	3.656+010	3.282+010	27.
15	8.208-001	6.120+010	5.457+010	28.
16	6.393-001	5.502+010	4.890+010	31.
17	4.979-001	5.705+010	5.060+010	34.
18	3.877-001	5.585+010	4.946+010	38.
19	3.020-001	5.183+010	4.586+010	41.
20	1.832-001	8.945+010	7.911+010	44.
21	1.111-001	6.995+010	6.191+010	46.
22	6.738-002	5.177+010	4.590+010	49.
23	4.087-002	4.290+010	3.815+010	50.
24	2.554-002	3.610+010	3.226+010	52.
25	1.989-002	1.731+010	1.558+010	52.
26	1.503-002	1.769+010	1.607+010	53.
27	9.119-003	2.852+010	2.623+010	53.
28	5.531-003	2.851+010	2.660+010	52.
29	3.355-003	2.913+010	2.768+010	52.
30	2.839-003	9.844+009	9.542+009	50.
31	2.404-003	9.890+009	9.802+009	49.
32	2.035-003	9.946+009	1.009+010	46.
33	1.234-003	2.990+010	3.105+010	44.
34	7.485-004	2.919+010	3.098+010	41.
35	4.540-004	2.746+010	2.969+010	38.
36	2.754-004	2.587+010	2.835+010	35.
37	1.670-004	2.553+010	2.820+010	32.
38	1.013-004	2.583+010	3.008+010	14.
39	6.144-005	2.628+010	2.878+010	31.
40	3.727-005	2.672+010	2.872+010	32.

TABLE 4.2.4.1.1.3 (Cont'd)

FERRET-SAND II RESULTS FOR
PRAIRIE ISLAND UNIT 1 CAPSULE V
(AVERAGE FOR CAPSULE)

GROUP	ENERGY (MeV)	A PRIORI FLUX* ($n/cm^2 \cdot s$)	ADJUSTED FLUX ($n/cm^2 \cdot s$)	% UNCERTAIN (1 σ)
41	2.260-005	2.696+010	2.820+010	34.
42	1.371-005	2.657+010	2.683+010	36.
43	8.315-006	2.549+010	2.465+010	38.
44	5.043-006	2.433+010	2.241+010	40.
45	3.059-006	2.374+010	2.073+010	41.
46	1.855-006	2.374+010	1.962+010	41.
47	1.125-006	2.420+010	1.894+010	40.
48	6.826-007	2.465+010	1.831+010	39.
49	4.140-007	2.494+010	1.766+010	37.
50	2.511-007	3.678+010	2.492+010	35.
51	1.523-007	5.130+010	3.360+010	33.
52	9.237-008	5.671+010	3.631+010	32.
53	1.000-010	1.725+011	1.042+011	23.
FLUX, E > 0.0 MeV		1.482+012	1.404+012	17.
FLUX, E < 0.414 eV		3.140+011	2.167+011	21.
FLUX, E > 0.1 MeV		5.378+011	5.233+011	24.
FLUX, E > 1.0 MeV		1.431+011	1.419+011	11.
dpa/s		2.459-010	2.410-010	16.
FLUENCE+, E > 1.0 MeV		6.077+018	6.027+018	11.
dpa+		1.045-002	1.024-002	16.

---

* ABSOLUTE CALCULATED FLUX (OR NORMALIZED TO Fe54(n,p)Mn54 REACTION RATE).

+ BASED ON 4.248+007 EFFECTIVE FULL POWER SECONDS OF EXPOSURE; UNITS OF n/cm^2 FOR FLUENCE AND TOTAL NUMBER OF DISPLACED ATOMS OF IRON PER TARGET ATOM OF IRON FOR dpa.

TABLE 4.2.4.1.1.4

COMPARISON OF MEASURED AND CALCULATED REACTION RATES USED IN THE ANALYSIS OF PRAIRIE ISLAND UNIT 1 CAPSULE V

REACTION	REACTION RATE (DPS/NUCLEUS) MEAS	A PRIORI CALC	ADJ CALC	RATIO MEAS/CALC A PRIORI	ADJ CALC
Np237(n,f)Cs137	3.93-013	4.42-013	3.99-013	.89	.98
U238(n,f)Cs137	4.54-014	4.83-014	4.45-014	.94	1.02
Co59(n,γ)Co60 (Cd)	4.10-012	3.64-012	3.98-012	1.13	1.03
Co59(n,γ)Co60	8.49-012	1.14-011	8.85-012	.75	.96
Fe54(n,p)Mn54	7.94-015	8.49-015	7.88-015	.94	1.01
Ni58(n,p)Co58	1.02-014	1.16-014	1.06-014	.88	.96
Cu63(n,α)Co60	6.72-017	6.86-017	6.62-017	.98	1.02

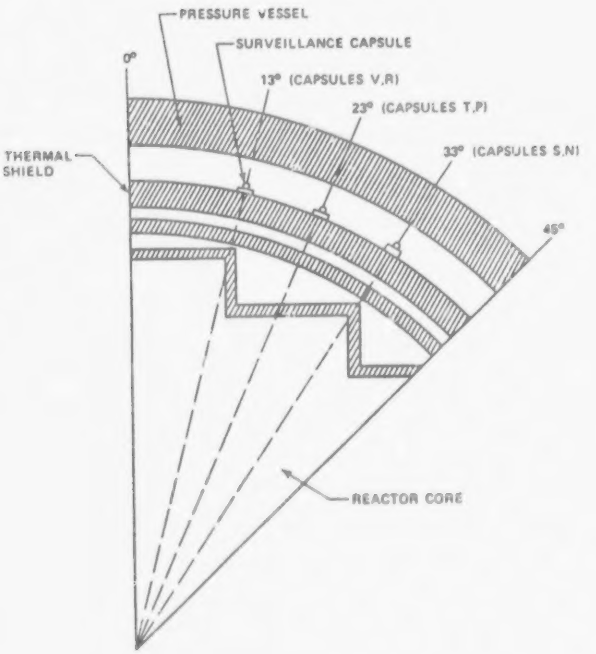
PRESSURE VESSEL
SURVEILLANCE CAPSULE
0°
13° (CAPSULES V,R)
23° (CAPSULES T,P)
33° (CAPSULES S,N)
THERMAL SHIELD
45°
REACTOR CORE

(a) Reactor Geometry.

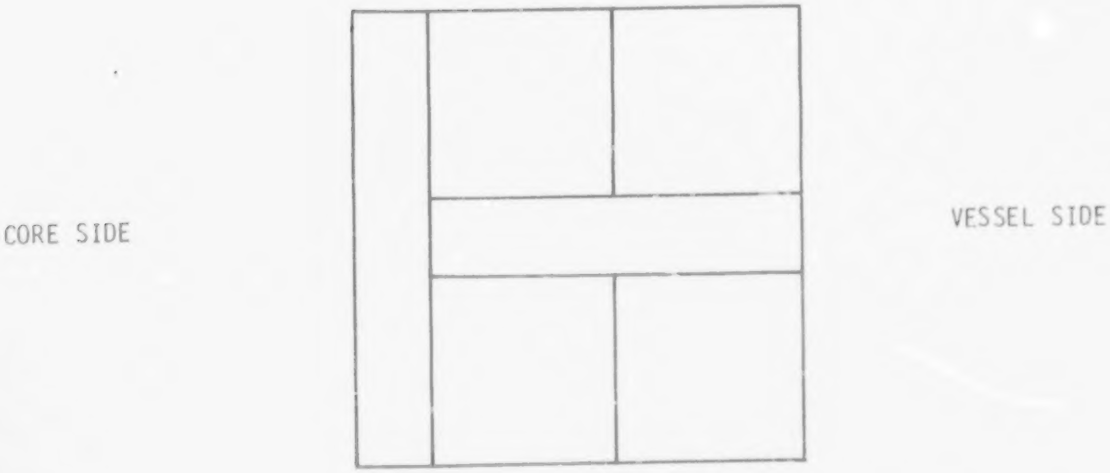
CORE SIDE
VESSEL SIDE

(b) Plan View of Surveillance Capsule

FIGURE 4.2.4.2.1.1. Orientation of the Capsule Relative to the Core and Vessel Wall - Prairie Island Unit 2 Capsule V.

TABLE 4.2.4.2.1.1

SUMMARY OF REACTOR OPERATIONS
PRAIRIE ISLAND UNIT 2 CAPSULE V

TIME PERIOD	START DATE	TIME INTERVAL	AVERAGE POWER LEVEL (MWt)	LOCAL POWER FACTOR
1	12/17/74	15.	125.	1.00
2	1/ 1/75	31.	797.	1.00
3	2/ 1/75	28.	1429.	1.00
4	3/ 1/75	31.	992.	1.00
5	4/ 1/75	30.	1518.	1.00
6	5/ 1/75	31.	1567.	1.00
7	6/ 1/75	30.	304.	1.00
8	7/ 1/75	31.	1245.	1.00
9	8/ 1/75	31.	1542.	1.00
10	9/ 1/75	30.	1422.	1.00
11	10/ 1/75	31.	1258.	1.00
12	11/ 1/75	30.	1574.	1.00
13	12/ 1/75	31.	834.	1.00
14	1/ 1/76	31.	496.	1.00
15	2/ 1/76	29.	1518.	1.00
16	3/ 1/76	31.	1481.	1.00
17	4/ 1/76	61.	1335.	1.00
18	6/ 1/76	30.	1091.	1.00
19	7/ 1/76	31.	1606.	1.00
20	8/ 1/76	31.	1628.	1.00
21	9/ 1/76	30.	1626.	1.00
22	10/ 1/76	21.	1376.	1.00
	10/22/76	DISCHARGED*		

---

*EFFECTIVE FULL POWER OPERATION TIME WAS 4.394+007 SECONDS AT A FULL POWER LEVEL OF 1650. MWt.

TABLE 4.2.4.2.1.2

REACTION RATE DATA AND CORRECTION FACTORS FOR PRAIRIE ISLAND UNIT 2 CAPSULE V

REACTION NAME	IDENT	TOR RATE (DPS/NUCL)	SATURATION FACTOR	GRADIENT FACTOR	IMPURITY FACTOR	AVG REACTION RATE (RPS/NUCL)	% UNCERT (1σ)
^{54}Fe(n,p)^{54}Mn	BOT	5.44-015	1.627+000	0.950	1.000	8.00-015	10.
	BOT MID	5.31-015	1.627+000	0.950	1.000		
	MID	5.11-015	1.627+000	0.950	1.000		
	TOP MID	4.83-015	1.627+000	0.950	1.000		
	TOP	5.18-015	1.627+000	0.950	1.000		
^{58}Ni(n,p)^{58}Co	MID	8.16-015	1.142+000	1.130	1.000	1.05-014	10.
^{63}Cu(n,α)^{60}Co	BOT MID	1.04-017	6.097+000	1.100	1.000	6.67-017	10.
	TOP MID	9.49-018	6.097+000	1.100	1.000		
^{237}Np(n,f)^{137}Cs	MID	8.94-016	3.189+001	1.000	1.000	4.55-013	10.
^{238}U(n,f)^{137}Cs	MID	1.05-016	3.189+001	1.000	0.847	4.71-014	10.
^{59}Co(n,γ)^{60}Co	BOT (B)	1.39-012	6.097+000	0.940	1.000	8.21-012	10.
	TOP (B)	1.47-012	6.097+000	0.940	1.000		
^{59}Co(n,γ)^{60}Co	* (Cd)	5.77-013	6.097+000	1.180	1.000	4.15-012	10.

Cd = Cadmium-Covered Dosimeter.
B = Bare Dosimeter.
* = Generic value for two-loop plants.

TABLE 4.2.4.2.1.3

FERRET-SAND II RESULTS FOR PRAIRIE ISLAND UNIT 2 CAPSULE V (AVERAGE FOR CAPSULE)

GROUP	ENERGY (MeV)	*A PRIORI FLUX* (n/cm^2•s)	ADJUSTED FLUX (n/cm^2•s)	% UNCERTAIN (1 σ)
1	1.492+001	3.914+006	3.773+006	41.
2	1.350+001	8.138+006	7.834+006	38.
3	1.162+001	3.773+007	3.625+007	34.
4	1.000+001	1.145+008	1.100+008	30.
5	8.607+000	2.897+008	2.780+008	26.
6	7.408+000	6.805+008	6.496+008	24.
7	6.065+000	2.391+009	2.274+009	20.
8	4.966+000	3.481+009	3.252+009	21.
9	3.679+000	5.958+009	5.510+009	21.
10	2.865+000	8.783+009	8.198+009	21.
11	2.231+000	1.687+010	1.599+010	21.
12	1.738+000	2.487+010	2.423+010	21.
13	1.353+000	3.495+010	3.477+010	21.
14	1.108+000	3.656+010	3.679+010	24.
15	8.208-001	6.120+010	6.269+010	24.
16	6.393-001	5.502+010	5.673+010	27.
17	4.979-001	5.705+010	5.905+010	30.
18	3.877-001	5.585+010	5.778+010	34.
19	3.020-001	5.183+010	5.349+010	37.
20	1.832-001	8.945+010	9.190+010	40.
21	1.111-001	6.995+010	7.136+010	43.
22	6.738-002	5.177+010	5.238+010	46.
23	4.087-002	4.290+010	4.303+010	48.
24	2.554-002	3.610+010	3.595+010	50.
25	1.989-002	1.731+010	1.715+010	51.
26	1.503-002	1.769+010	1.748+010	52.
27	9.119-003	2.852+010	2.824+010	52.
28	5.531-003	2.851+010	2.837+010	52.
29	3.355-003	2.913+010	2.927+010	51.
30	2.839-003	9.844+009	1.002+010	50.
31	2.404-003	9.890+009	1.023+010	48.
32	2.035-003	9.946+009	1.047+010	46.
33	1.234-003	2.990+010	3.207+010	44.
34	7.485-004	2.919+010	3.187+010	41.
35	4.540-004	2.746+010	3.044+010	38.
36	2.754-004	2.587+010	2.899+010	35.
37	1.670-004	2.553+010	2.878+010	32.
38	1.013-004	2.583+010	3.043+010	14.
39	6.144-005	2.628+010	2.931+010	31.
40	3.727-005	2.672+010	2.928+010	32.

TABLE 4.2.4.2.1.3 (Cont'd)

FERRET-SAND II RESULTS FOR
PRAIRIE ISLAND UNIT 2 CAPSULE V
(AVERAGE FOR CAPSULE)

GROUP	ENERGY (MeV)	A PRIORI FLUX* ($n/cm^2 \cdot s$)	ADJUSTED FLUX ($n/cm^2 \cdot s$)	% UNCERTAIN (1 σ)
41	2.260-005	2.696+010	2.873+010	34.
42	1.371-005	2.657+010	2.735+010	36.
43	8.315-006	2.549+010	2.515+010	38.
44	5.043-006	2.433+010	2.287+010	40.
45	3.059-006	2.374+010	2.118+010	41.
46	1.855-006	2.374+010	2.005+010	42.
47	1.125-006	2.420+010	1.937+010	41.
48	6.826-007	2.465+010	1.873+010	41.
49	4.140-007	2.494+010	1.807+010	39.
50	2.511-007	3.678+010	2.551+010	38.
51	1.523-007	5.130+010	3.440+010	36.
52	9.237-008	5.671+010	3.720+010	35.
53	1.000-010	1.725+011	1.066+011	29.
FLUX, E > 0.0 MeV		1.482+012	1.514+012	17.
FLUX, E < 0.414 eV		3.140+011	2.218+011	26.
FLUX, E > 0.1 MeV		5.378+011	5.961+011	20.
FLUX, E > 1.0 MeV		1.431+011	1.535+011	10.
dpa/s		2.459-010	2.670-010	13.
FLUENCE+, E > 1.0 MeV		6.286+018	6.746+018	10.
dpa+		1.081-002	1.173-002	13.

---

* ABSOLUTE CALCULATED FLUX (OR NORMALIZED TO Fe54(n,p)Mn54 REACTION RATE).

+ BASED ON 4.394+007 EFFECTIVE FULL POWER SECONDS OF EXPOSURE; UNITS OF n/cm^2 FOR FLUENCE AND TOTAL NUMBER OF DISPLACED ATOMS OF IRON PER TARGET ATOM OF IRON FOR dpa.

TABLE 4.2.4.2.1.4

COMPARISON OF MEASURED AND CALCULATED REACTION RATES USED IN THE ANALYSIS OF PRAIRIE ISLAND UNIT 2 CAPSULE V

REACTION	REACTION RATE (DPS/NUCLEUS) MEAS	 A PRIORI CALC	 ADJ CALC	RATIO MEAS/CALC A PRIORI	 ADJ CALC
Np237(n,f)Cs137	4.55-013	4.42-013	4.49-013	1.03	1.01
U238(n,f)Cs137	4.71-014	4.83-014	4.68-014	.97	1.01
Co59(n,γ)Co60 (Cd)	4.15-012	3.64-012	4.04-012	1.14	1.03
Co59(n,γ)Co60	8.21-012	1.14-011	9.02-012	.72	.91
Fe54(n,p)Mn54	8.00-015	8.49-015	7.99-015	.94	1.00
Ni58(n,p)Co58	1.05-014	1.16-014	1.08-014	.91	.97
Cu63(n,α)Co60	6.67-017	6.86-017	6.57-017	.97	1.01

BEST COPY AVAILABLE

235

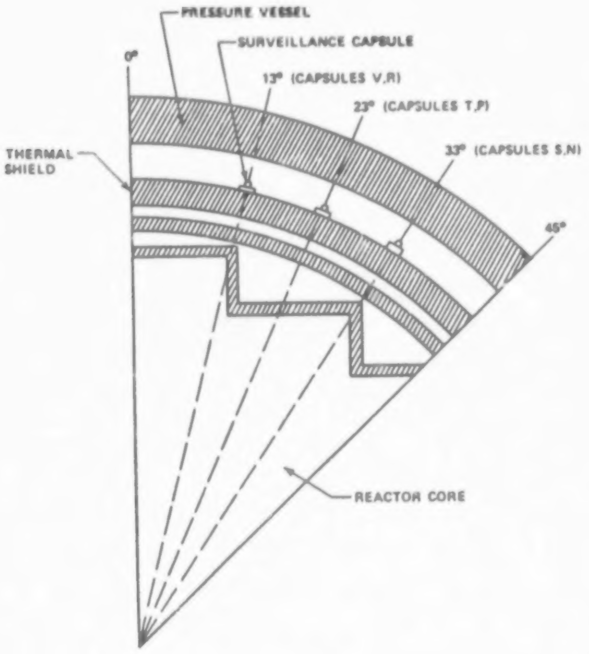
PRESSURE VESSEL
SURVEILLANCE CAPSULE
0°
13° (CAPSULES V,R)
23° (CAPSULES T,P)
33° (CAPSULES S,N)
THERMAL SHIELD
45°
REACTOR CORE

(a) Reactor Geometry.

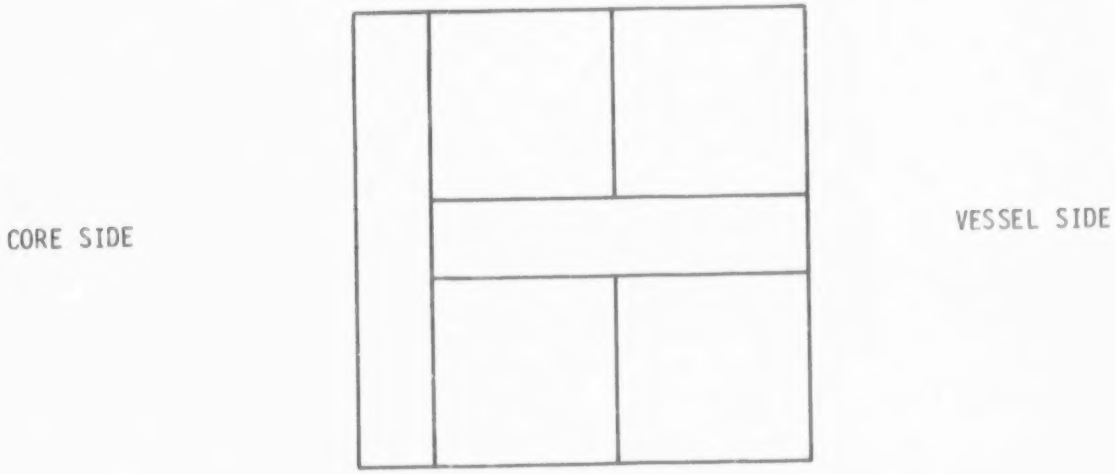
CORE SIDE
VESSEL SIDE

(b) Plan View of Surveillance Capsule

FIGURE 4.2.4.3.1.1. Orientation of the Capsule Relative to the Core and Vessel Wall - R. E. Ginna Unit 1 Capsule R.

TABLE 4.2.4.3.1.1

SUMMARY OF REACTOR OPERATIONS
R. E. GINNA UNIT 1 CAPSULE R

TIME PERIOD	START DATE	TIME INTERVAL	AVERAGE POWER LEVEL (MWt)	LOCAL POWER FACTOR
1	1/ 1/70	243.	711.	1.00
2	9/ 1/70	30.	1248.	1.00
3	10/ 1/70	31.	675.	1.00
4	11/ 1/70	30.	1204.	1.00
5	12/ 1/70	31.	1180.	1.00
6	1/ 1/71	31.	1151.	1.00
7	2/ 1/71	28.	1465.	1.00
8	3/ 1/71	31.	38.	1.00
9	4/ 1/71	30.	0.	1.00
10	5/ 1/71	31.	458.	1.00
11	6/ 1/71	30.	1189.	1.00
12	7/ 1/71	31.	1157.	1.00
13	8/ 1/71	31.	1277.	1.00
14	9/ 1/71	30.	1306.	1.00
15	10/ 1/71	31.	1324.	1.00
16	11/ 1/71	30.	1368.	1.00
17	12/ 1/71	31.	1303.	1.00
18	1/ 1/72	31.	1332.	1.00
19	2/ 1/72	29.	1421.	1.00
20	3/ 1/72	31.	1029.	1.00
21	4/ 1/72	30.	942.	1.00
22	5/ 1/72	31.	0.	1.00
23	6/ 1/72	30.	11.	1.00
24	7/ 1/72	31.	1138.	1.00
25	8/ 1/72	31.	1249.	1.00
26	9/ 1/72	30.	1310.	1.00
27	10/ 1/72	31.	459.	1.00
28	11/ 1/72	30.	549.	1.00
29	12/ 1/72	31.	1467.	1.00
30	1/ 1/73	31.	1234.	1.00
31	2/ 1/73	28.	1313.	1.00
32	3/ 1/73	31.	1312.	1.00
33	4/ 1/73	30.	1316.	1.00
34	5/ 1/73	31.	1319.	1.00
35	6/ 1/73	30.	1304.	1.00
36	7/ 1/73	31.	945.	1.00
37	8/ 1/73	31.	1316.	1.00
38	9/ 1/73	30.	1370.	1.00
39	10/ 1/73	31.	1140.	1.00
40	11/ 1/73	30.	1411.	1.00
41	12/ 1/73	31.	1286.	1.00
	1/ 1/74	DISCHARGED*		

---

*EFFECTIVE FULL POWER OPERATION TIME WAS 8.328+007 SECONDS AT A FULL POWER LEVEL OF 1520. MWt.

TABLE 4.2.4.3.1.2

REACTION RATE DATA AND CORRECTION FACTORS FOR R. E. GINNA UNIT 1 CAPSULE R

REACTION							
NAME	IDENT	TOR RATE (DPS/NUCL)	SATURATION FACTOR	GRADIENT FACTOR	IMPURITY FACTOR	AVG REACTION RATE (RPS/NUCL)	% UNCERT (1 σ)
^{54}Fe(n,p)^{54}Mn	W-13	7.96-015	1.397+000	0.950	1.000	1.06-014	10.
	R-14	7.57-015	1.397+000	0.950	1.000		
	R-18	7.88-015	1.397+000	0.950	1.000		
	W-14	6.22-015	1.397+000	1.180	1.000		
	R-15	6.51-015	1.397+000	1.180	1.000		
	P-19	7.08-015	1.397+000	1.180	1.000		
^{58}Ni(n,p)^{58}Co	MID	8.37-016	1.194+000	0.930	1.000	9.30-016	10.
^{63}Cu(n,α)^{60}Co	TOP	1.65-017	3.620+000	0.960	1.000	5.77-017	10.
	TOP MID	1.48-017	3.620+000	0.960	1.000		
	BOT MID	1.76-017	3.620+000	0.960	1.000		
	BOT	1.76-017	3.620+000	0.960	1.000		
^{237}Np(n,f)^{137}Cs	MID	1.67-015	1.720+001	1.000	1.000	4.59-013	10.
^{238}U(n,f)^{137}Cs	MID	1.71-015	1.720+001	1.000	0.806	3.95-013	10.
^{59}Co(n,γ)^{60}Co	* (Cd)	----	----	----	----	3.65-012	10.
^{59}Co(n,γ)^{60}Co	* (B)	----	----	----	----	7.91-012	10.

Cd = Cadmium-Covered Dosimeter.
B = Bare Dosimeter.
* = Generic value for two-loop plant.

TABLE 4.2.4.3.1.3

FERRET-SAND II RESULTS FOR
R. E. GINNA UNIT 1 CAPSULE R
(AVERAGE FOR CAPSULE)

GROUP	ENERGY (MeV)	A PRIORI FLUX* ($n/cm^2 \cdot s$)	ADJUSTED FLUX ($n/cm^2 \cdot s$)	% UNCERTAIN (1σ)
1	1.492+001	4.489+006	3.459+006	41.
2	1.350+001	9.332+006	7.106+006	37.
3	1.162+001	4.327+007	3.249+007	34.
4	1.000+001	1.313+008	9.733+007	30.
5	8.607+000	3.322+008	2.430+008	26.
6	7.408+000	7.804+008	5.617+008	24.
7	6.065+000	2.742+009	1.954+009	20.
8	4.966+000	3.992+009	2.795+009	22.
9	3.679+000	6.832+009	4.745+009	22.
10	2.865+000	1.007+010	7.077+009	23.
11	2.231+000	1.935+010	1.381+010	22.
12	1.738+000	2.852+010	2.098+010	21.
13	1.353+000	4.008+010	3.106+010	21.
14	1.108+000	4.193+010	3.514+010	24.
15	8.208-001	7.019+010	6.264+010	24.
16	6.393-001	6.310+010	5.801+010	27.
17	4.979-001	6.543+010	6.145+010	30.
18	3.877-001	6.404+010	6.081+010	33.
19	3.020-001	5.943+010	5.682+010	37.
20	1.832-001	1.026+011	9.814+010	40.
21	1.111-001	8.022+010	7.613+010	43.
22	6.738-002	5.937+010	5.554+010	46.
23	4.087-002	4.919+010	4.518+010	48.
24	2.554-002	4.140+010	3.725+010	50.
25	1.989-002	1.985+010	1.750+010	51.
26	1.503-002	2.028+010	1.757+010	52.
27	9.119-003	3.271+010	2.794+010	52.
28	5.531-003	3.269+010	2.764+010	52.
29	3.355-003	3.341+010	2.811+010	51.
30	2.839-003	1.129+010	9.492+009	50.
31	2.404-003	1.134+010	9.569+009	48.
32	2.035-003	1.141+010	9.686+009	46.
33	1.234-003	3.429+010	2.937+010	44.
34	7.485-004	3.348+010	2.893+010	41.
35	4.540-004	3.149+010	2.742+010	38.
36	2.754-004	2.967+010	2.598+010	35.
37	1.670-004	2.927+010	2.571+010	32.
38	1.013-004	2.962+010	2.665+010	14.
39	6.144-005	3.014+010	2.615+010	30.
40	3.727-005	3.065+010	2.625+010	32.

TABLE 4.2.4.3.1.3 (Cont'd)

FERRET-SAND II RESULTS FOR
R. E. GINNA UNIT 1 CAPSULE R
(AVERAGE FOR CAPSULE)

GROUP	ENERGY (MeV)	A PRIORI FLUX* ($n/cm^2 \cdot s$)	ADJUSTED FLUX ($n/cm^2 \cdot s$)	% UNCERTAIN ($1\ \sigma$)
41	2.260-005	3.092+010	2.588+010	34.
42	1.371-005	3.048+010	2.480+010	36.
43	8.315-006	2.923+010	2.302+010	38.
44	5.043-006	2.790+010	2.115+010	40.
45	3.059-006	2.722+010	1.979+010	41.
46	1.855-006	2.722+010	1.895+010	41.
47	1.125-006	2.775+010	1.850+010	41.
48	6.826-007	2.826+010	1.807+010	40.
49	4.140-007	2.860+010	1.760+010	39.
50	2.511-007	4.218+010	2.506+010	37.
51	1.523-007	5.883+010	3.402+010	36.
52	9.237-008	6.503+010	3.694+010	35.
53	1.000-010	1.978+011	1.069+011	28.
FLUX, E > 0.0 MeV		1.482+012	1.485+012	17.
FLUX, E < 0.414 eV		3.140+011	2.205+011	25.
FLUX, E > 0.1 MeV		5.378+011	6.042+011	21.
FLUX, E > 1.0 MeV		1.431+011	1.399+011	10.
dpa/s		2.459-010	2.586-010	14.
FLUENCE+, E > 1.0 MeV		1.191+019	1.165+019	10.
dpa+		2.048-002	2.154-002	14.

---

* ABSOLUTE CALCULATED FLUX (OR NORMALIZED TO Fe54(n,p)Mn54 REACTION RATE).

+ BASED ON 8.328+007 EFFECTIVE FULL POWER SECONDS OF EXPOSURE; UNITS OF n/cm^2 FOR FLUENCE AND TOTAL NUMBER OF DISPLACED ATOMS OF IRON PER TARGET ATOM OF IRON FOR dpa.

TABLE 4.2.4.3.1.4

COMPARISON OF MEASURED AND CALCULATED REACTION RATES USED IN THE ANALYSIS OF R. E. GINNA UNIT 1 CAPSULE R

REACTION	REACTION RATE (DPS/NUCLEUS) MEAS	A PRIORI CALC	ADJ CALC	RATIO MEAS/CALC A PRIORI	ADJ CALC
Np237(n,f)Cs137	4.59-013	5.06-013	4.41-013	.91	1.04
U238(n,f)Cs137	3.95-014	5.54-014	4.09-014	.71	.97
Co59(n,γ)Co60 (Cd)	3.65-012	4.17-012	3.58-012	.88	1.02
Co59(n,γ)Co60	7.91-012	1.30-011	8.53-012	.61	.93
Ni58(n,p)Co58	9.30-015	1.33-014	9.42-015	.70	.99
Cu63(n,α)Co60	5.77-017	7.87-017	5.69-017	.73	1.01
*Fe54(n,p)Mn54	1.06-014	9.83-015	6.97-015	1.08	1.52

----

* REACTION NOT USED TO ADJUST SPECTRUM

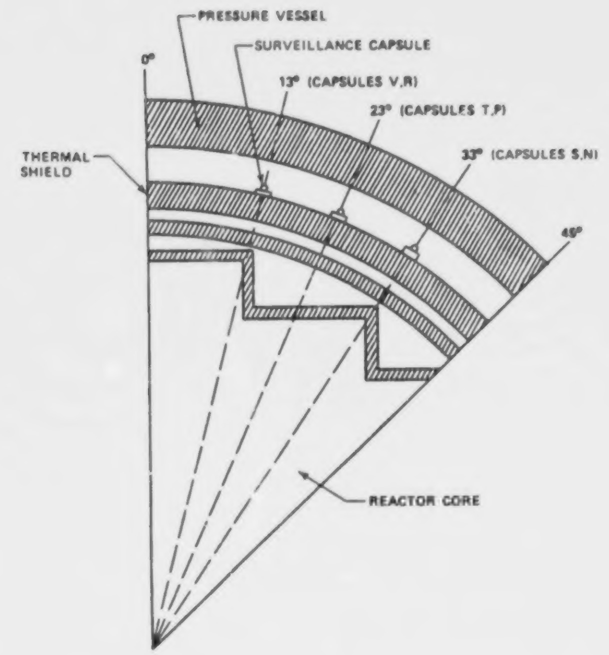
PRESSURE VESSEL
SURVEILLANCE CAPSULE
0°
13° (CAPSULES V,R)
23° (CAPSULES T,P)
33° (CAPSULES S,N)
THERMAL SHIELD
45°
REACTOR CORE

(a) Reactor Geometry.

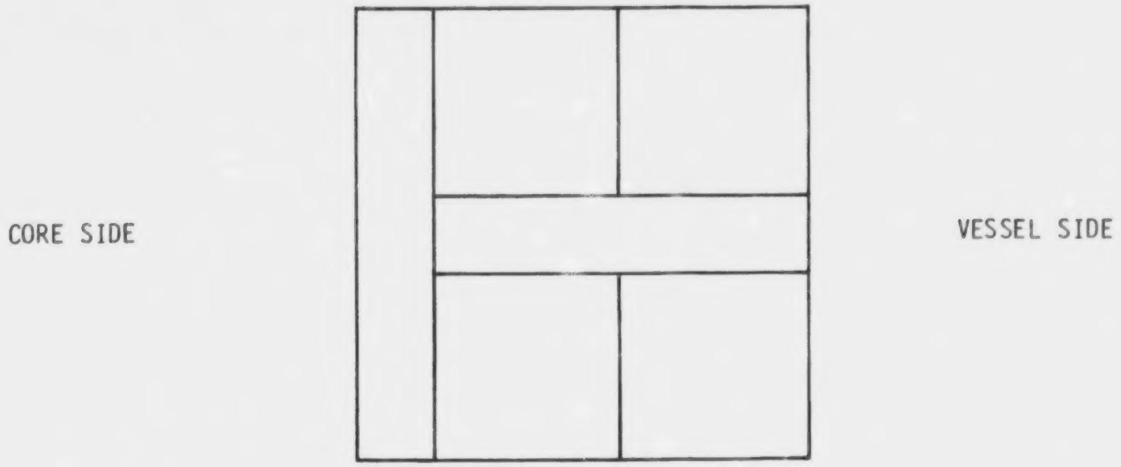
CORE SIDE
VESSEL SIDE

(b) Plan View of Surveillance Capsule

FIGURE 4.2.4.3.2.1. Orientation of the Capsule Relative to the Core and Vessel Wall - R. E. Ginna Unit 1 Capsule V.

TABLE 4.2.4.3.2.1

SUMMARY OF REACTOR OPERATIONS
R. E. GINNA UNIT 1 CAPSULE V

TIME PERIOD	START DATE	TIME INTERVAL	AVERAGE POWER LEVEL (MWt)	LOCAL POWER FACTOR
1	1/ 1/70	243.	711.	1.00
2	9/ 1/70	30.	1248.	1.00
3	10/ 1/70	31.	675.	1.00
4	11/ 1/70	30.	1204.	1.00
5	12/ 1/70	31.	1180.	1.00
6	1/ 1/71	31.	1151.	1.00
7	2/ 1/71	28.	1465.	1.00
8	3/ 1/71	31.	38.	1.00
9	4/ 1/71	30.	0.	1.00
10	5/ 1/71	31.	458.	1.00
11	6/ 1/71	30.	1189.	1.00
12	7/ 1/71	31.	1157.	1.00
13	8/ 1/71	31.	1277.	1.00
14	9/ 1/71	30.	1306.	1.00
15	10/ 1/71	31.	1324.	1.00
16	11/ 1/71	30.	1368.	1.00
17	12/ 1/71	31.	1303.	1.00
18	1/ 1/72	31.	1332.	1.00
19	2/ 1/72	29.	1421.	1.00
20	3/ 1/72	31.	1029.	1.00
21	4/ 1/72	30.	942.	1.00
	5/ 1/72	DISCHARGED*		

---

*EFFECTIVE FULL POWER OPERATION TIME WAS 4.612+007 SECONDS AT A FULL POWER LEVEL OF 1520. MWt.

TABLE 4.2.4.3.2.2

REACTION RATE DATA AND CORRECTION FACTORS FOR R. E. GINNA UNIT 1 CAPSULE V

REACTION NAME	IDENT	TOR RATE (DPS/NUCL)	SATURATION FACTOR	GRADIENT FACTOR	IMPURITY FACTOR	AVG REACTION RATE (RPS/NUCL)	% UNCERT (1σ)
^{54}Fe(n,p)^{54}Mn	W-1	4.82-015	1.715+000	0.950	1.000	7.90-015	10.
	R-1	5.02-015	1.715+000	0.950	1.000		
	S-6	4.25-015	1.715+000	0.950	1.000		
	P-7	5.02-015	1.715+000	0.950	1.000		
	W-2	3.98-015	1.715+000	1.180	1.000		
	R-3	3.81-015	1.715+000	1.180	1.000		
	S-8	3.94-015	1.715+000	1.180	1.000		
	P-9	4.10-015	1.715+000	1.180	1.000		
^{58}Ni(n,p)^{58}Co	MID	8.45-015	1.322+000	0.930	1.000	1.04-014	10.
^{63}Cu(n,α)^{60}Co	TOP	1.17-017	5.942+000	0.970	1.000	6.79-017	10.
	TOP MID	1.07-017	5.942+000	0.970	1.000		
	BOT MID	1.18-017	5.942+000	0.970	1.000		
	BOT	1.29-017	5.942+000	0.970	1.000		
^{237}Np(n,f)^{137}Cs	MID	4.87-016	3.050+001	1.000	1.000	2.37-013	10.
^{238}U(n,f)^{137}Cs	MID	9.15-017	3.050+001	1.000	0.862	4.01-014	10.

TABLE 4.2.4.3.2.3

FERRET-SAND II RESULTS FOR R. E. GINNA UNIT 1 CAPSULE V (AVERAGE FOR CAPSULE)

GROUP	ENERGY (MeV)	A PRIORI FLUX* (n/cm^2•s)	ADJUSTED FLUX (n/cm^2•s)	% UNCERTAIN (1 σ)
1	1.492+001	3.591+006	3.823+006	43.
2	1.350+001	7.466+006	8.037+006	39.
3	1.162+001	3.461+007	3.754+007	35.
4	1.000+001	1.050+008	1.144+008	30.
5	8.607+000	2.658+008	2.888+008	26.
6	7.408+000	6.243+008	6.714+008	24.
7	6.065+000	2.193+009	2.337+009	20.
8	4.966+000	3.194+009	3.309+009	21.
9	3.679+000	5.466+009	5.480+009	21.
10	2.865+000	8.058+009	7.797+009	21.
11	2.231+000	1.548+010	1.436+010	21.
12	1.738+000	2.282+010	2.036+010	22.
13	1.353+000	3.206+010	2.796+010	24.
14	1.108+000	3.354+010	2.920+010	31.
15	8.208-001	5.615+010	4.841+010	35.
16	6.393-001	5.048+010	4.334+010	39.
17	4.979-001	5.234+010	4.495+010	43.
18	3.877-001	5.124+010	4.422+010	47.
19	3.020-001	4.755+010	4.138+010	51.
20	1.832-001	8.206+010	7.217+010	54.
21	1.111-001	6.418+010	5.710+010	56.
22	6.738-002	4.750+010	4.274+010	58.
23	4.087-002	3.935+010	3.580+010	59.
24	2.554-002	3.312+010	3.041+010	61.
25	1.989-002	1.588+010	1.469+010	61.
26	1.503-002	1.623+010	1.511+010	62.
27	9.119-003	2.617+010	2.449+010	62.
28	5.531-003	2.615+010	2.456+010	63.
29	3.355-003	2.673+010	2.517+010	63.
30	2.839-003	9.031+009	8.518+009	63.
31	2.404-003	9.073+009	8.568+009	63.
32	2.035-003	9.125+009	8.623+009	63.
33	1.234-003	2.743+010	2.594+010	63.
34	7.485-004	2.678+010	2.533+010	63.
35	4.540-004	2.519+010	2.383+010	63.
36	2.754-004	2.373+010	2.245+010	63.
37	1.670-004	2.342+010	2.216+010	63.
38	1.013-004	2.370+010	2.242+010	63.
39	6.144-005	2.411+010	2.281+010	63.
40	3.727-005	2.452+010	2.320+010	63.

TABLE 4.2.4.3.2.3 (Cont'd)

FERRET-SAND II RESULTS FOR
R. E. GINNA UNIT 1 CAPSULE V
(AVERAGE FOR CAPSULE)

GROUP	ENERGY (MeV)	A PRIORI FLUX* ($n/cm^2 \cdot s$)	ADJUSTED FLUX ($n/cm^2 \cdot s$)	% UNCERTAIN ($1\ \sigma$)
41	2.260-005	2.473+010	2.340+010	63.
42	1.371-005	2.438+010	2.307+010	63.
43	8.315-006	2.339+010	2.213+010	63.
44	5.043-006	2.232+010	2.113+010	63.
45	3.059-006	2.178+010	2.061+010	63.
46	1.855-006	2.178+010	2.061+010	63.
47	1.125-006	2.220+010	2.101+010	63.
48	6.826-007	2.261+010	2.140+010	63.
49	4.140-007	2.288+010	2.166+010	63.
50	2.511-007	3.375+010	3.194+010	63.
51	1.523-007	4.706+010	4.455+010	63.
52	9.237-008	5.203+010	4.925+010	63.
53	1.000-010	1.582+011	1.498+011	63.
FLUX, E > 0.0 MeV		1.186+012	1.361+012	38.
FLUX, E < 0.414 eV		2.512+011	2.972+011	59.
FLUX, E > 0.1 MeV		4.303+011	4.725+011	33.
FLUX, E > 1.0 MeV		1.144+011	1.285+011	14.
dpa/s		1.967-010	2.203-010	22.
FLUENCE+, E > 1.0 MeV		5.278+018	5.925+018	14.
dpa+		9.074-003	1.016-002	22.

---

* ABSOLUTE CALCULATED FLUX (OR NORMALIZED TO Fe54(n,p)Mn54 REACTION RATE).

+ BASED ON 4.612+007 EFFECTIVE FULL POWER SECONDS OF EXPOSURE; UNITS OF n/cm^2 FOR FLUENCE AND TOTAL NUMBER OF DISPLACED ATOMS OF IRON PER TARGET ATOM OF IRON FOR dpa.

246

TABLE 4.2.4.3.2.4

COMPARISON OF MEASURED AND CALCULATED REACTION RATES USED IN THE ANALYSIS OF R. E. GINNA UNIT 1 CAPSULE V

	REACTION RATE (DPS/NUCLEUS)			RATIO MEAS/CALC	
REACTION	MEAS	A PRIORI CALC	ADJ CALC	A PRIORI	ADJ CALC
U238(n,f)Cs137	4.01-014	4.43-014	4.09-014	.90	.98
Fe54(n,p)Mn54	7.90-015	7.79-015	7.77-015	1.01	1.02
Ni58(n,p)Co58	1.04-014	1.06-014	1.04-014	.98	1.00
Cu63(n,α)Co60	6.79-017	6.29-017	6.74-017	1.08	1.01
*Np237(n,f)FP Cd	2.37-013	4.18-013	3.70-013	.57	.64

---

* REACTION NOT USED TO ADJUST SPECTRUM

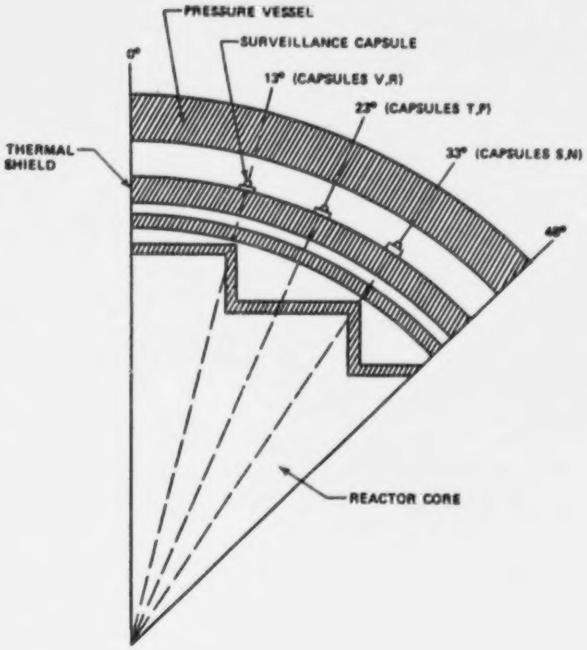
PRESSURE VESSEL
SURVEILLANCE CAPSULE
0°
13° (CAPSULES V,R)
23° (CAPSULES T,P)
33° (CAPSULES S,N)
THERMAL SHIELD
45°
REACTOR CORE

(a) Reactor Geometry.

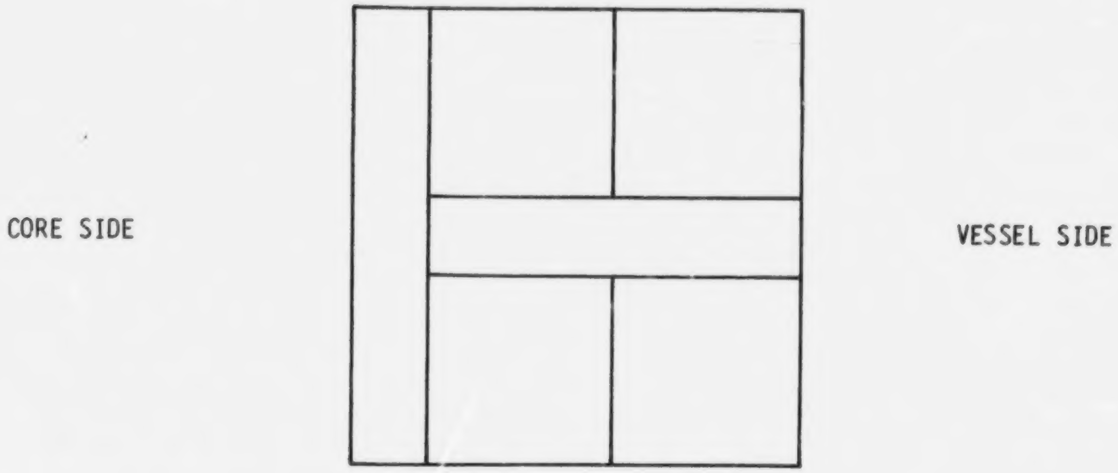
CORE SIDE
VESSEL SIDE

(b) Plan View of Surveillance Capsule

FIGURE 4.2.4.4.1.3. Orientation of the Capsule Relative to the Core and Vessel Wall - Kewaunee Capsule V.

TABLE 4.2.4.4.1.1

SUMMARY OF REACTOR OPERATIONS
KEWAUNEE CAPSULE V

TIME PERIOD	START DATE	TIME INTERVAL	AVERAGE POWER LEVEL (MWt)	LOCAL POWER FACTOR
1	4/14/74	17.	297.	1.00
2	5/ 1/74	31.	807.	1.00
3	6/ 1/74	30.	1201.	1.00
4	7/ 1/74	31.	1044.	1.00
5	8/ 1/74	31.	1576.	1.00
6	9/ 1/74	30.	911.	1.00
7	10/ 1/74	31.	427.	1.00
8	11/ 1/74	30.	1044.	1.00
9	12/ 1/74	31.	1219.	1.00
10	1/ 1/75	31.	1051.	1.00
11	2/ 1/75	28.	1381.	1.00
12	3/ 1/75	31.	1475.	1.00
13	4/ 1/75	30.	1148.	1.00
14	5/ 1/75	31.	1175.	1.00
15	6/ 1/75	30.	1081.	1.00
16	7/ 1/75	31.	1132.	1.00
17	8/ 1/75	31.	1581.	1.00
18	9/ 1/75	30.	840.	1.00
19	10/ 1/75	31.	1233.	1.00
20	11/ 1/75	30.	1143.	1.00
21	12/ 1/75	31.	1574.	1.00
22	1/ 1/76	31.	1487.	1.00
23	2/ 1/76	13.	1607.	1.00
	2/14/76	DISCHARGED*		

---

*EFFECTIVE FULL POWER OPERATION TIME WAS 4.057+007 SECONDS AT A FULL POWER LEVEL OF 1650. MWt.

249

TABLE 4.2.4.4.1.2

REACTION RATE DATA AND CORRECTION FACTORS FOR KEWAUNEE CAPSULE V

REACTION NAME	IDENT	TOR RATE (DPS/NUCL)	SATURATION FACTOR	GRADIENT FACTOR	IMPURITY FACTOR	AVG REACTION RATE (RPS/NUCL)	% UNCERT (1σ)
^{54}Fe(n,p)^{54}Mn	BOT	4.69-015	1.750+000	1.050	1.000	8.12-015	10.
	BOT MID	4.31-015	1.750+000	1.050	1.000		
	MID	4.36-015	1.750+000	1.050	1.000		
	TOP MID	4.17-015	1.750+000	1.050	1.000		
	TOP	4.57-015	1.750+000	1.050	1.000		
^{58}Ni(n,p)^{58}Co	MID	9.69-015	1.212+000	0.860	1.000	1.01-014	10.
^{63}Cu(n,α)^{60}Co	BOT MID	1.28-017	6.594+000	0.860	1.000	6.80-017	10.
	TOP MID	1.12-017	6.594+000	0.860	1.000		
^{237}Np(n,f)^{137}Cs	MID	8.68-016	3.452+001	1.000	1.000	4.78-013	10.
^{238}U(n,f)^{137}Cs	MID	9.88-017	3.452+001	1.000	0.855	4.86-014	10.
^{59}Co(n,γ)^{60}Co	TOP (B)	1.58-012	6.594+000	1.000	1.000	1.04-011	10.
^{59}Co(n,γ)^{60}Co	BOT (CD)	7.10-013	6.594+000	0.840	1.000	3.91-012	10.
	TOP (CD)	7.03-013	6.594+000	0.840	1.000		

CD = Cadmium-Covered Dosimeter.
B = Bare Dosimeter.

TABLE 4.2.4.4.1.3

FERRET-SAND II RESULTS FOR
KEWAUNEE CAPSULE V
(AVERAGE FOR CAPSULE)

GROUP	ENERGY (MeV)	A PRIORI FLUX* (n/cm^2•s)	ADJUSTED FLUX (n/cm^2•s)	% UNCERTAIN (1 σ)
1	1.492+001	4.704+006	4.016+006	41.
2	1.350+001	9.780+006	8.257+006	37.
3	1.162+001	4.534+007	3.782+007	34.
4	1.000+001	1.376+008	1.136+008	30.
5	8.607+000	3.481+008	2.846+008	26.
6	7.408+000	8.178+008	6.577+008	24.
7	6.065+000	2.873+009	2.277+009	20.
8	4.966+000	4.184+009	3.212+009	22.
9	3.679+000	7.160+009	5.400+009	21.
10	2.865+000	1.056+010	8.105+009	21.
11	2.231+000	2.028+010	1.597+010	21.
12	1.738+000	2.989+010	2.479+010	21.
13	1.353+000	4.200+010	3.613+010	21.
14	1.108+000	4.394+010	3.842+010	24.
15	8.208-001	7.356+010	6.640+010	24.
16	6.393-001	6.613+010	6.080+010	27.
17	4.979-001	6.857+010	6.392+010	30.
18	3.877-001	6.712+010	6.303+010	34.
19	3.020-001	6.229+010	5.868+010	37.
20	1.832-001	1.075+011	1.012+011	40.
21	1.111-001	8.407+010	7.865+010	43.
22	6.738-002	6.222+010	5.768+010	46.
23	4.087-002	5.156+010	4.726+010	48.
24	2.554-002	4.339+010	3.932+010	50.
25	1.989-002	2.080+010	1.864+010	51.
26	1.503-002	2.126+010	1.888+010	52.
27	9.119-003	3.428+010	3.022+010	52.
28	5.531-003	3.426+010	3.006+010	52.
29	3.355-003	3.501+010	3.065+010	51.
30	2.839-003	1.183+010	1.036+010	50.
31	2.404-003	1.189+010	1.043+010	49.
32	2.035-003	1.195+010	1.052+010	46.
33	1.234-003	3.593+010	3.178+010	44.
34	7.485-004	3.508+010	3.117+010	41.
35	4.540-004	3.300+010	2.944+010	38.
36	2.754-004	3.109+010	2.782+010	35.
37	1.670-004	3.068+010	2.750+010	32.
38	1.013-004	3.105+010	2.818+010	15.
39	6.144-005	3.158+010	2.818+010	30.
40	3.727-005	3.212+010	2.850+010	32.

TABLE 4.2.4.4.1.3 (Cont'd)

FERRET-SAND II RESULTS FOR
KEWAUNEE CAPSULE V
(AVERAGE FOR CAPSULE)

GROUP	ENERGY (MeV)	A PRIORI FLUX* ($n/cm^2 \cdot s$)	ADJUSTED FLUX ($n/cm^2 \cdot s$)	% UNCERTAIN ($1\ \sigma$)
41	2.260-005	3.240+010	2.846+010	33.
42	1.371-005	3.194+010	2.772+010	35.
43	8.315-006	3.064+010	2.620+010	38.
44	5.043-006	2.924+010	2.459+010	39.
45	3.059-006	2.853+010	2.356+010	40.
46	1.855-006	2.853+010	2.311+010	41.
47	1.125-006	2.908+010	2.311+010	41.
48	6.826-007	2.962+010	2.311+010	39.
49	4.140-007	2.998+010	2.299+010	38.
50	2.511-007	4.421+010	3.338+010	36.
51	1.523-007	6.165+010	4.599+010	34.
52	9.237-008	6.816+010	5.043+010	33.
53	1.000-010	2.073+011	1.500+011	26.
FLUX, E > 0.0 MeV		1.482+012	1.667+012	16.
FLUX, E < 0.414 eV		3.140+011	3.028+011	23.
FLUX, E > 0.1 MeV		5.378+011	6.402+011	20.
FLUX, E > 1.0 MeV		1.431+011	1.581+011	10.
dpa/s		2.459-010	2.818-010	13.
FLUENCE+, E > 1.0 MeV		5.804+018	6.414+018	10.
dpa+		9.978-003	1.143-002	13.

---

* ABSOLUTE CALCULATED FLUX (OR NORMALIZED TO Fe54(n,p)Mn54 REACTION RATE).

+ BASED ON 4.057+007 EFFECTIVE FULL POWER SECONDS OF EXPOSURE; UNITS OF n/cm^2 FOR FLUENCE AND TOTAL NUMBER OF DISPLACED ATOMS OF IRON PER TARGET ATOM OF IRON FOR dpa.

TABLE 4.2.4.4.1.4

COMPARISON OF MEASURED AND CALCULATED REACTION RATES USED IN THE ANALYSIS OF KEWAUNEE CAPSULE V

REACTION	REACTION RATE (DPS/NUCLEUS) MEAS	A PRIORI CALC	ADJ CALC	RATIO MEAS/CALC A PRIORI	ADJ CALC
Np237(n,f)Cs137	4.78-013	5.31-013	4.71-013	.90	1.02
U238(n,f)Cs137	4.86-014	5.81-014	4.76-014	.84	1.02
Co59(n,γ)Co60 (Cd)	3.91-012	4.37-012	3.88-012	.89	1.01
Co59(n,γ)Co60	1.04-011	1.37-011	1.07-011	.76	.97
Fe54(n,p)Mn54	8.12-015	1.02-014	7.97-015	.80	1.02
Ni58(n,p)Co58	9.84-015	1.39-014	1.06-014	.71	.93
Cu63(n,α)Co60	6.80-017	8.25-017	6.65-017	.82	1.02

253

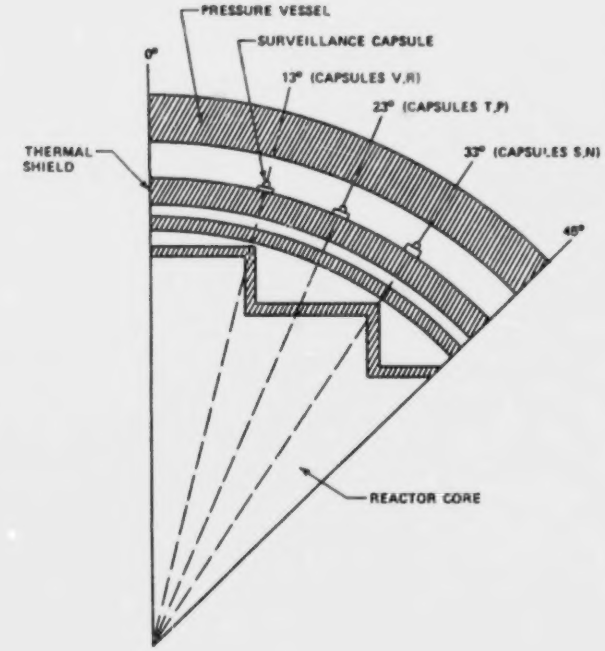
PRESSURE VESSEL
SURVEILLANCE CAPSULE
0°
13° (CAPSULES V,R)
23° (CAPSULES T,P)
33° (CAPSULES S,N)
THERMAL SHIELD
45°
REACTOR CORE

(a) Reactor Geometry.

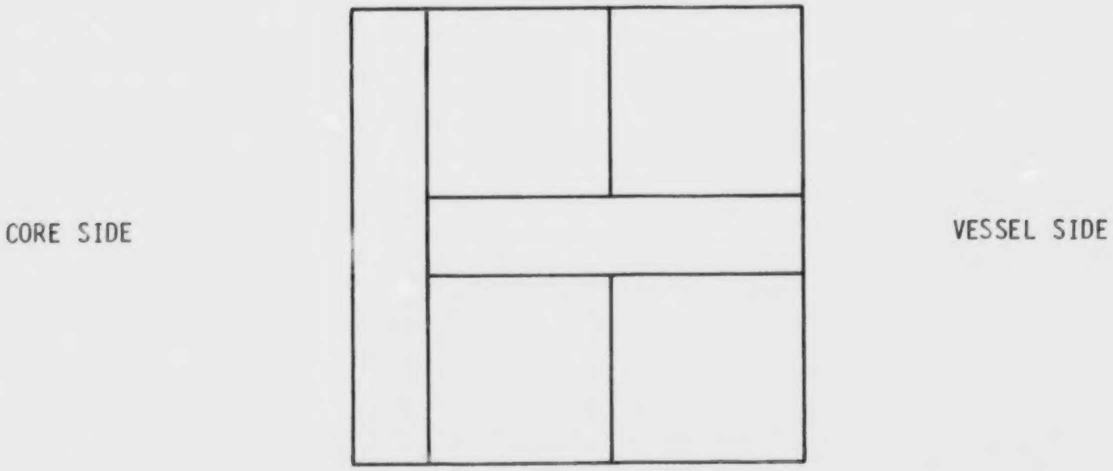
CORE SIDE
VESSEL SIDE

(b) Plan View of Surveillance Capsule

FIGURE 4.2.4.5.1.1. Orientation of the Capsule Relative to the Core and Vessel Wall - Point Beach Unit 1 Capsule S.

TABLE 4.2.4.5.1.1

SUMMARY OF REACTOR OPERATIONS
POINT BEACH UNIT 1 CAPSULE S

TIME PERIOD	START DATE	TIME INTERVAL	AVERAGE POWER LEVEL (MWt)	LOCAL POWER FACTOR
1	11/ 1/70	30.	247.	1.00
2	12/ 1/70	31.	610.	1.00
3	1/ 1/71	31.	971.	1.00
4	2/ 1/71	28.	978.	1.00
5	3/ 1/71	31.	1249.	1.00
6	4/ 1/71	30.	609.	1.00
7	5/ 1/71	31.	1114.	1.00
8	6/ 1/71	30.	1233.	1.00
9	7/ 1/71	31.	1254.	1.00
10	8/ 1/71	31.	1372.	1.00
11	9/ 1/71	30.	1238.	1.00
12	10/ 1/71	31.	1299.	1.00
13	11/ 1/71	30.	1071.	1.00
14	12/ 1/71	31.	1317.	1.00
15	1/ 1/72	182.	1393.	1.00
16	7/ 1/72	31.	1375.	1.00
17	8/ 1/72	31.	1485.	1.00
18	9/ 1/72	30.	1296.	1.00
19	10/ 1/72	92.	0.	1.00
20	1/ 1/73	59.	0.	1.00
21	3/ 1/73	31.	854.	1.00
22	4/ 1/73	30.	1084.	1.00
23	5/ 1/73	31.	1092.	1.00
24	6/ 1/73	30.	1236.	1.00
25	7/ 1/73	31.	1439.	1.00
26	8/ 1/73	31.	1345.	1.00
27	9/ 1/73	30.	1401.	1.00
28	10/ 1/73	31.	1275.	1.00
29	11/ 1/73	30.	1136.	1.00
30	12/ 1/73	31.	1268.	1.00
31	1/ 1/74	31.	1360.	1.00
32	2/ 1/74	28.	1449.	1.00
33	3/ 1/74	31.	1481.	1.00
34	4/ 1/74	30.	260.	1.00
35	5/ 1/74	31.	0.	1.00
36	6/ 1/74	30.	937.	1.00
37	7/ 1/74	31.	1451.	1.00
38	8/ 1/74	31.	1385.	1.00
39	9/ 1/74	30.	1379.	1.00
40	10/ 1/74	31.	1394.	1.00

TABLE 4.2.4.5.1.1 (Cont'd)

SUMMARY OF REACTOR OPERATIONS
POINT BEACH UNIT 1 CAPSULE S

TIME PERIOD	START DATE	TIME INTERVAL	AVERAGE POWER LEVEL (MWt)	LOCAL POWER FACTOR
41	11/ 1/74	30.	1303.	1.00
42	12/ 1/74	31.	1482.	1.00
43	1/ 1/75	31.	671.	1.00
44	2/ 1/75	28.	1334.	1.00
45	3/ 1/75	31.	0.	1.00
46	4/ 1/75	30.	1136.	1.00
47	5/ 1/75	31.	1481.	1.00
48	6/ 1/75	30.	1414.	1.00
49	7/ 1/75	31.	1488.	1.00
50	8/ 1/75	31.	1488.	1.00
51	9/ 1/75	30.	1455.	1.00
52	10/ 1/75	31.	1479.	1.00
53	11/ 1/75	16.	1425.	1.00
	11/17/75	DISCHARGED*		

---

*EFFECTIVE FULL POWER OPERATION TIME WAS 1.163+008 SECONDS AT A FULL POWER LEVEL OF 1488. MWt.

256

TABLE 4.2.4.5.1.2

REACTION RATE DATA AND CORRECTION FACTORS FOR POINT BEACH UNIT 1 CAPSULE S

REACTION NAME	IDENT	TOR RATE (DPS/NUCL)	SATURATION FACTOR	GRADIENT FACTOR	IMPURITY FACTOR	AVG REACTION RATE (RPS/NUCL)	% UNCERT (1σ)
^{54}Fe(n,p)^{54}Mn	C-37	3.73-015	1.265+000	0.950	1.000	4.66-015	10.
	R-26	3.69-015	1.265+000	0.950	1.000		
	WH-32	4.09-015	1.265+000	0.950	1.000		
	A-37	3.46-015	1.265+000	1.170	1.000		
	R-27	2.87-015	1.265+000	1.170	1.000		
	WW-31	3.21-015	1.265+000	1.170	1.000		
^{58}Ni(n,p)^{58}Co	MID	5.54-015	1.072+000	0.930	1.000	5.52-015	10.
^{63}Cu(n,α)^{60}Co	BOT MID	1.66-017	2.780+000	0.960	1.000	4.29-017	10.
	TOP MID	1.46-017	2.780+000	0.960	1.000		
	TOP	1.70-017	2.780+000	0.960	1.000		
^{237}Np(n,f)^{137}Cs	MID	1.08-015	1.248+001	1.000	1.000	2.15-013	10.
^{238}U(n,f)^{137}Cs	MID	1.29-016	1.248+001	1.000	0.840	2.25-014	10.
^{59}Co(n,γ)^{60}Co	B-M (B)	1.64-012	2.780+000	0.940	1.000	4.14-012	10.
	MID (B)	1.43-012	2.780+000	0.940	1.000		
	T-M (B)	1.71-012	2.780+000	0.940	1.000		
	TOP (B)	1.56-012	2.780+000	0.940	1.000		
^{59}Co(n,γ)^{60}Co	B-M (CD)	6.67-013	2.780+000	1.180	1.000	1.99-012	10.
	MID (CD)	5.40-013	2.780+000	1.180	1.000		
	T-M (CD)	6.18-013	2.780+000	1.180	1.000		
	TOP (CD)	5.97-013	2.780+000	1.180	1.000		

CD = Cadmium-Covered Dosimeter.
B = Bare Dosimeter.

TABLE 4.2.4.5.1.3

FERRET-SAND II RESULTS FOR
POINT BEACH UNIT 1 CAPSULE S
(AVERAGE FOR CAPSULE)

GROUP	ENERGY (MeV)	A PRIORI FLUX* ($n/cm^2 \cdot s$)	ADJUSTED FLUX ($n/cm^2 \cdot s$)	% UNCERTAIN ($1\ \sigma$)
1	1.492+001	2.258+006	2.515+006	41.
2	1.350+001	4.693+006	5.220+006	37.
3	1.162+001	2.176+007	2.408+007	34.
4	1.000+001	6.604+007	7.262+007	29.
5	8.607+000	1.671+008	1.818+008	26.
6	7.408+000	3.948+008	4.211+008	24.
7	6.065+000	1.397+009	1.466+009	20.
8	4.966+000	1.934+009	1.956+009	21.
9	3.679+000	3.102+009	3.039+009	21.
10	2.865+000	4.321+009	4.190+009	22.
11	2.231+000	8.255+009	7.872+009	22.
12	1.738+000	1.184+010	1.131+010	21.
13	1.353+000	1.619+010	1.576+010	22.
14	1.108+000	1.652+010	1.671+010	25.
15	8.208-001	2.704+010	2.820+010	24.
16	6.393-001	2.378+010	2.518+010	27.
17	4.979-001	2.449+010	2.631+010	30.
18	3.877-001	2.399+010	2.606+010	34.
19	3.020-001	2.197+010	2.411+010	37.
20	1.832-001	3.711+010	4.107+010	41.
21	1.111-001	2.857+010	3.174+010	44.
22	6.738-002	2.129+010	2.368+010	46.
23	4.087-002	1.781+010	1.979+010	48.
24	2.554-002	1.500+010	1.663+010	50.
25	1.989-002	7.159+009	7.929+009	51.
26	1.503-002	7.264+009	8.051+009	52.
27	9.119-003	1.178+010	1.311+010	52.
28	5.531-003	1.180+010	1.322+010	52.
29	3.355-003	1.194+010	1.354+010	51.
30	2.839-003	4.010+009	4.621+009	50.
31	2.404-003	4.019+009	4.721+009	48.
32	2.035-003	4.034+009	4.842+009	46.
33	1.234-003	1.215+010	1.492+010	44.
34	7.485-004	1.202+010	1.508+010	41.
35	4.540-004	1.127+010	1.441+010	38.
36	2.754-004	1.057+010	1.371+010	35.
37	1.670-004	1.050+010	1.373+010	32.
38	1.013-004	1.059+010	1.463+010	14.
39	6.144-005	1.072+010	1.390+010	31.
40	3.727-005	1.086+010	1.383+010	32.

TABLE 4.2.4.5.1.3 (Cont'd)

FERRET-SAND II RESULTS FOR POINT BEACH UNIT 1 CAPSULE S (AVERAGE FOR CAPSULE)

GROUP	ENERGY (MeV)	A PRIORI FLUX* (n/cm^2·s)	ADJUSTED FLUX (n/cm^2·s)	% UNCERTAIN (1 σ)
41	2.260-005	1.095+010	1.354+010	34.
42	1.371-005	1.085+010	1.293+010	36.
43	8.315-006	1.042+010	1.188+010	38.
44	5.043-006	9.930+009	1.076+010	40.
45	3.059-006	9.680+009	9.934+009	41.
46	1.855-006	9.675+009	9.382+009	41.
47	1.125-006	9.865+009	9.044+009	40.
48	6.826-007	1.005+010	8.731+009	39.
49	4.140-007	1.017+010	8.411+009	37.
50	2.511-007	1.454+010	1.150+010	34.
51	1.523-007	2.045+010	1.561+010	32.
52	9.237-008	2.308+010	1.721+010	31.
53	1.000-010	7.231+010	5.082+010	22.
FLUX, E > 0.0 MeV		5.556+011	6.998+011	16.
FLUX, E < 0.414 eV		1.152+011	1.036+011	19.
FLUX, E > 0.1 MeV		2.095+011	2.707+011	20.
FLUX, E > 1.0 MeV		6.021+010	7.266+010	10.
dpa/s		9.989-011	1.251-010	13.
FLUENCE+, E > 1.0 MeV		7.003+018	8.450+018	10.
dpa+		1.162-002	1.455-002	13.

---

* ABSOLUTE CALCULATED FLUX (OR NORMALIZED TO Fe54(n,p)Mn54 REACTION RATE).

+ BASED ON 1.163+008 EFFECTIVE FULL POWER SECONDS OF EXPOSURE; UNITS OF n/cm^2 FOR FLUENCE AND TOTAL NUMBER OF DISPLACED ATOMS OF IRON PER TARGET ATOM OF IRON FOR dpa.

TABLE 4.2.4.5.1.4

COMPARISON OF MEASURED AND CALCULATED REACTION RATES USED IN THE ANALYSIS OF POINT BEACH UNIT 1 CAPSULE S

REACTION	REACTION RATE (DPS/NUCLEUS) MEAS	A PRIORI CALC	ADJ CALC	RATIO MEAS/CALC A PRIORI	ADJ CALC
Fe54(n,p)Mn54	4.66-015	4.46-015	4.47-015	1.04	1.04
Ni58(n,p)Co58	5.52-015	6.03-015	5.86-015	.92	.94
Cu63(n,α)Co60	4.29-017	3.95-017	4.21-017	1.09	1.02
Np237(n,f)Cs137	2.15-013	2.00-013	2.10-013	1.07	1.02
U238(n,f)Cs137	2.25-014	2.36-014	2.30-014	.95	.98
Co59(n,γ)Co60 (Cd)	1.99-012	1.49-012	1.93-012	1.34	1.03
Co59(n,γ)Co60	4.14-012	4.70-012	4.28-012	.88	.97

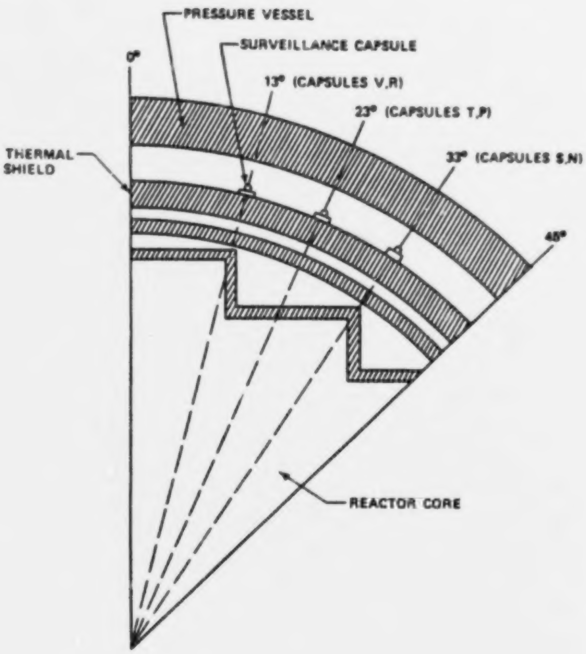
PRESSURE VESSEL
SURVEILLANCE CAPSULE
0°
13° (CAPSULES V,R)
23° (CAPSULES T,P)
33° (CAPSULES S,N)
THERMAL SHIELD
45°
REACTOR CORE

(a) Reactor Geometry.

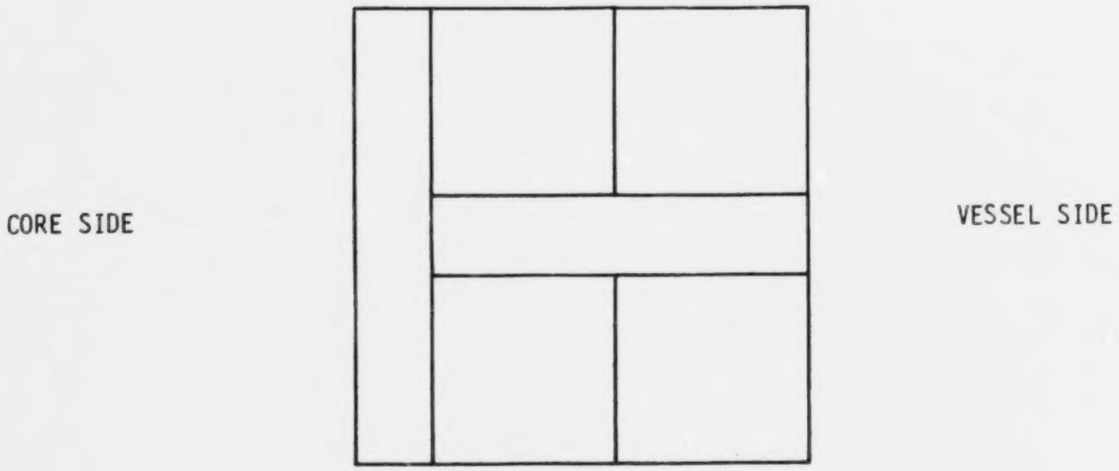
CORE SIDE
VESSEL SIDE

(b) Plan View of Surveillance Capsule

FIGURE 4.2.4.5.2.1. Orientation of the Capsule Relative to the Core and Vessel Wall - Point Beach Unit 1 Capsule R.

TABLE 4.2.4.5.2.1

SUMMARY OF REACTOR OPERATIONS
POINT BEACH UNIT 1 CAPSULE R

TIME PERIOD	START DATE	TIME INTERVAL	AVERAGE POWER LEVEL (MWt)	LOCAL POWER FACTOR
1	11/ 1/70	30.	247.	1.00
2	12/ 1/70	31.	610.	1.00
3	1/ 1/71	31.	971.	1.00
4	2/ 1/71	28.	978.	1.00
5	3/ 1/71	31.	1249.	1.00
6	4/ 1/71	30.	609.	1.00
7	5/ 1/71	31.	1114.	1.00
8	6/ 1/71	30.	1233.	1.00
9	7/ 1/71	31.	1254.	1.00
10	8/ 1/71	31.	1372.	1.00
11	9/ 1/71	30.	1238.	1.00
12	10/ 1/71	31.	1299.	1.00
13	11/ 1/71	30.	1071.	1.00
14	12/ 1/71	31.	1317.	1.00
15	1/ 1/72	182.	1393.	1.00
16	7/ 1/72	31.	1375.	1.00
17	8/ 1/72	31.	1485.	1.00
18	9/ 1/72	30.	1296.	1.00
19	10/ 1/72	92.	0.	1.00
20	1/ 1/73	59.	0.	1.00
21	3/ 1/73	31.	854.	1.00
22	4/ 1/73	30.	1084.	1.00
23	5/ 1/73	31.	1092.	1.00
24	6/ 1/73	30.	1236.	1.00
25	7/ 1/73	31.	1439.	1.00
26	8/ 1/73	31.	1345.	1.00
27	9/ 1/73	30.	1401.	1.00
28	10/ 1/73	31.	1275.	1.00
29	11/ 1/73	30.	1136.	1.00
30	12/ 1/73	31.	1268.	1.00
31	1/ 1/74	31.	1360.	1.00
32	2/ 1/74	28.	1449.	1.00
33	3/ 1/74	31.	1481.	1.00
34	4/ 1/74	30.	260.	1.00
35	5/ 1/74	31.	0.	1.00
36	6/ 1/74	30.	937.	1.00
37	7/ 1/74	31.	1451.	1.00
38	8/ 1/74	31.	1385.	1.00
39	9/ 1/74	30.	1379.	1.00
40	10/ 1/74	31.	1394.	1.00

TABLE 4.2.4.5.2.1 (Cont'd)

SUMMARY OF REACTOR OPERATIONS
POINT BEACH UNIT 1 CAPSULE R

TIME PERIOD	START DATE	TIME INTERVAL	AVERAGE POWER LEVEL (MWt)	LOCAL POWER FACTOR
41	11/ 1/74	30.	1303.	1.00
42	12/ 1/74	31.	1482.	1.00
43	1/ 1/75	31.	671.	1.00
44	2/ 1/75	28.	1334.	1.00
45	3/ 1/75	31.	0.	1.00
46	4/ 1/75	30.	1136.	1.00
47	5/ 1/75	31.	1481.	1.00
48	6/ 1/75	30.	1414.	1.00
49	7/ 1/75	31.	1488.	1.00
50	8/ 1/75	31.	1488.	1.00
51	9/ 1/75	30.	1455.	1.00
52	10/ 1/75	31.	1479.	1.00
53	11/ 1/75	16.	1425.	1.00
54	11/17/75	45.	0.	1.00
55	1/ 1/76	31.	974.	1.00
56	2/ 1/76	29.	1448.	1.00
57	3/ 1/76	31.	1473.	1.00
58	4/ 1/76	30.	1465.	1.00
59	5/ 1/76	31.	1395.	1.00
60	6/ 1/76	30.	1468.	1.00
61	7/ 1/76	31.	1472.	1.00
62	8/ 1/76	31.	1479.	1.00
63	9/ 1/76	30.	1495.	1.00
64	10/ 1/76	31.	36.	1.00
65	11/ 1/76	30.	190.	1.00
66	12/ 1/76	31.	1346.	1.00
67	1/ 1/77	31.	1485.	1.00
68	2/ 1/77	28.	1404.	1.00
69	3/ 1/77	31.	1478.	1.00
70	4/ 1/77	30.	1477.	1.00
71	5/ 1/77	31.	1437.	1.00
72	6/ 1/77	30.	1016.	1.00
73	7/ 1/77	31.	1413.	1.00
74	8/ 1/77	31.	1495.	1.00
75	9/ 1/77	30.	1372.	1.00
76	10/ 1/77	31.	164.	1.00
	11/ 1/77	DISCHARGED*		

---

*EFFECTIVE FULL POWER OPERATION TIME WAS 1.632+008 SECONDS AT A FULL POWER LEVEL OF 1495. MWt.

TABLE 4.2.4.5.2.2

REACTION RATE DATA AND CORRECTION FACTORS FOR POINT BEACH UNIT 1 CAPSULE R

REACTION NAME	IDENT	TOR RATE (DPS/NUCL)	SATURATION FACTOR	GRADIENT FACTOR	IMPURITY FACTOR	AVG REACTION RATE (RPS/NUCL)	% UNCERT (1σ)
$^{54}\mathrm{Fe}(n,p)^{54}\mathrm{Mn}$	C-13	6.11-015	1.284+000	0.950	1.000	8.05-015	10.
	R-10	6.69-015	1.284+000	0.950	1.000		
	WH-16	6.24-015	1.284+000	0.950	1.000		
	A-13	5.47-015	1.284+000	1.180	1.000		
	R-11	5.47-015	1.284+000	1.180	1.000		
	NW-15	5.59-015	1.284+000	1.180	1.000		
$^{58}\mathrm{Ni}(n,p)^{58}\mathrm{Co}$	MID	6.37-015	1.429+000	0.930	1.000	8.47-015	10.
$^{63}\mathrm{Cu}(n,\alpha)^{60}\mathrm{Co}$	BOT	3.51-017	2.214+000	0.960	1.000	6.96-017	10.
	BOT MID	3.43-017	2.214+000	0.960	1.000		
	TOP MID	2.87-017	2.214+000	0.960	1.000		
	TOP	3.27-017	2.214+000	0.960	1.000		
$^{237}\mathrm{Np}(n,f)^{137}\mathrm{Cs}$	MID	2.97-015	9.085+000	1.000	1.000	4.30-013	10.
$^{238}\mathrm{U}(n,f)^{137}\mathrm{Cs}$	MID	3.96-016	9.085+000	1.000	0.730	4.37-014	10.
$^{59}\mathrm{Co}(n,\gamma)^{60}\mathrm{Co}$	BOT (B)	3.42-012	2.214+000	0.930	1.000	7.67-012	10.
	B-M (B)	3.86-012	2.214+000	0.930	1.000		
	MID (B)	3.59-012	2.214+000	0.930	1.000		
	T-M (B)	3.81-012	2.214+000	0.930	1.000		
	TOP (B)	3.96-012	2.214+000	0.930	1.000		
$^{59}\mathrm{Co}(n,\gamma)^{60}\mathrm{Co}$	BOT (CD)	1.83-012	2.214+000	1.170	1.000	4.47-012	10.
	B-M (CD)	1.95-012	2.214+000	1.170	1.000		
	MID (CD)	1.69-012	2.214+000	1.170	1.000		
	T-M (CD)	1.55-012	2.214+000	1.170	1.000		
	TOP (CD)	1.60-012	2.214+000	1.170	1.000		

CD = Cadmium-Covered Dosimeter.
B = Bare Dosimeter.

TABLE 4.2.4.5.2.3

FERRET-SAND II RESULTS FOR POINT BEACH UNIT 1 CAPSULE R (AVERAGE FOR CAPSULE)

GROUP	ENERGY (MeV)	A PRIORI FLUX* (n/cm^2·s)	ADJUSTED FLUX (n/cm^2·s)	% UNCERTAIN (1 σ)
1	1.492+001	3.591+006	3.994+006	41.
2	1.350+001	7.466+006	8.296+006	37.
3	1.162+001	3.461+007	3.828+007	34.
4	1.000+001	1.050+008	1.157+008	29.
5	8.607+000	2.658+008	2.899+008	26.
6	7.408+000	6.243+008	6.636+008	24.
7	6.065+000	2.193+009	2.276+009	20.
8	4.966+000	3.194+009	3.110+009	21.
9	3.679+000	5.466+009	5.074+009	21.
10	2.865+000	8.058+009	7.492+009	22.
11	2.231+000	1.548+010	1.438+010	21.
12	1.738+000	2.282+010	2.196+010	21.
13	1.353+000	3.206+010	3.164+010	22.
14	1.108+000	3.354+010	3.365+010	24.
15	8.208-001	5.615+010	5.811+010	24.
16	6.393-001	5.048+010	5.312+010	27.
17	4.979-001	5.234+010	5.581+010	30.
18	3.877-001	5.124+010	5.510+010	34.
19	3.020-001	4.755+010	5.146+010	37.
20	1.832-001	8.206+010	8.909+010	40.
21	1.111-001	6.418+010	6.956+010	43.
22	6.738-002	4.750+010	5.125+010	46.
23	4.087-002	3.935+010	4.220+010	48.
24	2.554-002	3.312+010	3.531+010	50.
25	1.989-002	1.588+010	1.686+010	51.
26	1.503-002	1.623+010	1.722+010	52.
27	9.119-003	2.617+010	2.789+010	52.
28	5.531-003	2.615+010	2.814+010	52.
29	3.355-003	2.673+010	2.919+010	51.
30	2.839-003	9.031+009	1.006+010	50.
31	2.404-003	9.073+009	1.036+010	48.
32	2.035-003	9.125+009	1.070+010	46.
33	1.234-003	2.743+010	3.310+010	44.
34	7.485-004	2.678+010	3.319+010	41.
35	4.540-004	2.519+010	3.194+010	37.
36	2.754-004	2.373+010	3.058+010	35.
37	1.670-004	2.342+010	3.043+010	32.
38	1.013-004	2.370+010	3.288+010	13.
39	6.144-005	2.411+010	3.074+010	31.
40	3.727-005	2.452+010	3.040+010	32.

TABLE 4.2.4.5.2.3 (Cont'd)

FERRET-SAND II RESULTS FOR
POINT BEACH UNIT 1 CAPSULE R
(AVERAGE FOR CAPSULE)

GROUP	ENERGY (MeV)	A PRIORI FLUX* ($n/cm^2 \cdot s$)	ADJUSTED FLUX ($n/cm^2 \cdot s$)	% UNCERTAIN (1 σ)
41	2.260-005	2.473+010	2.938+010	34.
42	1.371-005	2.438+010	2.742+010	36.
43	8.315-006	2.339+010	2.463+010	38.
44	5.043-006	2.232+010	2.183+010	40.
45	3.059-006	2.178+010	1.965+010	41.
46	1.855-006	2.178+010	1.807+010	41.
47	1.125-006	2.220+010	1.696+010	41.
48	6.826-007	2.261+010	1.596+010	39.
49	4.140-007	2.288+010	1.502+010	38.
50	2.511-007	3.375+010	2.074+010	36.
51	1.523-007	4.706+010	2.750+010	34.
52	9.237-008	5.203+010	2.942+010	32.
53	1.000-010	1.582+011	8.193+010	25.
FLUX, E > 0.0 MeV		1.482+012	1.434+012	17.
FLUX, E < 0.414 eV		3.140+011	1.746+011	22.
FLUX, E > 0.1 MeV		5.378+011	5.637+011	20.
FLUX, E > 1.0 MeV		1.431+011	1.406+011	10.
dpa/s		2.459-010	2.497-010	13.
FLUENCE+, E > 1.0 MeV		2.335+019	2.294+019	10.
dpa+		4.014-002	4.075-002	13.

---

* ABSOLUTE CALCULATED FLUX (OR NORMALIZED TO Fe54(n,p)Mn54 REACTION RATE).

+ BASED ON 1.632+008 EFFECTIVE FULL POWER SECONDS OF EXPOSURE; UNITS OF n/cm^2 FOR FLUENCE AND TOTAL NUMBER OF DISPLACED ATOMS OF IRON PER TARGET ATOM OF IRON FOR dpa.

TABLE 4.2.4.5.2.4

COMPARISON OF MEASURED AND CALCULATED REACTION RATES USED IN THE ANALYSIS OF POINT BEACH UNIT 1 CAPSULE R

REACTION	REACTION RATE (DPS/NUCLEUS) MEAS	REACTION RATE (DPS/NUCLEUS) A PRIORI CALC	REACTION RATE (DPS/NUCLEUS) ADJ CALC	RATIO MEAS/CALC A PRIORI	RATIO MEAS/CALC ADJ CALC
Np237(n,f)Cs137	4.30-013	4.05-013	4.21-013	1.06	1.02
U238(n,f)Cs137	4.37-014	4.43-014	4.30-014	.99	1.02
Co59(n,γ)Co60 (Cd)	4.47-012	3.34-012	4.25-012	1.34	1.05
Co59(n,γ)Co60	7.67-012	1.04-011	8.18-012	.74	.94
Fe54(n,p)Mn54	8.05-015	7.79-015	7.56-015	1.03	1.06
Ni58(n,p)Co58	8.47-015	1.06-014	9.75-015	.80	.87
Cu63(n,α)Co60	6.96-017	6.29-017	6.70-017	1.11	1.04

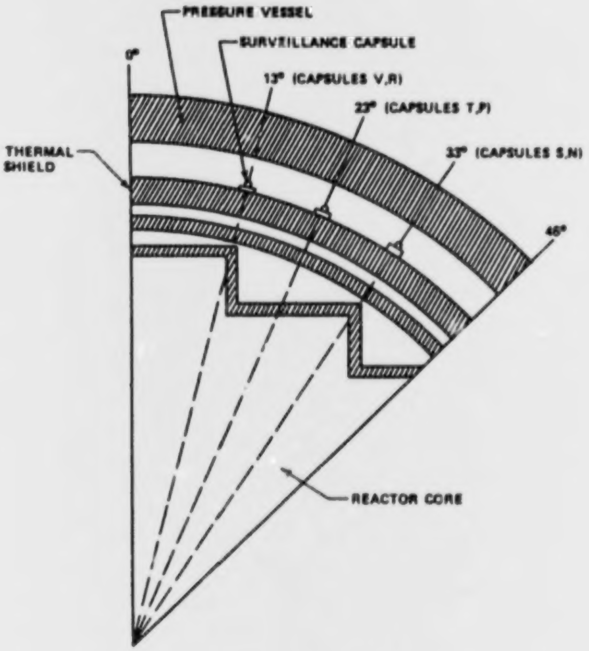
PRESSURE VESSEL
SURVEILLANCE CAPSULE
0°
13° (CAPSULES V,R)
23° (CAPSULES T,P)
33° (CAPSULES S,N)
THERMAL SHIELD
45°
REACTOR CORE

(a) Reactor Geometry.

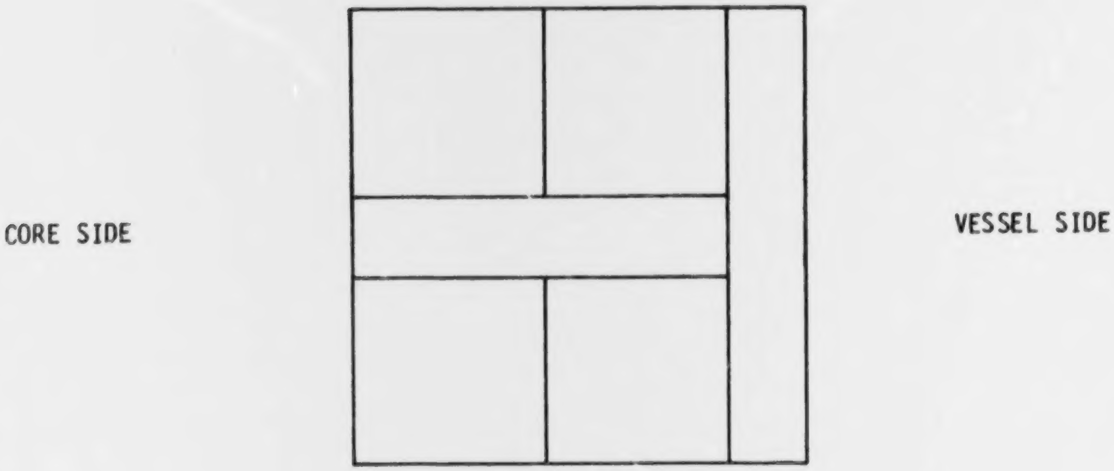
CORE SIDE
VESSEL SIDE

(b) Plan View of Surveillance Capsule

FIGURE 4.2.4.6.1.1. Orientation of the Capsule Relative to the Core and Vessel Wall - Point Beach Unit 2 Capsule V.

TABLE 4.2.4.6.1.1

SUMMARY OF REACTOR OPERATIONS
POINT BEACH UNIT 2 CAPSULE V

TIME PERIOD	START DATE	TIME INTERVAL	AVERAGE POWER LEVEL (MWt)	LOCAL POWER FACTOR
1	10/ 1/72	92.	369.	1.00
2	1/ 1/73	31.	284.	1.00
3	2/ 1/73	28.	278.	1.00
4	3/ 1/73	31.	740.	1.00
5	4/ 1/73	30.	743.	1.00
6	5/ 1/73	31.	1043.	1.00
7	6/ 1/73	30.	1300.	1.00
8	7/ 1/73	31.	1325.	1.00
9	8/ 1/73	31.	1397.	1.00
10	9/ 1/73	30.	1501.	1.00
11	10/ 1/73	31.	1474.	1.00
12	11/ 1/73	30.	1479.	1.00
13	12/ 1/73	31.	1424.	1.00
14	1/ 1/74	31.	1462.	1.00
15	2/ 1/74	28.	1458.	1.00
16	3/ 1/74	31.	1485.	1.00
17	4/ 1/74	30.	1495.	1.00
18	5/ 1/74	31.	1494.	1.00
19	6/ 1/74	30.	1229.	1.00
20	7/ 1/74	31.	1283.	1.00
21	8/ 1/74	31.	1494.	1.00
22	9/ 1/74	30.	1464.	1.00
23	10/ 1/74	31.	750.	1.00
	11/ 1/74	DISCHARGED*		

---

*EFFECTIVE FULL POWER OPERATION TIME WAS 4.805+007 SECONDS AT A FULL POWER LEVEL OF 1518. MWt.

TABLE 4.2.4.6.1.2

REACTION RATE DATA AND CORRECTION FACTORS FOR POINT BEACH UNIT 2 CAPSULE V

REACTION NAME	REACTION IDENT	TOR RATE (DPS/NUCL)	SATURATION FACTOR	GRADIENT FACTOR	IMPURITY FACTOR	AVG REACTION RATE (RPS/NUCL)	% UNCERT (1σ)
^{54}Fe(n,p)^{54}Mn	W-2 TEN	5.22-015	1.515+000	1.050	1.000	7.89-015	10.
	W-1 TEN	5.17-015	1.515+000	1.050	1.000		
	W-1 CHA	4.82-015	1.515+000	1.050	1.000		
	V-4 CHA	5.57-015	1.515+000	0.870	1.000		
	V-1 TEN	4.97-015	1.515+000	1.050	1.000		
^{63}Cu(n,α)^{60}Co	TOP	1.06-017	5.585+000	1.050	1.000	6.31-017	10.
	TOP MID	1.03-017	5.585+000	1.050	1.000		
	BOT MID	1.10-017	5.585+000	1.050	1.000		
	BOT	1.11-017	5.585+000	1.050	1.000		
^{58}Ni(n,p)^{58}Co	MID	6.87-015	1.222+000	1.040	1.000	8.73-015	10.
^{237}Np(n,f)^{137}Cs	MID	8.98-016	2.917+001	1.000	1.000	4.18-013	10.
^{238}U(n,f)^{137}Cs	MID	1.27-015	2.917+001	1.000	0.855	5.29-013	10.
^{59}Co(n,γ)^{60}Co	TOP (CD)	7.34-013	5.585+000	0.840	1.000	3.14-012	10.
	T-M (CD)	6.87-013	5.585+000	0.840	1.000		
	MID (CD)	6.07-013	5.585+000	0.840	1.000		
	B-M (CD)	6.87-013	5.585+000	0.840	1.000		
	BOT (CD)	6.28-013	5.585+000	0.840	1.000		
^{59}Co(n,γ)^{60}Co	TOP (B)	1.63-012	5.585+000	1.000	1.000	8.03-012	11.
	T-M (B)	1.46-012	5.585+000	1.000	1.000		
	MID (B)	1.19-012	5.585+000	1.000	1.000		
	B-M (B)	1.44-012	5.585+000	1.000	1.000		
	BOT (B)	1.48-012	5.585+000	1.000	1.000		

CD = Cadmium-Covered Dosimeter.
B = Bare Dosimeter.

270

TABLE 4.2.4.6.1.3

FERRET-SAND II RESULTS FOR POINT BEACH UNIT 2 CAPSULE V (AVERAGE FOR CAPSULE)

GROUP	ENERGY (MeV)	A PRIORI FLUX* $(n/cm^2 \cdot s)$	ADJUSTED FLUX $(n/cm^2 \cdot s)$	% UNCERTAIN $(1\ \sigma)$
1	1.492+001	3.586+006	3.380+006	41.
2	1.350+001	7.454+006	7.074+006	38.
3	1.162+001	3.456+007	3.307+007	34.
4	1.000+001	1.049+008	1.015+008	30.
5	8.607+000	2.654+008	2.601+008	26.
6	7.408+000	6.232+008	6.179+008	24.
7	6.065+000	2.188+009	2.192+009	20.
8	4.966+000	3.186+009	3.198+009	22.
9	3.679+000	5.457+009	5.514+009	22.
10	2.865+000	8.044+009	8.274+009	22.
11	2.231+000	1.541+010	1.624+010	23.
12	1.738+000	2.277+010	2.472+010	23.
13	1.353+000	3.201+010	3.483+010	23.
14	1.108+000	3.351+010	3.542+010	25.
15	8.208-001	5.600+010	5.857+010	25.
16	6.393-001	5.038+010	5.213+010	27.
17	4.979-001	5.227+010	5.342+010	31.
18	3.877-001	5.114+010	5.154+010	34.
19	3.020-001	4.740+010	4.704+010	38.
20	1.832-001	8.167+010	7.980+010	41.
21	1.111-001	6.385+010	6.150+010	44.
22	6.738-002	4.738+010	4.507+010	46.
23	4.087-002	3.930+010	3.700+010	49.
24	2.554-002	3.307+010	3.090+010	50.
25	1.989-002	1.585+010	1.472+010	51.
26	1.503-002	1.618+010	1.498+010	52.
27	9.119-003	2.610+010	2.414+010	52.
28	5.531-003	2.609+010	2.415+010	52.
29	3.355-003	2.663+010	2.471+010	51.
30	2.839-003	8.989+009	8.369+009	50.
31	2.404-003	9.028+009	8.441+009	49.
32	2.035-003	9.076+009	8.525+009	46.
33	1.234-003	2.730+010	2.576+010	44.
34	7.485-004	2.669+010	2.529+010	41.
35	4.540-004	2.514+010	2.390+010	38.
36	2.754-004	2.370+010	2.257+010	35.
37	1.670-004	2.337+010	2.224+010	32.
38	1.013-004	2.365+010	2.272+010	15.
39	6.144-005	2.406+010	2.272+010	30.
40	3.727-005	2.448+010	2.289+010	32.

TABLE 4.2.4.6.1.3 (Cont'td

FERRET-SAND II RESULTS FOR
POINT BEACH UNIT 2 CAPSULE V
(AVERAGE FOR CAPSULE)

GROUP	ENERGY (MeV)	A PRIORI FLUX* ($n/cm^2 \cdot s$)	ADJUSTED FLUX ($n/cm^2 \cdot s$)	% UNCERTAIN (1σ)
41	2.260-005	2.469+010	2.281+010	33.
42	1.371-005	2.434+010	2.213+010	35.
43	8.315-006	2.334+010	2.081+010	38.
44	5.043-006	2.228+010	1.942+010	39.
45	3.059-006	2.173+010	1.848+010	40.
46	1.855-006	2.173+010	1.800+010	40.
47	1.125-006	2.216+010	1.788+010	40.
48	6.826-007	2.257+010	1.775+010	38.
49	4.140-007	2.284+010	1.754+010	36.
50	2.511-007	3.371+010	2.533+010	34.
51	1.523-007	4.702+010	3.476+010	32.
52	9.237-008	5.197+010	3.802+010	30.
53	1.000-010	1.580+011	1.117+011	21.
FLUX, E > 0.0 MeV		1.436+012	1.349+012	16.
FLUX, E < 0.414 eV		3.045+011	2.274+011	18.
FLUX, E > 0.1 MeV		5.207+011	5.449+011	20.
FLUX, E > 1.0 MeV		1.386+011	1.514+011	11.
dpa/s		2.382-010	2.520-010	13.
FLUENCE+, E > 1.0 MeV		6.660+018	7.276+018	11.
dpa+		1.145-002	1.211-002	13.

---

* ABSOLUTE CALCULATED FLUX (OR NORMALIZED TO Fe54(n,p)Mn54 REACTION RATE).

+ BASED ON 4.805+007 EFFECTIVE FULL POWER SECONDS OF EXPOSURE; UNITS OF n/cm^2 FOR FLUENCE AND TOTAL NUMBER OF DISPLACED ATOMS OF IRON PER TARGET ATOM OF IRON FOR dpa.

272

TABLE 4.2.4.6.1.4

COMPARISON OF MEASURED AND CALCULATED REACTION RATES USED IN THE ANALYSIS OF POINT BEACH UNIT 2 CAPSULE V

REACTION	REACTION RATE (DPS/NUCLEUS) MEAS	A PRIORI CALC	ADJ CALC	RATIO MEAS/CALC A PRIORI	ADJ CALC
Np237(n,f)Cs137	4.18-013	4.04-013	4.20-013	1.03	1.00
U238(n,f)Cs137	5.29-014	4.42-014	4.70-014	1.20	1.12
Co59(n,γ)Co60 (Cd)	3.14-012	3.33-012	3.11-012	.94	1.01
Co59(n,γ)Co60	8.03-012	1.04-011	8.22-012	.77	.98
Fe54(n,p)Mn54	7.89-015	7.77-015	7.94-015	1.02	.99
Ni58(n,p)Co58	8.73-015	1.06-014	1.08-014	.82	.81
Cu63(n,α)Co60	6.31-017	6.28-017	6.26-017	1.00	1.01

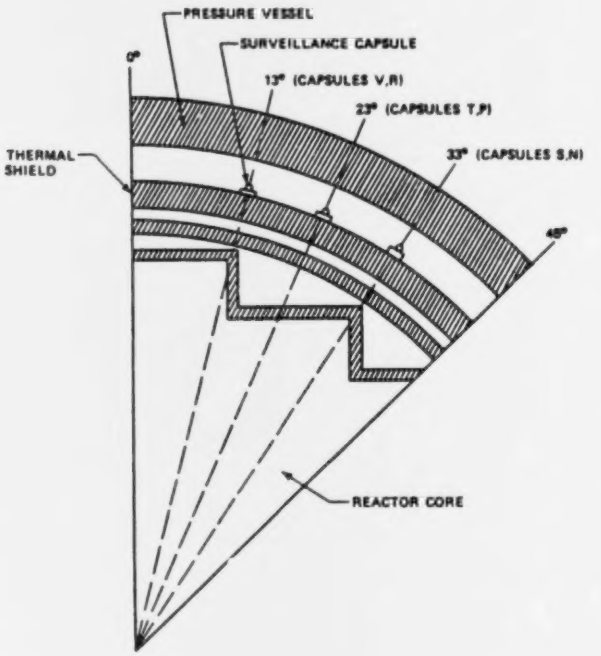
PRESSURE VESSEL
SURVEILLANCE CAPSULE
0°
13° (CAPSULES V,R)
23° (CAPSULES T,P)
33° (CAPSULES S,N)
THERMAL SHIELD
45°
REACTOR CORE

(a) Reactor Geometry.

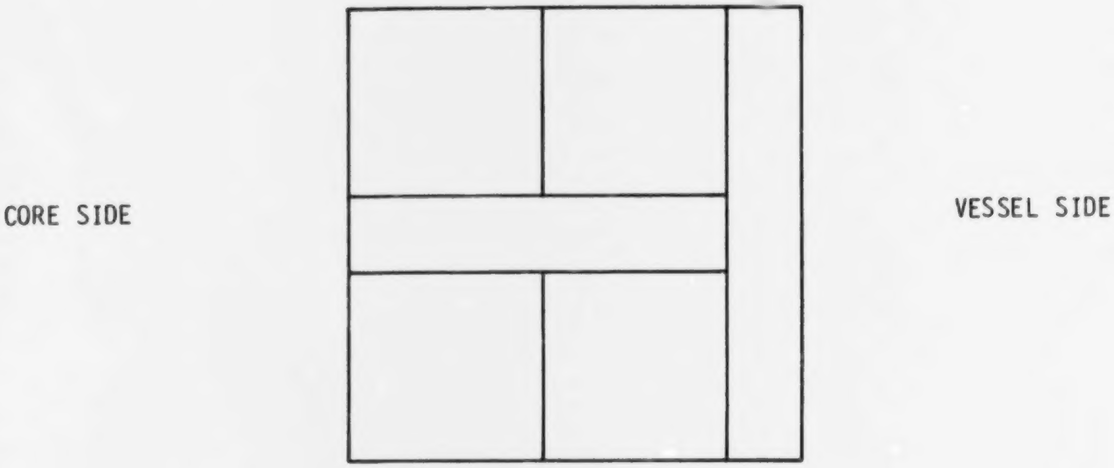
CORE SIDE
VESSEL SIDE

(b) Plan View of Surveillance Capsule

FIGURE 4.2.4.6.1.1. Orientation of the Capsule Relative to the Core and Vessel Wall - Point Beach Unit 2 Capsule T.

TABLE 4.2.4.6.2.1

SUMMARY OF REACTOR OPERATIONS
POINT BEACH UNIT 2 CAPSULE T

TIME PERIOD	START DATE	TIME INTERVAL	AVERAGE POWER LEVEL (MWt)	LOCAL POWER FACTOR
1	10/ 1/72	92.	369.	1.00
2	1/ 1/73	31.	284.	1.00
3	2/ 1/73	28.	278.	1.00
4	3/ 1/73	31.	740.	1.00
5	4/ 1/73	30.	743.	1.00
6	5/ 1/73	31.	1043.	1.00
7	6/ 1/73	30.	1300.	1.00
8	7/ 1/73	31.	1325.	1.00
9	8/ 1/73	31.	1397.	1.00
10	9/ 1/73	30.	1501.	1.00
11	10/ 1/73	31.	1474.	1.00
12	11/ 1/73	30.	1479.	1.00
13	12/ 1/73	31.	1424.	1.00
14	1/ 1/74	31.	1462.	1.00
15	2/ 1/74	28.	1458.	1.00
16	3/ 1/74	31.	1485.	1.00
17	4/ 1/74	30.	1495.	1.00
18	5/ 1/74	31.	1494.	1.00
19	6/ 1/74	30.	1229.	1.00
20	7/ 1/74	31.	1283.	1.00
21	8/ 1/74	31.	1494.	1.00
22	9/ 1/74	30.	1464.	1.00
23	10/ 1/74	31.	750.	1.00
24	11/ 1/74	30.	0.	1.00
25	12/ 1/74	31.	406.	1.00
26	1/ 1/75	31.	1497.	1.00
27	2/ 1/75	28.	1311.	1.00
28	3/ 1/75	31.	1454.	1.00
29	4/ 1/75	30.	1273.	1.00
30	5/ 1/75	31.	1183.	1.00
31	6/ 1/75	30.	1270.	1.00
32	7/ 1/75	31.	1430.	1.00
33	8/ 1/75	31.	1006.	1.00
34	9/ 1/75	30.	1385.	1.00
35	10/ 1/75	31.	1330.	1.00
36	11/ 1/75	30.	1354.	1.00
37	12/ 1/75	31.	1498.	1.00
38	1/ 1/76	31.	1439.	1.00
39	2/ 1/76	29.	1335.	1.00
40	3/ 1/76	31.	155.	1.00

TABLE 4.2.4.6.2.1 (Cont'd)

SUMMARY OF REACTOR OPERATIONS
POINT BEACH UNIT 2 CAPSULE T

TIME PERIOD	START DATE	TIME INTERVAL	AVERAGE POWER LEVEL (MWt)	LOCAL POWER FACTOR
41	4/ 1/76	30.	1351.	1.00
42	5/ 1/76	31.	1286.	1.00
43	6/ 1/76	30.	1400.	1.00
44	7/ 1/76	31.	1380.	1.00
45	8/ 1/76	31.	1374.	1.00
46	9/ 1/76	30.	1397.	1.00
47	10/ 1/76	31.	1500.	1.00
48	11/ 1/76	30.	1478.	1.00
49	12/ 1/76	31.	1482.	1.00
50	1/ 1/77	31.	1482.	1.00
51	2/ 1/77	28.	1485.	1.00
52	3/ 1/77	31.	135.	1.00
	4/ 1/77	DISCHARGED*		

---

*EFFECTIVE FULL POWER OPERATION TIME WAS 1.087+008 SECONDS AT A FULL POWER LEVEL OF 1518. MWt.

BLANK P

BLANK PAGE

BLANK PAGE

TABLE 4.2.4.6.2.2

REACTION RATE DATA AND CORRECTION FACTORS FOR POINT BEACH UNIT 2 CAPSULE T

REACTION		TOR RATE (DPS/NUCL)	SATURATION FACTOR	GRADIENT FACTOR	IMPURITY FACTOR	AVG REACTION RATE (RPS/NUCL)	% UNCERT (1σ)
NAME	IDENT						
^{54}Fe(n,p)^{54}Mn	E47	5.13-015	1.265+000	0.840	1.000	5.43-015	10.
	V37	5.02-015	1.265+000	0.840	1.000		
	E37	4.91-015	1.265+000	0.840	1.000		
	W32	4.16-015	1.265+000	1.050	1.000		
	H25	4.38-015	1.265+000	1.050	1.000		
	R30	3.95-015	1.265+000	1.050	1.000		
^{58}Ni(n,p)^{58}Co		5.06-015	1.374+000	1.040	1.000	7.23-015	10.
^{63}Cu(n,α)^{60}Co	BOT	1.79-017	2.872+000	1.050	1.000	4.88-017	10.
	BOT MID	1.65-017	2.872+000	1.050	1.000		
	TOP MID	1.43-017	2.872+000	1.050	1.000		
	TOP	1.59-017	2.872+000	1.050	1.000		
^{237}Np(n,f)^{137}Cs	MID	1.14-017	1.326+001	1.000	1.000	2.41-015	10.
^{238}U(n,f)^{137}Cs	MID	1.49-017	1.326+001	1.000	0.826	2.73-015	10.
^{59}Co(n,γ)^{60}Co	T-M (CD)	8.18-013	2.872+000	0.840	1.000	2.00-012	10.
	MID (CD)	7.96-013	2.872+000	0.840	1.000		
	B-M (CD)	8.70-013	2.872+000	0.840	1.000		
	TOP (CD)	8.33-013	2.872+000	0.840	1.000		
^{59}Co(n,γ)^{60}Co	T-M (B)	1.50-012	2.872+000	1.000	1.000	4.91-012	13.
	MID (B)	1.55-012	2.872+000	1.000	1.000		
	T-C (B)	1.95-012	2.872+000	1.000	1.000		
	TOP (B)	1.84-012	2.872+000	1.000	1.000		

CD = Cadmium-Covered Dosimeter.
B = Bare Dosimeter.

TABLE 4.2.4.6.2.3

FERRET-SAND II RESULTS FOR POINT BEACH UNIT 2 CAPSULE T (AVERAGE FOR CAPSULE)

GROUP	ENERGY (MeV)	A PRIORI FLUX* ($n/cm^2 \cdot s$)	ADJUSTED FLUX ($n/cm^2 \cdot s$)	% UNCERTAIN ($1\ \sigma$)
1	1.492+001	2.631+006	2.777+006	41.
2	1.350+001	5.470+006	5.790+006	38.
3	1.162+001	2.536+007	2.692+007	34.
4	1.000+001	7.697+007	8.185+007	30.
5	8.607+000	1.947+008	2.074+008	26.
6	7.408+000	4.590+008	4.900+008	24.
7	6.065+000	1.626+009	1.742+009	20.
8	4.966+000	2.239+009	2.415+009	21.
9	3.679+000	3.518+009	3.802+009	21.
10	2.865+000	4.334+009	4.662+009	22.
11	2.231+000	9.214+009	9.824+009	21.
12	1.738+000	1.312+010	1.385+010	21.
13	1.353+000	1.785+010	1.887+010	22.
14	1.108+000	1.825+010	1.955+010	25.
15	8.208-001	2.982+010	3.211+010	25.
16	6.393-001	2.623+010	2.824+010	28.
17	4.979-001	2.703+010	2.909+010	31.
18	3.877-001	2.648+010	2.847+010	34.
19	3.020-001	2.425+010	2.607+010	38.
20	1.832-001	4.098+010	4.405+010	41.
21	1.111-001	3.147+010	3.383+010	44.
22	6.738-002	2.333+010	2.507+010	46.
23	4.087-002	1.954+010	2.100+010	49.
24	2.554-002	1.649+010	1.773+010	50.
25	1.989-002	7.866+009	8.473+009	51.
26	1.503-002	7.959+009	8.600+009	52.
27	9.119-003	1.292+010	1.403+010	52.
28	5.531-003	1.294+010	1.415+010	52.
29	3.355-003	1.307+010	1.443+010	51.
30	2.839-003	4.384+009	4.897+009	50.
31	2.404-003	4.392+009	4.970+009	49.
32	2.035-003	4.406+009	5.057+009	46.
33	1.234-003	1.326+010	1.545+010	44.
34	7.485-004	1.317+010	1.555+010	41.
35	4.540-004	1.235+010	1.476+010	38.
36	2.754-004	1.157+010	1.396+010	35.
37	1.670-004	1.153+010	1.399+010	32.
38	1.013-004	1.162+010	1.458+010	14.
39	6.144-005	1.174+010	1.417+010	30.
40	3.727-005	1.186+010	1.416+010	32.

TABLE 4.2.4.6.2.3 (Cont'd)

FERRET-SAND II RESULTS FOR POINT BEACH UNIT 2 CAPSULE T (AVERAGE FOR CAPSULE)

GROUP	ENERGY (MeV)	A PRIORI FLUX* ($n/cm^2 \cdot s$)	ADJUSTED FLUX ($n/cm^2 \cdot s$)	% UNCERTAIN (1σ)
41	2.260-005	1.194+010	1.403+010	33.
42	1.371-005	1.187+010	1.364+010	36.
43	8.315-006	1.141+010	1.276+010	38.
44	5.043-006	1.085+010	1.177+010	39.
45	3.059-006	1.057+010	1.109+010	41.
46	1.855-006	1.056+010	1.071+010	41.
47	1.125-006	1.078+010	1.056+010	40.
48	6.826-007	1.099+010	1.042+010	39.
49	4.140-007	1.113+010	1.024+010	37.
50	2.511-007	1.615+010	1.445+010	35.
51	1.523-007	2.298+010	2.012+010	33.
52	9.237-008	2.609+010	2.251+010	32.
53	1.000-010	8.242+010	6.849+010	23.
FLUX, E > 0.0 MeV		7.493+011	7.832+011	16.
FLUX, E < 0.414 eV		1.588+011	1.358+011	21.
FLUX, E > 0.1 MeV		2.821+011	3.027+011	20.
FLUX, E > 1.0 MeV		8.111+010	8.652+010	9.
dpa/s		1.346-010	1.439-010	12.
FLUENCE+, E > 1.0 MeV		8.817+018	9.404+018	9.
dpa+		1.464-002	1.565-002	12.

---

* ABSOLUTE CALCULATED FLUX (OR NORMALIZED TO Fe54(n,p)Mn54 REACTION RATE).

+ BASED ON 1.087+008 EFFECTIVE FULL POWER SECONDS OF EXPOSURE; UNITS OF n/cm^2 FOR FLUENCE AND TOTAL NUMBER OF DISPLACED ATOMS OF IRON PER TARGET ATOM OF IRON FOR dpa.

TABLE 4.2.4.6.2.4

COMPARISON OF MEASURED AND CALCULATED REACTION RATES USED IN THE ANALYSIS OF POINT BEACH UNIT 2 CAPSULE T

	REACTION RATE (DPS/NUCLEUS)			RATIO MEAS/CALC	
REACTION	MEAS	A PRIORI CALC	ADJ CALC	A PRIORI	ADJ CALC
Np237(n,f)Cs137	2.41-013	2.21-013	2.39-013	1.09	1.01
U238(n,f)Cs137	2.73-014	2.61-014	2.77-014	1.05	.98
Co59(n,γ)Co60 (Cd)	2.00-012	1.63-012	1.97-012	1.23	1.02
Co59(n,γ)Co60	4.91-012	5.27-012	5.07-012	.93	.97
Fe54(n,p)Mn54	5.43-015	4.98-015	5.36-015	1.09	1.01
Ni58(n,p)Co58	7.23-015	6.73-015	7.22-015	1.07	1.00
Cu63(n,α)Co60	4.88-017	4.59-017	4.90-017	1.06	1.00

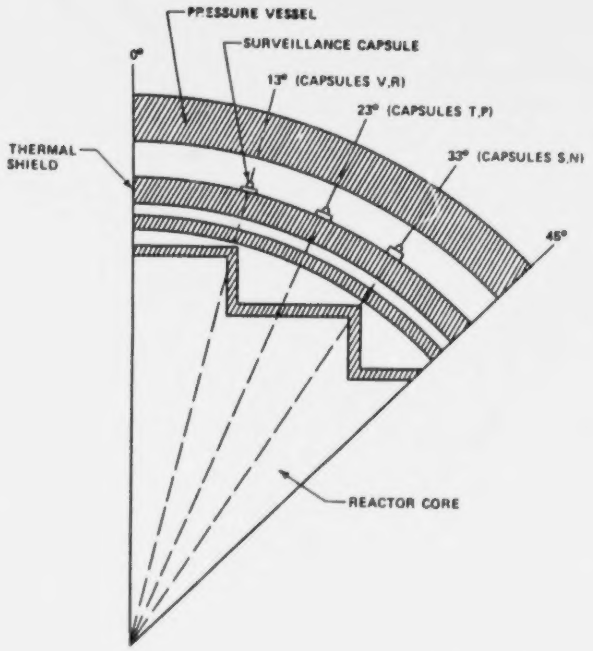
PRESSURE VESSEL
SURVEILLANCE CAPSULE
0°
13° (CAPSULES V,R)
23° (CAPSULES T,P)
33° (CAPSULES S,N)
THERMAL SHIELD
45°
REACTOR CORE

(a) Reactor Geometry.

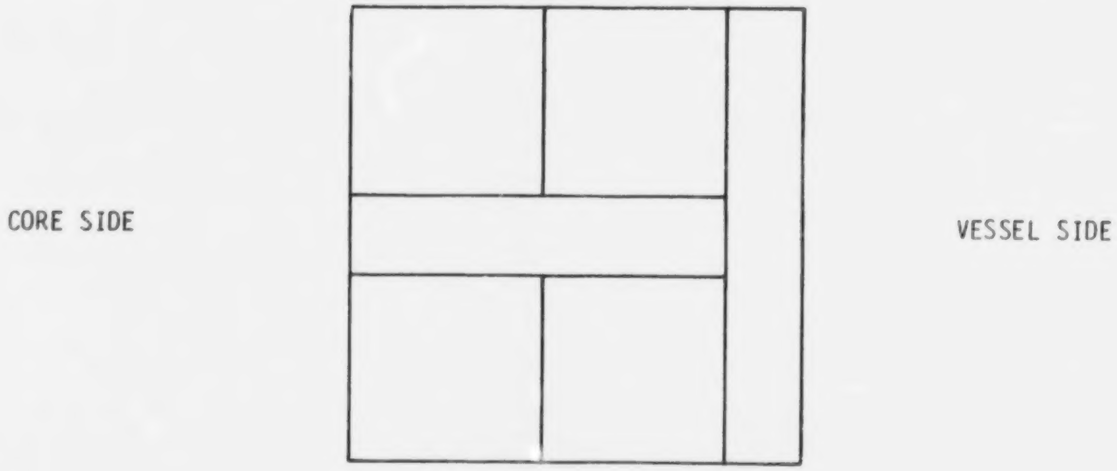
CORE SIDE
VESSEL SIDE

(b) Plan View of Surveillance Capsule

FIGURE 4.2.4.6.3.1. Orientation of the Capsule Relative to the Core and Vessel Wall - Point Beach Unit 2 Capsule R.

TABLE 4.2.4.6.3.1

SUMMARY OF REACTOR OPERATIONS
POINT BEACH UNIT 2 CAPSULE R

TIME PERIOD	START DATE	TIME INTERVAL	AVERAGE POWER LEVEL (MWt)	LOCAL POWER FACTOR
1	10/ 1/72	92.	369.	1.00
2	1/ 1/73	31.	284.	1.00
3	2/ 1/73	28.	278.	1.00
4	3/ 1/73	31.	740.	1.00
5	4/ 1/73	30.	743.	1.00
6	5/ 1/73	31.	1043.	1.00
7	6/ 1/73	30.	1300.	1.00
8	7/ 1/73	31.	1325.	1.00
9	8/ 1/73	31.	1397.	1.00
10	9/ 1/73	30.	1501.	1.00
11	10/ 1/73	31.	1474.	1.00
12	11/ 1/73	30.	1479.	1.00
13	12/ 1/73	31.	1424.	1.00
14	1/ 1/74	31.	1462.	1.00
15	2/ 1/74	28.	1458.	1.00
16	3/ 1/74	31.	1485.	1.00
17	4/ 1/74	30.	1495.	1.00
18	5/ 1/74	31.	1494.	1.00
19	6/ 1/74	30.	1229.	1.00
20	7/ 1/74	31.	1283.	1.00
21	8/ 1/74	31.	1494.	1.00
22	9/ 1/74	30.	1464.	1.00
23	10/ 1/74	31.	750.	1.00
24	11/ 1/74	30.	0.	1.00
25	12/ 1/74	31.	406.	1.00
26	1/ 1/75	31.	1497.	1.00
27	2/ 1/75	28.	1311.	1.00
28	3/ 1/75	31.	1454.	1.00
29	4/ 1/75	30.	1273.	1.00
30	5/ 1/75	31.	1183.	1.00
31	6/ 1/75	30.	1270.	1.00
32	7/ 1/75	31.	1430.	1.00
33	8/ 1/75	31.	1006.	1.00
34	9/ 1/75	30.	1385.	1.00
35	10/ 1/75	31.	1330.	1.00
36	11/ 1/75	30.	1354.	1.00
37	12/ 1/75	31.	1498.	1.00
38	1/ 1/76	31.	1439.	1.00
39	2/ 1/76	29.	1335.	1.00
40	3/ 1/76	31.	155.	1.00
41	4/ 1/76	30.	1351.	1.00
42	5/ 1/76	31.	1286.	1.00

TABLE 4.2.4.6.3.1 (Cont'd)

SUMMARY OF REACTOR OPERATIONS
POINT BEACH UNIT 2 CAPSULE R

TIME PERIOD	START DATE	TIME INTERVAL	AVERAGE POWER LEVEL (MWt)	LOCAL POWER FACTOR
43	6/ 1/76	30.	1400.	1.00
44	7/ 1/76	31.	1380.	1.00
45	8/ 1/76	31.	1374.	1.00
46	9/ 1/76	30.	1397.	1.00
47	10/ 1/76	31.	1500.	1.00
48	11/ 1/76	30.	1478.	1.00
49	12/ 1/76	31.	1482.	1.00
50	1/ 1/77	31.	1482.	1.00
51	2/ 1/77	28.	1485.	1.00
52	3/ 1/77	31.	135.	1.00
53	4/ 1/77	30.	293.	1.00
54	5/ 1/77	31.	1506.	1.00
55	6/ 1/77	30.	1497.	1.00
56	7/ 1/77	31.	1454.	1.00
57	8/ 1/77	31.	1322.	1.00
58	9/ 1/77	30.	1456.	1.00
59	10/ 1/77	31.	1497.	1.00
60	11/ 1/77	30.	1472.	1.00
61	12/ 1/77	31.	1485.	1.00
62	1/ 1/78	31.	1398.	1.00
63	2/ 1/78	28.	1474.	1.00
64	3/ 1/78	31.	972.	1.00
65	4/ 1/78	30.	495.	1.00
66	5/ 1/78	31.	1500.	1.00
67	6/ 1/78	30.	1472.	1.00
68	7/ 1/78	31.	1413.	1.00
69	8/ 1/78	31.	1428.	1.00
70	9/ 1/78	30.	1474.	1.00
71	10/ 1/78	31.	1488.	1.00
72	11/ 1/78	30.	1491.	1.00
73	12/ 1/78	31.	1431.	1.00
74	1/ 1/79	31.	1480.	1.00
75	2/ 1/79	28.	1480.	1.00
76	3/ 1/79	31.	994.	1.00
	4/ 1/79	DISCHARGED*		

---

*EFFECTIVE FULL POWER OPERATION TIME WAS 1.640+008 SECONDS AT A FULL POWER LEVEL OF 1518. MWt.

TABLE 4.2.4.6.3.2

REACTION RATE DATA AND CORRECTION FACTORS FOR POINT BEACH UNIT 2 CAPSULE R

REACTION NAME	IDENT	TOR RATE (DPS/NUCL)	SATURATION FACTOR	GRADIENT FACTOR	IMPURITY FACTOR	AVG REACTION RATE (RPS/NUCL)	% UNCERT (1σ)
$^{54}\mathrm{Fe}(n,p)^{54}\mathrm{Mn}$	V-13	8.53-015	1.151+000	0.860	1.000	7.75-015	10.
	E-23	7.89-015	1.151+000	0.860	1.000		
	E-13	6.92-015	1.151+000	0.860	1.000		
	A-9	6.43-015	1.151+000	1.050	1.000		
	R-14	6.57-015	1.151+000	1.050	1.000		
	W-16	6.37-015	1.151+000	1.050	1.000		
$^{63}\mathrm{Cu}(n,\alpha)^{60}\mathrm{Co}$	TOP	3.09-017	2.122+000	1.050	1.000	6.81-017	10.
	TOP MID	2.78-017	2.122+000	1.050	1.000		
	BOT MID	3.09-017	2.122+000	1.050	1.000		
	BOT	3.27-017	2.122+000	1.050	1.000		
$^{58}\mathrm{Ni}(n,p)^{58}\mathrm{Co}$	MID	9.39-015	1.140+000	1.050	1.000	1.12-014	10.
$^{237}\mathrm{Np}(n,f)^{137}\mathrm{Cs}$	MID	3.42-015	8.973+000	1.000	1.000	4.89-013	10.
$^{238}\mathrm{U}(n,f)^{137}\mathrm{Cs}$	MID	3.99-016	8.973+000	1.000	0.719	4.30-014	10.
$^{59}\mathrm{Co}(n,\gamma)^{60}\mathrm{Co}$	TOP (B)	5.44-012	2.122+000	1.000	1.000	9.83-012	19.
	T-M (B)	3.78-012	2.122+000	1.000	1.000		
	MID (B)	4.00-012	2.122+000	1.000	1.000		
	BOT (B)	5.30-012	2.122+000	1.000	1.000		
$^{59}\mathrm{Co}(n,\gamma)^{60}\mathrm{Co}$	TOP (CD)	2.11-012	2.122+000	0.860	1.000	3.90-012	10.
	T-M (CD)	2.04-012	2.122+000	0.860	1.000		
	MID (CD)	1.97-012	2.122+000	0.860	1.000		
	B-M (CD)	2.35-012	2.122+000	0.860	1.000		
	BOT (CD)	2.22-012	2.122+000	0.860	1.000		

CD = Cadmium-Covered Dosimeter.
B = Bare Dosimeter.

284

TABLE 4.2.4.6.3.3

FERRET-SAND II RESULTS FOR POINT BEACH UNIT 2 CAPSULE R (AVERAGE FOR CAPSULE)

GROUP	ENERGY (MeV)	A PRIORI FLUX* ($n/cm^2 \cdot s$)	ADJUSTED FLUX ($n/cm^2 \cdot s$)	% UNCERTAIN (1 σ)
1	1.492+001	3.699+006	4.065+006	41.
2	1.350+001	7.690+006	8.386+006	37.
3	1.162+001	3.565+007	3.847+007	34.
4	1.000+001	1.082+008	1.154+008	30.
5	8.607+000	2.737+008	2.882+008	26.
6	7.408+000	6.430+008	6.648+008	24.
7	6.065+000	2.259+009	2.306+009	20.
8	4.966+000	3.289+009	3.275+009	21.
9	3.679+000	5.630+009	5.512+009	21.
10	2.865+000	8.300+009	8.089+009	22.
11	2.231+000	1.594+010	1.558+010	22.
12	1.738+000	2.350+010	2.319+010	22.
13	1.353+000	3.303+010	3.381+010	22.
14	1.108+000	3.455+010	3.782+010	24.
15	8.208-001	5.783+010	6.649+010	24.
16	6.393-001	5.199+010	6.123+010	27.
17	4.979-001	5.391+010	6.472+010	30.
18	3.877-001	5.277+010	6.414+010	33.
19	3.020-001	4.897+010	6.010+010	37.
20	1.832-001	8.452+010	1.043+011	40.
21	1.111-001	6.610+010	8.140+010	43.
22	6.738-002	4.892+010	5.980+010	46.
23	4.087-002	4.054+010	4.899+010	48.
24	2.554-002	3.411+010	4.066+010	50.
25	1.989-002	1.635+010	1.921+010	51.
26	1.503-002	1.671+010	1.937+010	52.
27	9.119-003	2.695+010	3.087+010	52.
28	5.531-003	2.694+010	3.057+010	52.
29	3.355-003	2.753+010	3.106+010	51.
30	2.839-003	9.302+009	1.046+010	50.
31	2.404-003	9.345+009	1.050+010	49.
32	2.035-003	9.399+009	1.058+010	46.
33	1.234-003	2.825+010	3.192+010	44.
34	7.485-004	2.759+010	3.128+010	41.
35	4.540-004	2.595+010	2.953+010	38.
36	2.754-004	2.444+010	2.789+010	35.
37	1.670-004	2.412+010	2.755+010	32.
38	1.013-004	2.441+010	2.820+010	15.
39	6.144-005	2.483+010	2.816+010	30.
40	3.727-005	2.525+010	2.845+010	32.

TABLE 4.2.4.6.3.3 (Cont'd)

FERRET-SAND II RESULTS FOR
POINT BEACH UNIT 2 CAPSULE R
(AVERAGE FOR CAPSULE)

GROUP	ENERGY (MeV)	A PRIORI FLUX* ($n/cm^2 \cdot s$)	ADJUSTED FLUX ($n/cm^2 \cdot s$)	% UNCERTAIN (1 σ)
41	2.260-005	2.547+010	2.832+010	33.
42	1.371-005	2.511+010	2.748+010	36.
43	8.315-006	2.409+010	2.588+010	38.
44	5.043-006	2.299+010	2.419+010	40.
45	3.059-006	2.243+010	2.306+010	41.
46	1.855-006	2.243+010	2.250+010	41.
47	1.125-006	2.287+010	2.239+010	41.
48	6.826-007	2.329+010	2.227+010	40.
49	4.140-007	2.357+010	2.206+010	39.
50	2.511-007	3.476+010	3.189+010	37.
51	1.523-007	4.848+010	4.380+010	36.
52	9.237-008	5.359+010	4.793+010	35.
53	1.000-010	1.630+011	1.416+011	29.
FLUX, E > 0.0 MeV		1.482+012	1.662+012	17.
FLUX, E < 0.414 eV		3.140+011	2.873+011	26.
FLUX, E > 0.1 MeV		5.378+011	6.456+011	21.
FLUX, E > 1.0 MeV		1.431+011	1.534+011	10.
dpa/s		2.459-010	2.806-010	14.
FLUENCE+, E > 1.0 MeV		2.346+019	2.516+019	10.
dpa+		4.033-002	4.601-002	14.

---

* ABSOLUTE CALCULATED FLUX (OR NORMALIZED TO Fe54(n,p)Mn54 REACTION RATE).

+ BASED ON 1.640+008 EFFECTIVE FULL POWER SECONDS OF EXPOSURE; UNITS OF n/cm^2 FOR FLUENCE AND TOTAL NUMBER OF DISPLACED ATOMS OF IRON PER TARGET ATOM OF IRON FOR dpa.

TABLE 4.2.4.6.3.4

COMPARISON OF MEASURED AND CALCULATED REACTION RATES USED IN THE ANALYSIS OF POINT BEACH UNIT 2 CAPSULE R

	REACTION RATE (DPS/NUCLEUS)			RATIO MEAS/CALC	
REACTION	MEAS	A PRIORI CALC	ADJ CALC	A PRIORI	ADJ CALC
Np237(n,f)Cs137	4.89-013	4.17-013	4.73-013	1.17	1.03
U238(n,f)Cs137	4.30-014	4.57-014	4.56-014	.94	.94
Co59(n,γ)Co60 (Cd)	3.90-012	3.44-012	3.86-012	1.13	1.01
Co59(n,γ)Co60	9.83-012	1.07-011	1.03-011	.91	.95
Fe54(n,p)Mn54	7.75-015	8.02-015	7.94-015	.97	.98
Cu63(n,α)Co60	6.81-017	6.48-017	6.72-017	1.05	1.01
Ni58(n,p)Co58	1.12-014	1.09-014	1.10-014	1.02	1.02

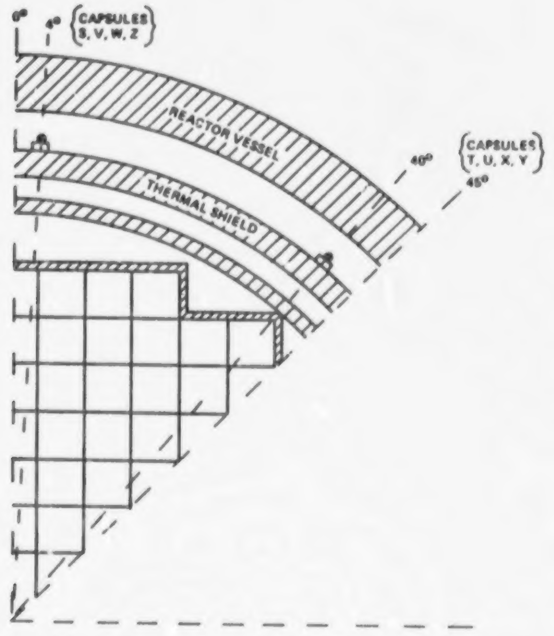
0°
4°
CAPSULES S, V, W, Z
REACTOR VESSEL
THERMAL SHIELD
40°
CAPSULES T, U, X, Y
45°

(a) Reactor Geometry.

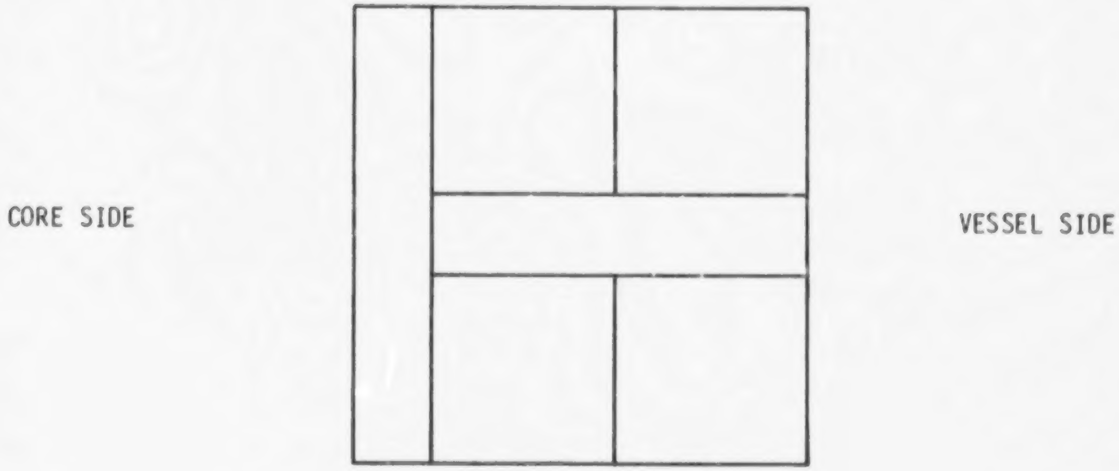
CORE SIDE
VESSEL SIDE

(b) Plan View of Surveillance Capsule

FIGURE 4.2.5.1.1.1. Orientation of the Capsule Relative to the Core and Vessel Wall - D. C. Cook Unit 1 Capsule T.

TABLE 4.2.5.1.1.1

SUMMARY OF REACTOR OPERATIONS
D. C. COOK UNIT 1 CAPSULE T

TIME PERIOD	START DATE	TIME INTERVAL	AVERAGE POWER LEVEL (MWt)	LOCAL POWER FACTOR
1	2/ 2/75	13.	169.	1.00
2	2/15/75	2.	0.	1.00
3	2/17/75	1.	227.	1.00
4	2/18/75	3.	0.	1.00
5	2/21/75	26.	1137.	1.00
6	3/19/75	16.	0.	1.00
7	4/ 4/75	82.	2447.	1.00
8	6/25/75	2.	0.	1.00
9	6/27/75	7.	2207.	1.00
10	7/ 4/75	19.	0.	1.00
11	7/23/75	81.	2486.	1.00
12	10/12/75	3.	0.	1.00
13	10/15/75	17.	2359.	1.00
14	11/ 1/75	14.	0.	1.00
15	11/15/75	48.	2428.	1.00
16	1/ 2/76	3.	0.	1.00
17	1/ 5/76	99.	2587.	1.00
18	4/13/76	27.	0.	1.00
19	5/10/76	53.	2714.	1.00
20	7/ 2/76	4.	0.	1.00
21	7/ 6/76	67.	3071.	1.00
22	9/11/76	8.	0.	1.00
23	9/19/76	63.	3120.	1.00
24	11/21/76	1.	0.	1.00
25	11/22/76	32.	2899.	1.00
	12/24/76	DISCHARGED*		

---

*EFFECTIVE FULL POWER OPERATION TIME WAS 3.991+007 SECONDS AT A FULL POWER LEVEL OF 3250. MWt.

TABLE 4.2.5.1.1.2

REACTION RATE DATA AND CORRECTION FACTORS FOR D. C. COOK UNIT 1 CAPSULE T

REACTION NAME	IDENT	TOR RATE (DPS/NUCL)	SATURATION FACTOR	GRADIENT FACTOR	IMPURITY FACTOR	AVG REACTION RATE (RPS/NUCL)	% UNCERT (1σ)
^{54}Fe(n,p)^{54}Mn	TOP	2.67-015	1.753+000	0.970	1.000	4.65-015	10.
	TOP MID	2.33-015	1.753+000	1.180	1.000		
	MID	2.33-015	1.753+000	1.180	1.000		
	BOT MID	2.33-015	1.753+000	1.180	1.000		
	BOT	2.49-015	1.753+000	0.970	1.000		
^{63}Cu(n,α)^{60}Co	TOP	7.85-018	6.687+000	0.970	1.000	5.43-017	10.
	MID	8.05-018	6.687+000	0.970	1.000		
	BOT	9.22-018	6.687+000	0.970	1.000		
^{58}Ni(n,p)^{58}Co	TOP	5.50-015	1.186+000	0.950	1.000	6.23-015	10.
	MID	5.41-015	1.186+000	0.950	1.000		
	BOT	5.67-015	1.186+000	0.950	1.000		
^{59}Co(n,γ)^{60}Co	TOP (CD)	1.79-013	6.687+000	1.180	1.000	1.34-012	10.
	BOT (CD)	1.60-013	6.687+000	1.180	1.000		
^{59}Co(n,γ)^{60}Co	TOP (B)	4.77-013	6.687+000	0.940	1.000	3.05-012	10.
	BOT (B)	4.92-013	6.687+000	0.940	1.000		
^{238}U(n,f)^{137}Cs	MID	4.74-016	3.508+001	1.000	0.926	2.57-013	10.
^{237}Np(n,f)^{137}Cs	MID	1.78-015	3.508+001	1.000	1.000	9.98-013	10.

CD = Cadmium-Covered Dosimeter.
B = Bare Dosimeter.

TABLE 4.2.5.1.1.3

FERRET-SAND II RESULTS FOR
D. C. COOK UNIT 1 CAPSULE T
(AVERAGE FOR CAPSULE)

GROUP	ENERGY (MeV)	A PRIORI FLUX* ($n/cm^2 \cdot s$)	ADJUSTED FLUX ($n/cm^2 \cdot s$)	% UNCERTAIN ($1\ \sigma$)
1	1.492+001	2.560+006	3.222+006	41.
2	1.350+001	5.322+006	6.727+006	37.
3	1.162+001	2.468+007	3.106+007	34.
4	1.000+001	7.489+007	9.355+007	29.
5	8.607+000	1.895+008	2.317+008	25.
6	7.408+000	4.463+008	5.185+008	23.
7	6.065+000	1.586+009	1.748+009	20.
8	4.966+000	2.221+009	2.180+009	21.
9	3.679+000	3.531+009	3.165+009	21.
10	2.865+000	5.042+009	4.276+009	23.
11	2.231+000	9.639+009	7.843+009	25.
12	1.738+000	1.395+010	1.112+010	30.
13	1.353+000	1.852+010	1.454+010	34.
14	1.108+000	1.846+010	1.437+010	38.
15	8.208-001	2.916+010	2.275+010	41.
16	6.393-001	2.529+010	1.997+010	44.
17	4.979-001	2.594+010	2.088+010	47.
18	3.877-001	2.558+010	2.108+010	50.
19	3.020-001	2.329+010	1.970+010	52.
20	1.832-001	3.862+010	3.353+010	53.
21	1.111-001	2.859+010	2.543+010	54.
22	6.738-002	2.017+010	1.833+010	55.
23	4.087-002	1.679+010	1.554+010	55.
24	2.554-002	1.407+010	1.322+010	55.
25	1.989-002	6.674+009	6.348+009	55.
26	1.503-002	6.734+009	6.470+009	55.
27	9.119-003	1.039+010	1.007+010	54.
28	5.531-003	1.021+010	9.959+009	54.
29	3.355-003	1.100+010	1.080+010	52.
30	2.839-003	3.801+009	3.757+009	51.
31	2.404-003	3.836+009	3.814+009	49.
32	2.035-003	3.860+009	3.860+009	47.
33	1.234-003	1.153+010	1.159+010	44.
34	7.485-004	1.109+010	1.120+010	41.
35	4.540-004	1.020+010	1.035+010	38.
36	2.754-004	9.351+009	9.514+009	35.
37	1.670-004	9.023+009	9.193+009	33.
38	1.013-004	9.241+009	9.518+009	15.
39	6.144-005	9.978+009	1.013+010	30.
40	3.727-005	1.068+010	1.079+010	31.

291

TABLE 4.2.5.1.1.3 (Cont'd)

FERRET-SAND II RESULTS FOR
D. C. COOK UNIT 1 CAPSULE T
(AVERAGE FOR CAPSULE)

GROUP	ENERGY (MeV)	A PRIORI FLUX* ($n/cm^2 \cdot s$)	ADJUSTED FLUX ($n/cm^2 \cdot s$)	% UNCERTAIN ($1\ \sigma$)
41	2.260-005	1.079+010	1.081+010	33.
42	1.371-005	1.027+010	1.020+010	35.
43	8.315-006	9.319+009	9.138+009	37.
44	5.043-006	9.126+009	8.826+009	39.
45	3.059-006	9.128+009	8.695+009	40.
46	1.855-006	9.131+009	8.559+009	40.
47	1.125-006	9.134+009	8.426+009	39.
48	6.826-007	9.138+009	8.301+009	38.
49	4.140-007	9.139+009	8.183+009	36.
50	2.511-007	9.024+009	7.976+009	34.
51	1.523-007	1.222+010	1.069+010	32.
52	9.237-008	2.016+010	1.749+010	30.
53	1.000-010	4.376+010	3.736+010	22.
FLUX, E > 0.0 MeV		6.736+011	5.626+011	22.
FLUX, E < 0.414 eV		1.010+011	8.170+010	19.
FLUX, E > 0.1 MeV		2.938+011	2.273+011	35.
FLUX, E > 1.0 MeV		8.956+010	6.790+010	22.
dpa/s		1.430-010	1.115-010	25.
FLUENCE+, E > 1.0 MeV		3.575+018	2.710+018	22.
dpa+		5.708-003	4.449-003	25.

---

* ABSOLUTE CALCULATED FLUX (OR NORMALIZED TO Fe54(n,p)Mn54 REACTION RATE).

+ BASED ON 3.991+007 EFFECTIVE FULL POWER SECONDS OF EXPOSURE; UNITS OF n/cm^2 FOR FLUENCE AND TOTAL NUMBER OF DISPLACED ATOMS OF IRON PER TARGET ATOM OF IRON FOR dpa.

TABLE 4.2.5.1.1.4

COMPARISON OF MEASURED AND CALCULATED
REACTION RATES USED IN THE ANALYSIS OF
D. C. COOK UNIT 1 CAPSULE T

REACTION	REACTION RATE (DPS/NUCLEUS)			RATIO MEAS/CALC	
	MEAS	A PRIORI CALC	ADJ CALC	A PRIORI	ADJ CALC
Fe54(n,p)Mn54	4.65-015	5.14-015	4.79-015	.91	.97
Ni58(n,p)Co58	6.23-015	6.94-015	6.36-015	.90	.98
Cu63(n,α)Co60	5.43-017	4.48-017	5.17-017	1.21	1.05
Co59(n,γ)Co60	3.05-012	3.35-012	3.08-012	.91	.99
Co59(n,γ)Co60 (Cd)	1.34-012	1.32-012	1.33-012	1.02	1.01
*Np237(n,f)FP Cd	9.98-013	2.28-013	1.85-013	4.38	5.38
*U238(n,f)FP Cd	2.57-013	2.82-014	2.37-014	9.12	10.85

---

* REACTION NOT USED TO ADJUST SPECTRUM

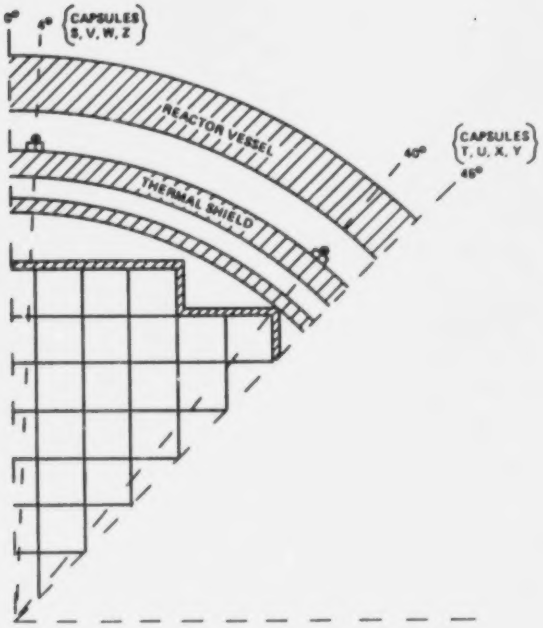
0°
4°
CAPSULES S, V, W, Z
REACTOR VESSEL
THERMAL SHIELD
40°
CAPSULES T, U, X, Y
45°

(a) Reactor Geometry.

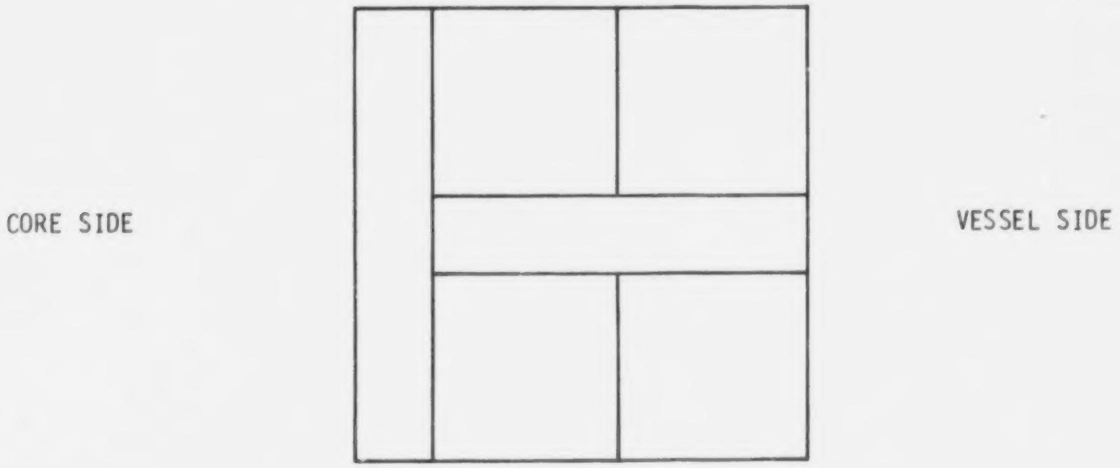
CORE SIDE
VESSEL SIDE

(b) Plan View of Surveillance Capsule

FIGURE 4.2.5.2.1.1. Orientation of the Capsule Relative to the Core and Vessel Wall - Indian Point Unit 2 Capsule T.

TABLE 4.2.5.2.1.1

SUMMARY OF REACTOR OPERATIONS
INDIAN POINT UNIT 2 CAPSULE T

TIME PERIOD	START DATE	TIME INTERVAL	AVERAGE POWER LEVEL (MWt)	LOCAL POWER FACTOR
1	8/ 1/73	24.	1165.	1.00
2	8/25/73	1.	0.	1.00
3	8/26/73	13.	1250.	1.00
4	9/ 8/73	13.	0.	1.00
5	9/21/73	8.	872.	1.00
6	9/29/73	2.	0.	1.00
7	10/ 1/73	12.	853.	1.00
8	10/13/73	105.	0.	1.00
9	1/26/74	4.	665.	1.00
10	1/30/74	51.	0.	1.00
11	3/22/74	28.	1501.	1.00
12	4/19/74	10.	0.	1.00
13	4/29/74	5.	1369.	1.00
14	5/ 4/74	1.	0.	1.00
15	5/ 5/74	6.	1308.	1.00
16	5/11/74	2.	0.	1.00
17	5/13/74	1.	201.	1.00
18	5/14/74	7.	0.	1.00
19	5/21/74	25.	1835.	1.00
20	6/15/74	2.	0.	1.00
21	6/17/74	36.	2122.	1.00
22	7/23/74	1.	0.	1.00
23	7/24/74	3.	2095.	1.00
24	7/27/74	10.	0.	1.00
25	8/ 6/74	32.	1835.	1.00
26	9/ 7/74	3.	0.	1.00
27	9/10/74	21.	2051.	1.00
28	10/ 1/74	11.	0.	1.00
29	10/12/74	29.	2390.	1.00
30	11/10/74	1.	0.	1.00
31	11/11/74	26.	2294.	1.00
32	12/ 7/74	1.	0.	1.00
33	12/ 8/74	25.	2346.	1.00
34	1/ 2/75	3.	0.	1.00
35	1/ 5/75	1.	1504.	1.00
36	1/ 6/75	1.	0.	1.00
37	1/ 7/75	25.	2432.	1.00
38	2/ 1/75	2.	0.	1.00
39	2/ 3/75	26.	2597.	1.00
40	3/ 1/75	34.	0.	1.00

TABLE 4.2.5.2.1.1 (Cont'd)

SUMMARY OF REACTOR OPERATIONS
INDIAN POINT UNIT 2 CAPSULE T

TIME PERIOD	START DATE	TIME INTERVAL	AVERAGE POWER LEVEL (MWt)	LOCAL POWER FACTOR
41	4/ 4/75	29.	2111.	1.00
42	5/ 3/75	1.	0.	1.00
43	5/ 4/75	86.	2514.	1.00
44	7/29/75	13.	0.	1.00
45	8/11/75	33.	1962.	1.00
46	9/13/75	1.	0.	1.00
47	9/14/75	33.	2197.	1.00
48	10/17/75	13.	0.	1.00
49	10/30/75	16.	2062.	1.00
50	11/15/75	1.	0.	1.00
51	11/16/75	50.	2327.	1.00
52	1/ 5/76	1.	0.	1.00
53	1/ 6/76	24.	2401.	1.00
54	1/30/76	6.	0.	1.00
55	2/ 5/76	55.	2517.	1.00
	3/31/76	DISCHARGED*		

---

*EFFECTIVE FULL POWER OPERATION TIME WAS 4.473+007 SECONDS AT A FULL POWER LEVEL OF 2760. MWt.

TABLE 4.2.5.2.1.2

REACTION RATE DATA AND CORRECTION FACTORS FOR INDIAN POINT UNIT 2 CAPSULE T

REACTION NAME	IDENT	TOR RATE (DPS/NUCL)	SATURATION FACTOR	GRADIENT FACTOR	IMPURITY FACTOR	AVG REACTION RATE (RPS/NUCL)	% UNCERT (1σ)
^{54}Fe(n,p)^{54}Mn	R-1	2.51-015	1.734+000	0.970	1.000	4.23-015	10.
	R-4	2.52-015	1.734+000	0.970	1.000		
	R-3	2.64-015	1.734+000	0.970	1.000		
	R-6	2.52-015	1.734+000	0.970	1.000		
	R-8	2.38-015	1.734+000	0.970	1.000		
^{58}Ni(n,p)^{58}Co	MID	5.30-015	1.268+000	0.950	1.000	6.39-015	10.
^{63}Cu(n,α)^{60}Co	TOP	8.06-018	6.101+000	0.950	1.000	4.34-017	11.
	BOT	6.92-018	6.101+000	0.950	1.000		
^{59}Co(n,γ)^{60}Co	TOP (CD)	2.31-013	6.101+000	1.180	1.000	1.62-012	10.
	MID (CD)	2.19-013	6.101+000	1.180	1.000		
	BOT (CD)	2.26-013	6.101+000	1.180	1.000		
^{59}Co(n,γ)^{60}Co	TOP (B)	4.89-013	6.101+000	0.940	1.000	2.96-012	10.
	MID (B)	5.54-013	6.101+000	0.940	1.000		
	BOT (B)	5.03-013	6.101+000	0.940	1.000		

CD = Cadmium-Covered Dosimeter.

B = Bare Dosimeter.

TABLE 4.2.5.2.1.3

FERRET-SAND II RESULTS FOR INDIAN POINT UNIT 2 CAPSULE T (AVERAGE FOR CAPSULE)

GROUP	ENERGY (MeV)	A PRIORI FLUX* (n/cm^2•s)	ADJUSTED FLUX (n/cm^2•s)	% UNCERTAIN (1 σ)
1	1.492+001	2.174+006	2.651+006	42.
2	1.350+001	4.519+006	5.476+006	38.
3	1.162+001	2.095+007	2.514+007	34.
4	1.000+001	6.358+007	7.553+007	30.
5	8.607+000	1.609+008	1.884+008	26.
6	7.408+000	3.789+008	4.338+008	24.
7	6.065+000	1.346+009	1.505+009	20.
8	4.966+000	1.886+009	2.016+009	21.
9	3.679+000	2.998+009	3.107+009	21.
10	2.865+000	4.281+009	4.364+009	22.
11	2.231+000	8.183+009	8.345+009	25.
12	1.738+000	1.184+010	1.212+010	29.
13	1.353+000	1.573+010	1.620+010	33.
14	1.108+000	1.567+010	1.620+010	37.
15	8.208-001	2.476+010	2.582+010	41.
16	6.393-001	2.147+010	2.266+010	45.
17	4.979-001	2.202+010	2.357+010	48.
18	3.877-001	2.171+010	2.357+010	51.
19	3.020-001	1.977+010	2.175+010	53.
20	1.832-001	3.279+010	3.653+010	55.
21	1.111-001	2.428+010	2.734+010	56.
22	6.738-002	1.713+010	1.946+010	57.
23	4.087-002	1.425+010	1.632+010	57.
24	2.554-002	1.195+010	1.377+010	58.
25	1.989-002	5.666+009	6.569+009	58.
26	1.503-002	5.717+009	6.663+009	57.
27	9.119-003	8.823+009	1.034+010	57.
28	5.531-003	8.665+009	1.021+010	57.
29	3.355-003	9.337+009	1.107+010	56.
30	2.839-003	3.227+009	3.851+009	55.
31	2.404-003	3.257+009	3.914+009	54.
32	2.035-003	3.277+009	3.968+009	53.
33	1.234-003	9.788+009	1.194+010	51.
34	7.485-004	9.415+009	1.157+010	50.
35	4.540-004	8.662+009	1.071+010	48.
36	2.754-004	7.939+009	9.868+009	47.
37	1.670-004	7.661+009	9.556+009	45.
38	1.013-004	7.846+009	9.963+009	39.
39	6.144-005	8.472+009	1.058+010	44.
40	3.727-005	9.066+009	1.129+010	44.

TABLE 4.2.5.2.1.3 (Cont'd)

FERRET-SAND II RESULTS FOR
INDIAN POINT UNIT 2 CAPSULE T
(AVERAGE FOR CAPSULE)

GROUP	ENERGY (MeV)	A PRIORI FLUX* (n/cm^2•s)	ADJUSTED FLUX (n/cm^2•s)	% UNCERTAIN (1 σ)
41	2.260-005	9.158+009	1.134+010	45.
42	1.371-005	8.723+009	1.072+010	46.
43	8.315-006	7.912+009	9.642+009	47.
44	5.043-006	7.748+009	9.349+009	47.
45	3.059-006	7.750+009	9.251+009	48.
46	1.855-006	7.752+009	9.151+009	49.
47	1.125-006	7.755+009	9.055+009	49.
48	6.826-007	7.759+009	8.965+009	49.
49	4.140-007	7.760+009	8.878+009	49.
50	2.511-007	7.661+009	8.687+009	49.
51	1.523-007	1.037+010	1.168+010	50.
52	9.237-008	1.711+010	1.915+010	50.
53	1.000-010	3.716+010	4.120+010	49.
FLUX, E > 0.0 MeV		6.736+011	6.045+011	29.
FLUX, E < 0.414 eV		1.010+011	8.959+010	44.
FLUX, E > 0.1 MeV		2.938+011	2.499+011	37.
FLUX, E > 1.0 MeV		8.956+010	7.342+010	22.
dpa/s		1.430-010	1.200-010	27.
FLUENCE+, E > 1.0 MeV		4.006+018	3.284+018	22.
dpa+		6.397-003	5.370-003	27.

---

* ABSOLUTE CALCULATED FLUX (OR NORMALIZED TO Fe54(n,p)Mn54 REACTION RATE).

+ BASED ON 4.473+007 EFFECTIVE FULL POWER SECONDS OF EXPOSURE; UNITS OF n/cm^2 FOR FLUENCE AND TOTAL NUMBER OF DISPLACED ATOMS OF IRON PER TARGET ATOM OF IRON FOR dpa.

TABLE 4.2.5.2.1.4

COMPARISON OF MEASURED AND CALCULATED REACTION RATES USED IN THE ANALYSIS OF INDIAN POINT UNIT 2 CAPSULE T

	REACTION RATE (DPS/NUCLEUS)			RATIO MEAS/CALC	
REACTION	MEAS	A PRIORI CALC	ADJ CALC	A PRIORI	ADJ CALC
Fe54(n,p)Mn54	4.22-015	4.27-015	4.48-015	.99	.94
Ni58(n,p)Co58	6.39-015	5.77-015	6.16-015	1.11	1.04
Cu53(n,α)Co60	4.34-017	3.73-017	4.26-017	1.16	1.02
Co59(n,γ)Co60 (Cd)	1.62-012	1.12-012	1.40-012	1.45	1.16
Co59(n,γ)Co60	2.96-012	2.84-012	3.32-012	1.04	.89

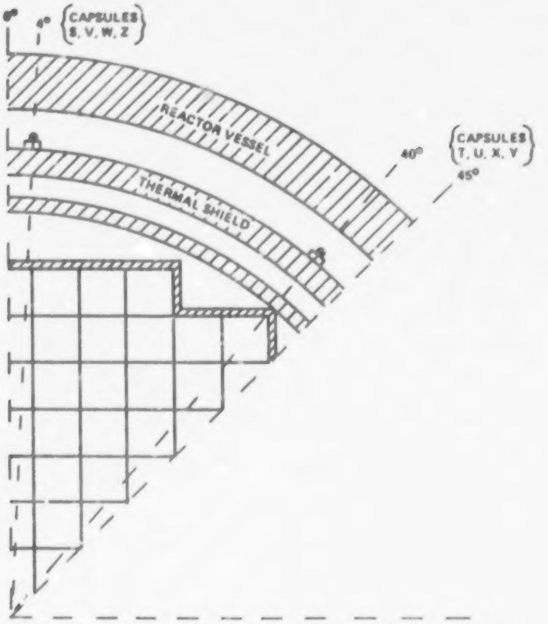
0°
4°
CAPSULES S, V, W, Z
REACTOR VESSEL
THERMAL SHIELD
40°
CAPSULES T, U, X, Y
45°

(a) Reactor Geometry.

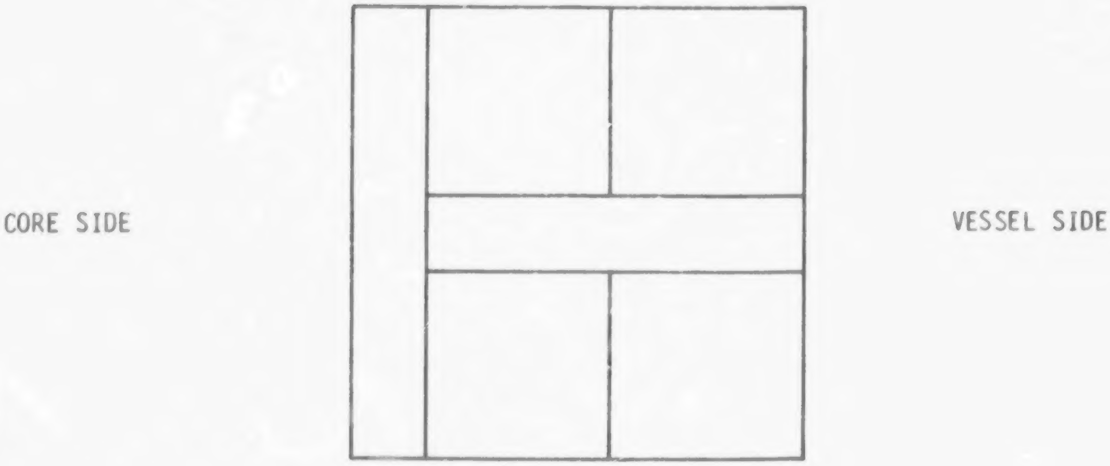
CORE SIDE
VESSEL SIDE

(b) Plan View of Surveillance Capsule

FIGURE 4.2.5.3.1.1. Orientation of the Capsule Relative to the Core and Vessel Wall - Indian Point Unit 3 Capsule T.

301

TABLE 4.2.5.3.1.1

SUMMARY OF REACTOR OPERATIONS
INDIAN POINT UNIT 3 CAPSULE T

TIME PERIOD	START DATE	TIME INTERVAL	AVERAGE POWER LEVEL (MWt)	LOCAL POWER FACTOR
1	4/ 8/76	146.	31.	1.00
2	9/ 1/76	30.	841.	1.00
3	10/ 1/76	31.	2168.	1.00
4	11/ 1/76	30.	2583.	1.00
5	12/ 1/76	31.	2268.	1.00
6	1/ 1/77	31.	1557.	1.00
7	2/ 1/77	28.	2687.	1.00
8	3/ 1/77	31.	2640.	1.00
9	4/ 1/77	30.	2054.	1.00
10	5/ 1/77	31.	2713.	1.00
11	6/ 1/77	30.	2688.	1.00
12	7/ 1/77	31.	2609.	1.00
13	8/ 1/77	31.	2684.	1.00
14	9/ 1/77	30.	2635.	1.00
15	10/ 1/77	31.	500.	1.00
16	11/ 1/77	30.	0.	1.00
17	12/ 1/77	31.	1120.	1.00
18	1/ 1/78	31.	2623.	1.00
19	2/ 1/78	28.	1729.	1.00
20	3/ 1/78	31.	2628.	1.00
21	4/ 1/78	30.	2245.	1.00
22	5/ 1/78	31.	2534.	1.00
23	6/ 1/78	7.	2619.	1.00
	6/ 8/78	DISCHARGED*		

---

*EFFECTIVE FULL POWER OPERATION TIME WAS 4.211+007 SECONDS AT A FULL POWER LEVEL OF 2760. MWt.

TABLE 4.2.5.3.1.2

REACTION RATE DATA AND CORRECTION FACTORS FOR INDIAN POINT UNIT 3 CAPSULE T

REACTION NAME	REACTION IDENT	TOR RATE (DPS/NUCL)	SATURATION FACTOR	GRADIENT FACTOR	IMPURITY FACTOR	AVG REACTION RATE (RPS/NUCL)	% UNCERT (1σ)
^{54}Fe(n,p)^{54}Mn	W-40	3.05-015	1.744+000	0.970	1.000	5.10-015	10.
	A-32	2.61-015	1.744+000	1.170	1.000		
	AT-58	2.43-015	1.744+000	1.170	1.000		
	W-37	2.79-015	1.744+000	0.970	1.000		
	B-9	2.99-015	1.744+000	0.970	1.000		
	AT-54	2.63-015	1.744+000	1.170	1.000		
^{58}Ni(n,p)^{58}Co	MID	5.16-015	1.261+000	0.950	1.000	6.18-015	10.
^{63}Cu(n,α)^{60}Co	MID	7.86-018	6.387+000	0.970	1.000	4.73-017	10.
	BOT	7.41-018	6.387+000	0.970	1.000		
^{59}Co(n,γ)^{60}Co	BOT (CD)	2.08-013	6.387+000	1.180	1.000	1.58-012	10.
	MID (CD)	2.09-013	6.387+000	1.180	1.000		
	TOP (CD)	2.12-013	6.387+000	1.180	1.000		
^{59}Co(n,γ)^{60}Co	BOT (B)	5.29-013	6.387+000	0.940	1.000	3.06-012	10.
	MID (B)	4.72-013	6.387+000	0.940	1.000		
	TOP (B)	5.26-013	6.387+000	0.940	1.000		

CD = Cadmium-Covered Dosimeter.
B = Bare Dosimeter.

303

303

TABLE 4.2.5.3.1.3

FERRET-SAND II RESULTS FOR
INDIAN POINT UNIT 3 CAPSULE T
(AVERAGE FOR CAPSULE)

GROUP	ENERGY (MeV)	A PRIORI FLUX* (n/cm^2•s)	ADJUSTED FLUX (n/cm^2•s)	% UNCERTAIN (1 σ)
1	1.492+001	2.741+006	2.783+006	41.
2	1.350+001	5.699+006	5.807+006	38.
3	1.162+001	2.642+007	2.693+007	34.
4	1.000+001	8.018+007	8.157+007	30.
5	8.607+000	2.029+008	2.049+008	26.
6	7.408+000	4.779+008	4.744+008	24.
7	6.065+000	1.698+009	1.657+009	20.
8	4.966+000	2.378+009	2.230+009	21.
9	3.679+000	3.781+009	3.417+009	21.
10	2.865+000	5.398+009	4.771+009	22.
11	2.231+000	1.032+010	8.884+009	25.
12	1.738+000	1.493+010	1.269+010	29.
13	1.353+000	1.983+010	1.668+010	33.
14	1.108+000	1.976+010	1.656+010	37.
15	8.208-001	3.122+010	2.614+010	41.
16	6.393-001	2.708+010	2.275+010	44.
17	4.979-001	2.777+010	2.348+010	47.
18	3.877-001	2.738+010	2.336+010	50.
19	3.020-001	2.493+010	2.150+010	51.
20	1.832-001	4.135+010	3.607+010	53.
21	1.111-001	3.061+010	2.701+010	54.
22	6.738-002	2.160+010	1.928+010	55.
23	4.087-002	1.797+010	1.622+010	55.
24	2.554-002	1.507+010	1.375+010	55.
25	1.989-002	7.145+009	6.590+009	55.
26	1.503-002	7.209+009	6.726+009	55.
27	9.119-003	1.113+010	1.051+010	54.
28	5.531-003	1.093+010	1.046+010	54.
29	3.355-003	1.177+010	1.145+010	52.
30	2.839-003	4.070+009	4.025+009	51.
31	2.404-003	4.107+009	4.136+009	49.
32	2.035-003	4.133+009	4.242+009	47.
33	1.234-003	1.234+010	1.291+010	44.
34	7.485-004	1.187+010	1.264+010	41.
35	4.540-004	1.092+010	1.181+010	38.
36	2.754-004	1.001+010	1.095+010	35.
37	1.670-004	9.660+009	1.064+010	32.
38	1.013-004	9.894+009	1.137+010	15.
39	6.144-005	1.068+010	1.172+010	30.
40	3.727-005	1.143+010	1.237+010	31.

304

TABLE 4.2.5.3.1.3 (Cont'd)

FERRET-SAND II RESULTS FOR
INDIAN POINT UNIT 3 CAPSULE T
(AVERAGE FOR CAPSULE)

GROUP	ENERGY (MeV)	A PRIORI FLUX* (n/cm^2•s)	ADJUSTED FLUX (n/cm^2•s)	% UNCERTAIN (1 σ)
41	2.260-005	1.155+010	1.226+010	33.
42	1.371-005	1.100+010	1.137+010	35.
43	8.315-006	9.977+009	9.996+009	38.
44	5.043-006	9.771+009	9.444+009	39.
45	3.059-006	9.773+009	9.085+009	40.
46	1.855-006	9.776+009	8.728+009	40.
47	1.125-006	9.779+009	8.388+009	40.
48	6.826-007	9.784+009	8.077+009	39.
49	4.140-007	9.785+009	7.796+009	37.
50	2.511-007	9.661+009	7.456+009	35.
51	1.523-007	1.308+010	9.844+009	33.
52	9.237-008	2.158+010	1.592+010	31.
53	1.000-010	4.685+010	3.332+010	24.
FLUX, E > 0.0 MeV		6.736+011	6.015+011	23.
FLUX, E < 0.414 eV		1.010+011	7.433+010	21.
FLUX, E > 0.1 MeV		2.938+011	2.520+011	35.
FLUX, E > 1.0 MeV		8.956+010	7.662+010	22.
dpa/s		1.430-010	1.234-010	25.
FLUENCE+, E > 1.0 MeV		3.772+018	3.226+018	22.
dpa+		6.023-003	5.196-003	25.

---

* ABSOLUTE CALCULATED FLUX (OR NORMALIZED TO Fe54(n,p)Mn54 REACTION RATE).

+ BASED ON 4.211+007 EFFECTIVE FULL POWER SECONDS OF EXPOSURE; UNITS OF n/cm^2 FOR FLUENCE AND TOTAL NUMBER OF DISPLACED ATOMS OF IRON PER TARGET ATOM OF IRON FOR dpa.

TABLE 4.2.5.3.1.4

COMPARISON OF MEASURED AND CALCULATED REACTION RATES USED IN THE ANALYSIS OF INDIAN POINT UNIT 3 CAPSULE T

	REACTION RATE (DPS/NUCLEUS)			RATIO MEAS/CALC	
REACTION	MEAS	A PRIORI CALC	ADJ CALC	A PRIORI	ADJ CALC
Fe54(n,p)Mn54	5.10-015	5.39-015	4.94-015	.95	1.03
Ni58(n,p)Co58	6.18-015	7.27-015	6.49-015	.85	.95
Cu63(n,α)Co60	4.73-017	4.71-017	4.66-017	1.00	1.02
Co59(n,γ)Co60 (Cd)	1.58-012	1.41-012	1.54-012	1.12	1.02
Co59(n,γ)Co60	3.06-012	3.58-012	3.14-012	.85	.97

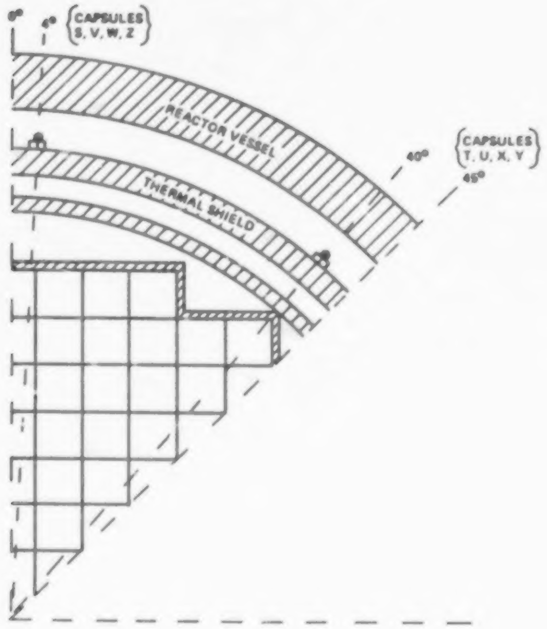
0°
4°
CAPSULES S, V, W, Z
REACTOR VESSEL
THERMAL SHIELD
40°
CAPSULES T, U, X, Y
45°

(a) Reactor Geometry.

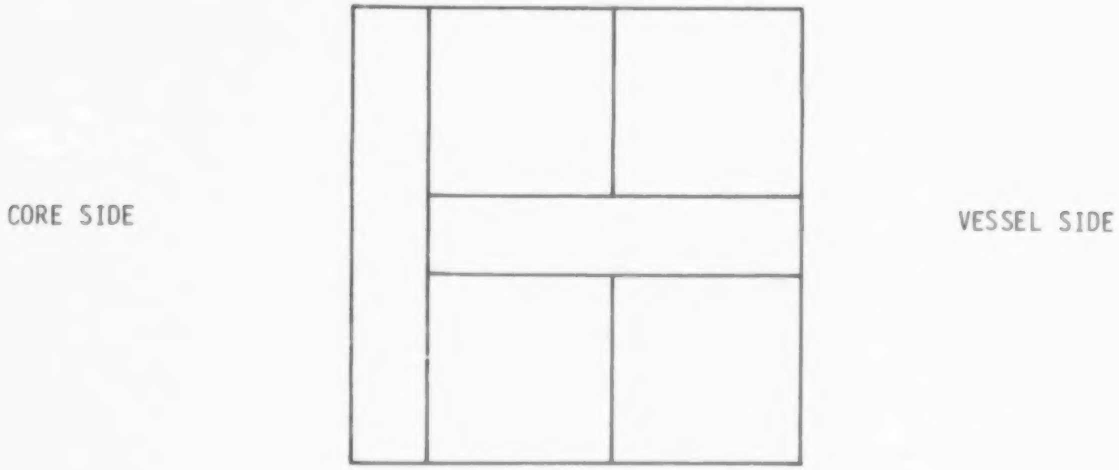
CORE SIDE
VESSEL SIDE

(b) Plan View of Surveillance Capsule

FIGURE 4.2.5.4.1.1. Orientation of the Capsule Relative to the Core and Vessel Wall - Zion Unit 1 Capsule T.

TABLE 4.2.5.4.1.1

SUMMARY OF REACTOR OPERATIONS
ZION UNIT 1 CAPSULE T

TIME PERIOD	START DATE	TIME INTERVAL	AVERAGE POWER LEVEL (MWt)	LOCAL POWER FACTOR
1	10/ 1/73	31.	1470.	1.00
2	11/ 1/73	30.	1770.	1.00
3	12/ 1/73	31.	1730.	1.00
4	1/ 1/74	90.	0.	1.00
5	4/ 1/74	30.	678.	1.00
6	5/ 1/74	31.	1420.	1.00
7	6/ 1/74	30.	1840.	1.00
8	7/ 1/74	31.	1520.	1.00
9	8/ 1/74	31.	1910.	1.00
10	9/ 1/74	30.	1450.	1.00
11	10/ 1/74	31.	2320.	1.00
12	11/ 1/74	30.	2070.	1.00
13	12/ 1/74	31.	2640.	1.00
14	1/ 1/75	31.	2250.	1.00
15	2/ 1/75	28.	1750.	1.00
16	3/ 1/75	31.	275.	1.00
17	4/ 1/75	30.	2440.	1.00
18	5/ 1/75	31.	1950.	1.00
19	6/ 1/75	30.	0.	1.00
20	7/ 1/75	31.	1830.	1.00
21	8/ 1/75	31.	2580.	1.00
22	9/ 1/75	30.	1690.	1.00
23	10/ 1/75	31.	2580.	1.00
24	11/ 1/75	30.	2590.	1.00
25	12/ 1/75	31.	2430.	1.00
26	1/ 1/76	31.	2520.	1.00
27	2/ 1/76	29.	2720.	1.00
28	3/ 1/76	31.	359.	1.00
	4/ 1/76	DISCHARGED*		

---

*EFFECTIVE FULL POWER OPERATION TIME WAS 3.789+007 SECONDS AT A FULL POWER LEVEL OF 3391. MWt.

308

TABLE 4.2.5.4.1.2

REACTION RATE DATA AND CORRECTION FACTORS FOR ZION UNIT 1 CAPSULE T

REACTION NAME	REACTION IDENT	TOR RATE (DPS/NUCL)	SATURATION FACTOR	GRADIENT FACTOR	IMPURITY FACTOR	AVG REACTION RATE (RPS/NUCL)	% UNCERT (1σ)
^{54}Fe(n,p)^{54}Mn	TOP	2.70-015	2.165+000	0.950	1.000	5.49-015	10.
	TOP MID	2.64-015	2.165+000	0.950	1.000		
	MID	2.62-015	2.165+000	0.950	1.000		
	BOT MID	2.70-015	2.165+000	0.950	1.000		
	BOT	2.70-015	2.165+000	0.950	1.000		
^{63}Cu(n,α)^{60}Co	TOP MID	7.97-018	7.280+000	1.050	1.000	4.84-017	37.
	BOT MID	4.69-018	7.280+000	1.050	1.000		
^{58}Ni(n,p)^{58}Co	TOP MID	4.45-015	1.821+000	0.860	1.000	6.84-015	10.
	MID	4.25-015	1.821+000	0.860	1.000		
	BOT MID	4.39-015	1.821+000	0.860	1.000		
^{237}Np(n,f)^{137}Cs	MID	3.53-016	3.717+001	1.000	1.000	2.09-013	10.
^{238}U(n,f)^{137}Cs	MID	4.74-017	3.717+001	1.000	0.901	2.65-014	10.
^{59}Co(n,γ)^{60}Co	TOP (B)	6.19-013	7.280+000	0.950	1.000	3.99-012	11.
	BOT (B)	5.33-013	7.280+000	0.950	1.000		
^{59}Co(n,γ)^{60}Co	TOP (CD)	2.52-013	7.280+000	1.170	1.000	1.99-012	12.
	BOT (CD)	2.14-013	7.280+000	1.170	1.000		

CD = Cadmium-Covered Dosimeter.
B = Bare Dosimeter.

TABLE 4.2.5.4.1.3

FERRET-SAND II RESULTS FOR
ZION UNIT 1 CAPSULE T
(AVERAGE FOR CAPSULE)

GROUP	ENERGY (MeV)	A PRIORI FLUX* ($n/cm^2 \cdot s$)	ADJUSTED FLUX ($n/cm^2 \cdot s$)	% UNCERTAIN (1 σ)
1	1.492+001	2.823+006	2.903+006	46.
2	1.350+001	5.870+006	6.053+006	43.
3	1.162+001	2.721+007	2.807+007	40.
4	1.000+001	8.258+007	8.490+007	36.
5	8.607+000	2.089+008	2.132+008	32.
6	7.408+000	4.922+008	4.966+008	28.
7	6.065+000	1.748+009	1.744+009	24.
8	4.966+000	2.449+009	2.402+009	22.
9	3.679+000	3.894+009	3.723+009	21.
10	2.865+000	5.560+009	5.164+009	22.
11	2.231+000	1.063+010	9.492+009	22.
12	1.738+000	1.538+010	1.327+010	21.
13	1.353+000	2.043+010	1.726+010	22.
14	1.108+000	2.035+010	1.712+010	25.
15	8.208-001	3.215+010	2.680+010	25.
16	6.393-001	2.789+010	2.327+010	28.
17	4.979-001	2.860+010	2.399+010	31.
18	3.877-001	2.820+010	2.391+010	35.
19	3.020-001	2.568+010	2.207+010	38.
20	1.832-001	4.259+010	3.723+010	42.
21	1.111-001	3.153+010	2.809+010	44.
22	6.738-002	2.225+010	2.022+010	47.
23	4.087-002	1.851+010	1.718+010	49.
24	2.554-002	1.552+010	1.471+010	51.
25	1.989-002	7.360+009	7.126+009	52.
26	1.503-002	7.426+009	7.352+009	52.
27	9.119-003	1.146+010	1.161+010	53.
28	5.531-003	1.125+010	1.170+010	52.
29	3.355-003	1.213+010	1.295+010	52.
30	2.839-003	4.192+009	4.607+009	50.
31	2.404-003	4.230+009	4.794+009	49.
32	2.035-003	4.257+009	4.978+009	46.
33	1.234-003	1.271+010	1.534+010	44.
34	7.485-004	1.223+010	1.519+010	41.
35	4.540-004	1.125+010	1.433+010	38.
36	2.754-004	1.031+010	1.340+010	35.
37	1.670-004	9.950+009	1.311+010	32.
38	1.013-004	1.019+010	1.442+010	14.
39	6.144-005	1.100+010	1.451+010	30.
40	3.727-005	1.178+010	1.529+010	32.

310

TABLE 4.2.5.4.1.3 (Cont'd)

FERRET-SAND II RESULTS FOR
ZION UNIT 1 CAPSULE T
(AVERAGE FOR CAPSULE)

GROUP	ENERGY (MeV)	A PRIORI FLUX* ($n/cm^2 \cdot s$)	ADJUSTED FLUX ($n/cm^2 \cdot s$)	% UNCERTAIN ($1\ \sigma$)
41	2.260-005	1.190+010	1.508+010	33.
42	1.371-005	1.133+010	1.392+010	36.
43	8.315-006	1.028+010	1.214+010	38.
44	5.043-006	1.006+010	1.138+010	40.
45	3.059-006	1.007+010	1.085+010	41.
46	1.855-006	1.007+010	1.033+010	41.
47	1.125-006	1.007+010	9.844+009	41.
48	6.826-007	1.008+010	9.404+009	40.
49	4.140-007	1.008+010	9.007+009	38.
50	2.511-007	1.018+010	8.753+009	36.
51	1.523-007	1.016+010	8.474+009	35.
52	9.237-008	1.065+010	8.696+009	33.
53	1.000-010	6.298+010	4.861+010	23.
FLUX, E > 0.0 MeV		6.938+011	6.657+011	16.
FLUX, E < 0.414 eV		1.041+011	8.355+010	21.
FLUX, E > 0.1 MeV		3.026+011	2.606+011	20.
FLUX, E > 1.0 MeV		9.225+010	8.017+010	10.
dpa/s		1.474-010	1.288-010	12.
FLUENCE+, E > 1.0 MeV		3.495+018	3.038+018	10.
dpa+		5.585-003	4.882-003	12.

---

* ABSOLUTE CALCULATED FLUX (OR NORMALIZED TO Fe54(n,p)Mn54 REACTION RATE).

+ BASED ON 3.789+007 EFFECTIVE FULL POWER SECONDS OF EXPOSURE; UNITS OF n/cm^2 FOR FLUENCE AND TOTAL NUMBER OF DISPLACED ATOMS OF IRON PER TARGET ATOM OF IRON FOR dpa.

TABLE 4.2.5.4.1.4

COMPARISON OF MEASURED AND CALCULATED REACTION RATES USED IN THE ANALYSIS OF ZION UNIT 1 CAPSULE T

REACTION	REACTION RATE (DPS/NUCLEUS) MEAS	A PRIORI CALC	ADJ CALC	RATIO MEAS/CALC A PRIORI	ADJ CALC
Fe54(n,p)Mn54	5.49-015	5.55-015	5.30-015	.99	1.04
Ni58(n,p)Co58	6.84-015	7.49-015	7.00-015	.91	.98
Cu63(n,α)Co60	4.84-017	4.85-017	4.86-017	1.00	1.00
Np237(n,f)Cs137	2.09-013	2.44-013	2.11-013	.86	.99
U238(n,f)Cs137	2.65-014	3.01-014	2.68-014	.88	.99
Co59(n,γ)Co60 (Cd)	1.99-012	1.45-012	1.93-012	1.37	1.03
Co59(n,γ)Co60	3.99-012	4.18-012	4.11-012	.96	.97

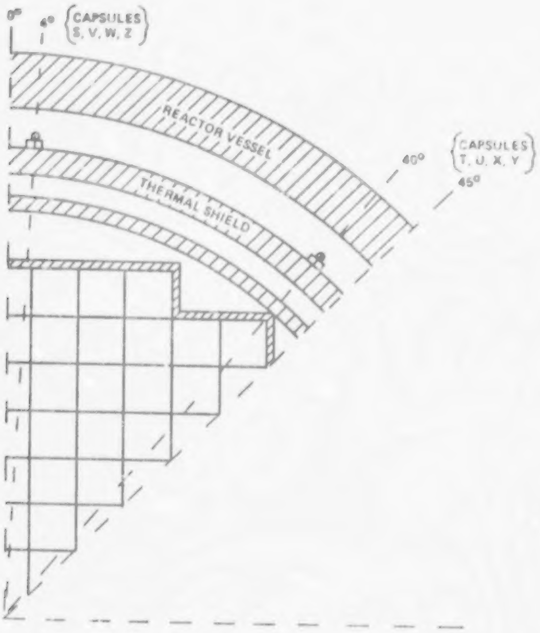
0°
4°
CAPSULES
S, V, W, Z
REACTOR VESSEL
THERMAL SHIELD
40°
CAPSULES
T, U, X, Y
45°

(a) Reactor Geometry.

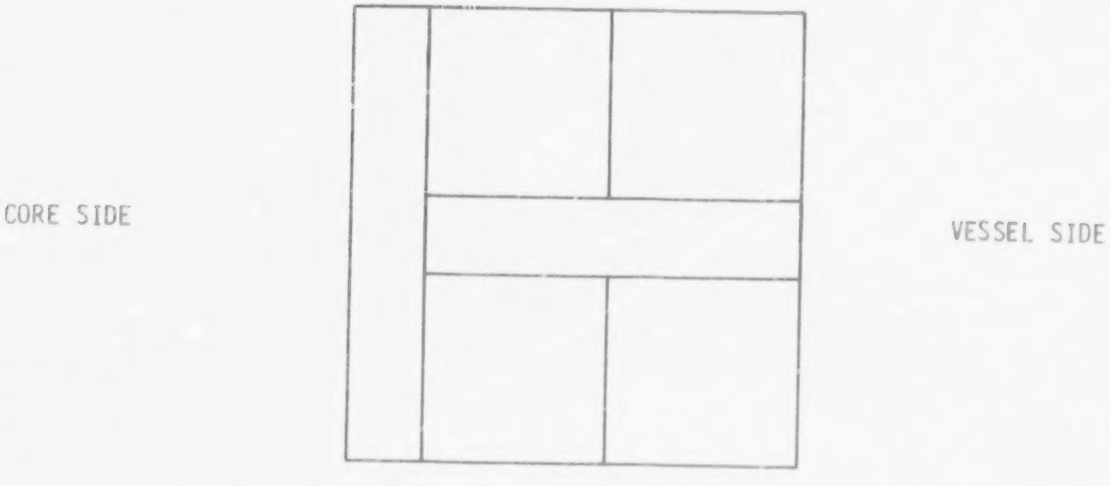
CORE SIDE
VESSEL SIDE

(b) Plan View of Surveillance Capsule

FIGURE 4.2.5.4.2.1. Orientation of the Capsule Relative to the Core and Vessel Wall - Zion Unit 1 Capsule U.

B/B

TABLE 4.2.5.4.2.1

SUMMARY OF REACTOR OPERATIONS
ZION UNIT 1 CAPSULE U

TIME PERIOD	START DATE	TIME INTERVAL	AVERAGE POWER LEVEL (MWt)	LOCAL POWER FACTOR
1	10/ 1/73	31.	1470.	1.00
2	11/ 1/73	30.	1770.	1.00
3	12/ 1/73	31.	1730.	1.00
4	1/ 1/74	90.	0.	1.00
5	4/ 1/74	30.	678.	1.00
6	5/ 1/74	31.	1420.	1.00
7	6/ 1/74	30.	1840.	1.00
8	7/ 1/74	31.	1520.	1.00
9	8/ 1/74	31.	1910.	1.00
10	9/ 1/74	30.	1450.	1.00
11	10/ 1/74	31.	2320.	1.00
12	11/ 1/74	30.	2070.	1.00
13	12/ 1/74	31.	2640.	1.00
14	1/ 1/75	31.	2250.	1.00
15	2/ 1/75	28.	1750.	1.00
16	3/ 1/75	31.	275.	1.00
17	4/ 1/75	30.	2440.	1.00
18	5/ 1/75	31.	1950.	1.00
19	6/ 1/75	30.	0.	1.00
20	7/ 1/75	31.	1830.	1.00
21	8/ 1/75	31.	2580.	1.00
22	9/ 1/75	30.	1690.	1.00
23	10/ 1/75	31.	2580.	1.00
24	11/ 1/75	30.	2590.	1.00
25	12/ 1/75	31.	2430.	1.00
26	1/ 1/76	31.	2520.	1.00
27	2/ 1/76	29.	2720.	1.00
28	3/ 1/76	31.	359.	1.00
29	4/ 1/76	61.	0.	1.00
30	6/ 1/76	30.	617.	1.00
31	7/ 1/76	31.	3070.	1.00
32	8/ 1/76	31.	2990.	1.00
33	9/ 1/76	30.	2470.	1.00
34	10/ 1/76	31.	912.	1.00
35	11/ 1/76	30.	2950.	1.00
36	12/ 1/76	31.	2460.	1.00
37	1/ 1/77	31.	3300.	1.00
38	2/ 1/77	28.	3150.	1.00
39	3/ 1/77	31.	2540.	1.00
40	4/ 1/77	30.	2370.	1.00

TABLE 4.2.5.4.2.1 (Cont'd)

SUMMARY OF REACTOR OPERATIONS
ZION UNIT 1 CAPSULE U

TIME PERIOD	START DATE	TIME INTERVAL	AVERAGE POWER LEVEL (MWt)	LOCAL POWER FACTOR
41	5/ 1/77	31.	3200.	1.00
42	6/ 1/77	30.	2060.	1.00
43	7/ 1/77	31.	2240.	1.00
44	8/ 1/77	31.	1780.	1.00
45	9/ 1/77	30.	373.	1.00
46	10/ 1/77	61.	0.	1.00
47	12/ 1/77	31.	2510.	1.00
48	1/ 1/78	31.	3340.	1.00
49	2/ 1/78	28.	3320.	1.00
50	3/ 1/78	31.	3240.	1.00
51	4/ 1/78	30.	3100.	1.00
52	5/ 1/78	31.	2450.	1.00
53	6/ 1/78	30.	3130.	1.00
54	7/ 1/78	31.	3140.	1.00
55	8/ 1/78	31.	2700.	1.00
56	9/ 1/78	30.	732.	1.00
57	10/ 1/78	31.	0.	1.00
58	11/ 1/78	30.	2260.	1.00
59	12/ 1/78	31.	3010.	1.00
60	1/ 1/79	31.	3230.	1.00
61	2/ 1/79	28.	3070.	1.00
62	3/ 1/79	31.	2590.	1.00
63	4/ 1/79	30.	2850.	1.00
64	5/ 1/79	31.	3200.	1.00
65	6/ 1/79	30.	1580.	1.00
66	7/ 1/79	31.	2770.	1.00
67	8/ 1/79	31.	2850.	1.00
68	9/ 1/79	30.	2610.	1.00
69	10/ 1/79	31.	1780.	1.00
	11/ 1/79	DISCHARGED*		

---

*EFFECTIVE FULL POWER OPERATION TIME WAS 1.123+008 SECONDS AT A FULL POWER LEVEL OF 3391. MWt.

315

TABLE 4.2.5.4.2.2

REACTION RATE DATA AND CORRECTION FACTORS FOR
ZION UNIT 1 CAPSULE U

REACTION		TOR RATE	SATURATION	GRADIENT	IMPURITY	AVG REACTION	% UNCERT
NAME	IDENT	(DPS/NUCL)	FACTOR	FACTOR	FACTOR	RATE (RPS/NUCL)	(1σ)
$^{54}\mathrm{Fe}(n,p)^{54}\mathrm{Mn}$	TOP	4.19-015	1.444+000	0.950	1.000	5.59-015	10.
	MID	4.02-015	1.444+000	0.950	1.000		
	BOT MID	4.10-015	1.444+000	0.950	1.000		
	BOT	3.99-015	1.444+000	0.950	1.000		
$^{63}\mathrm{Cu}(n,\alpha)^{60}\mathrm{Co}$	TOP MID	1.76-017	2.969+000	1.050	1.000	5.40-017	10.
	MID	1.70-017	2.969+000	1.050	1.000		
	BOT MID	1.74-017	2.969+000	1.050	1.000		
$^{58}\mathrm{Ni}(n,p)^{58}\mathrm{Co}$	TOP MID	5.41-015	1.408+000	0.860	1.000	6.56-015	10.
	MID	5.23-015	1.408+000	0.860	1.000		
	BOT MID	5.62-015	1.408+000	0.860	1.000		
$^{237}\mathrm{Np}(n,f)^{137}\mathrm{Cs}$	MID	1.18-015	1.301+001	1.000	1.000	2.44-013	10.
$^{238}\mathrm{U}(n,f)^{137}\mathrm{Cs}$	MID	1.62-016	1.301+001	1.000	0.893	3.14-014	10.
$^{59}\mathrm{Co}(n,\gamma)^{60}\mathrm{Co}$	TOP (B)	1.37-012	2.969+000	0.950	1.000	3.75-012	10.
	BOT (B)	1.29-012	2.969+000	0.950	1.000		
$^{59}\mathrm{Co}(n,\gamma)^{60}\mathrm{Co}$	TOP (CD)	6.97-013	2.969+000	1.170	1.000	2.34-012	10.
	BOT (CD)	6.53-013	2.969+000	1.170	1.000		

CD = Cadmium-Covered Dosimeter.
B = Bare Dosimeter.

TABLE 4.2.5.4.2.3

FERRET-SAND II RESULTS FOR ZION UNIT 1 CAPSULE U (AVERAGE FOR CAPSULE)

GROUP	ENERGY (MeV)	A PRIORI FLUX* ($n/cm^2\cdot s$)	ADJUSTED FLUX ($n/cm^2\cdot s$)	% UNCERTAIN ($1\ \sigma$)
1	1.492+001	2.796+006	3.224+006	41.
2	1.350+001	5.813+006	6.638+006	37.
3	1.162+001	2.695+007	3.040+007	34.
4	1.000+001	8.178+007	9.130+007	29.
5	8.607+000	2.069+008	2.276+008	26.
6	7.408+000	4.874+008	5.216+008	24.
7	6.065+000	1.732+009	1.798+009	20.
8	4.966+000	2.426+009	2.372+009	21.
9	3.679+000	3.856+009	3.628+009	21.
10	2.865+000	5.506+009	5.193+009	22.
11	2.231+000	1.053+010	1.004+010	22.
12	1.738+000	1.523+010	1.512+010	22.
13	1.353+000	2.023+010	2.034+010	22.
14	1.108+000	2.016+010	1.999+010	25.
15	8.208-001	3.184+010	3.197+010	25.
16	6.393-001	2.762+010	2.814+010	28.
17	4.979-001	2.833+010	2.929+010	31.
18	3.877-001	2.793+010	2.928+010	35.
19	3.020-001	2.543+010	2.697+010	38.
20	1.832-001	4.218+010	4.516+010	41.
21	1.111-001	3.123+010	3.371+010	44.
22	6.738-002	2.203+010	2.396+010	47.
23	4.087-002	1.833+010	2.009+010	49.
24	2.554-002	1.537+010	1.699+010	50.
25	1.989-002	7.288+009	8.149+009	51.
26	1.503-002	7.354+009	8.339+009	52.
27	9.119-003	1.135+010	1.311+010	52.
28	5.531-003	1.114+010	1.316+010	52.
29	3.355-003	1.201+010	1.457+010	51.
30	2.839-003	4.151+009	5.195+009	50.
31	2.404-003	4.189+009	5.427+009	48.
32	2.035-003	4.216+009	5.664+009	46.
33	1.234-003	1.259+010	1.755+010	44.
34	7.485-004	1.211+010	1.747+010	41.
35	4.540-004	1.114+010	1.657+010	38.
36	2.754-004	1.021+010	1.554+010	35.
37	1.670-004	9.854+009	1.521+010	32.
38	1.013-004	1.009+010	1.697+010	14.
39	6.144-005	1.090+010	1.671+010	30.
40	3.727-005	1.166+010	1.747+010	32.

317

TABLE 4.2.5.4.2.3 (Cont'd)

FERRET-SAND II RESULTS FOR ZION UNIT 1 CAPSULE U (AVERAGE FOR CAPSULE)

GROUP	ENERGY (MeV)	A PRIORI FLUX* (n/cm^2•s)	ADJUSTED FLUX (n/cm^2•s)	% UNCERTAIN (1 σ)
41	2.260-005	1.178+010	1.703+010	34.
42	1.371-005	1.122+010	1.548+010	36.
43	8.315-006	1.018+010	1.327+010	38.
44	5.043-006	9.966+009	1.219+010	40.
45	3.059-006	9.969+009	1.138+010	41.
46	1.855-006	9.971+009	1.061+010	41.
47	1.125-006	9.975+009	9.897+009	41.
48	6.826-007	9.980+009	9.271+009	40.
49	4.140-007	9.981+009	8.725+009	38.
50	2.511-007	9.855+009	8.163+009	36.
51	1.523-007	1.334+010	1.059+010	35.
52	9.237-008	2.201+010	1.689+010	33.
53	1.000-010	4.779+010	3.462+010	28.
FLUX, E > 0.0 MeV		6.870+011	7.501+011	16.
FLUX, E < 0.414 eV		1.030+011	7.900+010	24.
FLUX, E > 0.1 MeV		2.997+011	3.089+011	20.
FLUX, E > 1.0 MeV		9.136+010	9.030+010	10.
dpa/s		1.459-010	1.474-010	13.
FLUENCE+, E > 1.0 MeV		1.026+019	1.014+019	10.
dpa+		1.638-002	1.656-002	13.

---

* ABSOLUTE CALCULATED FLUX (OR NORMALIZED TO Fe54(n,p)Mn54 REACTION RATE).

+ BASED ON 1.123+008 EFFECTIVE FULL POWER SECONDS OF EXPOSURE; UNITS OF n/cm^2 FOR FLUENCE AND TOTAL NUMBER OF DISPLACED ATOMS OF IRON PER TARGET ATOM OF IRON FOR dpa.

TABLE 4.2.5.4.2.4

COMPARISON OF MEASURED AND CALCULATED REACTION RATES USED IN THE ANALYSIS OF ZION UNIT 1 CAPSULE U

REACTION	REACTION RATE (DPS/NUCLEUS)			RATIO MEAS/CALC	
	MEAS	A PRIORI CALC	ADJ CALC	A PRIORI	ADJ CALC
Fe54(n,p)Mn54	5.59-015	5.61-015	5.50-015	1.00	1.02
Cu63(n,α)Co60	5.40-017	4.90-017	5.23-017	1.10	1.03
Ni58(n,p)Co58	6.56-015	7.58-015	7.18-015	.87	.91
Np237(n,f)Cs137	2.44-013	2.42-013	2.45-013	1.01	1.00
U238(n,f)Cs137	3.14-014	2.98-014	2.95-014	1.05	1.06
Co59(n,γ)Co60	3.75-012	3.65-012	3.94-012	1.03	.95
Co59(n,γ)Co60 (Cd)	2.34-012	1.44-012	2.23-012	1.63	1.05

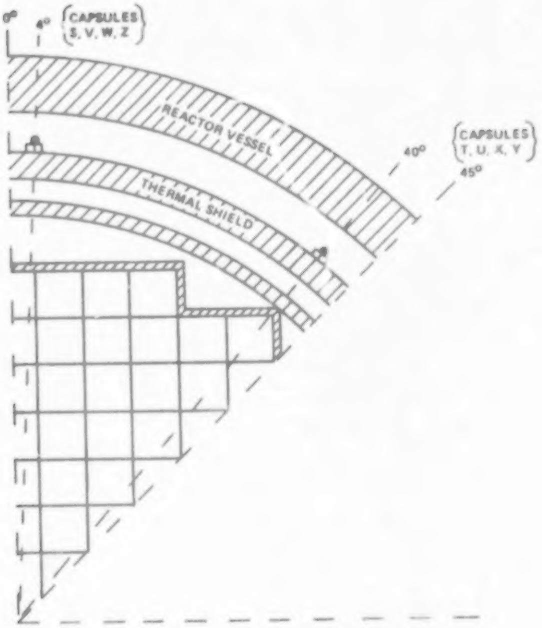
0°
4°
CAPSULES S, V, W, Z
REACTOR VESSEL
THERMAL SHIELD
40°
CAPSULES T, U, X, Y
45°

(a) Reactor Geometry.

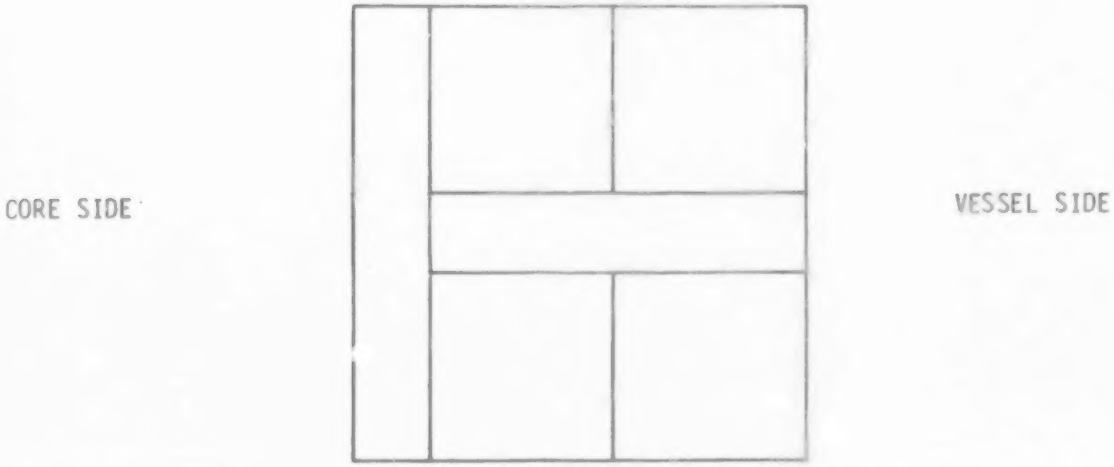
CORE SIDE
VESSEL SIDE

(b) Plan View of Surveillance Capsule

FIGURE 4.2.5.5.1.1. Orientation of the Capsule Relative to the Core and Vessel Wall - Zion Unit 2 Capsule U.

TABLE 4.2.5.5.1.1

SUMMARY OF REACTOR OPERATIONS
ZION UNIT 2 CAPSULE U

TIME PERIOD	START DATE	TIME INTERVAL	AVERAGE POWER LEVEL (MWt)	LOCAL POWER FACTOR
1	1/ 1/76	366.	3391.	1.00
2	1/ 1/77	98.	3391.	1.00
	4/ 9/77	DISCHARGED*		

---

*EFFECTIVE FULL POWER OPERATION TIME WAS 4.009+007 SECONDS AT A FULL POWER LEVEL OF 3391. MWt.

TABLE 4.2.5.5.1.2

REACTION RATE DATA AND CORRECTION FACTORS FOR ZION UNIT 2 CAPSULE U

REACTION NAME	 IDENT	TOR RATE (DPS/NUCL)	SATURATION FACTOR	GRADIENT FACTOR	IMPURITY FACTOR	AVG REACTION RATE (RPS/NUCL)	% UNCERT (1σ)
$^{54}Fe(n,p)^{54}Mn$	TOP			0.950	1.000	5.13-015	10.
	TOP MID			0.950	1.000		
	MID			0.950	1.000		
	BOT MID			0.950	1.000		
	BOT			0.950	1.000		
$^{58}Ni(n,p)^{58}Co$	TOP MID			0.860	1.000	6.88-015	10.
	MID			0.860	1.000		
	BOT MID			0.860	1.000		
$^{63}Cu(n,\alpha)^{60}Co$	TOP MID			1.050	1.000	4.80-017	10.
	MID			1.050	1.000		
	BOT MID			1.050	1.000		
$^{237}Np(n,f)^{137}Cs$	MID			1.000	1.000	1.79-013	10.
$^{238}U(n,f)^{137}Cs$	MID			1.000	0.901	2.27-014	10.
$^{59}Co(n,\gamma)^{60}Co$	TOP (B)			0.950	1.000	3.60-012	10.
	BOT (B)			0.950	1.000		
$^{59}Co(n,\gamma)^{60}Co$	TOP (CD)			1.170	1.000	1.06-012	10.
	BOT (CD)			1.170	1.000		

CD = Cadmium-Covered Dosimeter.
B = Bare Dosimeter.

TABLE 4.2.5.5.1.3

FERRET-SAND II RESULTS FOR
ZION UNIT 2 CAPSULE U
(AVERAGE FOR CAPSULE)

GROUP	ENERGY (MeV)	A PRIORI FLUX* ($n/cm^2 \cdot s$)	ADJUSTED FLUX ($n/cm^2 \cdot s$)	% UNCERTAIN ($1\ \sigma$)
1	1.492+001	2.741+006	2.750+006	41.
2	1.350+001	5.699+006	5.823+006	37.
3	1.162+001	2.642+007	2.735+007	34.
4	1.000+001	8.018+007	8.350+007	30.
5	8.607+000	2.029+008	2.107+008	26.
6	7.408+000	4.779+008	4.906+008	24.
7	6.065+000	1.698+009	1.728+009	20.
8	4.966+000	2.378+009	2.353+009	21.
9	3.679+000	3.781+009	3.577+009	21.
10	2.865+000	5.398+009	4.791+009	22.
11	2.231+000	1.032+010	8.481+009	22.
12	1.738+000	1.493+010	1.137+010	21.
13	1.353+000	1.983+010	1.453+010	22.
14	1.108+000	1.976+010	1.450+010	25.
15	8.208-001	3.122+010	2.247+010	25.
16	6.393-001	2.708+010	1.932+010	28.
17	4.979-001	2.777+010	1.980+010	31.
18	3.877-001	2.738+010	1.968+010	35.
19	3.020-001	2.493+010	1.817+010	38.
20	1.832-001	4.135+010	3.069+010	42.
21	1.111-001	3.061+010	2.318+010	44.
22	6.738-002	2.160+010	1.669+010	47.
23	4.087-002	1.797+010	1.414+010	49.
24	2.554-002	1.507+010	1.204+010	50.
25	1.989-002	7.145+009	5.778+009	52.
26	1.503-002	7.209+009	5.875+009	52.
27	9.119-003	1.113+010	9.102+009	52.
28	5.531-003	1.093+010	8.938+009	52.
29	3.355-003	1.177+010	9.598+009	51.
30	2.839-003	4.070+009	3.296+009	50.
31	2.404-003	4.107+009	3.297+009	49.
32	2.035-003	4.133+009	3.284+009	47.
33	1.234-003	1.234+010	9.699+009	44.
34	7.485-004	1.187+010	9.227+009	41.
35	4.540-004	1.092+010	8.403+009	38.
36	2.754-004	1.001+010	7.640+009	35.
37	1.670-004	9.660+009	7.330+009	33.
38	1.013-004	9.894+009	7.296+009	16.
39	6.144-005	1.068+010	8.095+009	30.
40	3.727-005	1.143+010	8.711+009	31.

TABLE 4.2.5.5.1.3 (Cont'd)

FERRET-SAND II RESULTS FOR
ZION UNIT 2 CAPSULE U
(AVERAGE FOR CAPSULE)

GROUP	ENERGY (MeV)	A PRIORI FLUX* ($n/cm^2 \cdot s$)	ADJUSTED FLUX ($n/cm^2 \cdot s$)	% UNCERTAIN (1σ)
41	2.260-005	1.155+010	8.881+009	33.
42	1.371-005	1.100+010	8.566+009	35.
43	8.315-006	9.977+009	7.893+009	37.
44	5.043-006	9.771+009	7.872+009	38.
45	3.059-006	9.773+009	8.031+009	39.
46	1.855-006	9.776+009	8.202+009	40.
47	1.125-006	9.779+009	8.378+009	39.
48	6.826-007	9.784+009	8.553+009	38.
49	4.140-007	9.785+009	8.722+009	36.
50	2.511-007	9.888+009	8.976+009	34.
51	1.523-007	9.860+009	9.078+009	32.
52	9.237-008	1.034+010	9.620+009	30.
53	1.000-010	6.115+010	5.847+010	16.
FLUX, E > 0.0 MeV		6.736+011	5.352+011	15.
FLUX, E < 0.414 eV		1.010+011	9.487+010	15.
FLUX, E > 0.1 MeV		2.938+011	2.190+011	20.
FLUX, E > 1.0 MeV		8.956+010	6.983+010	9.
dpa/s		1.431-010	1.113-010	12.
FLUENCE+, E > 1.0 MeV		3.590+018	2.799+018	9.
dpa+		5.735-003	4.459-003	12.

---

* ABSOLUTE CALCULATED FLUX (OR NORMALIZED TO Fe54(n,p)Mn54 REACTION RATE).

+ BASED ON 4.008+007 EFFECTIVE FULL POWER SECONDS OF EXPOSURE; UNITS OF n/cm^2 FOR FLUENCE AND TOTAL NUMBER OF DISPLACED ATOMS OF IRON PER TARGET ATOM OF IRON FOR dpa.

TABLE 4.2.5.5.1.4

COMPARISON OF MEASURED AND CALCULATED REACTION RATES USED IN THE ANALYSIS OF ZION UNIT 2 CAPSULE U

	REACTION RATE (DPS/NUCLEUS)			RATIO MEAS/CALC	
REACTION	MEAS	A PRIORI CALC	ADJ CALC	A PRIORI	ADJ CALC
Fe54(n,p)Mn54	5.13-015	5.39-015	5.02-015	.95	1.02
Ni58(n,p)Co58	6.88-015	7.27-015	6.72-015	.95	1.02
Cu63(n,α)Co60	4.80-017	4.71-017	4.79-017	1.02	1.00
Np237(n,f)Cs137	1.79-013	2.37-013	1.79-013	.76	1.00
U238(n,f)Cs137	2.27-014	2.92-014	2.38-014	.78	.95
Co59(n,γ)Co60 (Cd)	1.06-012	1.41-012	1.07-012	.75	.99
Co59(n,γ)Co60	3.60-012	4.06-012	3.57-012	.89	1.01

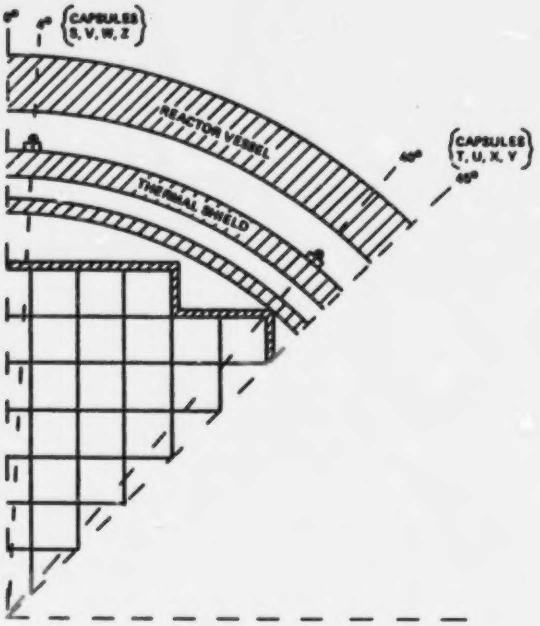
0°
4°
CAPSULES
S, V, W, Z
REACTOR VESSEL
THERMAL SHIELD
40°
CAPSULES
T, U, X, Y
45°

(a) Reactor Geometry.

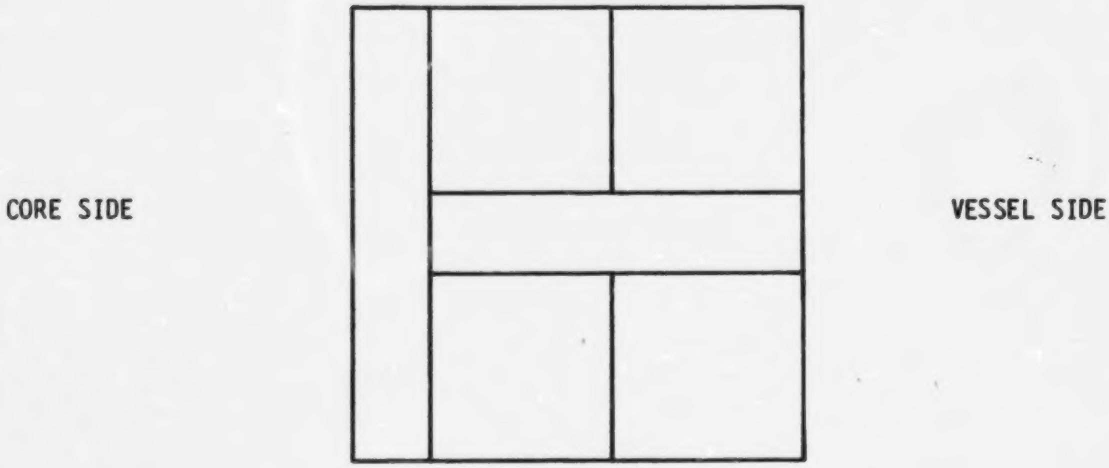
CORE SIDE
VESSEL SIDE

(b) Plan View of Surveillance Capsule

FIGURE 4.2.5.6.1.1. Orientation of the Capsule Relative to the Core and Vessel Wall - Salem Unit 1 Capsule T.

TABLE 4.2.5.6.1.1

SUMMARY OF REACTOR OPERATIONS
SALEM UNIT 1 CAPSULE T

TIME PERIOD	START DATE	TIME INTERVAL	AVERAGE POWER LEVEL (MWt)	LOCAL POWER FACTOR
1	3/ 1/77	31.	1803.	1.00
2	4/ 1/77	30.	1836.	1.00
3	5/ 1/77	31.	2016.	1.00
4	6/ 1/77	30.	1325.	1.00
5	7/ 1/77	31.	2017.	1.00
6	8/ 1/77	31.	2727.	1.00
7	9/ 1/77	30.	1651.	1.00
8	10/ 1/77	31.	0.	1.00
9	11/ 1/77	30.	104.	1.00
10	12/ 1/77	31.	2487.	1.00
11	1/ 1/78	31.	1811.	1.00
12	2/ 1/78	28.	3358.	1.00
13	3/ 1/78	31.	1543.	1.00
14	4/ 1/78	30.	0.	1.00
15	5/ 1/78	31.	0.	1.00
16	6/ 1/78	30.	1003.	1.00
17	7/ 1/78	31.	2651.	1.00
18	8/ 1/78	31.	2713.	1.00
19	9/ 1/78	30.	2814.	1.00
20	10/ 1/78	31.	721.	1.00
21	11/ 1/78	30.	1414.	1.00
22	12/ 1/78	31.	2208.	1.00
23	1/ 1/79	31.	3103.	1.00
24	2/ 1/79	28.	3016.	1.00
25	3/ 1/79	31.	2894.	1.00
26	4/ 1/79	3.	2856.	1.00
	4/ 4/79	DISCHARGED*		

---

*EFFECTIVE FULL POWER OPERATION TIME WAS 3.426+007 SECONDS AT A FULL POWER LEVEL OF 3483. MWt.

TABLE 4.2.5.6.1.2

REACTION RATE DATA AND CORRECTION FACTORS FOR SALEM UNIT 1 CAPSULE T

REACTION NAME	IDENT	TOR RATE (DPS/NUCL)	SATURATION FACTOR	GRADIENT FACTOR	IMPURITY FACTOR	AVG REACTION RATE (RPS/NUCL)	% UNCERT (1σ)
$^{54}\mathrm{Fe}(n,p)^{54}\mathrm{Mn}$	P8	2.43-015	2.174+000	0.980	1.000	5.21-015	10.
	P5	2.22-015	2.174+000	0.980	1.000		
	S1	2.54-015	2.174+000	0.980	1.000		
	E8	1.86-015	2.174+000	1.200	1.000		
	E5	2.05-015	2.174+000	1.200	1.000		
	R1	2.21-015	2.174+000	1.200	1.000		
$^{63}\mathrm{Cu}(n,\alpha)^{60}\mathrm{Co}$	TOP	6.90-018	7.916+000	0.960	1.000	5.21-017	10.
	BOT	6.80-018	7.916+000	0.960	1.000		
$^{58}\mathrm{Ni}(n,p)^{58}\mathrm{Co}$	MID	5.13-015	1.398+000	0.980	1.000	7.03-015	10.
$^{59}\mathrm{Co}(n,\gamma)^{60}\mathrm{Co}$	TOP (B)	4.30-013	7.916+000	0.980	1.000	3.56-012	10.
	MID (B)	4.63-013	7.916+000	0.980	1.000		
	BOT (B)	4.83-013	7.916+000	0.980	1.000		
$^{59}\mathrm{Co}(n,\gamma)^{60}\mathrm{Co}$	TOP (CD)	1.82-013	7.916+000	1.060	1.000	1.57-012	10.
	MID (CD)	1.85-013	7.916+000	1.060	1.000		
	BOT (CD)	1.94-013	7.916+000	1.060	1.000		

CD = Cadmium-Covered Dosimeter.
B = Bare Dosimeter.

TABLE 4.2.5.6.1.3

FERRET-SAND II RESULTS FOR SALEM UNIT 1 CAPSULE T (AVERAGE FOR CAPSULE)

GROUP	ENERGY (MeV)	A PRIORI FLUX* (n/cm^2•s)	ADJUSTED FLUX (n/cm^2•s)	% UNCERTAIN (1 σ)
1	1.492+001	2.741+006	3.109+006	41.
2	1.350+001	5.699+006	6.467+006	38.
3	1.162+001	2.642+007	2.988+007	34.
4	1.000+001	8.018+007	9.024+007	30.
5	8.607+000	2.029+008	2.258+008	26.
6	7.408+000	4.779+008	5.195+008	24.
7	6.065+000	1.698+009	1.803+009	20.
8	4.966+000	2.378+009	2.396+009	21.
9	3.679+000	3.781+009	3.649+009	21.
10	2.865+000	5.398+009	5.080+009	22.
11	2.231+000	1.032+010	9.536+009	25.
12	1.738+000	1.493+010	1.369+010	29.
13	1.353+000	1.983+010	1.808+010	33.
14	1.108+000	1.976+010	1.798+010	37.
15	8.208-001	3.122+010	2.847+010	41.
16	6.393-001	2.708+010	2.486+010	44.
17	4.979-001	2.777+010	2.576+010	47.
18	3.877-001	2.738+010	2.571+010	49.
19	3.020-001	2.493+010	2.372+010	51.
20	1.832-001	4.135+010	3.986+010	53.
21	1.111-001	3.061+010	2.987+010	54.
22	6.738-002	2.160+010	2.131+010	55.
23	4.087-002	1.797+010	1.791+010	55.
24	2.554-002	1.507+010	1.514+010	55.
25	1.989-002	7.145+009	7.236+009	55.
26	1.503-002	7.209+009	7.352+009	55.
27	9.119-003	1.113+010	1.142+010	54.
28	5.531-003	1.093+010	1.129+010	54.
29	3.355-003	1.177+010	1.226+010	52.
30	2.839-003	4.070+009	4.269+009	51.
31	2.404-003	4.107+009	4.343+009	49.
32	2.035-003	4.133+009	4.406+009	47.
33	1.234-003	1.234+010	1.327+010	44.
34	7.485-004	1.187+010	1.286+010	41.
35	4.540-004	1.092+010	1.191+010	38.
36	2.754-004	1.001+010	1.097+010	35.
37	1.670-004	9.660+009	1.062+010	33.
38	1.013-004	9.894+009	1.108+010	15.
39	6.144-005	1.068+010	1.174+010	30.
40	3.727-005	1.143+010	1.250+010	31.

TABLE 4.2.5.6.1.3 (Cont'd)

FERRET-SAND II RESULTS FOR
SALEM UNIT 1 CAPSULE T
(AVERAGE FOR CAPSULE)

GROUP	ENERGY (MeV)	A PRIORI FLUX* ($n/cm^2 \cdot s$)	ADJUSTED FLUX ($n/cm^2 \cdot s$)	% UNCERTAIN (1σ)
41	2.260-005	1.155+010	1.254+010	33.
42	1.371-005	1.100+010	1.182+010	35.
43	8.315-006	9.977+009	1.059+010	37.
44	5.043-006	9.771+009	1.023+010	39.
45	3.059-006	9.773+009	1.008+010	40.
46	1.855-006	9.776+009	9.930+009	40.
47	1.125-006	9.779+009	9.781+009	39.
48	6.826-007	9.784+009	9.641+009	38.
49	4.140-007	9.785+009	9.509+009	36.
50	2.511-007	9.661+009	9.271+009	34.
51	1.523-007	1.308+010	1.243+010	32.
52	9.237-008	2.158+010	2.034+010	30.
53	1.000-010	4.685+010	4.353+010	22.
FLUX, E > 0.0 MeV		6.736+011	6.629+011	22.
FLUX, E < 0.414 eV		1.010+011	9.508+010	19.
FLUX, E > 0.1 MeV		2.938+011	2.758+011	35.
FLUX, E > 1.0 MeV		8.956+010	8.282+010	22.
dpa/s		1.430-010	1.343-010	25.
FLUENCE+, E > 1.0 MeV		3.068+018	2.837+018	22.
dpa+		4.900-003	4.601-003	25.

---

* ABSOLUTE CALCULATED FLUX (OR NORMALIZED TO Fe54(n,p)Mn54 REACTION RATE).

+ BASED ON 3.426+007 EFFECTIVE FULL POWER SECONDS OF EXPOSURE; UNITS OF n/cm^2 FOR FLUENCE AND TOTAL NUMBER OF DISPLACED ATOMS OF IRON PER TARGET ATOM OF IRON FOR dpa.

TABLE 4.2.5.6.1.4

COMPARISON OF MEASURED AND CALCULATED REACTION RATES USED IN THE ANALYSIS OF SALEM UNIT 1 CAPSULE T

	REACTION RATE (DPS/NUCLEUS)			RATIO MEAS/CALC	
REACTION	MEAS	A PRIORI CALC	ADJ CALC	A PRIORI	ADJ CALC
Fe54(n,p)Mn54	5.21-015	5.39-015	5.29-015	.97	.99
Ni58(n,p)Co58	7.03-015	7.27-015	7.09-015	.97	.99
Cu63(n,α)Co60	5.21-017	4.71-017	5.10-017	1.11	1.02
Co59(n,γ)Co60 (Cd)	1.56-012	1.41-012	1.55-012	1.11	1.01
Co59(n,γ)Co60	3.56-012	3.58-012	3.59-012	.99	.99

4.3 COMBUSTION ENGINEERING SURVEILLANCE CAPSULES: SPECIFIC DETAILS

At present five capsules from Combustion Engineering plants have been reanalyzed. The a priori spectra for accelerated capsules out of the Palisade and Maine Yankee reactors are based on two-dimensional transport calculations by Stan Anderson of Westinghouse for the second accelerated capsule from Maine Yankee. Exact calculated spectra for the Palisade and Maine Yankee Capsule 1 could make some change in the exposures for these capsules if they are obtained at a later date. The a priori spectra for the vessel wall capsules for Maine Yankee and Fort Calhoun were calculated by the Brookhaven National Laboratory staff. The spectra for the capsules include the effect of reduced steel density in the capsule (i.e., about 50% water, 50% steel) whereas the accelerated capsules were assumed to be all steel. The effect of including water in the capsules is to reduce the flux and damage exposures 8 to 10%. As spectra for accelerated capsules flooded with water become available, the presently reported spectra and exposures will be updated.

The dosimetry information used to determine the exposures is summarized in one figure and four tables for each capsule reported. A general note explaining the number designation is in order. All tables identified with Section 4 of this NUREG report. The second number designates the reactor plant vendor (W = 2, CE = 3, B&W = 4, and GE = 5). The third number delineates between generic designs of the vendor. For further discussion of specific vendor generic plants see Sections 1 through 3. The fourth number designates tabulated information for a specific plant, and the fifth number designates the specific capsule. The last number refers to the table or figure number for the specific capsule information.

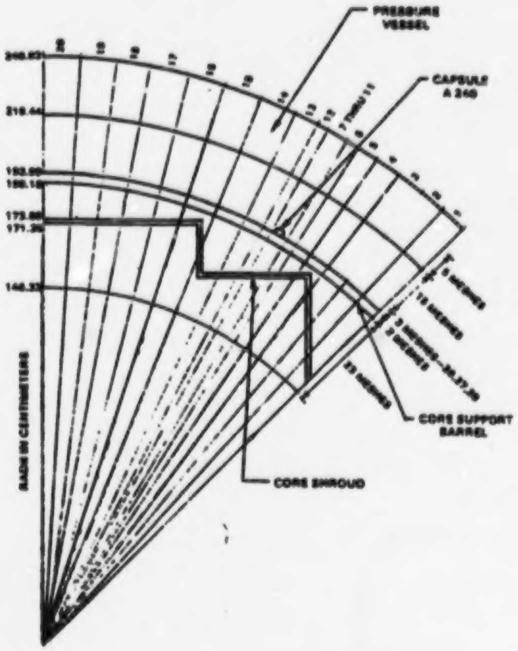
PRESSURE VESSEL
CAPSULE A 240
219.44
171.30
RADII IN CENTIMETERS
CORE SUPPORT BARREL
CORE SHROUD

(a) Reactor Geometry.

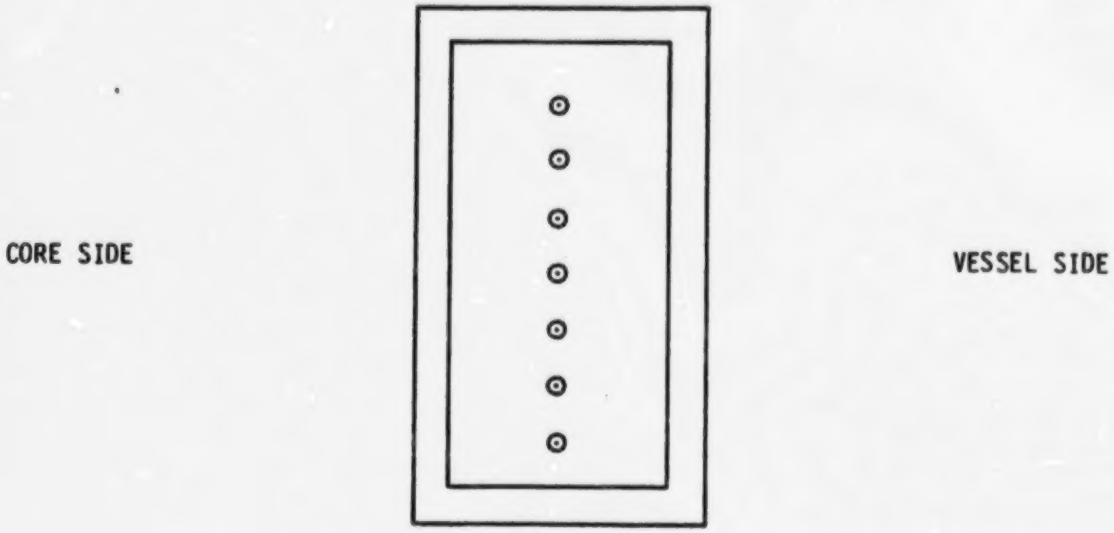
CORE SIDE
VESSEL SIDE

(b) Plan View of Surveillance Capsule.

FIGURE 4.3.1.1.1.1. Orientation of the Capsule Relative to the Core and Vessel Wall - Palisades Capsule A240.

BEST COPY AVAILABLE

333

TABLE 4.3.1.1.1.1

SUMMARY OF REACTOR OPERATIONS
PALISADES CAPSULE A240

TIME PERIOD	START DATE	TIME INTERVAL	AVERAGE POWER LEVEL (MWt)	LOCAL POWER FACTOR
1	9/27/75	95.	2540.	1.00
2	12/31/75	365.	2540.	1.00
3	12/30/76	365.	2540.	1.00
	12/30/77	DISCHARGED*		

---

*EFFECTIVE FULL POWER OPERATION TIME WAS 7.128+007 SECONDS AT A FULL POWER LEVEL OF 2540. MWt.

334

TABLE 4.3.1.1.1.2

REACTION RATE DATA AND CORRECTION FACTORS FOR PALISADES CAPSULE A240

REACTION		TOR RATE	SATURATION	GRADIENT	IMPURITY	AVG REACTION	% UNCERT
NAME	IDENT	(DPS/NUCL)	FACTOR	FACTOR	FACTOR	RATE (RPS/NUCL)	(1σ)
^{54}Fe(n,p)^{54}Mn	TOP			1.000	1.000	5.45-014	10.
	MID			1.000	1.000		
	BOT			1.000	1.000		
^{58}Ni(n,p)^{58}Co	TOP			1.000	1.000	7.14-014	10.
	MID			1.000	1.000		
	BOT			1.000	1.000		
^{63}Cu(n,α)^{60}Co	TOP			1.000	1.000	4.99-016	11.
	BOT			1.000	1.000		
^{46}Ti(n,p)^{46}Ti	BOT			1.000	1.000	9.68-015	10.

CD = Cadmium-Covered Dosimeter.
B = Bare Dosimeter.

TABLE 4.3.1.1.1.3

FERRET-SAND II RESULTS FOR PALISADES CAPSULE A240 (AVERAGE FOR CAPSULE)

GROUP	ENERGY (MeV)	A PRIORI FLUX* (n/cm^2•s)	ADJUSTED FLUX (n/cm^2•s)	% UNCERTAIN (1 σ)
1	1.492+001	2.796+007	2.996+007	44.
2	1.350+001	5.813+007	6.275+007	39.
3	1.162+001	2.695+008	2.919+008	35.
4	1.000+001	8.178+008	8.837+008	30.
5	8.607+000	2.069+009	2.224+009	26.
6	7.408+000	4.874+009	5.228+009	24.
7	6.065+000	1.732+010	1.869+010	19.
8	4.966+000	2.426+010	2.558+010	20.
9	3.679+000	3.856+010	3.877+010	21.
10	2.865+000	5.506+010	5.255+010	22.
11	2.231+000	1.053+011	9.796+010	25.
12	1.738+000	1.523+011	1.407+011	30.
13	1.353+000	2.023+011	1.852+011	34.
14	1.108+000	2.016+011	1.830+011	38.
15	8.208-001	3.184+011	2.878+011	43.
16	6.393-001	2.762+011	2.496+011	47.
17	4.979-001	2.833+011	2.570+011	50.
18	3.877-001	2.793+011	2.552+011	54.
19	3.020-001	2.543+011	2.346+011	56.
20	1.832-001	4.218+011	3.931+011	58.
21	1.111-001	3.123+011	2.942+011	60.
22	6.738-002	2.203+011	2.096+011	61.
23	4.087-002	1.833+011	1.760+011	62.
24	2.554-002	1.537+011	1.486+011	63.
25	1.989-002	7.288+010	7.092+010	63.
26	1.503-002	7.354+010	7.189+010	63.
27	9.119-003	1.135+011	1.113+011	64.
28	5.531-003	1.114+011	1.096+011	64.
29	3.355-003	1.201+011	1.183+011	64.
30	2.839-003	4.151+010	4.095+010	64.
31	2.404-003	4.189+010	4.135+010	64.
32	2.035-003	4.216+010	4.163+010	64.
33	1.234-003	1.259+011	1.244+011	64.
34	7.485-004	1.211+011	1.197+011	64.
35	4.540-004	1.114+011	1.101+011	64.
36	2.754-004	1.021+011	1.009+011	64.
37	1.670-004	9.854+010	9.738+010	64.
38	1.013-004	1.009+011	9.974+010	64.
39	6.144-005	1.090+011	1.077+011	64.
40	3.727-005	1.166+011	1.153+011	64.

TABLE 4.3.1.1.1.3 (Cont'd)

FERRET-SAND II RESULTS FOR
PALISADES CAPSULE A240
(AVERAGE FOR CAPSULE)

GROUP	ENERGY (MeV)	A PRIORI FLUX* ($n/cm^2 \cdot s$)	ADJUSTED FLUX ($n/cm^2 \cdot s$)	% UNCERTAIN ($1\ \sigma$)
41	2.260-005	1.178+011	1.164+011	64.
42	1.371-005	1.122+011	1.109+011	64.
43	8.315-006	1.018+011	1.006+011	64.
44	5.043-006	9.966+010	9.850+010	64.
45	3.059-006	9.969+010	9.852+010	64.
46	1.855-006	9.971+010	9.855+010	64.
47	1.125-006	9.975+010	9.858+010	64.
48	6.826-007	9.980+010	9.863+010	64.
49	4.140-007	9.981+010	9.864+010	64.
50	2.511-007	1.009+011	9.967+010	64.
51	1.523-007	1.006+011	9.940+010	64.
52	9.237-008	1.055+011	1.042+011	64.
53	1.000-010	6.237+011	6.164+011	64.
FLUX, E > 0.0 MeV		6.736+012	6.577+012	40.
FLUX, E < 0.414 eV		1.010+012	1.018+012	61.
FLUX, E > 0.1 MeV		2.938+012	2.767+012	39.
FLUX, E > 1.0 MeV		8.956+011	8.496+011	23.
dpa/s		1.431-009	1.364-009	28.
FLUENCE+, E > 1.0 MeV		6.386+019	6.058+019	23.
dpa+		1.020-001	9.723-002	28.

---

* ABSOLUTE CALCULATED FLUX (OR NORMALIZED TO Fe54(n,p)Mn54 REACTION RATE).

+ BASED ON 7.130+007 EFFECTIVE FULL POWER SECONDS OF EXPOSURE; UNITS OF n/cm^2 FOR FLUENCE AND TOTAL NUMBER OF DISPLACED ATOMS OF IRON PER TARGET ATOM OF IRON FOR dpa.

TABLE 4.3.1.1.1.4

COMPARISON OF MEASURED AND CALCULATED REACTION RATES USED IN THE ANALYSIS OF PALISADES CAPSULE A240

REACTION	REACTION RATE (DPS/NUCLEUS)			RATIO MEAS/CALC	
	MEAS	A PRIORI CALC	ADJ CALC	A PRIORI	ADJ CALC
Fe54(n,p)Mn54	5.45-014	5.50-014	5.51-014	.99	.99
Ni58(n,p)Co58	7.14-014	7.42-014	7.33-014	.96	.97
Cu63(n,α)Co60	4.99-016	4.80-016	5.09-016	1.04	.98
Ti46(n,p)Sc46	9.68-015	8.42-015	9.18-015	1.15	1.05

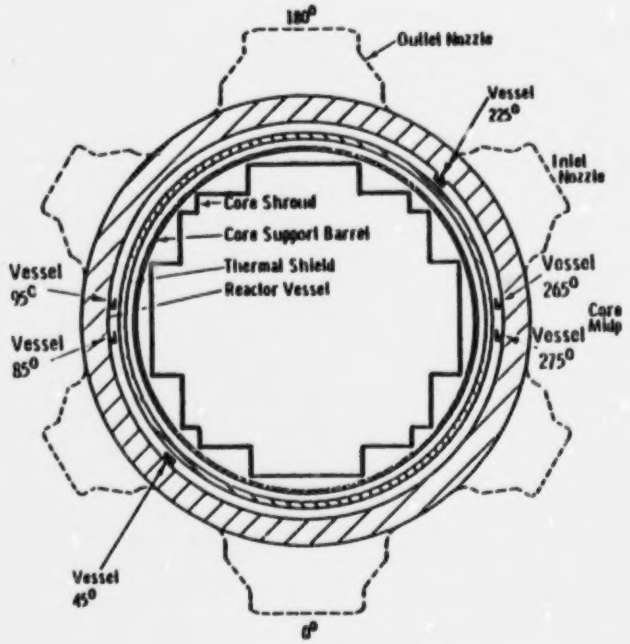
180°
Outlet Nozzle
Vessel 225°
Inlet Nozzle
Core Shroud
Core Support Barrel
Thermal Shield
Reactor Vessel
Vessel 95°
Vessel 265°
Core Midp
Vessel 85°
Vessel 275°
Vessel 45°
0°

(a) Reactor Geometry.

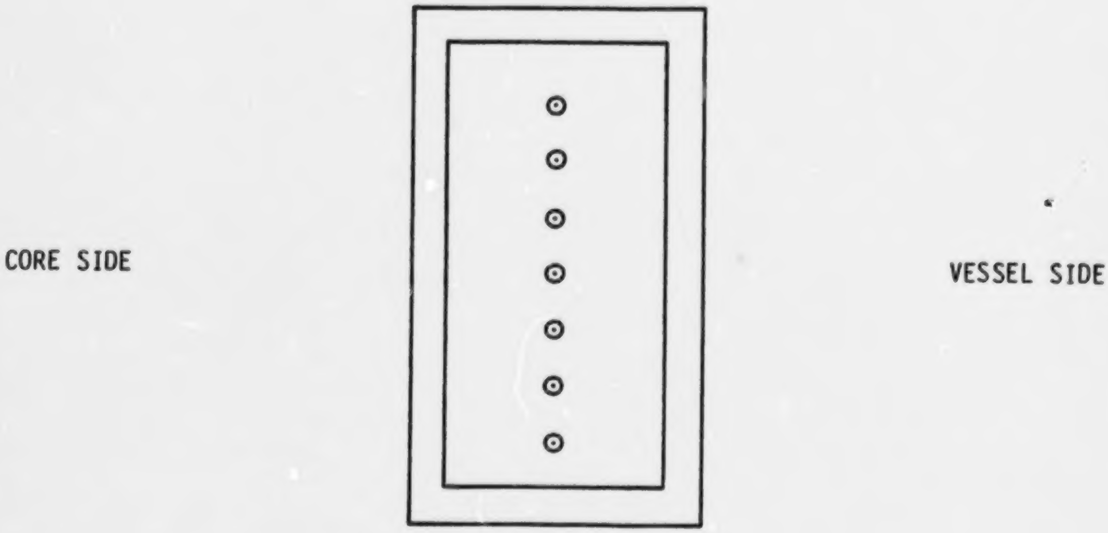
CORE SIDE
VESSEL SIDE

(b) Plan View of Surveillance Capsule.

FIGURE 4.3.2.1.1.1. Orientation of the Capsule Relative to the Core and Vessel Wall - Fort Calhoun Capsule W225.

TABLE 4.3.2.1.1.1

SUMMARY OF REACTOR OPERATIONS
FORT CALHOUN CAPSULE W225

TIME PERIOD	START DATE	TIME INTERVAL	AVERAGE POWER LEVEL (MWt)	LOCAL POWER FACTOR
1	2/26/75	365.	1680.	1.00
2	2/26/76	365.	1680.	1.00
3	2/25/77	218.	1680.	1.00
	10/ 1/77	DISCHARGED*		

---

*EFFECTIVE FULL POWER OPERATION TIME WAS 8.191+007 SECONDS AT A FULL POWER LEVEL OF 1680. MWt.

340

BEST COPY AVAILABLE

TABLE 4.3.2.1.1.2

REACTION RATE DATA AND CORRECTION FACTORS FOR FORT CALHOUN CAPSULE W225

REACTION							
NAME	IDENT	TOR RATE (DPS/NUCL)	SATURATION FACTOR	GRADIENT FACTOR	IMPURITY FACTOR	AVG REACTION RATE (RPS/NUCL)	% UNCERT (1σ)
^{54}Fe(n,p)^{54}Mn	2414			1.000	1.000	6.21-015	10.
	2441			1.000	1.000		
	2473			1.000	1.000		
^{58}Ni(n,p)^{58}Co	2414			1.000	1.000	9.25-015	10.
	2441			1.000	1.000		
	2473			1.000	1.000		
^{63}Cu(n,α)^{60}Co	2414			1.000	1.000	6.45-017	10.
	2441			1.000	1.000		
	2473			1.000	1.000		
^{46}Ti(n,p)^{46}Ti	2414			1.000	1.000	1.05-015	10.
	2441			1.000	1.000		
	2473			1.000	1.000		
^{238}U(n,f)^{137}Cs	2414 (CD)			1.000	0.893	2.74-014	10.
	2441 (CD)			1.000	0.893		
	2473 (CD)			1.000	0.893		
^{238}U(n,f)^{137}Cs	2414 (B)			1.000	0.337	3.10-014	22.
	2441 (B)			1.000	0.337		
	2473 (B)			1.000	0.337		

CD = Cadmium-Covered Dosimeter.
B = Bare Dosimeter.

TABLE 4.3.2.1.1.3

FERRET-SAND II RESULTS FOR FORT CALHOUN CAPSULE W225 (AVERAGE FOR CAPSULE)

GROUP	ENERGY (MeV)	A PRIORI FLUX* ($n/cm^2 \cdot s$)	ADJUSTED FLUX ($n/cm^2 \cdot s$)	% UNCERTAIN ($1\ \sigma$)
1	1.492+001	3.599+006	4.250+006	43.
2	1.350+001	7.483+006	8.808+006	38.
3	1.162+001	3.469+007	4.069+007	34.
4	1.000+001	1.053+008	1.234+008	29.
5	8.607+000	2.664+008	3.116+008	25.
6	7.408+000	5.748+008	6.641+008	23.
7	6.065+000	1.593+009	1.813+009	20.
8	4.966+000	2.999+009	3.332+009	20.
9	3.679+000	5.222+009	5.790+009	19.
10	2.865+000	4.707+009	5.313+009	22.
11	2.231+000	9.811+009	1.123+010	22.
12	1.738+000	9.994+009	1.147+010	24.
13	1.353+000	1.140+010	1.313+010	28.
14	1.108+000	1.012+010	1.166+010	34.
15	8.208-001	1.581+010	1.828+010	38.
16	6.393-001	1.321+010	1.533+010	42.
17	4.979-001	1.233+010	1.435+010	46.
18	3.877-001	1.096+010	1.278+010	50.
19	3.020-001	9.713+009	1.133+010	53.
20	1.832-001	1.623+010	1.891+010	55.
21	1.111-001	1.295+010	1.507+010	57.
22	6.738-002	1.078+010	1.252+010	59.
23	4.087-002	9.519+009	1.103+010	60.
24	2.554-002	8.530+009	9.864+009	61.
25	1.989-002	4.490+009	5.182+009	62.
26	1.503-002	4.984+009	5.742+009	62.
27	9.119-003	8.770+009	1.009+010	63.
28	5.531-003	8.568+009	9.848+009	63.
29	3.355-003	8.327+009	9.564+009	63.
30	2.839-003	2.719+009	3.121+009	63.
31	2.404-003	2.698+009	3.096+009	63.
32	2.035-003	2.693+009	3.089+009	63.
33	1.234-003	8.080+009	9.268+009	63.
34	7.485-004	8.089+009	9.277+009	63.
35	4.540-004	8.103+009	9.293+009	63.
36	2.754-004	8.120+009	9.312+009	63.
37	1.670-004	8.173+009	9.373+009	63.
38	1.013-004	8.315+009	9.535+009	63.
39	6.144-005	8.497+009	9.745+009	63.
40	3.727-005	8.532+009	9.784+009	63.

TABLE 4.3.2.1.1.3 (Cont'd)

FERRET-SAND II RESULTS FOR
FORT CALHOUN CAPSULE W225
(AVERAGE FOR CAPSULE)

GROUP	ENERGY (MeV)	A PRIORI FLUX* ($n/cm^2 \cdot s$)	ADJUSTED FLUX ($n/cm^2 \cdot s$)	% UNCERTAIN (1σ)
41	2.260-005	8.379+009	9.608+009	63.
42	1.371-005	8.250+009	9.460+009	63.
43	8.315-006	8.250+009	9.460+009	63.
44	5.043-006	8.258+009	9.469+009	63.
45	3.059-006	8.270+009	9.483+009	63.
46	1.855-006	8.283+009	9.498+009	63.
47	1.125-006	8.282+009	9.497+009	63.
48	6.826-007	7.747+009	8.883+009	63.
49	4.140-007	7.221+009	8.280+009	63.
50	2.511-007	1.270+010	1.457+010	63.
51	1.523-007	4.864+010	5.577+010	63.
52	9.237-008	8.227+010	9.433+010	63.
53	1.000-010	1.786+011	2.048+011	63.
FLUX, E > 0.0 MeV		6.812+011	7.828+011	43.
FLUX, E < 0.414 eV		3.294+011	3.778+011	60.
FLUX, E > 0.1 MeV		1.503+011	1.736+011	30.
FLUX, E > 1.0 MeV		6.224+010	7.115+010	14.
dpa/s		9.369-011	1.073-010	18.
FLUENCE+, E > 1.0 MeV		5.098+018	5.828+018	14.
dpa+		7.674-003	8.793-003	18.

---

* ABSOLUTE CALCULATED FLUX (OR NORMALIZED TO Fe54(n,p)Mn54 REACTION RATE).

+ BASED ON 8.191+007 EFFECTIVE FULL POWER SECONDS OF EXPOSURE; UNITS OF n/cm^2 FOR FLUENCE AND TOTAL NUMBER OF DISPLACED ATOMS OF IRON PER TARGET ATOM OF IRON FOR dpa.

TABLE 4.3.2.1.1.4

COMPARISON OF MEASURED AND CALCULATED REACTION RATES USED IN THE ANALYSIS OF FORT CALHOUN CAPSULE W225

REACTION	REACTION RATE (DPS/NUCLEUS)			RATIO MEAS/CALC	
	MEAS	A PRIORI CALC	ADJ CALC	A PRIORI	ADJ CALC
U238(n,f)Cs137	2.74-014	2.39-014	2.72-014	1.15	1.01
Ti46(n,p)Sc46	1.05-015	9.66-016	1.08-015	1.09	.98
Fe54(n,p)Mn54	6.21-015	5.85-015	6.54-015	1.06	.95
Ni58(n,p)Co58	9.25-015	7.67-015	8.81-015	1.21	1.05
Cu63(n,α)Co60	6.45-017	5.44-017	6.31-017	1.19	1.02

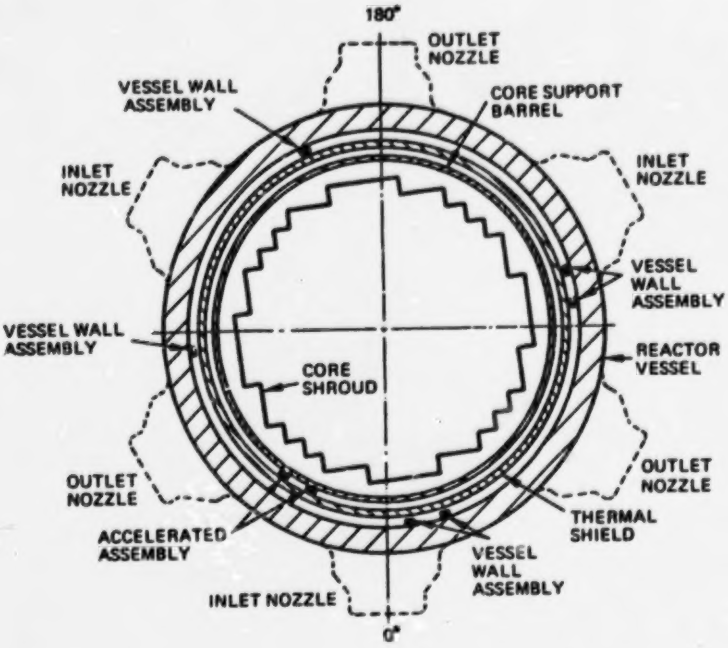
180°
OUTLET NOZZLE
VESSEL WALL ASSEMBLY
CORE SUPPORT BARREL
INLET NOZZLE
INLET NOZZLE
VESSEL WALL ASSEMBLY
VESSEL WALL ASSEMBLY
REACTOR VESSEL
CORE SHROUD
OUTLET NOZZLE
OUTLET NOZZLE
ACCELERATED ASSEMBLY
THERMAL SHIELD
VESSEL WALL ASSEMBLY
INLET NOZZLE
0°

(a) Reactor Geometry.

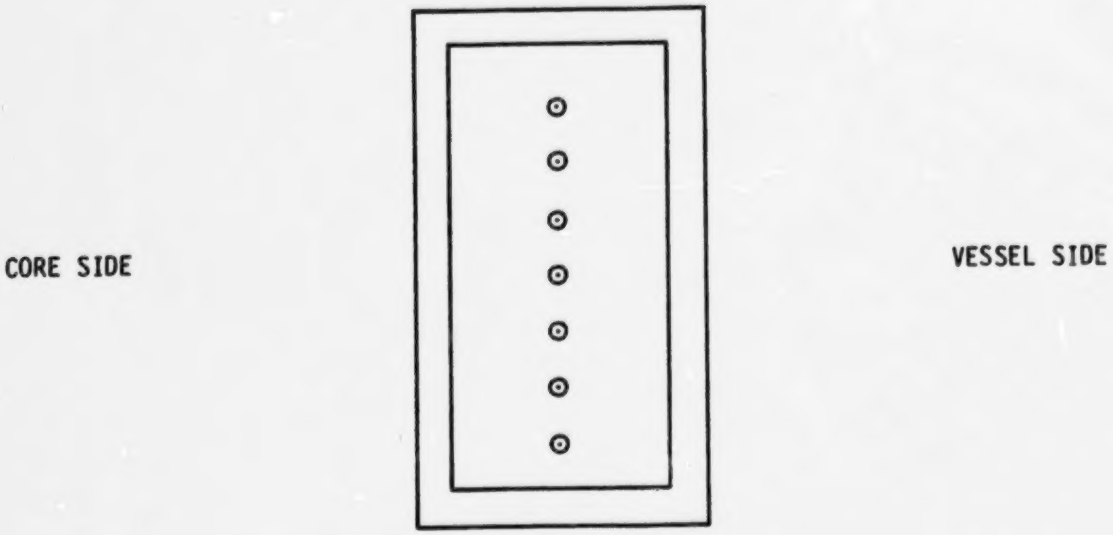
CORE SIDE
VESSEL SIDE

(b) Plan View of Surveillance Capsule.

FIGURE 4.3.3.1.1.1. Orientation of the Capsule Relative to the Core and Vessel Wall - Maine Yankee Capsule 1.

TABLE 4.3.3.1.1.1

SUMMARY OF REACTOR OPERATIONS
MAINE YANKEE CAPSULE 1

TIME PERIOD	START DATE	TIME INTERVAL	AVERAGE POWER LEVEL (MWt)	LOCAL POWER FACTOR
1	11/ 1/72	30.	556.	1.00
2	12/ 1/72	31.	1336.	1.00
3	1/ 1/73	31.	1602.	1.00
4	2/ 1/73	28.	926.	1.00
5	3/ 1/73	31.	1019.	1.00
6	4/ 1/73	30.	1807.	1.00
7	5/ 1/73	31.	1591.	1.00
8	6/ 1/73	30.	1269.	1.00
9	7/ 1/73	31.	0.	1.00
10	8/ 1/73	31.	754.	1.00
11	9/ 1/73	30.	663.	1.00
12	10/ 1/73	31.	1485.	1.00
13	11/ 1/73	30.	1916.	1.00
14	12/ 1/73	31.	1721.	1.00
15	1/ 1/74	31.	1932.	1.00
16	2/ 1/74	28.	1812.	1.00
17	3/ 1/74	31.	1820.	1.00
18	4/ 1/74	30.	1820.	1.00
19	5/ 1/74	31.	1854.	1.00
20	6/ 1/74	30.	1648.	1.00
	7/ 1/74	DISCHARGED*		

---

*EFFECTIVE FULL POWER OPERATION TIME WAS 2.777+007 SECONDS AT A FULL POWER LEVEL OF 2600. MWt.

TABLE 4.3.3.1.1.2

REACTION RATE DATA AND CORRECTION FACTORS FOR MAINE YANKEE CAPSULE 1

REACTION		TOR RATE (DPS/NUCL)	SATURATION FACTOR	GRADIENT FACTOR	IMPURITY FACTOR	AVG REACTION RATE (RPS/NUCL)	% UNCERT (1σ)
NAME	IDENT						
^{54}Fe(n,p)^{54}Mn	A2	2.01-014	2.369+000	1.000	1.000	4.63-014	10.
	D2	1.89-014	2.369+000	1.000	1.000		
	G2	1.96-014	2.369+000	1.000	1.000		
^{58}Ni(n,p)^{58}Co	A1	3.68-014	1.521+000	1.000	1.000	5.30-014	10.
	D1	3.35-014	1.521+000	1.000	1.000		
	G1	3.43-014	1.521+000	1.000	1.000		
^{63}Cu(n,α)^{60}Co	A1	3.69-017	9.498+000	1.000	1.000	3.84-016	11.
	D1	4.52-017	9.498+000	1.000	1.000		
	G1	3.93-017	9.498+000	1.000	1.000		
^{59}Co(n,γ)^{60}Co	A1 (CD)	8.87-013	9.498+000	1.000	1.000	9.90-012	16.
	D1 (CD)	1.22-012	9.498+000	1.000	1.000		
	G1 (CD)	1.02-012	9.498+000	1.000	1.000		
^{59}Co(n,γ)^{60}Co	A2 (B)	2.90-012	9.498+000	1.000	1.000	3.57-011	25.
	D2 (B)	4.74-012	9.498+000	1.000	1.000		
	G2 (B)	3.62-012	9.498+000	1.000	1.000		
^{46}Ti(n,p)^{46}Ti	A2	4.60-015	1.548+000	1.000	1.000	6.54-015	10.
	D2	4.13-015	1.548+000	1.000	1.000		
	G2	3.94-015	1.548+000	1.000	1.000		
^{238}U(n,f)^{103}Ru	A1 (CD)	4.84-015	1.486+000	1.000	0.862	7.91-014	22.
	D1 (CD)	3.32-015	1.486+000	1.000	0.862		
	G1 (CD)	3.38-015	1.486+000	1.000	0.862		

TABLE 4.3.3.1.1.2 (Cont'd)

REACTION RATE DATA AND CORRECTION FACTORS FOR
MAINE YANKEE UNIT 1 CAPSULE 1

REACTION		TOR RATE (DPS/NUCL)	SATURATION FACTOR	GRADIENT FACTOR	IMPURITY FACTOR	AVG REACTION RATE (RPS/NUCL)	% UNCERT (1σ)
NAME	IDENT						
$^{238}U(n,f)^{103}Ru$	A2 (B)	1.76-014	1.486+000	1.000	0.373	1.72-013	23.
	D2 (B)	2.44-014	1.486+000	1.000	0.373		
	G2 (B)	1.61-014	1.486+000	1.000	0.373		
$^{238}U(n,f)^{137}Cs$	A1 (CD)	1.07-016	5.032+001	1.000	0.862	6.08-014	23.
	D1 (CD)	7.18-017	5.032+001	1.000	0.862		
	G1 (CD)	7.36-017	5.032+001	1.000	0.862		
$^{238}U(n,f)^{137}Cs$	A2 (B)	4.71-016	5.032+001	1.000	0.373	1.78-013	26.
	D2 (B)	7.42-016	5.032+001	1.000	0.373		
	G2 (B)	4.96-016	5.032+001	1.000	0.373		
$^{238}U(n,f)^{141}Ce$	A1 (CD)	3.13-015	1.490+000	1.000	0.862	5.89-014	22.
	D1 (CD)	2.22-015	1.490+000	1.000	0.862		
	G1 (CD)	2.15-015	1.490+000	1.000	0.862		
$^{238}U(n,f)^{141}Ce$	A2 (B)	1.10-014	1.490+000	1.000	0.373	1.27-013	20.
	D2 (B)	1.54-014	1.490+000	1.000	0.373		
	G2 (B)	1.10-014	1.490+000	1.000	0.373		
$^{238}U(n,f)^{144}Ce$	A1 (CD)	2.12-015	2.254+000	1.000	0.862	7.92-014	13.
	D1 (CD)	1.73-015	2.254+000	1.000	0.862		
	G1 (CD)	1.71-015	2.254+000	1.000	0.862		
$^{238}U(n,f)^{144}Ce$	A2 (B)	6.57-015	2.254+000	1.000	0.373	1.26-013	10.
	G2 (B)	7.02-015	2.254+000	1.000	0.373		

CD = Cadmium-Covered Dosimeter.
B = Bare Dosimeter.

TABLE 4.3.3.1.1.3

FERRET-SAND II RESULTS FOR MAINE YANKEE CAPSULE 1 (AVERAGE FOR CAPSULE)

GROUP	ENERGY (MeV)	A PRIORI FLUX* (n/cm^2•s)	ADJUSTED FLUX (n/cm^2•s)	% UNCERTAIN (1 σ)
1	1.492+001	2.332+007	2.179+007	41.
2	1.350+001	4.847+007	4.579+007	38.
3	1.162+001	2.247+008	2.142+008	34.
4	1.000+001	6.820+008	6.540+008	30.
5	8.607+000	1.725+009	1.657+009	26.
6	7.408+000	4.072+009	3.887+009	24.
7	6.065+000	1.444+010	1.369+010	19.
8	4.966+000	2.010+010	1.891+010	20.
9	3.679+000	3.212+010	2.982+010	21.
10	2.865+000	4.535+010	4.131+010	22.
11	2.231+000	8.688+010	7.519+010	23.
12	1.738+000	1.246+011	1.027+011	27.
13	1.353+000	1.684+011	1.352+011	30.
14	1.108+000	1.693+011	1.364+011	35.
15	8.208-001	2.714+011	2.162+011	38.
16	6.393-001	2.382+011	1.885+011	42.
17	4.979-001	2.458+011	1.939+011	45.
18	3.877-001	2.408+011	1.903+011	48.
19	3.020-001	2.195+011	1.743+011	50.
20	1.832-001	3.666+011	2.935+011	52.
21	1.111-001	2.761+011	2.230+011	53.
22	6.738-002	1.999+011	1.630+011	54.
23	4.087-002	1.668+011	1.371+011	55.
24	2.554-002	1.401+011	1.159+011	55.
25	1.989-002	6.674+010	5.548+010	55.
26	1.503-002	6.777+010	5.642+010	55.
27	9.119-003	1.068+011	8.876+010	55.
28	5.531-003	1.060+011	8.779+010	54.
29	3.355-003	1.106+011	9.096+010	53.
30	2.839-003	3.782+010	3.081+010	52.
31	2.404-003	3.811+010	3.070+010	50.
32	2.035-003	3.831+010	3.048+010	48.
33	1.234-003	1.145+011	8.996+010	45.
34	7.485-004	1.110+011	8.610+010	43.
35	4.540-004	1.038+011	7.961+010	40.
36	2.754-004	9.678+010	7.356+010	37.
37	1.670-004	9.379+010	7.084+010	35.
38	1.013-004	9.503+010	6.954+010	21.
39	6.144-005	9.961+010	7.518+010	33.
40	3.727-005	1.036+011	7.876+010	33.

TABLE 4.3.3.1.1.3 (Cont'd)

FERRET-SAND II RESULTS FOR
MAINE YANKEE CAPSULE 1
(AVERAGE FOR CAPSULE)

GROUP	ENERGY (MeV)	A PRIORI FLUX* (n/cm^2•s)	ADJUSTED FLUX (n/cm^2•s)	% UNCERTAIN (1 σ)
41	2.260-005	1.045+011	8.030+010	34.
42	1.371-005	1.021+011	7.963+010	36.
43	8.315-006	9.664+010	7.677+010	38.
44	5.043-006	9.153+010	7.427+010	40.
45	3.059-006	9.018+010	7.490+010	41.
46	1.855-006	9.089+010	7.733+010	41.
47	1.125-006	9.191+010	8.011+010	41.
48	6.826-007	9.277+010	8.276+010	41.
49	4.140-007	9.332+010	8.512+010	40.
50	2.511-007	1.089+011	1.014+011	39.
51	1.523-007	1.532+011	1.450+011	38.
52	9.237-008	2.416+011	2.319+011	37.
53	1.000-010	5.245+011	5.152+011	33.
FLUX, E > 0.0 MeV		6.005+012	5.255+012	22.
FLUX, E < 0.414 eV		1.068+012	1.079+012	29.
FLUX, E > 0.1 MeV		2.446+012	2.074+012	33.
FLUX, E > 1.0 MeV		7.245+011	6.336+011	19.
dpa/s		1.178-009	1.025-009	23.
FLUENCE+, E > 1.0 MeV		2.012+019	1.759+019	19.
dpa+		3.272-002	2.846-002	23.

---

* ABSOLUTE CALCULATED FLUX (OR NORMALIZED TO Fe54(n,p)Mn54 REACTION RATE).

+ BASED ON 2.777+007 EFFECTIVE FULL POWER SECONDS OF EXPOSURE; UNITS OF n/cm^2 FOR FLUENCE AND TOTAL NUMBER OF DISPLACED ATOMS OF IRON PER TARGET ATOM OF IRON FOR dpa.

BEST COPY AVAILABLE

TABLE 4.3.3.1.1.4

COMPARISON OF MEASURED AND CALCULATED REACTION RATES USED IN THE ANALYSIS OF MAINE YANKEE CAPSULE 1

REACTION	REACTION RATE (DPS/NUCLEUS)			RATIO MEAS/CALC	
	MEAS	A PRIORI CALC	ADJ CALC	A PRIORI	ADJ CALC
Ni58(n,p)Co58	5.30-014	6.15-014	5.51-014	.86	.96
Cu63(n,α)Co60	3.84-016	4.00-016	3.81-016	.96	1.01
Co59(n,γ)Co60 (Cd)	9.90-012	1.35-011	1.02-011	.74	.97
Co59(n,γ)Co60	3.57-011	3.77-011	3.36-011	.95	1.06
Fe54(n,p)Mn54	4.63-014	4.65-014	4.30-014	1.00	1.08
Ti46(n,p)Sc46	6.54-015	7.15-015	6.67-015	.92	.98

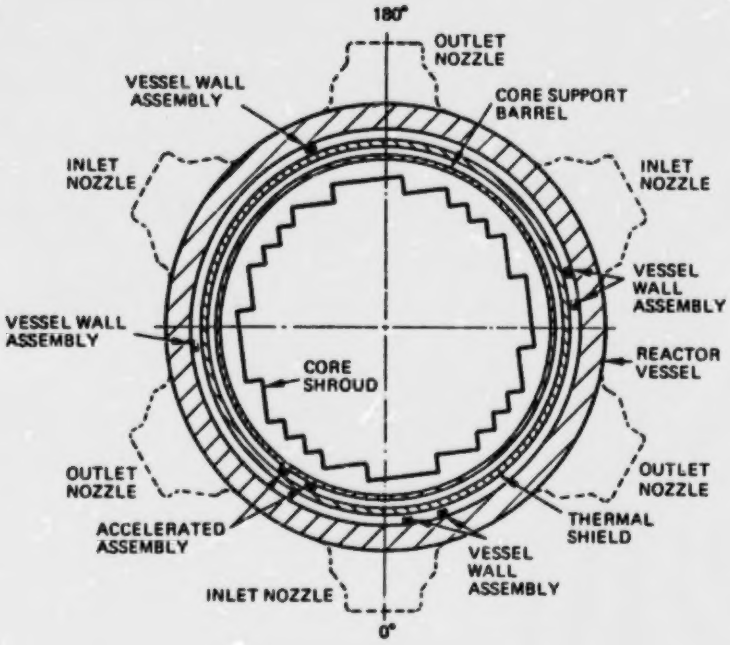
180°
OUTLET NOZZLE
VESSEL WALL ASSEMBLY
CORE SUPPORT BARREL
INLET NOZZLE
INLET NOZZLE
VESSEL WALL ASSEMBLY
VESSEL WALL ASSEMBLY
REACTOR VESSEL
CORE SHROUD
OUTLET NOZZLE
OUTLET NOZZLE
THERMAL SHIELD
ACCELERATED ASSEMBLY
VESSEL WALL ASSEMBLY
INLET NOZZLE
0°

(a) Reactor Geometry.

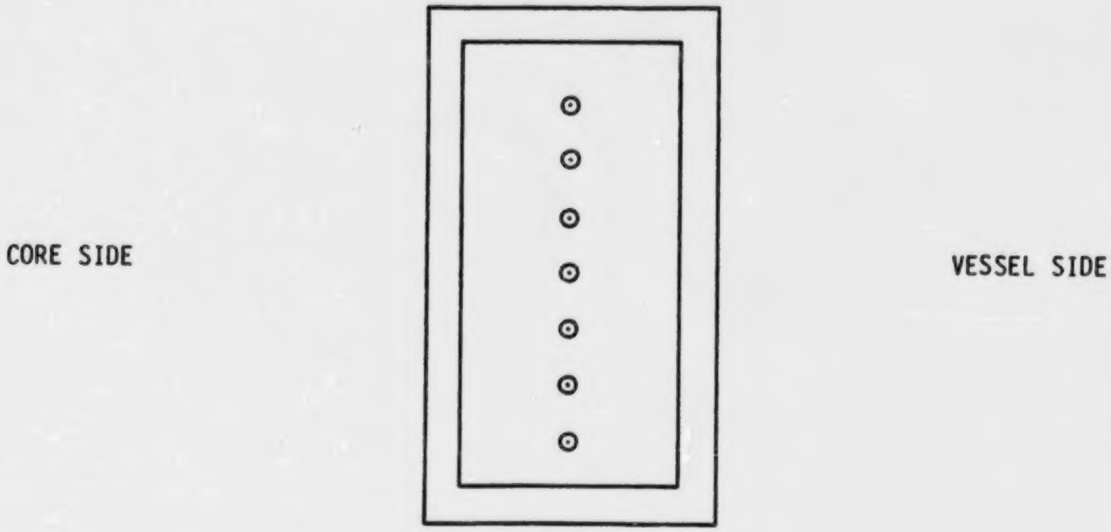
CORE SIDE
VESSEL SIDE

(b) Plan View of Surveillance Capsule.

FIGURE 4.3.3.1.2.1. Orientation of the Capsule Relative to the Core and Vessel Wall - Maine Yankee Capsule 2.

TABLE 4.3.3.1.2.1

SUMMARY OF REACTOR OPERATIONS
MAINE YANKEE CAPSULE 2

TIME PERIOD	START DATE	TIME INTERVAL	AVERAGE POWER LEVEL (MWt)	LOCAL POWER FACTOR
1	11/ 1/72	30.	556.	1.00
2	12/ 1/72	31.	1336.	1.00
3	1/ 1/73	31.	1602.	1.00
4	2/ 1/73	28.	926.	1.00
5	3/ 1/73	31.	1019.	1.00
6	4/ 1/73	30.	1807.	1.00
7	5/ 1/73	31.	1591.	1.00
8	6/ 1/73	30.	1269.	1.00
9	7/ 1/73	31.	0.	1.00
10	8/ 1/73	31.	754.	1.00
11	9/ 1/73	30.	663.	1.00
12	10/ 1/73	31.	1485.	1.00
13	11/ 1/73	30.	1916.	1.00
14	12/ 1/73	31.	1721.	1.00
15	1/ 1/74	31.	1932.	1.00
16	2/ 1/74	28.	1812.	1.00
17	3/ 1/74	31.	1820.	1.00
18	4/ 1/74	30.	1820.	1.00
19	5/ 1/74	31.	1854.	1.00
20	6/ 1/74	30.	1648.	1.00
21	7/ 1/74	92.	0.	1.00
22	10/ 1/74	31.	1113.	1.00
23	11/ 1/74	30.	1719.	1.00
24	12/ 1/74	31.	1955.	1.00
25	1/ 1/75	31.	1383.	1.00
26	2/ 1/75	28.	1838.	1.00
27	3/ 1/75	31.	2007.	1.00
28	4/ 1/75	30.	1948.	1.00
29	5/ 1/75	31.	109.	1.00
30	6/ 1/75	30.	23.	1.00
31	7/ 1/75	31.	1308.	1.00
32	8/ 1/75	31.	2171.	1.00
33	9/ 1/75	30.	2304.	1.00
34	10/ 1/75	31.	2382.	1.00
35	11/ 1/75	30.	1830.	1.00
36	12/ 1/75	31.	2280.	1.00
37	1/ 1/76	31.	2306.	1.00
38	2/ 1/76	29.	2184.	1.00
39	3/ 1/76	31.	2197.	1.00
40	4/ 1/76	30.	2301.	1.00

TABLE 4.3.3.1.2.1 (Cont'd)

SUMMARY OF REACTOR OPERATIONS
MAINE YANKEE CAPSULE 2

TIME PERIOD	START DATE	TIME INTERVAL	AVERAGE POWER LEVEL (MWt)	LOCAL POWER FACTOR
41	5/ 1/76	31.	2194.	1.00
42	6/ 1/76	30.	2036.	1.00
43	7/ 1/76	31.	2116.	1.00
44	8/ 1/76	31.	2236.	1.00
45	9/ 1/76	30.	1209.	1.00
46	10/ 1/76	31.	2192.	1.00
47	11/ 1/76	30.	2337.	1.00
48	12/ 1/76	31.	2322.	1.00
49	1/ 1/77	31.	2218.	1.00
50	2/ 1/77	28.	2226.	1.00
51	3/ 1/77	31.	1864.	1.00
52	4/ 1/77	30.	354.	1.00
53	5/ 1/77	31.	0.	1.00
54	6/ 1/77	30.	1204.	1.00
55	7/ 1/77	31.	2350.	1.00
56	8/ 1/77	31.	2392.	1.00
57	9/ 1/77	30.	2423.	1.00
58	10/ 1/77	31.	2444.	1.00
59	11/ 1/77	30.	2431.	1.00
60	12/ 1/77	31.	2397.	1.00
61	1/ 1/78	31.	2431.	1.00
62	2/ 1/78	28.	2220.	1.00
63	3/ 1/78	31.	2387.	1.00
64	4/ 1/78	30.	2332.	1.00
65	5/ 1/78	31.	2410.	1.00
66	6/ 1/78	30.	2114.	1.00
67	7/ 1/78	31.	913.	1.00
68	8/ 1/78	31.	107.	1.00
69	9/ 1/78	30.	1076.	1.00
70	10/ 1/78	31.	2226.	1.00
71	11/ 1/78	30.	2509.	1.00
72	12/ 1/78	31.	2519.	1.00
73	1/ 1/79	31.	2428.	1.00
74	2/ 1/79	28.	2473.	1.00
75	3/ 1/79	31.	1035.	1.00
76	4/ 1/79	30.	0.	1.00
77	5/ 1/79	31.	0.	1.00
78	6/ 1/79	30.	1940.	1.00
79	7/ 1/79	31.	2493.	1.00
80	8/ 1/79	31.	2470.	1.00

TABLE 4.3.3.1.2.1 (Cont'd)

SUMMARY OF REACTOR OPERATIONS
MAINE YANKEE CAPSULE 2

TIME PERIOD	START DATE	TIME INTERVAL	AVERAGE POWER LEVEL (MWt)	LOCAL POWER FACTOR
81	9/ 1/79	30.	18.	1.00
82	10/ 1/79	31.	2070.	1.00
83	11/ 1/79	30.	2449.	1.00
84	12/ 1/79	31.	2036.	1.00
85	1/ 1/80	11	[illegible]	1.00
	1/12/80	DISCHARGED*		

---

*EFFECTIVE FULL POWER OPERATION TIME WAS 1.446+008 SECONDS AT A FULL POWER LEVEL OF 2600. MWt.

TABLE 4.3.3.1.2.2

REACTION RATE DATA AND CORRECTION FACTORS FOR MAINE YANKEE CAPSULE 2

REACTION NAME	IDENT	TOR RATE (DPS/NUCL)	SATURATION FACTOR	GRADIENT FACTOR	IMPURITY FACTOR	AVG REACTION RATE (RPS/NUCL)	% UNCERT (1σ)
^{54}Fe(n,p)^{54}Mn	TOP	3.06-014	1.477+000	1.000	1.000	4.25-014	10.
	MID	2.64-014	1.477+000	1.000	1.000		
	BOT	2.94-014	1.477+000	1.000	1.000		
^{63}Cu(n,α)^{60}Co	TOP	1.52-016	2.489+000	1.000	1.000	3.66-016	10.
	MID	1.41-016	2.489+000	1.000	1.000		
	BOT	1.48-016	2.489+000	1.000	1.000		
^{58}Ni(n,p)^{58}Co	TOP	4.47-014	1.430+000	1.000	1.000	5.92-014	10.
	MID	3.98-014	1.430+000	1.000	1.000		
	BOT	3.98-014	1.430+000	1.000	1.000		
^{46}Ti(n,p)^{46}Ti	TOP	5.55-015	1.450+000	1.000	1.000	7.35-015	10.
	MID	4.57-015	1.450+000	1.000	1.000		
	BOT	5.08-015	1.450+000	1.000	1.000		
^{238}U(n,f)^{137}Cs	TOP (CD)	1.49-015	1.025+001	1.000	0.714	1.71-013	10.
	MID (CD)	1.30-015	1.025+001	1.000	0.714		
^{59}Co(n,γ)^{60}Co	TOP (B)	8.61-012	2.489+000	1.000	1.000	2.58-011	18.
	MID (B)	1.23-011	2.489+000	1.000	1.000		
	BOT (B)	1.02-011	2.489+000	1.000	1.000		
^{59}Co(n,γ)^{60}Co	TOP (CD)	2.44-012	2.489+000	1.000	1.000	6.71-012	12.
	MID (CD)	3.04-012	2.489+000	1.000	1.000		
	BOT (CD)	2.61-012	2.489+000	1.000	1.000		

CD = Cadmium-Covered Dosimeter.
B = Bare Dosimeter.

TABLE 4.3.3.1.2.3

FERRET-SAND II RESULTS FOR
MAINE YANKEE CAPSULE 2
(AVERAGE FOR CAPSULE)

GROUP	ENERGY (MeV)	A PRIORI FLUX* (n/cm^2·s)	ADJUSTED FLUX (n/cm^2·s)	% UNCERTAIN (1 σ)
1	1.492+001	2.177+007	1.966+007	41.
2	1.350+001	4.526+007	4.262+007	38.
3	1.162+001	2.098+008	2.049+008	34.
4	1.000+001	6.368+008	6.367+008	30.
5	8.607+000	1.611+009	1.635+009	26.
6	7.408+000	3.802+009	3.927+009	23.
7	6.065+000	1.348+010	1.434+010	19.
8	4.966+000	1.876+010	2.029+010	20.
9	3.679+000	2.999+010	3.096+010	20.
10	2.865+000	4.234+010	3.900+010	22.
11	2.231+000	8.112+010	6.653+010	22.
12	1.738+000	1.164+011	8.495+010	22.
13	1.353+000	1.572+011	1.078+011	25.
14	1.108+000	1.580+011	1.075+011	31.
15	8.208-001	2.534+011	1.651+011	34.
16	6.393-001	2.224+011	1.404+011	38.
17	4.979-001	2.295+011	1.420+011	42.
18	3.877-001	2.249+011	1.382+011	45.
19	3.020-001	2.049+011	1.264+011	48.
20	1.832-001	3.423+011	2.136+011	50.
21	1.111-001	2.578+011	1.635+011	52.
22	6.738-002	1.866+011	1.206+011	53.
23	4.087-002	1.557+011	1.024+011	54.
24	2.554-002	1.308+011	8.726+010	54.
25	1.989-002	6.232+010	4.200+010	55.
26	1.503-002	6.328+010	4.284+010	55.
27	9.119-003	9.969+010	6.739+010	54.
28	5.531-003	9.901+010	6.642+010	54.
29	3.355-003	1.033+011	6.838+010	53.
30	2.839-003	3.531+010	2.296+010	51.
31	2.404-003	3.558+010	2.262+010	49.
32	2.035-003	3.577+010	2.218+010	47.
33	1.234-003	1.070+011	6.458+010	45.
34	7.485-004	1.037+011	6.098+010	42.
35	4.540-004	9.692+010	5.569+010	39.
36	2.754-004	9.037+010	5.092+010	36.
37	1.670-004	8.758+010	4.862+010	34.
38	1.013-004	8.873+010	4.611+010	18.
39	6.144-005	9.301+010	5.121+010	31.
40	3.727-005	9.676+010	5.375+010	32.

TABLE 4.3.3.1.2.3 (Cont'd)

FERRET-SAND II RESULTS FOR
MAINE YANKEE CAPSULE 2
(AVERAGE FOR CAPSULE)

GROUP	ENERGY (MeV)	A PRIORI FLUX* ($n/cm^2 \cdot s$)	ADJUSTED FLUX ($n/cm^2 \cdot s$)	% UNCERTAIN (1 σ)
41	2.260-005	9.758+010	5.506+010	33.
42	1.371-005	9.534+010	5.499+010	35.
43	8.315-006	9.023+010	5.351+010	37.
44	5.043-006	8.546+010	5.234+010	38.
45	3.059-006	8.420+010	5.340+010	39.
46	1.855-006	8.486+010	5.580+010	40.
47	1.125-006	8.582+010	5.850+010	40.
48	6.826-007	8.662+010	6.114+010	39.
49	4.140-007	8.713+010	6.361+010	37.
50	2.511-007	1.017+011	7.674+010	36.
51	1.523-007	1.430+011	1.108+011	34.
52	9.237-008	2.256+011	1.786+011	32.
53	1.000-010	4.897+011	4.002+011	26.
FLUX, E > 0.0 MeV		5.905+012	3.939+012	20.
FLUX, E < 0.414 eV		1.050+012	8.300+011	23.
FLUX, E > 0.1 MeV		2.405+012	1.592+012	28.
FLUX, E > 1.0 MeV		7.124+011	5.343+011	13.
dpa/s		1.159-009	8.380-010	18.
FLUENCE+, E > 1.0 MeV		1.030+020	7.727+019	13.
dpa+		1.676-001	1.212-001	18.

---

* ABSOLUTE CALCULATED FLUX (OR NORMALIZED TO Fe54(n,p)Mn54 REACTION RATE).

+ BASED ON 1.446+008 EFFECTIVE FULL POWER SECONDS OF EXPOSURE; UNITS OF n/cm^2 FOR FLUENCE AND TOTAL NUMBER OF DISPLACED ATOMS OF IRON PER TARGET ATOM OF IRON FOR dpa.

TABLE 4.3.3.1.2.4

COMPARISON OF MEASURED AND CALCULATED REACTION RATES USED IN THE ANALYSIS OF MAINE YANKEE CAPSULE 2

REACTION	REACTION RATE (DPS/NUCLEUS) MEAS	A PRIORI CALC	ADJ CALC	RATIO MEAS/CALC A PRIORI	ADJ CALC
U238(n,f)Cs137	1.71-013	2.30-013	1.85-013	.74	.92
Ni58(n,p)Co58	5.92-014	5.74-014	5.60-014	1.03	1.06
Cu63(n,α)Co60	3.66-016	3.74-016	3.81-016	.98	.96
Fe54(n,p)Mn54	4.25-014	4.25-014	4.16-014	1.00	1.02
Ti46(n,p)Sc46	7.35-015	6.55-015	7.05-015	1.12	1.04
Co59(n,γ)Co60 (Cd)	6.71-012	1.26-011	6.91-012	.53	.97
Co59(n,γ)Co60	2.58-011	3.52-011	2.50-011	.73	1.03

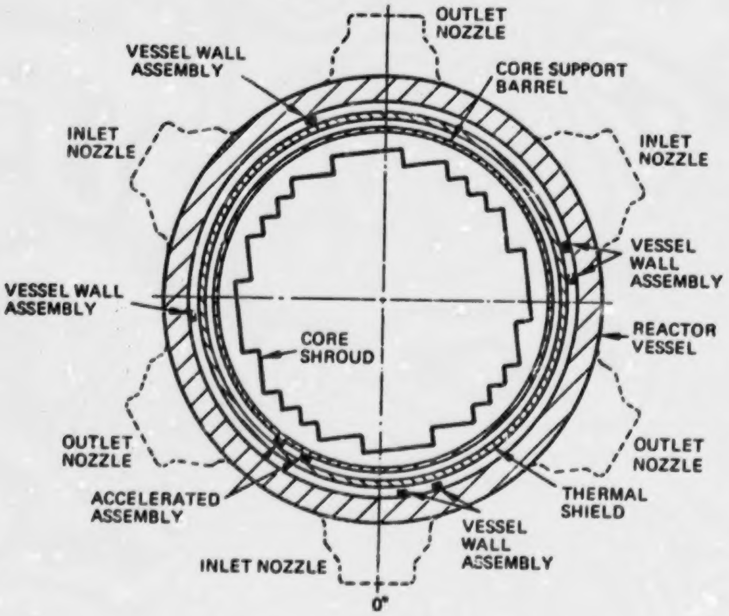
180°
OUTLET NOZZLE
VESSEL WALL ASSEMBLY
CORE SUPPORT BARREL
INLET NOZZLE
INLET NOZZLE
VESSEL WALL ASSEMBLY
VESSEL WALL ASSEMBLY
REACTOR VESSEL
CORE SHROUD
OUTLET NOZZLE
OUTLET NOZZLE
ACCELERATED ASSEMBLY
THERMAL SHIELD
VESSEL WALL ASSEMBLY
INLET NOZZLE
0°

(a) Reactor Geometry.

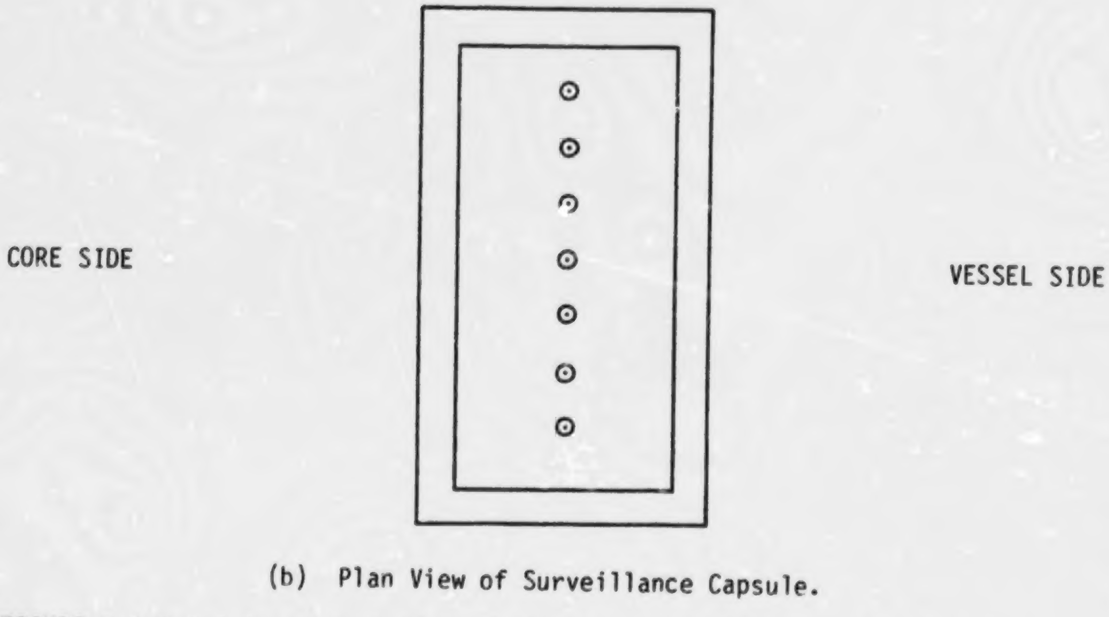
CORE SIDE
VESSEL SIDE

(b) Plan View of Surveillance Capsule.

FIGURE 4.3.3.1.3.1. Orientation of the Capsule Relative to the Core and Vessel Wall - Maine Yankee Capsule W263.

TABLE 4.3.3.1.3.1

SUMMARY OF REACTOR OPERATIONS
MAINE YANKEE CAPSULE W263

TIME PERIOD	START DATE	TIME INTERVAL	AVERAGE POWER LEVEL (MWt)	LOCAL POWER FACTOR
1	11/ 1/72	30.	556.	1.00
2	12/ 1/72	31.	1336.	1.00
3	1/ 1/73	31.	1602.	1.00
4	2/ 1/73	28.	926.	1.00
5	3/ 1/73	31.	1019.	1.00
6	4/ 1/73	30.	1807.	1.00
7	5/ 1/73	31.	1591.	1.00
8	6/ 1/73	30.	1269.	1.00
9	7/ 1/73	31.	0.	1.00
10	8/ 1/73	31.	754.	1.00
11	9/ 1/73	30.	663.	1.00
12	10/ 1/73	31.	1485.	1.00
13	11/ 1/73	30.	1916.	1.00
14	12/ 1/73	31.	1721.	1.00
15	1/ 1/74	31.	1932.	1.00
16	2/ 1/74	28.	1812.	1.00
17	3/ 1/74	31.	1820.	1.00
18	4/ 1/74	30.	1820.	1.00
19	5/ 1/74	31.	1854.	1.00
20	6/ 1/74	30.	1648.	1.00
21	7/ 1/74	92.	0.	1.00
22	10/ 1/74	31.	1113.	1.00
23	11/ 1/74	30.	1719.	1.00
24	12/ 1/74	31.	1955.	1.00
25	1/ 1/75	31.	1383.	1.00
26	2/ 1/75	28.	1838.	1.00
27	3/ 1/75	31.	2007.	1.00
28	4/ 1/75	30.	1948.	1.00
29	5/ 1/75	31.	109.	1.00
30	6/ 1/75	30.	23.	1.00
31	7/ 1/75	31.	1308.	1.00
32	8/ 1/75	31.	2171.	1.00
33	9/ 1/75	30.	2304.	1.00
34	10/ 1/75	31.	2382.	1.00
35	11/ 1/75	30.	1830.	1.00
36	12/ 1/75	31.	2280.	1.00
37	1/ 1/76	31.	2306.	1.00
38	2/ 1/76	29.	2184.	1.00
39	3/ 1/76	31.	2197.	1.00
40	4/ 1/76	30.	2301.	1.00

TABLE 4.3.3.1.3.1 (Cont'd)

SUMMARY OF REACTOR OPERATIONS
MAINE YANKEE CAPSULE W263

TIME PERIOD	START DATE	TIME INTERVAL	AVERAGE POWER LEVEL (MWt)	LOCAL POWER FACTOR
41	5/ 1/76	31.	2194.	1.00
42	6/ 1/76	30.	2036.	1.00
43	7/ 1/76	31.	2116.	1.00
44	8/ 1/76	31.	2236.	1.00
45	9/ 1/76	30.	1209.	1.00
46	10/ 1/76	31.	2192.	1.00
47	11/ 1/76	30.	2337.	1.00
48	12/ 1/76	31.	2322.	1.00
49	1/ 1/77	31.	2218.	1.00
50	2/ 1/77	28.	2226.	1.00
51	3/ 1/77	31.	1864.	1.00
52	4/ 1/77	30.	354.	1.00
53	5/ 1/77	31.	0.	1.00
54	6/ 1/77	30.	1204.	1.00
55	7/ 1/77	31.	2350.	1.00
56	8/ 1/77	31.	2392.	1.00
57	9/ 1/77	30.	2423.	1.00
58	10/ 1/77	31.	2444.	1.00
59	11/ 1/77	30.	2431.	1.00
60	12/ 1/77	31.	2397.	1.00
61	1/ 1/78	31.	2431.	1.00
62	2/ 1/78	28.	2220.	1.00
63	3/ 1/78	31.	2387.	1.00
64	4/ 1/78	30.	2332.	1.00
65	5/ 1/78	31.	2410.	1.00
66	6/ 1/78	30.	2114.	1.00
67	7/ 1/78	31.	913.	1.00
68	8/ 1/78	31.	107.	1.00
69	9/ 1/78	30.	1076.	1.00
70	10/ 1/78	31.	2226.	1.00
71	11/ 1/78	30.	2509.	1.00
72	12/ 1/78	31.	2519.	1.00
73	1/ 1/79	31.	2428.	1.00
74	2/ 1/79	28.	2473.	1.00
75	3/ 1/79	31.	1035.	1.00
76	4/ 1/79	30.	0.	1.00
77	5/ 1/79	31.	0.	1.00
78	6/ 1/79	30.	1940.	1.00
79	7/ 1/79	31.	2493.	1.00
80	8/ 1/79	31.	2470.	1.00

TABLE 4.3.3.1.3.1 (Cont'd)

SUMMARY OF REACTOR OPERATIONS
MAINE YANKEE CAPSULE W263

TIME PERIOD	START DATE	TIME INTERVAL	AVERAGE POWER LEVEL (MWt)	LOCAL POWER FACTOR
81	9/ 1/79	30.	18.	1.00
82	10/ 1/79	31.	2070.	1.00
83	11/ 1/79	30.	2449.	1.00
84	12/ 1/79	31.	2036.	1.00
85	1/ 1/80	11.	1591.	1.00
	1/12/80	DISCHARGED*		

---

*EFFECTIVE FULL POWER OPERATION TIME WAS 1.446+008 SECONDS AT A FULL POWER LEVEL OF 2600. MWt.

BEST COPY AVAILABLE

TABLE 4.3.3.1.3.2

REACTION RATE DATA AND CORRECTION FACTORS FOR MAINE YANKEE CAPSULE W263

REACTION NAME	IDENT	TOR RATE (DPS/NUCL)	SATURATION FACTOR	GRADIENT FACTOR	IMPURITY FACTOR	AVG REACTION RATE (RPS/NUCL)	% UNCERT (1σ)
$^{54}\mathrm{Fe}(n,p)^{54}\mathrm{Mn}$	TOP	2.84-015	1.477+000	1.000	1.000	4.00-015	10.
	MID	2.56-015	1.477+000	1.000	1.000		
	BOT	2.73-015	1.477+000	1.000	1.000		
$^{58}\mathrm{Ni}(n,p)^{58}\mathrm{Co}$	TOP	4.08-015	1.430+000	1.000	1.000	5.50-015	10.
	MID	3.46-015	1.430+000	1.000	1.000		
	BOT	3.99-015	1.430+000	1.000	1.000		
$^{63}\mathrm{Cu}(n,\alpha)^{60}\mathrm{Co}$	TOP	1.85-017	2.489+000	1.000	1.000	4.47-017	10.
	MID	1.70-017	2.489+000	1.000	1.000		
	BOT	1.85-017	2.489+000	1.000	1.000		
$^{46}\mathrm{Ti}(n,p)^{46}\mathrm{Ti}$	TOP	5.35-016	1.450+000	1.000	1.000	7.46-016	10.
	MID	5.01-016	1.450+000	1.000	1.000		
	BOT	5.08-016	1.450+000	1.000	1.000		
$^{238}\mathrm{U}(n,f)^{137}\mathrm{Cs}$	TOP	1.04-016	1.025+001	1.000	0.885	1.57-014	10.
	MID	9.80-017	1.025+001	1.000	0.885		
	BOT	1.09-016	1.025+001	1.000	0.885		
$^{59}\mathrm{Co}(n,\gamma)^{60}\mathrm{Co}$	TOP (B)	1.95-012	2.489+000	1.000	1.000	4.73-012	19.
	MID (B)	2.24-012	2.489+000	1.000	1.000		
	BOT (B)	1.51-012	2.489+000	1.000	1.000		
$^{59}\mathrm{Co}(n,\gamma)^{60}\mathrm{Co}$	TOP (CD)	2.75-013	2.489+000	1.000	1.000	7.09-013	10.
	MID (CD)	2.92-013	2.489+000	1.000	1.000		
	BOT (CD)	2.88-013	2.489+000	1.000	1.000		

CD = Cadmium-Covered Dosimeter.
B = Bare Dosimeter.

TABLE 4.3.3.1.3.3

FERRET-SAND II RESULTS FOR MAINE YANKEE CAPSULE 263 (AVERAGE FOR CAPSULE)

GROUP	ENERGY (MeV)	A PRIORI FLUX* (n/cm^2·s)	ADJUSTED FLUX (n/cm^2·s)	% UNCERTAIN (1 σ)
1	1.492+001	2.391+006	2.863+006	40.
2	1.350+001	4.971+006	6.047+006	37.
3	1.162+001	2.305+007	2.832+007	33.
4	1.000+001	6.995+007	8.663+007	29.
5	8.607+000	1.770+008	2.188+008	25.
6	7.408+000	3.818+008	4.606+008	23.
7	6.065+000	1.059+009	1.238+009	20.
8	4.966+000	1.993+009	2.173+009	20.
9	3.679+000	3.554+009	3.619+009	20.
10	2.865+000	3.198+009	3.141+009	22.
11	2.231+000	6.688+009	6.353+009	21.
12	1.738+000	6.483+009	6.025+009	23.
13	1.353+000	7.847+009	7.131+009	27.
14	1.108+000	6.487+009	5.788+009	32.
15	8.208-001	9.778+009	8.625+009	36.
16	6.393-001	8.176+009	7.178+009	39.
17	4.979-001	7.863+009	6.908+009	43.
18	3.877-001	6.940+009	6.125+009	46.
19	3.020-001	6.087+009	5.410+009	48.
20	1.832-001	1.007+010	9.030+009	51.
21	1.111-001	8.081+009	7.306+009	52.
22	6.738-002	6.932+009	6.320+009	53.
23	4.087-002	6.202+009	5.697+009	54.
24	2.554-002	5.442+009	5.032+009	55.
25	1.989-002	2.827+009	2.628+009	55.
26	1.503-002	3.131+009	2.926+009	55.
27	9.119-003	5.487+009	5.152+009	54.
28	5.531-003	5.328+009	5.025+009	53.
29	3.355-003	5.138+009	4.868+009	52.
30	2.839-003	1.667+009	1.587+009	51.
31	2.404-003	1.648+009	1.576+009	49.
32	2.035-003	1.637+009	1.572+009	47.
33	1.234-003	4.892+009	4.722+009	44.
34	7.485-004	4.912+009	4.759+009	41.
35	4.540-004	4.944+009	4.803+009	38.
36	2.754-004	4.982+009	4.848+009	35.
37	1.670-004	5.056+009	4.917+009	33.
38	1.013-004	5.191+009	5.086+009	15.
39	6.144-005	5.364+009	5.170+009	30.
40	3.727-005	5.485+009	5.236+009	31.

TABLE 4.3.3.1.3.3 (Cont'd)

FERRET-SAND II RESULTS FOR MAINE YANKEE CAPSULE W263 (AVERAGE FOR CAPSULE)

GROUP	ENERGY (MeV)	A PRIORI FLUX* ($n/cm^2 \cdot s$)	ADJUSTED FLUX ($n/cm^2 \cdot s$)	% UNCERTAIN (1 σ)
41	2.260-005	5.544+009	5.225+009	33.
42	1.371-005	5.585+009	5.175+009	35.
43	8.315-006	5.607+009	5.090+009	38.
44	5.043-006	5.610+009	4.973+009	39.
45	3.059-006	5.593+009	4.829+009	40.
46	1.855-006	5.561+009	4.668+009	41.
47	1.125-006	5.468+009	4.460+009	40.
48	6.826-007	5.224+009	4.144+009	39.
49	4.140-007	5.069+009	3.920+009	37.
50	2.511-007	9.773+009	7.390+009	35.
51	1.523-007	3.796+010	2.813+010	33.
52	9.237-008	6.421+010	4.684+010	31.
53	1.000-010	1.394+011	9.831+010	23.
FLUX, E > 0.0 MeV		4.818+011	3.919+011	16.
FLUX, E < 0.414 eV		2.564+011	1.846+011	21.
FLUX, E > 0.1 MeV		9.642+010	8.818+010	25.
FLUX, E > 1.0 MeV		4.131+010	3.922+010	12.
dpa/s		6.175-011	5.831-011	14.
FLUENCE+, E > 1.0 MeV		5.973+018	5.671+018	12.
dpa+		8.930-003	8.432-003	14.

---

* ABSOLUTE CALCULATED FLUX (OR NORMALIZED TO Fe54(n,p)Mn54 REACTION RATE).

+ BASED ON 1.446+008 EFFECTIVE FULL POWER SECONDS OF EXPOSURE; UNITS OF n/cm^2 FOR FLUENCE AND TOTAL NUMBER OF DISPLACED ATOMS OF IRON PER TARGET ATOM OF IRON FOR dpa.

TABLE 4.3.3.1.3.4

COMPARISON OF MEASURED AND CALCULATED REACTION RATES USED IN THE ANALYSIS OF MAINE YANKEE CAPSULE W263

	REACTION RATE (DPS/NUCLEUS)			RATIO MEAS/CALC	
REACTION	MEAS	A PRIORI CALC	ADJ CALC	A PRIORI	ADJ CALC
U238(n,f)Cs137	1.57-014	1.60-014	1.57-014	.98	1.00
Ni58(n,p)Co58	5.50-015	5.16-015	5.41-015	1.07	1.02
Cu63(n,α)Co60	4.47-017	3.62-017	4.33-017	1.24	1.03
Co59(n,γ)Co60 (Cd)	7.09-013	7.44-013	7.05-013	.95	1.00
Co59(n,γ)Co60	4.73-012	6.74-012	4.99-012	.70	.95
Fe54(n,p)Mn54	4.00-015	4.01-015	4.19-015	1.00	.95
Ti46(n,p)Sc46	7.46-016	6.58-016	7.40-016	1.13	1.01

4.4 BABCOCK AND WILCOX SURVEILLANCE CAPSULES: SPECIFIC DETAILS

At present five capsules from Babcock and Wilcox plants have been reanalyzed. The a priori spectra were provided by C. L. Whitmarsh of Babcock and Wilcox. See Section 1.4.1 for further details.

The dosimetry information used to determine the exposures is summarized in one figure and four tables for each capsule reported. A general note explaining the number designation is in order. All tables are identified with Section 4 of this NUREG report. The second number designates the reactor plant vendor (W = 2, CE = 3, B&W = 4, and GE = 5). The third number delineates between generic designs of the vendor. For further discussion of specific vendor generic plants see Sections 1 through 3. The fourth number designates tabulated information for a specific plant, and the fifth number designates the specific capsule. The last number refers to the table or figure number for the specific capsule information.

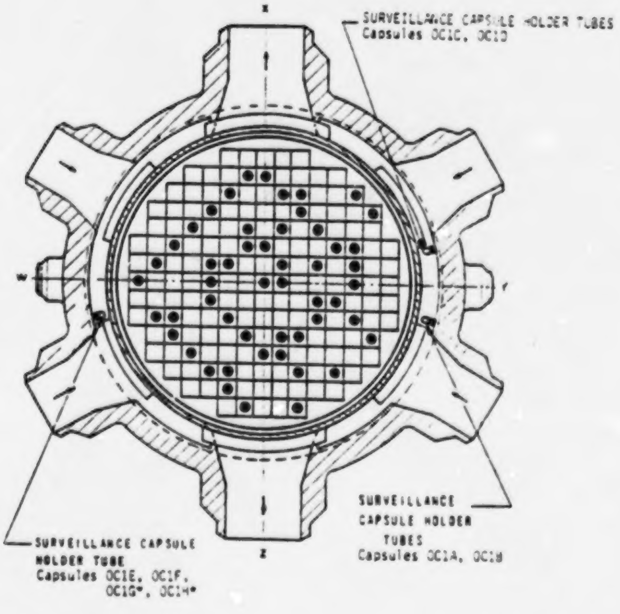
X
SURVEILLANCE CAPSULE HOLDER TUBES
Capsules OC1C, OC1D
W
Y
SURVEILLANCE CAPSULE HOLDER TUBE
Capsules OC1E, OC1F,
OC1G*, OC1H*
Z
SURVEILLANCE CAPSULE HOLDER TUBES
Capsules OC1A, OC1B

*Thermal aging capsules.

(a) Reactor Geometry.

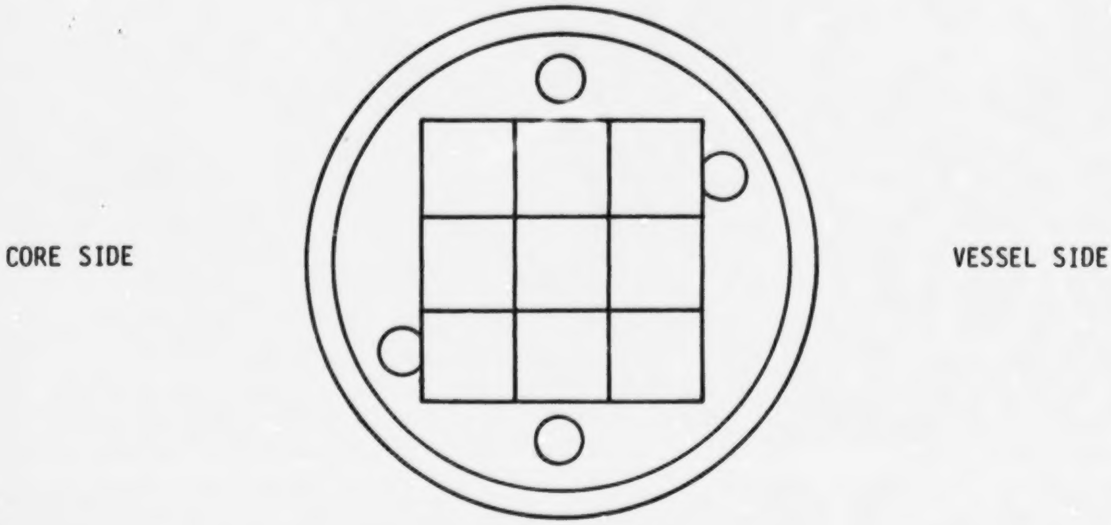
CORE SIDE
VESSEL SIDE

(b) Plan View of Surveillance Capsule.

FIGURE 4.4.1.1.1.1. Orientation of the Capsule Relative to the Core and Vessel Wall - Oconée Unit 1 Capsule F.

TABLE 4.4.1.1.1.1

SUMMARY OF REACTOR OPERATIONS
OCONEE UNIT 1 CAPSULE F

TIME PERIOD	START DATE	TIME INTERVAL	AVERAGE POWER LEVEL (MWt)	LOCAL POWER FACTOR
1	5/ 4/73	28.	282.	1.00
2	6/ 1/73	30.	693.	1.00
3	7/ 1/73	31.	1181.	1.00
4	8/ 1/73	31.	1130.	1.00
5	9/ 1/73	30.	1258.	1.00
6	10/ 1/73	31.	1746.	1.00
7	11/ 1/73	30.	1772.	1.00
8	12/ 1/73	31.	1284.	1.00
9	1/ 1/74	31.	1900.	1.00
10	2/ 1/74	28.	873.	1.00
11	3/ 1/74	31.	2157.	1.00
12	4/ 1/74	30.	2234.	1.00
13	5/ 1/74	31.	1977.	1.00
14	6/ 1/74	30.	77.	1.00
15	7/ 1/74	31.	1644.	1.00
16	8/ 1/74	31.	2363.	1.00
17	9/ 1/74	30.	2080.	1.00
18	10/ 1/74	18.	1592.	1.00
	10/19/74	DISCHARGED*		

---

*EFFECTIVE FULL POWER OPERATION TIME WAS 2.629+007 SECONDS AT A FULL POWER LEVEL OF 2568. MWt.

TABLE 4.4.1.1.1.2

REACTION RATE DATA AND CORRECTION FACTORS FOR OCONEE UNIT 1 CAPSULE F

REACTION		TOR RATE (DPS/NUCL)	SATURATION FACTOR	GRADIENT FACTOR	IMPURITY FACTOR	AVG REACTION RATE (RPS/NUCL)	% UNCERT (1σ)
NAME	IDENT						
$^{54}Fe(n,p)^{54}Mn$	FD5	1.34-015	2.366+000	0.847	1.000	2.56-015	10.
	FD6	9.70-016	2.366+000	1.000	1.000		
	FD7	1.09-015	2.366+000	1.000	1.000		
	FD8	9.61-016	2.366+000	1.181	1.000		
$^{58}Ni(n,p)^{58}Co$	FD5	3.46-015	1.475+000	0.768	1.000	3.90-015	10.
	FD6	2.64-015	1.475+000	1.000	1.000		
	FD7	2.61-015	1.475+000	1.000	1.000		
	FD8	2.04-015	1.475+000	1.303	1.000		
$^{137}Np(n,f)^{103}Ru$	FD5	5.94-015	1.409+000	0.771	1.000	1.12-013	10.
	FD6	4.17-015	1.409+000	1.000	1.000		
	FD7	4.41-015	1.409+000	1.000	1.000		
	FD8	3.53-015	1.409+000	1.297	1.000		
$^{237}Np(n,f)^{137}Cs$	FD5	1.59-016	5.303+001	0.765	1.000	9.97-014	10.
	FD6	1.13-016	5.303+001	1.000	1.000		
	FD7	1.16-016	5.303+001	1.000	1.000		
	FD8	9.29-017	5.303+001	1.307	1.000		
$^{237}Np(n,f)^{141}Ce$	FD5	3.90-015	1.397+000	0.743	1.000	7.26-014	10.
	FD6	2.65-015	1.397+000	1.000	1.000		
	FD7	2.85-015	1.397+000	1.000	1.000		
	FD8	2.16-015	1.397+000	1.345	1.000		
$^{237}Np(n,f)^{144}Ce$	FD5	2.21-015	2.244+000	0.767	1.000	8.68-014	10.
	FD6	1.50-015	2.244+000	1.000	1.000		
	FD7	1.60-015	2.244+000	1.000	1.000		
	FD8	1.30-015	2.244+000	1.303	1.000		

TABLE 4.4.1.1.1.2 (Cont'd)

REACTION RATE DATA AND CORRECTION FACTORS FOR
OCONEE UNIT 1 CAPSULE F

REACTION NAME	IDENT	TOR RATE (DPS/NUCL)	SATURATION FACTOR	GRADIENT FACTOR	IMPURITY FACTOR	AVG REACTION RATE (RPS/NUCL)	% UNCERT (1σ)
$^{238}U(n,f)^{137}Cs$	FD5	9.96-018	5.303+001	1.254	0.971	1.39-014	31.
	FD6	1.68-017	5.303+001	1.000	0.971		
	FD7	2.30-017	5.303+001	1.000	0.971		
	FD8	1.57-017	5.303+001	0.798	0.971		
$^{238}U(n,f)^{103}Ru$	FD5	1.27-015	1.409+000	0.762	0.971	2.17-014	10.
	FD6	9.96-016	1.409+000	1.000	0.971		
	FD7	1.01-015	1.409+000	1.000	0.971		
	FD8	7.39-016	1.409+000	1.312	0.971		
$^{238}U(n,f)^{141}Ce$	FD5	8.34-016	1.397+000	0.764	0.971	1.60-014	10.
	FD6	6.48-016	1.397+000	1.000	0.971		
	FD7	6.52-016	1.397+000	1.000	0.971		
	FD8	4.86-016	1.397+000	1.310	0.971		
$^{238}U(n,f)^{144}Ce$	FD5	4.82-016	2.244+000	0.773	0.971	1.80-014	10.
	FD6	3.78-016	2.244+000	1.000	0.971		
	FD7	3.79-016	2.244+000	1.000	0.971		
	FD8	2.88-016	2.244+000	1.294	0.971		
$^{59}Co(n,\gamma)^{60}Co$	FD5 (CD)	2.69-014	9.909+000	0.833	1.000	2.16-013	10.
	FD6 (CD)	2.15-014	9.909+000	1.000	1.000		
	FD7 (CD)	2.09-014	9.909+000	1.000	1.000		
	FD8 (CD)	1.87-014	9.909+000	1.200	1.000		
$^{59}Co(n,\gamma)^{60}Co$	FD5 (B)	1.71-013	9.909+000	0.657	1.000	1.10-012	10.
	FD6 (B)	1.11-013	9.909+000	1.000	1.000		
	FD7 (B)	1.09-013	9.909+000	1.000	1.000		
	FD8 (B)	7.39-014	9.909+000	1.522	1.000		

CD = Cadmium-Covered Dosimeter.
B = Bare Dosimeter.

TABLE 4.4.1.1.1.3

FERRET-SAND II RESULTS FOR OCONEE UNIT 1 CAPSULE F (AVERAGE FOR CAPSULE)

GROUP	ENERGY (MeV)	A PRIORI FLUX* (n/cm^2·s)	ADJUSTED FLUX (n/cm^2·s)	% UNCERTAIN (1 σ)
1	1.492+001	2.683+006	2.523+006	48.
2	1.350+001	5.579+006	5.218+006	45.
3	1.162+001	2.737+007	2.548+007	42.
4	1.000+001	8.747+007	8.113+007	38.
5	8.607+000	2.137+008	1.977+008	34.
6	7.408+000	3.589+008	3.318+008	30.
7	6.065+000	9.711+008	8.970+008	25.
8	4.966+000	1.447+009	1.337+009	22.
9	3.679+000	2.328+009	2.167+009	20.
10	2.865+000	2.229+009	2.089+009	24.
11	2.231+000	4.819+009	4.590+009	28.
12	1.738+000	4.724+009	4.528+009	33.
13	1.353+000	4.876+009	4.707+009	37.
14	1.108+000	3.916+009	3.795+009	41.
15	8.208-001	5.411+009	5.270+009	44.
16	6.393-001	4.036+009	3.946+009	47.
17	4.979-001	3.602+009	3.531+009	49.
18	3.877-001	3.180+009	3.121+009	51.
19	3.020-001	2.802+009	2.751+009	53.
20	1.832-001	4.626+009	4.539+009	54.
21	1.111-001	3.605+009	3.531+009	54.
22	6.738-002	2.894+009	2.827+009	55.
23	4.087-002	2.414+009	2.351+009	55.
24	2.554-002	2.020+009	1.959+009	55.
25	1.989-002	1.034+009	9.981+008	55.
26	1.503-002	1.141+009	1.094+009	55.
27	9.119-003	1.984+009	1.889+009	54.
28	5.531-003	1.904+009	1.796+009	54.
29	3.355-003	1.809+009	1.689+009	53.
30	2.839-003	5.800+008	5.352+008	51.
31	2.404-003	5.703+008	5.195+008	49.
32	2.035-003	5.639+008	5.067+008	47.
33	1.234-003	1.679+009	1.488+009	44.
34	7.485-004	1.690+009	1.479+009	41.
35	4.540-004	1.712+009	1.481+009	38.
36	2.754-004	1.745+009	1.497+009	35.
37	1.670-004	1.792+009	1.528+009	33.
38	1.013-004	1.853+009	1.533+009	15.
39	6.144-005	1.914+009	1.637+009	30.
40	3.727-005	1.913+009	1.651+009	31.

TABLE 4.4.1.1.1.3 (Cont'd)

FERRET-SAND II RESULTS FOR OCONEE UNIT 1 CAPSULE F (AVERAGE FOR CAPSULE)

GROUP	ENERGY (MeV)	A PRIORI FLUX* ($n/cm^2 \cdot s$)	ADJUSTED FLUX ($n/cm^2 \cdot s$)	% UNCERTAIN ($1\ \sigma$)
41	2.260-005	1.835+009	1.607+009	33.
42	1.371-005	1.740+009	1.552+009	35.
43	8.315-006	1.684+009	1.537+009	37.
44	5.043-006	1.655+009	1.552+009	39.
45	3.059-006	1.642+009	1.585+009	40.
46	1.855-006	1.627+009	1.619+009	40.
47	1.125-006	1.548+009	1.589+009	39.
48	6.826-007	1.415+009	1.497+009	37.
49	4.140-007	1.370+009	1.489+009	35.
50	2.511-007	1.737+009	1.937+009	33.
51	1.523-007	4.958+009	5.649+009	30.
52	9.237-008	7.985+009	9.256+009	27.
53	1.000-010	1.654+010	1.978+010	16.
FLUX, E > 0.0 MeV		1.302+011	1.305+011	17.
FLUX, E < 0.414 eV		3.259+010	3.811+010	13.
FLUX, E > 0.1 MeV		5.388+010	5.204+010	30.
FLUX, E > 1.0 MeV		2.785+010	2.656+010	21.
dpa/s		3.818-011	3.647-011	19.
FLUENCE+, E > 1.0 MeV		7.323+017	6.981+017	21.
dpa+		1.004-003	9.588-004	19.

---

* ABSOLUTE CALCULATED FLUX (OR NORMALIZED TO Fe54(n,p)Mn54 REACTION RATE).

+ BASED ON 2.629+007 EFFECTIVE FULL POWER SECONDS OF EXPOSURE; UNITS OF n/cm^2 FOR FLUENCE AND TOTAL NUMBER OF DISPLACED ATOMS OF IRON PER TARGET ATOM OF IRON FOR dpa.

TABLE 4.4.1.1.1.4

COMPARISON OF MEASURED AND CALCULATED REACTION RATES USED IN THE ANALYSIS OF OCONEE UNIT 1 CAPSULE F

	REACTION RATE (DPS/NUCLEUS)			RATIO MEAS/CALC	
REACTION	MEAS	A PRIORI CALC	ADJ CALC	A PRIORI	ADJ CALC
Fe54(n,p)Mn54	2.56-015	2.95-015	2.73-015	.87	.94
Ni58(n,p)Co58	3.90-015	3.85-015	3.68-015	1.01	1.06
Co59(n,γ)Co60 (Cd)	2.16-013	2.54-013	2.18-013	.85	.99
Co59(n,γ)Co60	1.10-012	9.93-013	1.09-012	1.11	1.01
*Np237(n,f)FP Cd	9.97-014	6.04-014	5.78-014	1.65	1.72
*U238(n,f)FP Cd	1.39-014	1.18-014	1.11-014	1.18	1.25

* REACTION NOT USED TO ADJUST SPECTRUM

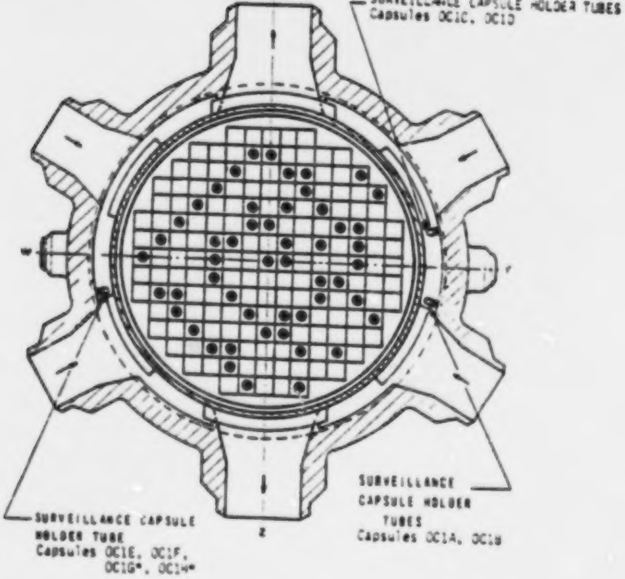
X
W
Y
Z
SURVEILLANCE CAPSULE HOLDER TUBES
Capsules OC1C, OC1D
SURVEILLANCE CAPSULE HOLDER TUBE
Capsules OC1E, OC1F,
OC1G*, OC1H*
SURVEILLANCE CAPSULE HOLDER TUBES
Capsules OC1A, OC1B

*Thermal aging capsules.

(a) Reactor Geometry.

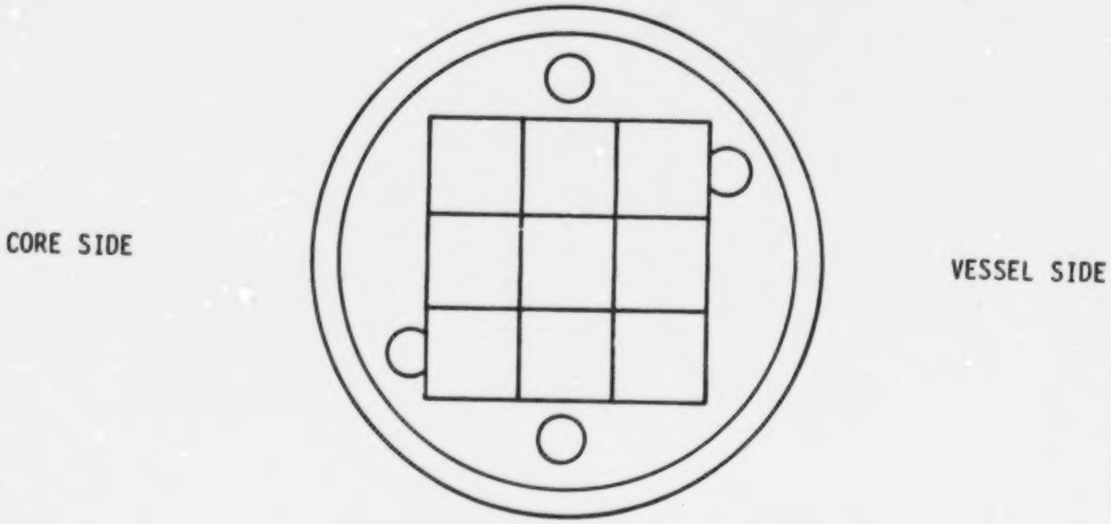
CORE SIDE
VESSEL SIDE

(b) Plan View of Surveillance Capsule.

FIGURE 4.4.1.1.2.1. Orientation of the Capsule Relative to the Core and Vessel Wall - Oconee Unit 1 Capsule E.

376

TABLE 4.4.1.1.2.1

SUMMARY OF REACTOR OPERATIONS
OCONEE UNIT 1 CAPSULE E

TIME PERIOD	START DATE	TIME INTERVAL	AVERAGE POWER LEVEL (MWt)	LOCAL POWER FACTOR
1	5/ 4/73	28.	282.	1.00
2	6/ 1/73	30.	693.	1.00
3	7/ 1/73	31.	1181.	1.00
4	8/ 1/73	31.	1130.	1.00
5	9/ 1/73	30.	1258.	1.00
6	10/ 1/73	31.	1746.	1.00
7	11/ 1/73	30.	1772.	1.00
8	12/ 1/73	31.	1284.	1.00
9	1/ 1/74	31.	1900.	1.00
10	2/ 1/74	28.	873.	1.00
11	3/ 1/74	31.	2157.	1.00
12	4/ 1/74	30.	2234.	1.00
13	5/ 1/74	31.	1977.	1.00
14	6/ 1/74	30.	77.	1.00
15	7/ 1/74	31.	1644.	1.00
16	8/ 1/74	31.	2363.	1.00
17	9/ 1/74	30.	2080.	1.00
18	10/ 1/74	18.	1592.	1.00
19	10/19/74	143.	0.	1.00
20	3/11/75	21.	1618.	1.00
21	4/ 1/75	30.	2183.	1.00
22	5/ 1/75	31.	2491.	1.00
23	6/ 1/75	30.	2414.	1.00
24	7/ 1/75	31.	1977.	1.00
25	8/ 1/75	31.	2260.	1.00
26	9/ 1/75	30.	2542.	1.00
27	10/ 1/75	31.	2568.	1.00
28	11/ 1/75	30.	2363.	1.00
29	12/ 1/75	31.	2131.	1.00
30	1/ 1/76	31.	2234.	1.00
31	2/ 1/76	7.	2517.	1.00
	2/ 8/76	DISCHARGED*		

---

*EFFECTIVE FULL POWER OPERATION TIME WAS 5.186+007 SECONDS AT A FULL POWER LEVEL OF 2568. MWt.

TABLE 4.4.1.1.2.2

REACTION RATE DATA AND CORRECTION FACTORS FOR OCONEE UNIT 1 CAPSULE E

REACTION NAME	REACTION IDENT	TOR RATE (DPS/NUCL)	SATURATION FACTOR	GRADIENT FACTOR	IMPURITY FACTOR	AVG REACTION RATE (RPS/NUCL)	% UNCERT (1σ)
$^{238}U(n,f)^{95}Zr$	ED1	6.21-016	1.141+000	1.000	0.971	1.40-014	10.
	ED2	8.34-016	1.141+000	0.773	0.971		
	ED3	4.98-016	1.141+000	1.294	0.971		
	ED4	6.72-016	1.141+000	1.000	0.971		
$^{238}U(n,f)^{103}Ru$	ED1	7.31-016	1.121+000	1.000	0.971	1.32-014	10.
	ED2	9.84-016	1.121+000	0.766	0.971		
	ED3	5.77-016	1.121+000	1.306	0.971		
	ED4	7.83-016	1.121+000	1.000	0.971		
$^{238}U(n,f)^{137}Cs$	ED1	2.72-017	2.723+001	1.000	0.971	1.25-014	10.
	ED2	2.91-017	2.723+001	0.930	0.971		
	ED3	2.51-017	2.723+001	1.076	0.971		
	ED4	3.22-017	2.723+001	1.000	0.971		
$^{238}U(n,f)^{141}Ce$	ED1	5.49-016	1.121+000	1.000	0.971	1.15-014	10.
	ED2	7.35-016	1.121+000	0.786	0.971		
	ED3	4.55-016	1.121+000	1.272	0.971		
	ED4	6.01-016	1.121+000	1.000	0.971		
$^{237}Np(n,f)^{95}Zr$	ED1	3.70-015	1.141+000	1.000	1.000	7.21-014	10.
	ED2	4.33-015	1.141+000	0.810	1.000		
	ED3	2.84-015	1.141+000	1.234	1.000		
	ED4	3.68-015	1.141+000	1.000	1.000		
$^{137}Np(n,f)^{103}Ru$	ED1	3.81-015	1.121+000	1.000	1.000	7.35-014	10.
	ED2	4.41-015	1.121+000	0.811	1.000		
	ED3	2.90-015	1.121+000	1.234	1.000		
	ED4	3.68-015	1.121+000	1.000	1.000		

TABLE 4.4.1.1.2.2 (Cont'd)

REACTION RATE DATA AND CORRECTION FACTORS FOR
OCONEE UNIT 1 CAPSULE E

REACTION NAME	IDENT	TOR RATE (DPS/NUCL)	SATURATION FACTOR	GRADIENT FACTOR	IMPURITY FACTOR	AVG REACTION RATE (RPS/NUCL)	% UNCERT (1σ)
^{237}Np(n,f)^{137}Cs	ED1	1.22-016	2.723+001	1.000	1.000	5.89-014	13.
	ED2	1.41-016	2.723+001	0.918	1.000		
	ED3	1.18-016	2.723+001	1.089	1.000		
	ED4	1.62-016	2.723+001	1.000	1.000		
^{237}Np(n,f)^{141}Ce	ED1	3.74-015	1.121+000	1.000	1.000	7.51-014	10.
	ED2	4.37-015	1.121+000	0.823	1.000		
	ED3	2.96-015	1.121+000	1.216	1.000		
	ED4	3.66-015	1.121+000	1.000	1.000		
^{58}Ni(n,p)^{58}Co	ED1	3.48-015	1.151+000	1.000	1.000	3.98-015	10.
	ED2	4.32-015	1.151+000	0.784	1.000		
	ED3	2.66-015	1.151+000	1.276	1.000		
	ED4	3.59-015	1.151+000	1.000	1.000		
^{54}Fe(n,p)^{54}Mn	ED1	1.81-015	1.631+000	1.000	1.000	2.97-015	10.
	ED2	2.10-015	1.631+000	0.853	1.000		
	ED3	1.52-015	1.631+000	1.173	1.000		
	ED4	1.89-015	1.631+000	1.000	1.000		
^{59}Co(n,γ)^{60}Co	ED1 (CD)	3.43-014	5.389+000	1.000	1.000	1.93-013	10.
	ED2 (CD)	3.84-014	5.389+000	0.946	1.000		
	ED3 (CD)	3.43-014	5.389+000	1.057	1.000		
	ED4 (CD)	3.60-014	5.389+000	1.000	1.000		
^{59}Co(n,γ)^{60}Co	ED1 (B)	2.65-013	5.389+000	1.000	1.000	1.41-012	10.
	ED2 (B)	2.95-013	5.389+000	0.849	1.000		
	ED3 (B)	2.12-013	5.389+000	1.178	1.000		
	ED4 (B)	2.84-013	5.389+000	1.000	1.000		

CD = Cadmium-Covered Dosimeter.
B = Bare Dosimeter.

TABLE 4.4.1.1.2.3

FERRET-SAND II RESULTS FOR OCONEE UNIT 1 CAPSULE E (AVERAGE FOR CAPSULE)

GROUP	ENERGY (MeV)	A PRIORI FLUX* ($n/cm^2 \cdot s$)	ADJUSTED FLUX ($n/cm^2 \cdot s$)	% UNCERTAIN ($1\ \sigma$)
1	1.492+001	3.686+006	3.279+006	47.
2	1.350+001	7.664+006	6.819+006	44.
3	1.162+001	3.710+007	3.312+007	41.
4	1.000+001	1.115+008	1.003+008	37.
5	8.607+000	2.493+008	2.268+008	33.
6	7.408+000	4.215+008	3.892+008	29.
7	6.065+000	1.004+009	9.397+008	25.
8	4.966+000	1.540+009	1.459+009	22.
9	3.679+000	2.635+009	2.555+009	20.
10	2.865+000	2.402+009	2.413+009	22.
11	2.231+000	4.490+009	4.713+009	22.
12	1.738+000	4.452+009	4.785+009	23.
13	1.353+000	4.840+009	5.176+009	24.
14	1.108+000	3.943+009	4.105+009	28.
15	8.208-001	5.541+009	5.710+009	29.
16	6.393-001	4.268+009	4.365+009	33.
17	4.979-001	3.907+009	3.950+009	36.
18	3.877-001	3.522+009	3.511+009	40.
19	3.020-001	3.168+009	3.107+009	43.
20	1.832-001	5.377+009	5.187+009	46.
21	1.111-001	4.297+009	4.080+009	48.
22	6.738-002	3.450+009	3.226+009	50.
23	4.087-002	2.857+009	2.634+009	52.
24	2.554-002	2.379+009	2.162+009	53.
25	1.989-002	1.216+009	1.090+009	53.
26	1.503-002	1.343+009	1.183+009	54.
27	9.119-003	2.343+009	2.025+009	53.
28	5.531-003	2.257+009	1.907+009	53.
29	3.355-003	2.156+009	1.775+009	52.
30	2.839-003	6.944+008	5.546+008	51.
31	2.404-003	6.840+008	5.283+008	49.
32	2.035-003	6.771+008	5.046+008	47.
33	1.234-003	2.016+009	1.449+009	45.
34	7.485-004	2.028+009	1.408+009	42.
35	4.540-004	2.054+009	1.382+009	39.
36	2.754-004	2.093+009	1.374+009	36.
37	1.670-004	2.150+009	1.386+009	33.
38	1.013-004	2.224+009	1.317+009	17.
39	6.144-005	2.297+009	1.476+009	30.
40	3.727-005	2.295+009	1.501+009	31.

TABLE 4.4.1.1.2.3 (Cont'd)

FERRET-SAND II RESULTS FOR
OCONEE UNIT 1 CAPSULE E
(AVERAGE FOR CAPSULE)

GROUP	ENERGY (MeV)	A PRIORI FLUX* ($n/cm^2 \cdot s$)	ADJUSTED FLUX ($n/cm^2 \cdot s$)	% UNCERTAIN (1 σ)
41	2.260-005	2.203+009	1.484+009	33.
42	1.371-005	2.088+009	1.464+009	34.
43	8.315-006	2.020+009	1.490+009	36.
44	5.043-006	1.986+009	1.553+009	38.
45	3.059-006	1.970+009	1.643+009	39.
46	1.855-006	1.952+009	1.742+009	39.
47	1.125-006	1.857+009	1.774+009	39.
48	6.826-007	1.698+009	1.733+009	37.
49	4.140-007	1.643+009	1.786+009	35.
50	2.511-007	2.085+009	2.404+009	33.
51	1.523-007	5.949+009	7.217+009	30.
52	9.237-008	9.582+009	1.211+010	28.
53	1.000-010	1.985+010	2.690+010	18.
FLUX, E > 0.0 MeV		1.483+011	1.490+011	13.
FLUX, E < 0.414 eV		3.911+010	5.042+010	15.
FLUX, E > 0.1 MeV		5.694+010	5.749+010	18.
FLUX, E > 1.0 MeV		2.803+010	2.886+010	10.
dpa/s		3.967-011	4.011-011	10.
FLUENCE+, E > 1.0 MeV		1.454+018	1.497+018	10.
dpa+		2.057-003	2.080-003	10.

---

* ABSOLUTE CALCULATED FLUX (OR NORMALIZED TO Fe54(n,p)Mn54 REACTION RATE).

+ BASED ON 5.186+007 EFFECTIVE FULL POWER SECONDS OF EXPOSURE; UNITS OF n/cm^2 FOR FLUENCE AND TOTAL NUMBER OF DISPLACED ATOMS OF IRON PER TARGET ATOM OF IRON FOR dpa.

TABLE 4.4.1.1.2.4

COMPARISON OF MEASURED AND CALCULATED REACTION RATES USED IN THE ANALYSIS OF OCONEE UNIT 1 CAPSULE E

REACTION	REACTION RATE (DPS/NUCLEUS)			RATIO MEAS/CALC	
	MEAS	A PRIORI CALC	ADJ CALC	A PRIORI	ADJ CALC
Np237(n,f)Cs137	5.89-014	6.02-014	6.05-014	.98	.97
U238(n,f)Cs137	1.25-014	1.16-014	1.19-014	1.07	1.05
Ni58(n,p)Co58	3.98-015	4.11-015	4.00-015	.97	1.00
Fe54(n,p)Mn54	2.97-015	3.16-015	3.06-015	.94	1.00
Co59(n,γ)Co60 (Cd)	1.93-013	3.05-013	1.98-013	.63	.97
Co59(n,γ)Co60	1.41-012	1.19-012	1.36-012	1.18	1.04

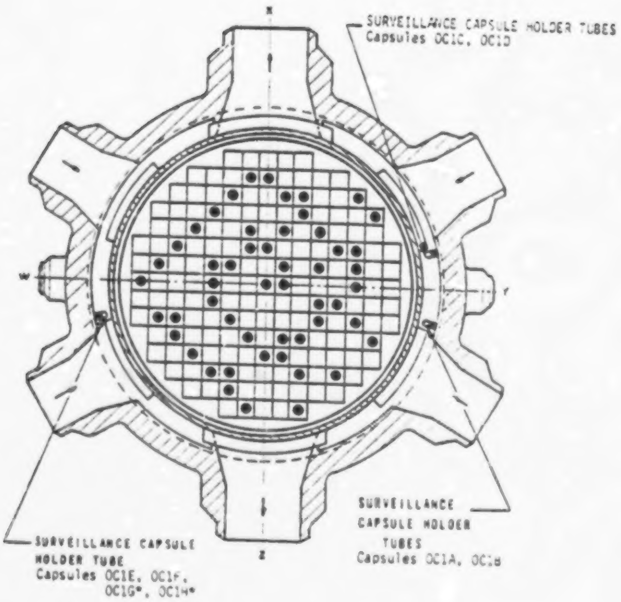
X
SURVEILLANCE CAPSULE HOLDER TUBES
Capsules OC1C, OC1D
W
Y
Z
SURVEILLANCE CAPSULE HOLDER TUBE
Capsules OC1E, OC1F, OC1G*, OC1H*
SURVEILLANCE CAPSULE HOLDER TUBES
Capsules OC1A, OC1B

*Thermal aging capsules.

(a) Reactor Geometry.

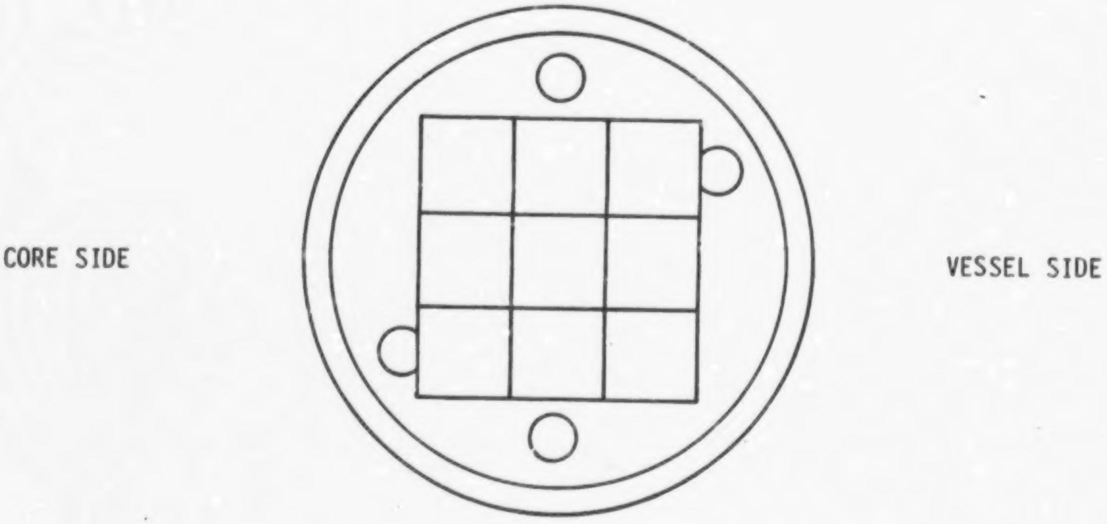
CORE SIDE
VESSEL SIDE

(b) Plan View of Surveillance Capsule.

FIGURE 4.4.1.2.1.1. Orientation of the Capsule Relative to the Core and Vessel Wall - Oconee Unit 2 Capsule C.

TABLE 4.4.1.2.1.1

SUMMARY OF REACTOR OPERATIONS
OCONEE UNIT 2 CAPSULE C

TIME PERIOD	START DATE	TIME INTERVAL	AVERAGE POWER LEVEL (MWt)	LOCAL POWER FACTOR
1	12/ 6/73	26.	976.	1.00
2	1/ 1/74	31.	154.	1.00
3	2/ 1/74	28.	0.	1.00
4	3/ 1/74	31.	0.	1.00
5	4/ 1/74	30.	0.	1.00
6	5/ 1/74	31.	282.	1.00
7	6/ 1/74	30.	1669.	1.00
8	7/ 1/74	31.	539.	1.00
9	8/ 1/74	31.	26.	1.00
10	9/ 1/74	30.	1284.	1.00
11	10/ 1/74	31.	565.	1.00
12	11/ 1/74	30.	2363.	1.00
13	12/ 1/74	31.	1669.	1.00
14	1/ 1/75	31.	1438.	1.00
15	2/ 1/75	28.	0.	1.00
16	3/ 1/75	31.	1592.	1.00
17	4/ 1/75	30.	1926.	1.00
18	5/ 1/75	31.	2260.	1.00
19	6/ 1/75	30.	2234.	1.00
20	7/ 1/75	31.	1823.	1.00
21	8/ 1/75	31.	1772.	1.00
22	9/ 1/75	30.	1130.	1.00
23	10/ 1/75	31.	1900.	1.00
24	11/ 1/75	30.	2260.	1.00
25	12/ 1/75	31.	2542.	1.00
26	1/ 1/76	31.	2388.	1.00
27	2/ 1/76	29.	1566.	1.00
28	3/ 1/76	31.	2363.	1.00
29	4/ 1/76	7.	1772.	1.00
	4/ 8/76	DISCHARGED*		

---

*EFFECTIVE FULL POWER OPERATION TIME WAS 3.802+007 SECONDS AT A FULL POWER LEVEL OF 2568. MWt.

384

TABLE 4.4.1.2.1.2

REACTION RATE DATA AND CORRECTION FACTORS FOR OCONEE UNIT 2 CAPSULE C

REACTION NAME	IDENT	TOR RATE (DPS/NUCL)	SATURATION FACTOR	GRADIENT FACTOR	IMPURITY FACTOR	AVG REACTION RATE (RPS/NUCL)	% UNCERT (1σ)
$^{54}Fe(n,p)^{54}Mn$	CD1	1.50-015	1.833+000	1.000	1.000	2.62-015	10.
	CD2	1.53-015	1.833+000	1.000	1.000		
	CD3	1.70-015	1.833+000	0.791	1.000		
	CD4	1.07-015	1.833+000	1.264	1.000		
$^{58}Ni(n,p)^{58}Co$	CD1	2.76-015	1.248+000	1.000	1.000	3.37-015	10.
	CD2	2.82-015	1.248+000	1.000	1.000		
	CD3	3.48-015	1.248+000	0.750	1.000		
	CD4	1.96-015	1.248+000	1.333	1.000		
$^{58}Fe(n,\gamma)^{59}Fe$	CD1	4.64-014	1.223+000	1.000	1.000	5.29-014	14.
	CD2	5.02-014	1.223+000	1.000	1.000		
	CD3	6.05-014	1.223+000	0.630	1.000		
	CD4	2.40-014	1.223+000	1.586	1.000		
$^{237}Np(n,f)^{95}Zr$	CD1	2.72-015	1.240+000	1.000	1.000	5.66-014	10.
	CD2	2.46-015	1.240+000	1.000	1.000		
	CD3	3.32-015	1.240+000	0.786	1.000		
	CD4	2.05-015	1.240+000	1.272	1.000		
$^{137}Np(n,f)^{103}Ru$	CD1	2.68-015	1.221+000	1.000	1.000	5.74-014	10.
	CD2	2.49-015	1.221+000	1.000	1.000		
	CD3	3.41-015	1.221+000	0.782	1.000		
	CD4	2.08-015	1.221+000	1.279	1.000		
$^{237}Np(n,f)^{137}Cs$	CD1	9.90-017	3.683+001	1.000	1.000	5.94-014	16.
	CD2	7.94-017	3.683+001	1.000	1.000		
	CD3	1.14-016	3.683+001	0.987	1.000		
	CD4	1.12-016	3.683+001	1.013	1.000		

TABLE 4.4.1.2.1.2 (Cont'd)

REACTION RATE DATA AND CORRECTION FACTORS FOR OCONEE UNIT 2 CAPSULE C

REACTION NAME	REACTION IDENT	TOR RATE (DPS/NUCL)	SATURATION FACTOR	GRADIENT FACTOR	IMPURITY FACTOR	AVG REACTION RATE (RPS/NUCL)	% UNCERT (1σ)
$^{237}Np(n,f)^{141}Ce$	CD1	1.94-015	1.220+000	1.000	1.000	4.12-014	10.
	CD2	1.72-015	1.220+000	1.000	1.000		
	CD3	2.40-015	1.220+000	0.768	1.000		
	CD4	1.42-015	1.220+000	1.302	1.000		
$^{237}Np(n,f)^{144}Ce$	CD1	1.31-015	1.751+000	1.000	1.000	4.96-014	10.
	CD2	1.07-015	1.751+000	1.000	1.000		
	CD3	1.51-015	1.751+000	0.786	1.000		
	CD4	9.36-016	1.751+000	1.272	1.000		
$^{237}Np(n,f)^{106}Ru$	CD1	1.44-015	1.999+000	1.000	1.000	1.15-013	14.
	CD2	1.47-015	1.999+000	1.000	1.000		
	CD3	1.29-015	1.999+000	0.879	1.000		
	CD4	9.96-016	1.999+000	1.138	1.000		
$^{238}U(n,f)^{95}Zr$	CD1	5.22-016	1.240+000	1.000	0.971	1.10-014	12.
	CD2	5.12-016	1.240+000	1.000	0.971		
	CD3	5.54-016	1.240+000	0.753	0.971		
	CD4	3.14-016	1.240+000	1.328	0.971		
$^{238}U(n,f)^{103}Ru$	CD1	6.27-016	1.221+000	1.000	0.971	1.06-014	14.
	CD2	6.23-016	1.221+000	1.000	0.971		
	CD3	6.70-016	1.221+000	0.728	0.971		
	CD4	3.55-016	1.221+000	1.373	0.971		
$^{238}U(n,f)^{137}Cs$	CD1	1.86-017	3.683+001	1.000	0.971	1.11-014	10.
	CD2	1.87-017	3.683+001	1.000	0.971		
	CD3	1.99-017	3.683+001	0.943	0.971		
	CD4	1.77-017	3.683+001	1.060	0.971		

TABLE 4.4.1.2.1.2 (Cont'd)

REACTION RATE DATA AND CORRECTION FACTORS FOR OCONEE UNIT 2 CAPSULE C

REACTION NAME	IDENT	TOR RATE (DPS/NUCL)	SATURATION FACTOR	GRADIENT FACTOR	IMPURITY FACTOR	AVG REACTION RATE (RPS/NUCL)	% UNCERT (1σ)
$^{238}U(n,f)^{141}Ce$	CD1	4.75-016	1.220+000	1.000	0.971	9.02-015	16.
	CD2	4.68-016	1.220+000	1.000	0.971		
	CD3	5.08-016	1.220+000	0.708	0.971		
	CD4	2.54-016	1.220+000	1.412	0.971		
$^{238}U(n,f)^{144}Ce$	CD1	3.01-016	1.751+000	1.000	0.971	1.02-014	10.
	CD2	2.84-016	1.751+000	1.000	0.971		
	CD3	3.22-016	1.751+000	0.780	0.971		
	CD4	1.96-016	1.751+000	1.281	0.971		
$^{238}U(n,f)^{106}Ru$	CD1	2.40-016	1.999+000	1.000	0.971	1.38-014	29.
	CD2	2.03-016	1.999+000	1.000	0.971		
	CD3	1.76-016	1.999+000	0.776	0.971		
	CD4	1.06-016	1.999+000	1.289	0.971		
$^{59}Co(n,\gamma)^{60}Co$	CD2 (CD)	1.50-013	7.022+000	1.000	1.000	8.27-013	19.
	CD3 (CD)	9.78-014	7.022+000	1.000	1.000		
	CD4 (CD)	2.09-013	7.022+000	0.535	1.000		
	CD1 (CD)	5.97-014	7.022+000	1.868	1.000		
$^{59}Co(n,\gamma)^{60}Co$	CD1 (B)	1.86-013	7.022+000	1.000	1.000	1.21-012	10.
	CD2 (B)	1.89-013	7.022+000	1.000	1.000		
	CD3 (B)	2.34-013	7.022+000	0.673	1.000		
	CD4 (B)	1.06-013	7.022+000	1.486	1.000		

CD = Cadmium-Covered Dosimeter.
B = Bare Dosimeter.

387

TABLE 4.4.1.2.1.3

FERRET-SAND II RESULTS FOR
OCONEE UNIT 2 CAPSULE C
(AVERAGE FOR CAPSULE)

GROUP	ENERGY (MeV)	A PRIORI FLUX* (n/cm^2•s)	ADJUSTED FLUX (n/cm^2•s)	% UNCERTAIN (1 σ)
1	1.492+001	3.072+006	3.584+006	47.
2	1.350+001	6.387+006	7.165+006	44.
3	1.162+001	3.091+007	3.341+007	41.
4	1.000+001	9.293+007	9.716+007	37.
5	8.607+000	2.078+008	2.114+008	33.
6	7.408+000	3.513+008	3.511+008	29.
7	6.065+000	8.369+008	8.224+008	25.
8	4.966+000	1.283+009	1.256+009	22.
9	3.679+000	2.196+009	2.179+009	20.
10	2.865+000	2.001+009	2.094+009	23.
11	2.231+000	3.741+009	4.151+009	22.
12	1.738+000	3.710+009	4.371+009	23.
13	1.353+000	4.033+009	4.938+009	24.
14	1.108+000	3.286+009	4.108+009	28.
15	8.208-001	4.617+009	5.985+009	29.
16	6.393-001	3.557+009	4.783+009	32.
17	4.979-001	3.255+009	4.522+009	36.
18	3.877-001	2.935+009	4.191+009	39.
19	3.020-001	2.640+009	3.857+009	42.
20	1.832-001	4.481+009	6.680+009	45.
21	1.111-001	3.581+009	5.438+009	47.
22	6.738-002	2.875+009	4.446+009	49.
23	4.087-002	2.381+009	3.757+009	51.
24	2.554-002	1.982+009	3.200+009	52.
25	1.989-002	1.014+009	1.679+009	53.
26	1.503-002	1.119+009	1.913+009	53.
27	9.119-003	1.952+009	3.475+009	53.
28	5.531-003	1.881+009	3.482+009	53.
29	3.355-003	1.797+009	3.472+009	52.
30	2.839-003	5.787+008	1.174+009	51.
31	2.404-003	5.700+008	1.216+009	49.
32	2.035-003	5.642+008	1.264+009	47.
33	1.234-003	1.680+009	3.938+009	45.
34	7.485-004	1.690+009	4.121+009	42.
35	4.540-004	1.712+009	4.303+009	39.
36	2.754-004	1.745+009	4.864+009	37.
37	1.670-004	1.792+009	4.720+009	35.
38	1.013-004	1.853+009	4.843+009	20.
39	6.144-005	1.914+009	4.832+009	33.
40	3.727-005	1.913+009	4.689+009	34.

TABLE 4.4.1.2.1.3 (Cont'd)

FERRET-SAND II RESULTS FOR
OCONEE UNIT 2 CAPSULE C
(AVERAGE FOR CAPSULE)

GROUP	ENERGY (MeV)	A PRIORI FLUX* ($n/cm^2 \cdot s$)	ADJUSTED FLUX ($n/cm^2 \cdot s$)	% UNCERTAIN (1σ)
41	2.260-005	1.835+009	4.325+009	36.
42	1.371-005	1.740+009	3.905+009	37.
43	8.315-006	1.684+009	3.574+009	39.
44	5.043-006	1.655+009	3.308+009	40.
45	3.059-006	1.642+009	3.079+009	41.
46	1.855-006	1.627+009	2.861+009	40.
47	1.125-006	1.548+009	2.553+009	39.
48	6.826-007	1.415+009	2.193+009	38.
49	4.140-007	1.370+009	1.999+009	35.
50	2.511-007	1.737+009	2.394+009	33.
51	1.523-007	4.958+009	6.502+009	30.
52	9.237-008	7.985+009	1.005+010	27.
53	1.000-010	1.654+010	1.971+010	19.
FLUX, E > 0.0 MeV		1.236+011	1.919+011	14.
FLUX, E < 0.414 eV		3.259+010	4.066+010	15.
FLUX, E > 0.1 MeV		4.745+010	6.102+010	20.
FLUX, E > 1.0 MeV		2.336+010	2.667+010	10.
dpa/s		3.306-011	3.883-011	11.
FLUENCE+, E > 1.0 MeV		8.881+017	1.014+018	10.
dpa+		1.257-003	1.476-003	11.

---

* ABSOLUTE CALCULATED FLUX (OR NORMALIZED TO Fe54(n,p)Mn54 REACTION RATE).

+ BASED ON 3.802+007 EFFECTIVE FULL POWER SECONDS OF EXPOSURE; UNITS OF n/cm^2 FOR FLUENCE AND TOTAL NUMBER OF DISPLACED ATOMS OF IRON PER TARGET ATOM OF IRON FOR dpa.

TABLE 4.4.1.2.1.4

COMPARISON OF MEASURED AND CALCULATED REACTION RATES USED IN THE ANALYSIS OF OCONEE UNIT 2 CAPSULE C

REACTION	REACTION RATE (DPS/NUCLEUS) MEAS	A PRIORI CALC	ADJ CALC	RATIO MEAS/CALC A PRIORI	ADJ CALC
Fe54(n,p)Mn54	2.62-015	2.64-015	2.67-015	.99	.98
Ni58(n,p)Co58	3.37-015	3.42-015	3.47-015	.98	.97
Fe58(n,γ)Fe59	5.29-014	2.68-014	4.63-014	1.98	1.14
Np237(n,f)Cs137	5.94-014	5.01-014	6.05-014	1.18	.98
U238(n,f)Cs137	1.11-014	9.69-015	1.07-014	1.15	1.04
Co59(n,γ)Co60 (Cd)	8.27-013	2.54-013	6.24-013	3.25	1.33
Co59(n,γ)Co60	1.21-012	9.93-013	1.54-012	1.22	.79

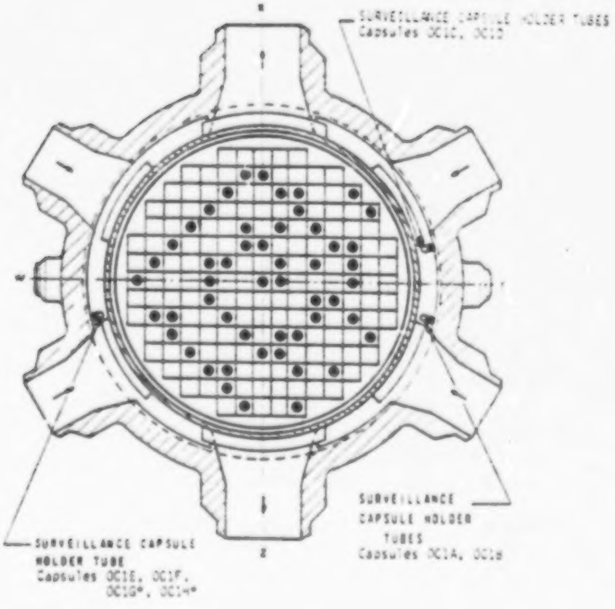
SURVEILLANCE CAPSULE HOLDER TUBES
Capsules OC1C, OC1D
SURVEILLANCE CAPSULE HOLDER TUBES
Capsules OC1A, OC1B
SURVEILLANCE CAPSULE HOLDER TUBE
Capsules OC1E, OC1F, OC1G*, OC1H*

*Thermal aging capsules.

(a) Reactor Geometry.

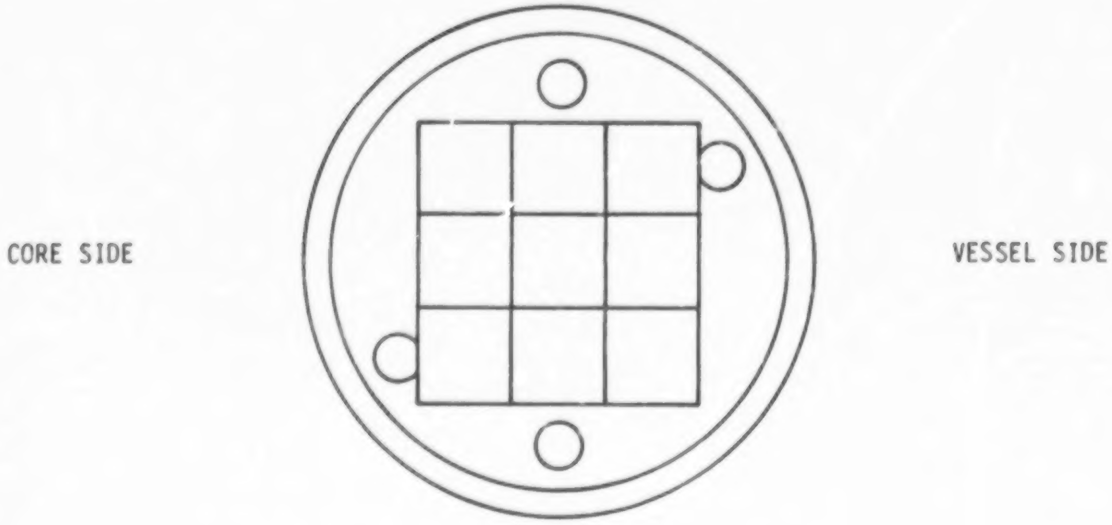
CORE SIDE
VESSEL SIDE

(b) Plan View of Surveillance Capsule.

FIGURE 4.4.1.3.1.1. Orientation of the Capsule Relative to the Core and Vessel Wall - Oconee Unit 3 Capsule A.

TABLE 4.4.1.3.1.1

SUMMARY OF REACTOR OPERATIONS
OCONEE UNIT 3 CAPSULE A

TIME PERIOD	START DATE	TIME INTERVAL	AVERAGE POWER LEVEL (MWt)	LOCAL POWER FACTOR
1	10/ 1/74	31.	411.	1.00
2	11/ 1/74	30.	1361.	1.00
3	12/ 1/74	31.	1387.	1.00
4	1/ 1/75	31.	1464.	1.00
5	2/ 1/75	28.	1695.	1.00
6	3/ 1/75	31.	1772.	1.00
7	4/ 1/75	30.	565.	1.00
8	5/ 1/75	31.	1207.	1.00
9	6/ 1/75	30.	1284.	1.00
10	7/ 1/75	31.	2388.	1.00
11	8/ 1/75	31.	2286.	1.00
12	9/ 1/75	30.	2183.	1.00
13	10/ 1/75	31.	1335.	1.00
14	11/ 1/75	30.	2414.	1.00
15	12/ 1/75	31.	2440.	1.00
16	1/ 1/76	31.	2337.	1.00
17	2/ 1/76	29.	1618.	1.00
18	3/ 1/76	24.	1258.	1.00
	3/25/76	DISCHARGED*		

---

*EFFECTIVE FULL POWER OPERATION TIME WAS 2.983+007 SECONDS AT A FULL POWER LEVEL OF 2568. MWt.

392

BLANK PAGE

BLANK PAGE

BLANK PAGE

TABLE 4.4.1.3.1.2 (Cont'd)

REACTION RATE DATA AND CORRECTION FACTORS FOR OCONEE UNIT 3 CAPSULE A

REACTION NAME	IDENT	TOR RATE (DPS/NUCL)	SATURATION FACTOR	GRADIENT FACTOR	IMPURITY FACTOR	AVG REACTION RATE (RPS/NUCL)	% UNCERT (1σ)
$^{238}U(n,f)^{141}Ce$	AD1	4.23-016	1.520+000	1.000	0.971	1.13-014	10.
	AD2	4.39-016	1.520+000	1.000	0.971		
	AD3	3.14-016	1.520+000	1.290	0.971		
	AD4	5.24-016	1.520+000	0.775	0.971		
$^{238}U(n,f)^{144}Ce$	AD1	2.52-016	2.006+000	1.000	0.971	1.07-014	10.
	AD2	2.57-016	2.006+000	1.000	0.971		
	AD3	1.89-016	2.006+000	1.303	0.971		
	AD4	3.20-016	2.006+000	0.767	0.971		
$^{238}U(n,f)^{106}Ru$	AD1	1.20-016	2.328+000	1.000	0.971	1.10-014	10.
	AD2	1.33-016	2.328+000	1.000	0.971		
	AD3	9.13-017	2.328+000	1.303	0.971		
	AD4	1.55-016	2.328+000	0.767	0.971		
$^{59}Co(n,\gamma)^{60}Co$	AD3 (CD)	1.89-014	8.753+000	1.000	1.000	2.08-013	29.
	AD4 (CD)	2.87-014	8.753+000	1.000	1.000		
$^{59}Co(n,\gamma)^{60}Co$	AD1 (B)	1.34-013	8.753+000	1.000	1.000	1.15-012	10.
	AD2 (B)	1.39-013	8.753+000	1.000	1.000		
	AD3 (B)	8.33-014	8.753+000	1.504	1.000		
	AD4 (B)	1.88-013	8.753+000	0.665	1.000		

CD = Cadmium-Covered Dosimeter.
B = Bare Dosimeter.

TABLE 4.4.1.3.1.3

FERRET-SAND II RESULTS FOR OCONEE UNIT 3 CAPSULE A (AVERAGE FOR CAPSULE)

GROUP	ENERGY (MeV)	A PRIORI FLUX* ($n/cm^2 \cdot s$)	ADJUSTED FLUX ($n/cm^2 \cdot s$)	% UNCERTAIN ($1\ \sigma$)
1	1.492+001	3.072+006	2.991+006	47.
2	1.350+001	6.387+006	6.143+006	44.
3	1.162+001	3.091+007	2.949+007	41.
4	1.000+001	9.293+007	8.840+007	37.
5	8.607+000	2.078+008	1.983+008	33.
6	7.408+000	3.513+008	3.390+008	29.
7	6.065+000	8.369+008	8.169+008	25.
8	4.966+000	1.283+009	1.274+009	22.
9	3.679+000	2.196+009	2.250+009	20.
10	2.865+000	2.001+009	2.165+009	22.
11	2.231+000	3.741+009	4.313+009	22.
12	1.738+000	3.710+009	4.489+009	23.
13	1.353+000	4.033+009	4.990+009	25.
14	1.108+000	3.286+009	4.056+009	28.
15	8.208-001	4.617+009	5.766+009	30.
16	6.393-001	3.557+009	4.466+009	34.
17	4.979-001	3.255+009	4.085+009	37.
18	3.877-001	2.935+009	3.659+009	40.
19	3.020-001	2.640+009	3.254+009	43.
20	1.832-001	4.481+009	5.447+009	46.
21	1.111-001	3.581+009	4.286+009	48.
22	6.738-002	2.875+009	3.385+009	50.
23	4.087-002	2.381+009	2.760+009	52.
24	2.554-002	1.982+009	2.263+009	53.
25	1.989-002	1.014+009	1.140+009	54.
26	1.503-002	1.119+009	1.240+009	54.
27	9.119-003	1.952+009	2.132+009	54.
28	5.531-003	1.881+009	2.017+009	54.
29	3.355-003	1.797+009	1.888+009	53.
30	2.839-003	5.787+008	5.951+008	52.
31	2.404-003	5.700+008	5.724+008	51.
32	2.035-003	5.642+008	5.526+008	49.
33	1.234-003	1.680+009	1.603+009	48.
34	7.485-004	1.690+009	1.573+009	46.
35	4.540-004	1.712+009	1.557+009	43.
36	2.754-004	1.745+009	1.585+009	41.
37	1.670-004	1.792+009	1.583+009	40.
38	1.013-004	1.853+009	1.508+009	30.
39	6.144-005	1.914+009	1.676+009	38.
40	3.727-005	1.913+009	1.695+009	38.

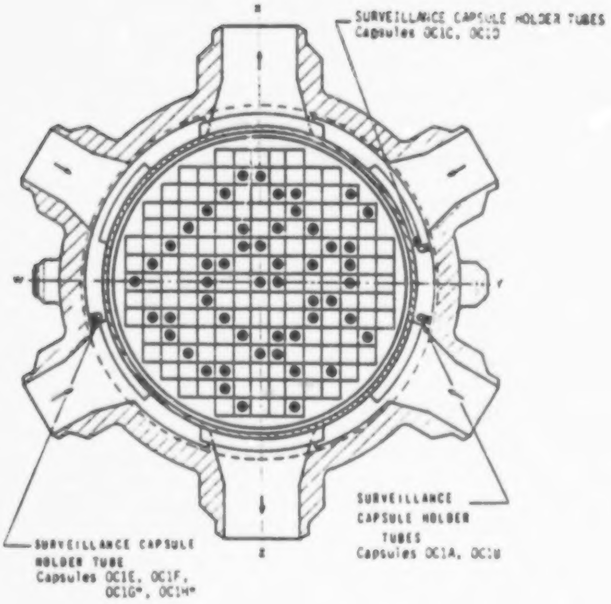
X
SURVEILLANCE CAPSULE HOLDER TUBES
Capsules OC1C, OC1D
W
Y
SURVEILLANCE
CAPSULE HOLDER
TUBES
Capsules OC1A, OC1B
Z
SURVEILLANCE CAPSULE
HOLDER TUBE
Capsules OC1E, OC1F,
OC1G*, OC1H*

*Thermal aging capsules.

(a) Reactor Geometry.

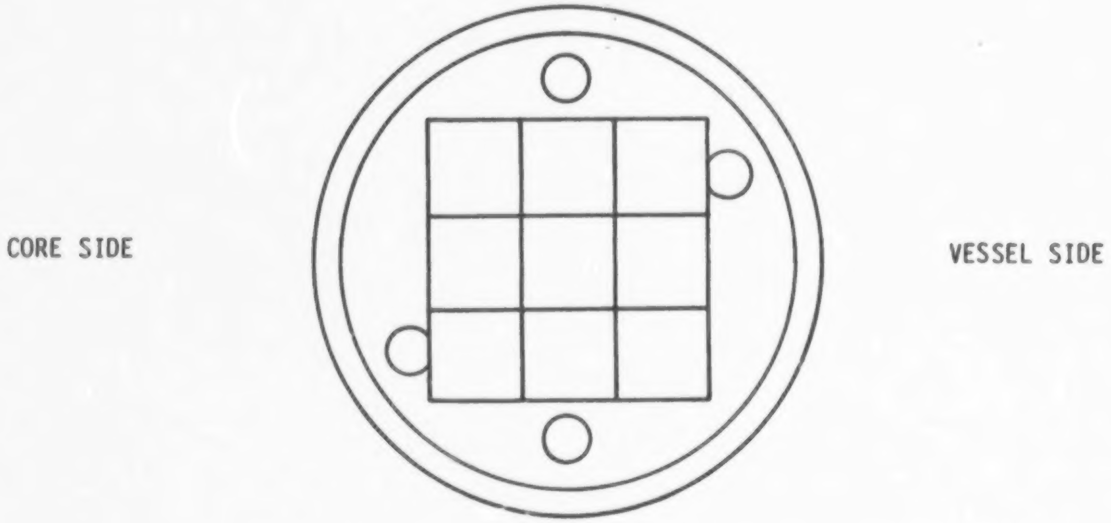
CORE SIDE
VESSEL SIDE

(b) Plan View of Surveillance Capsule.

FIGURE 4.4.1.4.1.1. Orientation of the Capsule Relative to the Core and Vessel Wall - Three Mile Island Unit 1 Capsule E.

395

TABLE 4.4.1.4.1.1

SUMMARY OF REACTOR OPERATIONS
THREE MILE ISLAND UNIT 1 CAPSULE E

TIME PERIOD	START DATE	TIME INTERVAL	AVERAGE POWER LEVEL (MWt)	LOCAL POWER FACTOR
1	6/16/74	15.	285.	1.00
2	7/ 1/74	31.	1060.	1.00
3	8/ 1/74	31.	1057.	1.00
4	9/ 1/74	30.	2375.	1.00
5	10/ 1/74	31.	1626.	1.00
6	11/ 1/74	30.	1996.	1.00
7	12/ 1/74	31.	2472.	1.00
8	1/ 1/75	31.	2335.	1.00
9	2/ 1/75	28.	2513.	1.00
10	3/ 1/75	31.	2428.	1.00
11	4/ 1/75	30.	1711.	1.00
12	5/ 1/75	31.	1748.	1.00
13	6/ 1/75	30.	1222.	1.00
14	7/ 1/75	31.	2456.	1.00
15	8/ 1/75	31.	2517.	1.00
16	9/ 1/75	30.	2152.	1.00
17	10/ 1/75	31.	1545.	1.00
18	11/ 1/75	30.	1427.	1.00
19	12/ 1/75	31.	2103.	1.00
20	1/ 1/76	31.	2294.	1.00
21	2/ 1/76	20.	2502.	1.00
	2/21/76	DISCHARGED*		

---

*EFFECTIVE FULL POWER OPERATION TIME WAS 4.036+007 SECONDS AT A FULL POWER LEVEL OF 2535. MWt.

TABLE 4.4.1.4.1.2 (Cont'd)

REACTION RATE DATA AND CORRECTION FACTORS FOR THREE MILE ISLAND UNIT 1 CAPSULE E

REACTION NAME	IDENT	TOR RATE (DPS/NUCL)	SATURATION FACTOR	GRADIENT FACTOR	IMPURITY FACTOR	AVG REACTION RATE (RPS/NUCL)	% UNCERT (1σ)
$^{237}Np(n,f)^{106}Ru$	ED1	5.81-016	1.867+000	1.000	1.000	5.75-014	35.
	ED2	6.52-016	1.867+000	0.862	1.000		
	ED3	4.85-016	1.867+000	1.160	1.000		
	ED4	1.05-015	1.867+000	1.000	1.000		
$^{59}Co(n,\gamma)^{60}Co$	ED1 (CD)	2.78-014	6.585+000	1.000	1.000	1.79-013	10.
	ED2 (CD)	3.37-014	6.585+000	0.800	1.000		
	ED3 (CD)	2.15-014	6.585+000	1.250	1.000		
	ED4 (CD)	2.71-014	6.585+000	1.000	1.000		
$^{59}Co(n,\gamma)^{60}Co$	ED1 (B)	1.85-013	6.585+000	1.000	1.000	1.09-012	10.
	ED2 (B)	2.33-013	6.585+000	0.663	1.000		
	ED3 (B)	1.02-013	6.585+000	1.509	1.000		
	ED4 (B)	1.70-013	6.585+000	1.000	1.000		

TABLE 4.4.1.4.1.3

FERRET-SAND II RESULTS FOR THREE MILE ISLAND UNIT 1 CAPSULE E (AVERAGE FOR CAPSULE)

GROUP	ENERGY (MeV)	A PRIORI FLUX* ($n/cm^2 \cdot s$)	ADJUSTED FLUX ($n/cm^2 \cdot s$)	% UNCERTAIN (1 σ)
1	1.492+001	3.032+006	2.886+006	47.
2	1.350+001	6.304+006	5.955+006	44.
3	1.162+001	3.051+007	2.874+007	41.
4	1.000+001	9.172+007	8.666+007	37.
5	8.607+000	2.051+008	1.956+008	33.
6	7.408+000	3.467+008	3.363+008	29.
7	6.065+000	8.260+008	8.139+008	25.
8	4.966+000	1.266+009	1.272+009	22.
9	3.679+000	2.167+009	2.254+009	20.
10	2.865+000	1.975+009	2.173+009	22.
11	2.231+000	3.693+009	4.351+009	22.
12	1.738+000	3.662+009	4.519+009	22.
13	1.353+000	3.981+009	4.973+009	24.
14	1.108+000	3.243+009	3.982+009	27.
15	8.208-001	4.557+009	5.607+009	28.
16	6.393-001	3.510+009	4.316+009	31.
17	4.979-001	3.213+009	3.924+009	35.
18	3.877-001	2.897+009	3.495+009	38.
19	3.020-001	2.605+009	3.092+009	41.
20	1.832-001	4.423+009	5.154+009	44.
21	1.111-001	3.535+009	4.042+009	47.
22	6.738-002	2.837+009	3.185+009	49.
23	4.087-002	2.350+009	2.591+009	51.
24	2.554-002	1.956+009	2.120+009	52.
25	1.989-002	1.001+009	1.065+009	53.
26	1.503-002	1.105+009	1.153+009	53.
27	9.119-003	1.927+009	1.974+009	53.
28	5.531-003	1.856+009	1.853+009	53.
29	3.355-003	1.773+009	1.717+009	52.
30	2.839-003	5.712+008	5.354+008	51.
31	2.404-003	5.626+008	5.083+008	49.
32	2.035-003	5.569+008	4.836+008	47.
33	1.234-003	1.658+009	1.382+009	45.
34	7.485-004	1.668+009	1.336+009	42.
35	4.540-004	1.689+009	1.305+009	39.
36	2.754-004	1.722+009	1.319+009	36.
37	1.670-004	1.768+009	1.303+009	33.
38	1.013-004	1.829+009	1.192+009	17.
39	6.144-005	1.889+009	1.372+009	30.
40	3.727-005	1.888+009	1.397+009	31.

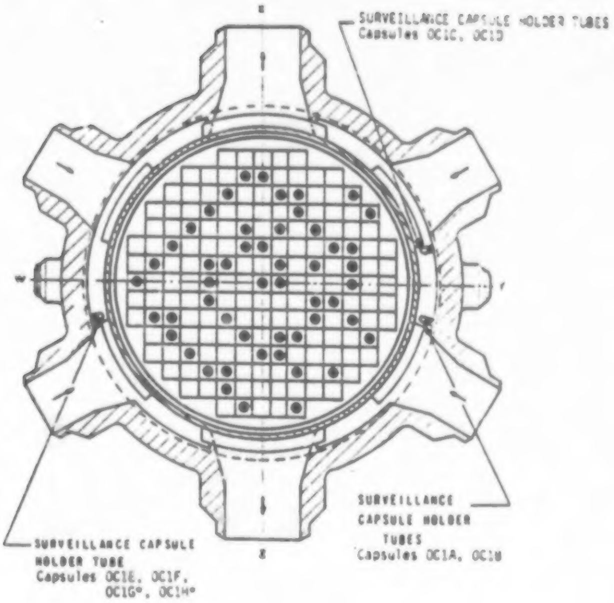
SURVEILLANCE CAPSULE HOLDER TUBES
Capsules OC1C, OC1D
W
Y
Z
SURVEILLANCE CAPSULE HOLDER TUBES
Capsules OC1A, OC1B
SURVEILLANCE CAPSULE HOLDER TUBE
Capsules OC1E, OC1F,
OC1G*, OC1H*

*Thermal aging capsules.

(a) Reactor Geometry.

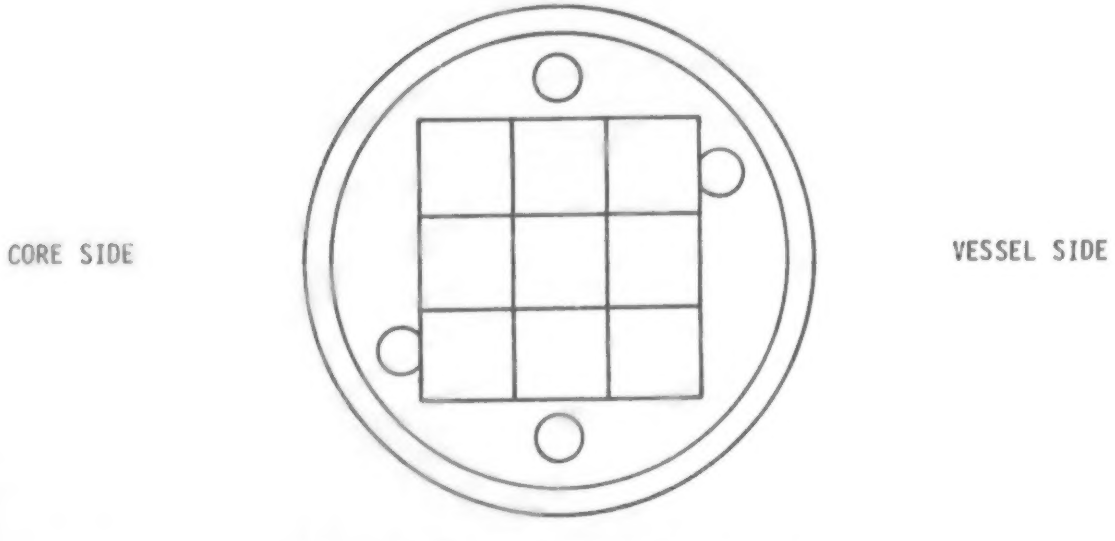
CORE SIDE
VESSEL SIDE

(b) Plan View of Surveillance Capsule.

FIGURE 4.4.1.5.1.1. Orientation of the Capsule Relative to the Core and Vessel Wall - Arkansas Nuclear One Unit 1 Capsule ANI-E.

BEST COPY AVAILABLE

399

TABLE 4.4.1.5.1.1

SUMMARY OF REACTOR OPERATIONS
ARKANSAS NUCLEAR ONE UNIT 1 CAPSULE ANI-E

TIME PERIOD	START DATE	TIME INTERVAL	AVERAGE POWER LEVEL (MWt)	LOCAL POWER FACTOR
1	8/ 1/74	31.	91.	1.00
2	9/ 1/74	30.	418.	1.00
3	10/ 1/74	31.	312.	1.00
4	11/ 1/74	30.	340.	1.00
5	12/ 1/74	31.	1525.	1.00
6	1/ 1/75	31.	2113.	1.00
7	2/ 1/75	28.	2231.	1.00
8	3/ 1/75	31.	969.	1.00
9	4/ 1/75	30.	0.	1.00
10	5/ 1/75	31.	1557.	1.00
11	6/ 1/75	30.	2162.	1.00
12	7/ 1/75	31.	2225.	1.00
13	8/ 1/75	31.	2391.	1.00
14	9/ 1/75	30.	2256.	1.00
15	10/ 1/75	31.	1936.	1.00
16	11/ 1/75	30.	1887.	1.00
17	12/ 1/75	31.	1572.	1.00
18	1/ 1/76	31.	1196.	1.00
19	2/ 1/76	29.	2450.	1.00
	3/ 1/76	DISCHARGED*		

---

*EFFECTIVE FULL POWER OPERATION TIME WAS 2.819+007 SECONDS AT A FULL POWER LEVEL OF 2568. MWt.

400

TABLE 4.4.1.5.1.2

REACTION RATE DATA AND CORRECTION FACTORS FOR ARKANSAS NUCLEAR ONE UNIT 1 CAPSULE ANI-E

REACTION NAME	IDENT	TOR RATE (DPS/NUCL)	SATURATION FACTOR	GRADIENT FACTOR	IMPURITY FACTOR	AVG REACTION RATE (RPS/NUCL)	% UNCERTAIN (1σ)
Fe54(n,p)Mn54	FE-ED1	1.24-015	2.197+000	1.000	1.000	2.67-015	5.
	FE-ED2	1.28-015	2.197+000	1.000	1.000		
	FE-ED3	8.99-016	2.197+000	1.304	1.000		
	FE-ED4	1.52-015	2.197+000	0.767	1.000		
Ni58(n,p)Co58	NI-ED1	2.47-015	1.387+000	1.000	1.000	3.39-015	5.
	NI-ED2	2.57-015	1.387+000	1.000	1.000		
	NI-ED3	1.81-015	1.387+000	1.310	1.000		
	NI-ED4	3.11-015	1.387+000	0.764	1.000		
Fe58(n,γ)Fe59	FE-ED1	3.24-014	1.352+000	1.000	1.000	4.17-014	8.
	FE-ED2	3.33-014	1.352+000	1.000	1.000		
	FE-ED3	1.83-014	1.352+000	1.559	1.000		
	FE-ED4	4.49-014	1.352+000	0.641	1.000		
U238(n,f)Zr95	U-ED1	4.34-016	1.378+000	1.000	0.967	1.18-014	5.
	U-ED2	4.65-016	1.378+000	1.000	0.967		
	U-ED3	3.39-016	1.378+000	1.331	0.967		
	U-ED4	6.01-016	1.378+000	0.751	0.967		
U238(n,f)Ru103	U-ED1	5.38-016	1.343+000	1.000	0.967	1.19-014	5.
	U-ED2	5.95-016	1.343+000	1.000	0.967		
	U-ED3	4.42-016	1.343+000	1.294	0.967		
	U-ED4	7.40-016	1.343+000	0.773	0.967		

401

BLANK PAGE

BLANK PAGE

BLANK PAGE

TABLE 4.4.1.5.1.2 (Cont'd)

REACTION RATE DATA AND CORRECTION FACTORS FOR
ARKANSAS NUCLEAR ONE UNIT 1 CAPSULE ANI-E

REACTION NAME	IDENT	TOR RATE (DPS/NUCL)	SATURATION FACTOR	GRADIENT FACTOR	IMPURITY FACTOR	AVG REACTION RATE (RPS/NUCL)	% UNCERTAIN (1σ)
U238(n,f)Cs137	U-ED1	1.24-017	4.944+001	1.000	0.967	1.10-014	7.
	U-ED2	1.45-017	4.944+001	1.000	0.967		
	U-ED3	1.04-017	4.944+001	1.355	0.967		
	U-ED4	1.92-017	4.944+001	0.738	0.967		
U238(n,f)Ce141	U-ED1	4.24-016	1.325+000	1.000	0.967	1.01-014	5.
	U-ED2	4.31-016	1.325+000	1.000	0.967		
	U-ED3	3.32-016	1.325+000	1.309	0.967		
	U-ED4	5.69-016	1.325+000	0.764	0.967		
U238(n,f)Ru106	U-ED1	1.19-016	2.426+000	1.000	0.967	1.12-014	7.
	U-ED2	1.31-016	2.426+000	1.000	0.967		
	U-ED3	8.40-017	2.426+000	1.365	0.967		
	U-ED4	1.56-016	2.426+000	0.732	0.967		
Np237(n,f)Cs137	NP-ED1	7.24-017	4.944+001	1.000	1.000	5.86-014	5.
	NP-ED2	7.24-017	4.944+001	1.000	1.000		
	NP-ED3	6.28-017	5.499+001	1.215	1.000		
	NP-ED4	9.26-017	4.944+001	0.823	1.000		
Np237(n,f)Zr95	NP-ED1	2.51-015	1.378+000	1.000	1.000	5.99-014	5.
	NP-ED2	2.55-015	1.378+000	1.000	1.000		
	NP-ED3	1.91-015	1.378+000	1.275	1.000		
	NP-ED4	3.10-015	1.378+000	0.784	1.000		

TABLE 4.4.1.5.1.2 (Cont'd)

REACTION RATE DATA AND CORRECTION FACTORS FOR ARKANSAS NUCLEAR ONE UNIT 1 CAPSULE ANI-E

REACTION NAME	REACTION IDENT	TOR RATE (DPS/NUCL)	SATURATION FACTOR	GRADIENT FACTOR	IMPURITY FACTOR	AVG REACTION RATE (RPS/NUCL)	% UNCERTAIN (1σ)
Np237(n,f)Ru103	NP-ED1	2.69-015	1.343+000	1.000	1.000	7.07-014	10.
	NP-ED2	2.87-015	1.343+000	1.000	1.000		
	NP-ED3	3.42-015	1.343+000	0.952	1.000		
Np237(n,f)Ce141	NP-ED1	2.04-015	1.325+000	1.000	1.000	6.38-014	27.
	NP-ED2	3.66-015	1.325-000	1.000	1.000		
	NP-ED3	1.44-015	1.325+000	1.664	1.000		
	NP-ED4	3.98-015	1.325+000	0.601	1.000		
Np237(n,f)Ru106	NP-ED1	5.68-016	2.426+000	1.000	1.000	5.41-014	17.
	NP-ED2	5.74-016	2.426+000	1.000	1.000		
	NP-ED3	3.12-016	2.426+000	1.371	1.000		
	NP-ED4	5.85-016	2.426+000	0.730	1.000		
Co59(n,γ)Co60 (Bare)	CO-ED1	1.17-013	9.232+000	1.000	1.000	1.02-012	8.
	CO-ED2	1.19-013	9.323+000	1.000	1.000		
	CO-ED3	6.95-014	9.232+000	1.484	1.000		
	CO-ED4	1.53-013	9.232+000	0.674	1.000		
Co59(n,γ)Co60 (Cd)	CO-ED1	1.08-013	9.232+000	1.000	1.000	9.56-013	24.
	CO-ED2	6.73-014	9.232+000	1.000	1.000		
	CO-ED3	9.52-014	9.232+000	1.255	1.000		
	CO-ED4	1.50-013	9.232+000	0.797	1.000		

2/03

TABLE 4.4.1.5.1.3

FERRET-SAND II RESULTS FOR
ARKANSAS NUCLEAR ONE UNIT 1 CAPSULE ANI-E
(AVERAGE FOR CAPSULE)

GROUP	ENERGY (MeV)	A PRIORI FLUX* (n/cm^2•s)	ADJUSTED FLUX (n/cm^2•s)	% UNCERTAIN (1σ)
1	1.492+001	3.072+006	3.260+006	47.
2	1.350+001	6.387+006	6.575+006	44.
3	1.162+001	3.091+007	3.098+007	41.
4	1.000+001	9.293+007	9.112+007	37.
5	8.607+000	2.078+008	2.008+008	33.
6	7.408+000	3.513+008	3.378+008	29.
7	6.065+000	8.369+008	8.021+008	25.
8	4.966+000	1.283+009	1.240+009	22.
9	3.679+000	2.196+009	2.177+009	20.
10	2.865+000	2.001+009	2.112+009	22.
11	2.231+000	3.741+009	4.226+009	22.
12	1.738+000	3.710+009	4.475+009	22.
13	1.353+000	4.033+009	5.064+009	24.
14	1.108+000	3.286+009	4.199+009	26.
15	8.208-001	4.617+009	6.096+009	27.
16	6.393-001	3.557+009	4.824+009	31.
17	4.979-001	3.255+009	4.509+009	34.
18	3.877-001	2.935+009	4.126+009	38.
19	3.020-001	2.640+009	3.749+009	41.
20	1.832-001	4.481+009	6.411+009	44.
21	1.111-001	3.581+009	5.157+009	47.
22	6.738-002	2.875+009	4.171+009	49.
23	4.087-002	2.381+009	3.493+009	50.
24	2.554-002	1.982+009	2.955+009	52.
25	1.989-002	1.014+009	1.545+009	53.
26	1.503-002	1.119+009	1.758+009	53.
27	9.119-003	1.952+009	3.199+009	53.
28	5.531-003	1.881+009	3.219+009	52.
29	3.355-003	1.797+009	3.231+009	52.
30	2.839-003	5.787+008	1.102+009	51.
31	2.404-003	5.700+008	1.154+009	49.
32	2.035-003	5.642+008	1.213+009	47.
33	1.234-003	1.680+009	3.821+009	45.
34	7.485-004	1.690+009	4.039+009	42.
35	4.540-004	1.712+009	4.250+009	40.
36	2.754-004	1.745+009	4.840+009	37.
37	1.670-004	1.792+009	4.687+009	36.
38	1.013-004	1.853+009	4.903+009	21.
39	6.144-005	1.914+009	4.721+009	34.
40	3.727-005	1.913+009	4.509+009	35.

TABLE 4.4.1.5.1.3 (Cont'd)

FERRET-SAND II RESULTS FOR ARKANSAS NUCLEAR ONE UNIT 1 CAPSULE ANI-E (AVERAGE FOR CAPSULE)

GROUP	ENERGY (MeV)	A PRIORI FLUX* (n/cm^2•s)	ADJUSTED FLUX (n/cm^2•s)	% UNCERTAIN (1σ)
41	2.260-005	1.835+009	4.064+009	37.
42	1.371-005	1.740+009	3.567+009	38.
43	8.315-006	1.684+009	3.157+009	40.
44	5.043-006	1.655+009	2.812+009	41.
45	3.059-006	1.642+009	2.511+009	42.
46	1.855-006	1.627+009	2.233+009	42.
47	1.125-006	1.548+009	1.906+009	41.
48	6.826-007	1.415+009	1.570+009	39.
49	4.140-007	1.380+009	1.388+009	37.
50	2.511-007	1.558+009	1.432+009	35.
51	1.523-007	1.521+009	1.303+009	33.
52	9.237-008	3.413+009	2.763+009	32.
53	1.000-010	2.473+010	1.723+010	19.
FLUX, E > 0.0 MeV		1.236+011	1.686+011	15.
FLUX, E < 0.414 eV		3.260+010	2.412+010	17.
FLUX, E > 0.1 MeV		4.745+010	6.072+010	18.
FLUX, E > 1.0 MeV		2.336+010	2.705+010	9.
dpa/s		3.311-011	3.879-011	10.
FLUENCE+, E > 1.0 MeV		6.963+017	8.064+017	9.
dpa+		9.869-004	1.156-003	10.

---

*ABSOLUTE CALCULATED FLUX (OR NORMALIZED TO Fe54(n,p)Mn54 REACTION RATE).

+BASED ON 2.981+007 EFFECTIVE FULL POWER SECONDS OF EXPOSURE; UNITS OF n/cm^2 FOR FLUENCE AND TOTAL NUMBER OF DISPLACED ATOMS OF IRON PER TARGET ATOM OF IRON FOR dpa.

TABLE 4.4.1.5.1.4

COMPARISON OF MEASURED AND CALCULATED REACTION RATES USED IN THE ANALYSIS OF ARKANSAS NUCLEAR ONE UNIT 1 CAPSULE ANI-E

REACTION	REACTION RATE (DPS/NUCLEUS)			RATIO MEAS/CALC	
	MEAS	A PRIORI CALC	ADJ CALC	A PRIORI	ADJ CALC
Fe54(n,p)Mn54	2.67-015	2.69-015	2.71-015	0.99	0.99
Ni58(n,p)Co58	3.39-015	3.49-015	3.51-015	0.97	0.97
Fe58(N,γ)Fe59	4.17-014	3.40-014	3.68-014	1.23	1.13
U238(n,f)FP*	1.12-014	9.69-015	1.08-014	1.16	1.04
Np237(n,f)FP*	6.14-014	5.01-014	6.14-014	1.22	1.00
Co59(n,γ)Co60	1.02-012	1.23-012	1.32-012	0.83	0.77
Co59(n,γ)Co60	9.56-013	2.54-013	6.14-013	3.76	1.56

---

*Average value determined from all fission products.

4.5 GENERAL ELECTRIC SURVEILLANCE CAPSULES: SPECIFIC DETAILS

At present, three capsules from General Electric (GE) plants have been reanalyzed. The a priori spectra were provided by S. L. Anderson of Westinghouse. (See Section 1.2.1 for further details.) It is noted that, due to the strong flux gradient through GE capsules, the exposures are reported for each individual basket, and the letters at the end of the Table numbers for Tables 4.5.1.2.1.3 and 4.5.1.2.1.4 indicate results for different baskets. Other then this, the table and figure numbering designation used here is the same as for the W, CE, and B&W sections, as described on pages 4.2.1, 4.3.1, and 4.4-1, respectively.

BEST COPY AVAILABLE

407

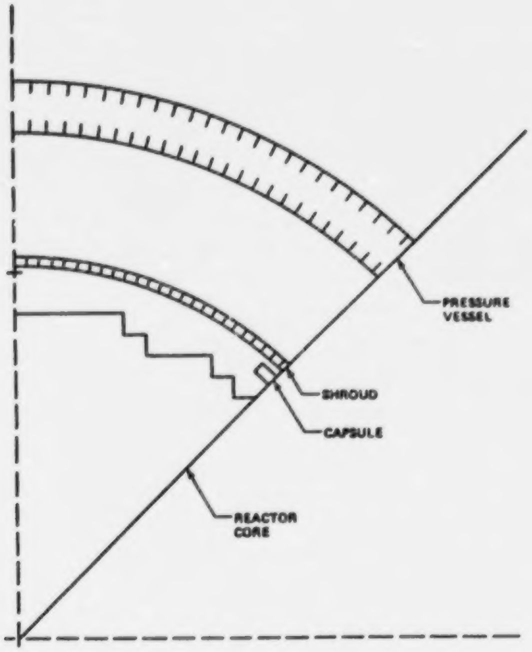
PRESSURE VESSEL
SHROUD
CAPSULE
REACTOR CORE

(a) Reactor Geometry.

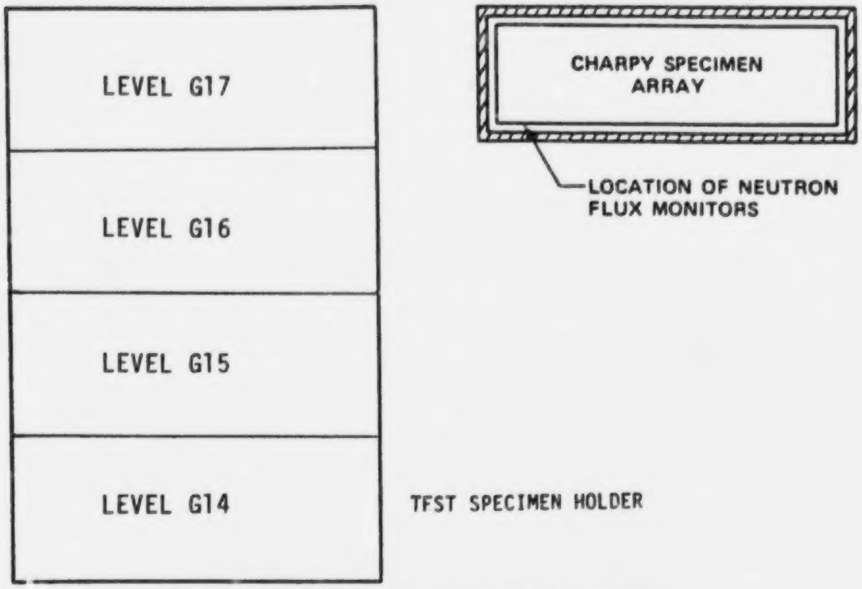
LEVEL G17
LEVEL G16
LEVEL G15
LEVEL G14
TFST SPECIMEN HOLDER
CHARPY SPECIMEN ARRAY
LOCATION OF NEUTRON FLUX MONITORS

(b) Plan View of Surveillance Capsule.

FIGURE 4.5.1.1.1.1. Orientation of the Capsule Relative to the Core and Vessel Wall - Dresden Unit 3 Capsule 4.

TABLE 4.5.1.1.1.1

SUMMARY OF REACTOR OPERATIONS
DRESDEN UNIT 3 CAPSULE 4

TIME PERIOD	START DATE	TIME INTERVAL	AVERAGE POWER LEVEL (MWt)	LOCAL POWER FACTOR
1	10/71-1/72	123.	1584.	1.00
2	2/72	29.	1693.	1.00
3	3/72	31.	2191.	1.00
4	4/72	30.	1456.	1.00
5	5/72	31.	1802.	1.00
6	6/72	30.	1713.	1.00
7	7/72	31.	1799.	1.00
8	8/72	31.	1963.	1.00
9	9/72	30.	1923.	1.00
10	10/72	31.	1966.	1.00
11	11/72	30.	1450.	1.00
12	12/72	31.	1873.	1.00
13	1/73	31.	2173.	1.00
14	2/73	28.	2105.	1.00
15	3/73	31.	210.	1.00
16	4/73	30.	0.	1.00
17	5/73	31.	0.	1.00
18	6/73	30.	1188.	1.00
19	7/73	31.	1769.	1.00
20	8/73	31.	1188.	1.00
21	9/73	30.	1933.	1.00
22	10/73	31.	1847.	1.00
23	11/73	30.	1794.	1.00
24	12/73	31.	1878.	1.00
25	1/74	31.	1430.	1.00
26	2/74	28.	1913.	1.00
27	3/74	31.	763.	1.00
28	4/74	30.	0.	1.00
29	5/74	31.	0.	1.00
30	6/74	30.	745.	1.00
31	7/74	31.	1170.	1.00
32	8/74	31.	2014.	1.00
33	9/74	30.	1476.	1.00
34	10/74	31.	2052.	1.00
35	11/74	30.	1243.	1.00
36	12/74	31.	1258.	1.00
37	1/75	31.	993.	1.00
38	2/75	28.	776.	1.00
39	3/75	31.	1165.	1.00
40	4/75	30.	581.	1.00
41	5/75	31.	0.	1.00
42	6/75	30.	0.	1.00
43	7/75	31.	0.	1.00
44	8/75	31.	0.	1.00

TABLE 4.5.1.1.1.1 (Cont'd)

SUMMARY OF REACTOR OPERATIONS
DRESDEN UNIT 3 CAPSULE 4

TIME PERIOD	START DATE	TIME INTERVAL	AVERAGE POWER LEVEL (MWt)	LOCAL POWER FACTOR
45	9/75	30.	561.	1.00
46	10/75	31.	2102.	1.00
47	11/75	30.	2108.	1.00
48	12/75	31.	1324.	1.00
49	1/76	31.	1754.	1.00
50	2/76	29.	1668.	1.00
51	3/76	31.	1708.	1.00
52	4/76	30.	1645.	1.00
53	5/76	31.	1430.	1.00
54	6/76	30.	1751.	1.00
55	7/76	31.	1680.	1.00
56	8/76	31.	1547.	1.00
57	9/76	30.	854.	1.00
58	10/76	31.	0.	1.00
59	11/76	30.	1215.	1.00
60	12/76	31.	2257.	1.00
61	1/77	31.	2411.	1.00
62	2/77	28.	2113.	1.00
63	3/77	31.	2325.	1.00
64	4/77	30.	1377.	1.00
65	5/77	31.	1466.	1.00
66	6/77	30.	1491.	1.00
67	7/77	31.	2032.	1.00
68	8/77	31.	2092.	1.00
69	9/77	30.	2166.	1.00
70	10/77	31.	1996.	1.00
71	11/77	30.	1691.	1.00
72	12/77	31.	1430.	1.00
73	1/78	31.	1549.	1.00
74	2/78	28.	1387.	1.00
75	3/78	31.	164.	1.00
76	4/78	30.	0.	1.00
77	5/78	31.	910.	1.00
78	6/78	30.	1981.	1.00
79	7/78	31.	1857.	1.00
80	8/78	31.	2282.	1.00
81	9/78	30.	1481.	1.00
82	10/78	31.	2322.	1.00
83	11/78	30.	2138.	1.00
84	12/78	31.	677.	1.00
	1/1/79	DISCHARGED*		

---

*EFFECTIVE FULL POWER OPERATION TIME WAS 8.483+007 SECONDS AT A FULL POWER LEVEL OF 2527. MWt.

TABLE 4.5.1.1.1.2

REACTION RATE DATA AND CORRECTION FACTORS FOR DRESDEN UNIT 3 CAPSULE 4

REACTION		TOR RATE	SATURATION	GRADIENT	IMPURITY	AVG REACTION	% UNCERTAIN
NAME	IDENT	(DPS/NUCL)	FACTOR	FACTOR	FACTOR	RATE (RPS/NUCL)	(1σ)
$^{54}Fe(n,p)^{54}Mn$	G-14	2.99-015	10.9	1.0	1.0	3.26-014	10.
	G-15	2.18-015				2.38-014	
	G-16	1.73-015				1.89-014	
	G-17	7.46-016				8.15-015	
$^{63}Cu(n,\alpha)^{60}Co$	G-14	1.22-016	3.94	1.0	1.0	4.81-016	10.
	G-15	9.36-017				3.68-016	
	G-16	7.30-017				2.87-017	
	G-17	3.85-017				1.51-017	

4/11

TABLE 4.5.1.1.1.3A

FERRET-SAND II RESULTS FOR DRESDEN UNIT 3 CAPSULE 4 BASKET G-14 (AVERAGE FOR CAPSULE)

GROUP	ENERGY (MeV)	A PRIORI FLUX* (n/cm^2•s)	ADJUSTED FLUX (n/cm^2•s)	% UNCERTAIN (1σ)
1	1.492+001	1.456+007	2.885+007	43.
2	1.350+001	3.026+007	6.000+007	39.
3	1.162+001	1.403+008	2.744+008	34.
4	1.000+001	4.258+008	8.193+008	30.
5	8.607+000	1.077+009	1.989+009	25.
6	7.408+000	2.547+009	4.265+009	23.
7	6.065+000	9.378+009	1.421+010	20.
8	4.966+000	1.455+010	1.788+010	22.
9	3.679+000	2.674+010	2.794+010	22.
10	2.865+000	3.032+010	2.958+010	25.
11	2.231+000	4.820+010	4.473+010	29.
12	1.738+000	4.166+010	3.781+010	34.
13	1.353+000	3.908+010	3.465+010	39.
14	1.108+000	2.503+010	2.201+010	43.
15	8.208-001	3.552+010	3.157+010	47.
16	6.393-001	2.754+010	2.513+010	50.
17	4.979-001	2.531+010	2.397+010	54.
18	3.877-001	2.327+010	2.301+010	56.
19	3.020-001	2.143+010	2.216+010	58.
20	1.832-001	3.768+010	4.067+010	60.
21	1.111-001	3.127+010	3.510+010	61.
22	6.738-002	2.575+010	2.989+010	62.
23	4.087-002	2.233+010	2.664+010	63.
24	2.554-002	1.903+010	2.320+010	63.
25	1.989-002	9.635+009	1.194+010	64.
26	1.503-002	1.058+010	1.326+010	64.
27	9.119-003	1.839+010	2.324+010	64.
28	5.531-003	1.817+010	2.310+010	64.
29	3.355-003	1.845+010	2.354+010	64.
30	2.839-003	6.228+009	7.967+009	64.
31	2.404-003	6.259+009	8.018+009	64.
32	2.035-003	6.300+009	8.077+009	64.
33	1.234-003	1.909+010	2.449+010	64.
34	7.485-004	1.936+010	2.484+010	64.
35	4.540-004	1.959+010	2.514+010	64.
36	2.754-004	1.981+010	2.542+010	64.
37	1.670-004	2.003+010	2.571+010	64.
38	1.013-004	2.027+010	2.602+010	64.
39	6.144-005	2.052+010	2.634+010	64.
40	3.727-005	2.079+010	2.669+010	64.

TABLE 4.5.1.1.1.3A (Cont'd)

FERRET-SAND II RESULTS FOR
DRESDEN UNIT 3 CAPSULE 4 BASKET G-14
(AVERAGE FOR CAPSULE)

GROUP	ENERGY (MeV)	A PRIORI FLUX* ($n/cm^2 \cdot s$)	ADJUSTED FLUX ($n/cm^2 \cdot s$)	% UNCERTAIN (1σ)
41	2.260-005	2.107+010	2.705+010	64.
42	1.371-005	2.137+010	2.743+010	64.
43	8.315-006	2.169+010	2.784+010	64.
44	5.043-006	2.196+010	2.819+010	64.
45	3.059-006	2.217+010	2.846+010	64.
46	1.855-006	2.277+010	2.923+010	64.
47	1.125-006	2.405+010	3.087+010	64.
48	6.826-007	2.521+010	3.236+010	64.
49	4.140-007	2.601+010	3.338+010	64.
50	2.511-007	7.656+010	9.827+010	64.
51	1.523-007	1.465+011	1.880+011	64.
52	9.237-008	1.765+011	2.266+011	64.
53	1.000-010	1.040+012	1.335+012	64.
FLUX, E > 0.0 MeV		2.408+012	2.954+012	49.
FLUX, E < 0.414 eV		1.465+012	1.881+012	62.
FLUX, E > 0.1 MeV		4.466+011	4.442+011	31.
FLUX, E > 1.0 MeV		2.513+011	2.470+011	20.
dpa/s		3.568-010	3.702-010	19.
FLUENCE+, E > 1.0 MeV		2.132+019	2.096+019	20.
dpa+		3.027-002	3.141-002	19.

---

*ABSOLUTE CALCULATED FLUX (OR NORMALIZED TO Fe54(n,p)Mn54 REACTION RATE).

+BASED ON 8.483+007 EFFECTIVE FULL POWER SECONDS OF EXPOSURE; UNITS OF n/cm^2 FOR FLUENCE AND TOTAL NUMBER OF DISPLACED ATOMS OF IRON PER TARGET ATOM OF IRON FOR dpa.

TABLE 4.5.1.1.1.4A

COMPARISON OF MEASURED AND CALCULATED REACTION RATES USED IN THE ANALYSIS OF DRESDEN UNIT 3 CAPSULE 4 BASKET G-14

	REACTION RATE (DPS/NUCLEUS)			RATIO MEAS/CALC	
REACTION	MEAS	A PRIORI CALC	ADJ CALC	A PRIORI	ADJ CALC
Fe54(n,p)Mn54	3.26-014	3.12-014	3.59-014	1.04	0.91
Cu63(n,α)Co60	4.81-016	2.66-016	4.39-016	1.81	1.09

414

TABLE 4.5.1.1.1.3B

FERRET-SAND II RESULTS FOR
DRESDEN UNIT 3 CAPSULE 4 BASKET G-15
(AVERAGE FOR CAPSULE)

GROUP	ENERGY (MeV)	A PRIORI FLUX* (n/cm^2•s)	ADJUSTED FLUX (n/cm^2•s)	% UNCERTAIN (1σ)
1	1.492+001	1.092+007	2.233+007	43.
2	1.350+001	2.269+007	4.640+007	39.
3	1.162+001	1.052+008	2.118+008	34.
4	1.000+001	3.193+008	6.314+008	29.
5	8.607+000	8.079+008	1.526+009	25.
6	7.408+000	1.910+009	3.240+009	23.
7	6.065+000	7.033+009	1.067+010	20.
8	4.966+000	1.091+010	1.320+010	22.
9	3.679+000	2.005+010	2.039+010	22.
10	2.865+000	2.274+010	2.148+010	25.
11	2.231+000	3.615+010	3.238+010	30.
12	1.738+000	3.125+010	2.732+010	34.
13	1.353+000	2.931+010	2.501+010	39.
14	1.108+000	1.877+010	1.589+010	43.
15	8.208-001	2.664+010	2.283+010	47.
16	6.393-001	2.066+010	1.822+010	50.
17	4.979-001	1.898+010	1.744+010	54.
18	3.877-001	1.745+010	1.682+010	56.
19	3.020-001	1.608+010	1.627+010	58.
20	1.832-001	2.826+010	2.997+010	60.
21	1.111-001	2.345+010	2.595+010	61.
22	6.738-002	1.931+010	2.216+010	62.
23	4.087-002	1.675+010	1.980+010	63.
24	2.554-002	1.427+010	1.727+010	63.
25	1.989-002	7.226+009	8.899+009	64.
26	1.503-002	7.935+009	9.898+009	64.
27	9.119-003	1.379+010	1.736+010	64.
28	5.531-003	1.363+010	1.726+010	64.
29	3.355-003	1.383+010	1.759+010	64.
30	2.839-003	4.671+009	5.954+009	64.
31	2.404-003	4.694+009	5.994+009	64.
32	2.035-003	4.725+009	6.038+009	64.
33	1.234-003	1.432+010	1.831+010	64.
34	7.485-004	1.452+010	1.857+010	64.
35	4.540-004	1.469+010	1.879+010	64.
36	2.754-004	1.485+010	1.901+010	64.
37	1.670-004	1.502+010	1.922+010	64.
38	1.013-004	1.520+010	1.946+010	64.
39	6.144-005	1.539+010	1.970+010	64.
40	3.727-005	1.559+010	1.995+010	64.

TABLE 4.5.1.1.1.3B (Cont'd)

FERRET-SAND II RESULTS FOR
DRESDEN UNIT 3 CAPSULE 4 BASKET G-15
(AVERAGE FOR CAPSULE)

GROUP	ENERGY (MeV)	A PRIORI FLUX* ($n/cm^2 \cdot s$)	ADJUSTED FLUX ($n/cm^2 \cdot s$)	% UNCERTAIN (1σ)
41	2.260-005	1.580+010	2.022+010	64.
42	1.371-005	1.603+010	2.051+010	64.
43	8.315-006	1.626+010	2.081+010	64.
44	5.043-006	1.647+010	2.108+010	64.
45	3.059-006	1.663+010	2.128+010	64.
46	1.855-006	1.708+010	2.185+010	64.
47	1.125-006	1.804+010	2.308+010	64.
48	6.826-007	1.890+010	2.419+010	64.
49	4.140-007	1.950+010	2.496+010	64.
50	2.511-007	5.742+010	7.347+010	64.
51	1.523-007	1.099+011	1.406+011	64.
52	9.237-008	1.324+011	1.694+011	64.
53	1.000-010	7.799+011	9.979+011	64.
FLUX, E > 0.0 MeV		1.806+012	2.200+012	49.
FLUX, E < 0.414 eV		1.099+012	1.406+012	62.
FLUX, E > 0.1 MeV		3.350+011	3.242+011	31.
FLUX, E > 1.0 MeV		1.885+011	1.798+011	20.
dpa/s		2.676-010	2.710-010	19.
FLUENCE+, E > 1.0 MeV		1.599+019	1.525+019	20.
dpa+		2.270-002	2.299-002	19.

---

*ABSOLUTE CALCULATED FLUX (OR NORMALIZED TO Fe54(n,p)Mn54 REACTION RATE).

+BASED ON 8.483+007 EFFECTIVE FULL POWER SECONDS OF EXPOSURE; UNITS OF n/cm^2 FOR FLUENCE AND TOTAL NUMBER OF DISPLACED ATOMS OF IRON PER TARGET ATOM OF IRON FOR dpa.

TABLE 4.5.1.1.1.4B

COMPARISON OF MEASURED AND CALCULATED REACTION RATES USED IN THE ANALYSIS OF DRESDEN UNIT 3 CAPSULE 4 BASKET G-15

REACTION	REACTION RATE (DPS/NUCLEUS) MEAS	A PRIORI CALC	ADJ CALC	RATIO MEAS/CALC A PRIORI	ADJ CALC
Fe54(n,p)Mn54	2.38-014	2.34-014	2.65-014	1.02	0.90
Cu63(n,α)Co60	3.68-016	2.00-016	3.34-016	1.84	1.10

417

TABLE 4.5.1.1.1.3C

FERRET-SAND II RESULTS FOR DRESDEN UNIT 3 CAPSULE 4 BASKET G-16 (AVERAGE FOR CAPSULE)

GROUP	ENERGY (MeV)	A PRIORI FLUX* (n/cm²•s)	ADJUSTED FLUX (n/cm²•s)	% UNCERTAIN (1σ)
1	1.492+001	9.097+006	1.741+007	43.
2	1.350+001	1.891+007	3.616+007	39.
3	1.162+001	8.768+007	1.650+008	34.
4	1.000+001	2.661+008	4.918+008	29.
5	8.607+000	6.732+008	1.190+009	25.
6	7.408+000	1.592+009	2.535+009	23.
7	6.065+000	5.861+009	8.381+009	20.
8	4.966+000	9.096+009	1.044+010	22.
9	3.679+000	1.671+010	1.620+010	22.
10	2.865+000	1.895+010	1.711+010	25.
11	2.231+000	3.012+010	2.583+010	29.
12	1.738+000	2.604+010	2.183+010	34.
13	1.353+000	2.442+010	2.001+010	39.
14	1.108+000	1.564+010	1.272+010	43.
15	8.208-001	2.220+010	1.829+010	47.
16	6.393-001	1.721+010	1.459+010	50.
17	4.979-001	1.582+010	1.396+010	54.
18	3.877-001	1.454+010	1.344+010	56.
19	3.020-001	1.340+010	1.299+010	58.
20	1.832-001	2.355+010	2.391+010	60.
21	1.111-001	1.954+010	2.068+010	61.
22	6.738-002	1.609+010	1.765+010	62.
23	4.087-002	1.396+010	1.576+010	63.
24	2.554-002	1.189+010	1.374+010	63.
25	1.989-002	6.022+009	7.076+009	64.
26	1.503-002	6.613+009	7.868+009	64.
27	9.119-003	1.149+010	1.379+010	64.
28	5.531-003	1.136+010	1.372+010	64.
29	3.355-003	1.153+010	1.398+010	64.
30	2.839-003	3.892+009	4.731+009	64.
31	2.404-003	3.912+009	4.762+009	64.
32	2.035-003	3.937+009	4.797+009	64.
33	1.234-003	1.193+010	1.455+010	64.
34	7.485-004	1.210+010	1.475+010	64.
35	4.540-004	1.224+010	1.493+010	64.
36	2.754-004	1.238+010	1.510+010	64.
37	1.670-004	1.252+010	1.527+010	64.
38	1.013-004	1.267+010	1.546+010	64.
39	6.144-005	1.283+010	1.565+010	64.
40	3.727-005	1.299+010	1.585+010	64.

418

TABLE 4.5.1.1.1.3C

FERRET-SAND II RESULTS FOR
DRESDEN UNIT 3 CAPSULE 4 BASKET G-16
(AVERAGE FOR CAPSULE)

GROUP	ENERGY (MeV)	A PRIORI FLUX* ($n/cm^2 \cdot s$)	ADJUSTED FLUX ($n/cm^2 \cdot s$)	% UNCERTAIN (1σ)
41	2.260-005	1.317+010	1.607+010	64.
42	1.371-005	1.336+010	1.629+010	64.
43	8.315-006	1.355+010	1.653+010	64.
44	5.043-006	1.373+010	1.675+010	64.
45	3.059-006	1.386+010	1.690+010	64.
46	1.855-006	1.423+010	1.736+010	64.
47	1.125-006	1.503+010	1.834+010	64.
48	6.826-007	1.575+010	1.922+010	64.
49	4.140-007	1.625+010	1.983+010	64.
50	2.511-007	4.785+010	5.837+010	64.
51	1.523-007	9.155+010	1.117+011	64.
52	9.237-008	1.103+011	1.346+011	64.
53	1.000-010	6.499+011	7.928+011	64.
FLUX, E > 0.0 MeV		1.505+012	1.749+012	49.
FLUX, E < 0.414 eV		9.159+011	1.117+012	62.
FLUX, E > 0.1 MeV		2.791+011	2.585+011	31.
FLUX, E > 1.0 MeV		1.571+011	1.432+011	20.
dpa/s		2.230-010	2.155-010	19.
FLUENCE+, E > 1.0 MeV		1.333+019	1.215+019	20.
dpa+		1.892-002	1.828-002	19.

---

*ABSOLUTE CALCULATED FLUX (OR NORMALIZED TO Fe54(n,p)Mn54 REACTION RATE).

+BASED ON 8.483+007 EFFECTIVE FULL POWER SECONDS OF EXPOSURE; UNITS OF n/cm^2 FOR FLUENCE AND TOTAL NUMBER OF DISPLACED ATOMS OF IRON PER TARGET ATOM OF IRON FOR dpa.

BEST COPY AVAILABLE

419

TABLE 4.5.1.1.1.4C

COMPARISON OF MEASURED AND CALCULATED REACTION RATES USED IN THE ANALYSIS OF DRESDEN UNIT 3 CAPSULE 4 BASKET G-16

REACTION	REACTION RATE (DPS/NUCLEUS) MEAS	A PRIORI CALC	ADJ CALC	RATIO MEAS/CALC A PRIORI	ADJ CALC
Fe54(n,p)Mn54	1.89-014	1.95-014	2.09-014	0.97	0.90
Cu63(n,α)Co60	2.87-016	1.66-016	2.61-016	1.72	1.10

420

TABLE 4.5.1.1.1.3D

FERRET-SAND II RESULTS FOR
DRESDEN UNIT 3 CAPSULE 4 BASKET G-17
(AVERAGE FOR CAPSULE)

GROUP	ENERGY (MeV)	A PRIORI FLUX* (n/cm^2•s)	ADJUSTED FLUX (n/cm^2•s)	% UNCERTAIN (1σ)
1	1.492+001	3.821+006	9.549+006	42.
2	1.350+001	7.943+006	1.980+007	38.
3	1.162+001	3.683+007	8.978+007	34.
4	1.000+001	1.118+008	2.663+008	29.
5	8.607+000	2.828+008	6.336+008	25.
6	7.408+000	6.687+008	1.291+009	23.
7	6.065+000	2.462+009	4.058+009	20.
8	4.966+000	3.820+009	4.705+009	22.
9	3.679+000	7.018+009	6.975+009	22.
10	2.865+000	7.960+009	7.215+009	26.
11	2.231+000	1.265+010	1.071+010	30.
12	1.738+000	1.094+010	8.974+009	35.
13	1.353+000	1.026+010	8.172+009	39.
14	1.108+000	6.570+009	5.191+009	43.
15	8.208-001	9.324+009	7.502+009	47.
16	6.393-001	7.229+009	6.051+009	51.
17	4.979-001	6.644+009	5.871+009	54.
18	3.877-001	6.109+009	5.744+009	57.
19	3.020-001	5.627+009	5.641+009	59.
20	1.832-001	9.890+009	1.054+010	60.
21	1.111-001	8.208+009	9.242+009	61.
22	6.738-002	6.759+009	7.975+009	62.
23	4.087-002	5.862+009	7.186+009	63.
24	2.554-002	4.996+009	6.310+009	63.
25	1.989-002	2.529+009	3.268+009	64.
26	1.503-002	2.777+009	3.647+009	64.
27	9.119-003	4.826+009	6.412+009	64.
28	5.531-003	4.770+009	6.387+009	64.
29	3.355-003	4.842+009	6.516+009	64.
30	2.839-003	1.635+009	2.207+009	64.
31	2.404-003	1.643+009	2.223+009	64.
32	2.035-003	1.654+009	2.240+009	64.
33	1.234-003	5.012+009	6.793+009	64.
34	7.485-004	5.081+009	6.890+009	64.
35	4.540-004	5.142+009	6.974+009	64.
36	2.754-004	5.199+009	7.052+009	64.
37	1.670-004	5.258+009	7.133+009	64.
38	1.013-004	5.322+009	7.219+009	64.
39	6.144-005	5.387+009	7.308+009	64.
40	3.727-005	5.457+009	7.403+009	64.

TABLE 4.5.1.1.1.3D (Cont'd)

FERRET-SAND II RESULTS FOR
DRESDEN UNIT 3 CAPSULE 4 BASKET G-17
(AVERAGE FOR CAPSULE)

GROUP	ENERGY (MeV)	A PRIORI FLUX* ($n/cm^2 \cdot s$)	ADJUSTED FLUX ($n/cm^2 \cdot s$)	% UNCERTAIN (1σ)
41	2.260-005	5.532+009	7.504+009	64.
42	1.371-005	5.609+009	7.610+009	64.
43	8.315-006	5.693+009	7.723+009	64.
44	5.043-006	5.765+009	7.821+009	64.
45	3.059-006	5.820+009	7.896+009	64.
46	1.855-006	5.976+009	8.107+009	64.
47	1.125-006	6.313+009	8.565+009	64.
48	6.826-007	6.617+009	8.976+009	64.
49	4.140-007	6.826+009	9.261+009	64.
50	2.511-007	2.010+010	2.726+010	64.
51	1.523-007	3.845+010	5.216+010	64.
52	9.237-008	4.634+010	6.287+010	64.
53	1.000-010	2.730+011	3.703+011	64.
FLUX, E > 0.0 MeV		6.320+011	8.061+011	50.
FLUX, E < 0.414 eV		3.847+011	5.218+011	62.
FLUX, E > 0.1 MeV		1.172+011	1.106+011	31.
FLUX, E > 1.0 MeV		6.598+010	6.088+010	20.
dpa/s		9.366-011	9.361-011	19.
FLUENCE+, E > 1.0 MeV		5.597+018	5.164+018	20.
dpa+		7.945-003	7.941-003	19.

---

*ABSOLUTE CALCULATED FLUX (OR NORMALIZED TO Fe54(n,p)Mn54 REACTION RATE).

+BASED ON 8.483+007 EFFECTIVE FULL POWER SECONDS OF EXPOSURE; UNITS OF n/cm^2 FOR FLUENCE AND TOTAL NUMBER OF DISPLACED ATOMS OF IRON PER TARGET ATOM OF IRON FOR dpa.

TABLE 4.5.1.1.1.4D

COMPARISON OF MEASURED AND CALCULATED REACTION RATES USED IN THE ANALYSIS OF DRESDEN UNIT 3 CAPSULE 4 BASKET G-17

REACTION	REACTION RATE (DPS/NUCLEUS) MEAS	A PRIORI CALC	ADJ CALC	RATIO MEAS/CALC A PRIORI	ADJ CALC
Fe54(n,p)Mn54	8.15-015	8.19-015	9.40-015	0.99	0.87
Cu63(n,α)Co60	1.51-016	6.99-017	1.33-016	2.16	1.14

BEST COPY AVAILABLE

423

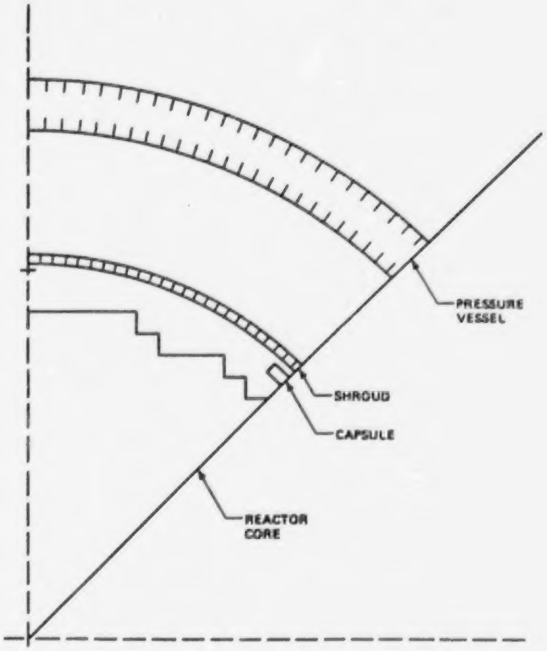
PRESSURE VESSEL
SHROUD
CAPSULE
REACTOR CORE

(a) Reactor Geometry.

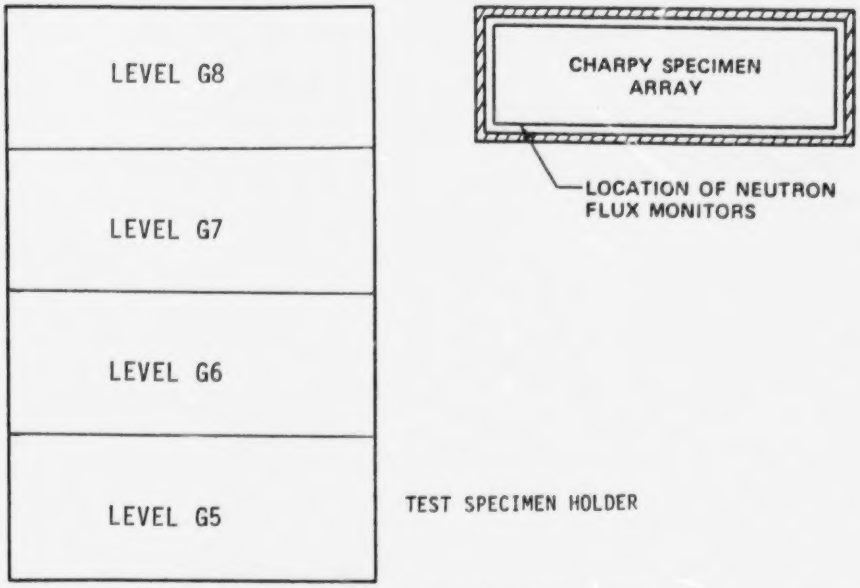
LEVEL G8
LEVEL G7
LEVEL G6
LEVEL G5
CHARPY SPECIMEN ARRAY
LOCATION OF NEUTRON FLUX MONITORS
TEST SPECIMEN HOLDER

(b) Plan View of Surveillance Capsule.

FIGURE 4.5.1.2.1.1. Orientation of the Capsule Relative to the Core and Vessel Wall - Quad Cities Unit 1 Capsule 3.

TABLE 4.5.1.2.1.1

SUMMARY OF REACTOR OPERATIONS
QUAD-CITIES UNIT 1 CAPSULE 3

TIME PERIOD	START DATE	TIME INTERVAL	AVERAGE POWER LEVEL (MWt)	LOCAL POWER FACTOR
1	6/72	30.	1321.	1.00
2	7/72	31.	809.	1.00
3	8/72	31.	1183.	1.00
4	9/72	30.	1497.	1.00
5	10/72	31.	1765.	1.00
6	11/72	30.	1876.	1.00
7	12/72	31.	1949.	1.00
8	1/73	31.	1941.	1.00
9	2/73	28.	1861.	1.00
10	3/73	31.	1918.	1.00
11	4/73	30.	1303.	1.00
12	5/73	31.	1137.	1.00
13	6/73	30.	2159.	1.00
14	7/73	31.	2124.	1.00
15	8/73	31.	1685.	1.00
16	9/73	30.	1562.	1.00
17	10/73	31.	1720.	1.00
18	11/73	30.	1768.	1.00
19	12/73	31.	2097.	1.00
20	1/74	31.	1502.	1.00
21	2/74	28.	2097.	1.00
22	3/74	31.	1981.	1.00
23	4/74	30.	0.	1.00
24	5/74	31.	0.	1.00
25	6/74	31.	0.	1.00
26	7/74	30.	261.	1.00
27	8/74	31.	1999.	1.00
28	9/74	30.	2192.	1.00
29	10/74	31.	1200.	1.00
30	11/74	30.	1911.	1.00
31	12/74	31.	2124.	1.00
32	1/75	31.	630.	1.00
33	2/75	28.	269.	1.00
34	3/75	31.	2242.	1.00
35	4/75	30.	2350.	1.00
36	5/75	31.	1441.	1.00
37	6/75	30.	1941.	1.00
38	7/75	31.	1765.	1.00
39	8/75	31.	1559.	1.00
40	9/75	30.	1886.	1.00
41	10/75	31.	1733.	1.00
42	11/75	30.	1597.	1.00
43	12/75	31.	1459.	1.00
44	1/76	31.	85.	1.00

TABLE 4.5.1.2.1.1 (Cont'd)

SUMMARY OF REACTOR OPERATIONS
QUAD-CITIES UNIT 1 CAPSULE 3

TIME PERIOD	START DATE	TIME INTERVAL	AVERAGE POWER LEVEL (MWt)	LOCAL POWER FACTOR
45	2/76	29.	0.	1.00
46	3/76	31.	537.	1.00
47	4/76	30.	1687.	1.00
48	5/76	31.	1692.	1.00
49	6/76	30.	1173.	1.00
50	7/76	31.	660.	1.00
51	8/76	31.	1248.	1.00
52	9/76	30.	2152.	1.00
53	10/76	31.	2029.	1.00
54	11/76	30.	1645.	1.00
55	12/76	31.	2152.	1.00
56	1/77	31.	1991.	1.00
57	2/77	28.	1652.	1.00
58	3/77	31.	1200.	1.00
59	4/77	30.	0.	1.00
60	5/77	31.	939.	1.00
61	6/77	30.	1675.	1.00
62	7/77	31.	1700.	1.00
63	8/77	31.	884.	1.00
64	9/77	30.	691.	1.00
65	10/77	31.	1323.	1.00
66	11/77	30.	1831.	1.00
67	12/77	31.	1926.	1.00
68	1/78	31.	2277.	1.00
69	2/78	28.	1770.	1.00
70	3/78	31.	2250.	1.00
71	4/78	30.	1404.	1.00
72	5/78	31.	1469.	1.00
73	6/78	30.	1692.	1.00
74	7/78	31.	1964.	1.00
75	8/78	31.	2074.	1.00
76	9/78	30.	1833.	1.00
77	10/78	31.	1592.	1.00
78	11/78	30.	1464.	1.00
79	12/78	31.	1474.	1.00
80	1/79	12.	1579.	1.00
	1/13/79	DISCHARGED*		

---

*EFFECTIVE FULL POWER OPERATION TIME WAS 1.243+008 SECONDS AT A FULL POWER LEVEL OF 2511. MWt.

426

TABLE 4.5.1.2.1.2

REACTION RATE DATA AND CORRECTION FACTORS FOR QUAD-CITIES UNIT 1 CAPSULE 3

REACTION NAME	IDENT	TOR RATE (DPS/NUCL)	SATURATION FACTOR	GRADIENT FACTOR	IMPURITY FACTOR	AVG REACTION RATE (RPS/NUCL)	% UNCERTAIN (1σ)
^{54}Fe(n,p)^{54}Mn	G-5	7.24-015	6.07	1.000	1.000	4.38-014	10.
	G-6	5.49-015				3.33-014	
	G-7	4.22-015				2.56-014	
	G-8	2.22-015				1.35-014	
^{58}Ni(n,p)^{58}Co	G-5	1.11-016	552.00	1.000	1.000	6.13-014	36.
	G-6	6.20-017				3.43-014	57.
	G-7	6.10-017				3.37-014	34.
	G-8	3.17-017				1.75-014	54.
^{63}Cu(n,α)^{60}Co	G-5	1.16-016	3.58	1.000	1.000	4.14-016	10.
	G-6	9.10-017				3.27-016	
	G-7	6.87-017				2.46-016	
	G-8	5.22-017				1.88-016	

TABLE 4.5.1.3.1.3A

FERRET-SAND II RESULTS FOR
QUAD-CITIES UNIT 1 CAPSULE 3 BASKET G-5
(AVERAGE FOR CAPSULE)

GROUP	ENERGY (MeV)	A PRIORI FLUX* ($n/cm^2 \cdot s$)	ADJUSTED FLUX ($n/cm^2 \cdot s$)	% UNCERTAIN (1σ)
1	1.492+001	2.062+007	2.293+007	44.
2	1.350+001	4.287+007	4.769+007	39.
3	1.162+001	1.987+008	2.206+008	35.
4	1.000+001	6.032+008	6.677+008	30.
5	8.607+000	1.526+009	1.679+009	26.
6	7.408+000	3.609+009	3.916+009	24.
7	6.065+000	1.329+010	1.423+010	20.
8	4.966+000	2.062+010	2.136+010	21.
9	3.679+000	3.787+010	3.815+010	21.
10	2.865+000	4.296+010	4.274+010	24.
11	2.231+000	6.828+010	6.755+010	27.
12	1.738+000	5.902+010	5.822+010	32.
13	1.353+000	5.536+010	5.441+010	37.
14	1.108+000	3.546+010	3.479+010	41.
15	8.208-001	5.032+010	4.945+010	45.
16	6.393-001	3.902+010	3.849+010	49.
17	4.979-001	3.586+010	3.558+010	52.
18	3.877-001	3.297+010	3.293+010	55.
19	3.020-001	3.037+010	3.054+010	58.
20	1.832-001	5.337+010	5.405+010	60.
21	1.111-001	4.430+010	4.513+010	61.
22	6.738-002	3.648+010	3.736+010	62.
23	4.087-002	3.163+010	3.253+010	63.
24	2.554-002	2.696+010	2.782+010	63.
25	1.989-002	1.365+010	1.412+010	64.
26	1.503-002	1.499+010	1.553+010	64.
27	9.119-003	2.605+010	2.703+010	64.
28	5.531-003	2.575+010	2.674+010	64.
29	3.355-003	2.613+010	2.715+010	64.
30	2.839-003	8.823+009	9.171+009	64.
31	2.404-003	8.867+009	9.219+009	64.
32	2.035-003	8.925+009	9.280+009	64.
33	1.234-003	2.705+010	2.813+010	64.
34	7.485-004	2.742+010	2.852+010	64.
35	4.540-004	2.775+010	2.886+010	64.
36	2.754-004	2.806+010	2.918+010	64.
37	1.670-004	2.838+010	2.951+010	64.
38	1.013-004	2.872+010	2.987+010	64.
39	6.144-005	2.907+010	3.024+010	64.
40	3.727-005	2.945+010	3.063+010	64.

428

TABLE 4.5.1.3.1.3A (Cont'd)

FERRET-SAND II RESULTS FOR
QUAD-CITIES UNIT 1 CAPSULE 3 BASKET G-5
(AVERAGE FOR CAPSULE)

GROUP	ENERGY (MeV)	A PRIORI FLUX* ($n/cm^2 \cdot s$)	ADJUSTED FLUX ($n/cm^2 \cdot s$)	% UNCERTAIN (1σ)
41	2.260-005	2.985+010	3.105+010	64.
42	1.371-005	3.027+010	3.148+010	64.
43	8.315-006	3.072+010	3.195+010	64.
44	5.043-006	3.111+010	3.236+010	64.
45	3.059-006	3.141+010	3.267+010	64.
46	1.855-006	3.225+010	3.354+010	64.
47	1.125-006	3.407+010	3.544+010	64.
48	6.826-007	3.571+010	3.714+010	64.
49	4.140-007	3.684+010	3.832+010	64.
50	2.511-007	1.085+011	1.128+011	64.
51	1.523-007	2.075+011	2.158+011	64.
52	9.237-008	2.501+011	2.601+011	64.
53	1.000-010	1.473+012	1.532+012	64.
FLUX, E > 0.0 MeV		3.411+012	3.520+012	48.
FLUX, E < 0.414 eV		2.076+012	2.159+012	62.
FLUX, E > 0.1 MeV		6.327+011	6.320+011	30.
FLUX, E > 1.0 MeV		3.561+011	3.549+011	19.
dpa/s		5.055-010	5.078-010	19.
FLUENCE+, E > 1.0 MeV		4.426+019	4.411+019	19.
dpa+		6.283-002	6.312-002	19.

---

*ABSOLUTE CALCULATED FLUX (OR NORMALIZED TO Fe54(n,p)Mn54 REACTION RATE).

+BASED ON 1.243+008 EFFECTIVE FULL POWER SECONDS OF EXPOSURE; UNITS OF n/cm^2 FOR FLUENCE AND TOTAL NUMBER OF DISPLACED ATOMS OF IRON PER TARGET ATOM OF IRON FOR dpa.

TABLE 4.5.1.3.1.4A

COMPARISON OF MEASURED AND CALCULATED REACTION RATES USED IN THE ANALYSIS OF QUAD-CITIES UNIT 1 CAPSULE 3 BASKET G-5

	REACTION RATE (DPS/NUCLEUS)			RATIO MEAS/CALC	
REACTION	MEAS	A PRIORI CALC	ADJ CALC	A PRIORI	ADJ CALC
Fe54(n,p)Mn54	4.38-014	4.42-014	4.51-014	0.99	0.97
Ni58(n,p)Co58	6.13-014	5.72-014	5.87-014	1.07	1.04
Cu63(n,α)Co60	4.14-016	3.77-016	4.08-016	1.10	1.01

TABLE 4.5.1.3.1.3B

FERRET-SAND II RESULTS FOR
QUAD-CITIES UNIT 1 CAPSULE 3 BASKET G-6
(AVERAGE FOR CAPSULE)

GROUP	ENERGY (MeV)	A PRIORI FLUX* (n/cm^2•s)	ADJUSTED FLUX (n/cm^2•s)	% UNCERTAIN (1σ)
1	1.492+001	1.577+007	1.840+007	43.
2	1.350+001	3.278+007	3.827+007	39.
3	1.162+001	1.520+008	1.767+008	35.
4	1.000+001	4.612+008	5.332+008	30.
5	8.607+000	1.167+009	1.332+009	26.
6	7.408+000	2.760+009	3.064+009	24.
7	6.065+000	1.016+010	1.099+010	20.
8	4.966+000	1.577+010	1.601+010	21.
9	3.679+000	2.896+010	2.782+010	21.
10	2.865+000	3.285+010	3.083+010	24.
11	2.231+000	5.221+010	4.805+010	28.
12	1.738+000	4.514+010	4.127+010	33.
13	1.353+000	4.233+010	3.841+010	37.
14	1.108+000	2.712+010	2.454+010	42.
15	8.208-001	3.848+010	3.493+010	46.
16	6.393-001	2.983+010	2.729+010	49.
17	4.979-001	2.742+010	2.538+010	53.
18	3.877-001	2.521+010	2.366+010	56.
19	3.020-001	2.322+010	2.211+010	58.
20	1.832-001	4.081+010	3.942+010	60.
21	1.111-001	3.388+010	3.315+010	61.
22	6.738-002	2.789+010	2.760+010	62.
23	4.087-002	2.419+010	2.416+010	63.
24	2.554-002	2.062+010	2.075+010	63.
25	1.989-002	1.044+010	1.056+010	64.
26	1.503-002	1.146+010	1.165+010	64.
27	9.119-003	1.992+010	2.030+010	64.
28	5.531-003	1.969+010	2.011+010	64.
29	3.355-003	1.998+010	2.044+010	64.
30	2.839-003	6.747+009	6.907+009	64.
31	2.404-003	6.781+009	6.946+009	64.
32	2.035-003	6.825+009	6.993+009	64.
33	1.234-003	2.068+010	2.120+010	64.
34	7.485-004	2.097+010	2.149+010	64.
35	4.540-004	2.122+010	2.175+010	64.
36	2.754-004	2.146+010	2.199+010	64.
37	1.670-004	2.170+010	2.225+010	64.
38	1.013-004	2.196+010	2.251+010	64.
39	6.144-005	2.223+010	2.279+010	64.
40	3.727-005	2.252+010	2.309+010	64.

TABLE 4.5.1.3.1.3B (Cont'd)

FERRET-SAND II RESULTS FOR QUAD-CITIES UNIT 1 CAPSULE 3 BASKET G-6 (AVERAGE FOR CAPSULE)

GROUP	ENERGY (MeV)	A PRIORI FLUX* (n/cm^2•s)	ADJUSTED FLUX (n/cm^2•s)	% UNCERTAIN (1σ)
41	2.260-005	2.283+010	2.340+010	64.
42	1.371-005	2.315+010	2.373+010	64.
43	8.315-006	2.349+010	2.408+010	64.
44	5.043-006	2.379+010	2.439+010	64.
45	3.059-006	2.402+010	2.462+010	64.
46	1.855-006	2.466+010	2.528+010	64.
47	1.125-006	2.606+010	2.671+010	64.
48	6.826-007	2.731+010	2.799+010	64.
49	4.140-007	2.817+010	2.888+010	64.
50	2.511-007	8.294+010	8.502+010	64.
51	1.523-007	1.587+011	1.627+011	64.
52	9.237-008	1.913+011	1.961+011	64.
53	1.000-010	1.126+012	1.155+012	64.
FLUX, E > 0.0 MeV		2.608+012	2.630+012	48.
FLUX, E < 0.414 eV		1.588+012	1.627+012	62.
FLUX, E > 0.1 MeV		4.839+011	4.548+011	30.
FLUX, E > 1.0 MeV		2.723+011	2.550+011	19.
dpa/s		3.865-010	3.682-010	19.
FLUENCE+, E > 1.0 MeV		3.384+019	3.170+019	19.
dpa+		4.805-002	4.576-002	19.

---

*ABSOLUTE CALCULATED FLUX (OR NORMALIZED TO Fe54(n,p)Mn54 REACTION RATE).

+BASED ON 1.243+008 EFFECTIVE FULL POWER SECONDS OF EXPOSURE; UNITS OF n/cm^2 FOR FLUENCE AND TOTAL NUMBER OF DISPLACED ATOMS OF IRON PER TARGET ATOM OF IRON FOR dpa.

TABLE 4.5.1.3.1.4B

COMPARISON OF MEASURED AND CALCULATED REACTION RATES USED IN THE ANALYSIS OF QUAD-CITIES UNIT 1 CAPSULE 3 BASKET G-6

REACTION	REACTION RATE (DPS/NUCLEUS) MEAS	A PRIORI CALC	ADJ CALC	RATIO MEAS/CALC A PRIORI	ADJ CALC
Fe54(n,p)Mn54	3.33-014	3.38-014	3.34-014	0.98	1.00
Ni58(n,p)Co58	3.43-014	4.38-014	4.27-014	0.78	0.80
Cu63(n,α)Co60	3.27-016	2.88-016	3.18-016	1.13	1.03

433

BEST COPY AVAILABLE

TABLE 4.5.1.3.1.3C

FERRET-SAND II RESULTS FOR (AVERAGE FOR CAPSULE)
QUAD-CITIES UNIT 1 CAPSULE 3 BASKET G-7

GROUP	ENERGY (MeV)	A PRIORI FLUX* ($n/cm^2 \cdot s$)	ADJUSTED FLUX ($n/cm^2 \cdot s$)	% UNCERTAIN (1σ)
1	1.492+001	1.213+007	1.804+007	43.
2	1.350+001	2.522+007	3.769+007	39.
3	1.162+001	1.169+008	1.747+008	35.
4	1.000+001	3.548+008	5.293+008	30.
5	8.607+000	8.976+008	1.326+009	26.
6	7.408+000	2.123+009	3.060+009	24.
7	6.065+000	7.815+009	1.100+010	20.
8	4.966+000	1.213+010	1.603+010	21.
9	3.679+000	2.228+010	2.782+010	21.
10	2.865+000	2.527+010	3.075+010	24.
11	2.231+000	4.016+010	4.779+010	28.
12	1.738+000	3.472+010	4.089+010	33.
13	1.353+000	3.257+010	3.791+010	37.
14	1.108+000	2.086+010	2.412+010	42.
15	8.208-001	2.960+010	3.419+010	46.
16	6.393-001	2.295+010	2.662+010	50.
17	4.979-001	2.109+010	2.467+010	53.
18	3.877-001	1.939+010	2.292+010	56.
19	3.020-001	1.786+010	2.137+010	58.
20	1.832-001	3.140+010	3.801+010	60.
21	1.111-001	2.606+010	3.191+010	61.
22	6.738-002	2.146+010	2.654+010	62.
23	4.087-002	1.861+010	2.321+010	63.
24	2.554-002	1.586+010	1.991+010	63.
25	1.989-002	8.029+009	1.013+010	64.
26	1.503-002	8.817+009	1.117+010	64.
27	9.119-003	1.532+010	1.946+010	64.
28	5.531-003	1.514+010	1.927+010	64.
29	3.355-003	1.537+010	1.959+010	64.
30	2.839-003	5.190+009	6.618+009	64.
31	2.404-003	5.216+009	6.655+009	64.
32	2.035-003	5.250+009	6.700+009	64.
33	1.234-003	1.591+010	2.031+010	64.
34	7.485-004	1.613+010	2.059+010	64.
35	4.540-004	1.632+010	2.084+010	64.
36	2.754-004	1.650+010	2.107+010	64.
37	1.670-004	1.669+010	2.131+010	64.
38	1.013-004	1.689+010	2.157+010	64.
39	6.144-005	1.710+010	2.184+010	64.
40	3.727-005	1.732+010	2.212+010	64.

TABLE 4.5.1.3.1.3C (Cont'd)

FERRET-SAND II RESULTS FOR (AVERAGE FOR CAPSULE)
QUAD-CITIES UNIT 1 CAPSULE 3 BASKET G-7

GROUP	ENERGY (MeV)	A PRIORI FLUX* (n/cm^2•s)	ADJUSTED FLUX (n/cm^2•s)	% UNCERTAIN (1σ)
41	2.260-005	1.756+010	2.242+010	64.
42	1.371-005	1.781+010	2.274+010	64.
43	8.315-006	1.807+010	2.308+010	64.
44	5.043-006	1.830+010	2.337+010	64.
45	3.059-006	1.848+010	2.359+010	64.
46	1.855-006	1.897+010	2.423+010	64.
47	1.125-006	2.004+010	2.559+010	64.
48	6.826-007	2.100+010	2.682+010	64.
49	4.140-007	2.167+010	2.767+010	64.
50	2.511-007	6.380+010	8.146+010	64.
51	1.523-007	1.221+011	1.559+011	64.
52	9.237-008	1.471+011	1.878+011	64.
53	1.000-010	8.665+011	1.106+012	64.
FLUX, E > 0.0 MeV		2.006+012	2.531+012	48.
FLUX, E < 0.414 eV		1.221+012	1.559+012	62.
FLUX, E > 0.1 MeV		3.722+011	4.467+011	30.
FLUX, E > 1.0 MeV		2.094+011	2.531+011	19.
dpa/s		2.973-010	3.642-010	19.
FLUENCE+, E > 1.0 MeV		2.603+019	3.147+019	19.
dpa+		3.696-002	4.527-002	19.

---

*ABSOLUTE CALCULATED FLUX (OR NORMALIZED TO Fe54(n,p)Mn54 REACTION RATE).

+BASED ON 1.243+008 EFFECTIVE FULL POWER SECONDS OF EXPOSURE; UNITS OF n/cm^2 FOR FLUENCE AND TOTAL NUMBER OF DISPLACED ATOMS OF IRON PER TARGET ATOM OF IRON FOR dpa.

TABLE 4.5.1.3.1.4C

COMPARISON OF MEASURED AND CALCULATED REACTION RATES USED IN THE ANALYSIS OF QUAD-CITIES UNIT 1 CAPSULE 3 BASKET G-7

	REACTION RATE (DPS/NUCLEUS)			RATIO MEAS/CALC	
REACTION	MEAS	A PRIORI CALC	ADJ CALC	A PRIORI	ADJ CALC
Fe54(n,p)Mn54	2.56-014	2.60-014	2.58-014	0.98	0.99
Ni58(n,p)Co58	3.37-014	3.37-014	3.34-014	1.00	1.01
Cu63(n,α)Co60	2.46-016	2.22-016	2.44-016	1.11	1.01

TABLE 4.5.1.3.1.3D

FERRET-SAND II RESULTS FOR
QUAD-CITIES UNIT 1 CAPSULE 3 BASKET G-8
(AVERAGE FOR CAPSULE)

GROUP	ENERGY (MeV)	A PRIORI FLUX* ($n/cm^2 \cdot s$)	ADJUSTED FLUX ($n/cm^2 \cdot s$)	% UNCERTAIN (1σ)
1	1.492+001	6.065+006	1.118+007	43.
2	1.350+001	1.261+007	2.326+007	39.
3	1.162+001	5.845+007	1.065+008	34.
4	1.000+001	1.774+008	3.184+008	30.
5	8.607+000	4.488+008	7.756+008	25.
6	7.408+000	1.061+009	1.679+009	23.
7	6.065+000	3.907+009	5.653+009	20.
8	4.966+000	6.064+009	7.240+009	21.
9	3.679+000	1.114+010	1.144+010	21.
10	2.865+000	1.263+010	1.218+010	25.
11	2.231+000	2.008+010	1.846+010	29.
12	1.738+000	1.736+010	1.563+010	34.
13	1.353+000	1.628+010	1.435+010	38.
14	1.108+000	1.043+010	9.124+009	42.
15	8.208-001	1.480+010	1.307+010	46.
16	6.393-001	1.148+010	1.038+010	50.
17	4.979-001	1.055+010	9.868+009	53.
18	3.877-001	9.696+009	9.440+009	56.
19	3.020-001	8.931+009	9.062+009	58.
20	1.832-001	1.570+010	1.657+010	60.
21	1.111-001	1.303+010	1.426+010	61.
22	6.738-002	1.073+010	1.211+010	62.
23	4.087-002	9.304+009	1.077+010	63.
24	2.554-002	7.930+009	9.368+009	63.
25	1.989-002	4.015+009	4.815+009	64.
26	1.503-002	4.408+009	5.346+009	64.
27	9.119-003	7.661+009	9.364+009	64.
28	5.531-003	7.572+009	9.304+009	64.
29	3.355-003	7.686+009	9.477+009	64.
30	2.839-003	2.595+009	3.207+009	64.
31	2.404-003	2.608+009	3.227+009	64.
32	2.035-003	2.625+009	3.251+009	64.
33	1.234-003	7.955+009	9.857+009	64.
34	7.485-004	8.066+009	9.997+009	64.
35	4.540-004	8.161+009	1.012+010	64.
36	2.754-004	8.252+009	1.023+010	64.
37	1.670-004	8.346+009	1.035+010	64.
38	1.013-004	8.447+009	1.047+010	64.
39	6.144-005	8.551+009	1.060+010	64.
40	3.727-005	8.662+009	1.074+010	64.

437

TABLE 4.5.1.3.1.3D (Cont'd)

FERRET-SAND II RESULTS FOR
QUAD-CITIES UNIT 1 CAPSULE 3 BASKET G-8
(AVERAGE FOR CAPSULE)

GROUP	ENERGY (MeV)	A PRIORI FLUX* (n/cm^2•s)	ADJUSTED FLUX (n/cm^2•s)	% UNCERTAIN (1σ)
41	2.260-005	8.780+009	1.089+010	64.
42	1.371-005	8.904+009	1.104+010	64.
43	8.315-006	9.036+009	1.120+010	64.
44	5.043-006	9.151+009	1.135+010	64.
45	3.059-006	9.238+009	1.145+010	64.
46	1.855-006	9.486+009	1.176+010	64.
47	1.125-006	1.002+010	1.242+010	64.
48	6.826-007	1.050+010	1.302+010	64.
49	4.140-007	1.084+010	1.343+010	64.
50	2.511-007	3.190+010	3.955+010	64.
51	1.523-007	6.103+010	7.567+010	64.
52	9.237-008	7.356+010	9.120+010	64.
53	1.000-010	4.333+011	5.372+011	64.
FLUX, E > 0.0 MeV		1.003+012	1.192+012	49.
FLUX, E < 0.414 eV		6.106+011	7.570+011	62.
FLUX, E > 0.1 MeV		1.861+011	1.822+011	30.
FLUX, E > 1.0 MeV		1.047+011	1.015+011	19.
dpa/s		1.487-010	1.514-010	19.
FLUENCE+, E > 1.0 MeV		1.302+019	1.261+019	19.
dpa+		1.848-002	1.882-002	19.

---

*ABSOLUTE CALCULATED FLUX (OR NORMALIZED TO Fe54(n,p)Mn54 REACTION RATE).

+BASED ON 1.243+008 EFFECTIVE FULL POWER SECONDS OF EXPOSURE; UNITS OF n/cm^2 FOR FLUENCE AND TOTAL NUMBER OF DISPLACED ATOMS OF IRON PER TARGET ATOM OF IRON FOR dpa.

TABLE 4.5.1.3.1.4D

COMPARISON OF MEASURED AND CALCULATED REACTION RATES USED IN THE ANALYSIS OF QUAD-CITIES UNIT 1 CAPSULE 3 BASKET G-8

	REACTION RATE (DPS/NUCLEUS)			RATIO MEAS/CALC	
REACTION	MEAS	A PRIORI CALC	ADJ CALC	A PRIORI	ADJ CALC
Fe54(n,p)Mn54	1.35-014	1.30-014	1.46-014	1.04	0.93
Ni58(n,p)Co58	1.75-014	1.68-014	1.88-014	1.04	0.93
Cu63(n,α)Co60	1.88-016	1.11-016	1.73-016	1.69	1.09

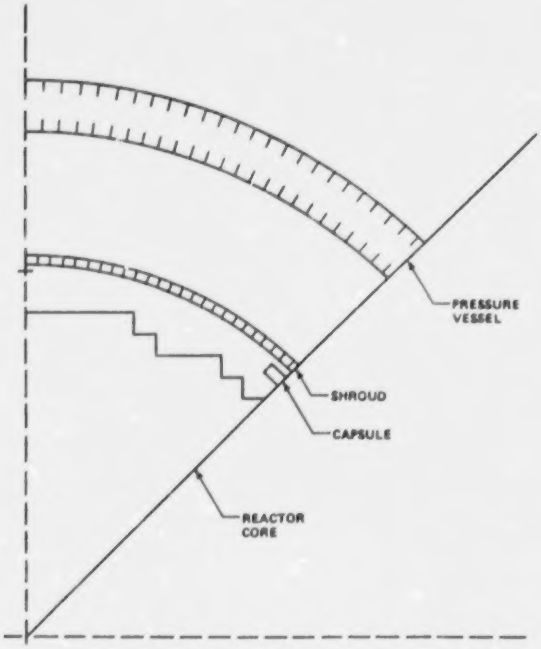
PRESSURE VESSEL
SHROUD
CAPSULE
REACTOR CORE

(a) Reactor Geometry.

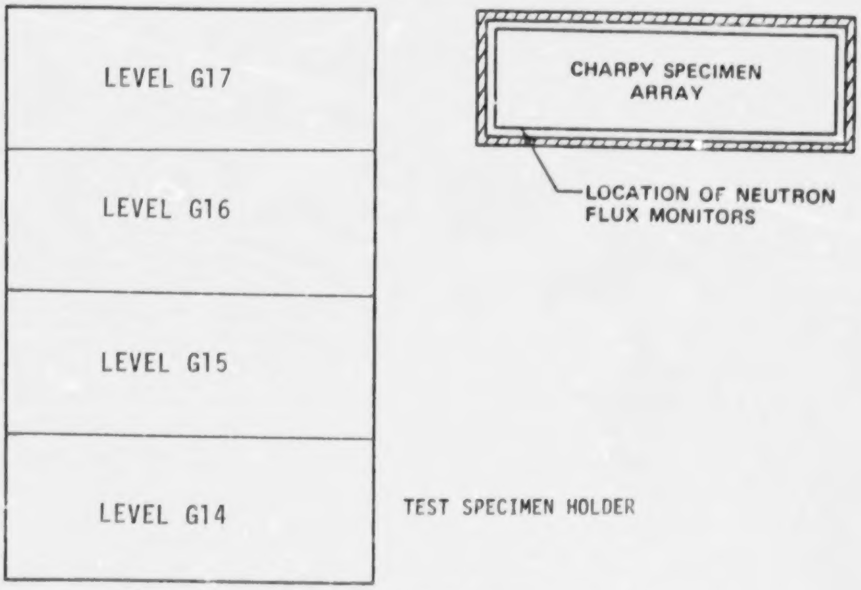
LEVEL G17
LEVEL G16
LEVEL G15
LEVEL G14
TEST SPECIMEN HOLDER
CHARPY SPECIMEN ARRAY
LOCATION OF NEUTRON FLUX MONITORS

(b) Plan View of Surveillance Capsule.

FIGURE 4.5.1.3.1.1. Orientation of the Capsule Relative to the Core and Vessel Wall - Quad Cities Unit 2 Capsule 3.

TABLE 4.5.1.3.1.1

SUMMARY OF REACTOR OPERATIONS
QUAD-CITIES UNIT 2 CAPSULE 3

TIME PERIOD	START DATE	TIME INTERVAL	AVERAGE POWER LEVEL (MWt)	LOCAL POWER FACTOR
1	6/72	30.	341.	1.00
2	7/72	31.	791.	1.00
3	8/72	31.	999.	1.00
4	9/72	30.	0.	1.00
5	10/72	31.	801.	1.00
6	11/72	30.	1861.	1.00
7	12/72	31.	1780.	1.00
8	1/73	31.	1650.	1.00
9	2/73	28.	2011.	1.00
10	3/73	31.	2378.	1.00
11	4/73	30.	1052.	1.00
12	5/73	31.	1630.	1.00
13	6/73	30.	2041.	1.00
14	7/73	31.	1996.	1.00
15	8/73	31.	1931.	1.00
16	9/73	30.	1783.	1.00
17	10/73	31.	1763.	1.00
18	11/73	30.	2079.	1.00
19	12/73	31.	2220.	1.00
20	1/74	31.	1911.	1.00
21	2/74	28.	2230.	1.00
22	3/74	31.	1642.	1.00
23	4/74	30.	1913.	1.00
24	5/74	31.	2036.	1.00
25	6/74	30.	932.	1.00
26	7/74	31.	1836.	1.00
27	8/74	31.	1966.	1.00
28	9/74	30.	444.	1.00
29	10/74	31.	1763.	1.00
30	11/74	30.	1723.	1.00
31	12/74	31.	1097.	1.00
32	1/75	31.	0.	1.00
33	2/75	28.	0.	1.00
34	3/75	31.	0.	1.00
35	4/75	30.	25.	1.00
36	5/75	31.	1697.	1.00
37	6/75	30.	1702.	1.00
38	7/75	31.	1512.	1.00
39	8/75	31.	866.	1.00
40	9/75	30.	1494.	1.00
41	10/75	31.	176.	1.00
42	11/75	30.	1469.	1.00
43	12/75	31.	2242.	1.00
44	1/76	31.	2406.	1.00
45	2/76	29.	1677.	1.00
46	3/76	31.	1888.	1.00

441

TABLE 4.5.1.3.1.1 (Cont'd)

SUMMARY OF REACTOR OPERATIONS
QUAD-CITIES UNIT 2 CAPSULE 3

TIME PERIOD	START DATE	TIME INTERVAL	AVERAGE POWER LEVEL (MWt)	LOCAL POWER FACTOR
47	4/76	30.	2240.	1.00
48	5/76	31.	1908.	1.00
49	6/76	30.	1695.	1.00
50	7/76	31.	1733.	1.00
51	8/76	31.	1650.	1.00
52	9/76	30.	537.	1.00
53	10/76	31.	0.	1.00
54	11/76	30.	1685.	1.00
55	12/76	31.	1836.	1.00
56	1/77	31.	2350.	1.00
57	2/77	28.	1597.	1.00
58	3/77	31.	691.	1.00
59	4/77	30	2325.	1.00
60	5/77	31.	1908.	1.00
61	6/77	30.	1843.	1.00
62	7/77	31.	1494.	1.00
63	8/77	31.	1032.	1.00
64	9/77	30.	1143.	1.00
65	10/77	31.	1667.	1.00
66	11/77	30.	1494.	1.00
67	12/77	31.	1820.	1.00
68	1/78	31.	728.	1.00
69	2/78	28.	0.	1.00
70	3/78	31.	1143.	1.00
71	4/78	30.	2172.	1.00
72	5/78	31.	1384.	1.00
73	6/78	30.	1268.	1.00
74	7/78	31.	2019.	1.00
75	8/78	31.	2257.	1.00
76	9/78	30.	2107.	1.00
77	10/78	31.	1931.	1.00
78	11/78	30.	1959.	1.00
79	12/78	31.	2164.	1.00
80	1/79	31.	2162.	1.00
81	2/79	28.	1918.	1.00
82	3/79	31.	1898.	1.00
83	4/79	30.	1715.	1.00
84	5/79	31.	1901.	1.00
85	6/79	30.	1836.	1.00
86	7/79	31.	1720.	1.00
87	8/79	31.	1549.	1.00
88	9/79	30.	1276.	1.00
89	10/79	31.	1240.	1.00
90	11/79	30.	896.	1.00
	12/1/79	DISCHARGED*		

---

*EFFECTIVE FULL POWER OPERATION TIME WAS 1.422+008 SECONDS AT A FULL POWER LEVEL OF 2511. MWt.

TABLE 4.5.1.3.1.2

REACTION RATE DATA AND CORRECTION FACTORS FOR QUAD-CITIES UNIT 2 CAPSULE 3

REACTION NAME	IDENT	TOR RATE (DPS/NUCL)	SATURATION FACTOR	GRADIENT FACTOR	IMPURITY FACTOR	AVG REACTION RATE (RPS/NUCL)	% UNCERTAIN (1σ)
54Fe(n,p)54Mn	G-14	7.91-015	4.92	1.000	1.000	3.89-014	10.
	G-15	6.65-015				3.27-014	
	G-16	4.65-015				2.29-014	
	G-17	4.41-015				2.18-014	
58Ni(n,p)58Co	G-14	1.80-016	276.00	1.000	1.000	4.95-014	29.
	G-15	1.52-016				4.21-014	29.
	G-16	1.03-016				2.84-014	14.
	G-17	7.96-017				2.20-014	41.
63Cu(n,α)60Co	G-14	1.14-016	3.15	1.000	1.000	3.59-016	10.
	G-15	9.74-017				3.07-016	
	G-16	6.60-017				2.08-016	
	G-17	6.37-017				2.02-016	

TABLE 4.5.1.2.1.3A

FERRET-SAND II RESULTS FOR
QUAD-CITIES UNIT 2 CAPSULE 3 BASKET G-14
(AVERAGE FOR CAPSULE)

GROUP	ENERGY (MeV)	A PRIORI FLUX* (n/cm²•s)	ADJUSTED FLUX (n/cm²•s)	% UNCERTAIN (1σ)
1	1.492+001	1.819+007	1.990+007	44.
2	1.350+001	3.782+007	4.140+007	39.
3	1.162+001	1.754+008	1.916+008	35.
4	1.000+001	5.322+008	5.797+008	30.
5	8.607+000	1.346+009	1.457+009	26.
6	7.408+000	3.184+009	3.398+009	24.
7	6.065+000	1.172+010	1.234+010	20.
8	4.966+000	1.819+010	1.853+010	21.
9	3.679+000	3.342+010	3.305+010	20.
10	2.865+000	3.790+010	3.702+010	23.
11	2.231+000	6.025+010	5.827+010	27.
12	1.738+000	5.208+010	5.020+010	32.
13	1.353+000	4.885+010	4.689+010	37.
14	1.108+000	3.129+010	2.999+010	41.
15	8.208-001	4.440+010	4.261+010	45.
16	6.393-001	3.443+010	3.317+010	49.
17	4.979-001	3.164+010	3.067+010	52.
18	3.877-001	2.909+010	2.840+010	55.
19	3.020-001	2.679+010	2.635+010	58.
20	1.832-001	4.709+010	4.666+010	59.
21	1.111-001	3.909+010	3.899+010	61.
22	6.738-002	3.219+010	3.229+010	62.
23	4.087-002	2.791+010	2.814+010	63.
24	2.554-002	2.379+010	2.408+010	63.
25	1.989-002	1.204+010	1.223+010	64.
26	1.503-002	1.323+010	1.345+010	64.
27	9.119-003	2.298+010	2.342+010	64.
28	5.531-003	2.272+010	2.317+010	64.
29	3.355-003	2.306+010	2.353+010	64.
30	2.839-003	7.785+009	7.949+009	64.
31	2.404-003	7.824+009	7.991+009	64.
32	2.035-003	7.875+009	8.044+009	64.
33	1.234-003	2.386+010	2.438+010	64.
34	7.485-004	2.420+010	2.472+010	64.
35	4.540-004	2.448+010	2.502+010	64.
36	2.754-004	2.476+010	2.529+010	64.
37	1.670-004	2.504+010	2.558+010	64.
38	1.013-004	2.534+010	2.589+010	64.
39	6.144-005	2.565+010	2.621+010	64.
40	3.727-005	2.599+010	2.655+010	64.

TABLE 4.5.1.2.1.3A (Cont'd)

FERRET-SAND II RESULTS FOR QUAD-CITIES UNIT 2 CAPSULE 3 BASKET G-14 (AVERAGE FOR CAPSULE)

GROUP	ENERGY (MeV)	A PRIORI FLUX* ($n/cm^2 \cdot s$)	ADJUSTED FLUX ($n/cm^2 \cdot s$)	% UNCERTAIN (1σ)
41	2.260-005	2.634+010	2.691+010	64.
42	1.371-005	2.671+010	2.729+010	64.
43	8.315-006	2.711+010	2.770+010	64.
44	5.043-006	2.745+010	2.805+010	64.
45	3.059-006	2.772+010	2.832+010	64.
46	1.855-006	2.846+010	2.908+010	64.
47	1.125-006	3.006+010	3.072+010	64.
48	6.826-007	3.151+010	3.219+010	64.
49	4.140-007	3.251+010	3.321+010	64.
50	2.511-007	9.570+010	9.778+010	64.
51	1.523-007	1.831+011	1.871+011	64.
52	9.237-008	2.207+011	2.255+011	64.
53	1.000-010	1.300+012	1.328+012	64.
FLUX, E > 0.0 MeV		3.009+012	3.049+012	48.
FLUX, E < 0.414 eV		1.832+012	1.872+012	62.
FLUX, E > 0.1 MeV		5.583+011	5.456+011	30.
FLUX, E > 1.0 MeV		3.142+011	3.065+011	19.
dpa/s		4.460-010	4.389-010	18.
FLUENCE+, E > 1.0 MeV		4.468+019	4.359+019	19.
dpa+		6.342-002	6.241-002	18.

---

*ABSOLUTE CALCULATED FLUX (OR NORMALIZED TO Fe54(n,p)Mn54 REACTION RATE).

+BASED ON 1.422+008 EFFECTIVE FULL POWER SECONDS OF EXPOSURE; UNITS OF n/cm^2 FOR FLUENCE AND TOTAL NUMBER OF DISPLACED ATOMS OF IRON PER TARGET ATOM OF IRON FOR dpa.

TABLE 4.5.1.2.1.4A
COMPARISON OF MEASURED AND CALCULATED REACTION RATES USED IN THE ANALYSIS OF QUAD-CITIES UNIT 2 CAPSULE 3 BASKET G-14

REACTION	REACTION RATE (DPS/NUCLEUS) MEAS	A PRIORI CALC	ADJ CALC	RATIO MEAS/CALC A PRIORI	ADJ CALC
Fe54(n,p)Mn54	3.89-014	3.90-014	3.91-014	1.00	0.99
Ni58(n,p)Co58	4.95-014	5.05-014	5.04-014	0.98	0.98
Cu63(n,α)Co60	3.59-016	3.33-016	3.54-016	1.08	1.01

TABLE 4.5.1.2.1.3B

FERRET-SAND II RESULTS FOR
QUAD-CITIES UNIT 2 CAPSULE 3 BASKET G-15
(AVERAGE FOR CAPSULE)

GROUP	ENERGY (MeV)	A PRIORI FLUX* ($n/cm^2 \cdot s$)	ADJUSTED FLUX ($n/cm^2 \cdot s$)	% UNCERTAIN (1σ)
1	1.492+001	1.456+007	1.700+007	43.
2	1.350+001	3.026+007	3.538+007	39.
3	1.162+001	1.403+008	1.638+008	35.
4	1.000+001	4.258+008	4.957+008	30.
5	8.607+000	1.077+009	1.245+009	26.
6	7.408+000	2.547+009	2.899+009	24.
7	6.065+000	9.378+009	1.052+010	20.
8	4.966+000	1.455+010	1.570+010	21.
9	3.679+000	2.674+010	2.786+010	20.
10	2.865+000	3.032+010	3.113+010	23.
11	2.231+000	4.820+010	4.893+010	27.
12	1.738+000	4.166+010	4.211+010	32.
13	1.353+000	3.908+010	3.928+010	37.
14	1.108+000	2.503+010	2.509+010	41.
15	8.208-001	3.552+010	3.564+010	45.
16	6.393-001	2.754+010	2.774+010	49.
17	4.979-001	2.531+010	2.565+010	52.
18	3.877-001	2.327+010	2.377+010	55.
19	3.020-001	2.143+010	2.207+010	58.
20	1.832-001	3.768+010	3.911+010	59.
21	1.111-001	3.127+010	3.270+010	61.
22	6.738-002	2.575+010	2.710+010	62.
23	4.087-002	2.233+010	2.362+010	63.
24	2.554-002	1.903+010	2.022+010	63.
25	1.989-002	9.635+009	1.027+010	64.
26	1.503-002	1.058+010	1.130+010	64.
27	9.119-003	1.839+010	1.968+010	64.
28	5.531-003	1.817+010	1.947+010	64.
29	3.355-003	1.845+010	1.978+010	64.
30	2.839-003	6.228+009	6.681+009	64.
31	2.404-003	6.259+009	6.717+009	64.
32	2.035-003	6.300+009	6.762+009	64.
33	1.234-003	1.909+010	2.049+010	64.
34	7.485-004	1.936+010	2.078+010	64.
35	4.540-004	1.959+010	2.103+010	64.
36	2.754-004	1.981+010	2.126+010	64.
37	1.670-004	2.003+010	2.151+010	64.
38	1.013-004	2.027+010	2.177+010	64.
39	6.144-005	2.052+010	2.203+010	64.
40	3.727-005	2.079+010	2.232+010	64.

TABLE 4.5.1.2.1.3B (Cont'd)

FERRET-SAND II RESULTS FOR
QUAD-CITIES UNIT 2 CAPSULE 3 BASKET G-15
(AVERAGE FOR CAPSULE)

GROUP	ENERGY (MeV)	A PRIORI FLUX* (n/cm^2·s)	ADJUSTED FLUX (n/cm^2·s)	% UNCERTAIN (1σ)
41	2.260-005	2.107+010	2.262+010	64.
42	1.371-005	2.137+010	2.294+010	64.
43	8.315-006	2.169+010	2.328+010	64.
44	5.043-006	2.196+010	2.358+010	64.
45	3.059-006	2.217+010	2.380+010	64.
46	1.855-006	2.277+010	2.444+010	64.
47	1.125-006	2.405+010	2.582+010	64.
48	6.826-007	2.521+010	2.706+010	64.
49	4.140-007	2.601+010	2.792+010	64.
50	2.511-007	7.656+010	8.219+010	64.
51	1.523-007	1.465+011	1.573+011	64.
52	9.237-008	1.765+011	1.895+011	64.
53	1.000-010	1.040+012	1.116+012	64.
FLUX, E > 0.0 MeV		2.408+012	2.562+012	48.
FLUX, E < 0.414 eV		1.465+012	1.573+012	62.
FLUX, E > 0.1 MeV		4.466+011	4.579+011	30.
FLUX, E > 1.0 MeV		2.513+011	2.577+011	19.
dpa/s		3.568-010	3.692-010	18.
FLUENCE+, E > 1.0 MeV		3.574+019	3.664+019	19.
dpa+		5.074-002	5.250-002	18.

---

* ABSOLUTE CALCULATED FLUX (OR NORMALIZED TO Fe54(n,p)Mn54 REACTION RATE).

+ BASED ON 1.422+008 EFFECTIVE FULL POWER SECONDS OF EXPOSURE; UNITS OF n/cm^2 FOR FLUENCE AND TOTAL NUMBER OF DISPLACED ATOMS OF IRON PER TARGET ATOM OF IRON FOR dpa.

TABLE 4.5.1.2.1.4B

COMPARISON OF MEASURED AND CALCULATED REACTION RATES USED IN THE ANALYSIS OF QUAD-CITIES UNIT 2 CAPSULE 3 BASKET G-15

	REACTION RATE (DPS/NUCLEUS)			RATIO MEAS/CALC	
REACTION	MEAS	A PRIORI CALC	ADJ CALC	A PRIORI	ADJ CALC
Fe54(n,p)Mn54	3.27-014	3.12-014	3.31-014	1.05	0.99
Ni58(n,p)Co58	4.21-014	4.04-014	4.26-014	1.04	0.99
Cu63(n,α)Co60	3.07-016	2.66-016	3.02-016	1.15	1.02

TABLE 4.5.1.2.1.3C

FERRET-SAND II RESULTS FOR QUAD-CITIES UNIT 2 CAPSULE 3 BASKET G-16 (AVERAGE FOR CAPSULE)

GROUP	ENERGY (MeV)	A PRIORI FLUX* (n/cm²•s)	ADJUSTED FLUX (n/cm²•s)	% UNCERTAIN (1σ)
1	1.492+001	1.061+007	1.153+007	44.
2	1.350+001	2.206+007	2.400+007	39.
3	1.162+001	1.023+008	1.111+008	35.
4	1.000+001	3.104+008	3.361+008	30.
5	8.607+000	7.854+008	8.446+008	26.
6	7.408+000	1.857+009	1.969+009	24.
7	6.065+000	6.838+009	7.155+009	20.
8	4.966+000	1.061+010	1.075+010	21.
9	3.679+000	1.949+010	1.915+010	20.
10	2.865+000	2.211+010	2.145+010	23.
11	2.231+000	3.514+010	3.367+010	26.
12	1.738+000	3.038+010	2.900+010	32.
13	1.353+000	2.849+010	2.708+010	36.
14	1.108+000	1.825+010	1.732+010	40.
15	8.208-001	2.590+010	2.460+010	45.
16	6.393-001	2.008+010	1.915+010	48.
17	4.979-001	1.846+010	1.770+010	52.
18	3.877-001	1.697+010	1.640+010	55.
19	3.020-001	1.563+010	1.522+010	57.
20	1.832-001	2.747+010	2.696+010	59.
21	1.111-001	2.280+010	2.253+010	61.
22	6.738-002	1.877+010	1.867+010	62.
23	4.087-002	1.628+010	1.627+010	63.
24	2.554-002	1.388+010	1.393+010	63.
25	1.989-002	7.025+009	7.074+009	63.
26	1.503-002	7.715+009	7.786+009	64.
27	9.119-003	1.341+010	1.355+010	64.
28	5.531-003	1.325+010	1.341+010	64.
29	3.355-003	1.345+010	1.362+010	64.
30	2.839-003	4.541+009	4.602+009	64.
31	2.404-003	4.564+009	4.627+009	64.
32	2.035-003	4.594+009	4.658+009	64.
33	1.234-003	1.392+010	1.412+010	64.
34	7.485-004	1.411+010	1.431+010	64.
35	4.540-004	1.428+010	1.448+010	64.
36	2.754-004	1.444+010	1.465+010	64.
37	1.670-004	1.461+010	1.481+010	64.
38	1.013-004	1.478+010	1.499+010	64.
39	6.144-005	1.496+010	1.518+010	64.
40	3.727-005	1.516+010	1.537+010	64.

TABLE 4.5.1.2.1.3C (Cont'd)

FERRET-SAND II RESULTS FOR QUAD-CITIES UNIT 2 CAPSULE 3 BASKET G-16 (AVERAGE FOR CAPSULE)

GROUP	ENERGY (MeV)	A PRIORI FLUX* (n/cm²•s)	ADJUSTED FLUX (n/cm²•s)	% UNCERTAIN (1σ)
41	2.260-005	1.537+010	1.558+010	64.
42	1.371-005	1.558+010	1.580+010	64.
43	8.315-006	1.581+010	1.604+010	64.
44	5.043-006	1.601+010	1.624+010	64.
45	3.059-006	1.617+010	1.640+010	64.
46	1.855-006	1.660+010	1.684+010	64.
47	1.125-006	1.754+010	1.779+010	64.
48	6.826-007	1.838+010	1.864+010	64.
49	4.140-007	1.896+010	1.923+010	64.
50	2.511-007	5.582+010	5.662+010	64.
51	1.523-007	1.068+011	1.083+011	64.
52	9.237-008	1.287+011	1.306+011	64.
53	1.000-010	7.582+011	7.690+011	64.
FLUX, E > 0.0 MeV		1.755+012	1.765+012	48.
FLUX, E < 0.414 eV		1.069+012	1.084+012	62.
FLUX, E > 0.1 MeV		3.257+011	3.154+011	29.
FLUX, E > 1.0 MeV		1.833+011	1.773+011	18.
dpa/s		2.602-010	2.539-010	18.
FLUENCE+, E > 1.0 MeV		2.606+019	2.521+019	18.
dpa+		3.700-002	3.610-002	18.

---

*ABSOLUTE CALCULATED FLUX (OR NORMALIZED TO Fe54(n,p)Mn54 REACTION RATE).

+BASED ON 1.422+008 EFFECTIVE FULL POWER SECONDS OF EXPOSURE; UNITS OF n/cm² FOR FLUENCE AND TOTAL NUMBER OF DISPLACED ATOMS OF IRON PER TARGET ATOM OF IRON FOR dpa.

TABLE 4.5.1.2.1.4C

COMPARISON OF MEASURED AND CALCULATED REACTION RATES USED IN THE ANALYSIS OF QUAD-CITIES UNIT 2 CAPSULE 3 BASKET G-16

	REACTION RATE (DPS/NUCLEUS)			RATIO MEAS/CALC	
REACTION	MEAS	A PRIORI CALC	ADJ CALC	A PRIORI	ADJ CALC
Fe54(n,p)Mn54	2.29-014	2.28-014	2.27-014	1.01	1.01
Ni58(n,p)Co58	2.84-014	2.94-014	2.90-014	0.96	0.98
Cu63(n,α)Co60	2.08-016	1.94-016	2.05-016	1.07	1.01

TABLE 4.5.1.2.1.3D

FERRET-SAND II RESULTS FOR
QUAD-CITIES UNIT 2 CAPSULE 3 BASKET G-17
(AVERAGE FOR CAPSULE)

GROUP	ENERGY (MeV)	A PRIORI FLUX* (n/cm^{2}•s)	ADJUSTED FLUX (n/cm^{2}•s)	% UNCERTAIN (1σ)
1	1.492+001	1.031+007	1.131+007	43.
2	1.350+001	2.143+007	2.352+007	39.
3	1.162+001	9.937+007	1.087+008	35.
4	1.000+001	3.016+008	3.284+008	30.
5	8.607+000	7.630+008	8.222+008	26.
6	7.408+000	1.804+009	1.903+009	24.
7	6.065+000	6.643+009	6.866+009	20.
8	4.966+000	1.031+010	1.016+010	21.
9	3.679+000	1.894+010	1.784+010	21.
10	2.865+000	2.148+010	1.987+010	24.
11	2.231+000	3.414+010	3.097+010	28.
12	1.738+000	2.951+010	2.663+010	33.
13	1.353+000	2.768+010	2.482+010	37.
14	1.108+000	1.773+010	1.587+010	41.
15	8.208-001	2.516+010	2.257+010	45.
16	6.393-001	1.951+010	1.760+010	49.
17	4.979-001	1.793+010	1.633+010	53.
18	3.877-001	1.648+010	1.518+010	55.
19	3.020-001	1.518+010	1.415+010	58.
20	1.832-001	2.669+010	2.517+010	60.
21	1.111-001	2.215+010	2.112+010	61.
22	6.738-002	1.824+010	1.755+010	62.
23	4.087-002	1.582+010	1.534+010	63.
24	2.554-002	1.348+010	1.316+010	63.
25	1.989-002	6.825+009	6.695+009	64.
26	1.503-002	7.494+009	7.379+009	64.
27	9.119-003	1.302+010	1.286+010	64.
28	5.531-003	1.287+010	1.273+010	64.
29	3.355-003	1.307+010	1.294+010	64.
30	2.839-003	4.411+009	4.371+009	64.
31	2.404-003	4.434+009	4.395+009	64.
32	2.035-003	4.462+009	4.425+009	64.
33	1.234-003	1.352+010	1.341+010	64.
34	7.485-004	1.371+010	1.360+010	64.
35	4.540-004	1.387+010	1.376+010	64.
36	2.754-004	1.403+010	1.392+010	64.
37	1.670-004	1.419+010	1.408+010	64.
38	1.013-004	1.436+010	1.425+010	64.
39	6.144-005	1.454+010	1.442+010	64.
40	3.727-005	1.473+010	1.461+010	64.

TABLE 4.5.1.2.1.3D (Cont'd)

FERRET-SAND II RESULTS FOR
QUAD-CITIES UNIT 2 CAPSULE 3 BASKET G-17
(AVERAGE FOR CAPSULE)

GROUP	ENERGY (MeV)	A PRIORI FLUX* ($n/cm^2 \cdot s$)	ADJUSTED FLUX ($n/cm^2 \cdot s$)	% UNCERTAIN (1σ)
41	2.260-005	1.493+010	1.481+010	64.
42	1.371-005	1.514+010	1.502+010	64.
43	8.315-006	1.536+010	1.524+010	64.
44	5.043-006	1.556+010	1.543+010	64.
45	3.059-006	1.571+010	1.558+010	64.
46	1.855-006	1.613+010	1.600+010	64.
47	1.125-006	1.704+010	1.690+010	64.
48	6.826-007	1.785+010	1.771+010	64.
49	4.140-007	1.842+010	1.828+010	64.
50	2.511-007	5.423+010	5.380+010	64.
51	1.523-007	1.038+011	1.029+011	64.
52	9.237-008	1.251+011	1.241+011	64.
53	1.000-010	7.365+011	7.307+011	64.
FLUX, E > 0.0 MeV		1.705+012	1.669+012	48.
FLUX, E < 0.414 eV		1.038+012	1.030+012	62.
FLUX, E > 0.1 MeV		3.164+011	2.920+011	30.
FLUX, E > 1.0 MeV		1.780+011	1.639+011	19.
dpa/s		2.527-010	2.359-010	19.
FLUENCE+, E > 1.0 MeV		2.532+019	2.331+019	19.
dpa+		3.594-002	3.355-002	19.

---

* ABSOLUTE CALCULATED FLUX (OR NORMALIZED TO Fe54(n,p)Mn54 REACTION RATE).

+ BASED ON 1.422+008 EFFECTIVE FULL POWER SECONDS OF EXPOSURE; UNITS OF n/cm^2 FOR FLUENCE AND TOTAL NUMBER OF DISPLACED ATOMS OF IRON PER TARGET ATOM OF IRON FOR dpa.

TABLE 4.5.1.2.1.4D

COMPARISON OF MEASURED AND CALCULATED REACTION RATES USED IN THE ANALYSIS OF QUAD-CITIES UNIT 2 CAPSULE 3 BASKET G-17

REACTION	REACTION RATE (DPS/NUCLEUS) MEAS	A PRIORI CALC	ADJ CALC	RATIO MEAS/CALC A PRIORI	ADJ CALC
Fe54(n,p)Mn54	2.18-014	2.21-014	2.13-014	0.99	1.02
Ni58(n,p)Co58	2.20-014	2.86-014	2.70-014	0.77	0.81
Cu63(n,α)Co60	2.02-016	1.89-016	1.98-016	1.07	1.02

455

5.0 SURVEILLANCE DATA DEVELOPMENT, EVALUATION, AND SPACIAL AND TEMPORAL EXTRAPOLATIONS

For additional background information, the reader is referred to: 1) ASTM Special Technical Publications STP 481 (1970), STP 616 (1977), STP 683 (1979), STP 698 (1980), STP 725 (1981), STP 784 (1983), STP 819 (1983), and the Annual Books of ASTM Standards (Part 45, "Nuclear Standards," on and before 1982; Volume 12.02, "Nuclear, Solar, and Geothermal Energy," for 1983 and thereafter); 2) the ASTM E706-84 Master Matrix for LWR-PV Surveillance Standards; 3) the EPRI Report NP-3319 (Pe84) and 4) the series of LWR-PV-SDIP reports (Mc85).

5.1 DETERMINATION OF NEUTRON DAMAGE

5.1.1 Introduction

The prediction of the amount of radiation damage to water-cooled reactor pressure vessels throughout their service life is required by 10CFR50, Appendix G, "Fracture Toughness Requirements," and Appendix H, "Reactor Vessel Material Surveillance Program Requirements," in order to ensure safe plant operation. The problem of predicting the vessel damage condition has been exacerbated by the uncertainties and scatter in existing physics-dosimetry-metallurgy data and by the difficulty of assigning uncertainties to predicted property change and exposure values (Ra82a).

What must be known is the maximum permitted damage (property change) allowable in service for the specific material (for example, ΔRT_{NDT}), the confidence limit (or safety margin) to be sure this maximum permitted damage is not exceeded, and the total damage to the component at critical points such as the belt line of the pressure vessel (Mc82,Ra82a). Accurate assessment of the total damage requires knowledge of the damage cross section or function giving the damage per unit exposure, the neutron flux-spectrum, and the neutron fluence.

As referenced above, programs are underway to improve the accuracy of damage analysis and thereby decrease the required safety margins. These programs aim to decrease uncertainties in the measured and calculated property change and neutron exposure values and thereby increase confidence in predicted vessel damage estimates. This increased confidence will be obtained by:

1) Interlaboratory physics, dosimetry, and metallurgy comparisons to ensure measurement accuracy.

2) Calibration measurements in benchmark fields to provide reference points for testing calculational accuracy.

3) Systematic analysis using least-squares codes to improve the exposure values for radiation embrittlement data bases and to define the uncertainties in the values.

4) Measurements in surveillance capsules and ex-vessel reactor cavities of operating LWR power plants to provide normalization points for interpolations and extrapolations into the vessel from both inside and outside, and to provide measured integral data that reflect the effects of core-loading changes on vessel and support structure exposures.

457

5.1.2 Evaluation of Neutron Damage

Neutron damage to reactor pressure vessels is evaluated based on data obtained at other irradiation locations (in both power and test reactors) and on calculations (see ASTM E706). Available data consist of measured values of damage to pressure vessel steel specimens irradiated in test reactors and at surveillance positions in power reactors at rates accelerated over those expected in the vessel itself. To correlate these data with the change in vessel properties to end-of-life requires both absolute and relative damage rates to be calculated for both the test piece irradiation and the vessel exposure locations. Thus property trend curves must be well known and understood in order to allow interpolations and extrapolations in space (radial and azimuthal lead factors) and time (exposures).

The property trend curves are developed for pressure vessel steels using data from power reactor surveillance and test reactor experiments. To correlate measured damage from these tests requires that the steel chemistry be well known so that effects of minor constituents (for example, copper, phosphorus, nickel, etc.) can be evaluated. In addition, however, it is important to know the exposure to each specimen (fluence $E > 1$ MeV, dpa, etc.) and differences in exposure that might result from differences in the neutron flux-spectra.

The present data base for damage rates (as characterized by ΔRT_{NDT}) uses fluence of neutrons with energy greater than 1 MeV as the exposure parameter. However, research and development work in thermal and fast reactors has shown that displacements per atom (dpa) provides improved correlations for data for different neutron environments. Although the differences between high-energy neutron spectra in various thermal reactors is smaller than the range experienced in fast reactors, correlations using dpa will result in improved trend curves, especially when the test reactor, surveillance, and ex-vessel cavity data are to be compared.

Past data on fluence of surveillance and test reactors have been based on very limited analysis. Both measurements and calculations have significant uncertainties. Recently Simons et al [Section 4.0 and Ref. (Si84)] have re-analyzed some of the power reactor surveillance data and produced revised fluence values. The revised values are almost all higher than earlier vendor/utility/service laboratory estimates, by up to a factor of about two. The more recent data show less change, however [see Figure 5.1.1 taken from Ref. (Si82)]. The present limiting accuracy for determining exposure values using least-squares analysis methods is estimated to be in the 5 to 15% (1σ) range (see Figure 5.1.1). Attainment of uncertainties approaching this range for LWR power plants can only be achieved by careful adherence to the four steps given previously.

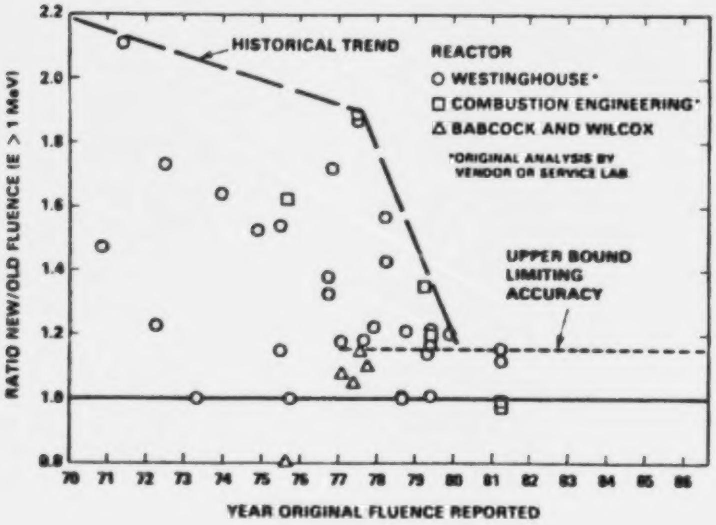

FIGURE 5.1.1. Relationship Between Re-evaluated and Original Surveillance Exposures.

5.1.3 Physics-Dosimetry Nuclear Data Needs

Attainment of neutron exposure values to limiting accuracies also requires consideration of the accuracy of the nuclear data used in dosimetry measurements, reactor calculations, and damage evaluations. The specifics of physics-dosimetry nuclear data needs [see Refs. (Ka82,Mc81,Mc82) and ASTM E 706 for the basis of these needs] were discussed at an IAEA Advisory Group Meeting (AGM) on Nuclear Data for Radiation Damage Assessment and Safety Aspects held on 12-16 October 1981 (St83b). At this meeting, conclusions and recommendations were made to indicate areas in which improvements could be made that would affect evaluation of neutron irradiation damage (Ko82). These conclusions and recommendations are summarized below. Considered at this meeting was not only pressure vessel damage, but also evaluations of damage to components for thermal, fast, and fusion reactors. Nuclear data for environment characterization and for radiation damage calculations and damage correlation estimates were discussed.

Nuclear data for environmental characterization are in reasonably good shape. Table 5.1.1 shows a comparison between calculated and measured integral cross sections for dosimetry reactions in the ^{235}U fission neutron spectrum (Fa76). Only values for $^{47}Ti(n,p)$, $^{27}Al(n,p)$, $^{127}I(n,2n)$, and $^{55}Mn(n,2n)$ show discrepancies of 10% or more. These and some of the other discrepancies (>5%) need to be considered when these reactions are used for fluence determinations.

TABLE 5.1.1

COMPARISON OF MEASURED AND CALCULATED CROSS SECTIONS IN THE ^{235}U FISSION NEUTRON SPECTRUM

Reaction	Effective Threshold (MeV)	Measured Value (mb)[a]	Quoted Error in Measured Value (%)[a]	Calculated Value (mb)[b]	Calculated/ Measured
^{115}In(n,γ)^{116}In	---	134.5	4.5	124.7	0.93
^{197}Au(n,γ)^{198}Au	---	83.5	6.0	78.3	0.94
^{63}Cu(n,γ)^{64}Cu	---	9.30	15.1	9.87	1.06
^{235}U(n,f)	---	1215	1.8	1236	1.02
^{239}Pu(n,f)	---	1826	3.0	1791	0.98
^{237}Np(n,f)	0.6	1340	4.0	1347	1.01
^{115}In(n,n')^{115}In	1.2	191	3.7	179	0.94
^{232}Th(n,f)	1.4	81	6.7	75.0	0.93
^{238}U(n,f)	1.5	308	2.7	305	0.99
^{47}Ti(n,p)^{47}Sc	2.2	17.1	6.0	22.5	1.32
^{58}Ni(n,p)^{58}Co	2.8	109	5.5	105.0	0.96
^{32}S(n,p)^{32}P	2.9	66.8	5.5	70.5	1.06
^{54}Fe(n,p)^{54}Mn	3.1	83	6.5	81.0	0.98
^{46}Ti(n,p)^{46}Sc	3.9	11.5	7.0	11.2	0.97
^{27}Al(n,p)^{27}Mg	4.4	3.86	6.5	4.26	1.10
^{56}Fe(n,p)^{56}Mn	6.0	1.035	7.2	1.036	1.00
^{59}Co(n,α)^{56}Mn	6.8	0.143	7.0	0.150	1.05
^{63}Cu(n,α)^{60}Co	6.8	0.58	7.0	0.558	0.96
^{27}Al(n,α)^{24}Na	7.2	0.708	7.0	0.719	1.02
^{48}Ti(n,p)^{48}Sc	7.6	0.269	7.0	0.282	1.05
^{127}I(n,2n)^{126}I	10.5	1.05	6.2	1.21	1.15
^{55}Mn(n,2n)^{54}Mn	11.6	0.244	6.1	0.201	0.82

---

[a] Taken from data in Ref. (Fa76) as updated by J. A. Grundl, March 1982. Uncertainties are 1σ values; mb = 10^{-31} m^2.

[b] Using ENDF/B-V dosimetry file 620-point cross sections and the ENDF/B-V Watt form for the ^{235}U fission spectrum.

Of more concern is the evaluation of cross-section uncertainties. It is recognized that not only are absolute cross-section errors necessary, but that the correlations between the cross sections at different energies and between different reaction cross sections must be known to do a proper statistical uncertainty evaluation. Production of data files containing this information is, therefore, recommended to receive more attention [ASTM E706 and Ref. (Ko82)]. To accomplish this end, it is required that experimental nuclear data measurements be properly documented so that correlations between different sources of error can be considered.

In addition, covariance uncertainty matrices should be generated for the various benchmark neutron fields to allow propagation of these uncertainties for introduction of integral data in cross-section evaluations [see Sections 5.2 and 5.3.

Nuclear data for radiation damage calculations and damage correlation estimates are more uncertain. These data include calculated displacement cross sections and cross sections for damage monitors (i.e., quartz, sapphire, metallurgical specimens, etc.). At the present time, it is recommended that ASTM [see Practice for Characterizing Neutron Exposures in Ferritic Steels in Terms of Displacements per Atom (dpa)(E693)] and EURATOM (Zi81) displacement cross sections be used for damage evaluation of pressure vessel steels. Uncertainties should be developed for dpa cross sections based on the nuclear data used in the cross-section calculations.

Considerable work on development of damage detectors remains to be done, both for the determination of the relationship between the measured damage and exposure and for the relationship between the measured damage and dpa.

5.1.4 Physics-Dosimetry-Metallurgy Standards

A series of ASTM standards described in ASTM E706 is currently in preparation. The interrelationship of these practices, guides, and methods for the prediction of neutron-induced changes in LWR pressure vessels and support structure steels is shown in Figure 1.0.1. Figure 1.0.2 gives the schedule for their preparation, balloting, acceptance, validation, and revision. Some of these are existing ASTM standards, and some are ASTM standards that have been newly proposed. The scope of each standard and the general requirements for content and consistency are discussed in the Master Matrix as well as writers' and users' information, justification, specific requirements for the practices, guides, and methods, and information on applicable documents and references.

Of particular interest for the application of physics-dosimetry for damage exposure determinations are the I-A, I-C, I-D, II-A, II-B, II-C, II-D, II-E, and III-A to III-E practices, guides, and methods. Use of the standardized methods for physics-dosimetry analyses, together with the benchmark testing (II-E) standard, will enable consistent and reliable results to be obtained. Integral values so obtained will be used for the evaluation of the ENDF/A cross section and uncertainty files (II-B) to ensure self-consistent fluence determinations utilizing the different types of dosimetry sets (Li82). This self-consistent data file will be established using least-squares adjustment methods (similar to those recommended in the II-A standard). This will be done to minimize discrepancies between evaluated data and measurements and to include cross-section correlations in the uncertainty analysis to ensure consistent and conservative error estimates.

5.1.5 Conclusions

Prediction of irradiation damage in a reactor pressure vessel is a complicated problem requiring a combination of calculations and measurements. Uncertainties in results can be reduced through the use of standardized and verified calculational techniques, measurement techniques, and nuclear data. These improvements will be realized through interlaboratory comparisons, benchmark verifications, and application of improved, more extensive measurement and calculational techniques.

5.2 TREND CURVE DATA DEVELOPMENT, TESTING, AND APPLICATIONS

As discussed in the 1984 Annual Report (Mc85a) and as a part of the LWR-PV-SDIP Program, statistically based data correlation studies have been made by HEDL and other program participants using existing PWR and BWR physics-dosimetry-metallurgical data in anticipation of the analysis of new fracture toughness and embrittlement data from the BSR-HSST, SUNY-NSTF, ORR-PSF, and other experiments. The reader is referred to Refs (Ma83b,Mc84,Mc85a,Mc84h, Gu84,Gu84a,Gu84b,Pe84,Ra84) for additional information and appropriate references.

In Section 4.1.3 and in Ref (Si84), Simons presents results of evaluation and reevaluation of exposure units and values for 47 PWR and BWR surveillance capsule reports for W, B&W, CE, and GE power plants. Using a consistent set of auxiliary data and dosimetry-adjusted reactor physics results, the revised fluence values (Table 4.1.3.3) for E > 1 MeV averaged 25% higher than the originally reported values. The range of fluence values (new/old) was from a low of 0.80 to a high of 2.38; see also Ref (Si82a,Mc84). These HEDL-derived FERRET-SAND II exposure parameter values have been used for the HEDL PWR and BWR trend curve data development and testing studies discussed here and in Ref (Mc85).

In Ref (Ra84), Randall discusses the basis for his Revision 2 of Reg. Guide 1.99. As stated, the Guide is being updated to reflect recent studies of the physical basis for neutron radiation damage and efforts to correlate damage to chemical composition and fluence. Revision 2 contains several significant changes. Welds and base metal are treated separately. Nickel content is added as a variable, and phosphorus is removed. The exponent in the fluence factor is reduced, especially at high fluences; and guidance is given for calculating attenuation of damage through the vessel wall.

For PV wall neutron fluence attenuation predictions, the preliminary results of PSF (Mc85a) comparisons lie within 10% but reaffirm slight deficiencies in the iron cross sections first brought to light by the PCA and PSF startup experiment comparisons (Mc81,Wi83), which show increasing disagreement the further into the PV one goes.

In the planned Revision 2 of Reg. Guide 1.99 (Ra84), the equation used for PV wall fluence attenuation by Randall is

$$\text{Fluence}(X) = \text{Fluence}(\text{Surface}) \cdot e^{-0.24X} , \qquad (1)$$

where X is the depth in the wall in inches, measured from the inside surface. This equation is based on transport calculations by Guthrie et al. (Gu82, Gu82a) for the dpa attenuation through an 8.0-inch vessel wall. These calculations did not account for the deficiencies in the iron cross sections mentioned above.

It has been recently noted by Fabry that the $^{6}Li(n,\alpha)$ spectrometry data (DeLeeuw, Mc81) in PCA are consistent with gas proton recoil spectrometry (Rogers, Mc81) and silicon damage measurements (DeLeeuw, Mc81), and they indicate larger proportions of neutrons below 1.0 MeV than predicted by ENDF/BIV; the discrepancy is on the order of 20%, in the same direction as NRE results reported by Roberts, Gold, and Preston in Ref (Mc85a), Section 2.2.1.1, "NRE Measurements." This confirmed result does affect the dpa/ϕ > 1 MeV transverse predictions through the reactor PV planned for use in Reg. Guide 1.99, Revision 2 (Ra84), and may adversely impinge upon eventual crack-arrest considerations in the safety analysis of ASME-III designed vessels. It is recommended, therefore, that:

1) A new simultaneous evaluation of all experimental data in PCA, the NESDIP replica, and the Mol Iron Shell Benchmarks should be performed, including the French DM results obtained during the PSF startup program,

2) Integral measurements using NRE as well as higher threshold-energy sensors [such as $^{58}Ni(n,p)$, $^{64}Zn(n,p)$, or $^{27}Al(n,\alpha)$] should be performed in the Mol Iron Shell Benchmarks, and

3) Continuous gamma-ray spectrometry experiments be conducted in the NESDIP benchmark, Phase 3, to resolve inelastic gamma-rays produced by fast neutron interactions in iron and thereby test the inelastic neutron transport cross section of iron.

In Refs (Gu84b) and (Mc84h), the effects of changes in different variables and use of different exposure parameter models for predicting the Charpy shift for the 30-point PSF weld, plate, and forging data base and a 30-point PWR weld data base are discussed in considerable detail.

The main comments and conclusions of Guthrie's study (Gu84b), based on the use of PSF and test reactor data, are:

1) In surveying the previously existing data available for the alloys in the PSF experiment, it has become apparent that the fluence exponent is dependent on temperature and flux level. For A302B alloy, the PWR surveillance data fell consistently below the higher flux level LITR data and showed a lower value for the fluence exponent. The overall scatter of the existing data is such that it is not clear that Charpy tests or K_{IC} tests can be used to uncover fine details in mechanisms.

2) Because of the possible rate effect (which was predicted by G. R. Odette in his PSF Blind Test submission), the PWR surveillance trend-curve laws cannot be expected to work as well in the PSF as might be expected from their stated standard deviations.

3) In applying existing Charpy shift laws to the PSF C_V data, we find that the largest observed shift occurred for the Rolls-Royce A533B weld (Code R), which had a high nickel content (1.58%)--well outside the

range of the data base used to develop the HEDL PWR Charpy shift equations (Gu84). A comparison of the HEDL equation applications and the Hawthorne values for ΔT_{cv30} are given in Ref (Gu84). The overall deviation is 31.6°F or 17.6°C (1σ). This is more than the standard deviation of the fit to the original data base and is due to the facts that 1) the Code R specimen is outside the recommended chemistry range, and 2) the rate effect has caused the predictions for ΔT_{cv30} to be biased low. The values in Ref (Gu84) should not be compared to blind test predictions since no use was made of SSC-1 results to guide the calculations and no correction has been attempted for rate effects.

4) There appears to be a rate effect in the PSF Charpy and compression data. The fluence exponent appears to increase with increased flux and appears to decrease with increased copper.

5) The similarity of the spectra at the separate irradiation positions severely limits the possible comments about damage functions.

6) No extra thermal neutron effect, beyond that already represented in the ASTM dpa cross section, was identifiable in the PSF data.

The main comments and conclusions of the study by McElroy et al. (Mc84h), based on the use of PSF, PWR, and BWR data, are:

1) There is a significant improvement (reduction) in the standard deviation of the fit for weld Charpy shift trend curves that includes the effect of low-energy thermal neutrons. For the 30-point weld data set, improvements of the amounts observed could occur at a frequency of ~4% by chance.

2) A knowledge of the actual boron content of PV steels and the use of a trend curve that employs an exposure parameter dose term, including the total production of dpa in iron and helium, could make significant improvements in lowering the standard deviation of the fit for the existing PWR surveillance capsule metallurgical weld data base.

3) Based on the trend curve model that includes the effect of thermal neutrons, for both PWR and BWR power plants, up to about 80% of the SS-clad/PV steel wall interface and surveillance capsule specimen dose term values could be attributed to helium production in PV steels, depending on the particular surveillance capsule design, Charpy specimen placement, steel boron content, and power plant operating conditions.

4) Existing PWR and BWR surveillance capsule derived embrittlement trend curves [based on the use of just fast fluence (E > 1 MeV) or dpa for the exposure term] cannot be expected to give reliable predictions of the combined fast and thermal neutron contributions to the Charpy shift at the SS-clad/PV steel wall interface, 1/4-T, 1/2-T, 3/4-T, or 1-T

465

locations. [It is noted that the PSF experiment provides physics-dosimetry-metallurgy data for predicting the Charpy shift in PV steels at deep in-wall locations, such as the 1/4-T, 1/2-T, and 3/4-T positions, where the T/F ratios are in the very low range of ∿0.14 to ∿0.53. However, even for these very low ratios, helium from both boron and steel high energy (n,α) reactions may still contribute 5% to 30% to the exposure parameter dose term value.]

5) None of the Charpy shift trend curve equations studied [see Table 1 of Ref (Mc84h)] except perhaps the one based on the use of an exposure parameter of fluence E > 0.1 MeV, appears to properly bound all the six PV steel observed PSF damage gradient curves. Based on the French simulated PV-wall DOMPAC Experiment (Mc84,Al83), Alberman concluded that for low temperature (< 100°C) irradiations, fast fluence (E > 1 MeV) is too "optimistic" and is not, therefore, a conservative neutron exposure parameter. He also concluded that, at low temperature, 95% of the measured damage (based on tungsten and graphite DM results) comes from neutrons with energy E > 0.1 MeV. This led him to conclude that the exposure parameter, fluence (E > 0.1 MeV), is perhaps "pessimistic" but has the advantage of being the lower threshold of all (displacement) damage models. Thus it takes into account all neutrons that create (displacement) damage.

6) The plant specific weld data sets used in the PWR and BWR data base studies, except for one, do not support a saturation effect at high fluences above ∿1 x 10^{19} n/cm^2 (E > 1 MeV). Consequently, the existing Reg. Guide 1.99 (Re77) upper bound (truncated) trend curve model shape (or plant specific curves) may have to be used for high fluence embrittlement predictions for PV steel welds, and perhaps forgings and plates.

7) Any significant thermal neutron contribution to PV steel embrittlement is, most probably, a result of (n,α) reactions in boron-10 rather than by neutron-induced Fe(n,γ) recoil reactions.

8) It appears that the current ASTM E693 dpa cross section should not be used to correlate highly thermalized light or heavy water moderated power or test reactor irradiation effects data because it significantly overestimates the low-energy thermal neutron dpa contribution.

9) The PV-wall SS-clad/PV steel interface surface T/F ratio for PWR and BWR power plants is expected to be in the range of 2 to 6 on the basis of surveillance capsule measurements, Westinghouse transport calculations, GE measurements, and the PSF experiment physics-dosimetry results.

10) Individual Charpy specimens (with natural boron content of ∿0.4 up to perhaps 5 wt ppm) in PWR and BWR surveillance capsules will be subject to ℄ neutron exposures with T/F ratios in the range of ∿0.5 to 5, depending on the surveillance capsule design, its placement, and the reactor operating conditions. The T/F variation for individual Charpy specimens, therefore, could be an important parameter for the correlation of a set of Charpy specimen results and derived ΔRT_{NDT} values.

11) From this study, that of Grant and Earp (Gr84), and others discussed in Ref (Mc84h), a final conclusion is: the PSF experiment and PWR and BWR surveillance program results clearly show that comparison of the effects of radiation damage on yield strength, hardness, RT_{NDT}, and USE will be needed to aid in improving and refining our knowledge of trend curves and PV wall damage gradients. Implicit in this are the current observations that the establishment of separate trend curves for welds, forgings, and plates will give increased understanding and accuracy in projections of the present and future metallurgical condition of PV steels.

As discussed in previous annual reports and as a part of the LWR-PV-SDIP Program, statistically based (as well as other) physics-dosimetry-metallurgy data analysis and correlation studies using research reactor data are also being made by ORNL, MEA, HEDL, UCSB, and other program participants. The reader is referred to Sections 2.3.1 and 2.3.2 of Ref (Mc85) and the Proceeding of the 5th ASTM-EURATOM Symposium for more information on the ORNL, MEA, HEDL, UCSB, and other studies.

5.3 THE USE OF ADJUSTMENT METHODS AND RELATED STATISTICAL ANALYSIS FOR THE EVALUATION OF PRESSURE VESSEL SURVEILLANCE RESULTS

NOTE: This section was written in 1982 and reflects the status of adjustment procedures and their applications at that time. Although all of the considerations and discussions in this section are still valid, considerable work has been done at ORNL, primarily regarding the LEPRICON and LSL code packages, toward realizing the stated goals. Details can be found in more recent NUREG and EPRI reports on this subject.

5.3.1 Introduction

Surveillance programs are required in 10 CFR 50, Appendix H, and Regulatory Guide 1.99 for pressurized light water reactors (LWR) in order to determine the extent of radiation damage in the reactor pressure vessel and associated components. The results from these programs are needed to determine the safety margins to prevent brittle fracture and rapid crack propagation in reactor pressure vessels as may be caused by stress in flawed structures during operation, testing, maintenance, or postulated accidents (Mc82). Requirements for the design and evaluation of surveillance procedures are given in ASTM Standard E706(IA)/E853 (As84). Surveillance capsules containing dosimeters and metallurgical specimens are attached at some place inside the pressure vessel at the start of reactor operation and are being removed according to a predetermined schedule during the life of the reactor.

The evaluation of surveillance capsule results is expected to provide the following information:

1) The sensitivity of the pressure vessel material and weldments to neutron irradiation damage is determined from the tests of the metallurgical specimen. This is done by correlating the shifts in nil ductility temperature and upper shelf energy to neutron exposure parameters such as fluence > 1.0 MeV or dpa, as determined from the capsule dosimetry.

2) The results from the capsule dosimetry are also used to verify and, if necessary, to correct the reactor physics calculations. These calculations are necessary to determine the damage exposure values inside the pressure vessel wall where direct measurements cannot be made.

Fairly large uncertainties are connected with both types of information and these meed to be considered in determining the safety margins. The task of combining and propagating uncertainties in the form of variances and covariances is the domain of statistical analysis that, in its simpler forms, is included in all routine surveillance evaluations. However, the underlying physical models are far from simple, and the application of spectrum adjustment (Zi82a) and more general least-squares fitting methods is not only more appropriate but also gives significantly improved uncertainty bounds in many cases.

Application of these more elaborate statistical methods to evaluation of surveillance results will be discussed in this paper. Corresponding to the two goals stated above, somewhat different procedures are needed for each task.

Emphasis will be on dosimetry analysis; however, improved analytical methods are also needed for the evaluation of metallurgical tests and transport calculations. A more detailed discussion of these methods can be found in (St82a) and (As82a), respectively.

5.3.2 Statistical Analysis in Support of Dosimetry for Metallurgical Tests

Metallurgical test specimen in surveillance capsules serve essentially the same purpose as those in materials test reactors and the analytical methods should thus be the same. Examples of detailed dosimetry analysis for materials test irradiations are described in (St83). The primary goal is to determine, as accurately as possible, the values of radiation damage parameters such as fluence > 1.0 MeV, fluence > 0.1 MeV, and dpa, at the location of the metallurgical samples. Good results are critically dependent on a good selection of dosimetry sensors and the distribution of dosimeters over all locations within the capsule. Single sensor gradient wires may be substituted at locations where multiple foil sets cannot be placed.

Several least-squares adjustment methods (Ma81)(Pe77a)(Sc79)(St82b) obtain best estimates for the damage exposure parameter values from a combination of measurements and calculations. There appears to be, however, some reluctance on the part of the evaluators to use these methods for routine surveillance capsule evaluations. Instead a scale factor is determined by comparing measured and calculated reaction rates, and this scale factor is then applied to the calculated exposure parameters values. It is not hard to see why this approach is preferred; it is simple and straight forward in contrast to the complex and unfamiliar adjustment procedures. In addition, the comparison of scale factors for different reaction rates provides an obvious check for the consistency between measurements and calculation and between different measurements; such inconsistencies are not always evident from the results of adjustment methods.

This simplified approach is nevertheless seriously flawed for the following reasons:

1) It is not clear a priori which of the ratios should be chosen as scale factor or, if a weighted average is used, what are the proper weights.

2) There is no easy and direct way to relate the uncertainties of the scale factors to those of the exposure parameter values which are derived from these scale factors.

3) Persistent biases may be introduced since an error in the scale factor applies to all determinations of exposure parameter values in the same capsule and, more seriously, to all capsules, which are based on essentially the same calculations.

To solve the first two problems the scale factor methods should be replaced by a more elaborate adjustment procedure. A reevaluation of surveillance results using adjustment methods has been performed in (Si82a) leading to considerable reduction of uncertainties. It may be noted that the results of adjustment procedures can still be interpreted in terms of scale factors, if a logarithmic adjustment is chosen. The calculated damage parameters, say dpa, is adjusted by a scale factor whose logarithm is a linear combination of the scale factor logarithm for different reaction rates. The weights in these linear combinations and the resulting variances and covariances for the adjusted damage parameters are determined from the variances and covariances of the measuring and calculational errors.* This interpretation of the adjustment procedures makes them not only more transparent but may eventually lead to further simplifications.

The problem of biases is a more serious one since the effective determination of the calculational biases requires the simultaneous processing of as many dosimeter sets as possible; as a minimum all available sets from the same reactor should be included and preferably a combination of sets obtained from different reactors of the same generic type provided the same transport calculation was performed. Unfortunately most currently available adjustment codes can process only one set at a time and the ones which can handle more than one may encounter computational difficulties if the number of different sets is large. A method based on a simplified assignment of flux covariances has been applied successfully to the HSST irradiation experiments at ORNL and is described in (St83). This method is also able to reduce the uncertainties of the exposure parameters below the values obtained from single set adjustments. This procedure is readily applicable to surveillance dosimetry.

An additional way of reducing biases in calculations and nuclear data is provided through the use of benchmark facilities.*,** The influence of cross section errors in particular is significantly reduced if the reaction rate measurements from a given dosimetry material is calibrated against measurements of the same material exposed to a benchmark field which is not too different from the field at the surveillance position. The necessary statistical analysis can be implemented as part of the adjustment code.

Adjustment procedures can also provide a guidance for the selection of dosimetry sensors. Obviously, the response function of the sensor material should match as closely as possible the response function of the damage exposure parameters. The reduction of uncertainties for different sets of dosimeters is investigated in (St82c). The ^{237}Np(n,f) reaction is among the best suited for the purposes of surveillance dosimetry. The ^{93}Nb(n,n') has a similarly advantageous response, but its nuclear data are still rather uncertain and counting is difficult. Other sensors such as ^{54}Fe(n,p), ^{46}Ti(n,p), ^{238}U(n,f), ^{63}Cu(n,α) should be included, not primarily for the reduction of uncertainties but for backup and verification.

Refs: * = (St83a), ** = (Mc81e).

470

5.3.3 Statistical Analysis for the Verification of Reactor Calculations and Extrapolation to End-Of-Life Conditions

The neutron fluence-spectrum at the surveillance capsules is only indirectly related to the fluences and thus the irradiation damage in the pressure vessel wall. Also current fuel management procedures may change so that the total accumulated fluence at the end-of-life (EOL) of the pressure vessel may not correspond to the rate of fluence accumulation during the time the surveillance program was in place. It follows that ultimately the determination of the radiation damage in the reactor vessel and of the length of its safe operating life rests with the accuracy of the reactor calculation. It is, therefore, necessary to determine uncertainty bounds for the calculated exposure parameter values and, if indicated, to correct calculational biases.

The determination of uncertainties for neutron transport calculations is not an easy task. Considerable research has been done by R. E. Maerker and coworkers.* The input uncertainties are due to errors in fuel loading, modeling, and nuclear constants. These can be converted into uncertainties for calculating exposure parameter values after sensitivities for the calculation to each of the input uncertainties has been established. Adjustment methods are then applied to make the calculations consistent with dosimetry measurements and to reduce the calculational uncertainties.

A large computational effort is needed to carry through a detailed analysis which cannot reasonably be performed anew for each new set of surveillance results. However a large amount of detail may not be necessary. Only the total variances and covariances enter into adjustment and verification procedure** and for these crude estimates may be sufficient in light of the fact that the input uncertainties for the sensitivity analysis are not too well known to begin with. In particular the variances and covariances obtained for one set of reactor calculations are likely to be applicable to calculations of other reactors. Further research is needed to convert this conjecture into factual data.

In order to detect calculational biases a large number of comparisons between calculated and measured reaction rates, including measurements in the cavity*** are desirable. This is even more important if corrections are considered. It should be kept in mind, however, that the primary objective is the verification of transport calculation including determination of credible and verifiable uncertainties (variances) for the calculated exposure parameter values within the pressure vessel wall. If the discrepancies between measured and calculated values are large, exceeding the assumed uncertainty bounds, then the statistical analysis is no longer valid. In this case the causes for the discrepancies need to be determined first, followed by better calculations and/or measurements.

Refs: * = (Ma81), ** = (St83a), *** = (Br82a).

5.3.4 Summary and Recommendations

The results from pressure vessel surveillance capsules provide valuable information for assessing the radiation damage in the pressure vessel wall and to establish safety margins for the operation of the reactor. To be fully effective, a careful statistical analysis of the surveillance data is needed. The mathematical model for assessing uncertainties in neutron transport and for the propagation of uncertainties from the input data to the desired output is rather complex and requires considerable computational effort. More conventional statistical methods are therefore used in current evaluations of surveillance data. More suitable analytical procedures are available now and can lead to considerable improvements if properly applied.*,** Simplifications are possible which preserve all essential features of the mathematical model while suppressing irrelevant and complicating details. Further research along these lines is needed to arrive at an optimal evaluation of surveillance data.

Refs: * = (Ma81), ** = (St83).

5.4 EVALUATION OF METHODS FOR REDUCING PRESSURE VESSEL FLUENCE

5.4.1 Pressure Vessel Radiation Embrittlement Calculations Programs

As part of the NRC/BNL "Pressure Vessel Radiation Embrittlement Calculations Program," the fluence reduction obtainable by 1) low-leakage fuel management in which the core peripheral assembly power is reduced and 2) selective replacement of peripheral assemblies with nonfuel-bearing "dummy" assemblies has been evaluated. This evaluation is intended as a generic scoping analysis. Plant-specific vessel fluence determinations will be made as required by the NRC (Au83).

Calculations have been performed using the DOT-3.5 discrete ordinates transport code together with the RSIC DLC-37/EPR (ENDF/B-IV) cross-section library for the Ft. Calhoun-1 (CE), H. B. Robinson-2 (Westinghouse), and Oconee-1 (B&W) reactors. The calculations indicate that up to a 40% vessel (>1.0 MeV) end-of-life fluence reduction may be obtained in low-leakage patterns in which the peripheral power is reduced by 50%. End-of-life fluence reductions by factors of ~4 may be obtained by fuel assembly replacement, with fluence accumulation rates reduced by factors of 9 to 12 and, in some cases, by factors as large as 18. In a specific case, the fluence reduction obtained will depend on the peripheral core geometry and remaining vessel lifetime.

Both low-leakage fuel management and assembly replacement achieve fluence reduction by shifting the core neutron source away from the vessel and toward the center of the core. As a result, the fluence reduction is accompanied by an increase in power peaking; and, in the cases analyzed, increases as large as 40% were obtained. It is expected that this power peaking increase will be partially offset by additional power flattening.

The impact of the proposed fluence reduction schemes on reactor design and operation has not been considered. The purpose of this study has been to determine the fluence reduction that could be achieved with the proposed schemes without drawing conclusions concerning the magnitude of the operational penalties that might be required to implement them. Also, the fluence reduction at vessel peak wall fluence and weld locations that can be obtained using part length fuel assemblies has not been considered but will be the subject of a future study. The results of these calculations are being used to identify plants in which fluence reduction and regulatory relief (e.g., through Appendix K) may be required.

5.4.2 Benchmarking of Pressure Vessel Fluence Calculations

Pressure vessel fluence benchmarking calculations are being performed for Maine Yankee, Ft. Calhoun-1, Arkansas-1 and the ORNL pool critical assembly benchmark experiment. The calculations are being performed with the DOT-3.5 discrete ordinates transport code and a collapsed 16-group ENDF/B-IV cross-section library. The calculational models include an accurate description of the core/shield/vessel configuration geometry and materials, and local core neutron source distribution. The effects of core depletion and axial fluence shape have been determined, and calculational uncertainties are being estimated.

5.5 W-NTD PROCEDURES

Since calculated fluence levels are based on conservative core power distributions derived from long-term operation, while capsule data are representatives of multiple-cycle operation, commitment to low-leakage fuel loading patterns may significantly reduce neutron flux levels. In addition, capsule lead factors could be changed, thus impacting the withdrawal schedule of remaining surveillance capsules. Interpretation of surveillance capsule data relative to pressure vessel condition should, therefore, reflect actual operating power distributions.

5.6 GE PROCEDURES

See Section 1.2 and Ref (St83a).

5.7 CE PROCEDURES

See Section 1.3 and Ref (St83a).

5.8 B&W PROCEDURES

Included in the DOT calculation of capsule flux analysis is the determination of flux distribution in the reactor pressure vessel. From this distribution, the maximum flux in the vessel is selected, multiplied by the capsule normalization factor and the vessel axial shape factor, and then combined with the irradiation time interval to produce vessel fluence. The axial factor relates a calculation in Rθ geometry to the axial location of maximum flux.

5.8.1 Plant Specific Fluence

For those reactors that have installed surveillance capsules, the calculated vessel flux represents average conditions for the irradiation period. For reactors without capsules, an additional calculation is performed with conditions and RPD corresponding to the time interval of vessel exposure. These data are normalized to the lates capsule calculation in a host reactor.

All vessel flux calculations are summarized in Table 5.8.1. Because of RPD variations from cycle to cycle and differences in full power between reactors, only comparable fuel cycles should be compared on a flux per unit power basis. Thus, all cycle 1 data are within a ±8% band. Differences in RPD distribution probably caused the high value for DB-1 (highest power at 2772 MWt) and the low value for CR-3 (lowest power at 2452 MWt). As expected, from analysis of the fuel shuffle scheme, later cycles created somewhat higher fluxes. Oconee 1 was unique from the standpoint of incore fuel arrangement for cycles 1 and 2; later cycles should be comparable to other 177FA reactors. Although the data in Table 5.8.1 were obtained from multiple calculations with plant specific conditions, the overall similarity between B&W 177FA reactors is quite evident.

5.8.2 Radial and Azimuthal Gradients

For the same type vessel, the radial gradient of fast flux through the pressure vessel is dependent only on the relative spectral shape of flux that reaches the vessel.* All B&W 177FA reactors have the same size vessel and are constructed of similar carbon steels. Thus, data in Figure 5.8.1 apply to all 177FA pressure vessels at all azimuthal locations.

The azimuthal flux gradient is primarily a function of core shape and RPD. Flux as a function of azimuthal angle is dependent on the circumferential source variation due to RPD distribution and to different attenuation path lengths due to the non-cylindrical core shape. Core shape, which is the same for all 177FA reactors, appears to be more influential on azimuthal

---

*Azimuthal and axial streaming of flux in the reactor cavity could affect the gradient near the outside surface.

478

TABLE 5.8.1

PRESSURE VESSEL FLUENCE

Reactor	Fuel Cycle	Cycle Length EFPD	Capsule Normalization Factor	Axial Shape Faetor	(b)Flux/Power
Oconee 1(c)	1	309	1.1	1.1	5.33
Oconee 2(c)	1	440	1.1	1.17	5.41
Oconee 3(c)	1A	345	1.1	1.18	5.41
TMI-1 (c)	1	471	1.1	1.1	5.65
ANO-1 (c)	1A	345	1.1	1.18	5.41
DB-1	1	374	0.98	1.17	5.81
CR-3	1A	269	0.89	1.22	4.98
Oconee 1(c)	2	291	1.1	1.1	8.10
Oconee 2	2→4	921	0.93(a)	1.17	6.11
Oconee 3	1B→5	1153	0.91(a)	1.17	6.04
ANO-1	1B→4	1047	1.07(a)	1.16	6.39
RS	1→3	1030	1.03(a)	1.17	7.00

(a) Normalized to capsule calculation in a host reactor

(b) Units are n/cm^{2}s/Mwt

(c) Calculations prior to 3/79 when procedure was updated

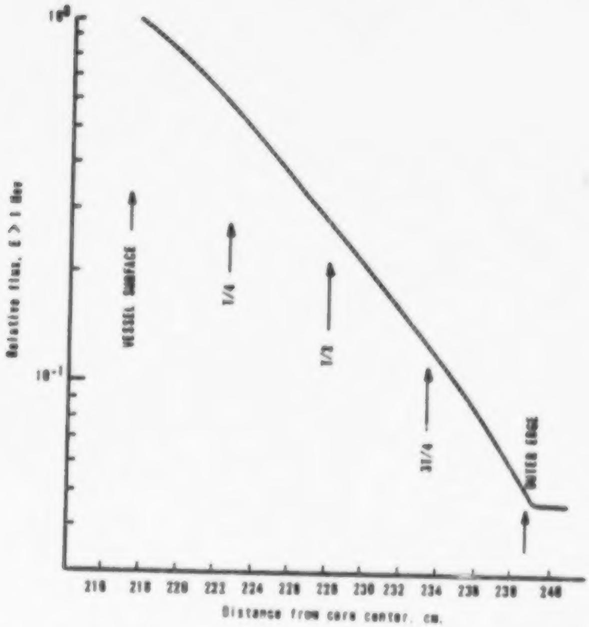

FIGURE 5.8.1. Radial Flux Gradient in a 177FA Reactor.

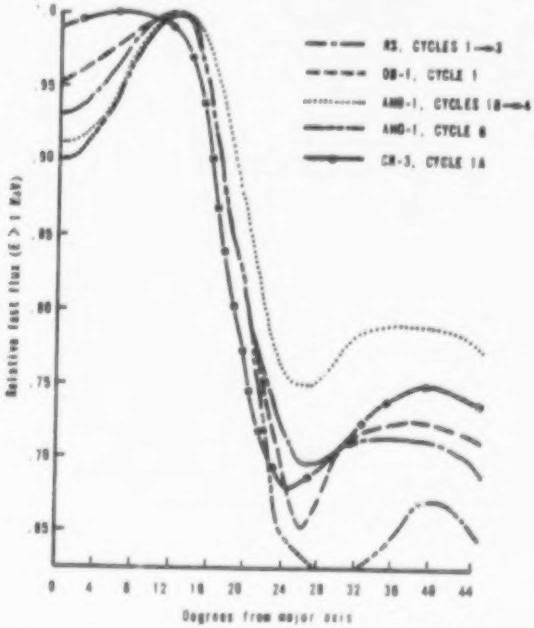

FIGURE 5.8.2. Azimuthal Flux Gradient in Selected 177FA Reactors at the Inside Surface of the Pressure Vessel.

flux shape at the inside vessel surface. Thus, gradients for selected fuel cycles (Figure 5.8.2) show a definite similarity between reactors and fuel cycles. Also, of note is the relatively small gradient compared to reactors of other vendors. The ANO-1 cycle 6 data were included because that is a low-leakage LBP cycle that represents a significant departure from the out-in fuel shuffle scheme used initially in the 177FA reactors. Most utilities with B&W reactors plan to use this low-leakage LBP fuel shuffle scheme after the first few cycles.

5.8.3 Fluence Lead Factors

Lead factors have been calculated which are the ratio of fast flux at selected locations to the inside vessel surface. Values in Table 5.8.2 are considered to be generic for 177FA reactors. Small differences caused by RPD distribution variations are observed in plant specific calculations.

5.8.4 Fluence Uncertainty

Uncertainties in fluence calculations have been estimated by comparison to integral measurements, when available, and from evaluation of each component to the analysis. Data that are summarized in Table 5.8.3 are based on the following:

Capsule -- Comparison of fast fluence to HEDL calculations (Si82a) for four capsules varied from -5 to -15% with a maximum uncertainty in the HEDL values of ±13%. Comparison of measured activities to Dosimetry Blind Test was <5%. Thus, total uncertainty for fast fluence derived from capsule activity is $\pm(13^2 + 5^2)^{.5} = \pm 14\%$.

TABLE 5.8.2

LEAD FACTORS FOR FAST FLUX

Location	Lead Factor (a)
Old capsule at 11°	1.8
New capsule at 11°	5.4
New capsule at 26.5°	3.9
Vessel T/4 at 11°	1/1.8
Vessel T/2 at 11°	1/3.6
Vessel 3T/4 at 11°	1/7.7

(a) relative to flux at the maximum vessel location, about 11° off axis at the inside vessel surface.

TABLE 5.8.3

FLUENCE CALCULATION UNCERTAINTIES

Calculation	Uncertainty (%)
Capsule (derived from measured activity)	± 14
Pressure vessel (maximum location for capsule irradiation time interval)	± 20
Pressure vessel (maximum location, long term extrapolation)	± 22
Pressure vessel welds	± 33

Pressure Vessel (Maximum Location with Capsule) -- Translation of capsule fluence to the maximum flux location in the vessel introduces some additional uncertainty. The radial location of the capsule is known only to ±0.635 cm (corresponds to ±9% fast flux).

Spatial extrapolation from capsule to vessel surface was shown in the PCA Blind Test to be within ±5%. Determination of azimuthal and axial position of maximum flux was estimated to be ±10%. Thus, total uncertainty for the maximum location in the pressure vessel for the time interval corresponding to a capsule irradiation is $\pm(14^2 + 9^2 + 5^2 + 10^2)^{.5} = \pm 20\%$.

Pressure Vessel (Long-Term Extrapolation) -- Time extrapolation of maximum vessel fluence to long term is based on future cycle designs and the assumption of an equilibrium cycle condition. Comparisons of flux determined from core leakage flux from criticality calculations to capsule fluence analyses have been within ±10%. Thus, total uncertainty for the long-term prediction of maximum fluence in the pressure vessel is $\pm(20^2 + 10^2)^{.5} = \pm 22\%$. No allowance is included to account for inability to predict an equilibrium cycle condition.

Pressure Vessel Welds -- Translation of maximum vessel fluence to weld locations introduces uncertainties relating to axial and azimuthal shape of fast flux in the pressure vessel. This effect was estimated to be ±25% based on location, large flux gradients, and the assumption of generic conditions. Thus, total uncertainty of vessel weld fluence is $\pm(22^2 + 25^2)^{.5} = \pm 33\%$.

5.9 SwRI PROCEDURES

5.9.1 Determination of Vessel Wall Exposure

The spatial and spectral distributions of neutrons in the reactor pressure vessel are calculated using a two-dimensional model and the DOT-IV discrete ordinates transport code. See Section 3.6.3 for details of the modeling and calculational procedures.

The azimuthal/radial and vertical/radial distributions of fluence rate, normalized to one fission neutron, are determined with R-Θ and R-Z calculations, respectively. Radial mesh dimensions through the pressure vessel wall are chosen to provide mesh points centered at 1/4 in. beneath the inside surface (I.D.), the one-quarter thickness (1/4T), the 1/2T, and the 3/4T positions.

The lead factors (ratio of normalized fluence rate at the surveillance capsule position to the peak vessel wall values) are computed for the selected exposure parameter. Exposures are usually expressed in terms of fluence greater than 1 MeV, but other threshold energies and displacements per atom (dpa) may also be used. The peak vessel wall exposures at the I.D., the 1/4T, and the 3/4T are determined as the product of the capsule exposure, derived as described in 3.6.4, and the appropriate capsule lead factor.

5.9.2 Verification of Fluence Rate Calculations

Southwest Research Institute is a service laboratory and, as such, has no facilities for verifying the fluence rate calculations for the pressure vessel. However, some power reactors have surveillance capsules placed near the vessel wall and in accelerated positions representative of several fluence rates. This provides an opportunity for comparing measured and calculated fluence rates at various radial and azimuthal locations.

An example is the LaCrosse Boiling Water Reactor (LACBWR) operated by Dairyland Power Cooperative. The vessel was fitted with twenty specimen/dosimeter capsules, four each at five azimuthal positions, and two vessel wall dosimeter capsules.

Four specimen/dosimeter capsules, two each from the 39.5° and 21.25° positions, and the two vessel wall dosimeter capsules (23° position) were removed during the 1975 refuelling outage (No77). The calculated and measured fluence rates for each position were as follows:

Position	Fluence Rate, n/cm^2-sec Calculated	 Measured
Wall (23°)	5.0	4.7
Capsule (39.5°)	7.2	6.8
Capsule (21.25°)	11.2	11.0

This provides a measure of confidence in the modeling techniques used in the discrete ordinates transport calculation, especially since the presence of an undetermined amount of voids in the steam separators complicate the problem.

Another way to evaluate these calculations, which minimizes the effect of the void concentration, is to compare the calculated and measured capsule lead factors:

Capsule Position	Lead Factor Calculated	 Measured	 Ratio
39.5°	1.44	1.45	1.01
21.25°	2.24	2.34	1.04

We have not conducted an analysis to establish the uncertainties in these calculations.

5.10 BMI PROCEDURES

See Section 3.5.

485

BIBLIOGRAPHY

BIBLIOGRAPHY

(Al83) A. A. Alberman et al., DOMPAC Dosimetry Experiment Neutron Simulation of the Pressure Vessel of a Pressurized-Water Reactor, Characterization of Irradiation Damage, CEA-R-5217, Centre d'Etudes Nucleaires de Saclay, France, May 1983.

(An78) S. L. Anderson, "Characterization of the Neutron Environment for Commercial LWR Pressure Vessel Surveillance Programs," Proc. of the 2nd ASTM-EURATOM Symposium on Reactor Dosimetry, Palo Alto, CA, October 3-7, 1977, NUREG/CP-0004, NRC, Washington, DC, Vol. 3, pp. 1093-1107, 1978.

(Ar83) A. L. Aronson et al., Evaluation of Methods for Reducing Pressure Vessel Fluence, BNL-NUREG-32876, NRC, Washington, DC, March 1983.

(As73) ASTM E185-73, "Recommended Practice for Surveillance Tests on Structural Materials in Nuclear Reactors," 1973 Annual Book of ASTM Standards, American Society for Testing and Materials, Philadelphia, PA, 1973.

(As77) ASTM A370-77, "Methods and Definitions for Mechanical Testing of Steel Products," 1977 Annual Book of ASTM Standards, American Society for Testing and Materials, Philadelphia, PA, 1977.

(As79a) "Nuclear Standards," 1979 Annual Book of ASTM Standards, American Society for Testing and Materials, Philadelphia, PA, Part 45, p. 999, 1979.

(As79c) ASTM E185-79, "Standard Practice for Surveillance Tests for Nuclear Reactor Vessels," 1979 Annual Book of ASTM Standards, American Society for Testing and Materials, Philadelphia, PA, Part 45, 1979.

(As82) ASTM E706-81a, "Master Matrix for LWR Pressure Vessel Surveillance Standards," 1982 Annual Book of ASTM Standards, American Society for Testing and Materials, Philadelphia, PA, Part 45, 1982. (See most recent version of ASTM E706, Annual Book of ASTM Standards, Section 12, Volume 12.02, current edition.)

(As82a) ASTM E482-82, "Standard Guide for Application of Neutron Transport Methods for Reactor Vessel Surveillance," 1982 Annual Book of ASTM Standards, American Society for Testing and Materials, Philadelphia, PA, Part 45, 1982.

(As82b) ASTM E854-81, "Standard Method for Application and Analysis of Solid State Track Recorder (SSTR) Monitors for Reactor Vessel Surveillance," 1982 Annual Book of ASTM Standards, American Society for Testing and Materials, Philadelphia, PA, Part 45, 1982.

(As83a) ASTM E910-82, "Standard Method for Application and Analysis of Helium Accumulation Fluence Monitors for Reactor Vessel Surveillance," 1983 Annual Book of ASTM Standards, American Society for Testing and Materials, Philadelphia, PA, Section 12, Volume 12.02, pp. 761-774, 1983.

(As83b) ASTM E844, "Standard Guide for Sensor Set Design and Irradiation for Reactor Surveillance," Annual Book of ASTM Standards, American Society for Testing and Materials, Philadelphia, PA, Volume 12.02, current edition.

(As84) ASTM E853, "Standard Practice for Analyses and Interpretation of Nuclear Reactor Surveillance Results," Annual Book of ASTM Standards, American Society for Testing and Materials, Philadelphia, PA, Section 12, Volume 12.02, current edition.

(As85) ASTM E706-(IIE), "Standard Guide for Benchmark Testing of Reactor Vessel Dosimetry," in ASTM E706, in Annual Book of ASTM Standards, American Society for Testing and Materials, Philadelphia, PA, current edition.

(As85a) ASTM E706-(IIID), "Standard Method for Application and Analysis of Damage Monitors for Reactor Vessel Surveillance," in ASTM E706, in Annual Book of ASTM Standards, American Society for Testing and Materials, Philadelphia, PA, current edition.

(As85b) ASTM E944, "Standard Guide for Application of Neutron Spectrum Adjustment Methods," Annual Book of ASTM Standards, American Society for Testing and Materials, Philadelphia, PA, current edition.

(As85c) ASTM E1005, "Standard Method for Application and Analysis of Radiometric Monitors for Reactor Vessel Surveillance," Annual Book of ASTM Standards, American Society for Testing and Materials, Philadelphia, PA, current edition.

(As85d) ASTM E1006, "Standard Practice for Analysis and Interpretation of Physics-Dosimetry Results for Test Reactors," Annual Book of ASTM Standards, American Society for Testing and Materials, Philadelphia, PA, current edition.

(As85e) ASTM E1018, "Standard Guide for Application of ENDF/A Cross Section and Uncertainty Files," Annual Book of ASTM Standards, American Society for Testing and Materials, Philadelphia, PA, current edition.

(As85f) ASTM E1035, "Standard Practice for Determining Radiation Exposure for Nuclear Reactor Support Structures, "Annual Book of ASTM Standards, American Society for Testing and Materials, Philadelphia, PA, current edition.

(Be67b) S. Berg and W. N. McElroy, A Computer Automated Iterative Method for Neutron Flux Spectra Determination by Foil Activation, AFWL-TR-67-41, Vol. 1, Air Force Weapons Laboratory, Kirkland AFB, NM, July 1967.

(Bo70) R. D. Bourquin, TIMH - A Computer Program for the Determination of Fluence with a Time-Varying Flux, BNWL-1492, Battelle Pacific Northwest Laboratory, Richland, WA, August 1970. (TIMWH is a modified version of the TIMH program.)

(Br82a) W. E. Brandon et al., "Neutron Dosimetry in the Pressure Vessel Cavity of Two Pressurized Water Reactors," Proc. of the 4th ASTM-EURATOM Symposium on Reactor Dosimetry, Gaithersburg, MD, March 22-26, 1982, NUREG/CP-0029, NRC, Washington, DC, Vol. 1, pp. 533-554, July 1982.

(Ce70) Program for Irradiation Surveillance of Reactor Vessel Materials, CEND-359, Combustion Engineering, Inc., Windsor, CT, January 1970.

(Cf83) Code of Federal Regulations, 10CFR50, "Domestic Licensing of Production and Utilization Facilities," "General Design Criteria for Nuclear Power Plants," Appendix A; "Fracture Toughness Requirements," Appendix G; "Reactor Vessel Material Surveillance Program Requirements," Appendix H; US Government Printing Office, Washington, DC, current edition.

(Da77) J. A. Davidson, S. L. Anderson and K. V. Scott, Analysis of Capsule V from Northern States Power Company Prairie Island Unit No. 1 Reactor Vessel Radiation Surveillance Program, WCAP-8916, Westinghouse Electric Corp., Pittsburgh, PA, August 1977.

(Da78a) J. A. Davidson, S. L. Anderson and R. P. Shogan, Analysis of Capsule T from the Wisconsin Electric Power Company Point Beach Nuclear Plant Unit No. 2 Reactor Vessel Radiation Surveillance Program, WCAP-9331, Westinghouse Electric Corp., Pittsburgh, PA, August 1978.

(Da79) J. A. Davidson, S. L. Anderson and W. T. Kaiser, Analysis of Capsule T from the Indian Point Unit 3 Reactor Vessel Radiation Surveillance Program, WCAP-9491, Westinghouse Electric Corp., Pittsburgh, PA, April 1979.

(Di82) W. J. Dircks, Pressurized Thermal Shock (PTS), and Enclosure A, "NRC Staff Evaluation of PTS," SECY-82-465, NRC, Washington, DC, November 1982.

(Fa76) A. Fabry et al., "Review of Microscopic Integral Cross Section Data in Fundamental Dosimetry Benchmark Neutron Fields," Neutron Cross Sections for Reactor Dosimetry, IAEA-208, International Atomic Energy Agency, Vienna, Austria, Vol. 1, p. 233, November 1976.

(Go82c) R. Gold, F. H. Ruddy and J. H. Roberts, "Photofission Observations in Reactor Environments Using Selected Fission Product Yields," Proc. of the 4th ASTM-EURATOM Symposium on Reactor Dosimetry, Gaithersburg, MD, March 22-26, 1982, NUREG/CP-0029, NRC, Washington, DC, Vol. 1, pp. 345-353, July 1982.

(Gr81) J. A. Grundl et al., "NRC-EPRI Studies of Pressure-Vessel-Cavity Neutron Fields," Proc. of the 9th Water Reactor Safety Information Meeting, Gaithersburg, MD, October 26-30, 1981, NUREG/CP-0024, Vol. 1-3, NRC, Washington, DC, March 1982.

(Gr82) J. A. Grundl et al., "NBS Compendium of Benchmark Neutron Fields for Reactor Dosimetry," 1982 Annual Book of ASTM Standards, Part 45, "Nuclear Standards," American Society for Testing and Materials, Philadelphia, PA, p. 1266, 1982.

(Gr83) J. A. Grundl, C. M. Eisenhauer and E. D. McGarry, "Neutron Flux Measurements in the Pressure Vessel Cavity of an Operating US Power Reactor, LWR-PV-SDIP Quarterly Progress Report, January 1982 - March 1982, NUREG/CR-2805, Vol. 1, HEDL-TME 82-18, NRC, Washington, DC, pp. NBS-3 - NBS-52, January 1983.

(Gr84) S. P. Grant and S. L. Earp, "Methods for Extending Life of a PWR Reactor Vessel After Long-Term Exposure to Fast Neutron Radiation, Proc. of the 12th ASTM Symposium on Effects of Radiation on Materials, ASTM STP 870, Williamsburg, VA, June 1984.

(Gu80) G. L. Guthrie, "Reanalysis of the Existing Data Base Relating Irradiation Embrittlement and Neutron Exposure of Pressure Vessel Steels," LWR-PV-SDIP Quarterly Progress Report, January 1980 - March 1980, NUREG/CR-1241, Vol. 1, HEDL-TME 80-4, NRC, Washington, DC, December 1980.

(Gu81) G. L. Guthrie, "An Investigation of the Dependence of Charpy Trend-Curve Saturation on Nickel or Copper Concentration," LWR-PV-SDIP Quarterly Progress Report, October - December 1980, NUREG/CR-1241, Vol. 4, HEDL-TME 80-6, NRC, Washington, DC, pp. HEDL-9 - HEDL-17, November 1981.

(Gu81a) G. L. Guthrie, "A Determination of the Effect of Irradiation Temperature on the Irradiation-Induced Charpy Shift," LWR-PV-SDIP Quarterly Progress Report, January - March 1981, NUREG/CR-2345, Vol. 1, HEDL-TME 81-33, NRC, Washington, DC, October 1981.

(Gu82) G. L. Guthrie, W. N. McElroy and S. L. Anderson, "A Preliminary Study of the Use of Fuel Management Techniques for Slowing Pressure Vessel Embrittlement," Proc. of the 4th ASTM-EURATOM Symposium on Reactor Dosimetry, Gaithersburg, MD, March 22-26, 1982, NUREG/CP-0029, NRC, Washington, DC, Vol. 1, pp. 111-120, July 1982.

(Gu82a) G. L. Guthrie, W. N. McElroy and S. L. Anderson, "Investigations of Effects of Reactor Core Loadings on PV Neutron Exposure," LWR-PV-SDIP Quarterly Progress Report, October 1981 - December 1981, NUREG/CR-2345, Vol. 4, HEDL-TME 81-36, NRC, Washington, DC, Section E and Appendix, pp. HEDL-35 - HEDL-36 & HEDL-A1 - HEDL-A46, October 1982.

(Gu82b) G. L. Guthrie, "Development of Trend Curve Formulas Using Surveillance Data," LWR-PV-SDIP Quarterly Progress Report, January 1982 - March 1982, NUREG/CR-2805, Vol. 1, HEDL-TME 82-18, NRC, Washington, DC, pp. HEDL-3 - HEDL-18, December 1982.

(Gu82c) G. L. Guthrie, "Development of Trend Curve Formulas Using Surveillance Data - II," LWR-PV-SDIP Quarterly Progress Report, April - June 1982, NUREG/CR-2805, Vol. 2, HEDL-TME 82-19, NRC, Washington, DC, pp. HEDL-3 - HEDL-13, December 1982.

(Gu83) G. L. Guthrie, "Charpy Trend Curve Formulas Derived from an Expanded Surveillance Data Base," LWR-PV-SDIP Quarterly Progress Report, October 1982 - December 1982, NUREG/CR-2805, Vol. 4, HEDL-TME 82-21, NRC, Washington, DC, pp. HEDL-3 - HEDL-13, July 1983.

(Gu83a) G. L. Guthrie, "Pressure Vessel Steel Irradiation Embrittlement Formulas Derived from PWR Surveillance Data," from the ANS Special Session on Correlations and Implications of Neutron Irradiation Embrittlement of Pressure Vessel Steels, Detroit, MI, June 12-16, 1983, Trans. Am. Nucl. Soc. 44, p. 222, June 1983.

(Gu83b) G. L. Guthrie, "Error Estimations in Applications of Charpy Trend Curve Formulas," LWR-PV-SDIP Quarterly Progress Report, January 1983 - March 1983, NUREG/CR-3391, Vol. 1, HEDL-TME 83-21, NRC, Washington, DC, pp. HEDL-3 - HEDL-13, November 1983.

(Gu83c) G. L. Guthrie, "Charpy Trend Curve Development Based on PWR Surveillance Data," Proc. of the 11th WRSR Information Meeting, Gaithersburg, MD, October 24-28, 1983, NUREG/CP-0048, NRC, Washington, DC, 1983.

(Gu84) G. L. Guthrie, "Charpy Trend Curves Based on 177 PWR Data Points," LWR-PV-SDIP Quarterly Progress Report, April 1983 - June 1983, NUREG/CR-3391, Vol. 2, HEDL-TME 83-22, NRC, Washington, DC, pp. HEDL-3 - HEDL-15, April 1984.

(Gu84a) G. L. Guthrie, W. N. McElroy and R. L. Simons, "Effect of Thermal Neutrons in Irradiation Embrittlement of PWR Pressure Vessel Plates and Welds," LWR-PV-SDIP Quarterly Progress Report, April 1983 - June 1983, NUREG/CR-3391, Vol. 2, HEDL-TME 83-22, NRC, Washington, DC, HEDL-16 - HEDL-21, April 1984.

(Gu84b) G. L. Guthrie, "HEDL Analysis of the PSF Experiment, "Attachment to Minutes of the 14th LWR-PV-SDIP Meeting, HEDL-7511, Hanford Engineering Development Laboratory, Richland, WA, p. A7-1, October 1-5, 1984.

(Gu84c) G. L. Guthrie, "Uncertainty Considerations in Development and Application of Charpy Trend-Curve Formulas," HEDL-SA-3205, presented at the 5th ASTM-EURATOM Symposium on Reactor Dosimetry, Geesthacht, FRG, September 24-28, 1984.

(Gu84d) G. L. Guthrie, E. P. Lippincott and E. D. McGarry, LWR-PV-SDIP: PSF Blind Test Workshop Minutes, HEDL-7467, Hanford Engineering Development Laboratory, Richland, WA, April 9-10, 1984.

(Gu84e) G. L. Guthrie, K. Carlson and G. R. Odette, "Embrittlement of Compression Specimens Irradiated in the SSC-1 and SSC-2 Capsules of the PSF Experiment," LWR-PV-SDIP Semiannual Progress Report, October 1983 - March 1984, NUREG/CR-3746, Vol. 1, HEDL-TME 84-20, NRC, Washington, DC, pp. HEDL-18 - HEDL-24, November 1984.

(Gu85) G. L. Guthrie, "HEDL Analysis of the Poolside Facility Experiment," LWR-PV-SDIP Semiannual Progress Report, April 1984 - September 1984, NUREG/CR-3746, Vol. 2, HEDL-TME 84-21, NRC, Washington, DC, pp. HEDL-28 - HEDL-52, March 1985.

(Gu85a) G. L. Guthrie, "Results of Measurements of Compression and Hardness Specimens of Reactor Pressure Vessel Steel Irradiated at the Oak Ridge Reactor," LWR-PV-SDIP Semiannual Progress Report, April 1984 - September 1984, NUREG/CR-3746, Vol. 2, HEDL-TME 84-21, NRC, Washington, DC, pp. HEDL-53 - HEDL-82, March 1985.

(He82) P. D. Hedgecock and J. S. Perrin, "Standards for Materials Behavior Under Neutron Irradiation," Proc. of the 4th ASTM-EURATOM Symposium on Reactor Dosimetry, Gaithersburg, MD, March 22-26, 1982, NUREG/CP-0029, NRC, Washington, DC, Vol. 2, pp. 829-837, July 1982.

(Ir70) D. R. Ireland and V. G. Scotti, Examination and Evaluation of Capsule A for the Connecticut Yankee Reactor Pressure Vessel Surveillance Program, Battelle Memorial Institute, Columbus Laboratories, Columbus, OH, October 30, 1970.

(Ka82) F. B. K. Kam, Ed., Proc. of the 4th ASTM-EURATOM Symposium on Reactor Dosimetry, Gaithersburg, MD, March 22-26, 1982, NUREG/CP-0029, NRC, Washington, DC, Vols. 1 and 2, July 1982.

(Ke82) L. S. Kellogg and E. P. Lippincott, "PSF Interlaboratory Comparison," Proc. of the 4th ASTM-EURATOM Symposium on Reactor Dosimetry, Gaithersburg, MD, March 22-26, 1982, NUREG/CP-0029, CONF-820321/V2, NRC, Washington, DC, Vol. 2, pp. 929-945, July 1982.

(Ko82) N. P. Kocherov, "Highlights from the IAEA Advisory Group Meeting on Nuclear Data for Radiation Damage Assessment and Related Safety Aspects," Proc. of the 4th ASTM-EURATOM Symposium on Reactor Dosimetry, Gaithersburg, MD, March 22-26, 1982, NUREG/CP-0029, NRC, Washington, DC, Vol. 2, pp. 873-875, July 1982.

(Li75) E. P. Lippincott, J. A. Ulseth, L. S. Kellogg, A. I. Davis and W. N. McElroy, *EBR-II 75D High Power Dosimetry Test*, HEDL-TME 75-86, Hanford Engineering Development Laboratory, Richland, WA, December 1975.

(Li82) E. P. Lippincott and W. N. McElroy, "ASTM Standard Recommended Guide on Application of ENDF/A Cross Section and Uncertainty File: Establishment of the File," *Proc. of the 4th ASTM-EURATOM Symposium on Reactor Dosimetry*, Gaithersburg, MD, March 22-26, 1982, *NUREG/CP-0029, NRC, Washington*, DC, Vol. 2, pp. 705-710, July 1982.

(Lo75) A. L. Lowe Jr et al., *Analysis of Capsule OCI-F from Duke Power Company, Oconee Unit No. 1 Reactor Vessel Materials Surveillance Program*, BAW-1421, Babcock & Wilcox, Lynchburg, VA, August 1975.

(Lo77) A. L. Lowe Jr et al., *Analysis of Capsule OCI-E from Duke Power Company, Oconee Nuclear Station - Unit 1*, BAW-1436, Babcock & Wilcox, Lynchburg, VA, September 1977.

(Lo77a) A. L. Lowe Jr et al., *Analysis of Capsule OCII-C from Duke Power Company, Oconee Nuclear Station - Unit 2*, BAW-1437, Babcock & Wilcox, Lynchburg, VA, May 1977.

(Lo77b) A. L. Lowe Jr et al., *Analysis of Capsule OCII-A from Duke Power Company, Oconee Nuclear Station - Unit 3*, BAW-1438, Babcock & Wilcox, Lynchburg, VA, July 1977.

(Lo77c) A. L. Lowe Jr et al., *Analysis of Capsule TMI-1E from Metropolitan Edison Company, Three Mile Island Nuclear Station - Unit 1*, BAW-1439, Babcock & Wilcox, Lynchburg, VA, January 1977.

(Lo77d) A. L. Lowe Jr et al., *Analysis of Capsule ANI-E from Arkansas Power & Light Company, Arkansas Nuclear Station - Unit 1*, BAW-1440, Babcock & Wilcox, Lynchburg, VA, April 1977.

(Lo81) A. L. Lowe Jr et al., *Analysis of Capsule CR3-B from Florida Power Corporation, Crystal River - Unit 3*, BAW-1679, Babcock & Wilcox, Lynchburg, VA, June 1981.

(Lo81a) A. L. Lowe Jr et al., *Analysis of Capsule ANI-B from Arkansas Power & Light Company, Arkansas Nuclear Station - Unit 1*, BAW-1698, Babcock & Wilcox, Lynchburg, VA, December 1981.

(Lo81b) A. L. Lowe Jr et al., *Analysis of Capsule OCII-A from Duke Power Company, Oconee Nuclear Station - Unit 2*, BAW-1699, Babcock & Wilcox, Lynchburg, VA, December 1981.

(Lo81c) A. L. Lowe Jr et al., *Analysis of Capsule OCIII-B from Duke Power Company, Oconee Nuclear Station - Unit 3*, BAW-1697, Babcock & Wilcox, Lynchburg, VA, October 1981.

(Lo81d) A. L. Lowe Jr et al., *Analysis of Capsule V Virginia Electric and Power Company, North Anna Unit No. 1 Reactor Vessel Materials Surveillance Program*, BAW-1638, Babcock & Wilcox, Lynchburg, VA, March 1981.

(Lo82) A. L. Lowe Jr et al., *Analysis of Capsule TEI-F from the Toledo Edison Company, Davis-Besse Nuclear Station - Unit 1*, BAW-1701, Babcock & Wilcox, Lynchburg, VA, January 1982.

(Lo82a) A. L. Lowe Jr et al., *Analysis of Capsule RSI-B from Sacramento Muncipal Utility District, Rancho Seco - Unit 1*, BAW-1702, Babcock & Wilcox, Lynchburg, VA, February 1982.

(Ma73a) T. R. Mager et al., *Analysis of Capsule V from the Rochester Gas and Electric Company, R. E. Ginna Unit No. 1 Reactor Vessel Radiation Surveillance Program*, FP-RA-1, Westinghouse Electric Corp., Pittsburgh, PA, April 1973.

(Ma78b) T. U. Marston and K. E. Stahlkopf, "Radiation Embrittlement: Significance of Its Effects on Integrity and Operation of LWR Pressure Vessels," *Nuclear Safety* *2*, (6), p. 724, November - December 1978.

(Ma80d) G. C. Martin, *Browns Ferry Unit 3 In-Vessel Neutron Spectral Analysis*, NEDO-24793, General Electric Company, San Jose, CA, August 1980.

(Ma81) R. E. Maerker, J. J. Wagschal and B. L. Broadhead, *Development and Demonstration of an Advanced Methodology for LWR Dosimetry Applications*, EPRI NP-2188, (Project 1399-1, Interim Report), Electric Power Research Institute, Palo Alto, CA, December 1981.

(Ma81c) G. C. Martin, *Brown Ferry Unit 3 Drywell Neutron Measurements*, NEDO-24946, General Electric Company, San Jose, CA, June 1981.

(Ma81d) G. C. Martin, *Browns Ferry Unit 3 Cavity Neutron Spectral Analysis*, EPRI NP-1997, Electric Power Research Institute, Palo Alto, CA, August 1981.

(Ma82e) R. E. Maerker and M. L. Williams, "Calculations of the Westinghouse Perturbation Experiment at the Poolside Facility," *Proc. of the 4th ASTM-EURATOM Symposium on Reactor Dosimetry*, Gaithersburg, MD, March 22-26, 1982, NUREG/CP-0029, NRC, Washington, DC, Vol. 1, pp. 131-141, July 1982.

(Ma82g) T. R. Mager et al., *Feasibility of and Methodology for Thermal Annealing of Embrittled Reactor Vessel: Detailed Technical Description of the Work*, EPRI NP-2712, Vol. 2, (Final Report, Project 1021-1), Electric Power Research Institute, Palo Alto, CA, November 1982.

(Ma82h) T. U. Marston and T. R. Mager, "EPRI Thermal Anneal Program RP1021-1," Report to ASME Section XI Subcommittee on Repairs and Replacements and to NRC, February 1982.

(Ma82j) G. C. Martin and H. A. Till, "Browns Ferry Unit 3 Cavity Neutron Spectral Analysis," Proc. of the 4th ASTM-EURATOM Symposium on Reactor Dosimetry, Gaithersburg, MD, March 22-26, 1982, NUREG/CP-0029, NRC, Washington, DC, Vol. 1, pp. 555-564, July 1982.

(Ma83) T. U. Marston, "A Brief on the Assessment of Relative Uncertainties," from the ANS Special Session on Correlations and Implications of Neutron Irradiation Embrittlement of Pressure Vessel Steels, Detroit, MI, June 12-16, 1983, Trans. Am. Nucl. Soc. 44, p. 221, 1983.

(Ma83b) T. R. Mager, T. U. Marston and S. E. Yanichko, "Assessing Steady-State Neutron Exposure Effects Through Analyses of Reactor Vessel Surveillance Data," Radiation Embrittlement and Surveillance of Nuclear Reactor Pressure Vessels: An International Study, ASTM STP 819, L. E. Steele, Ed., American Society for Testing and Materials, pp. 155-165, 1983.

(Mc67) W. N. McElroy, S. Berg and T. Crocket, A Computer-Automated Iterative Method of Neutron Flux Spectra Determined by Foil Activation, AFWL-TR-67-41, Vol. I-IV, Air Force Weapons Laboratory, Kirkland AFB, NM, July 1967.

(Mc75c) W. N. McElroy and L. S. Kellogg, "Fuels and Materials Fast-Reactor Dosimetry Data Development and Testing," Nucl. Technol. 25, (2), pp. 180-223, 1975.

(Mc81) W. N. McElroy, Ed., LWR-PV-SDIP: PCA Experiments and Blind Test, NUREG/CR-1861, HEDL-TME 80-87, NRC, Washington, DC, July 1981.

(Mc81a) W. N. McElroy et al., LWR-PV-SDIP 1980 Annual Report, NUREG/CR-1747, HEDL-TME 80-73, NRC, Washington, DC, April 1981.

(Mc81e) E. D. McGarry et al., "Benchmark Field Referencing," LWR-PV-SDIP: PCA Experiments and Blind Test, W. N. McElroy, Ed., NUREG/CR-1861, HEDL-TME 80-87, NRC, Washington, DC, pp. 2.2-1 - 2.2-27, July 1981.

(Mc82) W. N. McElroy et al., "Surveillance Dosimetry of Operating Power Plants," Proc. of the 4th ASTM-EURATOM Symposium on Reactor Dosimetry, Gaithersburg, MD, March 22-26, 1982, NUREG/CP-0029, NRC, Washington, DC, pp. 3-43, July 1982. (Serves as the LWR Pressure Vessel Surveillance Dosimetry Improvement Program 1981 Annual Report.)

(Mc82a) W. N. McElroy et al., LWR-PV-SDIP 1982 Annual Report, NUREG/CR-2805, Vol. 3, HEDL-TME 82-20, NRC, Washington, DC, December 1982.

(Mc82b) W. N. McElroy et al., "Verification of Effects of Fuel Management Schemes on the Condition of Pressure Vessels and Their Support Structures," HEDL-SA-2791 and Proc. of the 10th WRSR Information Meeting, Gaithersburg, MD, October 12-15, 1982, NUREG/CP-0041, Vol. 4, pp. 184-227, January 1983.

(Mc82c) P. McConnell et al., Irradiated Nuclear Pressure Vessel Steel Data Base, EPRI NP-2428, Electric Power Research Institute, Palo Alto, CA, June 1982.

(Mc84) W. N. McElroy et al., LWR-PV-SDIP 1983 Annual Report, NUREG/CR-3391, Vol. 3, HEDL-TME 83-23, NRC, Washington, DC, January 1984.

(Mc84h) W. N. McElroy et al., "Trend Curve Exposure Parameter Data Development and Testing," HEDL-SA-3126 and Proc. of the 5th ASTM-EURATOM Symposium on Reactor Dosimetry, Geesthacht, FRG, September 24-28, 1984.

(Mc84i) W. N. McElroy, LWR-PV-SDIP: PCA Experiments Blind Test and Physics-Dosimetry Support for the PSF Experiments, NUREG/CR-3318, HEDL-TME 84-1, NRC, Washington, DC, September 1984.

(Mc85) W. N. McElroy et al., LWR-PV-SDIP Semiannual Progress Report, April - September 1984, NUREG/CR-3746, Vol. 2, HEDL-TME 84-21, NRC, Washington, DC, March 1985.

(Mc85a) W. N. McElroy et al., LWR-PV-SDIP 1984 Annual Report, October 1, 1983 - September 30, 1984, NUREG/CR-3746, Vol. 3, HEDL-TME 84-31, NRC, Washington, DC, March 1985.

(Mp79) MPC Subcommittee 6 on Nuclear Materials, "Prediction of the Shift in the Brittle-Ductile Transition Temperature of LWR Pressure Vessel Materials," Final Report to ASTM Subcommittee E10.02, American Society for Testing and Materials, Philadelphia, PA, June 1979.

(No67) E. B. Norris, Influence of Neutron Irradiation on the Properties of Steels and Welds Typical of the ERR Pressure Vessel, SwRI 1228 P4-28, Southwest Research Institute, San Antonio, TX, January 1967.

(No68) D. R. Ireland and E. B. Norris, Influence of Neutron Irradiation on the Properties of Steels and Welds Typical of the ERR Pressure Vessel After Two Power Years Operation, SwRI 1228 P9-15, Southwest Research Institute, San Antonio, TX, March 1968.

(No71) E. B. Norris, Analysis of First Surveillance Material Capsule from San Onofre Unit 1, SwRI Project 07-2892, Southwest Research Institute, San Antonio, TX, May 1971.

(No72) E. B. Norris, Analysis of Second Surveillance Material Capsule from San Onofre Unit 1, Final Report, SwRI Project 07-2892, Southwest Research Institute, San Antonio, TX, June 1972.

(No73) E. B. Norris, Analysis of the First Vessel Material Surveillance Capsule Withdrawal from LaCrosse Boiling Water Reactor, Topical Report No. 1, SwRI Project 02-3467, Southwest Research Institute, San Antonio, TX, March 1973.

(No73a) E. B. Norris, Analysis of the First Material Surveillance Capsule from H. B. Robinson Unit No. 2, Final Report, SwRI Project 02-3574, Southwest Research Institute, San Antonio, TX, July 1973.

(No74) E. B. Norris, Vessel Material Surveillance Program for Pilgrim Nuclear Power Station, Topical Report No. 1, SwRI Project 02-3812-001, Southwest Research Institute, San Antonio, TX, August 1974.

(No75) E. B. Norris, Vessel Material Surveillance Program for Vermont Yankee Nuclear Power Station, Final Report, SwRI Project 02-4032, Southwest Research Institute, San Antonio, TX, May 1975.

(No76) E. B. Norris, Reactor Vessel Material Surveillance Program for Turkey Point Unit No. 4 -- Analysis of Capsule T, Final Report, SwRI Project 02-4221, Southwest Research Institute, San Antonio, TX, June 1976.

(No76a) E. B. Norris and J. F. Unruh, Pressure-Temperature Limitations for the Turkey Point Unit Nos. 3 and 4 Nuclear Power Plants, SwRI Project 02-4383-039, Southwest Research Institute, San Antonio, TX, June 1976.

(No76b) E. B. Norris, Reactor Vessel Material Surveillance Program for H. B. Robinson Unit No. 2 -- Analysis of Capsule V, Final Report, SwRI Project 02-4397, Southwest Research Institute, San Antonio, TX, October 1976.

(No77) E. B. Norris, Analysis of the Vessel Material Surveillance Capsules Withdrawn from LaCrosse Boiling Water Reactor During the 1975 Refueling, Final Report, SwRI Project 02-4074-001, Southwest Research Institute, San Antonio, TX, April 1977.

(No77a) E. B. Norris, Reactor Vessel Material Surveillance Program for Indian Point Unit No. 2 -- Analysis of Capsule T, Final Report, SwRI Project 02-4531, Southwest Research Institute, San Antonio, TX, June 1977.

(No77b) E. B. Norris, Reactor Vessel Material Surveillance Program for Donald C. Cook Unit No. 1 -- Analysis of Capsule T, Final Report, SwRI Project 02-4770, Southwest Research Institute, San Antonio, TX, December 1977.

(No78) E. B. Norris, *Analysis of the Vessel Wall Neutron Dosimeter from Browns Ferry Unit 1 Pressure Vessel*, Final Report, SwRI Project 02-4884-001, Southwest Research Institute, San Antonio, TX, August 1978.

(No79) E. B. Norris, *Reactor Vessel Material Surveillance Program for Capsule S -- Turkey Point Unit No. 3; Capsule S -- Turkey Point Unit No. 4*, Final Report, SwRI Projects 02-5131 and 02-5380, Southwest Research Institute, San Antonio, TX, May 1979.

(No79a) E. B. Norris, *Analysis of the Vessel Wall Neutron Dosimeter from Browns Ferry Unit 2 Pressure Vessel*, Final Report, SwRI Project 02-4884-002, Southwest Research Institute, San Antonio, TX, September 1979.

(No79b) E. B. Norris, *Analysis of the Vessel Wall Neutron Dosimeter from Browns Ferry Unit 3 Pressure Vessel*, Final Report, SwRI Project 02-4884-003, Southwest Research Institute, San Antonio, TX, September 1979.

(No80) E. B. Norris, *Reactor Vessel Material Surveillance Program for KO-RI Unit No. 1 -- Analysis of Capsule V*, Final Report, SwRI Project 17-5759-201, Southwest Research Institute, San Antonio, TX, June 1980.

(No80a) E. B. Norris, *Reactor Vessel Material Surveillance Program for Indian Point Unit No. 2 -- Analysis of Capsule Y*, Final Report, SwRI Project 02-5212, Southwest Research Institute, San Antonio, TX, November 1980.

(No80b) E. B. Norris, *Reactor Vessel Material Surveillance Program for Indian Point Unit No. 2 -- Analysis of Capsule T*, Supplement to Final Report, SwRI Project 02-4531, Southwest Research Institute, San Antonio, TX, December 1980.

(No81) E. B. Norris, *Reactor Vessel Material Surveillance Program for Donald C. Cook Unit No. 1 -- Analysis of Capsule X*, Final Report, SwRI Project 02-6159, Southwest Research Institute, San Antonio, TX, June 1981.

(No81a) E. B. Norris, *Pilgrim Nuclear Power Station Unit 1 Reactor Vessel Irradiation Surveillance Program*, Final Report, SwRI Project 02-5951, Southwest Research Institute, San Antonio, TX, July 1981.

(No81b) E. B. Norris, *Reactor Vessel Material Surveillance Program for Donald C. Cook Unit No. 2 -- Analysis of Capsule T*, Final Report, SwRI Project 02-5928, Southwest Research Institute, San Antonio, TX, September 1981.

(No81c) E. B. Norris, Analysis of the Vessel Material Surveillance Capsules Withdrawn from LaCrosse Boiling Water Reactor During the 1980 Refueling, Final Report, SwRI Project 02-6208-001, Southwest Research Institute, San Antonio, TX, October 1981.

(No81d) E. B. Norris, Evaluation of the Response of Ferritic Materials to an Elevated Temperature Radiation Environment, Final Report, SwRI Project 02-9247, Southwest Research Institute, San Antonio, TX, September 30, 1981.

(No82) E. B. Norris, "Spectral Analysis of a BWR Vessel," Proc. of the 4th ASTM-EURATOM Symposium on Reactor Dosimetry, Gaithersburg, MD, March 22-26, 1982, NUREG/CP-0029, NRC, Washington, DC, Vol. 2, p. 1043, July 1982.

(Nr80) NRC Staff, Presentation to Advisory Committee on Reactor Safeguards, Metal Components Subcommittee, Transcribed Proceedings of Meeting, Washington, DC, January 24, 1980.

(Nr82) NRC Staff, Presentation to Advisory Committee on Reactor Safeguards, Metal Components Subcommittee, Meeting on Reactor Vessel Integrity (RVI), Washington, DC, May 11-12, 1982.

(OaXX) CASK-40-Group Coupled Neutron and Gamma Ray Cross-Section Data, RSIC-DLC-23, Radiation Shielding Information Center, Oak Ridge, TN.

(Pa84) T. O. Passell, Analysis of the Browns Ferry Unit 3 Irradiation Experiments, Summary Report, EPRI NP-3719, Electric Power Research Institute, Palo Alto, CA, November 1984.

(Pe72) J. S. Perrin, J. W. Sheckherd and V. G. Scotti, Examination and Evaluation of Capsule F for the Connecticut Yankee Reactor Pressure Vessel Surveillance Program, NRC, Public Document Room, Washington, DC, March 30, 1972.

(Pe75) J. S. Perrin et al., Surry Unit No. 1 Pressure Vessel Irradiation Capsule Program: Examination and Analysis of Capsule T, Docket 50280-462, NRC, Public Document Room, Washington, DC, June 24, 1975.

(Pe75a) J. S. Perrin et al., Surry Unit No. 2 Pressure Vessel Irradiation Capsule Program: Examination and Analysis of Capsule X, NRC, Public Document Room, Washington, DC, September 2, 1975.

(Pe75b) J. S. Perrin et al., Point Beach Unit No. 2 Pressure Vessel Surveillance Program: Evaluation of Capsule V, NRC, Public Document Room, Washington, DC, June 10, 1975.

(Pe77) F. G. Perey, The Data Covariance Files for ENDF/B-V, ORNL/TM-5839, Oak Ridge National Laboratory, Oak Ridge, TN, July 1977.

499

(Pe77a) F. G. Perey, *Least Squares Dosimetry Unfolding: The Program STAY'SL, ORNL/TM-6062, Oak Ridge National Laboratory, Oak Ridge, TN, 1977.*

(Pe78) J. S. Perrin et al., *Zion Nuclear Plant Reactor Pressure Vessel Surveillance Program: Unit No. 1 Capsule T and Unit No. 2 Capsule U, BCL-585-4, Battelle Memorial Institute, Columbus Laboratories,* Columbus, OH, March 1978.

(Pe79b) J. S. Perrin et al., *Palisades Nuclear Plant Reactor Pressure Vessel Surveillance Program: Capsule A-240*, BCL-585-12, Battelle *Memorial Institute, Columbus Laboratories,* Columbus, OH, March 13, 1979.

(Pe80) J. S. Perrin et al., *Maine Yankee Nuclear Plant Reactor Pressure Vessel Surveillance Program: Capsule 263*, BCL-585-21, Battelle *Memorial Institute, Columbus Laboratories,* Columbus, OH, December 21, 1980.

(Pe82b) M. Petilli, "A New Analysis of the Experiment for Measurement of $\Phi > 1$ MeV in Pressure Vessel Cavity of U.S. Light Water Power Reactor Arkansas," *Proc. of the 4th ASTM-EURATOM Symposium on Reactor Dosimetry*, Gaithersburg, MD, March 22-26, 1982, NUREG/CP-0029, NRC, Washington, DC, Vol. 1, pp. 545-554, July 1982.

(Pe84) J. S. Perrin, R. A. Wullaert, G. R. Odette and M. P. Lombroso, *Physically Based Regression Correlations of Embrittlement Data from Reactor PV Surveillance Programs*, EPRI NP-3319, Electric Power Research Institute, Palo Alto, CA, January 1984.

(Ra79) P. N. Randall, "Regulatory Aspects of Radiation Embrittlement of Reactor Vessel Steels," *Proc. of an IAEA Specialists' Meeting on Irradiation Embrittlement, Thermal Annealing, and Surveillance of Reactor Pressure Vessels*, Vienna, Austria, February 26 - March 1, 1979, IWG-RRPC-79/2, December 1979.

(Ra81b) P. N. Randall, "The Status of Trend Curves and Surveillance Results in USNRC Regulatory Activities," *Proc. of an IAEA Specialists' Meeting*, Vienna, Austria, October 20, 1981.

(Ra82a) P. N. Randall, "Status of Regulatory Demands in the U.S. on the Application of Pressure Vessel Dosimetry," *Proc. of the 4th ASTM-EURATOM Symposium on Reactor Dosimetry*, Gaithersburg, MD, March 22-26, 1982, NUREG/CP-0029, NRC, Washington, DC, Vol. 2, pp. 1011-1022, July 1982.

(Ra83) P. N. Randall, "NRC Perspective of Safety and Licensing Issues Regarding Reactor Vessel Steel Embrittlement," from the ANS Special Session on Correlations and Implications of Neutron Irradiation Embrittlement of Pressure Vessel Steels, Detroit, MI, June 12-16, 1983, *Trans. Am. Nucl. Soc. 44*, p. 220, 1983.

(Ra84) P. N. Randall, "Basis for Revision 2 of US NRC Regulatory Guide 1.99," Proc. 10th MPA Seminar, Stuttgart, FRG, October 10, 1984.

(Re77) Regulatory Guide 1.99, Effects of Residual Elements on Predicted Radiation Damage to Reactor Vessel Materials, Rev. 1, NRC, Washington, DC, April 1977.

(Ru84a) F. H. Ruddy et al., "Standardized Physics-Dosimetry for US Pressure Vessel Cavity Surveillance Programs," HEDL-SA-3095 and Proc. of the 5th ASTM-EURATOM Symposium on Reactor Dosimetry, Geesthacht, FRG, September 24-28, 1984.

(SaXX) SAILWR - Coupled, Self-Shielded, 47 Neutron, 20 Gamma-Ray, P_3, Cross-Section Library for Light Water Reactors, RSIC-DLC-76, Radiation Shielding Information Center, Oak Ridge, TN.

(Sc79) F. A. Schmittroth, FERRET Data Analysis Code, HEDL-TME 79-40, Hanford Engineering Development Laboratory, Richland, WA, September 1979.

(Se78) W. L. Server and W. Oldfield, Nuclear Pressure Vessel Steel Data Base, EPRI NP-933, Electric Power Research Institute, Palo Alto, CA, 1978.

(Sh82) R. A. Shaw, "Browns Ferry and Arkansas Nuclear One Pressure Vessel Neutron Fluence Benchmarks," Proc. of the 4th ASTM-EURATOM Symposium on Reactor Dosimetry, Gaithersburg, MD, March 22-26, 1982, NUREG/CP-0029, NRC, Washington, DC, Vol. 1, pp. 513-518, July 1982.

(Si82) R. L. Simons, "Correlation of Macroscopic Material Properties with Microscopic Nuclear Data," Nuclear Data for Radiation Damage Assessment and Related Safety Aspects, IAEA-TECDOC-263, International Atomic Energy Agency, Vienna, Austria, p. 241, 1982.

(Si82a) R. L. Simons et al., "Re-evaluation of the Dosimetry for Reactor Pressure Vessel Surveillance Capsules," Proc. of the 4th ASTM-EURATOM Symposium on Reactor Dosimetry, Gaithersburg, MD, March 22-26, 1982, NUREG/CP-0029, NRC, Washington, DC, Vol. 2, pp. 903-916, July 1982.

(Si84) R. L. Simons et al., "Re-evaluation of the Physics-Dosimetry from PWR and BWR Pressure Vessel Surveillance Programs," HEDL-SA-3210 and Proc. of the 5th ASTM-EURATOM Symposium on Reactor Dosimetry, Geesthacht, FRG, September 24-28, 1984.

(So70) R. G. Soltesz, R. K. Disney, J. Jedruch and S. L. Ziegler, "Nuclear Rocket Shielding Methods, Modification, Updating and Input Data," Two-Dimensional Discrete Ordinates Transport Technique, WANL-PR(LL)-034, Vol. 5, Westinghouse Electric Corp., Pittsburgh, PA, August 1970.

(St80) J. Strosnider and C. Monseprate, with Appendix Prepared by L. D. Kenworthy and C. D. Tether, *MATSURV -- Computerized Reactor Pressure Vessel Materials Information System*, NUREG-0688, NRC, Washington, DC, October 1980.

(St81) *Standard Review Plan and Branch Technical Position MTEB 5.2: Fracture Toughness Requirements*, NUREG-75/087, NRC, Washington, DC, 1981.

(St82) F. W. Stallmann, "Workshop on Adjustment Codes and Uncertainties," *Proc. of the 4th ASTM-EURATOM Symposium on Reactor Dosimetry*, Gaithersburg, MD, March 22-26, 1982, NUREG/CP-0029, NRC, Washington, DC, Vol. 2, pp. 1219-1220, July 1982.

(St82a) F. W. Stallmann, *Curve Fitting and Uncertainty Analysis of Charpy Impact Data*, NUREG/CR-2408, ORNL/TM-8081, NRC, Washington, DC, 1982.

(St82b) F. W. Stallmann, "LSL - A Logarithmic Least Squares Adjustment Method," *Proc. of the 4th ASTM-EURATOM Symposium on Reactor Dosimetry*, Gaithersburg, MD, March 22-26, 1982, NUREG/CP-0029, NRC, Washington, DC, Vol. 2, pp. 1123-1128, July 1982.

(St82c) F. W. Stallmann, "Uncertainties in the Estimation of Radiation Damage Parameters," *Proc. of the 4th ASTM-ERATOM Syumposium on Reactor Dosimetry*, Gaithersburg, MD, March 22-26, 1982, NUREG/CP-0029, NRC, Washington, DC, Vol. 2, pp. 1155-1163, July 1982.

(St82d) F. W. Stallmann, "Evaluation and Uncertainty Estimates of Charpy Impact Data," *Proc. of the 4th ASTM-EURATOM Symposium on Reactor Dosimetry*, Gaithersburg, MD, March 22-26, 1982, NUREG/CP-0029, NRC, Washington, DC, Vol. 2, pp. 855-859, July 1982.

(St82e) F. W. Stallmann, "Pressure Vessel Benchmark Facility to Study Fracture Toughness of Irradiated Pressure Vessel Materials (BSR-HSST)," *LWR-PV-SDIP Quarterly Progress Report, April 1982 - June 1982*, NUREG/CR-2805, Vol. 2, HEDL-TME 82-19, NRC, Washington, DC, p. ORNL-17, December 1982.

(St83) F. W. Stallmann, C. A. Baldwin and F. B. K. Kam, *Neutron Spectral Characterization of the 4th Nuclear Regulatory Commission Heavy Section Steel Technology 1T-CT Irradiation Experiment: Dosimetry and Uncertainty Analysis*, NUREG/CR-3333, ORNL/TM-8789, Oak Ridge National Laboratory, Oak Ridge, TN, July 1983.

(St83a) L. E. Steele, Ed., *Status of USA Nuclear Reactor Pressure Vessel Surveillance for Radiation Effects*, ASTM STP 784, American Society for Testing and Materials, Philadelphia, PA, January 1983.

(St83b) L. E. Steele, Ed., Radiation Embrittlement and Surveillance of Nuclear Reactor Pressure Vessels: An International Study, ASTM STP 819, American Society for Testing and Materials, Philadelphia, PA, November 1983.

(St84) F. W. Stallmann, Determination of Damage Exposure Parameter Values in the PSF Metallurgical Irradiation Experiment, NUREG/CR-3814, ORNL/TM-9166, Oak Ridge National Laboratory, Oak Ridge, TN, 1984.

(St84b) F. W. Stallmann, Statistical Evaluation of the Metallurgical Test Data in the ORR-PSF-PVS Irradiation Experiment, NUREG/CR-3815, ORNL/TM-9207, NRC, Washington, DC, August 1984.

(Ta82) S. W. Tagert et al., Structural Mechanics Program: Progress in 1981, EPRI NP-2705-SR, Electric Power Research Institute, Palo Alto, CA, October 1982.

(Ti80) H. Till, "Neutron Radiometric and Calculation Benchmarking for LWR Pressure Vessel Radiation Effects," Proc. of the 3rd ASTM-EURATOM Symposium on Reactor Dosimetry, Ispra, Italy, October 1-5, 1979, EUR 6813, Commission of the European Communities, Vol. II, pp. 1275-1287, 1980.

(To82) H. Tourwé and G. Minsart, "Surveillance Capsule Perturbation Studies in the PSF 4/12 Configuration," Proc. of the 4th ASTM-EURATOM Symposium on Reactor Dosimetry, Gaithersburg, MD, March 22-26, 1982, NUREG/CP-0029, NRC, Washington, DC, Vol. 1, pp. 471-480, July 1982.

(Va79) J. D. Varsik and S. T. Byrne, An Empirical Evaluation of the Irradiation Sensitivity of Reactor Pressure Vessel Materials, ASTM STP 683, American Society for Testing and Materials, Philadelphia, PA, p. 252, 1979.

(Va81) J. D. Varsik, "Evaluation of Irradiation Response of Reactor Pressure Vessel Materials," Semiannual Progress Report No. 3, July - December 1980, EPRI RP-1553-1, TR-MCM-110, Combustion Engineering Inc., Windsor, CT, 1981.

(Va82) J. D. Varsik, S. M. Schloss and J. M. Koziol, Evaluation of Irradiation Response of Reactor Pressure Vessel Materials, EPRI NP-2720, Electric Power Research Institute, Palo Alto, CA, 1982.

(Va83) J. D. Varsik, "An Empirical Evaluation of a Transition Temperature Shift in LWR-PV-SDIP Steels," from the ANS Special Session on Correlations and Implications of Neutron Irradiation Embrittlement of Pressure Vessel Steels, Detroit, MI, June 12-16, 1983, Trans. Am. Nucl. Soc. 44, p. 223, 1983.

(Wi83) M. L. Williams et al., "Validation of Neutron Transport Calculations in Benchmark Facilities for Improved Damage Fluence Predictions," Proc. of the 11th WRSR Information Meeting, Gaithersburg, MD, October 24-28, 1983, NUREG/CP-0048, Vol. 1-6, NRC, Washington, DC, 1983.

(Ya67) S. E. Yanichko, Connecticut Yankee Reactor Vessel Radiation Surveillance Program, WCAP-7036, Westinghouse Electric Corp., Pittsburgh, PA, April 1967.

(Ya73) S. E. Yanichko et al., Analysis of Capsule S from Carolina Power and Light Company H. B. Robinson Unit No. 2 Reactor Vessel Radiation Surveillance Program, WCAP-8249, Westinghouse Electric Corp., Pittsburgh, PA, December 18, 1973.

(Ya74) S. E. Yanichko, T. R. Mager and S. Kang, Analysis of Capsule R from the Rochester Gas and Electric Corporation R. E. Ginna Unit No. 1 Reactor Vessel Radiation Surveillance Program, WCAP-8421, Westinghouse Electric Corp., Pittsburgh, PA, November 1974.

(Ya75) S. E. Yanichko, J. H. Phillips and S. L. Anderson, Analysis of Capsule T from the Florida Power and Light Company Turkey Point Unit No. 3 Reactor Vessel Radiation Surveillance Program, WCAP-8631, Westinghouse Electric Corp., Pittsburgh, PA, December 1975.

(Ya76) S. E. Yanichko and S. L. Anderson, Analysis of Capsule S from the Wisconsin Electric Power Company and Wisconsin-Michigan Power Company Point Beach Nuclear Plant Unit No. 1 Reactor Vessel Radiation Surveillance Program, WCAP-8739, Westinghouse Electric Corp., Pittsburgh, PA, 1976.

(Ya77) S. E. Yanichko, S. L. Anderson and K. V. Scott, Analysis of Capsule V from the Wisconsin Public Service Corporation Kewaunee Nuclear Plant Reactor Vessel Radiation Surveillance Program, WCAP-8908, Westinghouse Electric Corp., Pittsburgh, PA, January 1977.

(Ya78) S. E. Yanichko and S. L. Anderson, Analysis of Capsule R from the Wisconsin Electric Power Company Point Beach Nuclear Plant Unit No. 1 Reactor Vessel Radiation Surveillance Program, WCAP-9357, Westinghouse Electric Corp., Pittsburgh, PA, August 1978.

(Ya79) S. E. Yanichko, S. L. Anderson and W. T. Kaiser, Analysis of Capsule F from the Southern California Edison Company San Onofre Reactor Vessel Radiation Surveillance Program, WCAP-9520, Westinghouse Electric Corp., Pittsburgh, PA, May 1979.

(Ya79a) S. E. Yanichko et al., Analysis of Capsule R from the Wisconsin Electric Power Company Point Beach Nuclear Plant Unit No. 2 Reactor Vessel Radiation Surveillance Program, WCAP-9635, EPRI RP-1021-3, Westinghouse Electric Corp., Pittsburgh, PA, December 1975.

(Ya80) S. E. Yanichko et al., Analysis of Capsule T from the Salem Unit 1 Reactor Vessel Surveillance Program, WCAP-9678, Westinghouse Electric Corp., Pittsburgh, PA, February 1980.

(Ya81) S. E. Yanichko, S. L. Anderson and W. T. Kaiser, Analysis of Capsule V from Northern States Power Company Prairie Island Unit No. 2 Reactor Vessel Radiation Surveillance Program, WCAP-9877, Westinghouse Electric Corp., Pittsburgh, PA, March 1981.

(Ya81a) S. E. Yanichko et al., Analysis of Capsule U from the Commonwealth Edison Company Zion Nuclear Plant Unit No. 1 Reactor Vessel Radiation Surveillance Program, WCAP-9890, EPRI RP-1021-3, Westinghouse Electric Corp., Pittsburgh, PA, March 1981.

(Ya81b) S. E. Yanichko et al., Analysis of the Maine Yankee Reactor Vessel Second Accelerated Surveillance Capsule, WCAP-9875, EPRI RP-1021-3, Westinghouse Electric Corp., Pittsburgh, PA, March 1981.

(Ya81c) S. E. Yanichko et al., Analysis of the Third Capsule from the Commonwealth Edison Company Quad Cities Unit 1 Nuclear Plant Reactor Vessel Radiation Surveillance Program, WCAP-9920, EPRI RP-1021-3, Westinghouse Electric Corporation, Pittsburgh, PA, August 1981.

(Ya82) S. E. Yanichko et al., Analysis of the Fourth Capsule from the Commonwealth Edison Company Dresden Unit 3 Nuclear Plant Reactor Vessel Radiation Surveillance Program, WCAP-10030, EPRI PR-1021-3, Westinghouse Electric Corporation, Pittsburgh, PA, January 1982.

(Ya82a) S. E. Yanichko et al., Analysis of the Third Capsule from the Commonwealth Edison Company Quad Cities Unit 2 Nuclear Plant Reactor Vessel Radiation Surveillance Program, WCAP-10064, EPRI PR-1021-3, Westinghouse Electric Corporation, Pittsburgh, PA, April 1982.

(Zi81) W. Zijp et al., Damage Cross Section Library DAMSIG81, ECN-81-104, The Netherlands Energy Research Foundation, ENC, Petten, The Netherlands, July 1981.

(Zi82a) W. L. Zijp and F. W. Stallmann, "Workshop on Spectrum Adjustment Procedures," Proc. of the 4th ASTM-EURATOM Symposium on Reactor Dosimetry, Gaithersburg, MD, March 22-26, 1982, NUREG/CP-0029, NRC, Washington, DC, Vol. 2, pp. 1221-1230, July 1982.

DISTRIBUTION

R5

DOE-HQ/Office of Converter
Reactor Deployment
Nuclear Regulation & Safety Division
NE-12
Washington, DC 20545

JD Griffith, Deputy Director

DOE-HQ/Office of Breeder
Technology Projects (8)
NE-53
Washington, DC 20545

H. Alter, Asst Director, Safety
DF Bunch, Director, Office of Breeder Technology Projects
PB Hemmig, Asst Director, Reactor Physics Technology
JW Lewellen, Manager, Core Analysis Technology
DK Magnus, Director, Fuels & Core Materials
RJ Neuhold, Director, Safety & Physics
CM Purdy, Asst Director, Materials & Structures Tech
A. Van Echo, Manager, Metallurgy, Absorbers & Standards

DOE-RL/AMF
Laboratory Management
and Technology Services
P.O. Box 550, FED/210-B
Richland, WA 99352

KR Absher, Chief

Arizona State University (2)
College of Eng & Appl Sciences
Tempe, AZ 85287

JW McKlveen
B. Stewart

Argonne National Laboratory (2)
9700 South Cass Avenue
Argonne, IL 60439

RJ Armani
RR Heinrich, Bldg 316

Babcock & Wilcox Company (7)
P.O. Box 10935
Lynchburg, VA 24506-0935

LB Gross
SQ King
RH Lewis
AA Lowe Jr
NL Snidow
JF Walters
CL Whitmarsh

B&W Owners Group
Materials Committee (7)
Babcock & Wilcox Co
P.O. Box 10935
c/o C. J. Hudson
Lynchburg, VA 24506-0935

JA Janiszewski, GPU Nuclear Corp
DF Spond, Arkansas Power & Light Co
MA Haghi, Duke Power Co
RA Webb, Florida Power Corp
DL Cox/SW Rutter, Sacramento Municipal Utility District
RJ Gradomski, Toledo Edison Co
EA Merrick, Tennessee Valley Authority

Battelle
Pacific Northwest Laboratory
P.O. Box 999
Richland, WA 99352

L. Faust
EP Simonen

506

DISTRIBUTION (Cont'd)

Battelle Memorial Institute (5)
505 King Avenue
Columbus, OH 43201

RS Denning
RG Jung
LM Lowry
MP Manahan
JS Perrin

Bechtel Power Corporation
15740 Shady Grove Road
Gaithersburg, MD 20760

WC Hopkins

Brookhaven National Laboratory (4)
National Neutron Cross-Section Center
Upton, Long Island, NY 11973

AL Aronson
JF Carew
BA Magurno
S. Pearlstein, T-197

Burns & Roe Inc
633 Industrial Avenue
Paramus, NJ 07672

J. Celnik

Carolina Power & Light Co
P.O. Box 1551
Raleigh, SC 27602

SP Grant

Centre d'Etude de l'Energie Nucléaire
Studiecentrum voor Kernenergie (6)
Boeretang 200
B-2400 Mol, Belgium

J. Debrue
G. DeLeeuw
S. DeLeeuw
A. Fabry
G. Minsart
Ph Van Asbroeck

Combustion Engineering Inc (5)
1000 Prospect Hill Road
Windsor, CT 06095

S. Byrne
G. Cavanaugh
JJ Koziol
RG Shimko
D. Stephen

Comitato Nazional per Energia Nucléare
Centro di Studi Nucleari della Casaccia
Casella Postale 2400
Santa Maria di Galeria
I-00060 Rome, Italy

U. Farinelli

Commissariat a l'Energie Atomique
Centre d'Etudes Nucleaires de Saclay (6)
Boite Postale 2
91190 Gif-sur-Yvette, France

AA Alberman
C. Buchalet
(Framatome)
JM Cerles
JP Genthon
P. Mas
(Grenoble)
P. Petrequin

Commonwealth Edison
P.O. Box 767
Chicago, IL 60690

E. Steeve

EG&G Idaho Inc
P.O. Box 1625
Idaho Falls, ID 83415

JW Rogers

EG&G Ortec Inc
100 Midland Road
Oak Ridge, TN 37830

W. Zimmer

DISTRIBUTION (Cont'd)

Electric Power Research Institute (8)
3412 Hillview Avenue
P.O. Box 10412
Palo Alto, CA 94304

T. Griesback	AD Rossin
TU Marston	R. Shaw
O. Ozer	K. Stahlkopf
T. Passell	JJ Taylor

Energieonderzoek Centrum Nederland
Westerdionweg 3
Postfach 1
NL-1755 ZG, Petten, The Netherlands

WL Zijp

EURATOM
Joint Research Center Ispra (2)
I-21020 Ispra, Varese, Italy

R. Dierckx
H. Rief

Florida Power & Light Co
P.O. Box 529100
Miami, FL 33152

JB Sun

Fracture Control Corporation
5951 Encina Road, No. 105
Goleta, CA 93117

P. McConnell

General Electric Co (3)
Vallecitos Nuclear Center
P.O. Box 460
Pleasanton, CA 94566

JP Higgins	GC Martin
JN Kass	

Institüt für Kernenergetik
und Energiesysteme (IKE-Stüttgart) (2)
Pfaffenwaldring 31, Postfach 801140
D-7000 Stüttgart 80 (Vaihingen),
Federal Republic of Germany

G. Hehn
G. Prillinger

International Atomic Energy Agency (2)
Wagramerstrasse 5, Postfach 100
A-1400 Vienna, Austria

A. Sinev
JJ Schmidt

Italian Atomic Power Authority
National Electric Energy Agency (2)
Viale Regina Margherita 137
Rome, Italy

M. Galliani
F. Remondino

Japan
Atomic Energy Research Institute (2)
Tokai Research Establishment
Tokai-mura, Naka-gun
Ibaraki-ken, Japan

S. Mizazono
K. Sakurai

Kernforschungsanlage Jülich GmbH (3)
Postfach 1913
D-517 Jülich 1,
Federal Republic of Germany

D. Pachur	L. Weise
W. Schneider	

508

DISTRIBUTION (Cont'd)

Kraftwerk Union Aktiengesellschaft (5)
Postfach 3220
D-8520 Erlangen,
Federal Republic of Germany

A. Gerscha
U. Groschel
W. Hofmann
J. Koban
C. Leitz

Los Alamos National Laboratory (2)
P.O. Box 1663
Los Alamos, NM 87545

GE Hansen, Group N-2
L. Stewart

Maine Yankee Atomic Power Co
Edison Drive
Augusta, MA 04336

HF Jones Jr

Materials Engineering Associates Inc
111 Mel-Mara Drive
Oxen Hill, MD 20021

JR Hawthorne

Max-Planck-Institüt
für Plasma Physik
The NET Team
D-8046 Garching bei München,
Federal Republic of Germany

DR Harries, Technology

Metrology Control Corporation
Joseph Building, Suite 7
1393 George Washington Way
Richland, WA 99352

JH Roberts

National Bureau of Standards
Center of Radiation Research (6)
Gaithersburg, MD 20899

RS Caswell
CM Eisenhauer
DM Gilliam
JA Grundl
G. Lamaze
ED McGarry

Naval Research Laboratory
Engineering Materials Division
Thermostructural Materials Branch
Code 6390
Washington, DC 20375

LE Steele

Nuclear Regulatory Commission (18)
Office of Nuclear Regulatory Research
Division of Engineering Technology
Materials Engineering Branch
5650 Nicholson Road
Washington, DC 20555

Chief
Public Doc Rm (3)
M. Bolotski
M. Dunenseld
BJ Elliot
R. Gamble
W. Hazelton
KG Hoge
RE Johnson
L. Lois
S. Pawlicki
PN Randall
CZ Serpan
D. Sieno
A. Taboada
M. Vagin

Oak Ridge National Laboratory (7)
P.O. Box X
Oak Ridge, TN 37830

CA Baldwin, Bldg 3001
FBK Kam
AL Lotts
RE Maerker
LS Miller
R. Nanstad
FW Stallmann

DISTRIBUTION (Cont'd)

Rockwell International
Rocketdyne Division (2)
6633 Canoga Avenue
Canoga Park, CA 91304

H. Farrar IV
BM Oliver

Rolls-Royce & Associates Ltd (4)
P.O. Box 31
Derby DE2 8BJ, UK

M. Austin
P. Burch
AF Thomas
TJ Williams

S.A. Cockerill-Ougree
Recherches et Developments
Division de la Construction Mecanique
B-4100 Seraing, Belgium

J. Widart

Science Applications Inc (3)
P.O. Box 2325
La Jolla, CA 92037

W. Hagan
GL Simmons
VV Verbinski

Ship Research Institute
Tokai Branch Office
Tokai-mura, Naka-gun
Ibaraki-ken, Japan

K. Takeuchi

Southwest Research Institute
8500 Calebra Road
P.O. Box 28510
San Antonio, TX 78284

EB Norris

Swiss Federal Institute
for Reactor Research
CH-5303 Würenlingen, Switzerland

F. Hegedüs

United Kingdom Atomic Energy Authority
Atomic Energy Research Establishment (2)
Harwell, Oxon OX11 0RA, UK

LM Davies
AJ Fudge

United Kingdom Atomic Energy Authority
Atomic Energy Establishment (4)
Winfrith, Dorchester, Dorset, UK

J. Butler
CG Campbell
AK McCracken
J. Sanders

University of Arkansas (2)
Dept of Mechanical Engineering
Fayetteville, AR 72701

CO Cogburn
L. West

University of California
at Santa Barbara (2)
Dept of Chem & Nucl Engineering
Santa Barbara, CA 93106

G. Lucas
GR Odette

University of London
Reactor Center
Silwood Park, Sunnyhill,
Ascot, Berkshire SL5 7PY, UK

JA Mason

BEST COPY AVAILABLE

DISTRIBUTION (Cont'd)

University of Tokyo (2)
Dept of Nuclear Engineering
7-3-1, Hongo
Bunkyo-ku, Tokyo, 113 Japan

M. Nakazawa
J. Sekiguchi

Westinghouse
Research and Development Center (2)
1310 Beulah Road
Pittsburgh, PA 15235

FH Ruddy
JA Spitznagel

Westinghouse
Nuclear Energy Systems (5)
P.O. Box 355
Pittsburgh, PA 15230

SL Anderson
EP Lippincott
TR Mager
RC Shank
SE Yanichko

University of Missouri at Rolla (2)
Dept of Nuclear Engineering
Building C
Rolla, MO 65401

DR Edwards
N. Tsoulfanidis

HEDL (42)
c/o Supervisor, Documentation
P.O. Box 1970, W/C-123
Richland, WA 99352

HJ Anderson	W/C-28
RA Bennett	W/D-3
LD Blackburn	W/A-40
JM Dahlke	W/C-115
DG Doran	W/A-57
EA Evans	W/C-23
DS Gelles	W/A-65
R. Gold	W/C-39
GL Guthrie	W/A-40
BR Hayward	W/C-44
LA James	W/A-40
LS Kellogg	W/C-39
NE Kenny	W/C-115
RL Knecht	W/A-40
JJ Laidler	W/B-107
WY Matsumoto	W/C-33
WN McElroy (2)	W/C-39
JP McNeece	W/A-56
JE Nolan	W/B-65
RE Peterson	W/B-66
CC Preston	W/C-39
JM Ruggles	W/C-33
RE Schenter	W/A-58
FA Schmittroth	W/A-58
WF Sheely	W/C-44
FR Shober	W/E-3
RL Simons	W/A-65
HH Yoshikawa	W/C-44
Program Files (10)	W/C-39
Central Files (2)	W/C-110
Documentation	W/C-123

NRC FORM 335
(2-84)
NRCM 1102,
3201, 3202

U.S. NUCLEAR REGULATORY COMMISSION

BIBLIOGRAPHIC DATA SHEET

SEE INSTRUCTIONS ON THE REVERSE

1. REPORT NUMBER (Assigned by TIDC, add Vol. No., if any)
NUREG/CR-3319
HEDL-TME 85-3

2. TITLE AND SUBTITLE
LWR PRESSURE VESSEL SURVEILLANCE DOSIMETRY IMPROVEMENT PROGRAM: LWR POWER REACTOR SURVEILLANCE PHYSICS-DOSIMETRY DATA BASE COMPENDIUM

3. LEAVE BLANK

4. DATE REPORT COMPLETED

MONTH	YEAR
July	1985

5. AUTHOR(S)
Edited by W. N. McElroy

6. DATE REPORT ISSUED

MONTH	YEAR
August	1985

7. PERFORMING ORGANIZATION NAME AND MAILING ADDRESS (Include Zip Code)
Hanford Engineering Development Laboratory
P.O. Box 1970
Richland, WA 99352

8. PROJECT/TASK/WORK UNIT NUMBER

9. FIN OR GRANT NUMBER
B5988

10. SPONSORING ORGANIZATION NAME AND MAILING ADDRESS (Include Zip Code)
Division of Engineering Technology
Office of Nuclear Regulatory Research
U.S. Nuclear Regulatory Commission
Washington, DC 20555

11a. TYPE OF REPORT
Technical

b. PERIOD COVERED (Inclusive dates)

12. SUPPLEMENTARY NOTES

13. ABSTRACT (200 words or less)

This NRC physics-dosimetry compendium (Sections 1.0 through 4.0) is a collation of information and data developed from available research and commercial light water reactor vessel surveillance program (RVSP) documents and related surveillance capsule reports. The Section 4.0 data represents the results of the HEDL least-squares FERRET-SAND II Code re-evaluation of exposure units and values for 47 PWR and BWR surveillance capsules. Using a consistent set of auxiliary data and dosimetry-adjusted reactor physics results, the revised fluence values for E > 1 MeV averaged 25% higher than the originally reported values. The range of fluence values (new/old) was from a low of 0.80 to a high of 2.38.

These HEDL-derived FERRET-SAND II exposure parameter values are being used for NRC-supported HEDL and other PWR and BWR trend curve data development and testing studies, which support Revision 2 of Regulatory Guide 1.99. These trend curves are used by the utilities and by the NRC to account for neutron radiation damage in setting pressure/temperature limits, in analysing fractures, and in predicting neutron-induced changes in reactor PV steel fracture toughness and embrittlement during the vessel's service life.

The status of the development and application of new advancements in LWR reactor surveillance programs is discussed, such as cavity physics-dosimetry for improving the reliability of current and end-of-life (EOL) predictions on the metallurgical conditions of pressure vessels and their support structures.

14. DOCUMENT ANALYSIS - a. KEYWORDS/DESCRIPTORS
LWR pressure vessel surveillance
Physics-dosimetry data base
Compendium

b. IDENTIFIERS/OPEN-ENDED TERMS

15. AVAILABILITY STATEMENT
Unlimited

16. SECURITY CLASSIFICATION
(This page)
Unclassified
(This report)
Unclassified

17. NUMBER OF PAGES

18. PRICE

512

BEST COPY AVAILABLE